

INFORMATION TO USERS

This manuscript has been reproduced from the microfilm master. UMI films the text directly from the original or copy submitted. Thus, some thesis and dissertation copies are in typewriter face, while others may be from any type of computer printer.

The quality of this reproduction is dependent upon the quality of the copy submitted. Broken or indistinct print, colored or poor quality illustrations and photographs, print bleedthrough, substandard margins, and improper alignment can adversely affect reproduction.

In the unlikely event that the author did not send UMI a complete manuscript and there are missing pages, these will be noted. Also, if unauthorized copyright material had to be removed, a note will indicate the deletion.

Oversize materials (e.g., maps, drawings, charts) are reproduced by sectioning the original, beginning at the upper left-hand corner and continuing from left to right in equal sections with small overlaps. Each original is also photographed in one exposure and is included in reduced form at the back of the book.

Photographs included in the original manuscript have been reproduced xerographically in this copy. Higher quality 6" x 9" black and white photographic prints are available for any photographs or illustrations appearing in this copy for an additional charge. Contact UMI directly to order.

U·M·I

University Microfilms International
A Bell & Howell Information Company
300 North Zeeb Road, Ann Arbor, MI 48106-1346 USA
313 761-4700 800 521-0600

Order Number 9236318

**Molecular engineering of liquid crystal polymers by living
polymerization**

Lee, Myongsoo, Ph.D.

Case Western Reserve University, 1992

U·M·I
300 N. Zeeb Rd.
Ann Arbor, MI 48106

MOLECULAR ENGINEERING OF LIQUID CRYSTAL POLYMERS BY LIVING
POLYMERIZATION

by

MYONGSOO LEE

Submitted in partial fulfillment of the requirements
for the Degree of Doctor of Philosophy

Thesis Advisor: Professor Virgil Percec

Department of Macromolecular Science
CASE WESTERN RESERVE UNIVERSITY

May, 1992

CASE WESTERN RESERVE UNIVERSITY

GRADUATE STUDIES

We hereby approve the thesis of

Myongsoo Lee
candidate for the Ph. D

degree.*

Signed:

Leroy R. Sullivan
(Chairman)

B. J. Skelton
John R. Skelton
JP Skelton

Date January 16, 1992

*We also certify that written approval has
been obtained for any proprietary material
contained therein.

I grant to Case Western Reserve University the right to use this work, irrespective of any copyright, for the University's own purposes without cost to the University or to its students, agents and employees. I further agree that the University may reproduce and provide single copies of the work, in any format other than in or from microforms, to the public for the cost of reproduction.

Thompson Lee

MOLECULAR ENGINEERING OF LIQUID CRYSTAL POLYMERS BY LIVING POLYMERIZATION

Abstract

by

MYONGSOO LEE

This dissertation is concerned with the synthesis and living cationic polymerization of ω -[(4-cyano-4'-biphenyl)oxy]alkyl vinyl ethers with alkyl groups from two to eleven methylene units. The phase transitions of polymers are described and compared to those of the ω -[(4-cyano-4'-biphenyl)oxy]alkyl ethyl ethers which are models of the monomeric structural units of the corresponding polymers. In addition, the influence of molecular weight on the phase transitions of the polymers is discussed.

Polymers containing flexible spacers with either 11 or 10 methylene unit exhibit an enantiotropic S_A phase, and above a certain molecular weight both polymers show a second smectic (S_X , unidentified) phase. Polymers with either 6 or 8 methylene units exhibit nematic and S_A phases at low degrees of polymerization. However, above a certain molecular weight the nematic phase disappears and a second smectic phase (S_X) appears. Polymers with medium length spacers containing an odd number of methylene units ($n=7,9$) exhibit an enantiotropic S_A phase and polymers with spacer lengths ($n=3$ and 4) exhibit an enantiotropic nematic mesophase irrespective of molecular weight. However, polymer containing a flexible spacer with 2 methylene units has a nematic mesophase only at low degrees of polymerization, and polymer with 5 methylene units exhibits the unusual isotropic-nematic- S_{AD} -reentrant nematic sequence above a certain

molecular weight. These results demonstrate that the transition temperature, nature, and number of mesophases are molecular weight dependent.

In the second part, the synthesis and characterization of statistical binary copolymers based on ω -[(4-cyano-4'-biphenyl)oxy]alkyl vinyl ethers with different spacer lengths are described. These binary copolymers were synthesized with constant degree of polymerization and narrow molecular weight distributions. It is demonstrated that the structural units of all binary copolymers behave as an ideal solution. This behavior allows the molecular engineering of materials having specified phase transition temperatures and corresponding thermodynamic parameters in a straightforward manner by living copolymerizations.

The synthesis and characterization of poly{ ω -[(4-cyano-4'-biphenyl)oxy]alkyl vinyl ether-co-(2S,3S)-(+)-2-chloro-3-methylpentyl 4'-(8-vinyloxyoctyloxy)biphenyl-4-carboxylate}X/Y {poly[(6-n)-co-(15-8)]X/Y} (where X/Y represents the molar ratio of the two structural units) with constant degree of polymerization and narrow molecular weight distribution are also described. In contrast to binary copolymers based on structural units containing the same mesogen but different spacer lengths, which behave as an ideal solution derived from the two structural units, this second class of statistical binary copolymers containing dissimilar mesogens having isomorphic structural units behave as a non-ideal solution.

In Part III, the synthesis and characterization of macromonomers and block copolymers based on mesogenic units are described. These experiments demonstrate that living cationic polymerization of mesogenic vinyl ether can be used in the synthesis of mesogenic macromonomers and mesogenic block copolymers. All of block copolymers are shown to possess a microphase separated morphology by their thermal behavior, as determined with DSC and optical polarized microscopy.

DEDICATION

This dissertation is dedicated to my wife, Hyungja, to my son, Joohyung and to my daughter, Joyce.

ACKNOWLEDGMENT

I would first like to express my heartiest thanks to my advisor, Professor Virgil Percec for his guidance, support and inspiration throughout this research. His admirable foresight and creativity led to the completion of this research.

Thanks are due to Dr. Tsukruk for the X-ray scattering studies of Chapter 3 and Dr. Rinaldi for 2D ^1H -NMR experiments. Special thanks are also extended to the members of Prof. Percec's group for their helpful suggestions, discussion and moral support.

Also, I would like to acknowledge the financial support from the Office of Naval Research.

TABLE OF CONTENTS

ABSTRACT.....	ii
DEDICATION.....	iv
ACKNOWLEDGMENT.....	vi
LIST OF SCHEMES AND FIGURES.....	xi
LIST OF TABLES.....	xxvi
CHAPTER 1. General Introduction.....	1
1.1. Thermotropic Liquid Crystals.....	1
1.2. Side Chain Liquid Crystal Polymers.....	3
1.2.1. Influence of Flexible Spacer	
1.2.2. Influence of Polymer Backbone	
1.2.3. Influence of Molecular Weight	
1.2.4. Living Cationic Polymerization of Mesogenic Vinyl Ethers	
1.3. General Experimental	18
References.....	20
PART I. INFLUENCE OF MOLECULAR WEIGHT ON THE PHASE TRANSITIONS OF POLY{ ω -[(4-CYANO-4'- BIPHENYL)OXY]ALKYL VINYL ETHER}S.....	24
CHAPTER 2. Synthesis and Characterization of Poly{ ω -[(4-Cyano-4'- Biphenyl)oxy]alkyl Vinyl Ether}s with Decanyl and Undecanyl Groups.....	25
2.1. Introduction.....	25
2.2. Experimental.....	26
2.2.1. Techniques	
2.2.2. Materials	
2.2.3. Synthesis of Monomers	
2.2.4. Cationic Polymerization	
2.3. Results and Discussion.....	35
References.....	67

CHAPTER 3. Structural Rearrangements During Mesomorphic Phase Transitions in Poly{ 10-[(4-Cyano-4'-Biphenyl)oxy]decanyl Vinyl Ether}	69
3.1. Introduction.....	69
3.2. Experimental.....	69
3.2.1. Materials	
3.2.2. Techniques	
3.3. Results and Discussion.....	73
3.3.1. Low-Temperature Smectic Phase	
3.3.2. High-Temperature Smectic Phase	
3.4. Conclusions.....	90
References.....	91
CHAPTER 4. Influence of Molecular Weight on the Phase Transitions of Poly{ 8-[(4-Cyano-4'-Biphenyl)oxy]octyl Vinyl Ether} and Poly{ 6-[(4-Cyano-4'-Biphenyl)oxy]hexyl Vinyl Ether}	92
4.1. Introduction.....	92
4.2. Experimental.....	93
4.2.1. Materials	
4.2.2. Synthesis of Monomers	
4.3.3. Cationic Polymerization	
4.3. Results and Discussion.....	99
References.....	124
CHAPTER 5. Influence of Molecular Weight on the Phase Transitions of Poly{ ω -[(4-Cyano-4'-Biphenyl)oxy]alkyl Vinyl Ether}s with Nonyl, Heptyl and Pentyl Alkyl Groups.....	126
5.1. Introduction.....	126
5.2. Experimental.....	127
5.2.1. Materials	
5.2.2. Synthesis of Monomers	
5.3.3. Cationic Polymerization	
5.3. Results and Discussion.....	136
References.....	163

CHAPTER 6. Influence of Molecular Weight on the Phase Transitions of Poly{ ω -[(4-Cyano-4'-Biphenyl)oxy]alkyl Vinyl Ether}s with Butyl, Propyl and Ethyl Alkyl Groups.....	165
6.1. Introduction.....	165
6.2. Experimental.....	165
6.2.1. Materials	
6.2.2. Synthesis of Monomers	
6.3.3. Cationic Polymerization	
6.3. Results and Discussion.....	173
References.....	201
PART II. MOLECULAR ENGINEERING OF LIQUID CRYSTALLINE PHASES BY COPOLYMERIZATION.....	202
CHAPTER 7. Synthesis and Characterization of Binary Copolymers of Poly{ ω -[(4-Cyano-4'-Biphenyl)oxy]alkyl Vinyl Ether}s Containing Undecanyl and Hexyl, Pentyl and Propyl, Undecanyl and Propyl, and Undecanyl and Pentyl Pairs of Alkyl Groups.....	203
7.1. Introduction.....	203
7.1.1. Isomorphism of Liquid Crystals	
7.1.2. Copolymerization.	
7.2. Experimental.....	207
7.2.1. Materials	
7.2.2. Monomer Synthesis	
7.2.3. Cationic Polymerization and Copolymerization	
7.3. Results and Discussion.....	209
7.3.1. Poly[(6-11)-co-(6-6)]	
7.3.2. Poly[(6-5)-co-(6-3)]	
7.3.1. Poly[(6-11)-co-(6-3)]	
7.3.1. Poly[(6-11)-co-(6-5)]	
References.....	256
CHAPTER 8. Synthesis and Characterization of Binary Copolymers of Poly{ ω -[(4-Cyano-4'-Biphenyl)oxy]alkyl Vinyl Ether}s Containing Undecanyl and Ethyl, and Octyl and Ethyl Pairs of Alkyl Groups.....	260
8.1. Introduction.....	260
8.2. Experimental.....	261
8.2.1. Materials	
8.2.2. Synthesis of Monomers	

8.2.3. Cationic Polymerization	
8.3. Results and Discussion.....	262
8.3.1. Poly[(6-8)-co-(6-2)]	
8.3.2. Poly[(6-11)-co-(6-2)]	
References.....	288
CHAPTER 9. Synthesis and Characterization of Binary Copolymers of 11-[(4-Cyano-4'-Biphenyl)oxy]undecanyl Vinyl Ether with (2S,3S)-(+)-2-Chloro-3-Methylpentyl-4'-(8-Vinyloxyoctyloxy)biphenyl-4-Carboxylate, and of (2S,3S)-(+)-2-Chloro-3-Methylpentyl-4'-(8-Vinyloxyoctyloxy)biphenyl-4-Carboxylate with 3-[(4-Cyano-4'-Biphenyl)oxy]propyl Vinyl Ether	289
9.1. Introduction.....	289
9.2. Experimental.....	291
9.2.1. Materials	
9.2.2. Synthesis of Monomers	
9.2.3. Cationic Polymerization and Copolymerization	
9.3. Results and Discussion.....	292
9.3.1. Poly[(6-11)-co-(15-8)]X/Y	
9.3.2. Poly[(15-8)-co-(6-3)]X/Y	
References.....	319
PART III. MOLECULAR ENGINEERING OF LIQUID CRYSTAL POLYMERS BY END FUNCTIONALIZATION AND BLOCK COPOLYMERIZATION.....	322
CHAPTER 10. Synthesis and Characterization of Macromonomers and Block Copolymers based on ω -[(4-Cyano-4'-Biphenyl)oxy]Alkyl Vinyl Ethers.....	323
10.1. Introduction.....	323
Part A. Synthesis and Characterization of Poly{3-[(4-Cyano-4'-Biphenyl)oxy]propyl Vinyl Ether} Macromonomers.....	324
10.2. Experimental.....	324
10.2.1. Materials	
10.2.2. Synthesis of Monomers	
10.2.3. Polymerizations	
10.3. Results and Discussion.....	326

Part B: Synthesis and Characterization of AB Block Copolymers Based on ω -(4-cyano-4'-biphenyl)oxy]alkyl Vinyl Ether, and 1H,1H,2H,2H-Perfluorodecyl Vinyl Ether, and of 2-(4-Biphenyloxy)ethyl Vinyl Ether with 1H,1H,2H,2H-Perfluorodecyl Vinyl Ether.....	334
10.4. Experimental.....	334
10.4.1. Materials	
10.4.2. Techniques	
10.4.3. Synthesis of Monomers	
10.4.4. Synthesis of Block Copolymers	
10.5. Results and Discussion.....	336
References.....	354
BIBLIOGRAPHY	355

LIST OF SCHEMES AND FIGURES

CHAPTER 1

- Figure 1. Schematic representation of molecular arrangements in liquid and different types of liquid crystal phases
- Scheme I. Synthesis of liquid crystalline polymers by radical polymerization
- Scheme II. Synthesis of liquid crystalline polymers by polymer homologous reactions.
- Figure 2. Schematic structure of liquid crystalline side chain polymers showing the necessity of decoupling the mesogenic groups and the polymer main chain through flexible spacers
- Figure 3. Schematic representation of the theoretical distortion of the statistical random coil conformation of the polymer backbone in the nematic and smectic phases. (b) Two possible modes of distortion of the random coil conformation of a rigid (left) and a flexible (right) polymer backbone. R_{\parallel} refers to the radius of gyration parallel to the magnetic field. The radius of gyration perpendicular to the magnetic field is labelled as R_{\perp} .
- Figure 4. (a) Schematic plot of free energies vs. temperature for a scheme that does not show a mesophase. G_k , G_{lc} and G_i are, respectively, the free energies of the crystalline, mesomorphic (virtual) and isotropic liquid states. $T_{k-i}=T_m$ is the crystalline melting point. Heavy line corresponds to the most stable state at a given temperature. (b) Schematic plot of free energies vs. temperature for system in Figure 4a but with raised G_i (to G_i') and the mesophase is uncovered. Heavy line corresponds to the most stable state at a given temperature.
- Figure 5. The broadening of the temperature range of an enantiotropic mesophase of the monomeric structural unit (M_0) by increasing the degree of polymerization. The upper part (a) describes the influence of molecular weight on the dependence between the free energies of the crystalline (G_k), liquid crystalline (G_{lc}) and isotropic (G_i) phases and transition temperatures. The translation of this dependence into the dependence phase transition temperature-molecular weight is presented in the lower part (b).
- Figure 6. Transformation of a virtual or monotropic mesophase of the monomeric structural unit (M_0) into an enantiotropic mesophase by increasing the degree of polymerization. The upper part (a) describes the influence of molecular weight on the dependence between the free energies of the crystalline (G_k), liquid crystalline (G_{lc}) and isotropic (G_i) phases and transition temperatures. The translation of this dependence into the dependence phase transition temperature-molecular weight is presented in the lower part (b).

Scheme III. Two general living cationic polymerization systems. 1) Active carbocation propagating species stabilized by their counterion 2) active carbocation stabilized by a Lewis base.

CHAPTER 2

Scheme I. Synthesis of monomers and model Compounds.

Scheme II. Cationic polymerization of 6-10 and 6-11

Scheme III. Chain transfer and termination reactions.

Figure 1. Representative 300-MHz 1-D ^1H -NMR spectrum of poly(6-10) with theoretical DP=4

Figure 2a. The aromatic region of the 300-MHz 2-D ^1H -NMR spectrum of poly(6-10) with theoretical DP=4.

Figure 2b. The aliphatic region of the 300-MHz 2-D ^1H -NMR spectrum of poly(6-10) with theoretical DP=4.

Figure 3. GPC traces of poly(6-10) with different molecular weights. The degrees of polymerization of each sample are printed on the figure.

Figure 4. The dependence of the number average molecular weight (M_n) determined by GPC; \square and by NMR; \blacktriangle and of the polydispersity (M_w/M_n); Δ of poly(6-10) on the $[M]_0/[I]_0$ ratio.

Figure 5a. Heating and cooling DSC traces of 7-10 (a, b), 6-10 (c, d) and 8-10 (e, f).

Figure 5b. Heating and cooling DSC traces of 7-11 (a, b), 6-11 (c, d) and 8-11 (e, f).

Figure 6a. DSC traces displayed during the first heating scan by poly(6-10) with different DP determined by GPC.

Figure 6b. DSC traces displayed during the second heating scan by poly(6-10) with different DP determined by GPC.

Figure 6c. DSC traces displayed during the first cooling scan by poly(6-10) with different DP determined by GPC.

Figure 7a The dependence of phase transition temperatures on the degree of polymerization of poly(6-10) (data from the first heating scan): O-T_g; \blacksquare -T_{k-S_A}; \square -T_{S_A-i}

- Figure 7b. The dependence of phase transition temperatures on the degree of polymerization of poly(6-10) (data from the second heating scan): O-Tg; Δ -Ts_{X-sA}; \square -Ts_{A-i}
- Figure 7c. The dependence of phase transition temperatures on the degree of polymerization of poly(6-10) (data from the first cooling scan): \blacksquare -Ti-s_A; \blacktriangle -Ts_{A-sX}; \bullet -Tg.
- Figure 8a. DSC traces displayed during the first heating scan by poly(6-11) with different DP.
- Figure 8b. DSC traces displayed during the second heating scan by poly(6-11) with different DP.
- Figure 8c. DSC traces displayed during the first cooling scan by poly(6-11) with different DP.
- Figure 9a. The dependence of phase transition temperatures on the degree of polymerization of poly(6-11). DP=1 corresponds to 8-11. (data from first heating) (fh) and (second heating scans) (sh) are presented in Figure 8a. \square -Tk-s_A(fh); O-Tg(fh); Δ -Ts_{A-i}(fh); \bullet -Tk-s_A(sh); \bullet -Tg(sh); \blacksquare -Ts_{X-sA}(sh); \blacktriangle -Ts_{A-i}(sh).
- Figure 9b. The dependence of phase transition temperatures on the degree of polymerization of poly(6-11). DP=1 corresponds to 8-11. (data from the cooling scan). \blacksquare -Ti-s_A; \blacklozenge -Ts_{A-k}; \blacktriangle -Ts_{A-sX}; \bullet -Tg.
- Figure 10. Representative optical polarized micrographs (100x) of poly(6-11) with DP=31: a) the s_A displayed at 148°C; b) the s_X displayed at 30°C.

CHAPTER 3

- Scheme I. The structure of poly{ 10-[(4-cyano-4'-biphenyl)oxy]decanyl vinyl ether} poly(6-10)
- Figure 1. Heating and cooling DSC traces (20 °C/min) of poly(6-10) with DP=19: A) first heating scan; B) second and subsequent heating scan; C) first and subsequent cooling scan.
- Figure 2. Wide-angle-X-ray scattering curves of poly(6-10) at different temperatures.
- Figure 3. Small angle X-ray scattering curves of poly(6-10) at different temperatures.

- Figure 4. Split of the WAXS for the smectic E phase of poly(6-10) by Lorentz profiles.
- Figure 5a. One-dimensional correlation functions $G(x)$ of poly(6-10) in the smectic E and smectic A phases
- Figure 5b. One-dimensional correlation functions $G(x)$ of poly(6-10) in the smectic E phase after cooling and annealing
- Figure 6. Molecular models of the liquid crystalline poly(6-10): (a) model of double-layered packing with overlapping of the mesogenic groups (main periodicity and half periodicity are shown), (b) possible changes of the arrangement of the biphenyl mesogenic groups as a result of torsional rotation.
- Figure 7. Wide-angle X-ray scattering curves of poly(6-10) at 35°C after cooling and annealing during 1 day.
- Figure 8. The dependence of d-spacing of poly(6-10) on temperature.
- Figure 9. Small-angle X-ray scattering curves of poly(6-10) obtained during annealing.

CHAPTER 4

- Scheme I. Synthesis of monomers and model compounds
- Scheme II. Cationic polymerization of 6-8 and 6-6
- Figure 1. The dependence of the number average molecular weight (M_n) and of the polydispersity (M_w/M_n) of poly(6-8) on the $[M]_0/[I]_0$ ratio.
- Figure 2a. Heating and cooling DSC traces of 7-8 (a, b), 6-8 (c, d) and 8-8 (e, f).
- Figure 2b. Heating and cooling DSC traces of 7-6 (a,b), 6-6 (c,d) and 8-6 (e,f).
- Figure 3a. DSC traces displayed during the first heating scan by poly (6-8) with different degrees of polymerization (DP). DP is printed on the top of each DSC scan.
- Figure 3b. DSC traces displayed during the second heating scan by poly (6-8) with different degrees of polymerization (DP). DP is printed on the top of each DSC scan.
- Figure 3c. DSC traces displayed during the first cooling scan by poly (6-8) with different degrees of polymerization (DP). DP is printed on the top of each DSC scan.

- Figure 4a. The dependence of phase transition temperatures on the degree of polymerization of poly(6-8). DP=1 corresponds to 8-8. (Data from first heating scan): O-Tg; \square -Ts_A-n; Δ -Tn-i; \bullet -Ts_X-s_A.
- Figure 4b. The dependence of phase transition temperatures on the degree of polymerization of poly(6-8). DP=1 corresponds to 8-8. (Data from second heating scan): O-Tg; \square -Ts_A-n; Δ -Tn-i; \bullet -Ts_X-s_A.
- Figure 4c. The dependence of phase transition temperatures on the degree of polymerization of poly(6-8). DP=1 corresponds to 8-8. (Data from first cooling scan): \square -Ti-s_A; Δ -Ti-n; \bullet -Ts_A-s_X; O-Tg; \bullet -Tk.
- Figure 5. Representative optical polarized micrographs (100x) of : a) 8-8 at 53°C on the cooling scan (nematic phase); b) 8-8 at 47°C on the cooling scan (s_A phase).
- Figure 6a. DSC traces displayed during the first heating scan by poly(6-6) with different degrees of polymerization (DP). DP is printed on the top of each DSC scan.
- Figure 6b. DSC traces displayed during the second heating scan by poly(6-6) with different degrees of polymerization (DP). DP is printed on the top of each DSC scan.
- Figure 6c. DSC traces displayed during the first cooling scan by poly(6-6) with different degrees of polymerization (DP). DP is printed on the top of each DSC scan.
- Figure 7a. The dependence of the phase transition temperatures on the degree of polymerization of poly(6-6). DP=1 corresponds to 8-6. (data from first heating scan): O-Tg; \square -Ts_A-n or Ts_A-i; Δ -Tn-i; \bullet -Ts_X-s_A; \bullet -Tm;
- Figure 7b. The dependence of the phase transition temperatures on the degree of polymerization of poly(6-6). DP=1 corresponds to 8-6. (data from second heating scan): O-Tg; \square -Ts_A-n or Ts_A-i; Δ -Tn-i; \bullet -Ts_X-s_A; \bullet -Tm.
- Figure 7c. The dependence of the phase transition temperatures on the degree of polymerization of poly(6-6). DP=1 corresponds to 8-6. (data from second heating scan): Δ -Tg; \square -Ts_A-n or Ts_A-i; O-Tn-i; \square -Ts_X-s_A; \square -Tm.

CHAPTER 5

- Scheme I. Synthesis of 5-[(4-cyano-4'-biphenyl)oxy]pentyl vinyl ether (6-5) and 7-[(4-cyano-4'-biphenyl)oxy]heptyl vinyl ether (6-7).
- Scheme II. Cationic polymerization of 6-9, 6-7 and 6-5.

- Figure 1. The mechanism of formation of the re-entrant nematic (n_{re}) mesophase
- Figure 2. The dependence of the number average molecular weight (M_n) and of the polydispersity (M_w/M_n) of poly(6-5) on the $[M]_0/[I]_0$ ratio.
- Figure 3a. Heating and cooling DSC scans of 7-9 (a, b), 6-9 (c, d) and 8-9 (e, f).
- Figure 3b. Heating and cooling DSC scans of 7-7 (a, b), 6-7 (c, d) and 8-7 (e, f).
- Figure 3c. Heating and cooling DSC scans of 7-5 (a, b), 6-5 (c, d) and 8-5 (e, f).
- Figure 4a. DSC traces displayed during the second heating scan by poly(6-9) with different degrees of polymerization (DP). DP is printed on the top of each DSC scan.
- Figure 4b. DSC traces displayed during the first cooling scan by poly(6-9) with different degrees of polymerization (DP). DP is printed on the top of each DSC scan.
- Figure 5a. The dependence of phase transition temperatures on the degree of polymerization of poly(6-9). (data from second heating scan): ○-T_g; □-T_{SA-i}.
- Figure 5b. The dependence of phase transition temperatures on the degree of polymerization of poly(6-9). (data from first cooling scan): ●-T_g; ■-T_{SA-i}.
- Figure 6a. DSC traces displayed during the second heating scan by poly(6-7) with different degrees of polymerization (DP). DP is printed on the top of each DSC scan.
- Figure 6b. DSC traces displayed during the first cooling scan by poly(6-7) with different degrees of polymerization (DP). DP is printed on the top of each DSC scan.
- Figure 7a. The dependence of phase transition temperatures on the degree of polymerization of poly(6-7). (data from second heating scan): ○-T_g; □-T_{SA-i}.
- Figure 7b. The dependence of phase transition temperatures on the degree of polymerization of poly(6-7). (data from first cooling scan): ●-T_g; ■-T_{SA-i}.
- Figure 8a. DSC traces displayed during the second heating scan by poly(6-5) with different degrees of polymerization (DP). DP is printed on the top of each DSC scan.
- Figure 8b. DSC traces displayed during the first cooling scan by poly(6-5) with different degrees of polymerization (DP). DP is printed on the top of each DSC scan.

- Figure 9a. The dependence of phase transition temperatures on the degree of polymerization of poly(6-5). (data from second heating scan): O-Tg; ▲-T_{nre}-s_{Ad}; □-T_{sAd}-n; Δ-T_{n-i}
- Figure 9b. The dependence of phase transition temperatures on the degree of polymerization of poly(6-5). (data from first cooling scan): O-Tg; Δ-T_{sAd}-n_{re}; ■-T_n-s_{Ad}; ▲-T_i-n.
- Figure 10. Representative optical polarized micrographs (100x) of the phases exhibited by poly(6-5) with degree of polymerization of 30: a) high temperature n phase at 109.2°C; b) transition from n to s_{Ad} phase at 102.4 °C; c) s_{Ad} phase 89.7°C; d) n_{re} phase at 54.2°C.

CHAPTER 6

- Scheme I. Synthesis of 2-[(4-cyano-4'-biphenyl)oxy]ethyl vinyl ether (6-2), 3-[(4-cyano-4'-biphenyl)oxy]propyl vinyl ether (6-3) and 4-[4-cyano-4'-biphenyl)oxy]butyl vinyl ether (6-4).
- Scheme II. Cationic polymerization of 6-2, 6-3 and 6-4.
- Figure 1. The dependence of the number average molecular weight (M_n) and of the polydispersity (M_w/M_n) of poly(6-2) (a), poly(6-3) (b) and poly(6-4) (c) on the [M]₀/[I]₀ ratio.
- Figure 2a. DSC traces displayed during the first heating scan by poly(6-2) with different degrees of polymerization (DP). DP is printed on the top of each DSC scan.
- Figure 2b. DSC traces displayed during the second heating scan by poly(6-2) with different degrees of polymerization (DP). DP is printed on the top of each DSC scan.
- Figure 2c. DSC traces displayed during the first cooling scan by poly(6-2) with different degrees of polymerization (DP). DP is printed on the top of each DSC scan.
- Figure 3. The dependence of phase transition temperatures on the degree of polymerization of poly(6-2). Data from first heating scan (fh) and second heating scan (sh): Δ-T_{n-i}(fh); □-T_{x-n}(fh); O-T_g(fh); ▲-T_{n-i}(sh); ●-T_g(sh).
- Figure 4a. DSC traces displayed during the first heating scan by poly(6-3) with different degrees of polymerization (DP). DP is printed on the top of each DSC scan.

- Figure 4b. DSC traces displayed during the second heating scan by poly(6-3) with different degrees of polymerization (DP). DP is printed on the top of each DSC scan.
- Figure 4c. DSC traces displayed during the first cooling scan by poly(6-3) with different degrees of polymerization (DP). DP is printed on the top of each DSC scan.
- Figure 5. The dependence of phase transition temperatures on the degree of polymerization of poly(6-3). Data from first cooling scan: Δ -T_{n-i}; O-T_g.
- Figure 6a. DSC traces displayed during the first heating scan by poly (6-4) with different degrees of polymerization (DP). DP is printed on the top of each DSC scan.
- Figure 6b. DSC traces displayed during the second heating scan by poly (6-4) with different degrees of polymerization (DP). DP is printed on the top of each DSC scan.
- Figure 6c. DSC traces displayed during the first cooling scan by poly (6-4) with different degrees of polymerization (DP). DP is printed on the top of each DSC scan.
- Figure 7. The dependence of phase transition temperatures on the degree of polymerization of poly(6-4). Data from first heating scan: Δ -T_{n-i}; \square -T_{x-n}; O-T_g.
- Figure 8. The dependence of phase transition temperatures on the length (n) of flexible spacer $[-(\text{CH}_2)_n-]$ of poly(6-n) at similar degrees of polymerization. a) data from second heating scan at DP=30: O-T_g; \blacklozenge -T_{sX-sA}; \square -T_{sA-i}; Δ -T_{n-i}; b) data from second heating scan at DP=23; O-T_g; \blacklozenge -T_{sX-sA}; \square -T_{sA-i}; Δ -T_{n-i}; c) data from second heating scan at DP=13: O-T_g; \square -T_{sA-i}; Δ -T_{n-i}; d) data from second heating scan at DP=4: O-T_g; \square -T_{sA-i}; Δ -T_{n-i}.
- Figure 9. The dependence of phase transition temperatures on the length (n) of flexible $[-(\text{CH}_2)_n-]$ spacer of poly(6-n) at similar degrees of polymerization. a) data from first heating scan at DP=30: O-T_g; \blacklozenge -T_{sX-sA(n)}; \blacksquare -T_{k-sA}; \square -T_{sA-i}; Δ -T_{n-i}; b) data from first heating scan at DP=23; O-T_g; \blacklozenge -T_{sX-sA(n)}; \blacksquare -T_{k-sA}; \square -T_{sA-i}; Δ -T_{n-i}; c) data from first heating scan at DP=13: O-T_g; \blacklozenge -T_{sX-sA(n)}; \blacksquare -T_{k-sA}; \square -T_{sA-i}; Δ -T_{n-i}; d) data from first heating scan at DP=4: O-T_g; \blacklozenge -T_{sX-n}; \blacksquare -T_{k-sA}; \square -T_{sA-i}; Δ -T_{n-i}.

CHAPTER 7

Scheme I. Cationic copolymerization of 6-n and 6-m.

- Figure 1a. DSC traces displayed during the first heating scan by poly(6-11), poly(6-6) and by poly[(6-11)-co-(6-6)]X/Y.
- Figure 1b. DSC traces displayed during the second heating scan by poly(6-11), poly(6-6) and by poly[(6-11)-co-(6-6)]X/Y.
- Figure 1c. DSC traces displayed during the first cooling scan by poly(6-11), poly(6-6) and by poly[(6-11)-co-(6-6)]X/Y.
- Figure 2a. The dependence of phase transition temperatures on the composition of poly[(6-11)-co-(6-6)]X/Y (data from the first heating scan): O-T_g; ◇-T_{SX-SA}; ■-T_{k-SA}; □-T_{SA-i}
- Figure 2b. The dependence of phase transition temperatures on the composition of poly[(6-11)-co-(6-6)]X/Y. (data from the second heating scan): O-T_g; ◇-T_{SX-SA}; □-T_{SA-i}
- Figure 2c. The dependence of phase transition temperatures on the composition of poly[(6-11)-co-(6-6)]X/Y (data from the first cooling scan): ■-T_{i-SA}; ◆-T_{SA-SX}; ●-T_g.
- Figure 2d. The dependence of the enthalpy changes associated with the mesomorphic-isotropic and isotropic-mesomorphic phase transitions on the composition of poly[(6-11)-co-(6-6)]X/Y. □-ΔH_{SA-i} (data from the first heating scan); Δ-ΔH_{SA-i} (data from the second heating scan); O-ΔH_{i-SA} (data from the first cooling scan).
- Figure 3a. DSC traces displayed during the first heating scan by poly(6-5), poly(6-3) and by poly[(6-5)-co-(6-3)]X/Y.
- Figure 3b. DSC traces displayed during the second heating scan by poly(6-5), poly(6-3) and by poly[(6-5)-co-(6-3)]X/Y.
- Figure 3c. DSC traces displayed during the first cooling scan by poly(6-5), poly(6-3) and by poly[(6-5)-co-(6-3)]X/Y.
- Figure 4a. The dependence of phase transition temperatures on the composition of poly[(6-5)-co-(6-3)]X/Y (data from the first heating scan): O-T_g; ◇-T_{X-n}; □-T_{SA-n}; Δ-T_{n-i}

- Figure 4b. The dependence of phase transition temperatures on the composition of poly[(6-5)-co-(6-3)]X/Y (data from the second heating scan): O-T_g; □-T_{sA-n}; Δ-T_{n-i}
- Figure 4c. The dependence of phase transition temperatures on the composition of poly[(6-5)-co-(6-3)]X/Y (data from the first cooling scan): ▲-T_{i-n}; ■-T_{n-sA}; ●-T_g
- Figure 4d. The dependence of the enthalpy changes associated with the mesomorphic-isotropic and isotropic-mesomorphic phase transitions on the composition of poly[(6-11)-co-(6-6)]X/Y. □-ΔH_{sA-i} (data from the first heating scan); Δ-ΔH_{sA-i} (data from the second heating scan); O-ΔH_{i-sA} (data from the first cooling scan).
- Figure 5a. DSC traces displayed during the first heating scan by poly(6-11), poly(6-3) and by poly[(6-11)-co-(6-3)]X/Y.
- Figure 5b. DSC traces displayed during the second heating scan by poly(6-11), poly(6-3) and by poly[(6-11)-co-(6-3)]X/Y.
- Figure 5c. DSC traces displayed during the first cooling scan by poly(6-11), poly(6-3) and by poly[(6-11)-co-(6-3)]X/Y.
- Figure 6a. The dependence of phase transition temperatures on the composition of poly[(6-11)-co-(6-3)]X/Y (data from the first heating scan): O-T_g; ◇-T_{X-sA}; ■-T_{k-sA}; ●-T_{n_{re}-sAd}; □-T_{sA-i}; Δ-T_{n-i}
- Figure 6b. The dependence of phase transition temperatures on the composition of poly[(6-11)-co-(6-3)]X/Y. (data from the secon heatig scan): O-T_g; ◇-T_{sX-sA}; ●-T_{n_{re}-sAd}; □-T_{sA-i}; Δ-T_{n-i}
- Figure 6c. The dependence of phase transition temperatures on the composition of poly[(6-11)-co-(6-3)]X/Y (data from the first cooling scan): ▲-T_{i-n}; ■-T_{i-sA}; ●-T_{sAd-n_{re}}; ◆-T_{sA-sX}; ●-T_g.
- Figure 6d. The dependence of the enthalpy changes associated with the mesomorphic-isotropic and isotropic-mesomorphic phase transitions on the composition of poly[(6-11)-co-(6-3)]X/Y. □-ΔH_{sA-i} (data from the first heating scan); Δ-ΔH_{sA-i} (data from the second heating scan); O-ΔH_{i-sA} (data from the first cooling scan).
- Figure 7: Representative optical polarized micrographs (100x) of the phases exhibited by poly[(6-11)-co-(6-3)]3/7 with degree of polymerization of 20: a) n phase at 99°C; b) transition from n to s_{Ad} at 92.5°C; c) s_{Ad} phase at 83.3°C; d) transition from s_{Ad} to n_{re} at 55.6°C; e) n_{re} phase at 52.9°C

- Figure 8a. DSC traces displayed during the first heating scan by poly(6-11), poly(6-5) and by poly[(6-11)-co-(6-5)]X/Y.
- Figure 8b. DSC traces displayed during the second heating scan by poly(6-11), poly(6-5) and by poly[(6-11)-co-(6-5)]X/Y.
- Figure 8c. DSC traces displayed during the first cooling scan by poly(6-11), poly(6-5) and by poly[(6-11)-co-(6-5)]X/Y.
- Figure 9a. The dependence of phase transition temperatures on composition of poly[(6-11)-co-(6-5)]X/Y: (data from first heating scan): O-Tg; ■-Tk-s_A; □-Ts_A-i or -Ts_A-n; Δ-Tn-i; ▲-Tn_{re}-s_{Ad}
- Figure 9b. The dependence of phase transition temperatures on composition of poly[(6-11)-co-(6-5)]X/Y: (data from second heating scan): O-Tg; ◇-Ts_X-s_A; □-Ts_A-i or -Ts_A-n; Δ-Tn-i; ▲-Tn_{re}-s_{Ad}
- Figure 9c. The dependence of phase transition temperatures on composition of poly[(6-11)-co-(6-5)]X/Y: (data from first cooling scan): ●-Tg; ▲-Ti-n; ■-Ti-s_A or Tn-s_A; Δ-Ts_{Ad}-n_{re}; ◆-Ts_A-s_X
- Figure 9d. The dependence of s_A-n and s_A-i phase transition temperatures on composition of poly[(6-11)-co-(6-5)]X/Y: (■) data calculated by Schroeder-van Laar equation; (□) experimental data from the first heating scan.
- Figure 9e. The dependence of the enthalpy changes associated with the mesomorphic-isotropic and isotropic-mesomorphic phase transitions : □-ΔHn-i (data from the first heating scan); Δ-ΔHn-i (data from the second heating scan); O-ΔHi-n (data from the first cooling scan) versus copolymer composition.

CHAPTER 8

Scheme I. Cationic copolymerization of (6-n) with (6-2)

- Figure 1a. DSC traces displayed during the first heating scan by poly(6-8), poly(6-2) and by poly[(6-8)-co-(6-2)]X/Y.
- Figure 1b. DSC traces displayed during the second heating scan by poly(6-8), poly(6-2) and by poly[(6-8)-co-(6-2)]X/Y.
- Figure 1c. DSC traces displayed during the first cooling scan by poly(6-8), poly(6-2) and by poly[(6-8)-co-(6-2)]X/Y.

- Figure 2a. The dependence of phase transition temperatures on composition of poly[(6-8)-co-(6-2)]X/Y (data from the first heating scan): O-T_g; ◇-T_{sX-sA}; Δ-T_{n-i}; □-T_{sA-i}; ▲-T_{n_{re}-sAd}
- Figure 2b. The dependence of phase transition temperatures on composition of poly[(6-8)-co-(6-2)]X/Y (data from the second heating scan): O-T_g; Δ-T_{n-i}; □-T_{sA-i}; ▲-T_{n_{re}-sAd};
- Figure 2c. The dependence of phase transition temperatures on composition of poly[(6-8)-co-(6-2)]X/Y (data from the first cooling scan): ●-T_g; ▲-T_{i-n}; ■-T_{i-sA}; Δ-T_{sAd-n_{re}}
- Figure 2d. The dependence of the enthalpy changes associated with the mesomorphic-isotropic and isotropic-mesomorphic phase transitions on the composition of poly[(6-8)-co-(6-2)]X/Y. □-ΔH_{sA-i} (data from the first heating scan); Δ-ΔH_{sA-i} (data from the second heating scan); O-ΔH_{i-sA} (data from the first cooling scan).
- Figure 3a. DSC traces displayed during the first heating scan by poly(6-11), poly(6-2) and by poly[(6-11)-co-(6-2)]X/Y.
- Figure 3b. DSC traces displayed during the second heating scan by poly(6-11), poly(6-2) and by poly[(6-11)-co-(6-2)]X/Y.
- Figure 3c. DSC traces displayed during the first cooling scan by poly(6-11), poly(6-2) and by poly[(6-11)-co-(6-2)]X/Y.
- Figure 4a. The dependence of phase transition temperatures on composition of poly[(6-11)-co-(6-2)]X/Y (data from the first heating scan): O-T_g; ◇-T_{sX-sA}; Δ-T_{n-i}; □-T_{sA-i}; ▲-T_{n_{re}-sAd}
- Figure 4b. The dependence of phase transition temperatures on composition of poly[(6-11)-co-(6-2)]X/Y (data from the second heating scan): O-T_g; Δ-T_{n-i}; □-T_{sA-i}; ▲-T_{n_{re}-sAd};
- Figure 4c. The dependence of phase transition temperatures on composition of poly[(6-11)-co-(6-2)]X/Y (data from the first cooling scan): ●-T_g; ▲-T_{i-n}; ■-T_{i-sA}; Δ-T_{sAd-n_{re}}
- Figure 4d. The dependence of the enthalpy changes associated with the mesomorphic-isotropic and isotropic-mesomorphic phase transitions on the composition of poly[(6-11)-co-(6-2)]X/Y. □-ΔH_{sA-i} (data from the

first heating scan); $\Delta\text{-}\Delta H_{SA-i}$ (data from the second heating scan); $O\text{-}\Delta H_{i-SA}$ (data from the first cooling scan).

- Figure 5. Representative optical polarized micrographs (100x) of the phases exhibited by poly[(6-8)-co-(6-2)]6/4 with degree of polymerization of 20: a) n phase at 103°C; b) transition from n to s_{Ad} at 98°C; c) s_{Ad} phase at 83°C d) n_{re} phase at 55°C

CHAPTER 9

Scheme I. Cationic copolymerization of 6-n with 15-8

- Figure 1. The aromatic region of the 200 MHz ^1H -NMR spectrum of poly[(15-8)-co-(6-3)]5/5.
- Figure 2a. DSC traces displayed during the first heating scan of poly(6-11), poly(15-8) and of [poly(6-11)-co-(15-8)]X/Y.
- Figure 2b. DSC traces displayed during the second heating scan of poly(6-11), poly(15-8) and of [poly(6-11)-co-(15-8)]X/Y.
- Figure 2c. DSC traces displayed during the first cooling scan of poly(6-11), poly(15-8) and of [poly(6-11)-co-(15-8)]X/Y.
- Figure 3a. The dependence of phase transition temperatures on the composition of [poly(6-11)-co-(15-8)]X/Y copolymers (data from first heating scan): O -T_g; ■ -T_k; ◇ -T_{SX-SA(SC*)}; □ -T_{SC*-SA}; □ -T_{SA-i};
- Figure 3b. The dependence of s_A -n and s_A -i phase transition temperatures on composition of poly[(6-11)-co-(6-5)]X/Y: (Δ) data calculated by Schroeder-van Laar equation; (□) experimental data from the first heating scan
- Figure 3c. The dependence of phase transition temperatures on the composition of [poly(6-11)-co-(15-8)]X/Y copolymers (data from second heating scan): O -T_g; ■ -T_k; ◇ -T_{SX-SA(SC*)}; □ -T_{SC*-SA}; □ -T_{SA-i}
- Figure 3d. The dependence of phase transition temperatures on the composition of [poly(6-11)-co-(15-8)]X/Y copolymers (data from first cooling scan): ● -T_g; ■ -T_k; ◇ -T_{SA(SC*)-SX}; □ -T_{SA-SC*}; ■ -T_{i-SA}
- Figure 3e. The dependence of the enthalpy changes associated with the mesomorphic-isotropic and isotropic-mesomorphic phase transitions on the composition of [poly(6-11)-co-(15-8)]X/Y: □ - ΔH_{SA-i} (data from

first heating scan); Δ - ΔH_{sA-i} (data from second heating scan); O- ΔH_{i-sA} (data from first cooling scan)

- Figure 4a. DSC traces displayed during the first heating scan of poly(15-8), poly(6-3) and of [poly(15-8)-co-(6-3)]X/Y.
- Figure 4b. DSC traces displayed during the second heating scan of poly(15-8), poly(6-3) and of [poly(15-8)-co-(6-3)]X/Y.
- Figure 4c. DSC traces displayed during the first cooling scan of poly(15-8), poly(6-3) and of [poly(15-8)-co-(6-3)]X/Y.
- Figure 5a. The dependence of phase transition temperatures on the composition of [poly(15-8)-co-(6-3)]X/Y copolymers (data from first heating scan): O - T_g; ■ - T_k; ◇ - T_{X-n(Ch)}; ◇ - T_{sX-sA(SC*)}; □ - s_{C*}-s_A; □ - T_{sA-i}; Δ - T_{n(Ch)-i}
- Figure 5b. The dependence of phase transition temperatures on the composition of [poly(15-8)-co-(6-3)]X/Y copolymers (data from second heating scan): O - T_g; ◇ - T_{sX-sA(SC*)}; □ - s_{C*}-s_A; □ - T_{sA-i}; Δ - T_{n(Ch)-i}
- Figure 5c. The dependence of phase transition temperatures on the composition of [poly(15-8)-co-(6-3)]X/Y copolymers (data from first cooling scan): ● - T_g; ◇ - T_{sA(SC*)-sX}; □ - s_A-s_{C*}; ■ - T_{i-sA}; Δ - T_{i-n(Ch)}
- Figure 5d. The dependence of the enthalpy changes associated with the mesomorphic-isotropic and isotropic-mesomorphic phase transitions on the composition of [poly(15-8)-co-(6-3)]X/Y: □- ΔH_{sA-i} (data from first heating scan); Δ - ΔH_{sA-i} (data from second heating scan); O- ΔH_{i-sA} (data from first cooling scan)
- Figure 6. Representative optical polarized micrograph (100x) of: (a) [poly(15-8)-co-(6-3)]8/2 at 85 °C on the cooling scan (cholesteric phase).

CHAPTER 10

Scheme I. Synthesis of macromonomers

- Figure 1. GPC traces of (A) poly(6-3)-I, (B) poly(6-3)-II and (C) poly(6-3)-III
- Figure 2. 200 MHz ¹H-NMR spectrum of poly(6-3)-I.
- Figure 3. 200 MHz ¹H-NMR spectrum of poly(6-3)-II.
- Figure 4. 200 MHz ¹H-NMR spectrum of poly(6-3)-III.

- Figure 5. The DSC scans (20 °C/min) of poly(6-3)-I: (a) first heating scan, (b) second heating scan, (c) first cooling scan; of poly(6-3)-II: (d) first heating scan, (e) second heating scan, (f) first cooling scan; and of poly(6-3)-III: (d) first heating scan, (e) second heating scan, (f) first cooling scan
- Scheme II. Synthesis of block copolymers
- Figure 6. GPC traces of poly[(6-2)-b-CF8]5/5 (a) and of poly(6-2) (DP=12) (b)
- Figure 7. 300 MHz ¹H-NMR spectrum of poly[(6-2)-b-CF8]5/5
- Figure 8. DSC traces displayed by the first heating (a), second heating (b) and the first cooling scans (c) of poly[(6-2)-b-CF8]5/5
- Figure 9. DSC traces displayed by the first heating (a), second heating (b) and the first cooling scans (c) of poly[BEVE-b-CF8]5/5
- Figure 10. Representative optical polarized micrograph (100x) of the mesophase displayed by poly[(6-2)-b-CF8]5/5 at 190 °C after annealing 1 day.
- Figure 11. DSC traces displayed by the first heating (a), second heating (b) and the first cooling scans (c) of poly[(6-3)-b-CF8]5/5
- Figure 12. Representative optical polarized micrographs (100x) of the mesophase displayed by poly(6-3) (DP=16) at 90 °C (a) and poly[(6-3)-b-CF8]5/5 at 90 °C after annealing overnight.
- Figure 13. DSC traces displayed by the first heating (a), second heating (b) and the first cooling scans (c) of poly[(6-9)-b-CF8]7/3
- Figure 14. Representative optical polarized micrographs (100x) of the mesophase displayed by poly(6-9) (DP=16) (a) and poly[(6-9)-b-CF8]7/3 (b) at 130 °C.
- Figure 15. DSC traces displayed by the first heating (a), second heating (b) and the first cooling scans (c) of poly[(6-11)-b-CF8]7/3

LIST OF TABLES

CHAPTER 2

- Table I. ^1H -NMR Chemical Shifts of Poly(6-10)
- Table II. Integration Ratio of Polymer Chain Ends
- Table III. Thermal Characterization of 4-Cyano-4'-(ω -hydroxyalkan-1-yloxy)biphenyls (7-10) and (7-11), ω -[(4-Cyano-4'-biphenyl)oxy]alkyl Vinyl Ethers (6-10) and (6-11), and of ω -[(4-Cyano-4'-biphenyl)oxy]alkyl Ethyl Ethers (8-10) and (8-11).
- Table IV. Cationic Polymerization of 10-[4-Cyano-4'-biphenyl)oxy]decanyl Vinyl Ether (6-10) (polymerization temperature, 0°C; polymerization solvent, methylene chloride; $[M]_0=0.265$; $[(\text{CH}_3)_2\text{S}]_0/[I]_0=10$; polymerization time, 1hr) and Characterization of the Resulting Polymers
- Table V. Cationic Polymerization of 11-[4-Cyano-4'-biphenyl)oxy]undecanyl Vinyl Ether (6-11) (polymerization temperature, 0°C; polymerization solvent, methylene chloride; $[M]_0=0.255$; $[(\text{CH}_3)_2\text{S}]_0/[I]_0=10$; polymerization time, 1hr) and Characterization of the Resulting Polymers.

CHAPTER 3

- Table I. Cationic Polymerization of 6-10 and Characterization of the Resulting Polymer
- Table II. Structural characteristic of poly(6-10)

CHAPTER 4

- Table I. Thermal Characterization of 4-Cyano-4'-(ω -hydroxyalkan-1-yloxy)biphenyls (7-8) and (7-6), ω -[(4-Cyano-4'-biphenyl)oxy]alkyl Vinyl Ethers (6-8) and (6-6), and of ω -[(4-Cyano-4'-biphenyl)oxy]alkyl Ethyl Ethers (8-8) and (8-6).
- Table II. Cationic Polymerization of 8-[4-Cyano-4'-biphenyl)oxy]octyl Vinyl Ether (6-8) (polymerization temperature, 0°C; polymerization solvent, methylene chloride; $[M]_0=0.285$; $[(\text{CH}_3)_2\text{S}]_0/[I]_0=10$; polymerization time, 1hr) and Characterization of the Resulting Polymers.

Table III. Cationic Polymerization of 6-[4-Cyano-4'-biphenyl]oxy]hexyl Vinyl Ether (6-6) (polymerization temperature, 0°C; polymerization solvent, methylene chloride; $[M]_0=0.311$; $[(CH_3)_2S]_0/[I]_0=10$; polymerization time, 1hr) and Characterization of the Resulting Polymers.

CHAPTER 5

Table I. Cationic Polymerization of 9-[4-Cyano-4'-biphenyl]oxy]nonyl Vinyl Ether (6-9) (polymerization temperature, 0°C; polymerization solvent, methylene chloride; $[M]_0=0.275$; $[(CH_3)_2S]_0/[I]_0=10$; polymerization time, 1hr) and Characterization of the Resulting Polymers.

Table II. Cationic Polymerization of 7-[4-Cyano-4'-biphenyl]oxy]heptyl Vinyl Ether (6-7) (polymerization temperature, 0°C; polymerization solvent, methylene chloride; $[M]_0=0.298$; $[(CH_3)_2S]_0/[I]_0=10$; polymerization time, 1hr) and Characterization of the Resulting Polymers.

Table III. Cationic Polymerization of 5-[4-Cyano-4'-biphenyl]oxy]pentyl Vinyl Ether (6-5) (polymerization temperature, 0°C; polymerization solvent, methylene chloride; $[M]_0=0.325$; $[(CH_3)_2S]_0/[I]_0=10$; polymerization time, 1hr) and Characterization of the Resulting Polymers.

Table IV. Thermal Characterization of 4-Cyano-4'-(ω -hydroxyalkan-1-yloxy)biphenyls (7-5), (7-7) and (7-9), ω -[(4-Cyano-4'-biphenyl)oxy]alkyl Vinyl Ethers (6-5), (6-7) and (6-9), and of ω -[(4-Cyano-4'-biphenyl)oxy]alkyl Ethyl Ethers (8-5), (8-7) and (8-9).

CHAPTER 6

Table I. Cationic Polymerization of 2-[4-Cyano-4'-biphenyl]oxy]ethyl Vinyl Ether (6-2) (polymerization temperature, 0°C; polymerization solvent, methylene chloride; $[M]_0=0.387$; $[(CH_3)_2S]_0/[I]_0=10$; polymerization time, 1hr) and Characterization of the Resulting Polymers.

Table II. Cationic Polymerization of 3-[4-Cyano-4'-biphenyl]oxy]propyl Vinyl Ether (6-3) (polymerization temperature, 0°C; polymerization solvent, methylene chloride; $[M]_0=0.358$; $[(CH_3)_2S]_0/[I]_0=10$; polymerization time, 1hr) and Characterization of the Resulting Polymers.

Table III. Cationic Polymerization of 4-[4-Cyano-4'-biphenyl]oxy]butyl Vinyl Ether (6-4) (polymerization temperature, 0°C; polymerization solvent, methylene chloride; $[M]_0=0.341$; $[(CH_3)_2S]_0/[I]_0=10$; polymerization time, 1hr) and Characterization of the Resulting Polymers.

Table IV. Thermal Characterization of 4-Cyano-4'-(ω -hydroxyalkan-1-yloxy)biphenyls (7-2, 7-3 and 7-4), ω -[(4-Cyano-4'-biphenyl)oxy]alkyl Vinyl Ethers (6-2, 6-3 and 6-4) and ω -[(4-Cyano-4'-biphenyl)oxy]alkyl Ethyl Ethers (8-2, 8-3 and 8-4)

CHAPTER 7

Table I. Cationic Copolymerization of 6-11 with 6-6 (polymerization temperature, 0°C; polymerization solvent, methylene chloride; $[M]_0=[6-11]+[6-6]=0.256-0.312M$; $[M]_0/[I]_0=20$; $[(CH_3)_2S]_0/[I]_0=10$; polymerization time, 1hr) and Characterization of the Resulting Polymers.

Table II. Cationic Copolymerization of 6-5 with 6-3 (polymerization temperature, 0°C; polymerization solvent, methylene chloride; $[M]_0=[6-5]+[6-3]=0.326-0.358M$; $[M]_0/[I]_0=20$; $[(CH_3)_2S]_0/[I]_0=10$; polymerization time, 1hr) and Characterization of the Resulting Polymers.

Table III. Cationic Copolymerization of 6-11 with 6-3 (polymerization temperature, 0°C; polymerization solvent, methylene chloride; $[M]_0=[6-11]+[6-3]=0.256-0.358M$; $[M]_0/[I]_0=20$; $[(CH_3)_2S]_0/[I]_0=10$; polymerization time, 1hr) and Characterization of the Resulting Polymers.

Table IV. Cationic Copolymerization of 6-11 with 6-5 (polymerization temperature, 0°C; polymerization solvent, methylene chloride; $[M]_0=[6-11]+[6-5]=0.256-0.326M$; $[M]_0/[I]_0=20$; $[(CH_3)_2S]_0/[I]_0=10$; polymerization time, 1hr) and Characterization of the Resulting Polymers.

CHAPTER 8

Table I. Cationic Copolymerization of 6-8 with 6-2 (polymerization temperature, 0°C; polymerization solvent, methylene chloride; $[M]_0=[6-8]+[6-2]=0.285-0.377M$; $[M]_0/[I]_0=20$; $[(CH_3)_2S]_0/[I]_0=10$; polymerization time, 1hr) and Characterization of the Resulting Polymers. Data on first line are

Table II. Cationic Copolymerization of 6-11 with 6-2 (polymerization temperature, 0°C; polymerization solvent, methylene chloride; $[M]_0=[6-11]+[6-2]=0.256-0.358M$; $[M]_0/[I]_0=20$; $[(CH_3)_2S]_0/[I]_0=10$; polymerization time, 1hr) and Characterization of the Resulting Polymers.

CHAPTER 9

- Table I. Cationic Copolymerization of 6-11 with 15-8 (polymerization temperature, 0°C; polymerization solvent, methylene chloride; $[M]_0=[\underline{6-11}]+[\underline{15-8}]=0.205-0.256\text{M}$; $[M]_0/[I]_0=20$; $[(\text{CH}_3)_2\text{S}]_0/[I]_0=10$; polymerization time, 1hr) and Characterization of the Resulting Copolymers.
- Table II. Cationic Copolymerization of 6-3 with 15-8 (polymerization temperature, 0°C; polymerization solvent, methylene chloride; $[M]_0=[\underline{6-3}]+[\underline{13-8}]=0.205-0.358\text{M}$; $[M]_0/[I]_0=20$; $[(\text{CH}_3)_2\text{S}]_0/[I]_0=10$; polymerization time, 1hr) and Characterization of the Resulting Copolymers. Data on first line

CHAPTER 10

- Table I. Synthesis of Poly{3-[(4-Cyano-4'-biphenyl)oxy]propyl Vinyl Ether} Macromonomers
- Table II. Thermal Transitions and Their Corresponding Thermodynamic Parameters of the Macromonomers of Poly(6-3)
- Table III; Block Copolymers of Mesogenic Vinyl Ethers (M) and CF8 via Sequential Living Polymerization by $\text{CF}_3\text{SO}_3\text{H}/(\text{CH}_3)_2\text{S}$. ($[M]_0/[I]_0=15$, $[(\text{CH}_3)_2\text{S}]_0/[I]_0=20$)
- Table IV. Thermal characterization of the AB block copolymers and of the parent homopolymers. Data on first line are from first heating and cooling scans. Data on the second line are from the second heating scans.

Chapter 1

GENERAL INTRODUCTION

1.1.-THERMOTROPIC LIQUID CRYSTALS

Liquid crystal is a term that is now commonly used to describe materials that exhibit partially ordered fluid phases that are intermediate between the three dimensionally ordered crystalline state and the disordered or isotropic fluid state. Phases with positional and/or orientational long-range order in one or two dimensions are termed mesophases. As a consequence of the molecular order, liquid crystal phases are anisotropic, i.e., their properties are a function of direction.

Although liquid crystalline behavior has been known since 1888 when Reinitzer¹ observed that cholesteryl benzoate melted to form a turbid melt that eventually cleared at a higher temperature, the first liquid crystalline compounds with completely known structure were derivatives of azoxybenzene synthesized by Gattermann in 1890.² Furthermore, Vorlander systematically investigated in a large number of compounds the relations among molecular structure and liquid crystalline properties. Up to 1908³ he obtained about 170 liquid crystalline compounds from which he was able to derive a general rule about the chemical structures of liquid crystals: the liquid crystalline shape is obtained by an utmost linear shape of the molecule. He also emphasized the increasing mesogeneity by elongation of the aromatic core of the molecule. In principle his rule has been valid up to now.

Modern-day interest in liquid crystalline polymers had its origin with the molecular theories of Onsager⁴ and Flory⁵. They predicted that rod-like molecules would spontaneously order above a critical concentration that depended on the axial ratio of the molecule. However, the first thermotropic liquid crystalline polymers were

reported only in the mid-1970's by Roviello and Sirigu⁶ and Jackson and Kuhfuss⁷ although patented research on main-chain liquid crystalline polymers were performed in the early 1970's.⁸ The discovery of these new polymeric materials stimulated considerable research not only because of their potential as high strength fibers but also because of their academic interest in the theoretical scheme of structural order in the fluid phases.

Thermotropic liquid crystalline polymers can be classified into two major categories: main-chain liquid crystalline polymers, where the mesogens constitute the polymer backbone and side chain liquid crystalline polymers, where the mesogens are attached to the polymer backbone as pendant groups. The study of these systems is so well established that a number of reviews have been written on both main chain⁹⁻¹⁰ and side chain liquid crystalline polymers.¹¹⁻¹⁵

Depending on their thermodynamic stability with respect to the crystalline phase, thermotropic mesophases can be virtual (unstable with respect to the crystalline phase), monotropic (metastable with respect to the crystalline phase), or enantiotropic (stable with respect to the crystalline phase).^{16,17} Virtual mesophases exist only below the melting and crystallization temperature and therefore can not be observed. Monotropic mesophases can be observed only during cooling due to the fact that the crystallization process is kinetically controlled and therefore is supercooled, while the liquid crystalline phase is thermodynamically controlled and is not supercooled. Enantiotropic mesophases can be observed both on heating and cooling.

Almost all pure compounds exhibiting thermotropic mesomorphism have pronounced anisotropy of shape. The majority of liquid crystalline substances are based on rod-like molecules. They are conventionally classified into three types: nematic, cholesteric and smectic (Figure 1). Characteristic for the nematic phase is a parallel

orientation of the molecules with an axis that corresponds to the long axis of the mesogen. If an optically active compound is dissolved in a nematic phase, then the structure acquires a spontaneous twist about an axis perpendicular to director in the cholesteric (chiral nematic) phase. The same twisted structure can be also found with cholesteric derivatives. While the nematic phase exhibit a one-dimensional degree of order, smectic phases can exhibit a two-dimensional or a three dimensional order.¹⁸ Molecules are arranged parallel to each other in smectic phases which are perpendicular to the layer (smectic A) or the tilted angle (smectic C) to the layer.

1.2.-SIDE CHAIN LIQUID CRYSTALLINE POLYMER

Many reviews have recently been published on the development of side chain liquid crystalline polymers. Academic interest has focused largely on characterizing these systems and understanding their structure-property relationships.^{12-14,20-22} Electrooptic phenomena exhibited by these polymers have also been considered in terms of potential device applications.²³

In side chain liquid crystalline polymers the mesogenic groups are connected to an existing polymer backbone either directly or via flexible spacer units. Direct linkage^{15,24} except in a few cases²⁵⁻²⁷ gives only glasses with an anisotropy of structure that is lost at the glass transition. Coupled with steric interactions between the side groups, the tendency toward a statistical distribution of chain conformations hinders the ordered arrangement of the mesogenic groups and mesophase formation is suppressed. Decoupling of the side groups by using a flexible spacer allows the main chain motion to occur without disturbance of the anisotropic arrangement of the side chains.

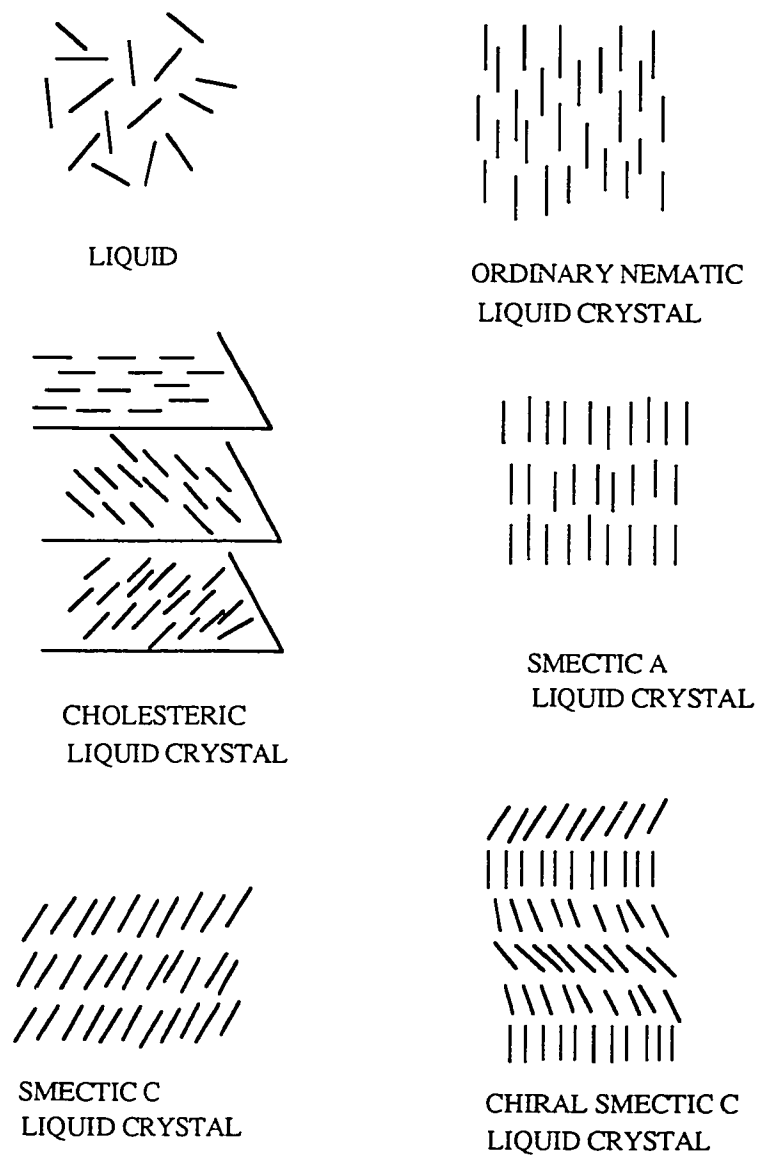


Figure 1. Schematic representation of molecular arrangements in liquid and different types of liquid crystal phases

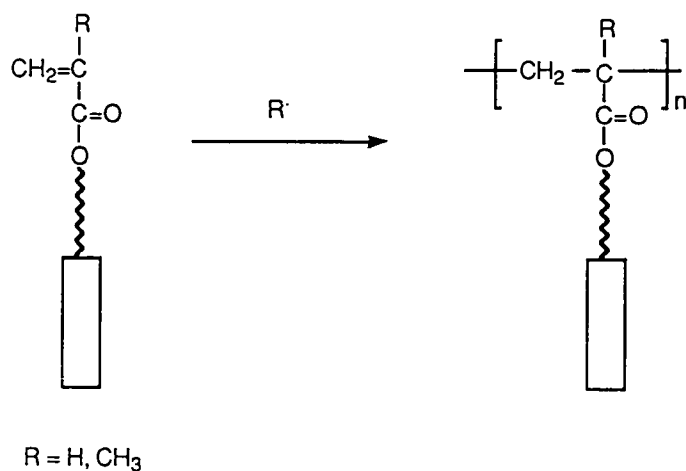
The most common backbones so far considered are poly-acrylate, poly-methacrylate and polysiloxane systems. Typical spacer groups consist of between 2 and 11 methylene units. Side chain liquid crystalline polymers of the acrylate and methacrylate type have been the most widely synthesized because they can be prepared easily by free radical polymerization²⁸⁻³¹(Scheme I).

Anionic,³² group transfer^{33,34} and cationic polymerizations³⁵⁻³⁷ have been used to obtain different tacticities, molecular weights and molecular weight distributions and to vary the nature of the polymer backbone. Polycondensation reactions^{38,39} have been successfully applied to preparation of side chain liquid crystalline polyesters with flexible, semi-flexible and rigid backbones. Chemical modification of reactive polymers such as sodium polyacrylates⁴⁰ or sodium polyitaconates⁴¹ has also been reported (Scheme II).

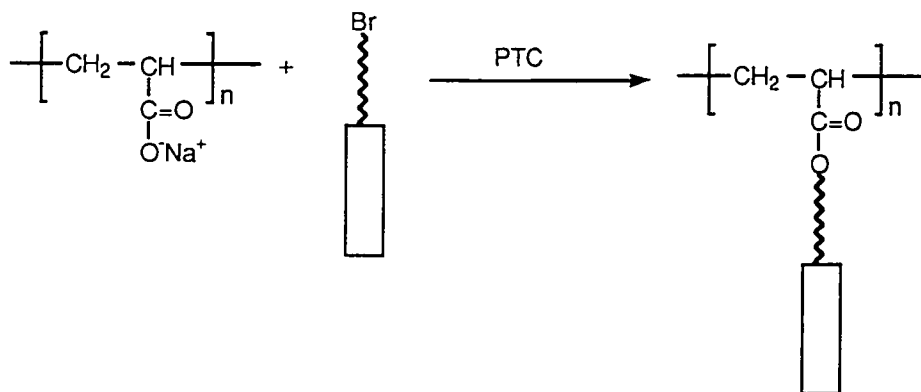
Side chain liquid crystalline polysiloxanes are usually prepared by an addition process, commencing with a preformed polymer backbone which contains reactive functional groups (Si-H) to which the mesogenic groups are appended.^{42,43} During the reaction, monitoring is carried out to ensure complete reaction of the Si-H functions with the terminal alkene which is to constitute the mesogenic side chain. The process is known as hydrosilylation.

1.2.1.-INFLUENCE OF FLEXIBLE SPACER

Attainment of a thermotropic liquid crystalline mesophase from a backbone containing mesogenic side groups requires reconciliation of the main chain's tendency to form a statistical random coil conformation and the side groups' tendency to arrange anisotropically. This is shown in Figure 2. The principle that the motions of both the main chain and the side groups are coupled when the mesogenic groups are directly



Scheme I. Synthesis of liquid crystalline polymer by radical polymerization



Scheme II. Synthesis of liquid crystalline polymer by polymer homologous reaction.
(PTC = phase transfer catalyst)

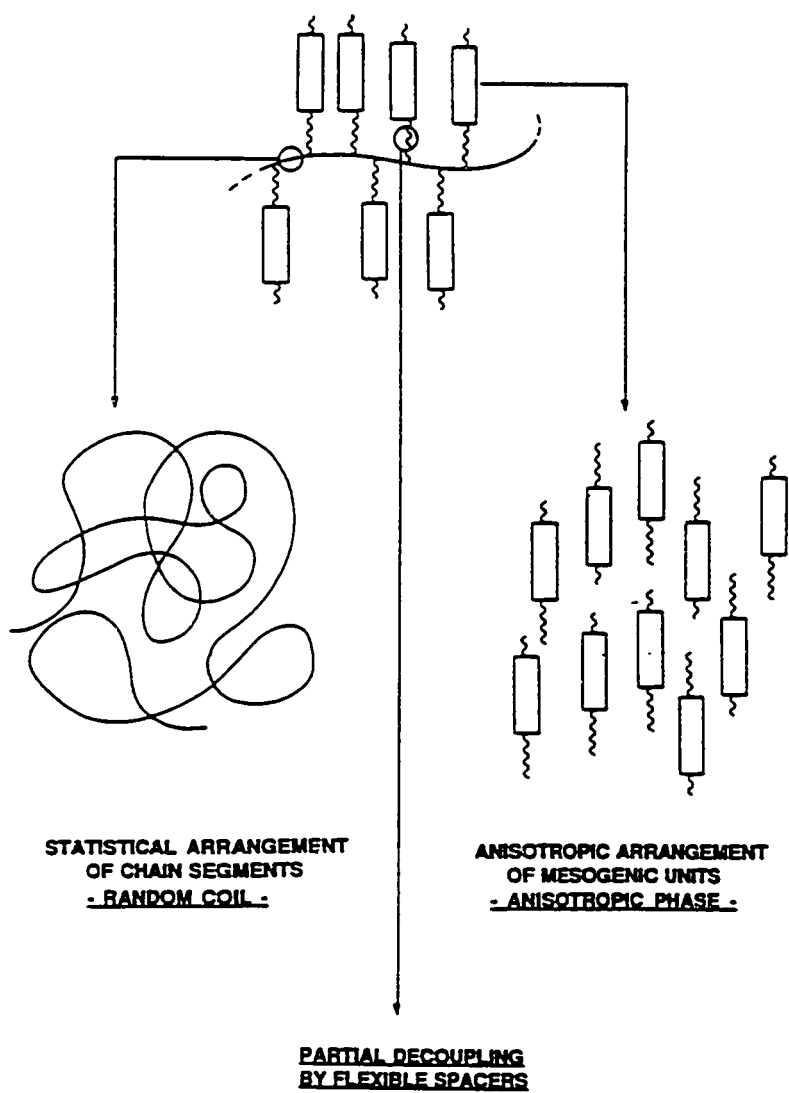


Figure 2. Schematic structure of liquid crystalline side chain polymers showing the necessity of decoupling the mesogenic groups and the polymer main chain through flexible spacers

attached to the flexible backbone is well accepted. In this case, the conformation of the main chain is disturbed when the side groups adopt an anisotropic arrangement. In order to balance the competition between the backbone's random-coil conformation and the side groups alignment, Ringsdorf and co-workers predicted that the motion of the polymer main chain must be decoupled from that of the anisotropically orientable mesogenic side groups in the fluid state.^{44,45} Based on spacer model, the side groups should be able to self-orient into an anisotropic mesophase even when the main chain adopts a random coil statistical conformation. The spacer concept therefore assumes that the main chain should do little to hinder the orientation of the mesogenic side groups; that is, for a given mesogen and spacer, the nature of polymer backbone should theoretically not affect the type of mesophase formed and its thermal stability. Subsequent work by Ringsdorf and Spiess⁴⁶⁻⁴⁸ demonstrated that complete decoupling does not occur although a spacer helps to decouple the mesogenic groups from the main chain, and that decoupling becomes more effective with increasing spacer length. Therefore, the nature of the highest temperature mesophase is determined mainly by spacer length. Long spacers have tendency to form smectic phases, while short spacers have tendency to form nematic phases. However, for identical spacer length, the nature of polymer backbone dictates the degree of decoupling.

1.2.2.-INFLUENCE OF POLYMER BACKBONE

Several publications⁴⁹⁻⁵² have pointed out that not only the nature and length of the flexible spacer, but also the nature of the polymer backbone influences the range of thermal stability of the mesophases. At constant molecular weight, the rigidity of the polymer backbone determines the thermodynamic stability of the mesophase. In fact, it has been mentioned by several research groups that for the same spacer length and

mesogenic unit, the broadest thermal stability of the mesophase is always obtained with the most flexible backbone.^{10,12} This trend can be explained by assuming that a more flexible backbone uses less energy to get distorted and therefore generates a more decoupled polymer system.

However, contrary to all expectations the entropy change of isotropization is higher for those polymers which are based on more rigid backbones and therefore, exhibit lower isotropization temperatures (Figure 3).⁵³ This contradiction between the values of the entropy change and the isotropization temperatures can be accounted for by a different mechanism of distortion of different polymer backbones as outlined in Figure 3, that is, while a rigid backbone gets more extended and therefore, in the smectic phase it can cross the smectic layer, in the case of a flexible backbone it gets squeezed between the smectic layers. The higher configurational entropy of the flexible backbone versus that of the rigid backbone in the smectic phase can account for the difference between the entropy change of isotropization from Figure 3. These conclusions are, however, only valid for polymer molecular weights that are high enough for their phase transitions to be molecular weight independent.

1.2.3.-INFLUENCE OF MOLECULAR WEIGHT

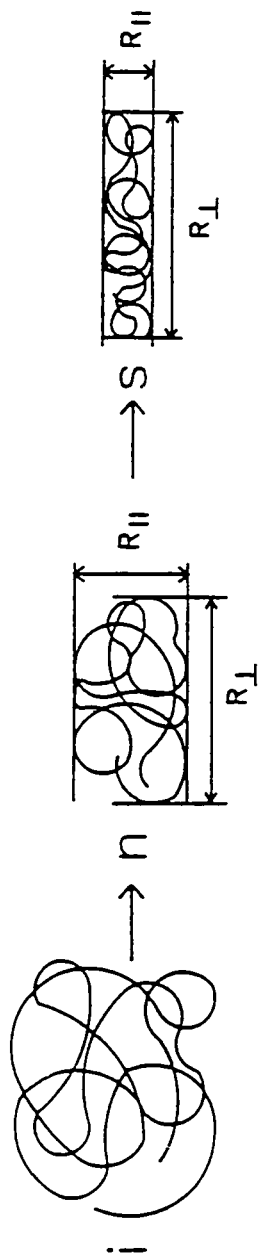
Recently, a simple thermodynamic scheme has been presented which correlates the thermodynamic stability of a certain phase with the rigidity of the molecule.^{16,17} According to basic thermodynamic relationship of free energy;

$$dG = VdP - SdT \quad (\text{eq. 1})$$

If we consider constant pressure, then equation 1 becomes

$$dG = -SdT \quad (\text{eq. 2})$$

a Theoretical (M. Warner)



b Experimental (Saclay Group)

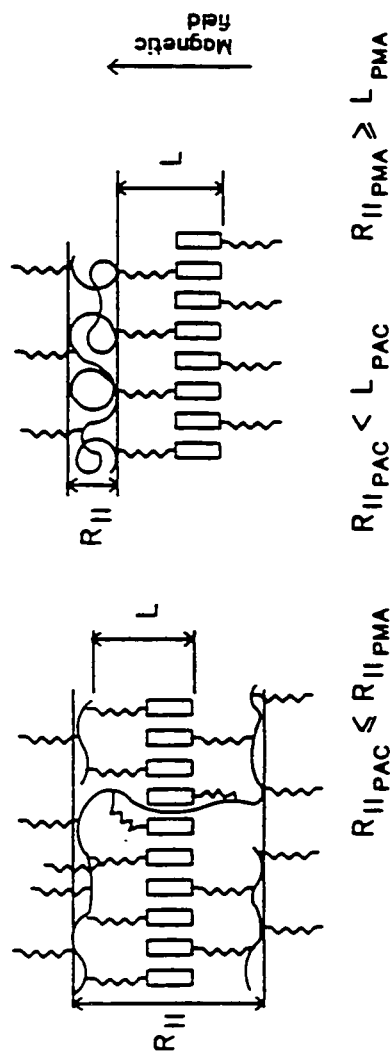


Figure 3. Schematic representation of the theoretical distortion of the statistical random coil conformation of the polymer backbone in the nematic and smectic phases. (b) Two possible modes of distortion of the random coil conformation of a rigid (left) and a flexible (right) polymer backbone. R_{II} refers to the radius of gyration parallel to the magnetic field. The radius of gyration perpendicular to the magnetic field is labelled as R_L .

As seen from Figure 4a, and as follows from equation 2, the free energies of both crystal (G_k) and isotropic liquid (G_i) decrease with increasing temperature where the decrease in G_i is steeper, due to $S_i > S_l > S_k$. In this case, the most stable phases are crystal and isotropic liquid. Therefore, the mesophase is virtual which is unrealizable. In order to create a stable mesophase a section of the G_{lc} versus T curve will need to be brought below both G_k and G_i . This can be achieved by raising G_i (Figure 4b) which arises from the lowering of the melt entropy (i.e., by increasing the molecular weight).

Upon increasing the molecular weight from monomer to polymer, the entropy of the liquid phase (S_i) decreases. The decrease of the entropies of liquid crystalline and crystalline phases is lower than that of the isotropic phase. The decrease of entropy of the crystalline phases can be negligible because it is very small. The decrease in S_i and S_{lc} tends asymptotically to zero with increasing molecular weight and therefore, G_i and G_{lc} increase with the increase of the polymer molecular weight. Above a certain molecular weight, G_i remains constant. Figures 5 and 6 transform the free energy (G) versus transition temperature (T) dependence into a transition temperature (T) versus molecular weight dependence. The T versus M plot in Figures 5,6 demonstrate that both melting and isotropization temperatures increase with molecular weight up to a certain range of M values beyond which T_{k-lc} and T_{lc-i} remain approximately constant above a certain molecular weight. However, the slope of the increase of T_{lc-i} steeper than that of T_{k-lc} . Figure 5 demonstrates that when monomer structural unit displays an enantiotropic mesophase, the resulting polymer will display a broader enantiotropic mesophase. In addition, Figure 6 demonstrates that when the monomer structural unit displays a monotropic mesophase, the resulting polymer will display an enantiotropic mesophase. This effect agrees with experimental data reported for the case of both main chain^{54,55} and side chain^{43,56} liquid crystalline polymers.

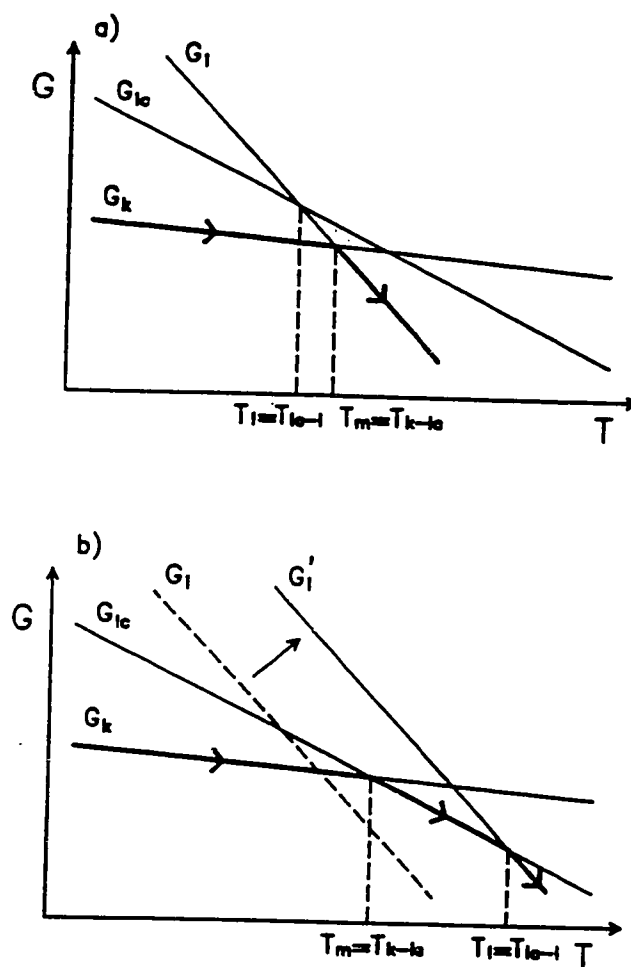


Figure 4. (a) Schematic plot of free energies vs. temperature for a scheme that does not show a mesophase. G_k , G_{lc} and G_i are, respectively, the free energies of the crystalline, mesomorphic (virtual) and isotropic liquid states. $T_{k-i} = T_m$ is the crystalline melting point. Heavy line correspond to the most stable state at a given temperature. (b) Schematic plot of free energies vs. temperature for system in Figure 4a but with raised G_i (to G_i') and the mesophase is uncovered. Heavy line correspond to the most stable state at a given temperature.

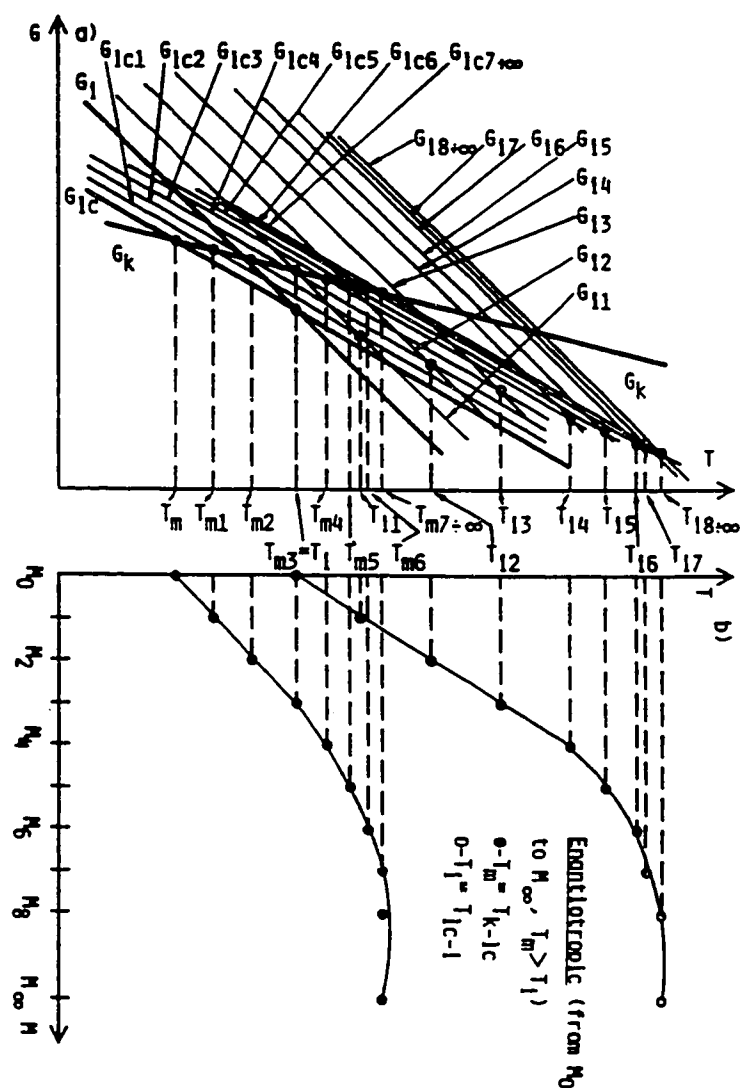


Figure 5. The broadening of the temperature range of an enantiotropic mesophase of the monomeric structural unit (M_0) by increasing the degree of polymerization. The upper part (a) describes the influence of molecular weight on the dependence between the free energies of the crystalline (G_k), liquid crystalline (G_{lc}) and isotropic (G_i) phases and transition temperatures. The translation of this dependence into the dependence into the dependence phase transition temperature-molecular weight is presented in the lower part (b).

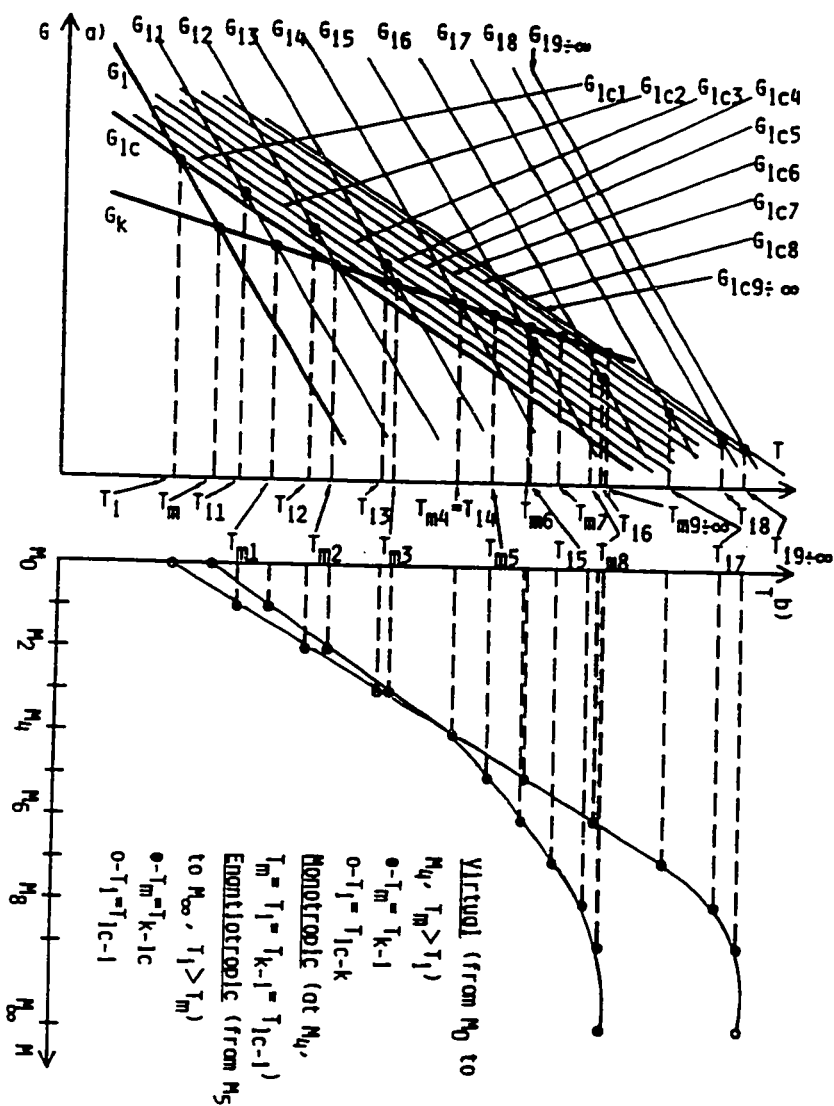


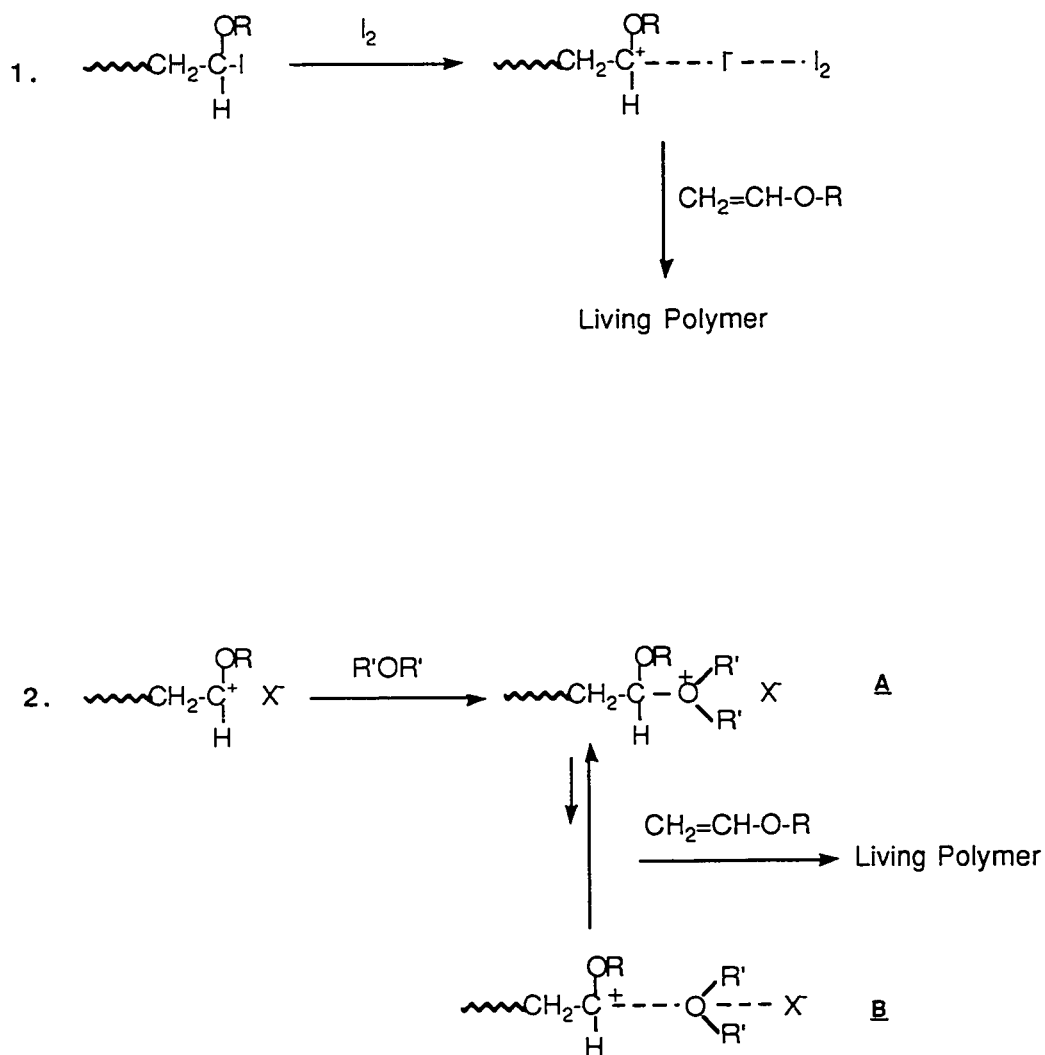
Figure 6. Transformation of a virtual or monotropic mesophase of the monomeric structural unit (M_0) into an enantiotropic mesophase by increasing the degree of polymerization. The upper part (a) describes the influence of molecular weight on the dependence between the free energies of the crystalline (G_K), liquid crystalline (G_{LC}) and isotropic (G_I) phases and transition temperatures. The translation of this dependence into the dependence into the dependence phase transition temperature-molecular weight is presented in the lower part (b).

1.2.4.-LIVING CATIONIC POLYMERIZATION OF MESOGENIC VINYL ETHERS

Vinyl ethers have a strong electron donating alkoxy substituent and therefore readily undergo polymerization on treatment with an acidic initiator. The polymerization is cationic in nature. The existence of an ether oxygen in the pendant group renders the cationic polymerization of vinyl ethers considerably different from those of nonpolar hydrocarbon monomers, such as styrene and isobutylene.

The most important development in this field is the discovery of living cationic polymerization of vinyl ethers which has allowed control of the molecular weight and structure of poly(vinyl ether) in 1984 by Higashimura and Sawamoto.^{57,58} To obtain stable active chain ends for living cationic polymerization one must suppress chain transfer and chain termination. This can be accomplished by formation of a covalent species from the growing carbocation chain ends capable of inserting monomer itself or regenerating carbocations reversibly at very low concentrations.⁶¹

Higashimura^{59,60} has reported two general living carbocation systems each with variations for polymerizations of vinyl ethers. In one the active carbocationic propagating species is stabilized by its counterion. In the other it is stabilized by a Lewis base. In the first case a quite nucleophilic counterion such as iodide ion (Scheme III, equation 1) is used to maintain a covalent bond with the growing active carbocation during the polymerization, and the covalent chain end is activated by mild Lewis acids. Then the insertion of this activated chain end by monomer molecules leads to living polymer. In the second method,^{62,63} a Lewis base such as ethyl acetate, 1,4-dioxane, 2,6-dimethylpyridine and dimethyl sulfide is used to stabilize a carbocation end group generated from reaction of monomer with a proton source ($\text{H}_2\text{O}/\text{EtAlCl}_2$, $\text{CH}_3\text{CO}_2\text{H}/\text{EtAlCl}_2$) through its nucleophilic interaction. An oxonium ion species A or



Scheme III. Two general living cationic polymerization systems. 1) Active carbocation propagating species stabilized by their counterion 2) active carbocation stabilized by a Lewis base.

a solvated carbocation **B** is proposed as the species reacting with the monomer⁵⁷ (Scheme III, equation 2). Although phenomenologically well established, however, the function of added base in inducing living polymerization is still obscure and awaits further study as pointed out in recent papers.^{64,65}

Living cationic polymerization of vinyl ethers represents an interesting preparative technique which can be used in the design of side chain liquid crystalline polymers since it can tolerate many different functional groups and can lead to controlled molecular weight and molecular weight distribution. To date, mesogenic vinyl ethers have been polymerized by Percec et al.³⁵⁻³⁷ In addition, it has been demonstrated that a variety of mesogenic vinyl ethers can be polymerized through a living mechanism leading to polymers of narrow molecular weight distribution and controlled molecular weight.⁶⁶⁻⁶⁹

So far, there is general agreement that there is an increase of the mesomorphic-mesomorphic phase transition temperatures up to a certain degree of polymerization, above which they become molecular weight independent.^{43,56,66-68,69-71} In addition, several publications have demonstrated that the number and the type of mesophases is also molecular weight dependent.^{56,67,71} Systematic elucidation of this phenomenon requires the synthesis of polymers with well defined molecular weights, and narrow molecular weight distributions.

This dissertation is concerned with the preparation and the mesomorphic behavior of the side chain liquid crystalline poly(vinylether)s by living polymerization. In part I, the synthesis and living cationic polymerization of ω -[(4-cyano-4'-biphenyl)oxy]alkyl vinyl ethers containing flexible spacers with 2 to 11 methylene units and the mesomorphic behavior of the resulting polymers are described. All

polymerizations showed living character within these experimental range of molecular weights. The results of this work constitute a systematic investigation of the influence of molecular weight on mesomorphic phase behavior in this class of polymers. In particular, the transition temperatures, nature and number of the mesophases in these materials are shown to be molecular weight dependent.

Part II described the preparation of statistical binary copolymers of ω -[(4-cyano-4'-biphenyl)oxy]alkyl vinyl ether having different spacer lengths. The molecular weights, molecular weight distributions and compositions of these copolymers were all well defined. It is shown that when the two structural units of the copolymer are isomorphic within a certain mesophase, both the phase transition temperature and the enthalpy changes associated with a particular mesophase display a continuous dependence on composition. It is demonstrated that the structural units of all binary copolymers behave as an ideal solution. In contrast to the ideal solution behavior of binary copolymers based on structural units containing the same mesogen but different spacer lengths, a second class of copolymers based on structural units which are isomorphic but contain dissimilar mesogens is shown to display non-ideal solution behavior.

In Part III, the synthesis and characterization of macromonomers and block copolymers based on mesogenic units are described. These experiments demonstrate that living cationic polymerization of mesogenic vinyl ethers can also be used in the synthesis of mesogenic macromonomers and mesogenic block copolymers. The thermal behavior of all block copolymers determined by DSC and optical polarized microscopy shows a microphase separated morphology.

1.3-GENERAL EXPERIMENTAL

^1H -NMR (200 MHz) spectra were recorded on a Varian XL-200 spectrometer. TMS was used as internal standard. A Perkin Elmer DSC-4 differential scanning calorimeter, equipped with a TADS 3600 data station was used to determine the thermal transitions which were reported as the maxima and minima of their endothermic and exothermic peaks respectively. In all cases, heating and cooling rates were $20^\circ\text{C}/\text{min}$ unless otherwise specified. Glass transition temperatures (T_g) were read at the middle of the change in the heat capacity. For certain polymer samples, the first heating scans sometimes differ from the second and subsequent heating scans. At the proper place, this difference will be mentioned. However, the second and subsequent heating scans are identical. The first heating scans can be reobtained after proper thermal treatment of the polymer sample. Both the first and the second DSC heating scans will be reported and discussed. A Carl-Zeiss optical polarized microscope (magnification: 100x) equipped with a Mettler FP 82 hot stage and a Mettler FP 800 central processor was used to observe the thermal transitions and to analyze the anisotropic textures.^{72,73} Molecular weights were determined by gel permeation chromatography (GPC) with a Perkin Elmer series 10 LC instrument equipped with LC-100 column oven, LC-600 autosampler and a Nelson analytical 900 series integrator data station. The measurements were made at 40°C using the UV detector. A set of Perkin Elmer PL gel columns of 10^4 and 500 \AA with CHCl_3 as solvent ($1\text{ml}/\text{min}$) and a calibration plot constructed with polystyrene standards was used to determine the molecular weights. Therefore, all molecular weights discussed in this paper are relative to polystyrene. High pressure liquid chromatography (HPLC) experiments were performed with the same instrument.

REFERENCES

1. F. Reinitzer, *Monatsh. Chem.* **9**, 421 (1888)
2. L. Gatterman and A. Rischke, *Ber. Deut. Chem. Ges.*, **23**, 1738 (1890)
3. D. Vorlander, *Kristallinisch-flussige Substanzen*, Enke Verlag, Stuttgart, (1908)
4. L. Onsager, *Ann. N. Y. Acad. Sci.*, **51**, 627 (1949)
5. P. J. Flory, *Proc. Royal Soc., London*, **234A**, 73 (1956)
6. A. Roviello and A. Sirigu, *J. Polym. Sci.: Polym. Lett.*, **13**, 455 (1975)
7. W. J. Jackson and H. F. Kuhfuss, *J. Polym. Sci.: Polym. Chem.*, **14**, 2043 (1976)
8. H. F. Kuhfuss and W. J. Jackson. *U. S. Patent*, 3,778,410 (1973); 3,804,805 (1974)
9. A. Caferri, W. R. Krigbaum and R. B. Meyer, "Polymer Liquid Crystals", Academic Press, New York (1982)
10. C. K. Ober, J. I. Jin and R. W. Lenz, *Adv. Polym. Sci.*, **59**, 103 (1984)
11. H. Finkelmann and G. Rehage, *Adv. Polym. Sci.*, **60/61**, 99 (1984)
12. C. B. McArdle, "Side Chain Liquid Crystalline Polymers", Chapman and Hall, New York, 1989
13. N. A. Plate and V. P. Shibaev, "Comb Shaped Polymers and Liquid Crystals", Plenum, New York, 1987
14. V. P. Shibaev and N. A. Plate, *Pure and Appl. Chem.*, **57**, 1589 (1985)
15. A. Blumstein, "Liquid Crystalline Order in Polymers", Academic Press, New York 1978
16. V. Percec and A. Keller, *Macromolecules*, **23**, 4347 (1990)
17. A. Keller, G. Ungar and V. Percec, "Advances in Liquid Crystalline Polymers", (R. A. Weiss and C. K. Ober Ed.), ACS Symposium Series 435, Am. Chem. Soc., Washington D. C., 1990
18. G. W. Gray and J. W. Goodby, "Smectic Liquid Crystals", Leonard Hill, Glasgow, 1984

19. C. Noel, "Polymeric Liquid Crystals", (A. Blumstein Ed.), Plenum Press, New York, 1985
20. C. Noel, *Makromol. Chem., Makromol. Symp.*, **22**, 95 (1988)
21. T. S. Chung, *Polym. Eng. Sci.*, **26**, 901 (1986)
22. C. Noel, "Recent Advances in Liquid Crystalline Polymers", (L. L. Chapoy Ed.), Elsevier Applied Science, **2**, 297 (1988)
23. H. J. Coles, "Developments in Crystalline Polymers", (D. C. Bassett Ed.), Elsevier Applied Science, **2**, 297 (1988)
24. V. P. Shibaev and N. A. Plate, *Vyskomol. Soed. Ser.*, **A19**, 23 (1977)
25. A. K. Alimoglu, A. Ledwith, P. A. Gemmell, G. W. Gray and D. Lacey, *Polymer*, **25**, 1342 (1987)
26. R. Duran and P. Gramain, *Makromol. Chem.*, **188**, 2001 (1987)
27. A. Frosini, G. Levita, D. Lupinacci and P. L. Magagnini, *Mol. Cryst. Liq. Cryst.*, **66**, 21 (1981)
28. G. Decobert, J. C. Dubois, S. Esselin and C. Noel, *Liq. Cryst.*, **1**, 307 (1986)
29. R. Zentel and H. Ringsdorf, *Makromol. Chem., Rapid Commun.*, **5**, 393 (1984)
30. J. Horvath, K. Nyitrai, F. Cser and G. Hardy, *Eur. Polym. J.*, **21**, 251 (1985)
31. M. Portugall, H. Ringsdorf and R. Zentel, *Makromol. Chem.*, **183**, 2311 (1982)
32. B. Hahn, J. H. Wendorff, M. Portugall and H. Ringsdorf, *Coll. Polym. Sci.*, **259**, 875 (1981)
33. W. Kreuder, O. W. Webster and H. Ringsdorf, *Makromol. Chem., Rapid Commun.*, **7**, 5 (1986)
34. C. Pugh and V. Percec, *ACS Polym. Prepr.*, **26(2)**, 303 (1985)
35. J. Rodriguez-Parada and V. Percec, *J. Polym. Sci., Polym. Chem. Ed.*, **24**, 1363 (1986)
36. J. Rodriguez-Parada and V. Percec, *J. Polym. Sci., Polym. Chem. Ed.*, **25**, 2269 (1986)
37. V. Percec and D. Tomazos, *Polym. Bull.*, **18**, 239 (1987)
38. B. Reck and H. Ringsdorf, *Makromol. Chem., Rapid Commun.*, **6**, 291 (1985)

39. R. Berg, V. Krone and H. Ringsdorf, *Makromol. Chem., Rapid Commun.*, **7**, 381 (1986)
40. P. Keller, *Macromolecules*, **17**, 2937 (1984)
41. P. Keller, *Macromolecules*, **18**, 2337 (1985)
42. H. Finkelmann and G. Rehage, *Makromol. Chem., Rapid Commun.*, **1**, 31, (1980)
43. V. Percec and B. Hahn, *Macromolecules*, **22**, 1588 (1989)
44. H. Finkelmann, M. Happ, M. Portugall and H. Ringsdorf, *Makromol. Chem.*, **179**, 2541 (1978)
45. H. Finkelmann, H. Ringsdorf and J. H. Wendorff, *Makromol. Chem.*, **179**, 273 (1978)
46. C. Boeffel, B. Hisgen, U. Pschorn, H. Ringsdorf and F. W. Spiess, *Israel J. Chem.*, **23**, 388 (1983)
47. H. Geib, B. Hisgen, U. Pschorn, H. Ringsdorf and F. W. Spiess, *J. Am. Chem. Soc.*, **104**, 917 (1982)
48. H. W. Spiess, *Pure Appl. Chem.*, **57**, 1617 (1985)
49. C. Pugh and V. Percec, *Polym. Bull.*, **16**, 513 (1986)
50. C. Pugh and V. Percec, *Polym. Bull.*, **16**, 521 (1986)
51. C. S. Hsu, J. M. Rodrigues-Parada and V. Percec, *Makromol. Chem.*, **188**, 1017 (1987)
52. C. S. Hsu, J. M. Rodrigues-Parada and V. Percec, *J. Polym. Sci.; Polym. Chem.*, **25**, 2425 (1987)
53. V. Percec and D. Tomazos, *Polymer*, **31**, 1658 (1990)
54. A. Blumstein, S. Vilasager, S. Ponrathnam, S. B. Clough R. B. Blumstein and G. Maret, *J. Polym. Sci.; Polym. Chem. Ed.* **20**, 877 (1982)
55. V. Percec and H. Nava and H. Jonsson, *J. Polym. Sci.; Polym. Chem. Ed.* **25**, 1943 (1987)
56. S. G. Kostromin, R. V. Talrose, V. P. Shibaev and N. A. Plate, *Makromol. Chem., Rapid Commun.*, **3**, 803 (1982)
57. M. Sawamoto, *Prog. Polym. Sci.*, **16**, 111 (1991)
58. T. Higashimura and M. Sawamoto, *Adv. Polym. Sci.*, **62**, 49 (1984)

59. M. Miyamoto, M. Sawamoto and T. Higashimura, *Macromolecules*, **17**, 265 (1984)
60. M. Sawamoto and T. Higashimura, *Makromol. Chem., Makromol. Symp.*, **3**, 83 (1986)
61. K. Matyjaszewski, *Makromol. Chem., Makromol. Symp.*, **13/14**, 457 (1988)
62. T. Higashimura, S. Aoshima and Y. Kishimoto, *Polym. Bull.*, **18**, 111 (1987)
63. T. Higashimura and S. Aoshima, *Macromolecules*, **22**, 1009 (1989)
64. C. G. Cho, B. A. Feit and O. W. Webster, *Macromolecules*, **23**, 1918 (1990)
65. C. H. Lin and K. Matyjaszewski, *Polym. Prepr., Am. Chem. Soc. Div. Polym. Chem.*, **31(1)**, 599 (1990)
66. T. Sagane and R. W. Lenz, *Polym. J.* **20**, 923 (1988); *Macromolecules*, **22**, 3763 (1989); *Polymer*, **30**, 2269 (1989)
67. V. Percec, Q. Zheng and M. Lee, *J. Mater. Sci.*, **1**, 611 (1991)
68. V. Percec, C. S. Wang and M. Lee, *Polym. Bull.*, **26**, 15 (1991)
69. H. Jonsson, V. Percec and A. Hult, *Polym. Bull.*, **25**, 115 (1991)
70. H. Stevens, G. Rehage and H. Finkelmann, *Macromolecules*, **17**, 851 (1984)
71. V. Percec, D. Tomazos and C. Pugh, *Macromolecules*, **22**, 3259 (1989)
72. D. Demus and L. Richter, "Textures of Liquid Crystals" Verlag Chemie, Weinheim 1978
73. G. W. Gray and J. W. Goodby, "Smectic Liquid Crystals, Textures and Structures", Leonard Hill, Glasgow, 1984

PART I. INFLUENCE OF MOLECULAR WEIGHT ON PHASE
TRANSITIONS OF POLY{ ω -[(4-CYANO-4'-
BIPHENYL)OXY]ALKYL VINYL ETHER}S

Chapter 2

SYNTHESIS AND CHARACTERIZATION OF POLY{ ω -[(4-CYANO-4'-BIPHENYL)OXY]ALKYL VINYL ETHER}S WITH DECANYL AND UNDECANYL GROUPS

2.1.-INTRODUCTION

The mechanism by which the polymer molecular weight influences the phase behavior of side chain liquid crystalline polymers (LCP) represents an open subject of discussion.¹⁻¹⁰ The molecular weight-phase transition dependence is the first factor which should be elucidated before a molecular design of side chain LCP can be accomplished. So far, the only trend which is generally accepted consists of the enlargement of the temperature range of the mesophase with the increase of the polymer molecular weight.¹⁻¹⁰

This dependence was recently explained based on thermodynamic principles assuming that the phase behavior of the polymer is dictated by that of the monomeric structural unit. However, there is only a single experiment in the literature which compares the phase behavior of a polymer with different molecular weights to that of its monomeric structural unit.⁷ When the mesophases of the monomeric unit and of the polymers are identical, the overall dependence of phase transitions on molecular weight could be explained as described in Chapter I.^{11,12} The least understood situation refers to polymers which display various mesophases at different molecular weights.^{4,7,9-10} Elucidation of this phenomenon requires the synthesis of polymers with well defined molecular weights, narrow molecular weight distributions as well as of their model compounds. So far, side chain liquid crystalline polymers with narrow molecular weight distribution were prepared by group transfer polymerization of

mesogenic methacrylates,⁷ by cationic polymerization of mesogenic vinyl and propenyl ethers,^{8-10,13,14} and by polymer homologous reactions.¹⁵

This chapter will present a novel and general procedure for the preparation of mesogenic vinyl ethers containing two or more than two methylenic units in the flexible spacer. Then it will describe the living cationic polymerization of 10-[(4-cyano-4'-biphenyl)oxy]decanyl vinyl ether (6-10) and 11-[(4-cyano-4'-biphenyl)oxy]undecanyl vinyl ether (6-11), and the influence of molecular weight on their phase transitions will be discussed by comparison to that of 10-[(4-cyano-4'-biphenyl)oxy]decanyl ethyl ether (8-10) and 11-[(4-cyano-4'-biphenyl)oxy]undecanyl ethyl ether (8-11) which represent the model compounds of the monomeric structural units of poly(6-10) and poly(6-11).

2.2.-EXPERIMENTAL

2.2.1.-Techniques

The 1-D ¹H and 2-D ¹H-NMR (COSY) spectra were recorded at 299.55 MHz on a VXR-300 NMR Spectrometer equipped with a 5 mm indirect detection probe in CDCl₃ at room temperature. 1-D spectra were obtained with a 5,600 Hz spectral width, 2.926 s acquisition time, 4 μs 13° pulse, 0 s relaxation delay and 2,048 transients. The 2-D ¹H-NMR (COSY) spectrum was obtained with a 2,775.5 spectral width, 0.184 s acquisition time, 13 μs 90° pulse, 1 s delay between transients and 32 transients.

2.2.2.-Materials

4-Phenylphenol (98%), 1,10-phenanthroline (anhydrous, 99%), palladium (II) diacetate (all from Lancaster Synthesis), ferric chloride anhydrous (98%, Fluka), copper (I) cyanide (99%), 9-borabicyclo[3.3.1]nonane (9-BBN, crystalline, 98%), 9-

bromononan-1-ol (97%), 10-bromodecan-1-ol (90%) and the other reagents (all from Aldrich) were used as received. Methyl sulfide (anhydrous, 99%, Aldrich) was refluxed over 9-BBN and then distilled under argon. Dichloromethane (99.6%, Aldrich) used as a polymerization solvent was first washed with concentrated sulfuric acid, then with water, dried over anhydrous magnesium sulfate, refluxed over calcium hydride and freshly distilled under argon before each use. N-Methyl-2-pyrrolidone (98%, Lancaster Synthesis) was dried by azeotropic distillation with benzene, shaken with barium oxide, filtered, and fractionally distilled under reduced pressure. Trifluoromethane sulfonic acid (triflic acid, 98%, Aldrich) was distilled under argon.

2.2.3.-Synthesis of Monomers

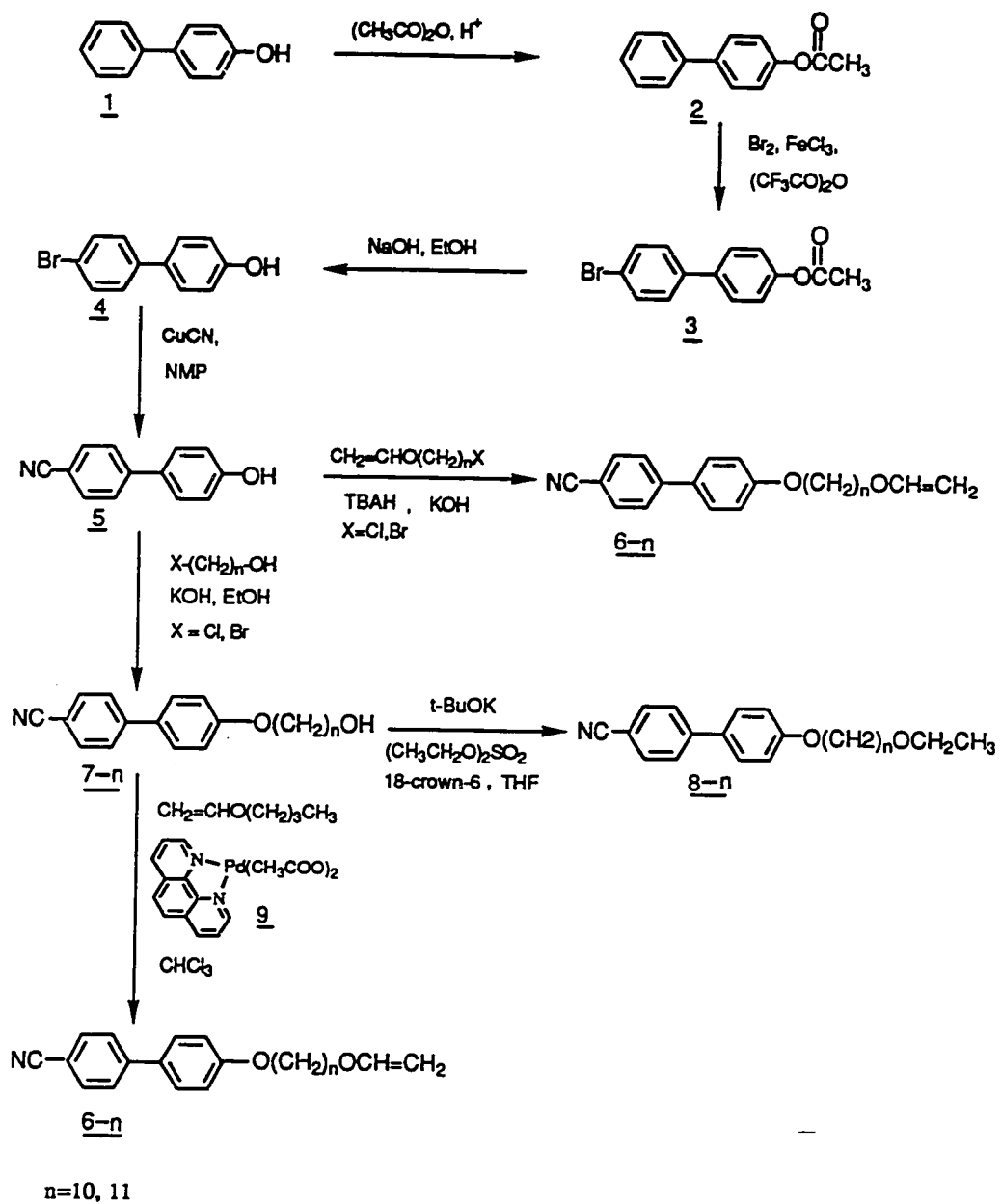
Scheme I outlines the general methods used in the synthesis of vinyl ethers.

1,10-Phenanthroline Palladium (II) Diacetate (9)

1,10-Phenanthroline palladium (II) diacetate was synthesized according to a literature procedure.¹⁶ mp 227°C (lit. 16, mp 234°C).

4-Phenylphenol Acetate (2)

To a mixture of 70g (0.41 mol) of 4-phenylphenol in 77.4 ml (0.82 mol) of acetic anhydride were added a few drops of concentrated H₂SO₄. The resulting solution was stirred at 60°C for 1 hr, cooled to room temperature, diluted with 300 ml of cold water and left stirring overnight. The resulting white crystals were filtered, washed with cold water, dried and recrystallized from ethanol to yield 87.2 g (92%) of **2**. Purity: 98% (HPLC). mp 86-87°C. ¹H-NMR (CDCl₃, TMS, d, ppm): 2.32 (3



Scheme I. Synthesis of Monomers and Model Compounds

protons, OCOCH_3 , s), 7.15 (2 aromatic protons, o to acetoxy, d), 7.44-7.58 (7 aromatic protons, m).

4-Acetoxy-4'-Bromobiphenyl (3)

Trifluoroacetic anhydride (14.2 ml, 0.1 mol) and FeCl_3 (0.2 g, 1.23 mmol) were added sequentially to an ice cooled solution of 4-phenyl phenol acetate (21.2 g, 0.1 mol) in 400 ml of dry CCl_4 . Bromine (16 g, 0.1 mol) was dropwise added and the reaction mixture was stirred at 0°C for 7 hr and at room temperature for other 7 hr. The CCl_4 was removed in a rotavapor and the resulting solid was washed with methanol and recrystallized from n-hexane to yield 20.5 g (66.8%) of white crystals. Purity: 99% (HPLC). mp $128\text{-}130^\circ\text{C}$ (lit. 17, 18, mp 130°C). $^1\text{H-NMR}$ (CDCl_3 , TMS, d, ppm): 2.32 (3 protons, OCOCH_3 , s), 7.18 (2 aromatic protons, o to acetoxy, d), 7.44-7.53 (2 aromatic protons, m to acetoxy, and 4 aromatic protons, o and m to Br, m).

4-Bromo-4'-Hydroxybiphenyl (4)

4-Acetoxy-4'-bromobiphenyl (20.5 g, 0.07 mol) was hydrolyzed by refluxing for 2 hr with a solution of 20 g NaOH in 400 ml of 80% aqueous ethanol. The ethanol was removed on a rotavapor and the obtained solid was dissolved in distilled water. The water solution was neutralized with dilute hydrochloric acid and the obtained solid was filtered, dried and recrystallized from a mixture of ethanol/water (3/2) to yield 16.5 g (94.6%). Purity: 98% (HPLC). mp $165\text{-}167^\circ\text{C}$ (lit. 20, mp $166\text{-}167^\circ\text{C}$). $^1\text{H-NMR}$ (Acetone- d_6 , TMS, d, ppm) : 4.8 (1 proton, -OH, s), 6.95 (2 aromatic protons, o to -OH, d), 7.49-7.55 (2 aromatic protons, m to -OH, and 4 aromatic protons, o and m to Br, m).

4-Cyano-4'-Hydroxybiphenyl (5)

A mixture of 4-bromo-4'-hydroxybiphenyl (20 g, 0.08 mol) and CuCN (10 g, 0.11 mol) in dry N-methyl-2-pyrrolidone (68 ml) was refluxed for 6 hr. After cooling, the reaction mixture was poured into a mixture of hydrated ferric chloride (31.7 g), concentrated hydrochloric acid (8 ml), and water (47 ml), and the resulting mixture was stirred at 60°C for 20 min. The mixture was extracted with chloroform, and the chloroform solution was successively washed with 5N hydrochloric acid, 10% aqueous sodium bicarbonate, water and dried over anhydrous magnesium sulfate. The chloroform was removed in a rotavapor, the obtained solid was dissolved in a minimum volume of hot acetone and sufficient petroleum ether was added to produce turbidity. The solution was refrigerated and the crystalline product was filtered, dried and recrystallized several times from toluene to yield 11.8 g (75.3%) of 4-cyano-4'-hydroxybiphenyl. Purity: 98% (HPLC). mp 195-198°C (lit. 18, mp 196-199°C). ¹H-NMR (Acetone-d₆, TMS, d, ppm): 3.80 (1 proton, -OH, s), 7.61 (2 aromatic protons, o to hydroxy, d), 7.61 (2 aromatic protons, o to hydroxy, d), 7.61 (2 aromatic protons, m to -OH, d), 7.79 (4 aromatic protons, o and m to -CN, s).

Synthesis of 4-cyano-4'-(10-hydroxydecan-1-yloxy)biphenyl (7-10)

4-Cyano-4'-hydroxybiphenyl (3.9 g, 0.02 mol), potassium hydroxide (1.12 g, 0.02 mol) and few crystals of potassium iodide were dissolved in a mixture of ethanol/water (7/3) (141.5 ml). 10-Bromodecan-1-ol (5 g, 0.21 mol) was added to the resulting solution which was heated to reflux for 24 hr. After cooling, the mixture was poured into water and then filtered. The obtained solid was recrystallized from methanol and then benzene, to yield 4.1 g (58.3%) of white crystals. mp, 97.4°C (DSC). ¹H-NMR (CDCl₃, TMS, d, ppm): 1.02-1.93 (16 protons, -(CH₂)₈-, m), 3.65

(2 protons, $-\text{CH}_2\text{OH}$, t), 4.01 (2 protons, PhOCH_2- , t), 7.02 (2 aromatic protons, o to alkoxy, d), 7.51 (2 aromatic protons, m to alkoxy, d), 7.66 (4 aromatic protons, o and m to-CN, d of d).

4-Cyano-4'-(11-Hydroxyundecan-1-yloxy)biphenyl (7-11)

4-Cyano-4'-hydroxybiphenyl (15.7 g, 0.08 mol), potassium hydroxide (4.5 g, 0.08 mol) and a few crystals of potassium iodide were dissolved in a mixture of ethanol-water (4:1) (440 ml). 11-Bromoundecan-1-ol (22.6 g, 0.09 mol) was added to the resulting solution which was heated to reflux for 24 hr. The ethanol was removed on a rotavapor and the resulting solid was washed successively with water, dilute aqueous NaOH and water. Recrystallization from methanol yielded 22.7 g (78%) of white crystals. mp 92°C (DSC). $^1\text{H-NMR}$ (CDCl_3 , TMS, d, ppm): 1.01-1.95 (18 protons, $-(\text{CH}_2)_9-$, m), 7.02 (2 aromatic protons, o to alkoxy, d), 7.51 (2 aromatic protons, m to alkoxy, d), 7.68 (4 aromatic protons, o and m to -CN, d of d).

Synthesis of 10-[(4-cyano-4'-biphenyl)oxy]decanyl vinyl ether (6-10)

4-Cyano-4'-(10-hydroxydecan-1-yloxy)biphenyl (1.50 g, 4.27 mmol) was added to a mixture of 1,10-phenanthroline palladium (II) diacetate (0.17 g, 0.42 mmol), n-butyl vinyl ether (23.3 ml) and dry chloroform (18 ml). The mixture was heated to 60°C for 6 hr. After cooling, it was filtered to remove the catalyst and the solvent was distilled in a rotavapor. The product was purified by column chromatography (silica gel, CH_2Cl_2 eluent) and then recrystallized from n-hexane to yield 1.2 g (74.7%) of white crystals. Purity: 99.9% (HPLC). mp, 65.4°C, Tn-i, 69.8°C (DSC). $^1\text{H-NMR}$ (CDCl_3 , TMS, d, ppm): 1.02-1.93 (16 protons, $-(\text{CH}_2)_8-$, m), 3.67 (2 protons, $-\text{CH}_2\text{O}-$, t), 4.01 (3 protons, $-\text{OCH}=\text{CH}_2$ trans and PhOCH_2- ,

m), 4.14 and 4.20 (1 proton, $-\text{OCH}=\underline{\text{CH}}_2$ cis, d), 6.49 (1 proton, $\text{OCH}=\underline{\text{CH}}_2$, q), 7.01 (2 aromatic protons, o to alkoxy, d), 7.50 (2 aromatic protons, m to alkoxy, d), 7.65 (4 aromatic protons, o and m to-CN, d of d).

11-[(4-Cyano-4'-Biphenyl)oxy]undecanyl Vinyl Ether (6-11)

4-Cyano-4'-(11-hydroxyundecan-1-yloxy)biphenyl (3.7 g, 0.01 mol) was added to a mixture of 1,10-phenanthroline palladium (II) diacetate (0.4 g, 1 mmol), n-butyl vinyl ether (15 ml) and dry chloroform (3.85 ml). The mixture was heated at 60°C for 6 hr. After cooling and filtration (to remove the catalyst) the solvent was distilled in a rotavapor and the product was purified by column chromatography (silica gel, CH_2Cl_2 eluent) to yield 3.8 g (91%) of white crystals. Purity: 99% (HPLC). mp 71°C (DSC). $^1\text{H-NMR}$ (CDCl_3 , TMS, d, ppm): 1.01-1.95 (18 protons, $-(\text{CH}_2)_9-$, m), 3.68 (2 protons, $-\text{CH}_2\text{O}-$, t), 4.01 (3 protons, $-\text{OCH}=\underline{\text{CH}}_2$ trans, and PhOCH_2- , m), 4.15 and 4.22 (1 proton, $\text{OCH}=\underline{\text{CH}}_2$ cis, d), 6.47 (1 proton, $\text{OCH}=\underline{\text{CH}}_2$, q), 7.01 (2 aromatic protons, o to alkoxy, d), 7.51 (2 aromatic protons, m to alkoxy, d), 7.66 (4 aromatic protons, o and m to -CN, d of d).

11-Bromoundecanyl Vinyl Ether

11-Bromoundecan-1-ol (2 g, 7.96 mmol) was added to a mixture of 1,10-phenanthroline palladium (II) diacetate (0.32 g, 0.8 mmol), n-butyl vinyl ether (42.5 ml) and chloroform (10 ml). The mixture was heated at 60°C for 6 hr. After cooling and filtration (to remove the catalyst) the solvent was distilled in a rotavapor and the product was purified by column chromatography (silica gel, methylene chloride eluent) to yield 1.96 g (89%) of a liquid. $^1\text{H-NMR}$ (CDCl_3 , TMS, d, ppm) : 1.0-2.1 (18 protons, $-(\text{CH}_2)_9-$, m), 3.45 (2 protons, $-\underline{\text{CH}}_2\text{Br}$, t), 3.71 (2 protons, $-\underline{\text{CH}}_2\text{O}-$, t),

4.03 (1 proton, $-\text{OCH}=\underline{\text{CH}}_2$ trans, d), 4.20 (1 proton, $-\text{OCH}=\underline{\text{CH}}_2$ cis, d), 6.57 (1 proton, $-\text{OCH}=\underline{\text{CH}}_2$, q).

Synthesis of 6-11 by the Etherification of 5 with 11-Bromoundecanyl Vinyl Ether

6-11 was also synthesized by the etherification of 5 with 11-bromoundecanyl vinyl ether, by following the synthetic procedure used for the preparation of 7-11. The purification of 6-11 was performed as in its previous synthesis. Yield: 60%.

Synthesis of 10-[(4-cyano-4'-biphenyl)oxy]decanyl ethyl ether (8-10)

4-Cyano-4'-(10-hydroxydecan-1-yloxy)biphenyl (0.3 g, 0.85 mmol) was added to a solution containing potassium t-butoxide (0.096 g, 0.85 mmol), a catalytic amount of 18-crown-6 and dry tetrahydrofuran (10 ml). Diethyl sulfate (0.114 ml, 0.94 mmol) was added and the reaction mixture was refluxed for 4 hr under argon. After cooling, the reaction mixture was poured into chloroform. The chloroform solution was extracted with 10% aqueous KOH, washed with water, dried over magnesium sulfate and the solvent was removed in a rotavapor. The resulting product was purified by column chromatography (silica gel, CH_2Cl_2 eluent) and then was recrystallized from methanol to yield 0.23 g (54.2%) of white crystals. Purity: 99% (HPLC). mp, 69.1°C (DSC). $^1\text{H-NMR}$ (CDCl_3 , TMS, d, ppm): 1.20 (3 protons, $-\text{OCH}_2\underline{\text{CH}}_3$, t), 1.30-1.93 (16 protons, $-(\underline{\text{CH}}_2)_8-$, m), 3.41 (4 protons, $\underline{\text{CH}}_2\text{OCH}_2\underline{\text{CH}}_3$, m), 4.01 (2 protons, PhOCH_2 , t), 7.02 (2 aromatic protons, o to alkoxy, d), 7.51 (2 aromatic protons, m to alkoxy, d), 7.66 (4 aromatic protons, o and m to $-\text{CN}$, d of d).

11-[(4-Cyano-4'-Biphenyl)oxy]undecanyl Ethyl Ether (8-11)

4-Cyano-4'-hydroxybiphenyl (3.9 g, 0.01 mol) was added to a solution containing potassium t-butoxide (1.12 g, 0.01 mol), 18-crown-6 (2.6 mg, 0.01 mmol) and dry tetrahydrofuran (78 ml). Diethyl sulfate (1.54 g, 0.01 mol) was added and the reaction mixture was refluxed for 3 hr. After cooling, the reaction mixture was extracted with chloroform, washed with water, dried over magnesium sulfate and the chloroform was removed in a rotavapor. The resulting product was purified by column chromatography (silica gel, methylene chloride eluent) to yield 2.43 g (62%) of white crystals. Purity: 99% (HPLC). mp 51.0°C, s_A -i 60.1°C (DSC). $^1\text{H-NMR}$ (CDCl_3 , TMS, d, ppm): 1.20 (3 protons, $-\text{OCH}_2\text{CH}_3$, t), 1.30-1.81 (18 protons, $-(\text{CH}_2)_9-$, m), 3.41 (4 protons, $-\text{CH}_2\text{OCH}_2-$, m), 4.00 (2 protons, $-\text{CH}_2\text{OPh}$, t), 7.01 (2 aromatic protons, o to alkoxy, d), 7.51 (2 aromatic protons, o and m to $-\text{CN}$, d of d).

2.2.4.-Cationic Polymerizations

Polymerizations were carried out in glass flasks equipped with teflon stopcocks and rubber septa under argon atmosphere at 0°C for 1 hr. All glassware was dried overnight at 180°C. The monomer was further dried under vacuum overnight in the polymerization flask. Then the flask was filled with argon, cooled to 0°C and the methylene chloride, dimethyl sulfide and triflic acid were added via a syringe. The monomer concentration was about 10 wt% of the solvent volume and the dimethyl sulfide concentration was 10 times larger than that of the initiator. The polymer molecular weight was controlled by the monomer/initiator ($[\text{M}]_0/[\text{I}]_0$) ratio. After quenching the polymerization with ammoniacal methanol, the reaction mixture was precipitated into methanol. The filtered polymers were dried and precipitated from methylene chloride solutions into methanol until GPC traces showed no traces of monomer. Tables IV and V summarize the polymerization results. Although polymer

yields are lower than expected due to losses during the purification process, conversions were almost quantitative in all cases.

2.3.-RESULTS AND DISCUSSION

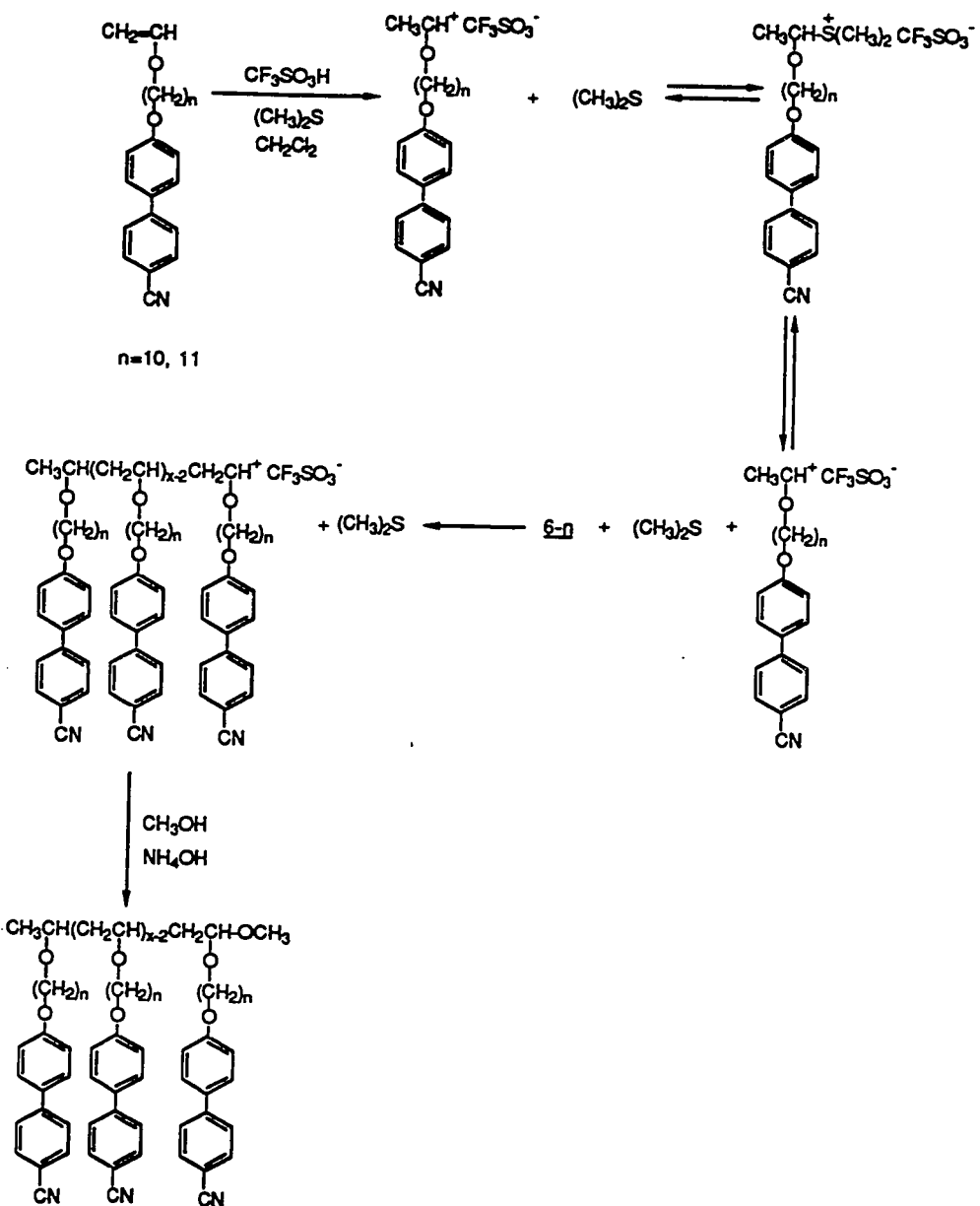
The synthesis of 6-10, 6-11, 8-10 and 8-11 is outlined in Scheme I. 6-11 was synthesized both by the transesterification of 7-11 and with n-butyl vinyl ether and by etherification of 5 with 11-bromoundecanyl vinyl ether. The novel part of this synthesis consists of 7-10, 7-11 and of 11-bromoundecan-1-ol with n-butyl vinyl ether in the presence of 1,10-phenanthroline palladium (II) diacetate (9). The vinyl interchange reaction between vinyl ethers and alcohols catalyzed by 9 can be performed under mild reaction conditions.^{16,19} Experiments performed in our laboratory have demonstrated that this reaction tolerates a variety of functional groups. Therefore, this reaction can be used in the synthesis of vinyl ethers containing mesogenic groups attached through various spacer lengths. Previously, mesogenic vinyl ethers were synthesized by the phase transfer catalyzed etherification of a mesogenic phenol with chloroethyl vinyl ether.^{8-10,13,20} This procedure allowed the preparation of monomers containing only two methylenic units in the flexible spacer. 1,10-Phenanthroline palladium (II) diacetate was also used to catalyze the transesterification of ω -bromoalkan-1-ols with n-butyl vinyl ether. The synthesis of 11-bromoundecanyl vinyl ether by this reaction, followed by the alkylation of 5 with 11-bromoundecanyl vinyl ether was also used in the preparation of 6-11. However, although 6-10 can be synthesized by the etherification of 4-cyano-4'-biphenyl with 10-bromodecanyl vinyl ether, the preferred route consists of the transesterification of 7-10.

As shown previously,^{8-10,14,15,21-23} living cationic polymerization of vinyl ethers tolerates a variety of functional groups. We prefer to perform this polymerization

with triflic acid/dimethyl sulfide initiator system, since under these conditions the polymerization can be carried out in methylene chloride at 0°C.²⁴ Scheme II outlines the polymerization mechanism. It is essential that the monomers used in these polymerization experiments are completely free of protonic impurity. The resulting polymers contain acetal chain ends and therefore, they should be manipulated in the absence of acids.

Figure 1 shows the 1-D ¹H-NMR spectrum of poly(6-10) with a theoretical degree of polymerization of four together with the proton assignments. The aromatic region of the 2-D ¹H-NMR spectrum of poly(6-10) is presented in Figure 2a while the aliphatic part of the same spectrum in Figure 2b. The off-diagonal cross-peaks from Figure 2a,b indicate which protons are J-coupled and support the assignment of the proton resonances from Figure 1. The chemical shifts of these assignments are summarized in Table 1. The signals due to the methyl (signal a), methoxy (signal f) and acetal, -CH₂(O)CH₂O-, (signal e) chain end can be easily integrated. Their experimental ratios (i.e., f/a≈1 and a/e≈3.0) correspond to the theoretical values expected for a polymer resulted from a polymerization free of chain transfer and termination reactions (Table II). The calculated degree of polymerization (DP=n/2e=3.4) is very close to the theoretical one i.e., [M]₀/[I]₀=4.0.

In addition, the NMR spectra of this polymer do not show any unsaturated chain ends which would result from chain transfer reaction. Only a very small signal at 9.8 ppm can be observed. This signal is due to a -CHO chain end which results from the termination reaction (Scheme III). However, it represents less than 1% of the total concentration of the methoxy chain end. The ¹H-NMR spectra of poly(6-10)s with degree of polymerization up to 30 were analyzed and show the same behavior. These results demonstrate that a quantitative functionalization of the poly(6-10) prepared with



Scheme II. Cationic polymerization of 6-10 and 6-11

Figure 1. Representative 300-MHz 1-D ¹H-NMR spectrum of poly(6-10) with theoretical DP=4

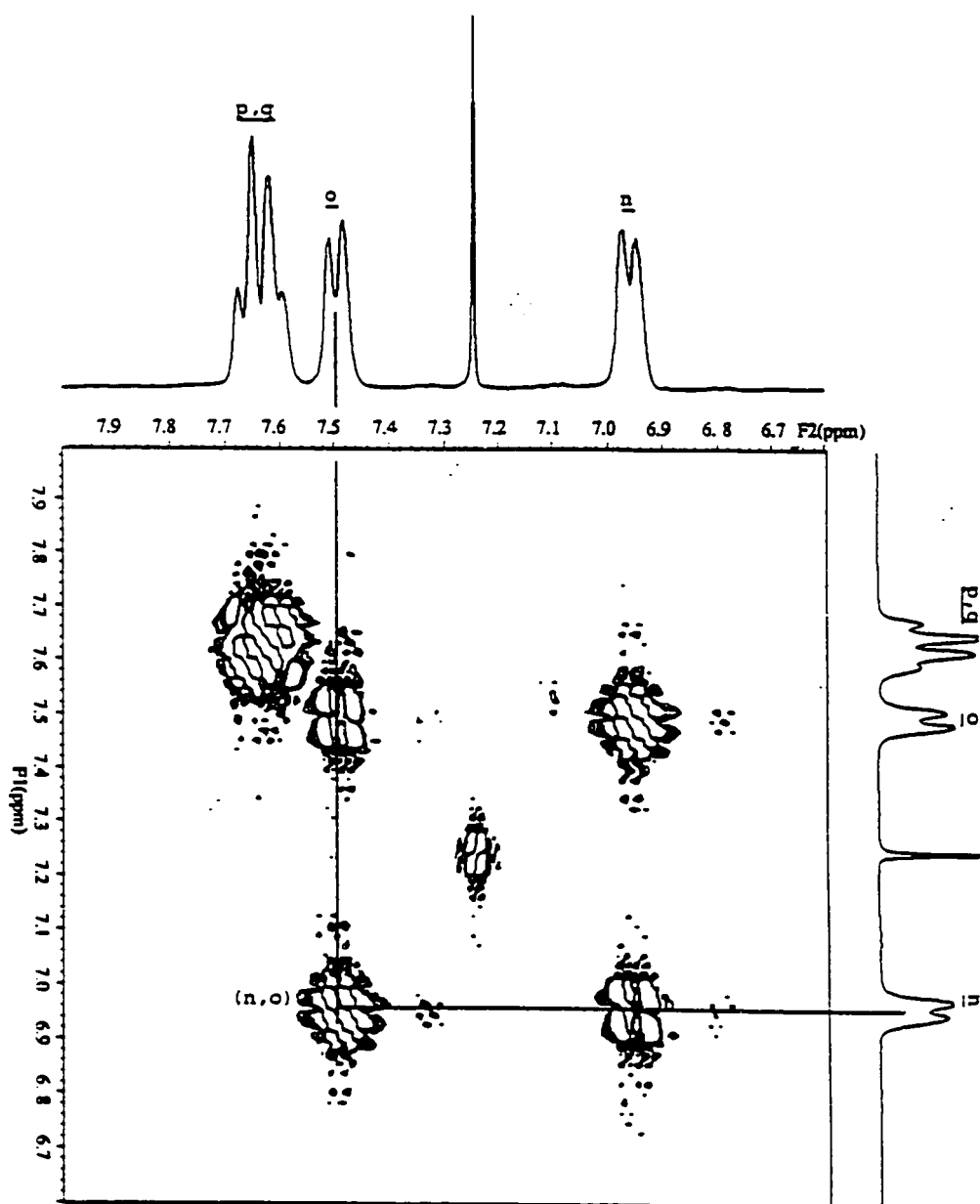


Figure 2a. The aromatic region of the 300-MHz 2-D ^1H -NMR spectrum of poly(6-10) with theoretical DP=4.

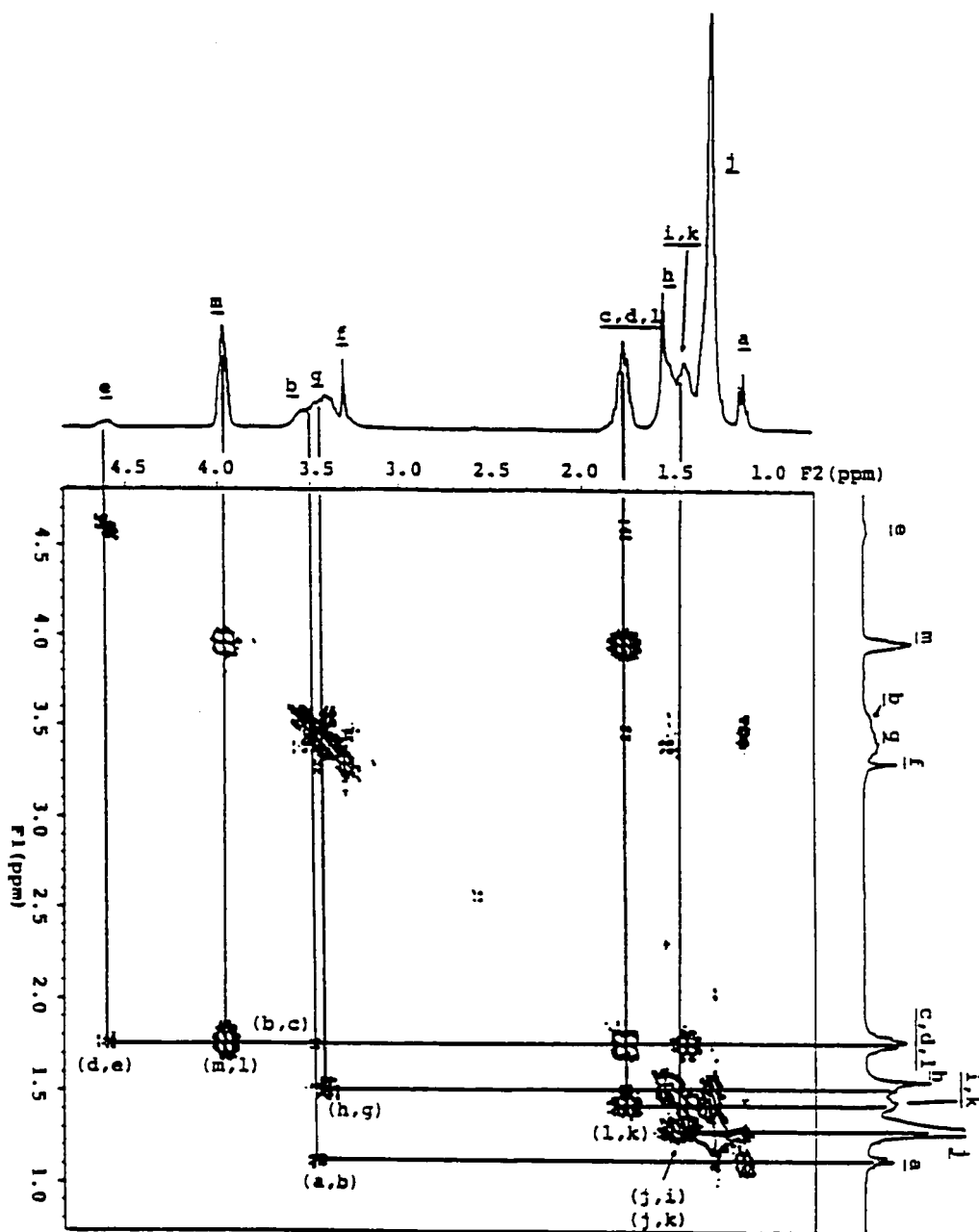


Figure 2b. The aliphatic region of the 300-MHz 2-D ^1H -NMR spectrum of poly(6-10) with theoretical DP=4.

Table I. ^1H -NMR Chemical Shifts of Poly(6-10)

proton	label	chemical shift (ppm)	nature of signal
polymer backbone	a	1.12	d
	b	3.50	m
	c	1.75	m
	d	1.75	m
	e	4.60	m
	f	3.30	s
flexible spacer	g	3.43	m
	h	1.53	m
	i	1.42	m
	j	1.29	m
	k	1.44	m
	l	1.78	m
	m	3.90	t
aromatic proton	n	6.94	d
	o	7.47	d
	p	7.65	d of d
	q	7.65	d of d

Table II. Integration Ratio of Polymer Chain Ends

proton	integration ratio (NMR)	theoretical ratio
f/a	0.96 ^a	1.0
n/e	6.8 ^b	8.0
a/e	2.87	3.0

^a Number of methoxy end groups/polymer chain^b DP (NMR)=6.8/2=3.4

Table III. Thermal Characterization of 4-Cyano-4'-(ω -hydroxyalkan-1-yloxy)biphenyls (7-10) and (7-11), ω -[(4-Cyano-4'-biphenyl)oxy]alkyl Vinyl Ethers (6-10) and (6-11), and of ω -[(4-Cyano-4'-biphenyl)oxy]alkyl Ethyl Ethers (8-10) and (8-11).

Compound	phase transitions (0°C) and corresponding enthalpy changes (kcal/mol)	
	heating	cooling
<u>7-10</u>	k 97.4 (10.0) i [n 97.2 (0.45) i]*	i 94.2 (0.52) n 75.5 (8.3) k
<u>6-10</u>	k 65.4 (8.4) i [n 69.8 (0.36) i]*	i 66.1 (0.43) n 52.6 (8.19) k
<u>8-10</u>	k 69.1 (12.9) i [s _A 65.0 (0.71) i]*	i 57.1 (0.72) s _A 27.9 (8.66) k
<u>7-11</u>	k 92.0 (12.4) i [n 95.2 (0.46) i]*	i 92.3 (0.49) n 77.0 (9.36) k
<u>6-11</u>	k 71.3 (11.10) i [s _A 60.8 (0.29) n 70.6 (0.32)]* i	i 58.9 (0.55) n 54.2 s _A 39.7 (0.55) k
<u>8-11</u>	k 51.0 (9.80) s _A 60.1 (0.74) i	i 56.8 (0.72) s _A 27.8 (8.72) k

*[] virtual data

* overlapped peaks

Table IV. Cationic Polymerization of 10-[4-Cyano-4'-biphenyl]oxy]decanyl Vinyl Ether (6-10) (polymerization temperature, 0°C; polymerization solvent, methylene chloride; $[M]_0/[I]_0=0.265$; $[(CH_3)_2S]_0/[I]_0=10$; polymerization time, 1 hr) and Characterization of the Resulting Polymers. Data on first line are from first heating and cooling scans. Data on second line are from second heating scan.

Sample No.	$[M]_0/[I]_0$	Polymer yield(%)	Mw/Mn		DP		phase transitions(°C)		and corresponding enthalpy changes (kcal/mru)	
			Max 10 ⁻³	G P C	4	3	heating	cooling		
1	4	71	1.4	1.15	4	3	g 3.6 k 51.1 (3.77) s _A 116.6 (0.83) i g 0.0 s _A 115.9 (0.86) i	i 110.9 (0.82) s _A -5.5 g		
2	7	66	2.6	1.13	7	6	g 8.7 k 49.7 (2.70) s _A 128.1 (0.78) i g 2.7 s _A 127.6 (0.80) i	i 122.0 (0.79) s _A -0.1 g		
3	10	78	4.2	1.08	11	10	g 11.8 k 53.4 (2.34) s _A 139.5 (0.77) i g 6.4 s _A 138.6 (0.76) i	i 132.4 (0.74) s _A 2.7 g		
4	15	74	6.1	1.09	16	14	g 12.7 k 53.8 (2.68) s _A 147.0 (0.78) i g 14.8 s _X 37.0 (0.62) s _A 147.8 (0.76) i	i 142.9 (0.73) s _A 24.9 (0.58) s _X 9.8 g		
5	20	85	7.3	1.14	19	21	g 15.5 k 55.0 (2.39) s _A 153.7 (0.76) i g 16.2 s _X 44.9 (0.68) s _A 152.9 (0.74) i	i 147.3 (0.72) s _A 37.4 (0.80) s _X 11.8 g		
6	25	83	9.6	1.10	25	27	g 16.2 k 55.2 (2.35) s _A 155.2 (0.75) i g 16.0 s _X 48.2 90.69) s _A 154.1 (0.72) i	i 149.1 (0.71) s _A 41.8 (0.84) s _X 12.2 g		
7	30	73	10.9	1.09	28	33	g 17.4 k 56.1 (2.35) s _A 156.5 (0.78) i g 16.5 s _X 50.6 (0.91) s _A 157.0 (0.71) i	i 151.2 (0.70) s _A 44.1 (0.84) s _X 12.8 g		

Table V. Cationic Polymerization of 11-[4-Cyano-4'-biphenyl]oxy]undecanyl Vinyl Ether (6-11) (polymerization temperature, 0°C; polymerization solvent, methylene chloride; $[M]_0=0.255$; $[(CH_3)_2S]_0/[I]_0=10$; polymerization time, 1hr) and Characterization of the Resulting Polymers. Data on first line are from first heating and cooling scans. Data on second line are from second heating scan.

Sample No.	$[M]_0/[I]_0$	Polymer yield(%)	$\overline{M}_n \cdot 10^{-3}$	$\overline{M}_w/\overline{M}_n$	D P	phase transitions(°C) and corresponding enthalpy changes (kcal/mru)	
						heating	cooling
1	3	75	1.1	1.04	3	k 50.1 (3.75) sA 96.4 (0.65) i g 3.6 k 67.1 (3.05) sA 90.2 (0.60) i	i 85.4 (0.65) sA 31.7 k -1.7 g
2	4	75	1.7	1.04	4	g 8.2 k 53.3 (3.33) sA 108.3 (0.83) i g -1.0 sA 106.5 (0.74) i	i 103.7 (0.81) sA 0.2 g
3	7	71	2.7	1.08	7	g 12.5 k 59.7 (3.34) sA 133.5 (0.81) i g 9.1 sA 125.8 (0.76) i	i 115.1 (0.69) sA 2.0 g
4	15	75	5.7	1.05	14	g 17.0 k 66.3 (3.29) sA 155.2 (0.82) i g 14.7 sA 150.1 (0.77) i	i 141.4 (0.78) sA 8.3 g
5	20	72	7.7	1.09	19	g 16.0 k 65.0 (2.95) sA 159.9 (0.82) i g 14.9 sX 50.7 (1.68) sA 148.7 (0.70) i	i 142.3 (0.74) sA 19.7 (0.70) sX 9.1 g
6	25	81	9.8	1.04	25	g 19.8 k 66.0 (3.31) sA 155.0 (0.80) i g 14.7 sX 50.0 (0.48) sA 146.8 (0.70) i	i 141.0 (0.78) sA 15.0 (0.29) sX 9.7 g
7	30	78	12.0	1.10	31	g 21.3 k 66.5 (2.76) sA 164.9 (0.77) i g 16.7 sX 51.6 (1.03) sA 160.8 (0.71) i	i 155.7 (0.72) sA 19.5 (0.42) sX 11.4 g

this initiation system is possible and that the number average molecular weight of the polymers with degrees of polymerization up to 30 can be determined by ^1H -NMR spectroscopy (Table IV, Figure 4).

Tables IV and V summarize the polymerization results. In both tables, conversions are less than quantitative due to polymer losses during the purification process. However, at the end of the polymerization, GPC traces showed that the conversion was almost quantitative. Figure 3 presents the GPC traces of poly(6-10)s with different degrees of polymerization. Although the molecular weights of the resulting polymers were determined by GPC using polystyrene as calibration standard and therefore have only relative meaning, they demonstrate that the ratio $[\text{M}]_0/[\text{I}]_0$ provides a very good control of the molecular weight. Figure 4 presents the plots of the dependences of the number average molecular weight (determined by both NMR and GPC) and of M_w/M_n versus the ratio between the initial monomer 6-10 and initiator concentrations $[\text{M}]_0/[\text{I}]_0$. This figure demonstrates that within this range of molecular weights the cationic polymerization of 6-10 shows a living character. Similar figure for poly(6-11) demonstrates that 6-11 also polymerizes through a living mechanism within this experimental range of molecular weight.

Heating and cooling DSC traces of 7-10, 7-6 and 8-10 are shown in Figure 5a. 7-10 and 8-10 exhibit a monotropic nematic and a monotropic smectic A mesophase respectively, while 6-10 an enantiotropic nematic mesophase. The transition from this nematic phase to the isotropic phase was determined by reheating the sample in the DSC instrument from a temperature which is above the crystallization temperature.

The DSC traces of 7-11, 6-11 and 8-11 are presented in Figure 5b. 7-11 displays a monotropic nematic mesophase. 6-11 presents a monotropic nematic and a monotropic s_A phase. The parameters of these two phase transitions from the heating

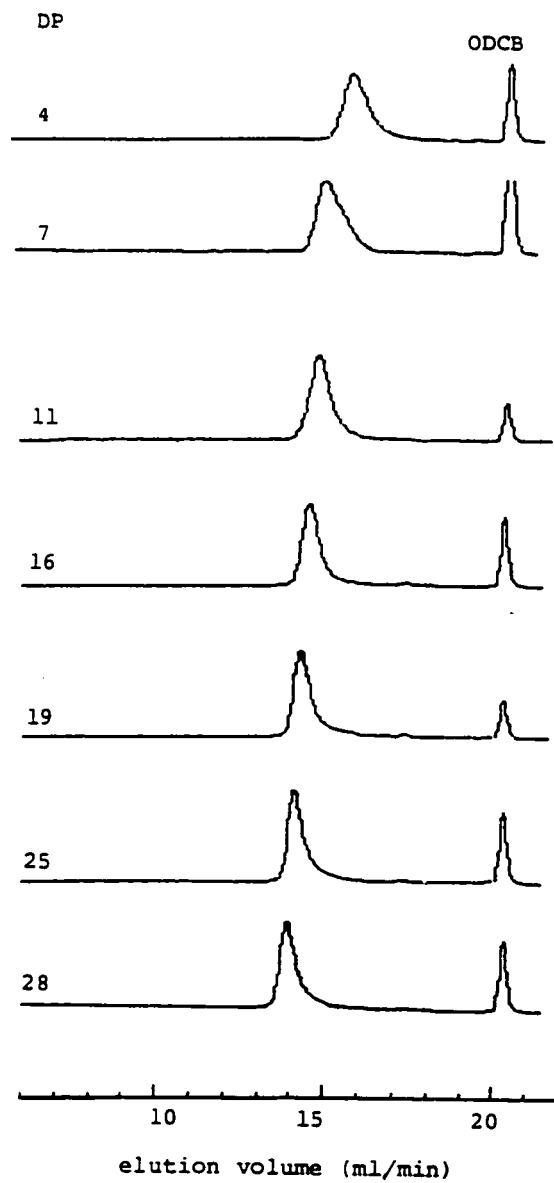


Figure 3. GPC traces of poly(6-10) with different molecular weights. The degrees of polymerization of each sample are printed on the figure.

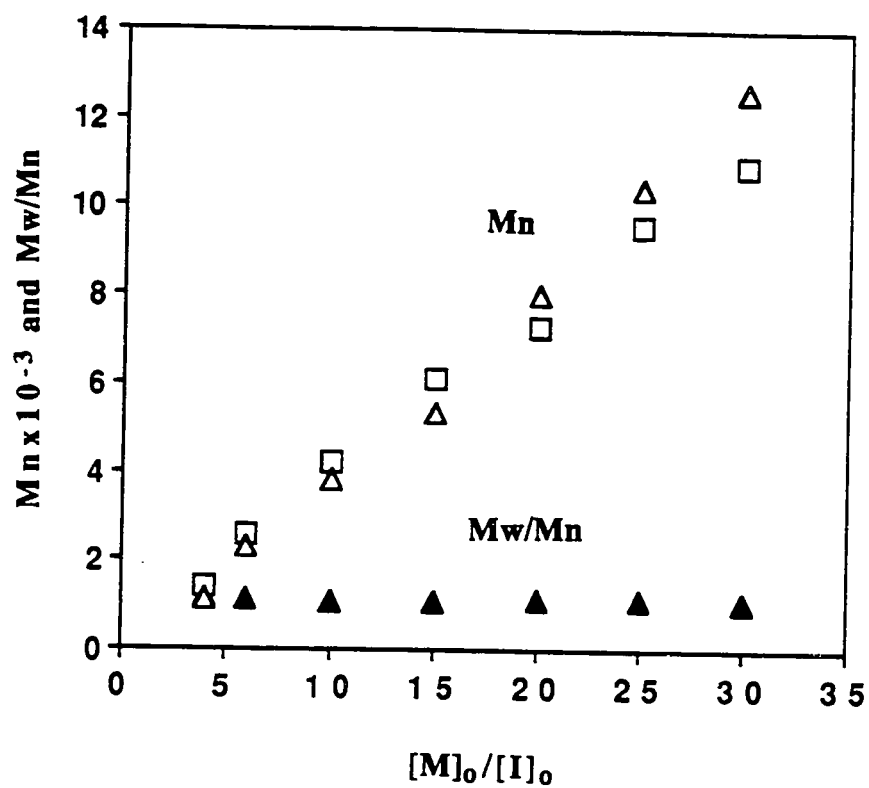


Figure 4. The dependence of the number average molecular weight (M_n) by determined by GPC; \square and by NMR; Δ and of the polydispersity (M_w/M_n); \blacktriangle of poly(6-10) on the $[M]_0/[I]_0$ ratio.

scans were obtained by reheating the sample before it reached the crystallization temperature. 8-11 presents an enantiotropic s_A mesophase (Figure 5b). Table III summarizes all these thermal transitions and their corresponding thermodynamic parameters.

The DSC traces of poly(6-10) obtained from the first and second heating and from the first cooling scans are presented in Figure 6a, b, c. The first and second DSC heating scans of poly(6-10) are different and therefore, both are shown in Figure 6a, b. In the first DSC heating scan, poly(6-10)s exhibit a crystalline melting followed by an enantiotropic s_A mesophase (Figure 6a). In the first cooling scan, poly(6-10)s with degree of polymerization up to sixteen exhibit the transition from the isotropic to the s_A phase followed by a glass transition temperature (Figure 6c). Poly(6-10)s with higher degrees of polymerization exhibit the transition from the isotropic to s_A followed by a transition from the s_A to a s_X (unidentified smectic phase). On the subsequent heating (Figure 6b) and cooling (Figure 6c) scans, depending on the degree of polymerization, poly(6-10) exhibit either an enantiotropic s_A or enantiotropic s_A and s_X phases (Table IV). However, if we anneal the polymer sample above the glass transition temperature after cooling and reheating, side chain crystallization occurs again and the polymer exhibits the same DSC heating scan as the first heating scan (Figure 6a). The dependence of molecular weight of the mesomorphic behavior of poly(6-10) is plotted in Figure 7a for the first heating scan, in Figure 7b for the second and subsequent heating scans and in Figure 7c for the first and subsequent cooling scans.

The model of the monomeric structural unit 8-11 exhibits a monotropic smectic A, while the poly(6-11) display a s_A mesophase. This result demonstrates that the transition from monomeric structural unit to polymer can generate the transformation of a monotropic mesophase into an enantiotropic one. This dependence can be explained

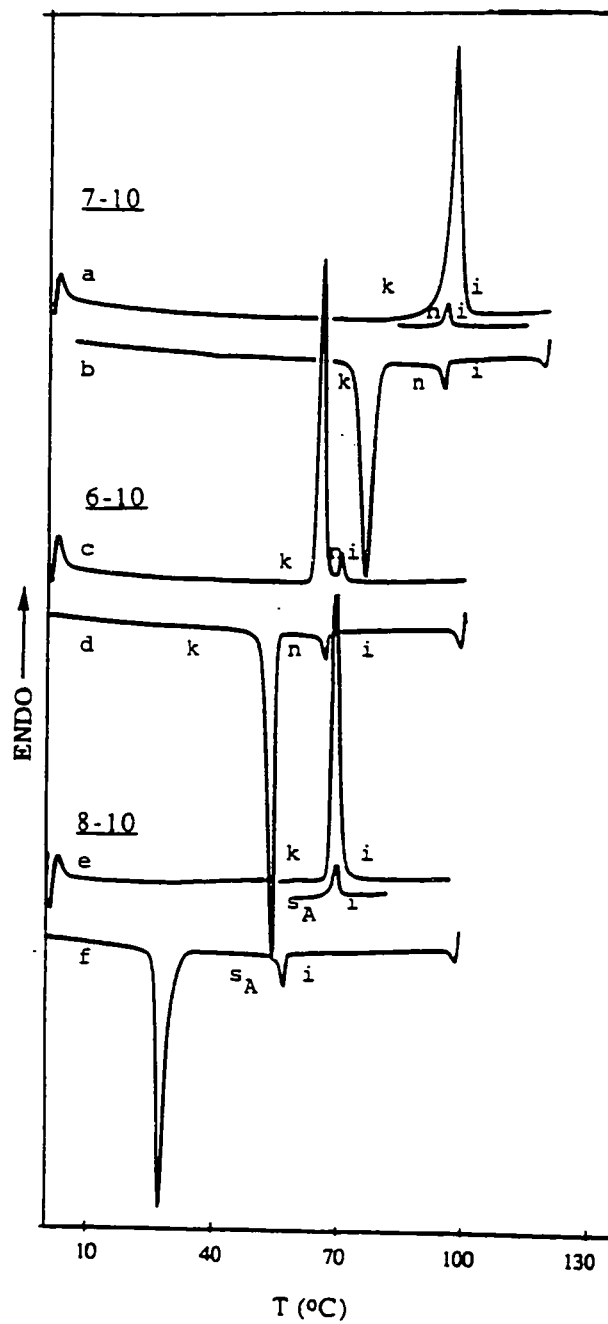


Figure 5a. Heating and cooling DSC traces of 7-10 (a, b), 6-10 (c, d) and 8-10 (e, f).

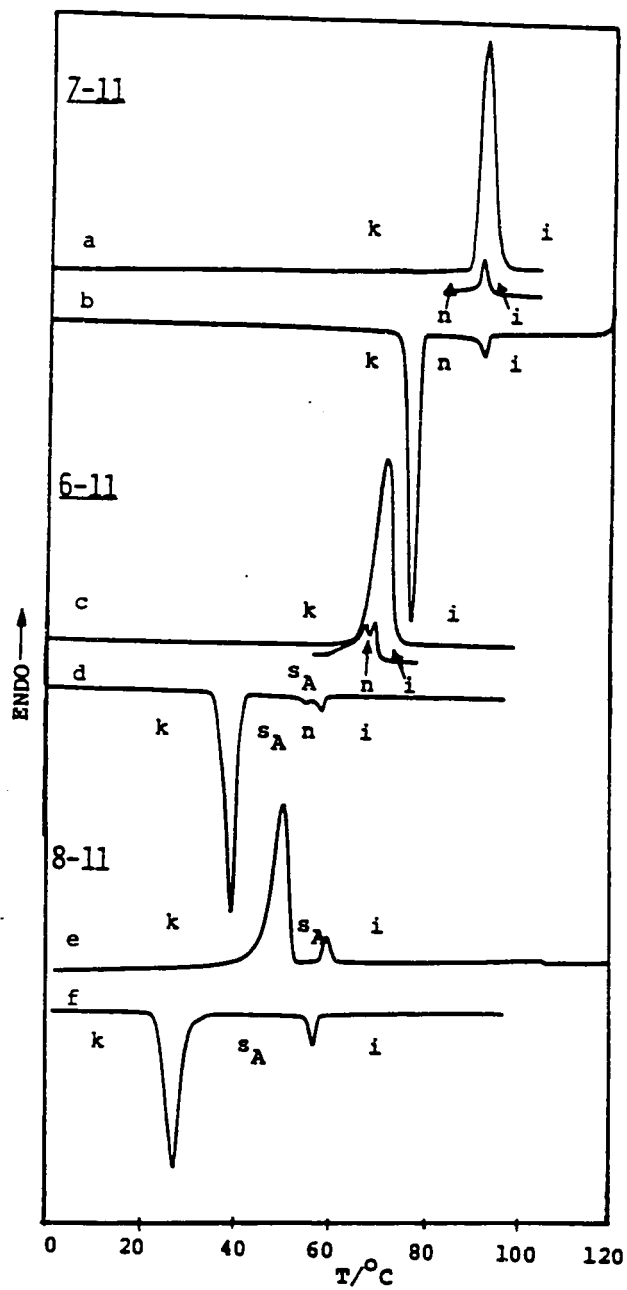


Figure 5b. Heating and cooling DSC traces of 7-11 (a, b), 6-11 (c, d) and 8-11 (e, f).

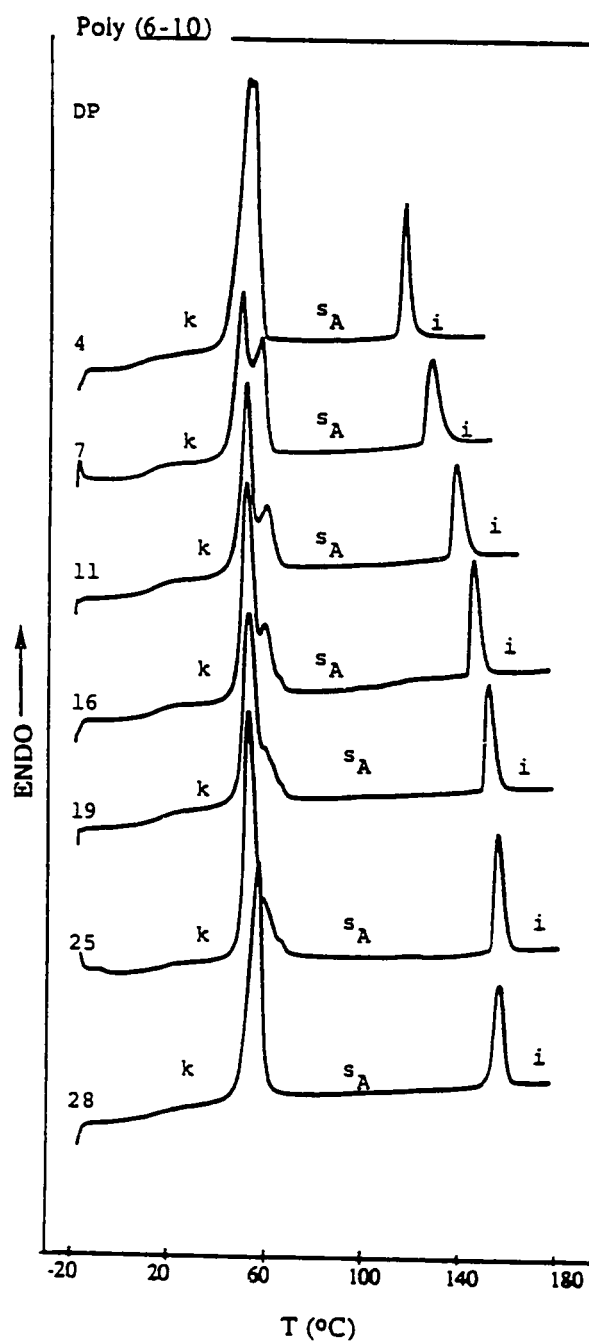


Figure 6a. DSC traces displayed during the first heating scan by poly(6-10) with different DP determined by GPC.

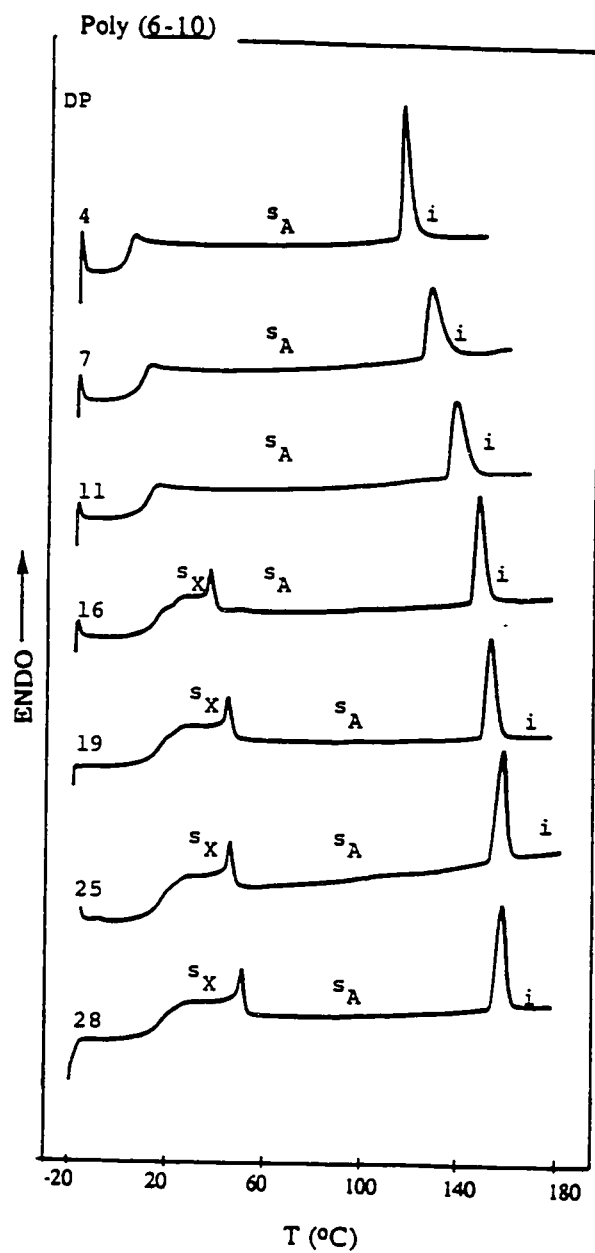


Figure 6b. DSC traces displayed during the second heating scan by poly(6-10) with different DP determined by GPC.

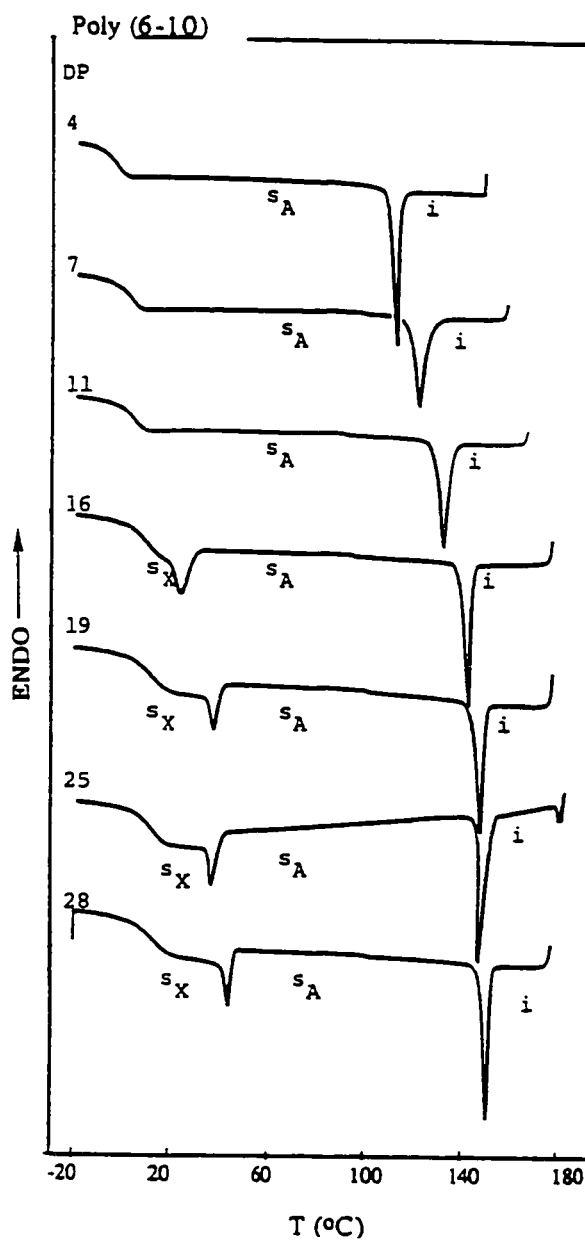


Figure 6c. DSC traces displayed during the first cooling scan by poly(6-10) with different DP determined by GPC.

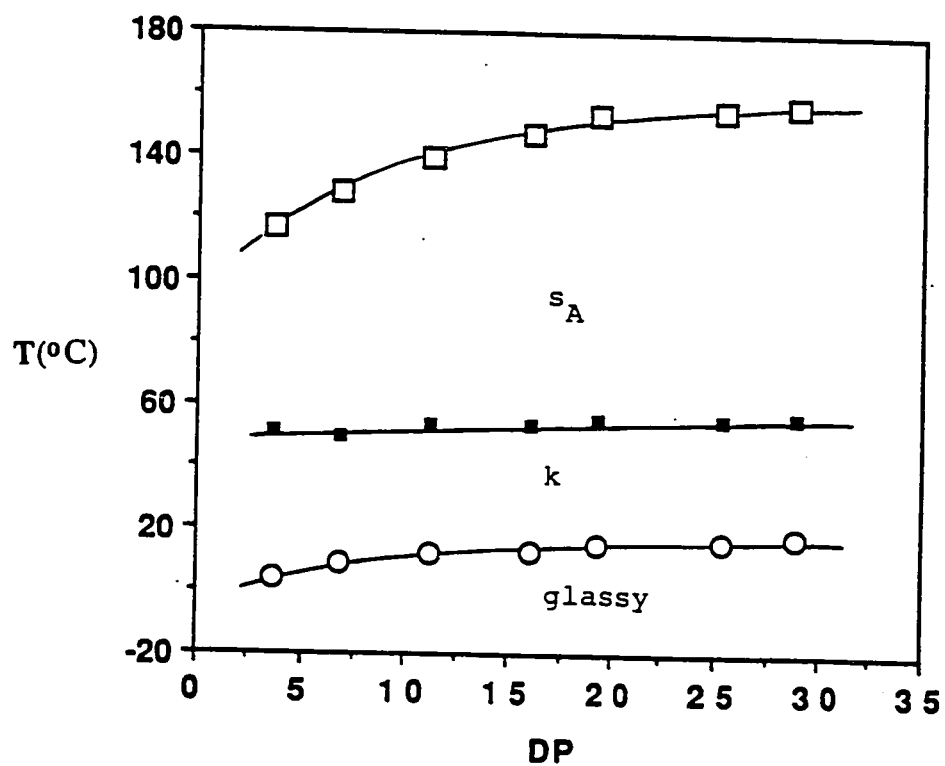


Figure 7a The dependence of phase transition temperatures on the degree of polymerization of poly(6-10) (data from the first heating scan): O- T_g ; ■- T_c - s_A ; □- T_{sA} -i

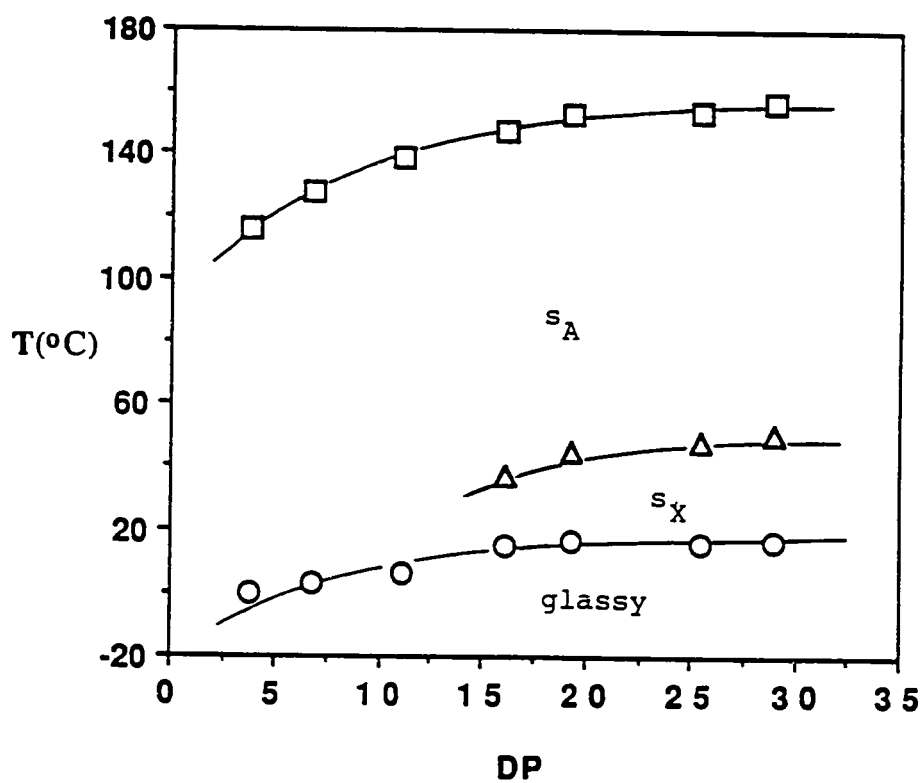


Figure 7b. The dependence of phase transition temperatures on the degree of polymerization of poly(6-10) (data from the second heating scan): O-Tg; Δ -Ts_{X-sA}; \square -Ts_{A-i}

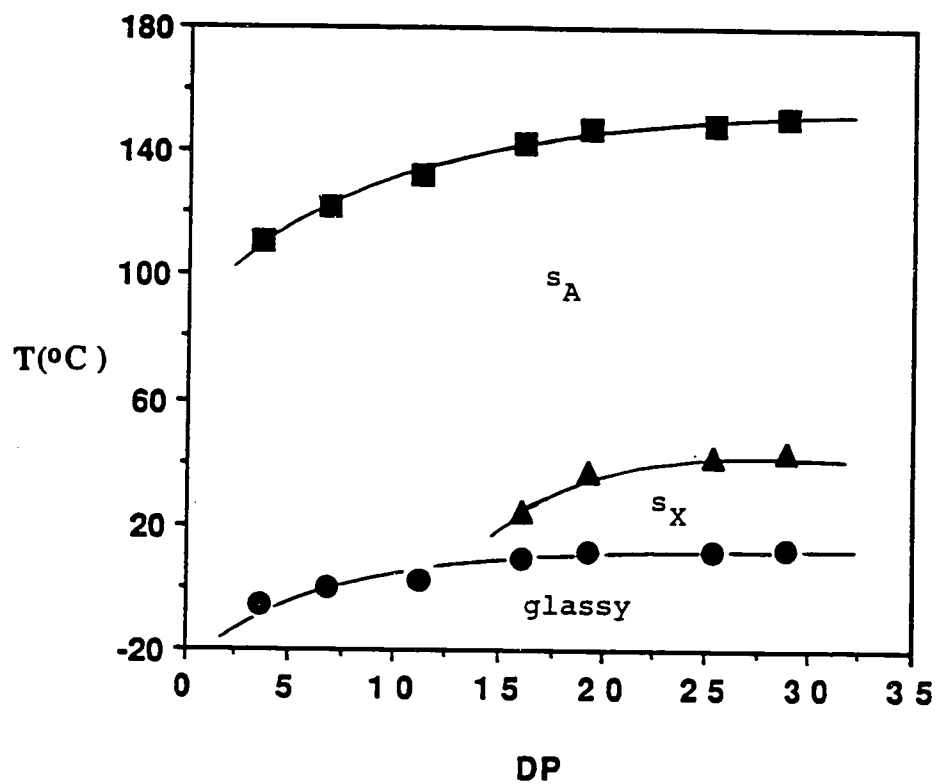


Figure 7c

The dependence of phase transition temperatures on the degree of polymerization of poly(6-10) (data from the first cooling scan): ■- T_{sA} ; ▲- T_{sX} ; ●- T_g .

on the basis of thermodynamic principles assuming that the phase behavior of the polymer is determined by that of the monomeric structural unit.^{11,12}

Figure 8a,b,c displays the first and second heating and the cooling DSC scans of poly(6-11). Poly(6-11) presents a mesomorphic behavior which resembles that of poly(6-10). In the first heating scan all polymers display a crystalline melting followed by a s_A phase (Figure 8a). In the second and subsequent heating scans only poly(6-11) with a degree of polymerization 3 presents a melting transition followed by a s_A phase. This statement is supported by the very small change in the heat capacity at the glass transition in the first versus second heating scans, by optical polarized microscopy observations, and by the difference between the temperature transition and the enthalpy change associated with the corresponding transition from the heating and cooling scans. Polymers with degrees of polymerization from 4 to 14 show only the s_A phase while polymers with higher degrees of polymerization display a s_X (i.e., an unidentified smectic phase) and a s_A mesophase (Figure 8b). On the cooling DSC scans (Figure 8c) we observe the crystallization peak only in the case of the lowest molecular weight polymer (degree of polymerization 3). The onset of the s_X phase formation from the cooling DSC scans can be observed only for the polymers with degrees of polymerization from 19 to 31. The formation of this s_X phase continues on the heating scan. The uncovering of the s_X phase is due to the very low rate of crystallization. Nevertheless, under proper annealing conditions all these polymers crystallize again. Consequently, under equilibrium conditions, the s_X phase of poly(6-11) is only monotropic. Therefore, the kinetically controlled crystallization process influences the relative thermodynamic stability of various mesophases. This effect was observed previously for other polymer samples.⁷ All these results are summarized in Table V.

Figure 9a plots the dependence between the various phase transition temperatures collected from the first and second heating scans and the degree of polymerization of poly(6-11). The data for the model compound of the monomeric structural unit, 8-11, which corresponds to a degree of polymerization equal to one, are also included. The thermal transition temperatures collected from the cooling scan are plotted in Figure 9b. Both the enlargement of the range of temperature of the s_A phase with the increase of the degree of polymerization, and the formation of the s_X mesophase above a certain degree of polymerization are in agreement with theoretical predictions.^{11,12} That is, the mesophase of the polymer is identical to that of the monomeric structural unit. This assumes that the monomeric unit should also display a virtual s_A mesophase.

It is generally accepted¹ that the polymerization of a mesogenic monomer which displays a nematic mesophase frequently leads to a polymer which displays a smectic mesophase. This is the case with the monomer 6-11 which displays a monotropic nematic and a monotropic s_A mesophase while poly(6-11) exhibits only a s_A mesophase. However, as previously mentioned⁷ we believe that it is correct to compare the mesophase displayed by polymer only with the mesophase displayed by the model compound which corresponds to the monomeric structural unit. Under these circumstances, both the model of the monomeric structural unit 8-11 and the poly(6-11) display an enantiotropic s_A mesophase. Several representative textures displayed by the s_A and s_X mesophases of poly(6-11) are presented in Figure 10.

In conclusion, the results described in this chapter demonstrate that the mesogenic vinyl ethers can be polymerized under living condition and provide a systematic investigation on the molecular weight effect on the phase behavior of side chain liquid crystalline polymers. With an increase of molecular weight from

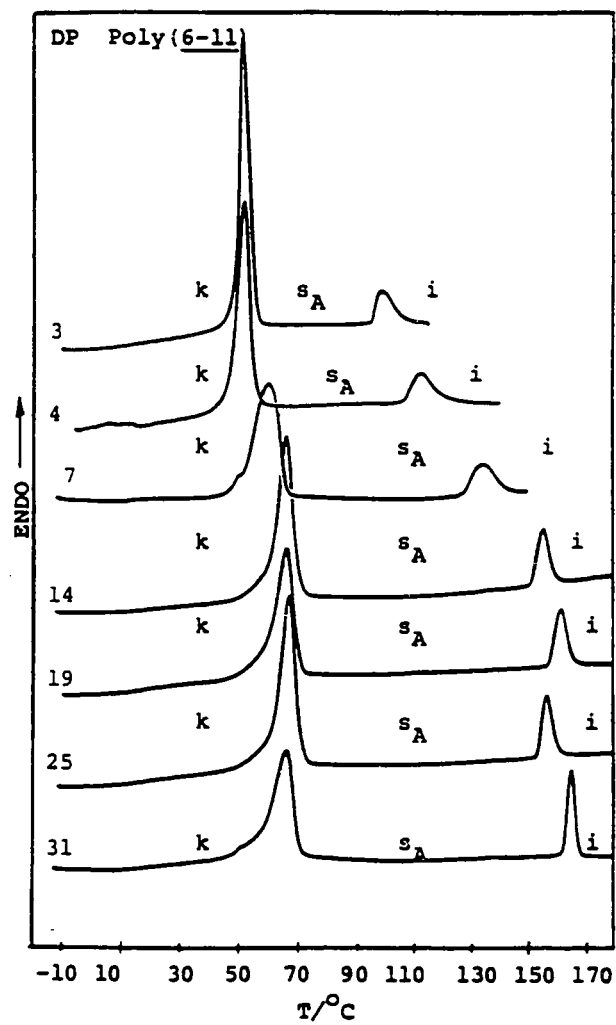


Figure 8a. DSC traces displayed during the first heating scan by poly(6-11) with different DP.

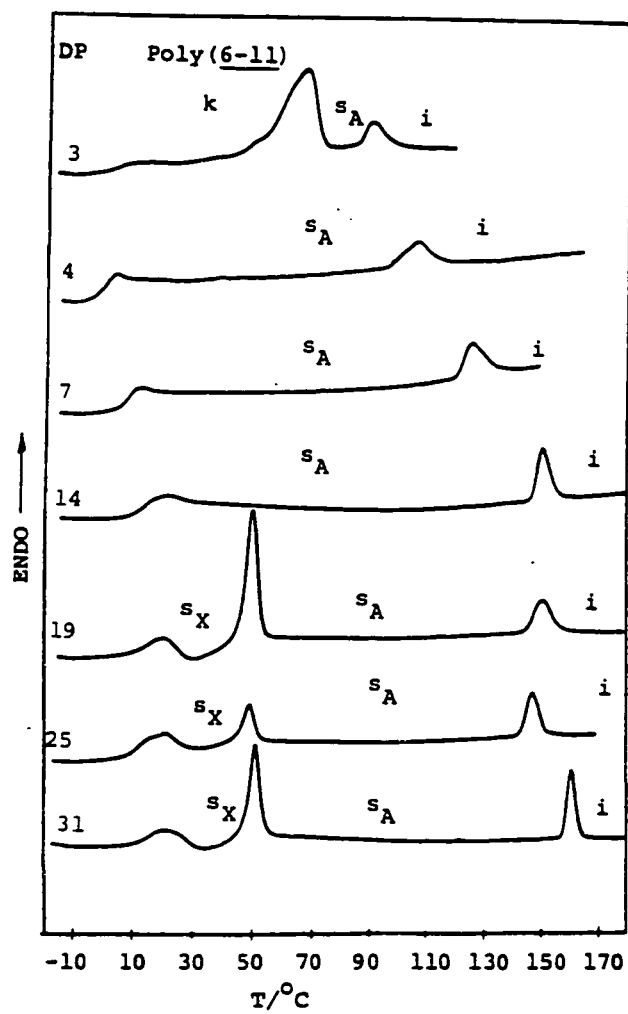


Figure 8b. DSC traces displayed during the second heating scan by poly(6-11) with different DP.

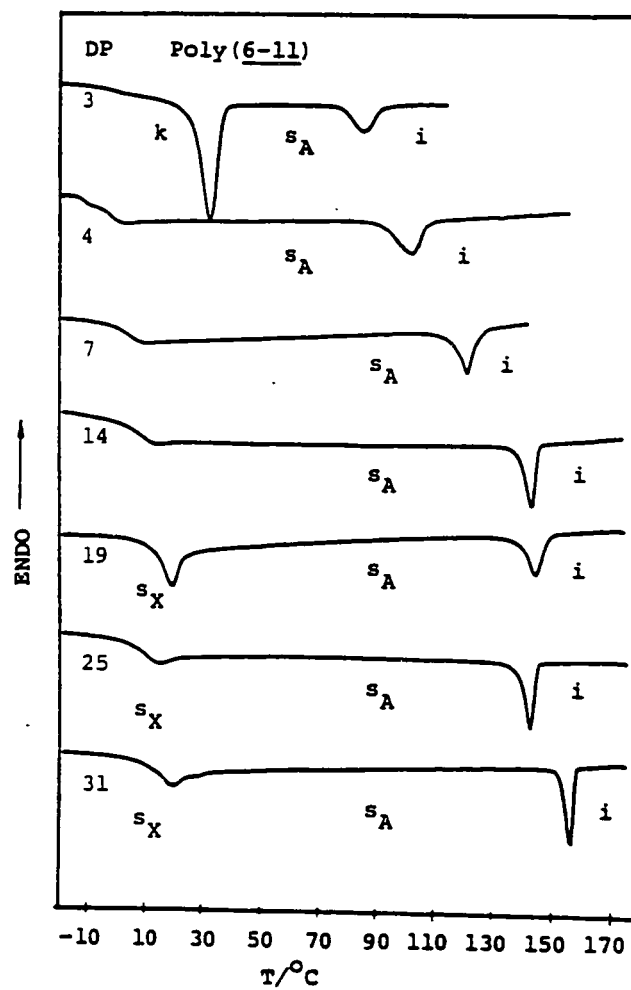


Figure 8c. DSC traces displayed during the first cooling scan by poly(6-11) with different DP.

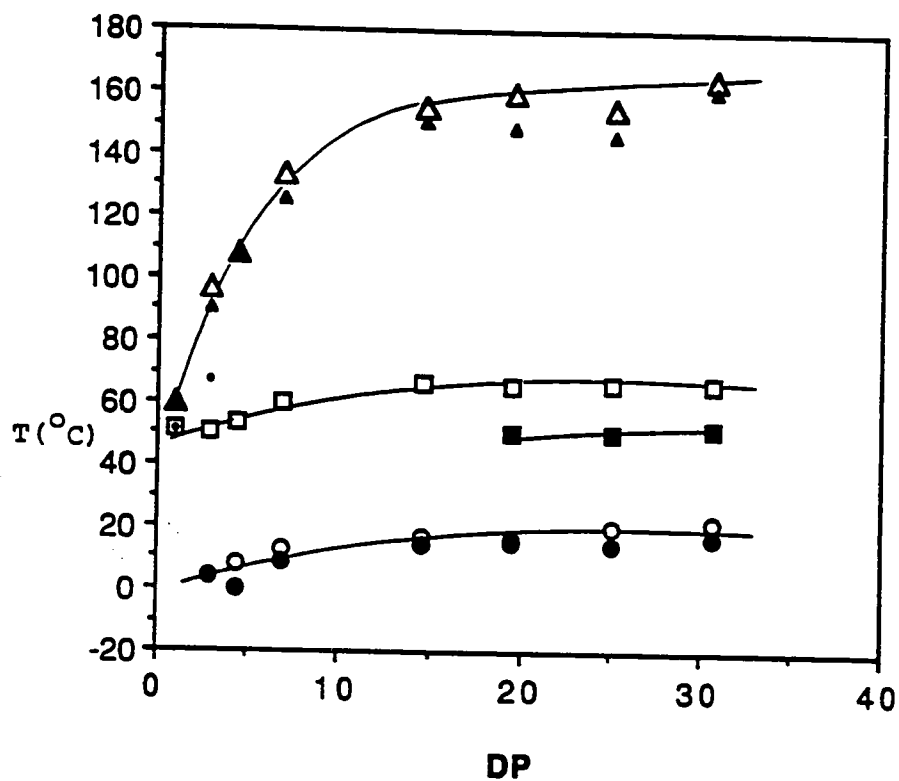


Figure 9a. The dependence of phase transition temperatures on the degree of polymerization of poly(6-11). DP=1 corresponds to 8-11. (data from first heating) (fh) and (second heating scans) (sh) are presented in Figure 8a. \square - $T_{k-sA}(fh)$; \circ - $T_g(fh)$; Δ - $T_{sA-i}(fh)$; \bullet - $T_{k-sA}(sh)$; \bullet - $T_g(sh)$; \blacksquare - $T_{sX-sA}(sh)$; \blacktriangle - $T_{sA-i}(sh)$.

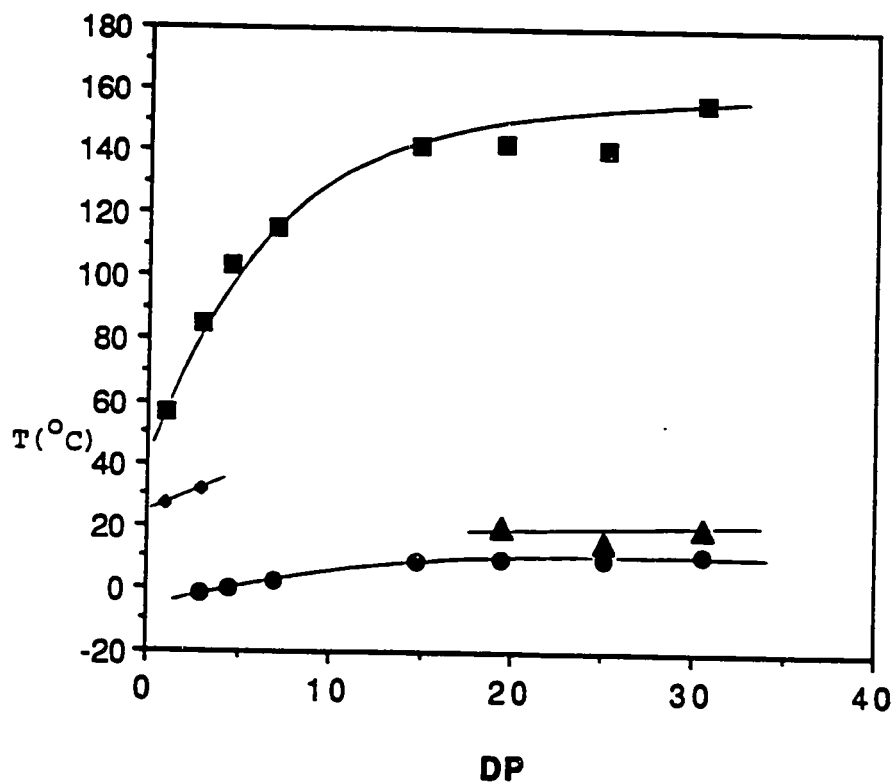


Figure 9b. The dependence of phase transition temperatures on the degree of polymerization of poly(6-11). DP=1 corresponds to 8-11. (data from the cooling scan). ■-Ti-sA; ♦-TsA-k; ▲-TsA-sX; ●-Tg.

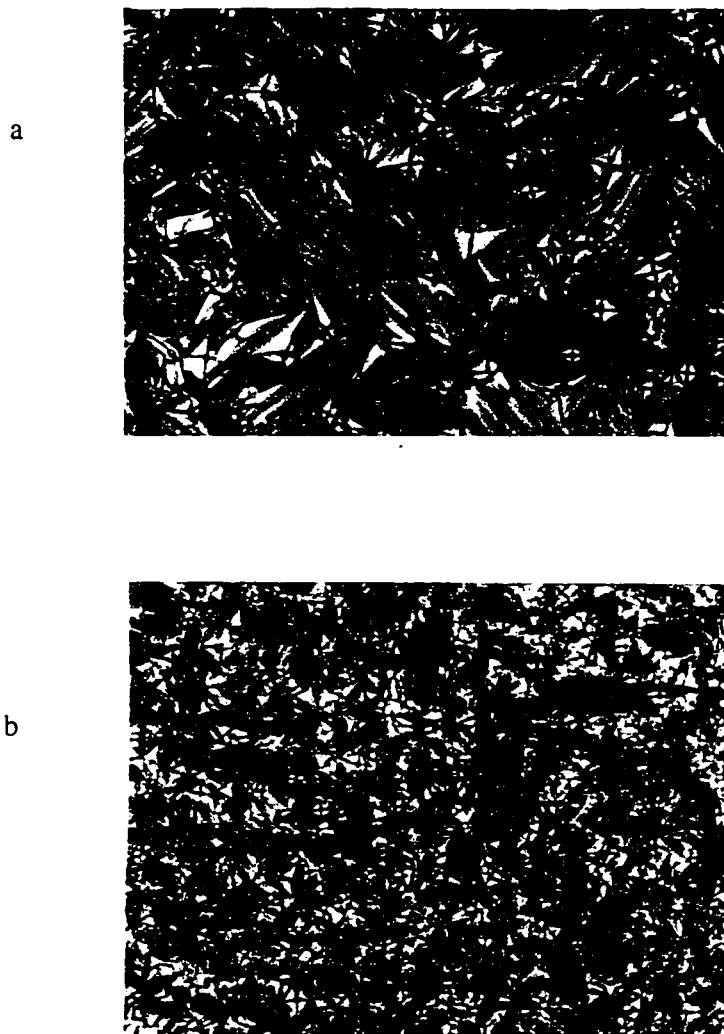


Figure 10. Representative optical polarized micrographs (100x) of poly(6-11) with DP=31: a) the s_A displayed at 148°C; b) the s_X displayed at 30°C.

monomeric structural unit, a monotropic mesophase transforms into an enantiotropic one in case of poly(6-10) and the range of temperature of the s_A phase enlarges in case of poly(6-11). In addition, both poly(6-10) and poly(6-11) exhibit s_X phase above certain molecular weight.

REFERENCES

1. V. Percec and C. Pugh, in "Side Chain Liquid Crystal Polymers", McArdle, C. B. Ed., Chapman and Hall, New York, 1989, p. 30 and references cited therein
2. S. G. Kostromin, R. V. Talroze, V. P. Shibaev and N. A. Plate, *Makromol. Chem., Rapid Commun.*, **3**, 803 (1982)
3. H. Stevens, G. Rehage and H. Finkelmann, *Macromolecules*, **17**, 851 (1984)
4. V. Shibaev, *Mol. Cryst. Liq. Cryst.*, **155**, 189 (1988)
5. S. Uchida, K. Morita, K. Miyoshi, K. Hashimoto and K. Kawasaki, *Mol. Cryst. Liq. Cryst.*, **155**, 93 (1988)
6. V. Percec and B. Hahn, *Macromolecules*, **22**, 1588 (1989)
7. V. Percec, D. Tomazos and C. Pugh, *Macromolecules*, **22**, 3259 (1989)
8. T. Sagane and R. W. Lenz, *Polym. J.*, **20**, 923 (1988)
9. T. Sagane and R. W. Lenz, *Polymer*, **30**, 2269 (1989)
10. T. Sagane and R. W. Lenz, *Macromolecules*, **22**, 3763 (1989)
11. V. Percec and A. Keller, *Macromolecules*, **23**, 4347 (1990)
12. A. Keller, G. Ungar and V. Percec, in "Advances in Liquid Crystalline Polymers", C. K. Ober and R. A. Weiss, Eds., ACS Symposium Series 435; Washington D.C., p.308 (1990)
13. J. M. Rodriguez-Parada and V. Percec, *J. Polym. Sci.:Part A: Polym. Chem.*, **24**, 1363 (1986)
14. R. Rodenhouse, V. Percec and A. E. Feiring, *J. Polym. Sci: Part C:Polym. Lett.*, **28**, 345 (1990)
15. J. Adams and W. Gronski, *Makromol. Chem., Rapid Commun.*, **10**, 553(1989)
16. J. E. McKeon and P. Fitton, *Tetrahedron*, **28**, 233 (1972)
17. C. S. Hsu, J. M. Rodriguez-Parada and V. Percec, *J. Polym. Sci. Part A:Polym. Chem.*, **25**, 2425 (1987)
18. G. W. Gray, H. J. Harrison, J. A. Nash, J. Constant, D. S. Hulme, J. Kirton and E. P. Raynes, in "Ordered Fluids and Liquid Crystals", Vol. II, R. S. Porter and J. F. Johnson, Eds., Plenum, New York, 1974, p.617
19. J. E. McKeon, P. Fitton and A. A. Griswold, *Tetrahedron*, **28**, 227 (1972)

20. V. Percec and D. Tomazos, *Polym. Bull.*, **18**, 239 (1987)
21. T. Higashimura, S. Aoshima and M. Sawamoto, *Makromol. Chem., Macromol. Symp.*, **13/14**, 457 (1988)
22. M. Sawamoto, S. Aoshima and T. Higashimura, *Makromol. Chem., Macromol. Symp.*, **13/14**, 513 (1988)
23. T. Higashimura and M. Sawamoto, in "Comprehensive Polymer Science", Vol.3, G. Allen and J. Bevington Eds., Pergamon Press, Oxford, 1989, p.684
24. C. G. Cho, B. A. Feit and O. W. Webster, *Macromolecules*, **23**, 1918 (1990)

Chapter 3
STRUCTURAL REARRANGEMENTS DURING MESOMORPHIC PHASE
TRANSITIONS IN POLY{10-[4-CYANO-4'-BIPHENYL)OXY]DECANYL VINYL
ETHER}

3.1.-INTRODUCTION

Poly{10-[(4-cyano-4'-biphenyl)oxy]decanyl vinyl ether}[poly(6-10)] with degrees of polymerization higher than 16 exhibits an unidentified smectic mesophase followed by an enantiotropic smectic A mesophase as described in previous chapter. In order to provide a complete elucidation of the phase behavior of poly(6-10), we must understand the structural arrangement of the polymer side groups in its different liquid crystalline states.

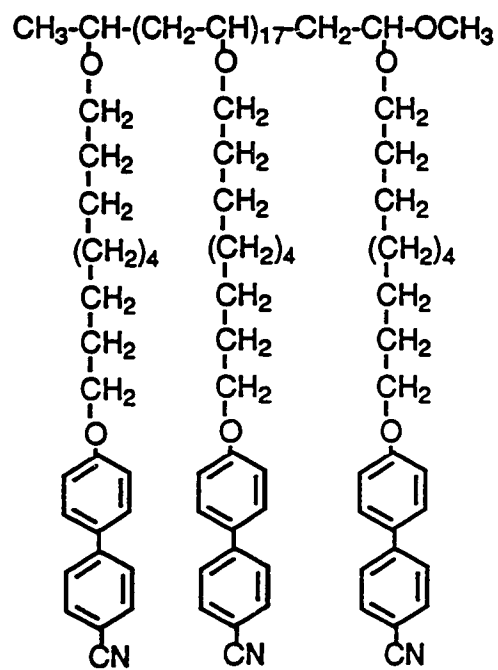
This chapter discusses the phase behavior and the structural rearrangements of the layer and intralayer ordering during the phase transitions between the liquid crystalline states of poly(6-10) with a degree of polymerization of 19.

3.2.-EXPERIMENTAL

3.2.1.-Materials

The synthesis of 10-[(4-cyano-4'-biphenyl)oxy]decanyl vinyl ether (6-10), its living cationic polymerization initiated with $\text{CF}_3\text{SO}_3\text{H}/\text{S}(\text{CH}_3)_2$ in CH_2Cl_2 at 0°C and the characterization of the resulted polymers were presented in Chapter 2. Table 1 summerizes the polymerization results. The structure of this polymer is shown in Scheme I.

3.2.2-Techniques



Scheme I. The structure of poly{ 10-[(4-cyano-4'-biphenyl)oxy]decanyl vinyl ether} poly(6-10)

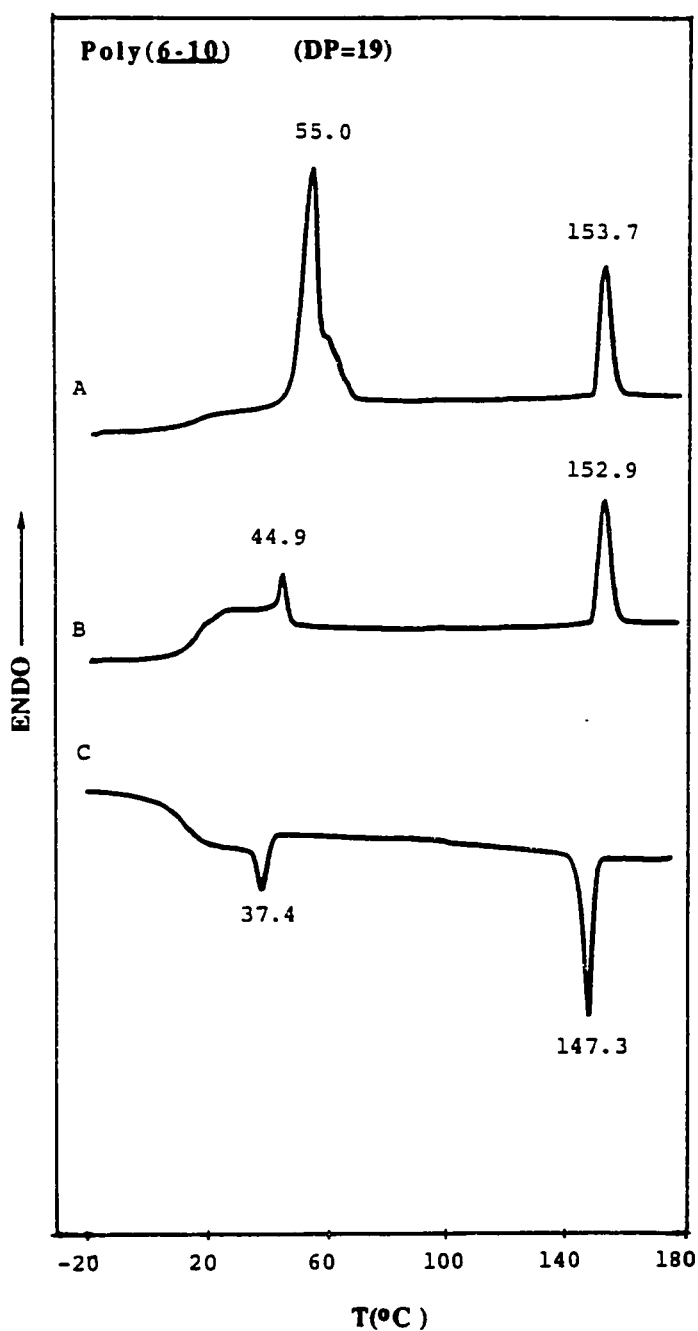


Figure 1. Heating and cooling DSC traces (20 $^{\circ}\text{C}/\text{min}$) of poly(6-10) with DP=19: A) first heating scan; B) second and subsequent heating scan; C) first and subsequent cooling scan.

Table I. Cationic Polymerization of 6-10 and Characterization of the Resulting Polymer

[M] ₀ /[I] ₀	Mn×10 ⁻³	Mw/Mn (GPC)	DP	phase transitions (°C) and corresponding enthalpy changes	
				heating	cooling
20	7.3	1.14	19	g 15.5 k 55.0 (2.39) s _A 153.7 i 147.3 (0.72) s _A 37.4 (0.76) i g 16.2 s _X 44.9 (0.68) s _A 152.9 (0.74) i	(0.80) s _X 11.8 g

Before the X-ray experiments, the polymer sample was heated to isotropic temperature then was cooled very slow to the liquid crystalline state during 10 hours and then was annealed at 35°C during 1 day . The oriented sample was obtained by very slow step-by-step cooling from the isotropic state to 35°C during 1 week in a magnetic field of 1 T. X-ray wide-angle scattering (WAXS) curves were recorded on a Siemens D-500 diffractometer. Small-angle X-ray scattering (SAXS) curves were obtained on a compact Kratky camera with positional detector. X-ray photo-patterns on oriented sample were obtained on flat cameras with different distances from the sample-film. In all cases a Ni-filtered $\text{CuK}\alpha$ radiation was used. Before the measurements the sample was kept at the desired temperature for at least 1 hour. The accuracy of the temperature of the thermostated sample was about $\pm 1^\circ$

The analysis of the SAXS data was made by using the programs FFSAXS. This program includes the smoothing of the data by cubic polynoms, the subtraction of the background and calculation of the one-dimensional correlation functions $G(x)$ by cosine-Fourier transform of the Lorenz corrected data. The analysis of the WAXS data was performed by using the program FIT which includes the smoothing of the data by splines, the subtraction of the diffuse background and the fit the observed maxima by various scattering functions. Additional experimental details on the characterization by WAXS and SAXS and on the processing of the results were presented elsewhere.¹

The spatial arrangement and the geometric sizes of the molecular fragments was analyzed for two conjugated monomeric units by the modeling program INSIGHT and the most favourable conformation was calculated by using the program DISCOVER.

3.3.-RESULTS AND DISCUSSION

A poly(6-10) with degree of polymerization equal to 19 and $M_w/M_n=1.14$ was used in all investigations. The DSC thermograms of this polymer are shown in Figure 1. Both in the heating and cooling scans, the low temperature unidentified smectic phase is separated from the high temperature smectic A phase by a first order transition (Figure 1). On the optical polarized microscope, the high temperature mesophase exhibits a focal conic texture which is characteristic to a smectic A phase, while the low temperature phase shows a broken focal conic texture. To elucidate the possible structure and the nature of mesomorphic transition between these two phases, first the structure of the low-temperature phase and the parameters of structural packing in the smectic A phase were determined. Later we will discuss the corresponding structural rearrangements during this phase transition.

3.3.1.-Low Temperature Smectic Phase

On the WAXS curves obtained at low temperatures two different sets of scattering peaks were observed: two very strong sharp peaks at 2.6° and 5.2° overlapped with a diffuse halo at $6-7^\circ$ and a modulated broad peak consisting of some overlapped maxima in the range of 20° (Figure 2). On the corresponding SAXS curves these two sharp peaks are visible more clear and an additional diffuse halo around 1° is also detected (Figure 3). The d-spacings of these X-ray data were calculated according to the Bragg's law and are presented in Table 2.

In the X-ray patterns of the polymer oriented in the magnetic field one can observe a meridional arrangement of the SAXS reflexions while all three sharp WAXS reflexions are concentrated in the very spreaded equatorial arcs (Figures 2 and 3).

The presence on the WAXS curves of three overlapped peaks points out to the formation of ordered intralayered packing of the mesogenic groups in low-temperature

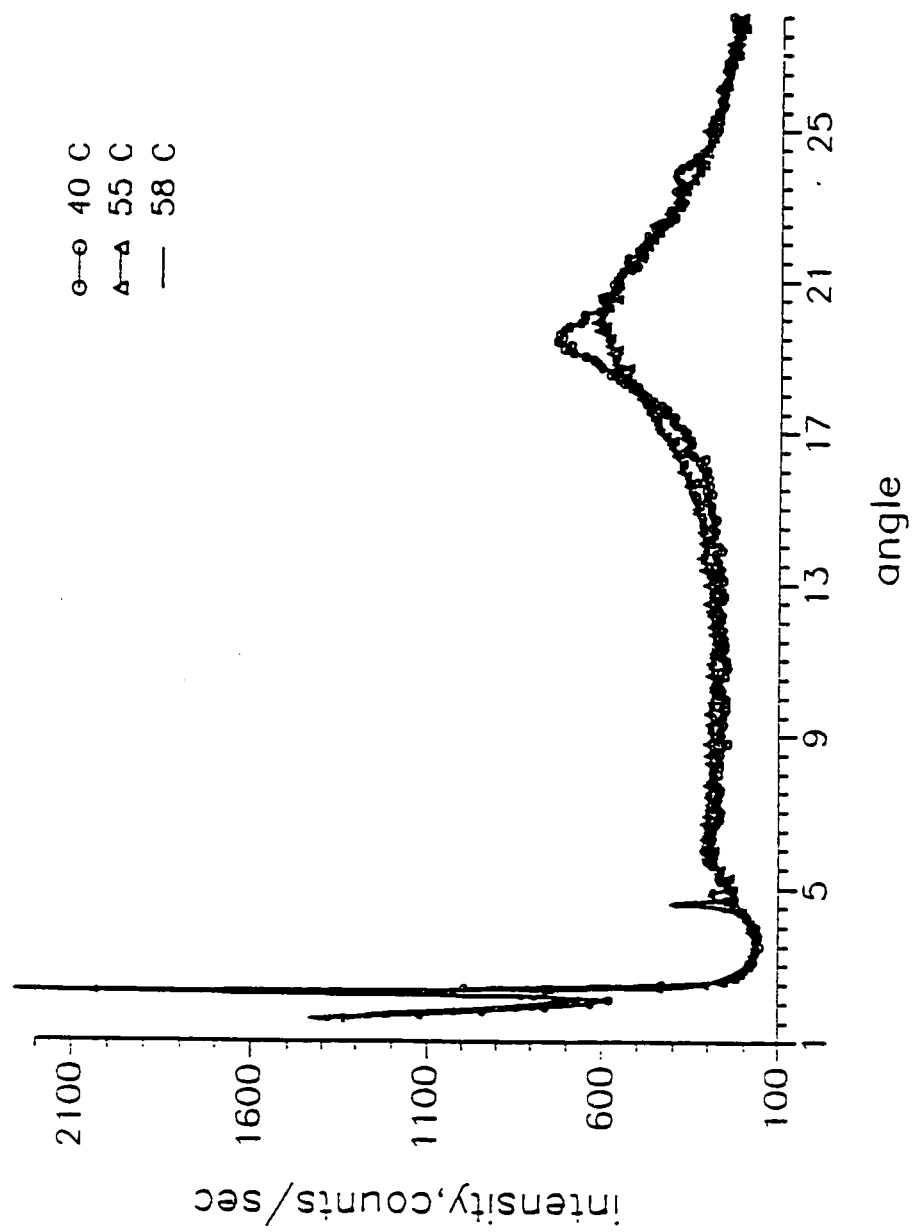


Figure 2. Wide-angle-X-ray scattering curves of poly(6-10) at different temperatures.

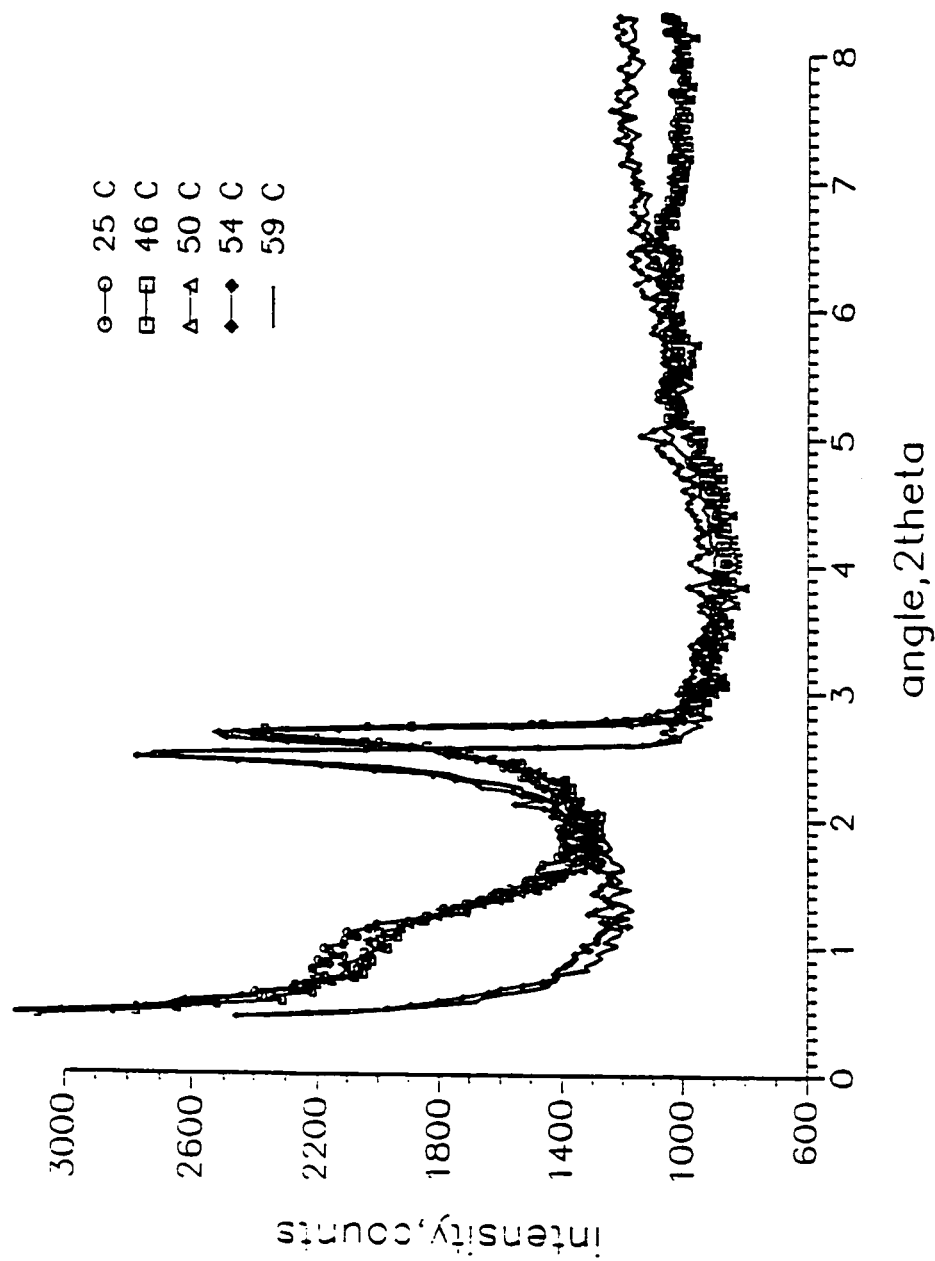


Figure 3. Small angle X-ray scattering curves of poly(6-10) at different temperatures.

Table II. Structural characteristic of poly(6-10)

	Temperature (°C)	d-spacings (nm)									
		1	2	3	4	5	6	7	ξ	ξ_{\perp}	
LC I											
state	25, cooled		3.17	1.59					45		
	25, annealed 2 hr	8.8 w	3.33	1.63	1.3 w	0.454				0.5	
	25, annealed 1 day	8.8 w	3.36	1.65	1.3 w	0.457	0.41	0.374	35	1.4	
LC II											
state	59		3.52	1.76	1.2 w	0.45			>100	0.4	

the accuracy of d-spacings in SAXS region is 0.5 nm for sharp peaks and 0.1 nm for weak ones;
in WAXS region the accuracy is 0.005 nm; w-weak intensity

smectic phase. The WAXS maximum was splitted in three sharp maxima of a Lorentz shape with half-widths of about 2° (Table 2, Figure 4). The absolute values of the intralayered correlation lengths ξ_{\perp} are in the range of 1.4 nm. This value is much higher than the typical values for disordered smectic phases (0.3-0.6 nm) but slightly lower than the typical ones observed for an ordered smectic phase in side chain liquid crystalline polymers¹⁻³. The correlations in the intralayered ordering ($L \approx 3-4 \xi_{\parallel}$) are expanded to 5-6 nm. Thus the regions with ordered intralayered packing include more than one hundred mesogenic groups which corresponds to the existence of a two dimensional lattice. As judged from the X-ray patterns, the mesogenic side groups are oriented along the direction of the magnetic field (Figures 2 and 3) and are arranged into layers orthogonally to the smectic plane.

The presence in WAXS angular region of the three sharp peaks orthogonally arranged according to the SAXS layered reflections is typical for a smectic E phase with orthorhombic symmetry of the two dimensional lattice^{3,4}. The position of all reflexes are indexed quite well as the 020, 100 and 110 reflections of the orthorhombic unit cell with the parameters: $a=0.4$ nm, $b=0.914$ nm and $c=3.36$ nm. Such a lattice is formed by the herringbone packed mesogenic groups with two different orientations of their short axes in the layered planes.^{2,3} Thus from the analysis of all available data we can conclude that the phase from the low temperature is a smectic E phase with two-dimensional intralayered packing of orthorhombic symmetry.^{4,5}

Let us consider the perfection of the one-dimensional ordering and the possible models of longitudinal packing of the macromolecular fragments in this phase. In order to characterize the perfection of the one-dimensional order we calculated the one-dimensional correlation function $G(x)$ (Figure 5). The $G(x)$ is common for lamellar phases of damping oscillations with a main period of 6.6 nm. The value of the

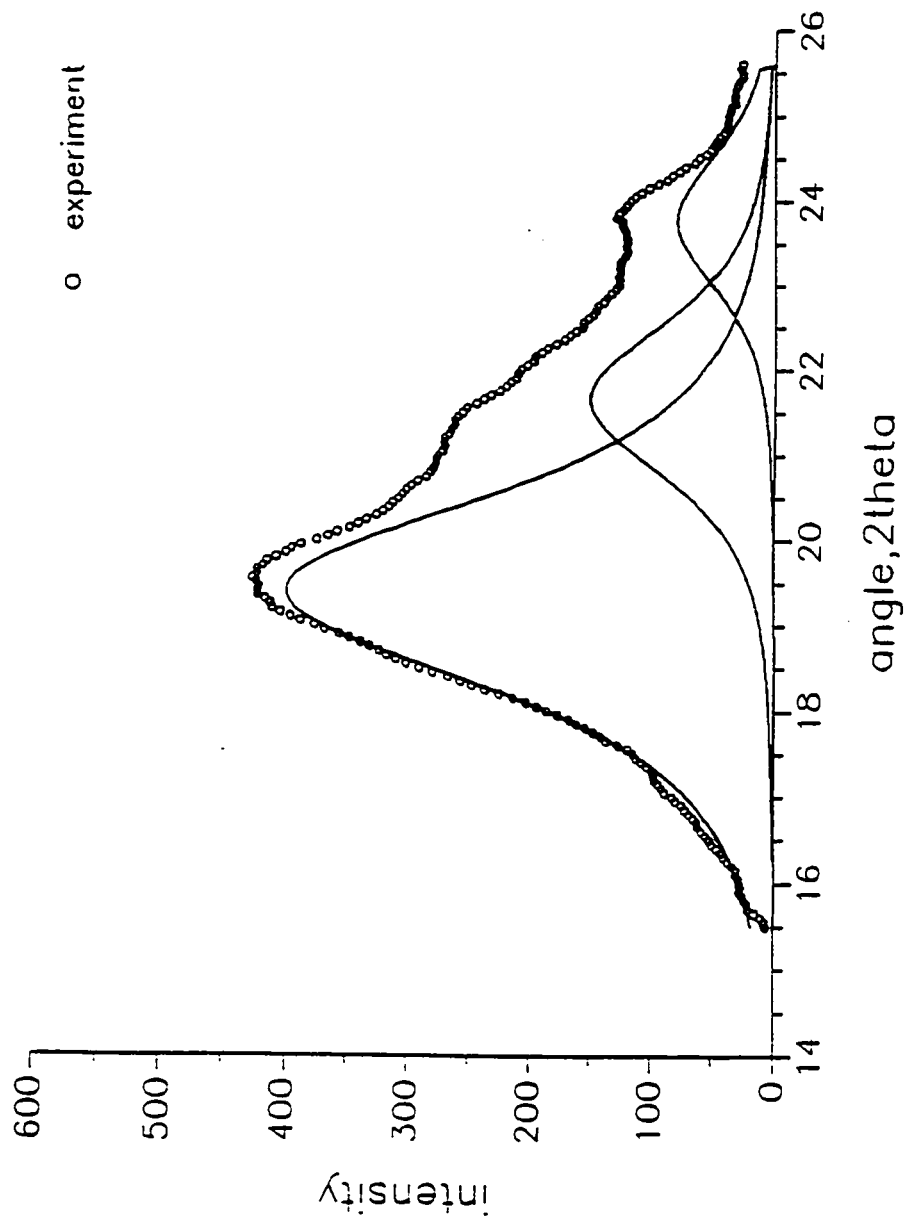


Figure 4. Split of the WAXS for the smectic E phase of poly(6-10) by Lorentz profiles.

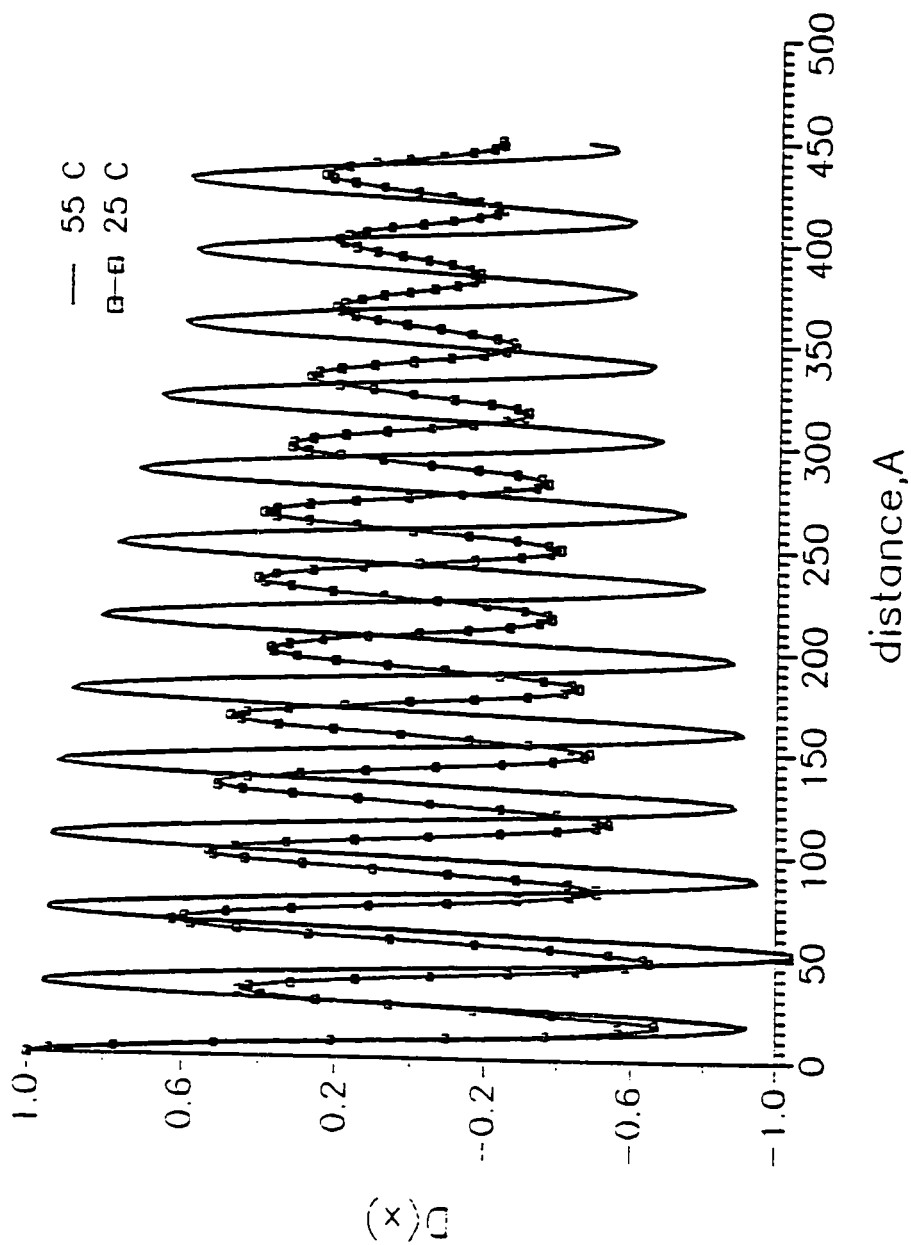


Figure 5a. One-dimensional correlation functions $G(x)$ of poly(6-10) in the smectic E and smectic A phases

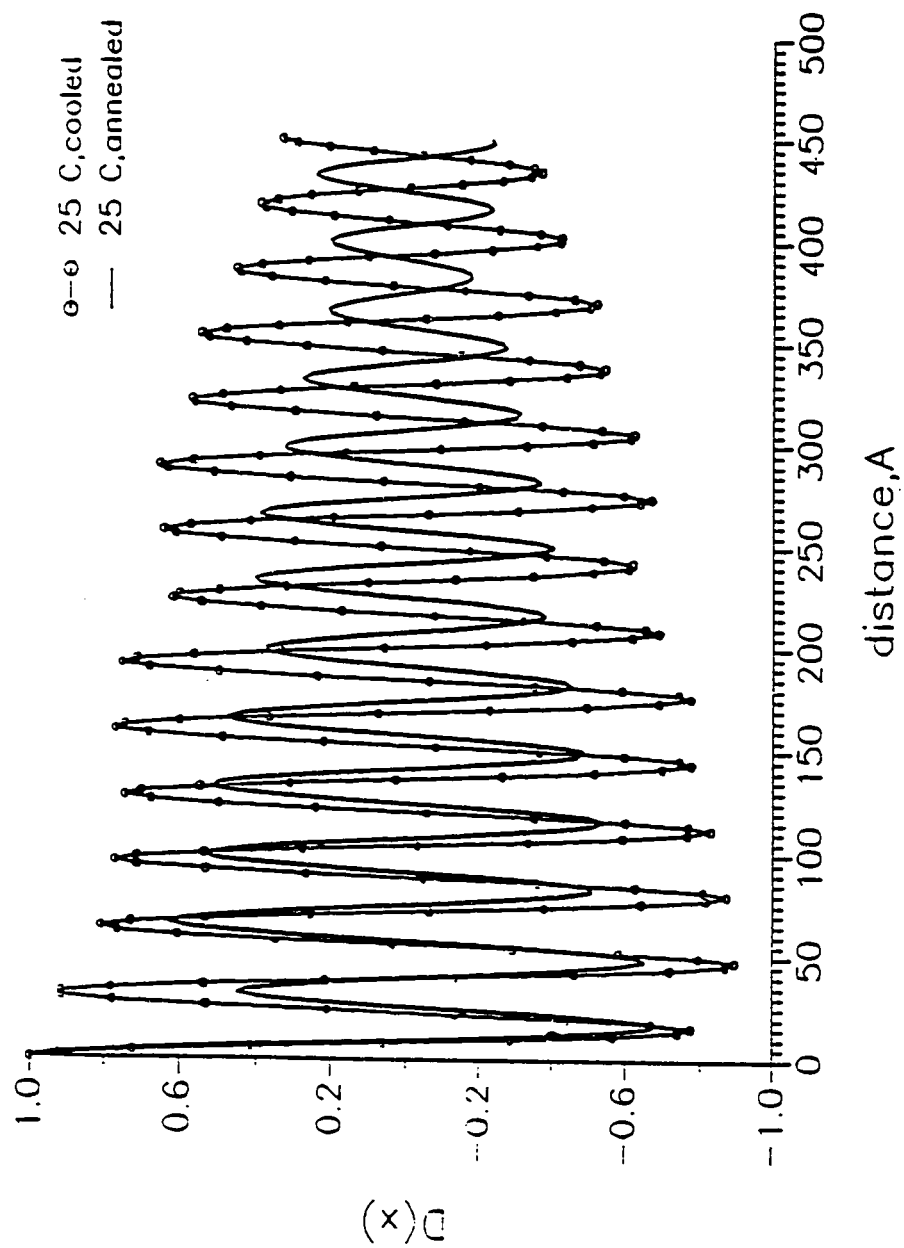


Figure 5b. One-dimensional correlation functions $G(x)$ of poly(6-10) in the smectic E phase after cooling and annealing

longitudinal correlation length $\xi_{||}$ calculated from $G(x)$ ¹ is equal to 35 nm. This value is also typical for smectic ordered phases of side-chain polymers with a high concentration of defects formed by the coil-like flexible backbones.^{1,2}

As deduced from the highest intensity of the second maximum of $G(x)$, the main period of density distribution which corresponds to the thickness of the layers is equal to 6.6nm. Such a periodicity fits quite well to the common double-layered structures of the cyano-containing mesogenic groups with partial overlapping of the side fragments (Figure 6). As judged from conformational calculations, the cyano biphenyl mesogenic groups are arranged at definite angle according to the orthogonal direction of the methylene spacer as shown in Figure 4, and in the framework of the proposed packing they are fully overlapped. The main periodicity of 6.6 nm is determined by the distance between the backbones arranged in the same plane (Figure 6). This distance is twice higher than the d-spacing calculated from the position of the first SAXS peak (Table 2). We also observe an additional maximum at 3.3 nm which points out to the existence of an additional half-period density wave. This situation is very similar to that discussed in details for other ordered side-chain smectic polymers¹⁻³ and demonstrates the existence of an additional periodicity normal to the smectic planes between dense packed mesogenic groups of the neighboring molecules (Figure 7). As it is well known for layered structures, the existence of such additional half-periods in density distribution leads to the extinction of the odd orders of reflections^{4,5}. Thus for the layered packing of the polymer studied, the first order of the reflection with $d=6.6\text{nm}$ should be extincted and the observed SAXS peaks are 2 and 4 orders of reflections of the proposed double-layered packing. Thus from this discussion we can conclude that the low-temperature phase in this polymer is a smectic E phase with

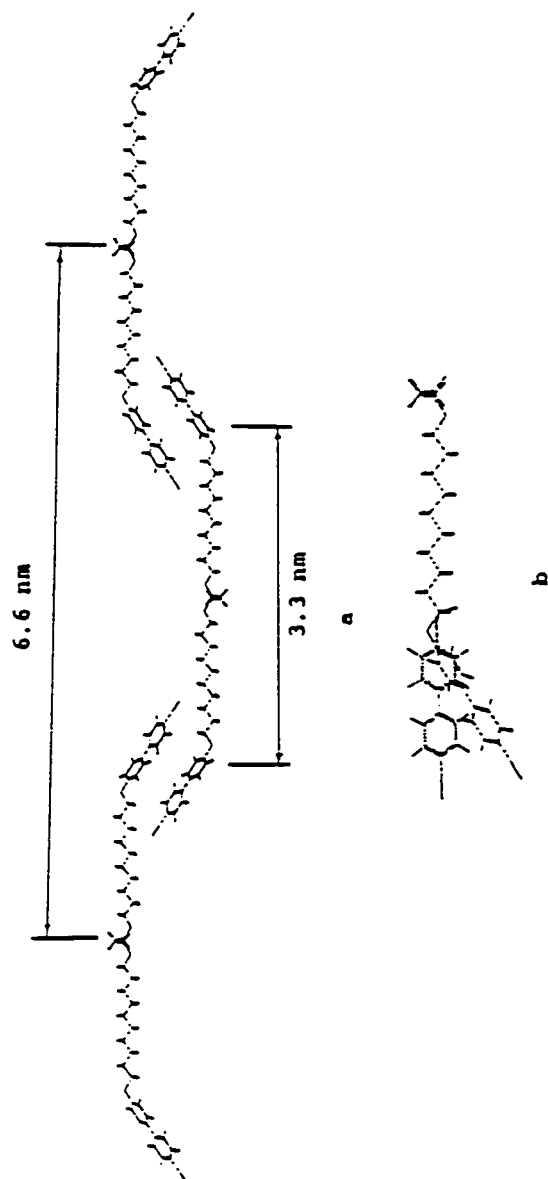


Figure 6. Molecular models of the liquid crystalline poly(6-10): (a) model of double-layered packing with overlapping of the mesogenic groups (main periodicity and half periodicity are shown), (b) possible changes of the arrangement of the biphenyl mesogenic groups as a result of torsional rotation.

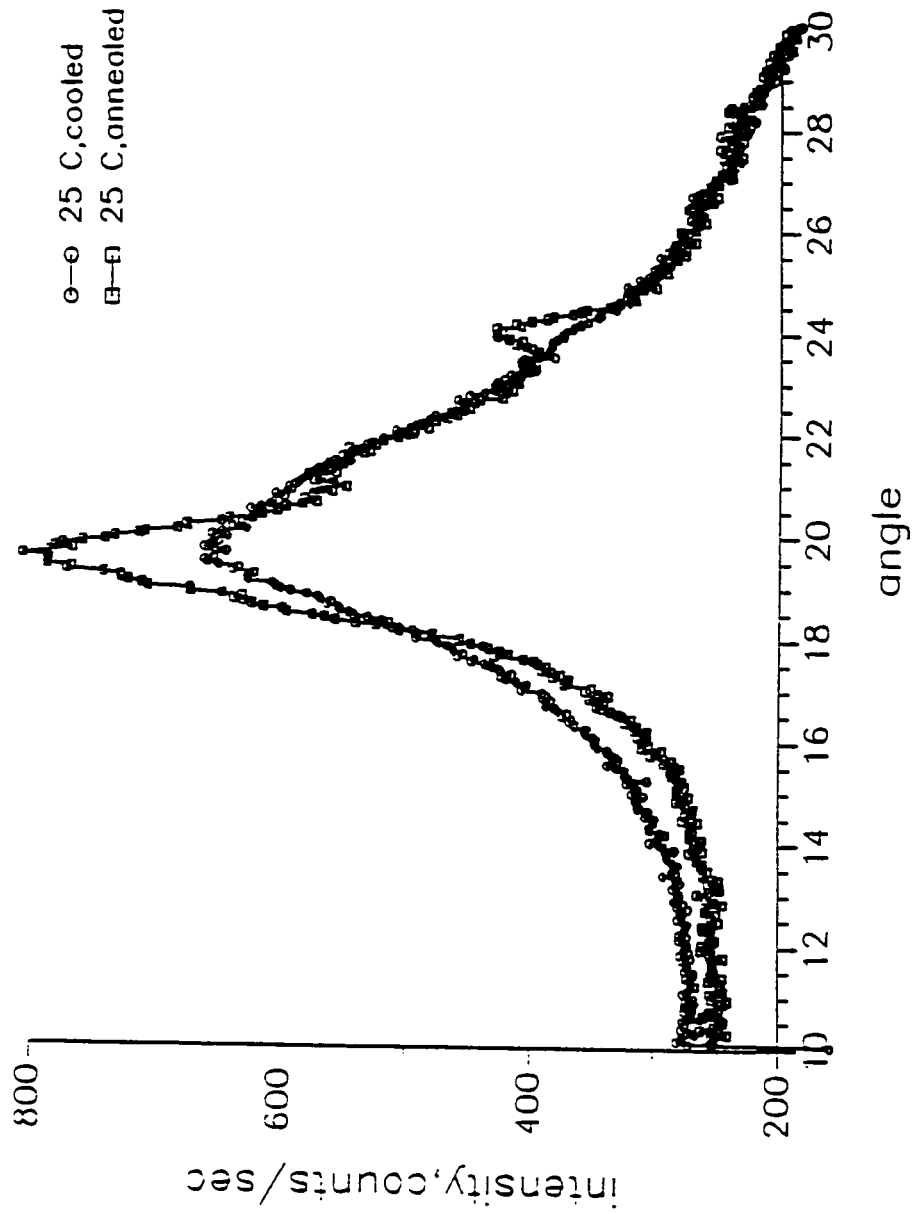


Figure 7. Wide-angle X-ray scattering curves of poly(6-10) at 35°C after cooling and annealing during 1 day.

orthorhombic intralayered order and double-layered longitudinal packing and with overlapped cyanobiphenyl mesogenic groups in the side chains.

3.3.2.-High-Temperature Smectic Phase

As was mentioned above the high-temperature phase in this polymer is most probably the common disordered smectic A phase.⁴ From the obtained data we can conclude that the well defined layered structure is maintained in this phase only with a slightly changed periodicity and liquid-like quasi-hexagonal ordering into layers (Figure 2,3). As a result of the two dimensional melting of the intralayered lattice only a short-range order is detected in this phase. The short-range order in the intralayered packing of the mesogenic groups is expanded only on $L=1-2$ nm which is typical for a smectic A mesophase. The thickness of layers of 7 nm is only slightly higher as compared to the initial double-layered packing. The perfection of the one-dimensional order in the smectic A phase is much higher as compared to the ordered smectic E phase. The value of the longitudinal correlation lengths $\xi_{||}$ is resolution limited and is not lower than 100 nm (Figure 5).

Thus the high temperature phase in this liquid crystalline polymer is a common disordered smectic A phase with interdigitated double-layered packing, long range longitudinal ordering and short-range order into layers. It is obvious from the comparison of the structural data of these two phases that during the phase transformation smectic E-smectic A, different changes of the structural ordering are observed such as: melting of the intralayered ordering, change of the thickness of the layered packing and the disappearance of the SAXS diffused halo. All these structural changes will be discussed in the next subchapter.

3.3.4.-Structural Changes Observed During the Cycle: Heating-Cooling-Annealing Intralayered Packing

The heating of the polymer up to T_1 leads only to minor changes of the WAXS scattering while an increase of temperature to above T_1 provides the appearance of the diffuse halo (Figure 2). These changes of WAXS scattering occur in a very narrow temperature interval (2-4°) near T_1 and correspond to the so called two dimensional-melting of the intralayer packing during the transition from the ordered to the disordered smectic phase.^{1,2} The orthorombic symmetry of the intralayer packing of the smectic E phase is broken and a common quasi-hexagonal short-range order is formed. The corresponding intralayer correlation length drops abruptly about 3-4 times (from 1.4 to 0.4 nm).

During the cooling of the high-temperature phase, the phase transformation occurs at $T_1=37^\circ$ (according to the DSC data with rate of 20 °C/min). But on the WAXS curve this phase transition occurs during 2 hours at room temperature. After the sample was slowly cooled at 35 °C for 10 hr the initial overlapped sharp peaks are restored and the ordered intralayered ordering which characterizes the smectic E phase is formed. Consequently, as a result of cooling from smectic A state in a glassy state we have generated a metastable structure with liquid-like intralayered order coexisting with the partially transformed ordered phase. This metastable structure could be transformed into the initial ordered smectic E state by prolonged annealing at temperatures higher than the glass transition temperature. This observation is also confirmed by the observed changes of DSC traces for samples with different thermal prehistory.

Layer Packing

During the transformation from smectic E to smectic A phase an increase of the intensity of the SAXS maximum and of the corresponding d-spacings as well as the disappearance of the diffuse halo from around 1° are observed simultaneously (Figure 3). All these changes occur very sharply in a narrow interval of 2°C width, i.e., from 54 to 56°C (see for example Figure 8). The longitudinal correlations increase sharply also after the transition from the smectic E into the smectic A phase (Figure 5). The increase of the thickness of the smectic layers during the melting of the intralayered packing can be explained very easily by the free rotation of the mesogenic groups in the smectic A phase. As can be seen from Figure 5 the introduction of only one gauche-conformer into the side chain, leads to the arrangement of the biphenyl moieties along the overall direction of the side chains. Correspondingly the projection of one side chain normal to the smectic plane increases with 0.15-0.2 nm. This leads to an increase of the overall thickness of the initial double-layered packing of 0.3-0.4 nm which corresponds to the observed value (Table 2).

The SAXS curve of the polymer cooled to room temperature from the isotropic state differs from the initial one. The sharp maximum shifts to the higher angles and the diffuse one from around 1° is not restored (Figure 8). After annealing at 35°C for two hours the sharp peak is shifted to the lower angles and the diffuse maximum at 1° appears. A longer annealing time of about 1 day leads to a full restoration of the initial curve of the annealed sample (Figure 9, Table 2). The longitudinal correlations are lowered very strongly during cooling and the height of the second maximum on $G(x)$ increases (Figure 5b). All these data are the result of the quick cooling of the polymer from the isotropic state into the glassy state with a freezing of the smectic A-like structure containing the liquid-like intralayer ordering. The development of the ordered

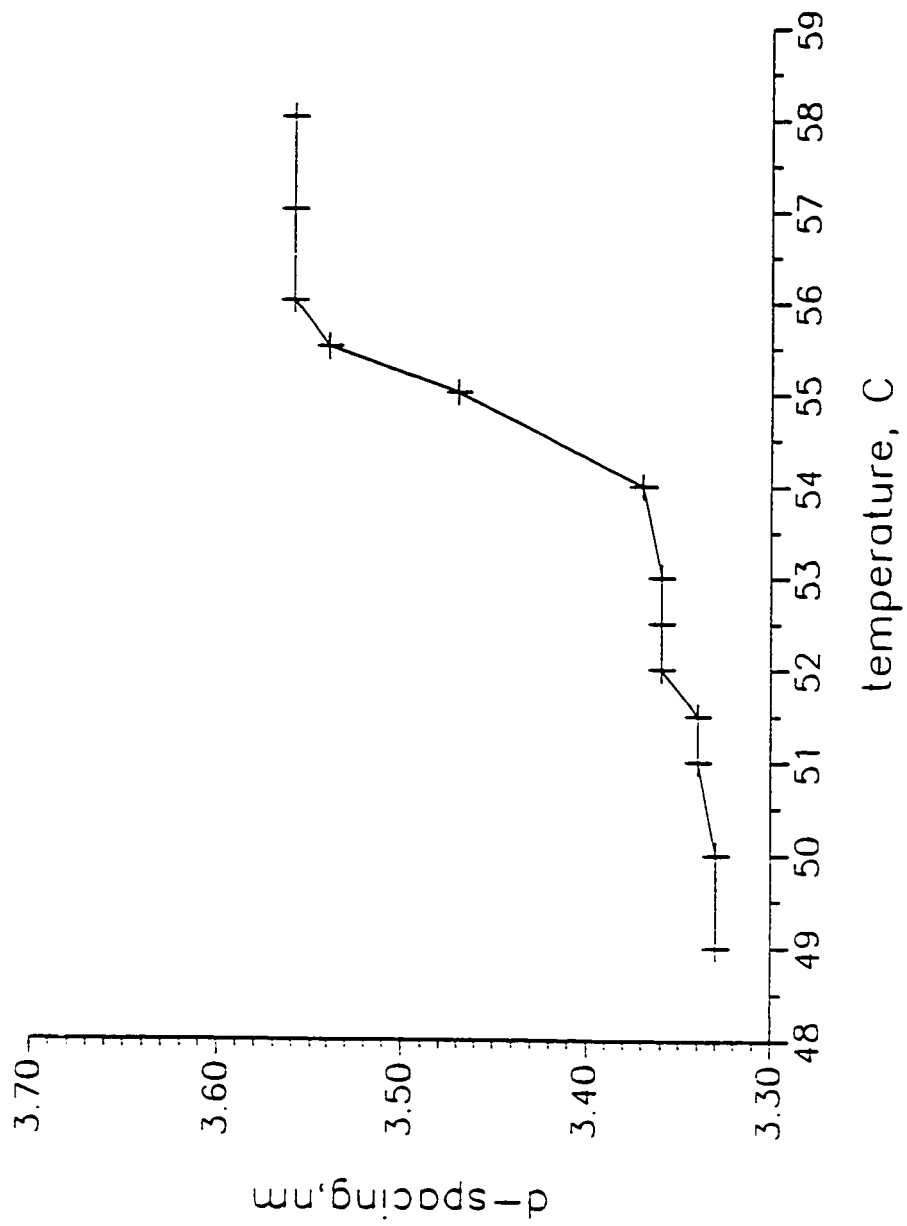


Figure 8. The dependence of d-spacing of poly(6-10) on temperature.

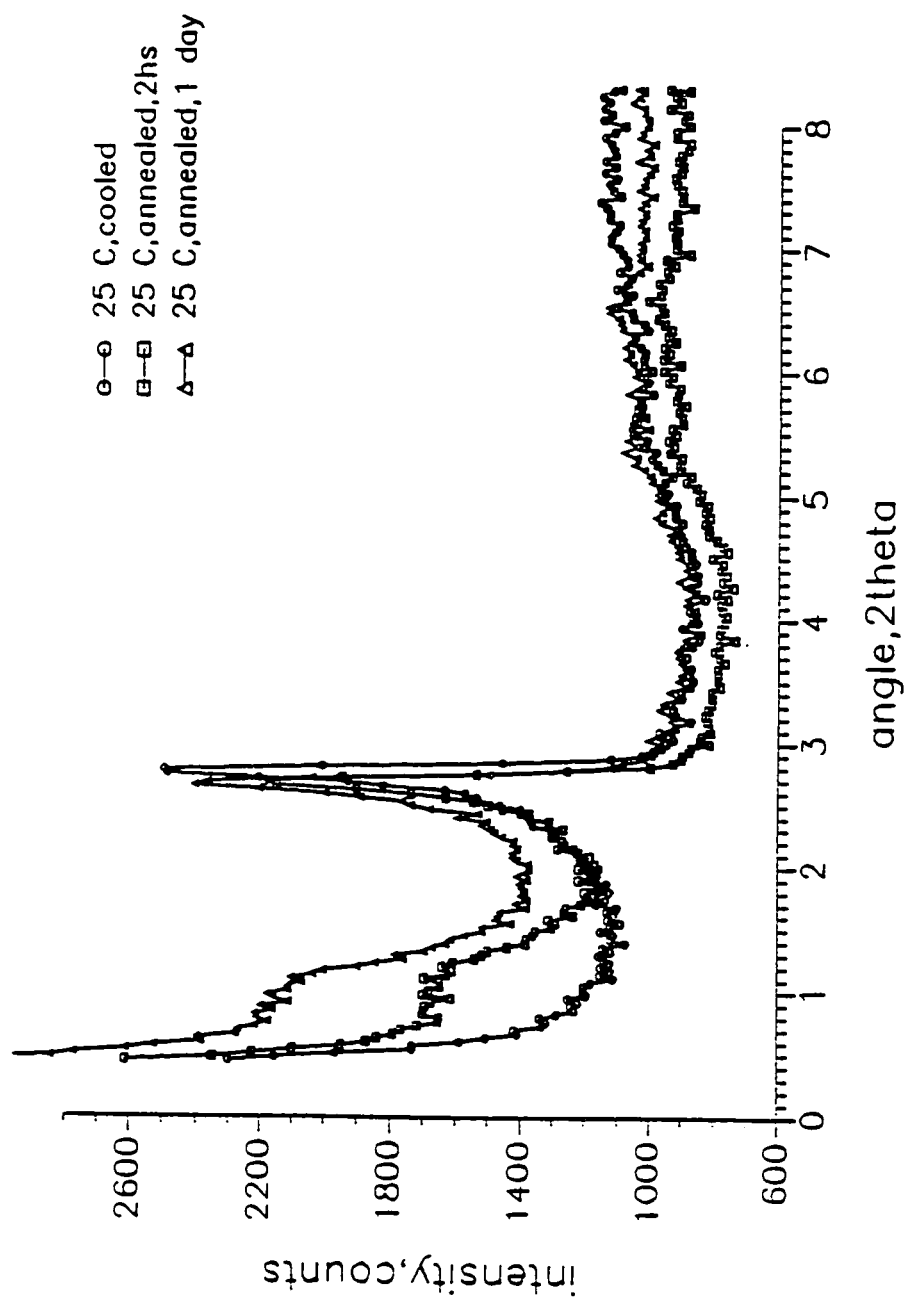


Figure 9. Small-angle X-ray scattering curves of poly(6-10) obtained during annealing.

smectic E phase at a temperature higher than T_g is a very slow process and the formation of the orthorombic lattice in the intralayer packing of the mesogenic groups with conformational changes in side groups is accompanied by the appropriated changes of the layer ordering.

3.4.-CONCLUSIONS

The side chain liquid crystalline polymer, poly(6-10), exhibits two different smectic phases: at low temperature an ordered smectic E phase with orthorombic intralayer packing of the mesogenic groups, and at high temperatures a common disordered smectic A phase. In both phases a double-layered longitudinal packing of the macromolecular fragments with a thickness of 6.6 nm-7 nm and overlapping of the slightly tilted mesogenic groups is realized. During the phase transition from the smectic E to the smectic A a melting of the intralayered packing occurs which leads also to the slight changes of the thickness of the smectic layers as a result of the conformational disordering of the side chains. A smectic A-like structure could be freezed in the glassy state by quick cooling. The development of the ordered smectic E phase as a result of annealing at temperatures higher than T_g is a very slow process since it requires the formation of the ordered intralayered orthorombic packing of mesogenic groups.

REFERENCES

1. V. Tsukruk, V. Shilov and Y. Lipatov, *Macromolecules*, **19**, 1308 (1986)
2. (a) V. Tsukruk, V. Shilov and Y. Lipatov, *Acta Polym.*, **36**, 403 (1985); (b) V. Tsukruk, V. Shilov and Y. Lipatov, *J. Macromol. Sci., Macromol. Chem. Phys.*, **C24**, 173 (1984).
3. C. Noel, in "Side Chain Liquid Crystal Polymers" McArdle, C. B., Eds., Chapman and Hall, New York, 1989, p. 159
4. W. Hefrich, *J. Phys. (Paris) Coll.*, **40**, C3 (1979)
5. G. W. Gray and G. W. Goodby, "Smectic Liquid Crystals, Leonard Hill, Glasgow, 1984

Chapter 4

INFLUENCE OF MOLECULAR WEIGHT ON THE PHASE TRANSITIONS OF POLY{8-[(4-CYANO-4'-BIPHENYL)OXY]OCTYL VINYL ETHER} AND OF POLY{6-[(4-CYANO-4'-BIPHENYL)OXY]HEXYL VINYL ETHER}

4.1.-INTRODUCTION

The most elementary step towards the molecular design of side chain liquid crystalline polymers represents the elucidation of the mechanism by which the polymer molecular weight influences its phase behavior as becomes apparent from the previous chapter. In previous chapter, the phase behavior of the polymers with different molecular weights was compared to that of the model compound of its monomeric structural unit. In both poly(6-10) and poly(6-11) the model compound of the monomeric structural unit and the polymers with different molecular weights display the same type of the highest temperature mesophase. The second smectic mesophase also appears above a certain molecular weight in both cases. This trend can be easily explained based on thermodynamics.^{1,2} There are additional examples in the literature where a polymer displays various mesophases at different molecular weights.^{3,5,6} However, no information is available on the phase behavior of the models of their monomeric structural units. Elucidation of this phenomenon requires the synthesis and characterization of polymers with well defined molecular weights, narrow molecular weight distributions as well as of the model compounds of their monomeric structural units.

This chapter describes the synthesis and living cationic polymerization of 8-[(4-(cyano-4'-biphenyl)oxy)octyl vinyl ether (6-8) and 6-[(4-(cyano-4'-biphenyl)oxy)hexyl vinyl ether (6-6) and the mesomorphic behavior of the resulting polymers with different

molecular weights. The phase behavior of these polymers will be compared to that of 8-[(4-cyano-4'-biphenyl)oxy]octyl ethyl ether (8-8) and 6-[(4-cyano-4'-biphenyl)oxy]hexyl ethyl ether (8-6), which represents the model of the monomeric structural unit of poly{8-[4(cyano-4'-biphenyl)oxy]octyl vinyl ether} [poly(6-8)] and poly{6-[4(cyano-4'-biphenyl)oxy]hexyl vinyl ether} [poly(6-6)] .

4.2.-EXPERIMENTAL

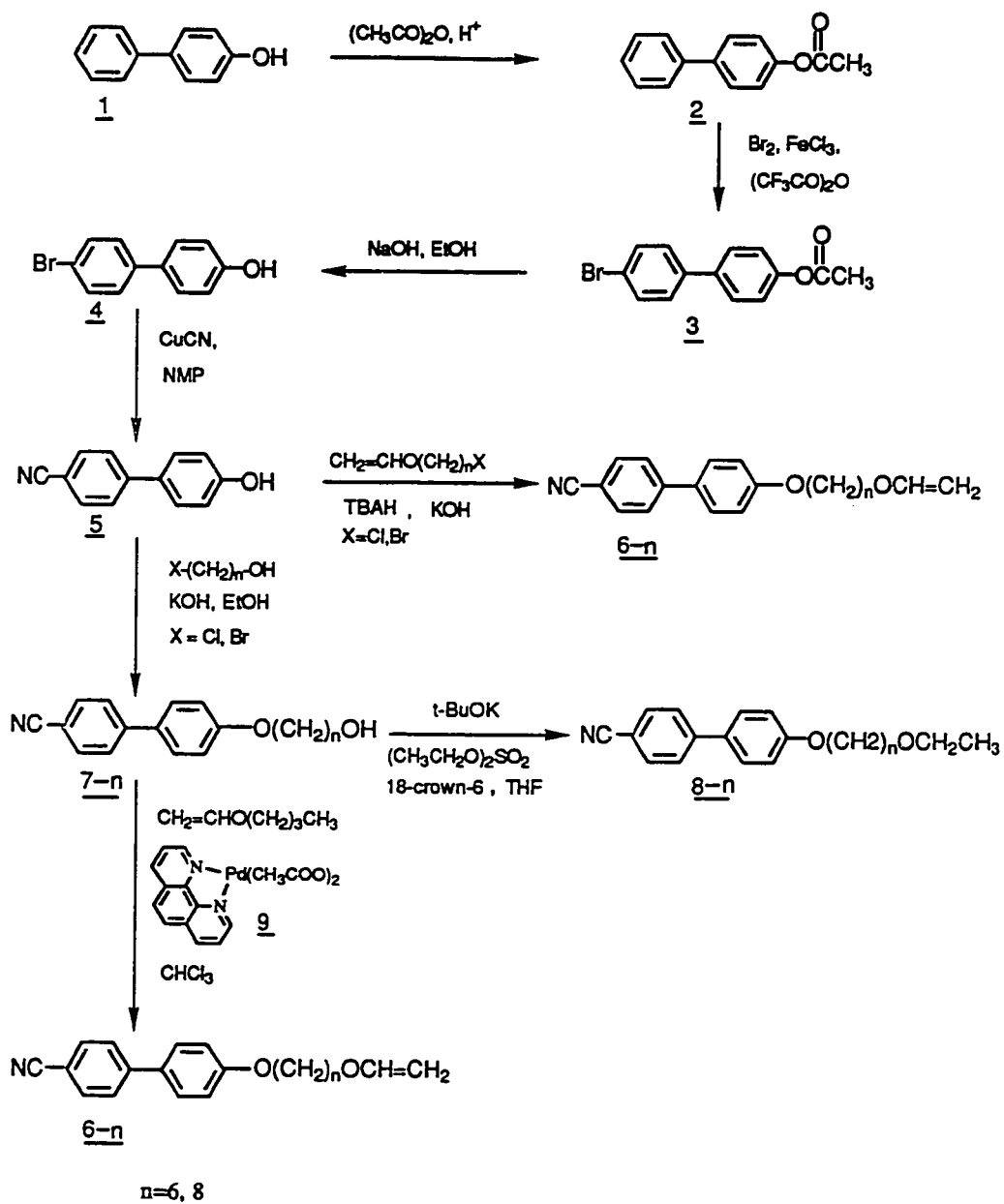
4.2.1-Materials

4-Phenylphenol (98%), 1,10-phenanthroline (anhydrous, 99%), palladium (II) acetate (all from Lancaster Synthesis), ferric chloride anhydrous (98%, Fluka), copper (I) cyanide (99%), n-butyl vinyl ether (98%), 9-borabicyclo[3.3.1]nonane (9-BBN, crystalline, 98%), 8-bromo-1-octanol (95%) and the other reagents (all from Aldrich) were used as received. Methyl sulfide (anhydrous, 99%, Aldrich) was refluxed over 9-BBN and then distilled under argon. Dichloromethane (99.6%, Aldrich) used as a polymerization solvent was first washed with concentrated sulfuric acid, then with water, dried over anhydrous magnesium sulfate, refluxed over calcium hydride and freshly distilled under argon before each use. N-Methyl-2-pyrrolidone (98%, Lancaster Synthesis) was dried by azeotropic distillation with benzene, shaken with barium oxide, filtered, and fractionally distilled under reduced pressure. Trifluoromethane sulfonic acid (triflic acid, 98%, Aldrich) was distilled under argon.

4.2.2.-Synthesis of monomers

Scheme I outlines the synthesis of monomers and model compounds.

1,10-Phenanthroline Palladium (II) Diacetate (9)



Scheme I. Synthesis of monomers and model compounds.

1,10-Phenanthroline palladium (II) diacetate was synthesized according to a literature procedure.⁶ mp 227°C. (lit. 6, mp 234°C).

4-Cyano-4'-Hydroxybiphenyl (5)

5 was synthesized as reported in a previous chapter. Purity: 98% (HPLC). mp 195-198°C. (lit. 7,8, mp 196-199°C). ¹H-NMR (Acetone-d₆, TMS, d, ppm): 3.80 (1 proton, OH, s), 7.01 (2 aromatic protons, o to -OH, d), 7.61 (2 aromatic protons, m to -OH, d), 7.70 (4 aromatic protons, o and m to -CN, s).

4-Cyano-4'-(8-hydroxyoctan-1-yloxy)biphenyl (7-8)

4-Cyano-4'-hydroxybiphenyl (5.8 g, 0.0297 mol), potassium hydroxide (1.66 g, 0.0297 mol) and few crystals of potassium iodide were dissolved in a mixture of ethanol-water (4/1) (165 ml). 8-Bromo-1-octanol (6.8 g, 0.033 mol) was added to the resulting solution which was heated to reflux for 24 hr. The ethanol was removed on a rotavapor and the resulting solid was washed successively with water, dilute aqueous NaOH and water. Recrystallization from methanol yielded 5.8 g (60.3%) of white crystals. Purity: 98 % (HPLC). ¹H-NMR (CDCl₃, TMS, d, ppm): 1.01-1.95 (12 protons, -(CH₂)₆-, m), 3.66 (2 protons, -CH₂OH, t), 4.01 (2 protons, PhOCH₂-, t), 7.01 (2 aromatic protons, o to alkoxy, d), 7.66 (4 aromatic protons, o and m to -CN, d of d). Thermal characterization of 7-8 is reported in Table I.

4-Cyano-4'-(6-hydroxyhexan-1-yloxy)biphenyl (7-6)

4-Cyano-4'-hydroxybiphenyl (126 g, 0.082 mol), potassium hydroxide (4.6 g, 0.082 mol) and few crystals of potassium iodide were dissolved in a mixture of ethanol-water (4/1) (450 ml). 6-Chloro-1-hexanol (12.3 g, 0.09 mol) was added to the

resulting solution which was heated to reflux for 24 hr. The ethanol was removed on a rotavapor and the resulting solid was washed successively with water, dilute aqueous NaOH and water. Recrystallization from methanol yielded 17 g (70.2%) of white crystals. Purity: 98% (HPLC). $^1\text{H-NMR}$ (CDCl_3 , TMS, δ , ppm): 1.01-1.95 (8 protons, $-(\text{CH}_2)_4-$, m), 3.64 (2 protons, $-\text{CH}_2\text{OH}$, t), 4.00 (2 protons, PhOCH_2- , t), 7.01 (2 aromatic protons, $-\text{CH}_2\text{OH}$, t), 7.55 (2 aromatic protons, m to alkoxy, d), 7.66 (4 aromatic protons, o and m to $-\text{CN}$, d of d). Thermal transitions of 7-6 are reported in Table I.

8-[4-Cyano-4'-biphenyl]oxyloctyl Vinyl Ether (6-8)

7-8 (4.5 g, 0.0139 mmol) was added to a mixture of 1,10-phenanthroline palladium (II) diacetate (0.55 g, 1.39 mmol), n-butyl vinyl ether (76 ml) and dry chloroform (70 ml). The mixture was heated at 60°C for 6 hr. After cooling and filtration (to remove the catalyst) the solvent was distilled in a rotavapor and the product was purified by column chromatography (silica gel, methylene chloride eluent) to yield 3.4 g (69.9%) of white crystals. Purity: 99% (HPLC). $^1\text{H-NMR}$ (CDCl_3 , TMS, δ , ppm): 1.01-1.95 (12 protons, $-(\text{CH}_2)_6-$, m), 3.68 (2 protons, $-\text{CH}_2\text{O}-$, t), 4.00 (3 protons, $\text{OCH}=\text{CH}_2$, trans, and PhOCH_2- , m), 4.14 and 4.21 (1 proton, $-\text{OCH}=\text{CH}_2$ cis, d), 6.49 (1 proton, $-\text{OCH}=\text{CH}_2$, q), 7.01 (2 aromatic protons, o to alkoxy, d), 7.50 (2 aromatic protons, m to alkoxy, d), 7.66 (4 aromatic protons, o and m to $-\text{CN}$, d of d). Thermal transitions of 6-8 are reported in Table I.

6-[4-Cyano-4'-biphenyl]oxylohexyl Vinyl Ether (6-6)

7-6 (2 g, 6.77 mmol) was added to a mixture of 1,10-phenanthroline palladium (II) diacetate (0.27 g, 0.677 mmol), n-butyl vinyl ether (36 ml) and dry chloroform (10

ml). The mixture was heated at 60°C for 6 hr. After cooling and filtration (to remove the catalyst) the solvent was distilled in a rotavapor and the product was purified by column chromatography (silica gel, methylene chloride eluent) to yield 1.85 g (85%) of white crystals. Purity: 99% (HPLC). $^1\text{H-NMR}$ (CDCl_3 , TMS, d, ppm): 1.01-1.95 (8 protons, $-(\text{CH}_2)_4-$, m), 3.70 (2 protons, $-\text{CH}_2\text{O}-$, t), 4.00 (3 protons, $-\text{OCH}=\text{CH}_2$, trans and PhOCH_2 , m), 4.14 and 4.21 (1 proton, $-\text{OCH}=\text{CH}_2$, cis, d), 6.45 (1 proton, $-\text{OCH}=\text{CH}_2$, q), 7.01 (2 aromatic protons, o to alkoxy, d), 7.50 (2 aromatic protons, m to alkoxy, d), 7.66 (4 aromatic protons, o and m to $-\text{CN}$, d of d).

8-[4-Cyano-4'-biphenyl]oxyloctyl Ethyl Ether (8-8)

7-8 (3.23 g, 0.01 mol) was added to a solution containing potassium t-butoxide (1.12 g, 0.01 mol) and 18-crown-6 (2.6 mg, 0.01 mmol) in dry tetrahydrofuran (78 ml). Diethyl sulfate (1.54 g, 0.01 mol) was added and the reaction mixture was refluxed for 3 hr. After cooling, the reaction mixture was extracted with chloroform, washed with water, dried over magnesium sulfate and the chloroform was removed in a rotavapor. The resulting product was purified by column chromatography (silica gel, methylene chloride eluent) to yield 2.2 g (63%) of white crystals. Purity: 99% (HPLC). $^1\text{H-NMR}$ (CDCl_3 , TMS, d, ppm): 1.20 (3 protons, $-\text{OCH}_2\text{CH}_3$, t), 1.30-1.81 (12 protons, $-(\text{CH}_2)_6-$, m), 3.41 (4 protons, $-\text{CH}_2\text{OCH}_2\text{CH}_3$, m), 4.00 (2 protons, $-\text{CH}_2\text{OPh}$, t), 7.01 (4 aromatic protons, m to alkoxy, d), 7.66 (4 aromatic protons, o and m to $-\text{CN}$, d of d). Thermal transitions of 8-8 are reported in Table I.

6-[4-Cyano-4'-biphenyl]oxylohexyl Ethyl Ether (8-6)

7-6 (2.95 g, 0.01 mol) was added to a solution containing potassium t-butoxide (1.12 g, 0.01 mol) and 18-crown-6 (2.6 mg, 0.01 mmol) in 78 ml of dry

tetrahydrofuran. Diethyl sulfate (1.54 g, 0.01 mol) was added and the reaction mixture was refluxed for 3 hr. After cooling, the reaction mixture was extracted with chloroform, washed with water, dried over magnesium sulfate and the chloroform was removed in a rotavapor. The resulting product was purified by column chromatography (silica gel, methylene chloride eluent) to yield 2.1 g (67%) of white crystals. Purity: 99% (HPLC). $^1\text{H-NMR}$ (CDCl_3 , TMS, δ , ppm): 1.21 (3 protons, $-\text{OCH}_2\text{CH}_3$, t), 1.46-1.82 (8 protons, $-(\text{CH}_2)_4-$, m), 3.43 (4 protons, $-\text{CH}_2\text{OCH}_2\text{CH}_3$, m), 4.01 (2 protons, $-\text{CH}_2\text{OPh}$, t), 7.02 (2 aromatic protons, o to alkoxy, d), 7.51 (2 aromatic protons, m to alkoxy, d), 7.68 (4 aromatic protons, o and m to $-\text{CN}$, d of d). Thermal transitions of 8-6 are reported in Table I.

4.2.3.-Cationic Polymerizations

Polymerizations were carried out in glass flasks equipped with teflon stopcocks and rubber septa under argon atmosphere at 0°C for 1 hr. All glassware was dried overnight at 130°C . The monomer was further dried under vacuum overnight in the polymerization flask. Then the flask was filled with argon, cooled to 0°C and the requested amounts of methylene chloride, dimethyl sulfide and triflic acid were added via a syringe. The monomer concentration was about 10 wt% of the solvent volume and the dimethyl sulfide concentration was 10 times larger than that of the initiator. The polymer molecular weight was controlled by the monomer/initiator ratio. At the end of the polymerization the reaction mixtures were precipitated into methanol containing few drops of NH_4OH . The filtered polymers were dried and precipitated from methylene chloride solutions into methanol until GPC traces showed no traces of monomer. Tables II and III summarize the polymerization results. Although the polymer yields

are lower than expected due to losses during the purification process, the conversions were almost quantitative in all cases.

4.3.-RESULTS AND DISCUSSION

The synthesis of 6-8, 6-6, 8-8 and 8-6 is outlined in Scheme I. Both 6-8 and 6-6 are synthesized by the vinyl ether interchange reaction with 1,10-phenanthroline palladium (II) diacetate under mild reaction condition.^{7,10}

As shown previously,^{4-6,11,12,13-15} living cationic polymerization of vinyl ethers tolerates a variety of functional groups. We prefer to perform this polymerization with triflic acid/dimethylsulfide initiator, since this polymerization can be carried out in methylene chloride at 0°C.^{16,17} Scheme II outlines the polymerization mechanism. Under our polymerization conditions, the poly(vinylether)s contain acetal chain ends (Scheme II) and therefore, they should be manipulated in the absence of acids.

The polymerization results are presented in Tables II and III. The molecular weights and the molecular weight distributions of both sets are presented in Tables II and III. All polymers display narrow molecular weight distribution. Although the number average molecular weights were determined by GPC using polystyrene as a calibration standard, the ratio of $[M]_0/[I]_0$ provides a very good control of molecular weight. The dependences of the number average molecular weight (M_n) and of M_w/M_n versus the ratio between the initial monomer and initiator concentration $[M]_0/[I]_0$ are plotted in Figure 1. Both plots show the living character of these polymerizations. Similar plots for poly(6-6) demonstrate that 6-6 polymerizes also through a living mechanism.

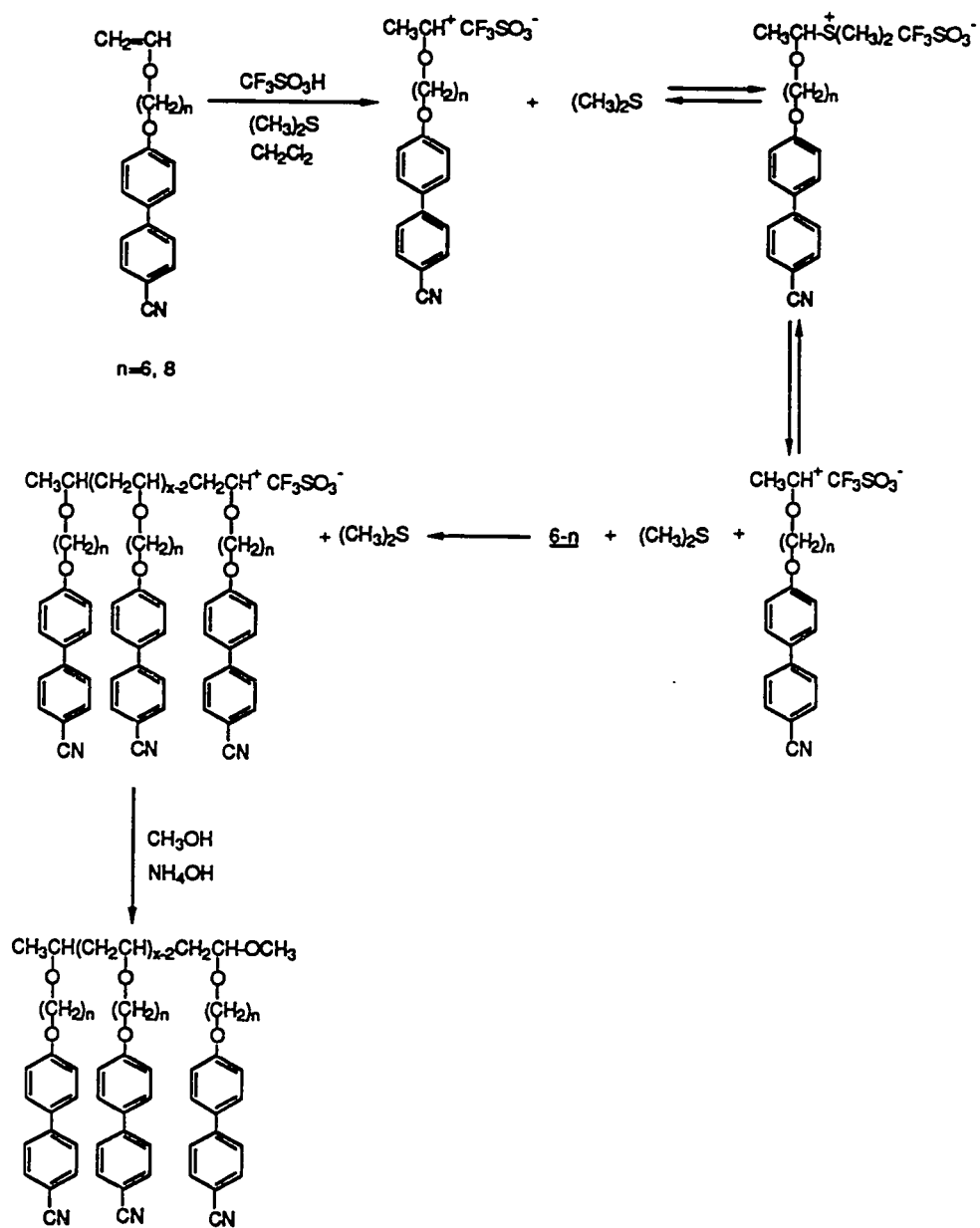
Figure 2a displays the heating and cooling DSC traces of 4-cyano-4'-(8-hydroxyoctan-1-yloxy)biphenyl (7-8), 8-[4-cyano-4'-biphenyloxy]octyl vinyl ether (6-

Table I. Thermal Characterization of 4-Cyano-4'-(ω -hydroxyalkan-1-yloxy)biphenyls (7-8) and (7-6), ω -[(4-Cyano-4'-biphenyl)oxy]alkyl Vinyl Ethers (6-8) and (6-6), and of ω -[(4-Cyano-4'-biphenyl)oxy]alkyl Ethyl Ethers (8-8) and (8-6).

Compound	phase transitions (0°C) and corresponding enthalpy changes (kcal/mol)	
	heating	cooling
<u>7-8</u>	k 87.7 (9.1) n 104.0 (0.23) i	i 100.4 (0.38) n 57.7 (6.09) k
<u>6-8</u>	k 54.0 (8.31) n 70.8 (0.27) i	i 67.3 (0.31) n 27.9 (4.68) k
<u>8-8</u>	k 62.9 (8.77) i [s _A 58.5 (0.26) n 61.0 (0.39)i]*	i 53.1 (0.37) n 46.9 (0.015) s _A 23.7 (7.21) k
<u>7-6</u>	k 93.5 (8.01) n 110.9 (0.25) i	i 107.8 (0.33) n 71.04 (5.66) k
<u>6-6</u>	k 75.5 (5.95) i [n 75.9 (0.35) i]	i 68.2 (0.31) n 55.8 (5.22) k
<u>8-6</u>	k 64.6 (8.67) [n 60.0 (0.12)] i	i 46.7 (0.13) n 27.1 (7.21) k

*[] virtual data

* overlapped peaks



Scheme II. Cationic polymerization of 6-8 and 6-6

Table II. Cationic Polymerization of 8-[4-Cyano-4'-biphenyl]oxyoctyl Vinyl Ether (6.8) (polymerization temperature, 0°C; polymerization solvent, methylene chloride; $[M]_0=0.285$; $[(CH_3)_2S]_0/[I]_0=10$; polymerization time, 1hr) and Characterization of the Resulting Polymers. Data on first line are from first heating and cooling scans. Data on second line are from second heating scan.

Sample No.	$[M]_0/[I]_0$	Polymer yield(%)	$M_w \cdot 10^{-3}$	M_w/M_n	D P	phase transitions(°C) and corresponding enthalpy changes (kcal/mru)	
						heating	cooling
1	2	42	0.8	1.11	2	g -6.4 sA 65.1 (-) ^a n 67.4 (0.28) i g -6.7 sA 63.8 (-) ^a n 65.6 (0.31) i	i 65.0 (0.29) n 63.5 (-) ^a sA -6.4 g
2	4	68	1.5	1.06	4	g 4.9 sA 110.9 (0.48) i g 2.5 sA 110.5 (0.47) i	i 105.6 (0.46) sA 0.1 g
3	6	65	2.0	1.07	5	g 5.8 sA 114.3 (0.51) i g 4.2 sA 114.0 (0.51) i	i 109.2 (0.50) sA 2.5 g
4	8	69	2.9	1.09	8	g 9.2 sA 125.6 (0.47) i g 7.5 sA 125.8 (0.47) i	i 120.5 (0.46) sA 7.5 g
5	10	71	3.6	1.09	10	g 12.6 sA 127.5 (0.43) i g 8.3 sA 127.3 (0.43) i	i 122.8 (0.46) sA 7.8 g
6	13	76	4.3	1.06	12	g 15.7 sX 36.4 (0.31) sA 136.4 (0.58) i g 9.2 sA 134.8 (0.46) i	i 128.8 (0.45) sA 7.9g
7	18	86	6.3	1.11	18	g 23.2 sX 49.4 (0.27) sA 145.0 (0.50) i g 17.5 sX 49.1 (0.27) 144.9 (0.44) i	i 139.6 (0.30) sA 40.9 (0.44) sX 12.5g
8	23	85	7.9	1.09	22	g 22.5 sX 67.1 (0.27) sA 154.1 (0.48) i g 18.7 sX 62.1 (0.28) sA 151.1 (0.43) i	i 141.6 (0.32) sA 49.7 (0.40) sX 13.3g
9	30	69	10.9	1.11	31	g 22.7 sX 69.0 (0.34) sA 155.1 (0.41) i g 21.5 sX 67.9 (0.31) sA 155.3 (0.40) i	i 150.0 (0.32) sA 62.8 (0.39) sX 19.2 g

^a overlapped peaks

Table III. Cationic Polymerization of 6-[4-Cyano-4'-biphenyl]oxy]hexyl Vinyl Ether (6-6) (polymerization temperature, 0°C; polymerization solvent, methylene chloride; $[M]_0 = 0.31$ l; $[(CH_3)_2S]_0/[I]_0 = 10$; polymerization time, 1hr) and Characterization of the Resulting Polymers. Data on first line are from first heating and cooling scans. Data on second line are from second heating scan.

Sample No.	$[M]_0/[I]_0$	Polymer yield(%)	Mnx 10 ⁻³	Mw/Mn	D P	phase transitions(°C) and corresponding enthalpy changes (kcal/mru)	
						heating	cooling
1	4	63	1.1	1.02	3	g 12.1 sA 90.8 (-) ^a n 95.7 (0.22) i g 12.1 sA 91.4 (-) ^a n 95.1 (0.21) i	i 91.5 (0.21) n 86.7 (-) ^a sA 3.3 g
2	5	61	1.7	1.03	5	g 16.4 sA 98.7 (-) ^a n 100.8 (0.28) i g 13.2 sA 99.2 (-) ^a n 101.2 (0.20) i	i 97.5 (0.20) n 94.8 (-) ^a sA 7.2 g
3	7	76	2.4	1.07	8	g 17.9 sA 101.9 (-) ^a n 102.8 (0.25) i g 16.4 sA 101.5 (-) ^a n 102.6 (0.19) i	i 100.7 (0.19) n 98.8 (-) ^a sA 4.8 g
4	9	84	2.9	1.03	9	g 17.7 sX 37.3 (0.21) sA 107.8 (0.17) i g 17.5 sA 104.0 (0.14) i	i 102.4 (0.19) n 100.8 (-) ^a sA 3.5 g
5	11	72	3.6	1.10	12	g 26.2 sX 45.6 (0.30) sA 109.1 (0.15) i g 15.6 sA 104.0 (0.14) i	i 105.0 (0.19) sA 5.6 g
6	13	75	4.4	1.05	14	g 28.9 sX 47.7 (0.45) sA 112.2 (0.15) i g 15.7 sA 112.7 (0.21) i	i 111.9 (0.19) sA 3.7 g
7	23	85	7.5	1.09	23	g 24.3 sX 52.0 (0.25) sA 117.1 (0.15) i g 23.2 sX 53.9 (0.23) sA 117.4 (0.14) i	i 113.4 (0.18) sA 36.2 (0.06) sX 12.7g
8	30	87	9.4	1.10	29	g 28.9 sX 73.9 (0.32) sA 124.8 (0.12) i g 29.5 sX 67.1 (0.46) sA 120.5 (0.15) i	i 117.6 (0.15) sA 54.1 (0.29) sX 25.8 g

^a overlapped peaks

8) and of 8-[(4-cyano-4'-biphenyl)oxy]octyl ethyl ether (8-8). 7-8 and 6-8 present an enantiotropic nematic mesophase. The model compound of the monomeric structural unit of poly(6-8), i.e., 8-8 presents a monotropic nematic and a monotropic s_A mesophase. The s_A -nematic and nematic-isotropic transitions from the heating scan of 8-8 were determined by reheating the sample in the DSC instrument from the above the temperature at which this compound crystallizes (Figure 2a). Heating and cooling DSC traces of 7-6, 6-6 and 8-6 are presented in Figure 2b. 7-6 displays an enantiotropic nematic mesophase. 6-6 and 8-6 display a monotropic nematic mesophase. The nematic-isotropic transition temperatures and their corresponding thermodynamic parameters were determined by cooling the sample up to before it reaches the crystallization temperature and then reheating it (Figure 2b). All these thermal transitions and the corresponding enthalpy changes are summarized in Table I.

Figure 3 presents the first heating, the second heating and the cooling DSC scans of poly(6-8). First and subsequent cooling scans of each polymer are identical. With the exception of the poly(6-8) which has a degree of polymerization equal to 12, all other polymers display first and subsequent heating scans which are almost identical. The case of poly(6-8) with DP=12 will be discussed later. Poly(6-8) with a degree of polymerization of 2 displays an enantiotropic s_A phase and an enantiotropic nematic phase which are almost overlapped on both their heating (Figure 3a,b) and cooling (Figure 3c) scans. Therefore, this dimer resembles the phase behavior of the model of the monomeric structural unit, 8-8, except that the dimer does not crystallize and its thermal transitions are shifted towards higher temperatures (Tables I and II).

Poly(6-8)s with degrees of polymerization from 4 to 10 display only an enantiotropic s_A mesophase. Poly(6-8) with degrees of polymerization equal and higher than 12 display a s_X (i.e., a smectic phase which was not yet identified) and an

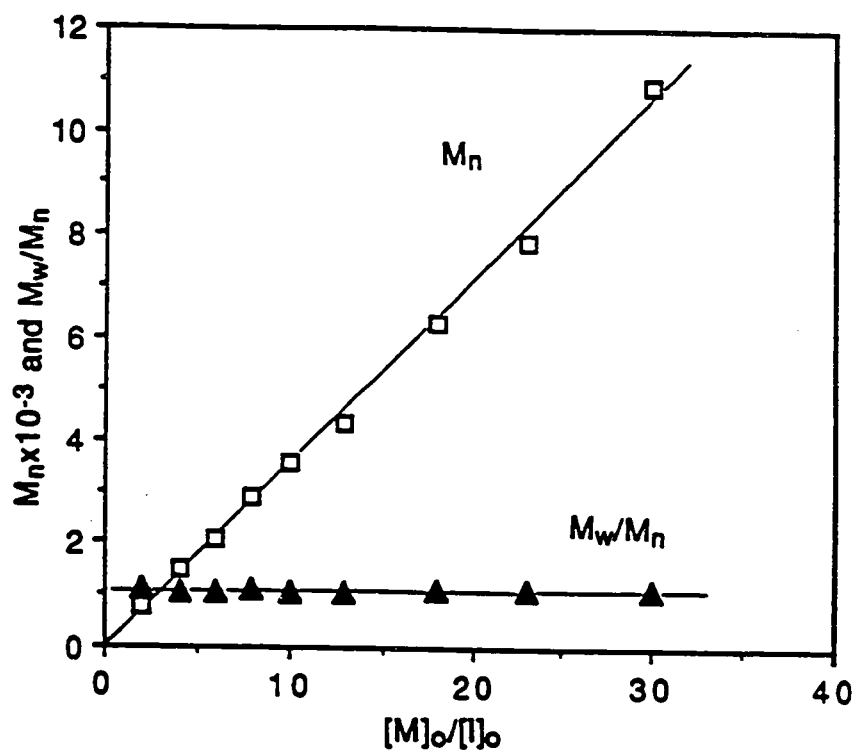


Figure 1. The dependence of the number average molecular weight (M_n) and of the polydispersity (M_w/M_n) of poly(6-8) on the $[M]_0/[I]_0$ ratio.

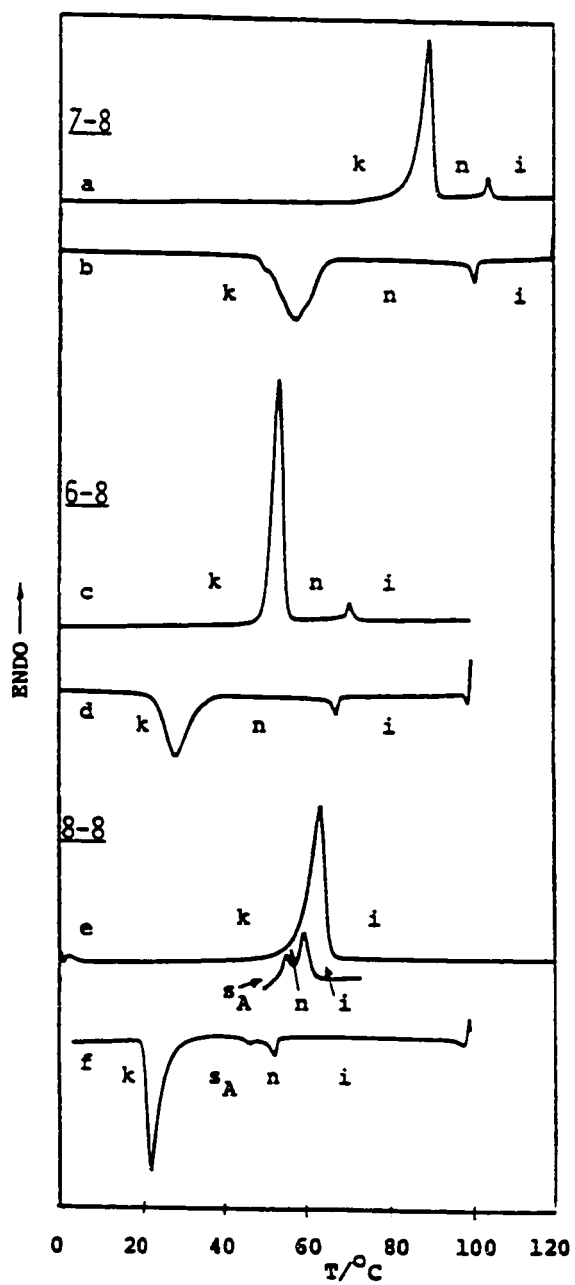


Figure 2a. Heating and cooling DSC traces of 7-8 (a, b), 6-8 (c, d) and 8-8 (e, f).

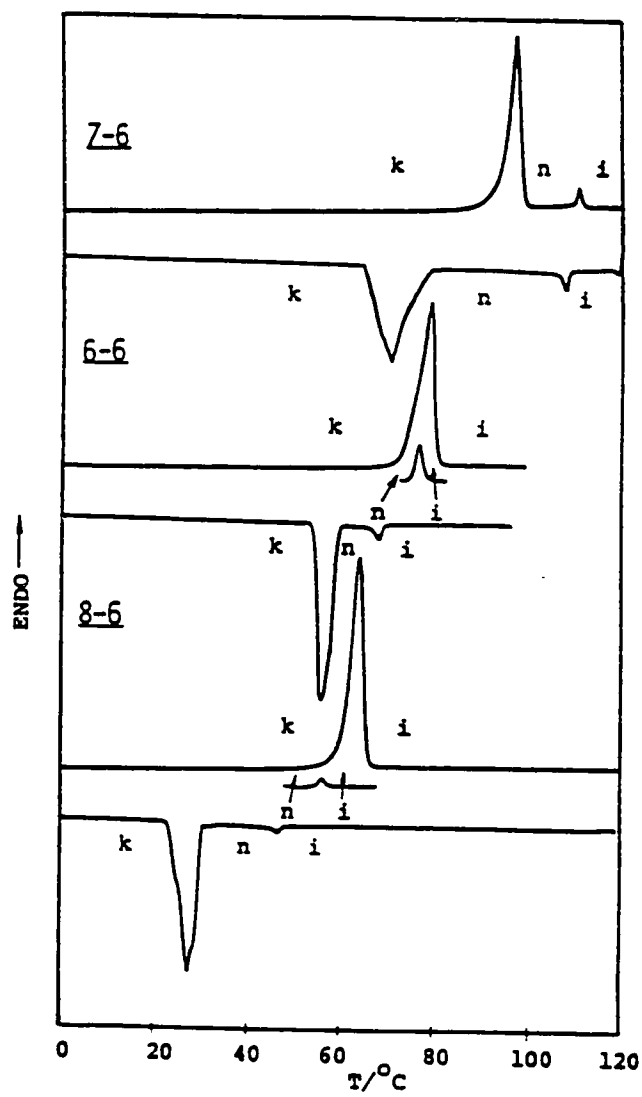


Figure 2b. Heating and cooling DSC traces of 7-6 (a,b), 6-6 (c,d) and 8-6 (e,f).

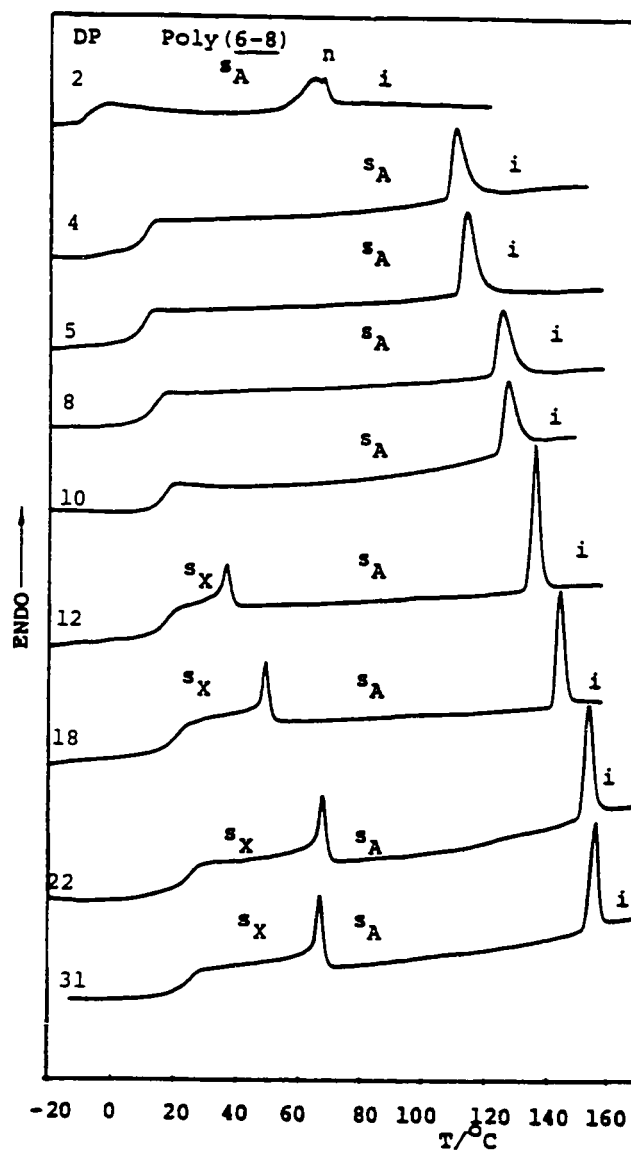


Figure 3a. DSC traces displayed during the first heating scan by poly (6-8) with different degrees of polymerization (DP). DP is printed on the top of each DSC scan.

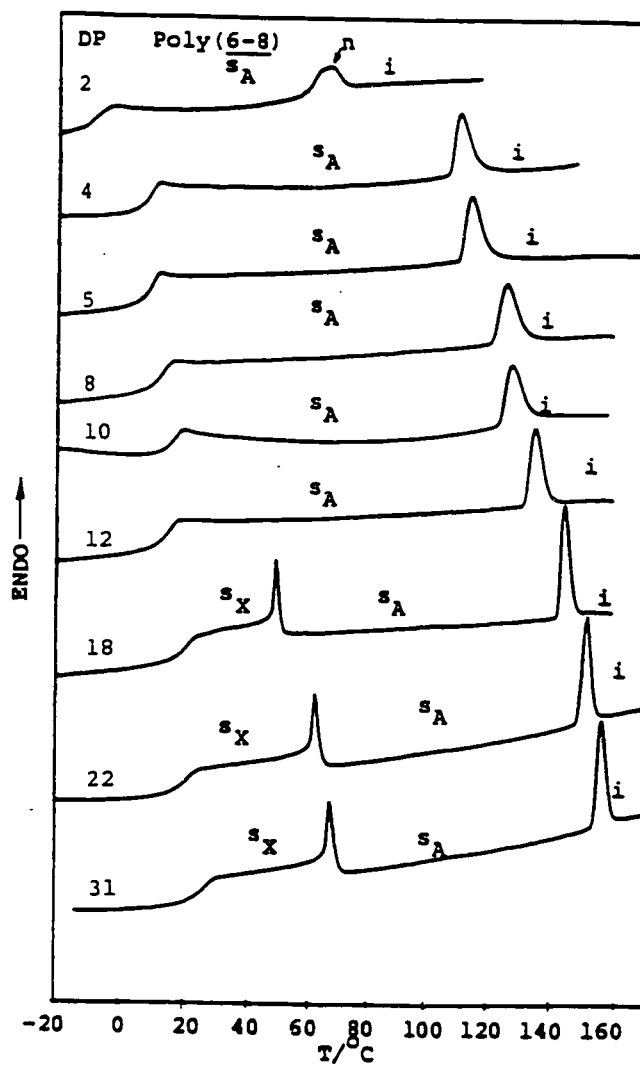


Figure 3b. DSC traces displayed during the second heating scan by poly (6-8) with different degrees of polymerization (DP). DP is printed on the top of each DSC scan.

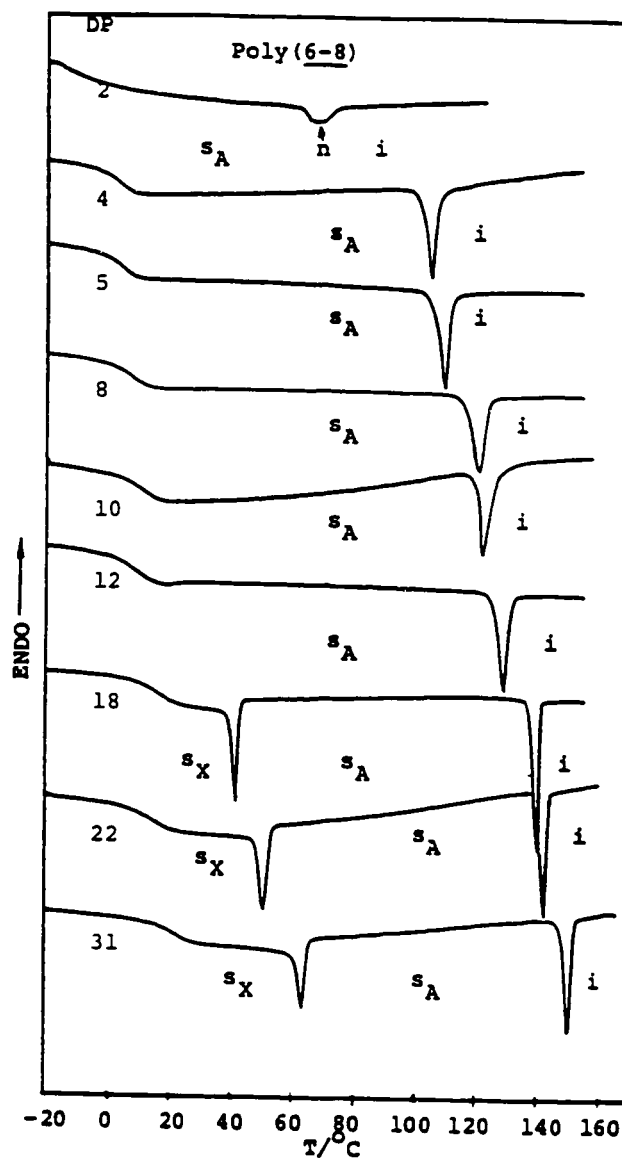


Figure 3c. DSC traces displayed during the first cooling scan by poly (6-8) with different degrees of polymerization (DP). DP is printed on the top of each DSC scan.

enantiotropic s_A phase. The s_X phase is enantiotropic in the case of polymers with degrees of polymerization from 18 to 31 and appears only on the first heating scan in the case of the polymers with a degree of polymerization equal to 12. This behavior is due to the kinetic effect provided by the close proximity of this phase transition to the glass transition of the polymer. All these phase transition temperatures and their corresponding thermodynamic parameters are summarized in Table II.

The thermal transition temperatures from the first heating, second heating and cooling scans of all polymers are plotted as a function of the degree of polymerization in Figure 4. The phase transition temperatures of the model compound of the monomeric structural unit (8-8) from Figure 2 and Table I are also included. However, the melting and crystallization temperatures are not plotted since they would overlap the other data. Nevertheless, we have to recall that both the nematic and the s_A phase of 8-8 are monotropic.

Figure 4,a,b,c provides us with the following conclusion. On increasing the degree of polymerization from monomer to dimer, both the nematic and s_A phase transition temperature become enantiotropic. This effect is both due to the decreased rate of crystallization of the dimer, which represents a kinetic effect, and due to the increase of the two phase transition temperatures with the increase of the molecular weight, which represents a thermodynamic effect. However, on increasing the degree of polymerization from 2 to 4, the polymer does not display anymore the nematic mesophase. Although only from two data points, we can assume that this change represents a continuous dependence of molecular weight. This result is simply due to the fact that the slope of the dependence temperature transition of the s_A phase versus polymerization degree is higher than that of the slope relating the dependence of the nematic temperature transition versus degree of polymerization.

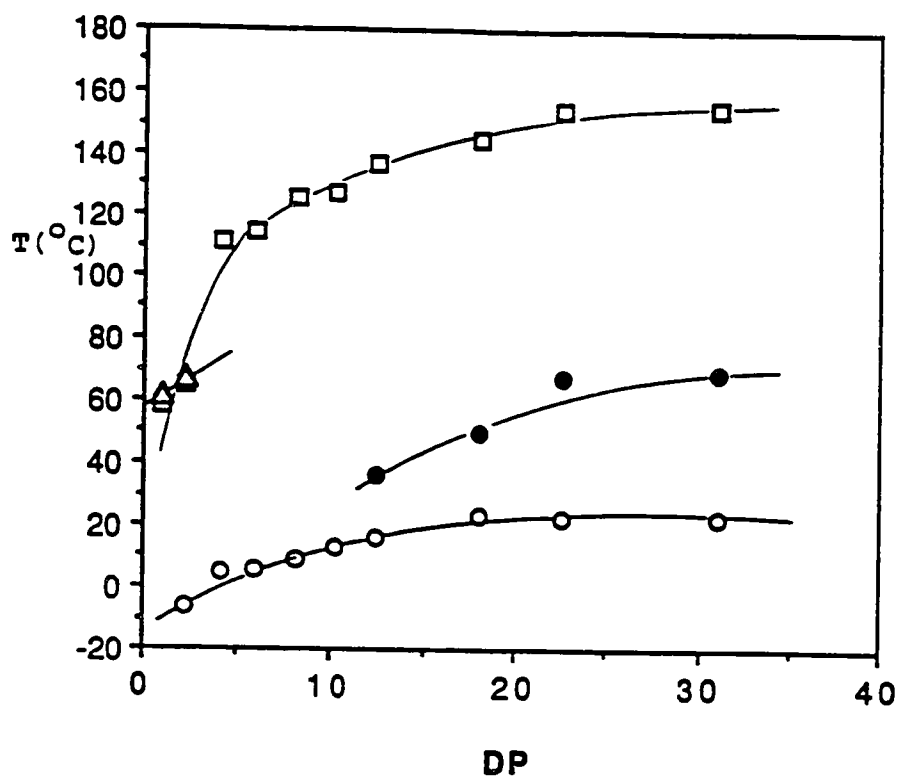


Figure 4a. The dependence of phase transition temperatures on the degree of polymerization of poly(6-8). DP=1 corresponds to 8-8 (data from first heating scan): O-Tg; \square -TsA-n; Δ -Tn-i; \bullet -TsX-sA.

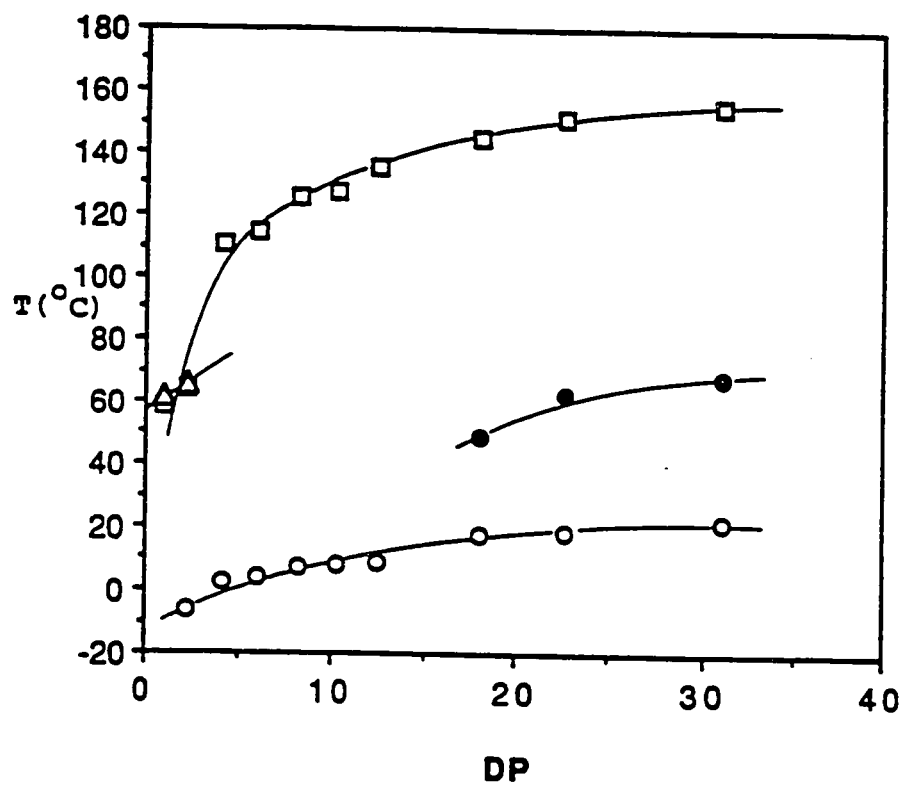


Figure 4b. The dependence of phase transition temperatures on the degree of polymerization of poly(6-8). DP=1 corresponds to 8-8 (data from second heating scan): O-Tg; □-TsA-n; Δ-Tn-i; ●-TsX-sA.

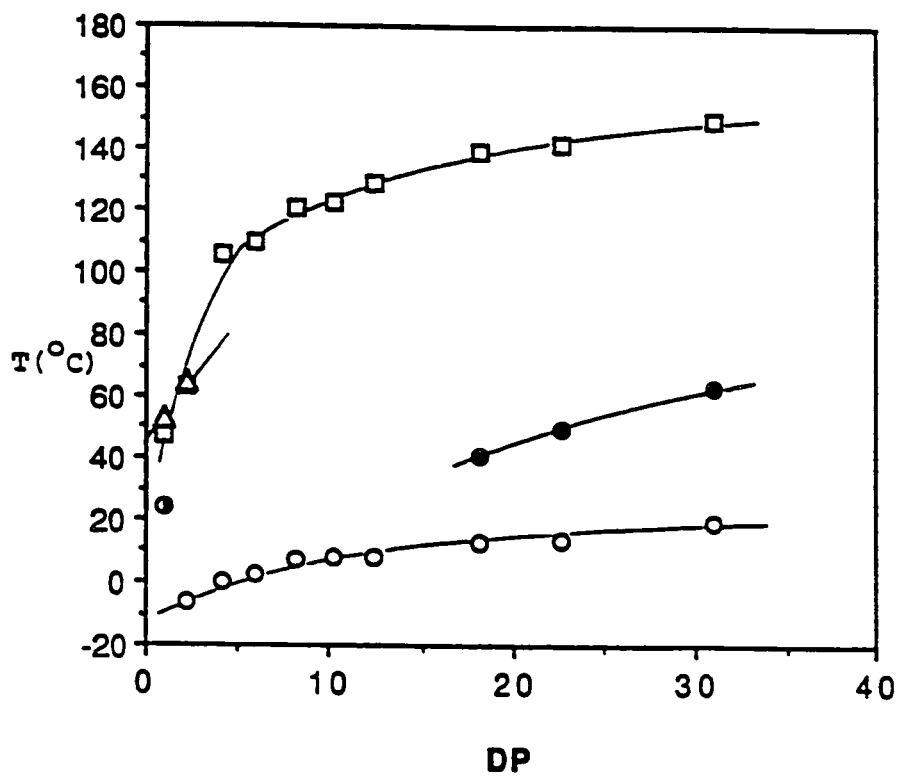


Figure 4c. The dependence of phase transition temperatures on the degree of polymerization of poly(6-8). DP=1 corresponds to 8-8 (data from first cooling scan): \square -Ti-sA; Δ -Ti-n; \bullet -TsA-sX; \circ -Tg; \ominus -Tk.

Figure 5 presents some representative textures displayed by the nematic and s_A exhibited by 8-8 (degree of polymerization of 1). The nematic and s_A mesophases of poly(6-8) with a degree of polymerization of 2 exhibit the same textures as those of 8-8.

The DSC traces of the first heating, second heating and cooling scans of poly(6-6) are presented in Figure 6. All cooling scans are identical. The phase transition temperatures which are not influenced by kinetics are identical on the first, second and subsequent heating scans. Only phase transitions which are located in the close proximity of the glass transition temperature are dependent on the thermal history of the sample. Poly(6-6) with degrees of polymerization from 3 to 8 display enantiotropic s_A and nematic mesophases irrespective of the DSC scan we consider for their characterization (Figure 6).

Polymers with degrees of polymerization from 9 to 29 display a s_X (i.e., an unidentified smectic phase) mesophase in the first heating scan. Only poly(6-6) with degrees of polymerization from 23 to 29 display an enantiotropic s_X phase. The s_X phase does not appear on the second heating and cooling scans for polymer samples with degrees of polymerization ranging from 9 to 14. However, after proper annealing conditions, the s_X mesophase reappears on the first heating scan. That is, for polymer samples with degrees of polymerization from 9 to 14, under equilibrium conditions the s_X phase is "inverse" monotropic. This behavior demonstrates that mesophases located in the close proximity of the glass transition temperature are subjected to strong kinetic influences.

The phase transition temperatures collected from the first, second and cooling DSC scans are plotted in Figure 7. The phase transition temperatures of the model compound of the monomeric structural unit (8-6), are also plotted and correspond to a

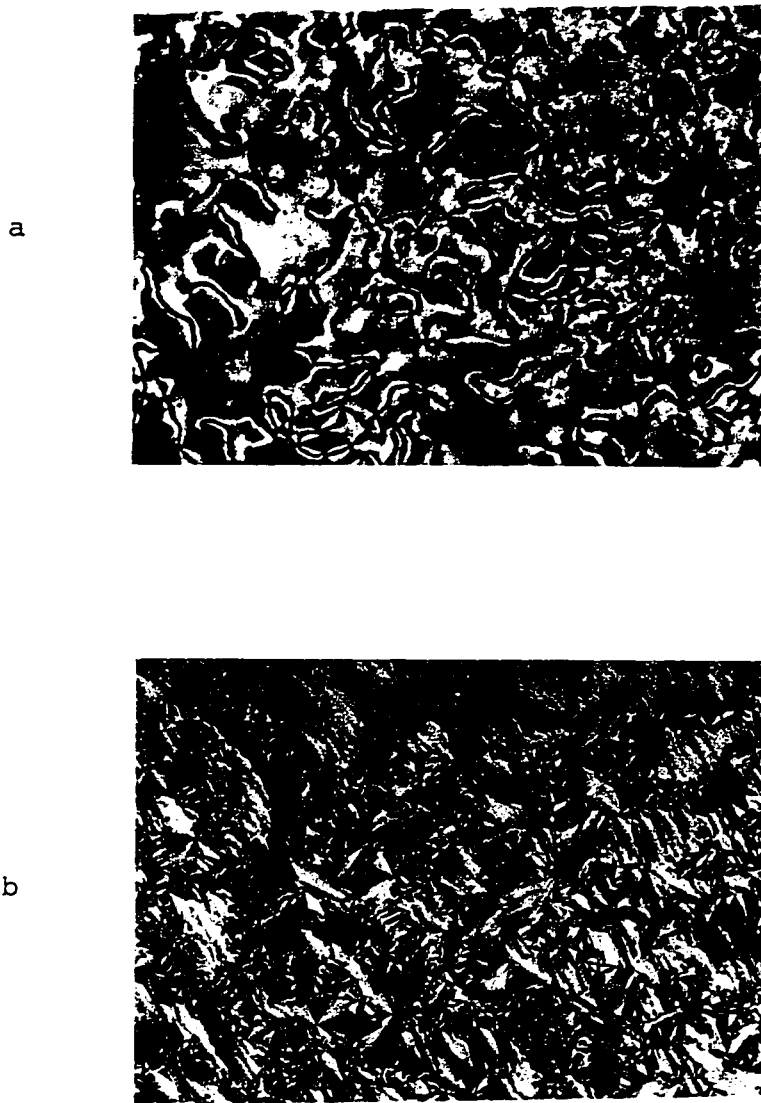


Figure 5. Representative optical polarized micrographs (100x) of : a) 8-8 at 53°C on the cooling scan (nematic phase); b) 8-8 at 47°C on the cooling scan (SA phase).

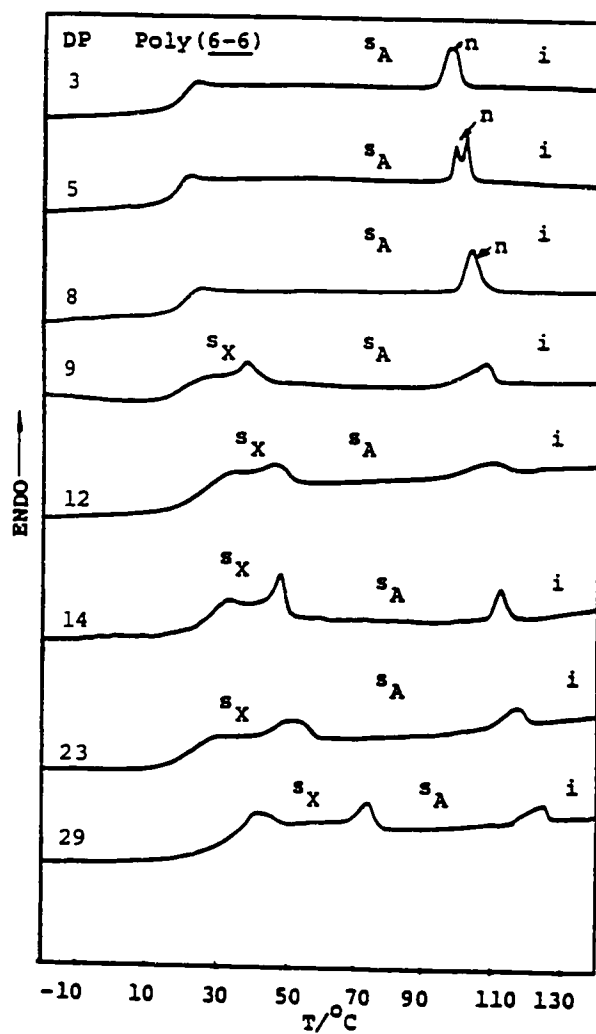


Figure 6a. DSC traces displayed during the first heating scan by poly(6-6) with different degrees of polymerization (DP). DP is printed on the top of each DSC scan.

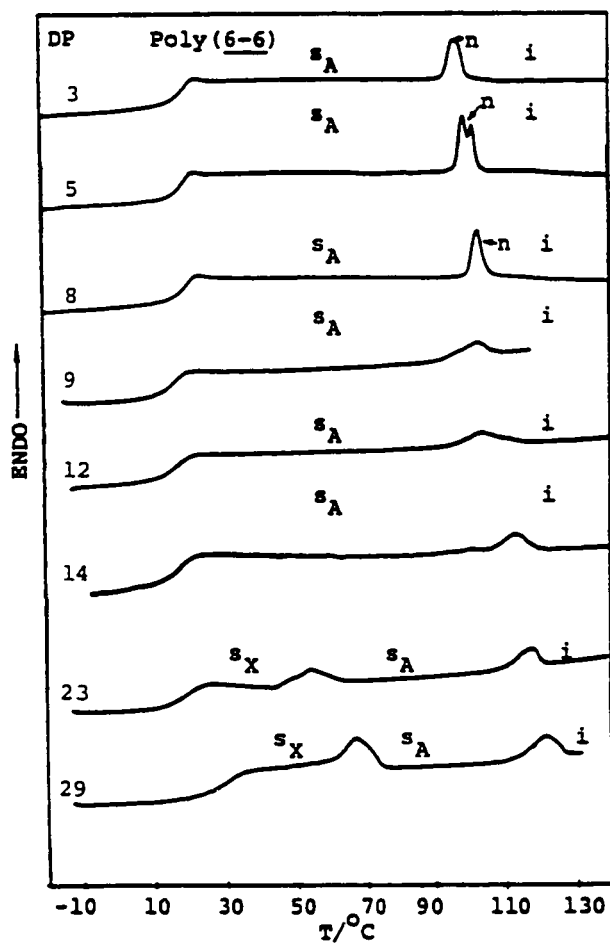


Figure 6b. DSC traces displayed during the second heating scan by poly(6-6) with different degrees of polymerization (DP). DP is printed on the top of each DSC scan.

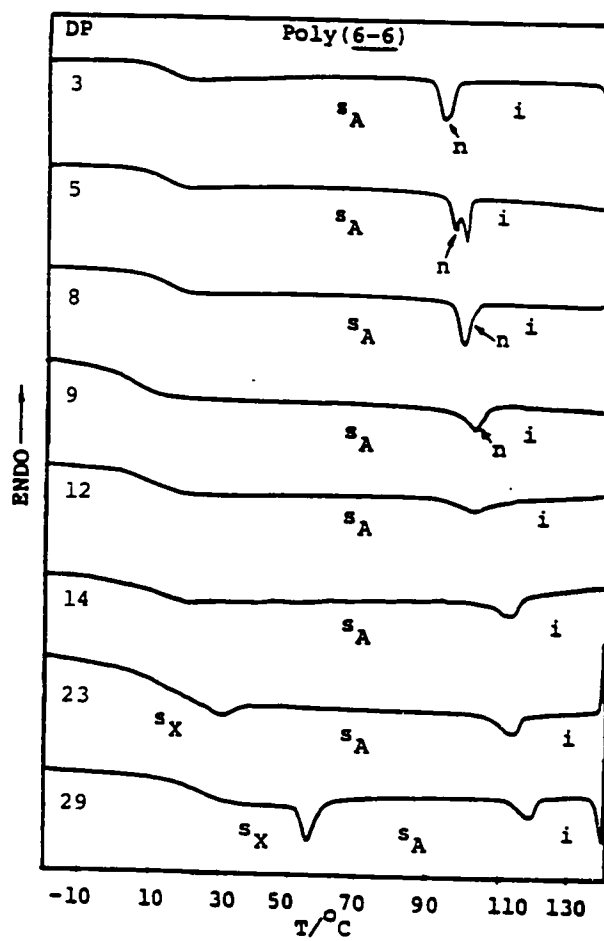


Figure 6c. DSC traces displayed during the first cooling scan by poly(6-6) with different degrees of polymerization (DP). DP is printed on the top of each DSC scan.

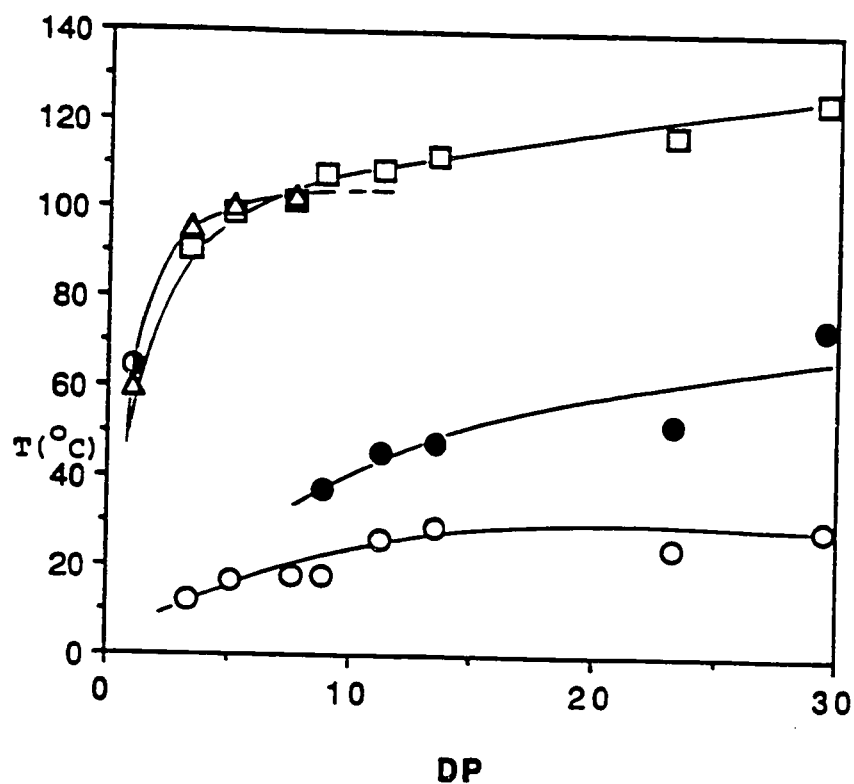


Figure 7a. The dependence of the phase transition temperatures on the degree of polymerization of poly(6-6). DP=1 corresponds to 8-6 (data from first heating scan): O-Tg; \square -TsA-n or TsA-i; Δ -Tn-i; \bullet -TsX-sA; \bullet -Tm;

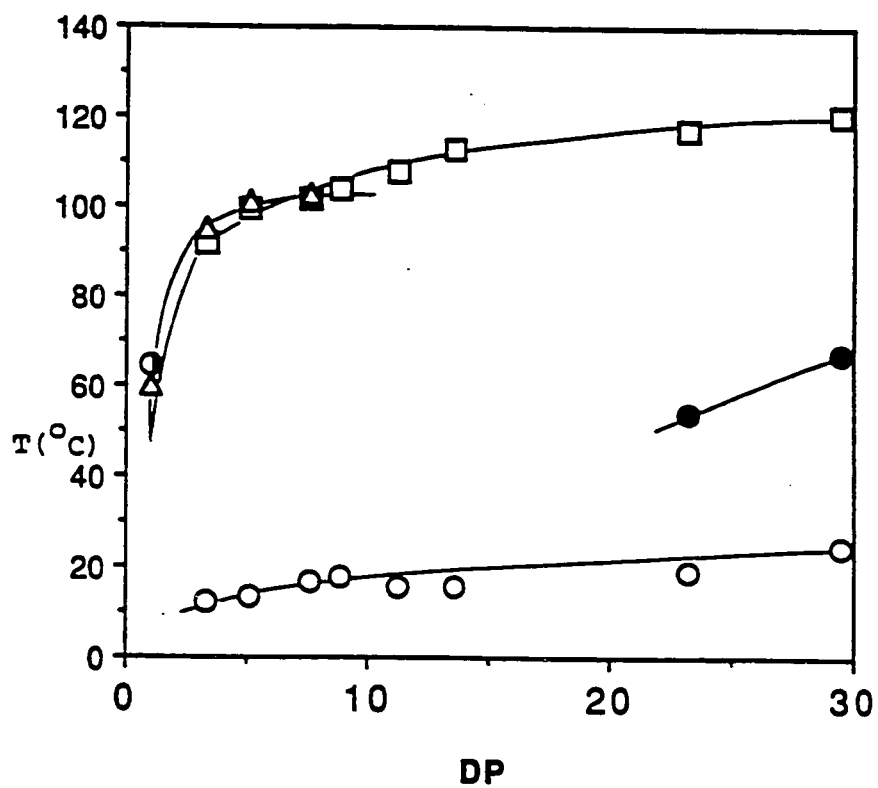


Figure 7b. The dependence of the phase transition temperatures on the degree of polymerization of poly(6-6). DP=1 corresponds to 8-6 (data from second heating scan): O-Tg; \square -TsA-n or TsA-i; Δ -Tn-i; \bullet -TsX-sA; \bullet -Tm.

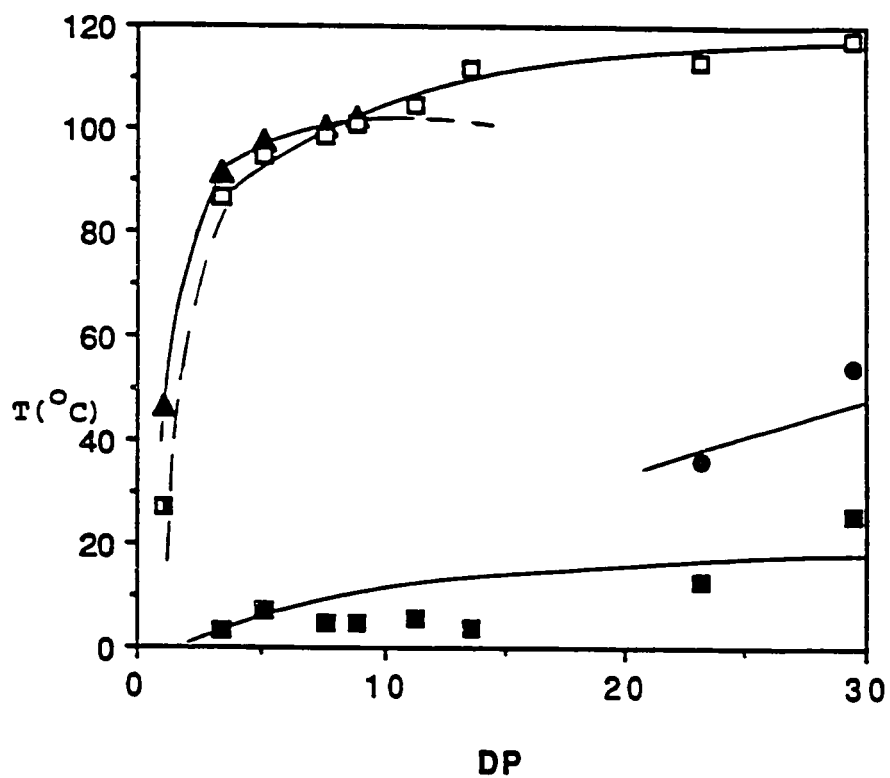


Figure 7c. The dependence of the phase transition temperatures on the degree of polymerization of poly(6-6). DP=1 corresponds to 8-6 (data from first cooling scan): ■-T_g; □-T_{sA-n} or T_{sA-i}; ▲-T_{n-i}; ●-T_{sX-sA}; ■-T_m.

degree of polymerization equal to 1. The plots from Figure 7 demonstrate a clear trend. Both the nematic-isotropic and the s_A -nematic or s_A -isotropic as well as their reversed transition temperatures display continuous dependences of polymerization degree. Let us assume that 8-6 displays a virtual s_A mesophase. Under these conditions, the dependence of the nematic-isotropic transition temperature versus polymerization degree has a higher slope than the dependence of the s_A -nematic, s_A -isotropic transition temperature versus polymerization degree. Above the degree of polymerization where these two dependences intersect each other, the nematic mesophase should appear below the s_A mesophase and therefore it becomes "virtual". This behavior can explain the change of the highest temperature mesophase from nematic to smectic upon increasing the degree of polymerization.

It is generally accepted that many nematic monomers lead to smectic side chain liquid crystalline polymers.¹⁸ However, it is not correct to compare the phase behavior of monomers with that of the corresponding polymers since as observed from Figure 2, small changes in the chemical structure of the monomer changes drastically their phase behavior. Most frequently, the mesomorphic behavior of the monomer is different from that of the model compound of the monomeric structural unit as described in previous chapter. To our knowledge, this is the first time when is experimentally observed that the change of the mesophase of the monomeric structural unit represents a continuous dependence of molecular weight. Such a dependence was previously demonstrated only for the case of a main chain liquid crystalline polymer.²⁰

REFERENCES

1. V. Percec and A. Keller, *Macromolecules*, **23**, 4347 (1990)
2. A. Keller, G. Ungar and V. Percec, in "Advances in Liquid Crystalline Polymers", C. K. Ober and R. A. Weiss, Eds., ACS Symposium Series 435; Washington D.C., p.308 (1990)
3. V. Shibaev, *Mol. Cryst. Liq. Cryst.*, **155**, 189 (1988)
4. T. Sagane and R. W. Lenz, *Polym. J.*, **20**, 923 (1988)
5. T. Sagane and R. W. Lenz, *Polymer*, **30**, 2269 (1989)
6. T. Sagane and R. W. Lenz, *Macromolecules*, **22**, 3763 (1989)
7. J. E. McKeon and P. Fitton, *Tetrahedron*, **28**, 233 (1972)
8. C. S. Hsu, J. M. Rodriguez-Parada and V. Percec, *J. Polym. Sci. Part A: Polym. Chem.*, **25**, 2425 (1987)
9. G. W. Gray, H. J. Harrison, J. A. Nash, J. Constant, D. S. Hulme, J. Kirton and E. P. Raynes, in "Ordered Fluids and Liquid Crystals", Vol. II, R. S. Porter and J. F. Johnson, Eds., Plenum, New York, 1974, p.617
10. J. E. McKeon, P. Fitton and A. A. Griswold, *Tetrahedron*, **28**, 227 (1972)
11. J. M. Rodriguez-Parada and V. Percec, *J. Polym. Sci:Part A: Polym. Chem.*, **24**, 1363 (1986)
12. R. Rodenhouse, V. Percec and A. E. Feiring, *J. Polym. Sci: Part C: Polym. Lett.*, **28**, 345 (1990)
13. T. Higashimura, S. Aoshima and M. Sawamoto, *Makromol. Chem., Macromol. Symp.*, **13/14**, 457 (1988)
14. M. Sawamoto, S. Aoshima and T. Higashimura, *Makromol. Chem., Macromol. Symp.*, **13/14**, 513 (1988)
15. T. Higashimura and M. Sawamoto, in "Comprehensive Polymer Science", Vol.3, G. Allen and J. Bevington Eds., Pergamon Press, Oxford, 1989, p.684
16. C. G. Cho, B. A. Feit and O. W. Webster, *Macromolecules*, **23**, 1918 (1990)
17. C. H. Lin and K. Matyjaszewski, *Polym. Prepr., Am. Chem. Soc.*, **31**(1), 599 (1990)

18. V. Percec and C. Pugh, in "Side Chain Liquid Crystal Polymers", McArdle, C. B. Ed., Chapman and Hall, New York, 1989, p. 30 and references cited therein
19. R. S. Kumar, S. B. Clough and A. Blumstein, *Mol. Cryst. Liq. Cryst.*, **157**, 387 (1988)
20. V. Percec, D. Tomazos and C. Pugh, *Macromolecules*, **22**, 3259 (1989)
21. M. Warner, In "Side Chain Liquid Crystal Polymers" C. B. McArdle Ed., Chapman and Hall, New York, 1989, p 7 and references cited therein.
22. C. Noel, In "Side Chain Liquid Crystal Polymers", C. B. McArdle Ed., Chapman and Hall, New York, 1989, p 159.
23. G. Pepy, J. P. Cotto, F. Hardouin, P. Keller, M. Lambert, F. Mousa, L. Noirez, A. Lapp and C. Strazzielle, *Makromol. Chem. Macromol. Symp.*, **15**, 251 (1988)
24. Percec, V. Tomazos, D. *Polymer*, **31**, 1658 (1990)

Chapter 5

INFLUENCE OF MOLECULAR WEIGHT ON THE PHASE TRANSITIONS OF POLY{ ω -[(4-CYANO-4'-BIPHENYL)OXY]ALKYL VINYL ETHER}S WITH NONYL, HEPTYL AND PENTYL ALKYL GROUPS

5.1.-INTRODUCTION

Several polymerization methods were investigated in order to develop living polymerization procedures for the preparation of side chain liquid crystalline polymers with well defined molecular weight and narrow molecular weight distribution. They include cationic polymerization of mesogenic vinyl ethers,^{1,2} group transfer polymerization of mesogenic methacrylates,³ and polymerization of methacrylates with methyl aluminum porphyrin catalysts.⁴ Cationic polymerization has been proved to be the most successful since it can be used to polymerize mesogenic vinyl ethers containing a large variety of functional groups.⁵⁻¹⁵ The results described in previous chapters have also shown that cationic polymerization of ω -[(4-cyano-4'-biphenyl)oxy]alkyl vinyl ethers with alkyl groups 8 to 11 follows a living mechanism and have demonstrated that the phase behavior of the resulting polymers is molecular weight dependent.

It is known that the highly polar cyano group attached to one end of the biphenyl group causes the formation of an antiparallel near-neighbor pairing that may result in partial bilayer smectic A phase (s_{Ad}). In that type of structure, it may exhibit unusual smectic A-reentrant nematic transition. Since the reentrant nematic phase (n_{re}) was discovered in 1975 in low molar mass liquid crystals,¹⁶ it received substantial theoretical and experimental interest.¹⁷ The first side chain liquid crystalline polymer exhibiting a n_{re} phase was reported in 1986.^{18,19} This polymer was based on a

polyacrylate backbone, six methylenic units in the flexible spacer, and 4-cyano-4'-oxybiphenyl side groups. In the mean time, several other polyacrylates containing mesogenic units with cyano groups and spacer lengths with five or six atoms were reported to exhibit the unusual i - n - s_{Ad} - n_{re} sequence.¹⁹⁻²⁵

The most probable mechanism for the generation of a n_{re} phase is presented in Figure 1.^{17d} The most stable s_A phase of mesogens containing cyano groups is based on layers containing dimers of mesogens. On cooling, the nematic phase formed directly from the isotropic phase contains both dimeric mesogens and monomeric mesogens and so does the first s_A phase. In order to go from less ordered s_A phase to the s_A phase based on dimeric mesogens, a n_{re} phase is required (Figure 1).

This chapter describes the synthesis, the living cationic polymerization and the phase behavior of the resulting polymers of the following three monomers from the series of ω -[(4-cyano-4'-biphenyl)oxy]alkyl vinyl ethers, i.e., synthesis of 9-[(4-cyano-4'-biphenyl)oxy]nonyl vinyl ether (6-9), 7-[(4-cyano-4'-biphenyl)oxy]heptyl vinyl ether (6-7) and 5-[(4-cyano-4'-biphenyl)oxy]pentyl vinyl ether (6-5). Therefore, this chapter will elucidate the phase behavior of the polymers with medium length spacers containing an odd number of methylene units.

5.2.-EXPERIMENTAL

5.2.1-Materials

4-Cyano-4'-hydroxybiphenyl of higher purity than 99.9% and 1,10-phenanthroline palladium (II) diacetate were synthesized as described previously.^{13,18} Methyl sulfide (anhydrous, 99%, Aldrich) was refluxed over 9-borabicyclo[3.3.1]nonane (crystalline, 98%, Aldrich) and then distilled under argon. Dichloromethane (99.6%, Aldrich) used as polymerization solvent was first washed

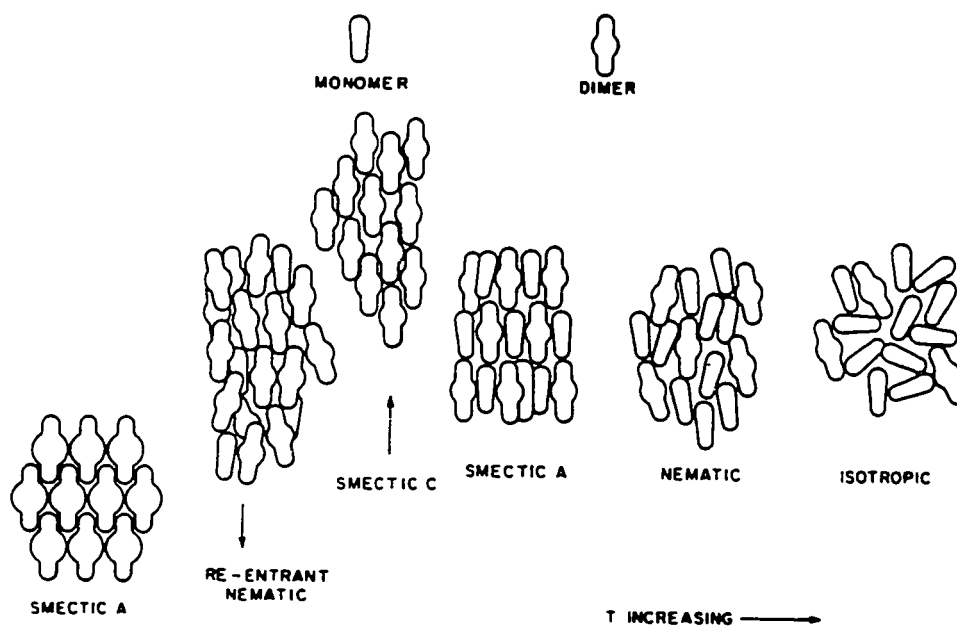


Figure 1. The mechanism of formation of the re-entrant nematic (n_{re}) mesophase.

with concentrated sulfuric acid, then with water, dried over magnesium sulfate, refluxed over calcium hydride and freshly distilled under argon before each use. Trifluoromethane sulfonic acid (triflic acid, 98%, Aldrich) was distilled under vacuum. 7-Bromoheptanol (95%, Aldrich), 5-bromovaleric acid (97%, Aldrich) and the other reagents were used as received.

5.2.2. Synthesis of Monomers

Scheme I outlines the general methods used in the synthesis of monomers and model compounds.

Synthesis of 4-cyano-4'-(9-hydroxynonan-1-yloxy)biphenyl (7-9)

4-Cyano-4'-hydroxybiphenyl (4.37 g, 0.0224 mol) and potassium carbonate (9.29 g, 0.067 mol) were added to a mixture of acetone-DMSO (10:1) (110 ml). 9-Bromononan-1-ol (5 g, 0.0224 mol) was added to the resulting solution which was heated to reflux for 24 hr. After cooling, the mixture was poured into water and then filtered. The obtained solid was recrystallized from methanol and then benzene, to yield 5.6 g (74.1%) of white crystals. mp, 81.4°C, T_{n-i} , 98.9°C (DSC). $^1\text{H-NMR}$ (CDCl_3 , TMS, δ , ppm): 1.01-1.95 (14 protons, $-(\text{CH}_2)_7-$, m), 3.65 (2 protons, $-\text{CH}_2\text{OH}$, t), 4.00 (2 protons, PhOCH_2- , t), 7.00 (2 aromatic protons, o to alkoxy, d), 7.51 (2 aromatic protons, m to alkoxy, d), 7.66 (4 aromatic protons, o and m to-CN, d of d).

Synthesis of 9-[4-(4-cyano-4'-biphenyl)oxy]nonyl vinyl ether (6-9)

4-Cyano-4'-(9-hydroxynonan-1-yloxy)biphenyl (4.0 g, 0.012 mol) was added to a mixture of 1,10-phenanthroline palladium (II) diacetate (0.48 g, 1.2 mmol), n-

Scheme 1: Synthesis of monomers and model compounds.

butyl vinyl ether (64.6 ml) and dry chloroform (17.1 ml). The mixture was heated to 60°C for 6 hr. After cooling, it was filtered to remove the catalyst and the solvent was distilled in a rotavapor. The product was purified by column chromatography (silica gel, CH₂Cl₂ eluent) and then recrystallized from n-hexane to yield 3.6 g (83.6%) of white crystals. Purity: 99.6% (HPLC). mp, 63.1°C (DSC). ¹H-NMR (CDCl₃, TMS, δ, ppm): 1.05-1.95 (16 protons, -(CH₂)₇-, m), 3.68 (2 protons, -CH₂O-, t), 4.01 (3 protons, -OCH=CH₂ trans and PhOCH₂-, m), 4.13 and 4.22 (1 proton, -OCH=CH₂ cis, d), 6.50 (1 proton, OCH=CH₂, q), 7.02 (2 aromatic protons, o to alkoxy, d), 7.56 (2 aromatic protons, m to alkoxy, d), 7.69 (4 aromatic protons, o and m to-CN, d of d).

Synthesis of 9-[(4-cyano-4'-biphenyl)oxy]nonyl ethyl ether (8-9)

4-Cyano-4'-(9-hydroxynonan-1-yloxy)biphenyl (0.5 g, 1.48 mmol) was added to a solution containing potassium t-butoxide (0.166 g, 1.48 mmol), a catalytic amount of 18-crown-6 and dry tetrahydrofuran (10 ml). Diethyl sulfate (0.197 ml, 1.5 mmol) was added and the reaction mixture was refluxed for 4 hr under argon. After cooling, the reaction mixture was poured into chloroform. The chloroform solution was extracted with 10% aqueous KOH, washed with water, dried over magnesium sulfate and the solvent was removed in a rotavapor. The resulting product was purified by column chromatography (silica gel, CH₂Cl₂ eluent) and then was recrystallized from methanol to yield 0.32 g (59.2%) of white crystals. Purity: 99% (HPLC). mp, 75.4°C (DSC). ¹H-NMR (CDCl₃, TMS, δ, ppm): 1.19 (3 protons, -OCH₂CH₃, t), 1.29-1.98 (14 protons, -(CH₂)₇-, m), 3.40 (4 protons, CH₂OCH₂CH₃, m), 4.01 (2 protons, PhOCH₂, t), 7.01 (2 aromatic protons, o to alkoxy, d), 7.50 (2 aromatic protons, m to alkoxy, d), 7.65 (4 aromatic protons, o and m to -CN, d of d).

Synthesis of 4-cyano-4'-(7-hydroxyheptan-1-yloxy)biphenyl (7-7)

4-Cyano-4'-hydroxybiphenyl (5.0 g, 0.0256 mol) and potassium carbonate (10.61 g, 0.0768 mol) were added to a mixture of acetone-DMSO (10:1) (110 ml). 7-Bromoheptan-1-ol (5 g, 0.0256 mol) was added to the resulting solution which was heated to reflux for 24 hr. After cooling, the mixture was poured into water and then filtered. The obtained solid was recrystallized from methanol and then benzene, to yield 5.5 g (69.4%) of white crystals. mp, 76.9°C, T_{n-i} , 103.2°C (DSC). $^1\text{H-NMR}$ (CDCl_3 , TMS, δ , ppm): 1.10-1.95 (10 protons, $-(\text{CH}_2)_5-$, m), 3.67 (2 protons, $-\text{CH}_2\text{OH}$, t), 4.00 (2 protons, PhOCH_2- , t), 7.02 (2 aromatic protons, o to alkoxy, d), 7.52 (2 aromatic protons, m to alkoxy, d), 7.67 (4 aromatic protons, o and m to-CN, d of d).

Synthesis of 7-[(4-cyano-4'-biphenyl)oxy]heptyl vinyl ether (6-7)

4-Cyano-4'-(7-hydroxyheptan-1-yloxy)biphenyl (3.0 g, 9.7 mmol) was added to a mixture of 1,10-phenanthroline palladium (II) diacetate (0.39 g, 0.97 mmol), n-butyl vinyl ether (52.9 ml) and dry chloroform (14 ml). The mixture was heated to 60°C for 6 hr. After cooling and filtration (to remove the catalyst) the solvent was distilled in a rotavapor and the product was purified by column chromatography (silica gel, CH_2Cl_2 eluent) and then recrystallized from n-hexane to yield 2.8 g (86.2%) of white crystals. Purity: 99.5% (HPLC). mp, 58.7°C (DSC). $^1\text{H-NMR}$ (CDCl_3 , TMS, δ , ppm): 1.10-1.95 (10 protons, $-(\text{CH}_2)_5-$, m), 3.69 (2 protons, $-\text{CH}_2\text{O}-$, t), 4.01 (3 protons, $-\text{OCH}=\text{CH}_2$ trans and PhOCH_2- , m), 4.14 and 4.21 (1 proton, $-\text{OCH}=\text{CH}_2$ cis, d), 6.53 (1 proton, $\text{OCH}=\text{CH}_2$, q), 7.01 (2 aromatic protons, o to alkoxy, d), 7.51

(2 aromatic protons, m to alkoxy, d), 7.66 (4 aromatic protons, o and m to-CN, d of d).

Synthesis of 7-[4-cyano-4'-biphenyl]oxy]heptyl ethyl ether (8-7)

4-Cyano-4'-(7-hydroxyheptan-1-yloxy)biphenyl (1.0 g, 3.23mmol) was added to a solution containing potassium t-butoxide (0.36 g, 3.23 mmol), a catalytic amount of 18-crown-6 and dry tetrahydrofuran (20 ml). Diethyl sulfate (0.44 ml, 3.35 mmol) was added and the reaction mixture was refluxed for 4 hr under argon. After cooling, the reaction mixture was poured into chloroform. The chloroform solution was extracted with 10% aqueous KOH, washed with water, dried over magnesium sulfate and the solvent was removed in a rotavapor. The resulting product was purified by column chromatography (silica gel, CH₂Cl₂ eluent) and then was recrystallized from methanol to yield 0.62 g (52.8%) of white crystals. Purity: 99% (HPLC). mp, 56.0°C (DSC). ¹H-NMR (CDCl₃, TMS, δ, ppm): 1.20 (3 protons, -OCH₂CH₃, t), 1.26-1.90 (10 protons, -(CH₂)₅-, m), 3.48 (4 protons, CH₂OCH₂CH₃, m), 4.02 (2 protons, PhOCH₂, t), 7.01 (2 aromatic protons, o to alkoxy, d), 7.50 (2 aromatic protons, m to alkoxy, d), 7.67 (4 aromatic protons, o and m to -CN, d of d).

Synthesis of 5-bromopentan-1-ol

A solution of 1-bromovaleric acid (15.0 g, 0.083 mol) in dry tetrahydrofuran (190 ml) was added dropwise into an ice cooled solution of borane/THF complex (1M) (155 ml). The reaction mixture was stirred at 0°C for 2 hr, allowed to come to room temperature, stirred 15 more hrs, and the mixture was again cooled with ice. Water was added dropwise to the ice cooled reaction mixture. Afterwards, a saturated aqueous K₂CO₃ solution was added to the reaction mixture which separates into two layers. The

aqueous layer was extracted two times with tetrahydrofuran, the organic layers were combined, dried over anhydrous magnesium sulfate and the solvent was removed on a rotavapor to yield 13.3 g (96%) of liquid. Purity: 100% (IR and NMR). $^1\text{H-NMR}$ (CDCl_3 , TMS, δ , ppm): 1.57 (4 protons, $\text{BrCH}_2\text{CH}_2\text{CH}_2-$, m), 1.90 (2 protons, $-\text{CH}_2\text{CH}_2\text{OH}$, m), 3.43 (2 protons, BrCH_2- , t), 3.67 (2 protons, $-\text{CH}_2\text{OH}$, t).

4-Cyano-4'-(5-hydroxypentan-1-yloxy)biphenyl (7-5)

Sodium metal (1.229g, 0.0534 mol) was dissolved in 305 ml of absolute ethanol, then 4-cyano-4'-hydroxybiphenyl (10.43 g, 0.0534 mol) was added, and the mixture was stirred for 45 minutes at room temperature. The ethanol was removed in a rotavapor to leave the salt. Dried N-methyl-pyrrolidinone (25 ml) and 5-bromo-1-pentanol (8.93g, 0.0535 mol) were added, and the mixture was heated at 110 °C for 30 hours. After cooling, the reaction mixture was poured into water and the precipitate was dissolved in CHCl_3 and washed with dilute NaOH and water. It was purified by column chromatography (silica gel, ethyl acetate/hexanes 6/4 eluent), and then it was recrystallized from chloroform to yield 7.53g (50.1%) of white crystals. Purity: 99.9% (HPLC). mp, 95.4°C (DSC). $^1\text{H-NMR}$ (CDCl_3 , TMS, δ , ppm): 1.64-1.86 (6 protons, $-(\text{CH}_2)_3-$, m), 3.71 (2 protons, $-\text{CH}_2\text{OH}$, t), 4.03 (2 protons, PhOCH_2- , t), 6.99 (2 aromatic protons, o to alkoxy, d), 7.54 (2 aromatic protons, m to alkoxy, d), 7.66 (4 protons, o and m to -CN, d of d).

5-[4-Cyano-4'-biphenyl)oxylpentyl vinyl ether (6-5)

4-Cyano-4'-(4-hydroxypentan-1-yloxy)biphenyl (2.80g, 9.95 mmol) was added to a mixture of 1,10-phenanthroline palladium (II) diacetate (0.193g, 0.477 mmol), n-butyl vinyl ether (45 ml, 0.348 mol), and dry chloroform (15 ml). The

mixture was heated to 60°C for 18 hours. After cooling and filtration (to remove the catalyst) the solvent was distilled in a rotavapor and the product was purified by column chromatography (silica gel, CH₂Cl₂ and then petroleum ether/ethyl ether=6/4 eluent) to yield 2.80g (91%) of white crystals. Purity: 99% (HPLC). mp, 52.4°C (DSC). ¹H-NMR (CDCl₃, TMS, δ, ppm): 1.57-1.93 (6 protons, -(CH₂)₃-, m), 3.73 (2 protons, -CH₂OCH=CH₂, t), 4.03 (3 protons, -OCH=CH₂ trans and PhOCH₂-, m), 4.15 and 4.22 (1 proton, OCH=CH₂ cis, d), 6.49 (1 proton, OCH=CH₂, q), 6.99 (2 aromatic protons, o to alkoxy, d), 7.53 (2 aromatic protons, m to alkoxy, d), 7.66 (4 aromatic protons, m and o to -CN, d of d).

5-[(4-Cyano-4'-biphenyl)oxy]pentyl ethyl ether (8-5)

4-Cyano-4'-(5-hydroxypentan-1-yloxy)biphenyl (0.4974g, 1.77 mmol) and potassium t-butoxide (0.2105g, 1.782 mmol) were refluxed in dry THF (20 ml) for 75 minutes. A few crystals of 18-crown-6 and diethyl sulfate (0.3017 g, 1.918 mmol) (98%, Aldrich) were added, and the reaction mixture was refluxed for 12 hours. After cooling, the reaction mixture was poured into chloroform. The chloroform solution was extracted with 10% aqueous KOH, washed with water, dried over magnesium sulfate and the solvent was removed in a rotavapor. The resulting product was purified by column chromatography (silica gel, CH₂Cl₂ eluent) to yield 0.26g (48%) white crystals. Purity: 99.85% (HPLC). mp, 53.5°C (DSC). ¹H-NMR (CDCl₃, TMS, δ, ppm): 1.21 (3 protons, OCH₂CH₃, t), 1.60-1.92 (6 protons, -(CH₂)₃-, m), 3.48 (4 protons, CH₂OCH₂CH₃, m), 4.02 (2 protons, PhOCH₂, t), 6.99 (2 aromatic protons, o to alkoxy, d), 7.53 (2 aromatic protons, m to alkoxy, d), 7.66 (4 aromatic protons, o and m to -CN, d of d).

5.2.3.-Cationic Polymerizations

Polymerizations were carried out in glass flasks equipped with teflon stopcocks and rubber septa under argon atmosphere at 0°C for 1 hr. All glassware was dried overnight at 130°C. The monomer was further dried under vacuum overnight in the polymerization flask. Then the flask was filled with argon, cooled to 0°C and the methylene chloride, dimethyl sulfide and triflic acid were added via a syringe. The monomer concentration was about 10 wt% of the solvent volume and the dimethyl sulfide concentration was 10 times larger than that of the initiator. The polymer molecular weight was controlled by the monomer/initiator ($[M]_0/[I]_0$) ratio. After quenching the polymerization with ammoniacal methanol, the reaction mixture was precipitated into methanol. The filtered polymers were dried and precipitated from methylene chloride solutions into methanol until GPC traces showed no traces of monomer. Tables I and II summarize the polymerization results. Although the polymer yields are lower than expected due to losses during the purification process, the conversions were almost quantitative in all cases.

5.3.-RESULTS AND DISCUSSION

Polymerization results are presented in Tables I, II and III. All polymers display a narrow molecular weight distribution. Figure 2 plots the dependences of M_n and M_w/M_n versus $[M]_0/[I]_0$ ratio for poly(6-9). The number average molecular weight (M_n) of poly (6-9) exhibits a linear dependence on $[M]_0/[I]_0$ as shown in Figure 2 although it is relative to polystyrene. Similar plots for poly(6-7) and poly(6-5) demonstrate that within this range of molecular weights the polymerizations of 6-5 and 6-7 show a living character (Tables II and III). The mechanism of this polymerization reaction is outlined in scheme II.

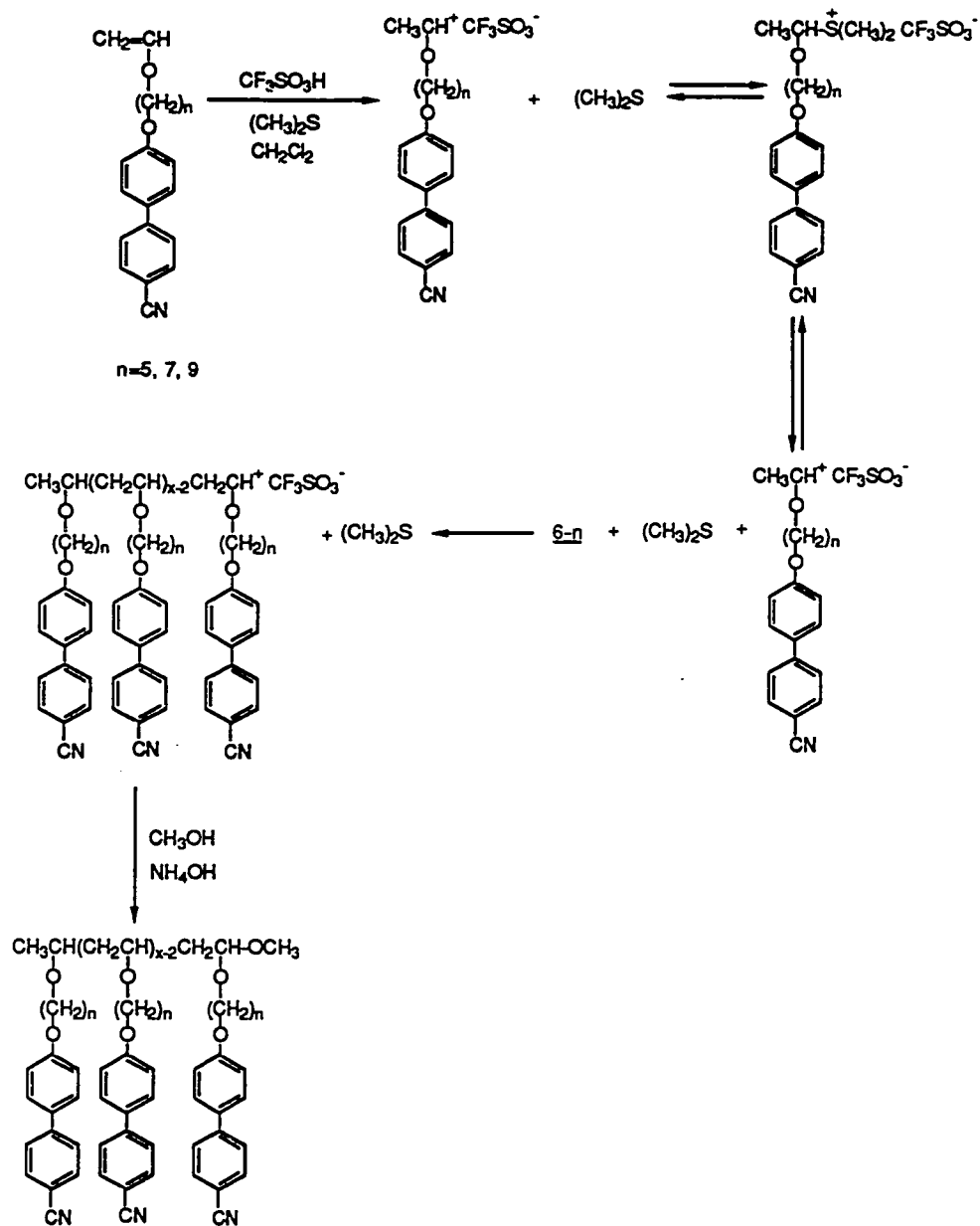
Scheme II. Cationic polymerization of 6-9, 6-7 and 6-5

Table I. Cationic Polymerization of 9-[4-Cyano-4'-biphenyl]oxylnonyl Vinyl Ether (6-9) (polymerization temperature, 0°C; polymerization solvent, methylene chloride; $[M]_0=0.275$; $[(CH_3)_2S]_0/[I]_0=10$; polymerization time, 1hr) and Characterization of the Resulting Polymers. Data on first line are from first heating and cooling scans. Data on second line are from second heating scan.

Sample No.	[M] ₀ /[I] ₀	Polymer yield(%)	G P C		phase transitions (°C) and corresponding enthalpy changes (kcal/mru)		
			Mux.10 ⁻³	Mw/Mn	D P	heating	cooling
1	2	44	0.9	1.54	3	g -1.6 s _A 104.1 (0.70) i g -1.6 s _A 103.8 (0.71) i	i 100.3 (0.71) s _A -6.7 g
2	4	31	1.8	1.13	5	g 5.8 s _A 120.6 (0.67) i g 5.0 s _A 120.2 (0.70) i	i 114.7 (0.69) s _A 0.8 g
3	6	56	2.0	1.24	6	g 11.7 s _A 125.1 (0.60) i g 9.2 s _A 124.4 (0.64) i	i 119.7 (0.64) s _A 3.3 g
4	8	62	2.9	1.07	8	g 10.1 s _A 131.8(0.64) i g 9.4 s _A 131.9 (0.65) i	i 124.3 (0.63) s _A 4.2 g
5	10	68	3.8	1.20	10	g 12.0 s _A 135.9 (0.62) i g 11.1 s _A 135.9 (0.63) i	i 130.0 (0.63) s _A 5.0 g
6	13	63	4.5	1.20	12	g 13.3 s _A 141.5 (0.62) i g 12.5 s _A 141.0 (0.60) i	i 136.7 (0.61) s _A 7.5 g
7	18	65	5.9	1.28	16	g 13.3 s _A 144.7 (0.62) i g 12.7 s _A 144.7 (0.62) i	i 138.7 (0.61) s _A 7.5 g
8	23	69	8.4	1.16	22	g 13.8 s _A 149.9 (0.60) i g 13.0 s _A 150.7 (0.59) i	i 145.8 (0.59) s _A 9.8 g
9	30	74	11.6	1.12	32	g 14.2 s _A 153.8 (0.62) i g 14.2 s _A 153.6 (0.59) i	i 149.0 (0.58) s _A 10.0 g

Table II. Cationic Polymerization of 7-[4-Cyano-4'-biphenyl]heptyl Vinyl Ether (6-7) (polymerization temperature, 0°C; polymerization solvent, methylene chloride; $[M]_0=0.298$; $[(CH_3)_2SiO]/[I]_0=10$; polymerization time, 1hr) and Characterization of the Resulting Polymers. Data on first line are from first heating and cooling scans. Data on second line are from second heating scan.

Sample No.	$[M]_0/[I]_0$	Polymer yield(%)	$M_{nx}10^{-3}$	M_w/M_n	D P	phase transitions(°C) and corresponding enthalpy changes (kcal/mru)	
						heating	cooling
1	2	44	1.1	1.12	3	g 5.3 sA 89.5 (0.43) i g 5.1 sA 89.7 (0.44) i	i 85.8 (0.43) sA 0.1 g
2	4	31	1.7	1.18	5	g 10.8 sA 108.0 (0.42) i g 10.8 sA 108.8 (0.80) i	i 104.6 (0.40) sA 7.1 g
3	6	56	2.3	1.14	7	g 13.2 sA 116.0 (0.39) i g 13.0 sA 116.0 (0.40) i	i 111.3 (0.39) sA 8.6 g
4	8	62	2.4	1.09	8	g 14.3 sA 120.1(0.39) i g 14.1 sA 120.6 (0.39) i	i 115.6 (0.39) sA 9.2 g
5	10	68	2.9	1.05	9	g 15.6 sA 123.1 (0.36) i g 15.6 sA 123.5 (0.74) i	i 117.7 (0.39) sA 10.6 g
6	13	63	4.4	1.16	13	g 17.6 sA 131.3 (0.36) i g 17.6 sA 132.0 (0.37) i	i 127.7 (0.36) sA 12.4 g
7	18	65	5.4	1.34	16	g 19.5 sA 133.0 (0.38) i g 18.8 sA 133.5 (0.71)	i 128.7 (0.36) sA 14.7 g
8	23	69	7.9	1.20	24	g 20.4 sA 137.3 (0.38) i g 20.1 sA 137.6 (0.35) i	i 132.2 (0.36) sA 14.9 g
9	30	74	8.8	1.15	26	g 21.2 sA 140.3 (0.34) i g 20.8 sA 140.8 (0.35) i	i 134.0 (0.34) sA 15.0 g

Table III. Cationic Polymerization of 5-[4-Cyano-4'-biphenyl]oxypentyl Vinyl Ether (6-5) (polymerization temperature, 0°C; polymerization solvent, methylene chloride; $[M]_0=0.325$; $[(CH_3)_2S]_0/[I]_0=10$; polymerization time, 1hr) and Characterization of the Resulting Polymers. Data on first line are from first heating and cooling scans. Data on second line are from second heating scan.

Sample No.	$[M]_0/[I]_0$	Polymer yield(%)	$M_n \times 10^{-3}$	Mw/Mn		D P	phase transitions(°C) and corresponding enthalpy changes (kcal/mru)	
				G	P C		heating	cooling
1	4	76	1.4	1.10	5		g 19.2 n 95.2 (0.11) i g 18.7 n 94.3 (0.15) i	i 91.1 (0.13) n 13.2 g
2	6	79	1.9	1.11	6		g 24.7 n 98.3 (0.14) i g 22.2 n 97.7 (0.14) i	i 93.2 (0.15) n 16.5 g
3	9	82	3.1	1.21	10		g 29.8 n_{re} 55 (-) ^a s _A 80.1 n 100.8 (0.11)* i g 27.5 n_{re} 55 (-) ^a s _A 78.2 n 100.8 (0.12)* i	i 96.5 (0.14)* n 76.0 s _A 55 (-) ^a n _{re} 21.4 g
4	13	87	3.9	1.13	13		g 33.8 n_{re} 60 (-) ^a s _A 90.1 n 104.4 (0.14)* i g 33.2 n_{re} 60 (-) ^a s _A 89.1 n 103.2 (0.13)* i	i 101.4 (0.14)* n 84.2 s _A 60 (-) ^a n _{re} 28.2 g
5	18	82	5.2	1.15	17		g 35.4 n_{re} 65 (-) ^a s _A 95.0 n 112.3 (0.12)* i g 33.8 n_{re} 65 (-) ^a s _A 95.6 n 112.0 (0.13)* i	i 107.1 (0.10)* n 93.3 s _A 65 (-) ^a n _{re} 30.4 g
6	23	85	7.5	1.21	25		g 38.2 n_{re} 68 (-) ^a s _A 99.1 n 113.6 (0.14)* i g 36.8 n_{re} 68 (-) ^a s _A 102.7 n 113.8 (0.14)* i	i 109.6 (0.11)* n 96.3 s _A 68 (-) ^a n _{re} 35.0 g
7	30	88	9.5	1.12	31		g 39.3 n_{re} 69 (-) ^a s _A 104.9 n 115.4 (0.12)* i g 37.5 n_{re} 69 (-) ^a s _A 104.4 n 115.5 (0.10)* i	i 111.7 (0.11)* n 101.8 s _A 69 (-) ^a n _{re} 34.2 g

* overlapped peaks

^a data obtained from optical polarized microscopy

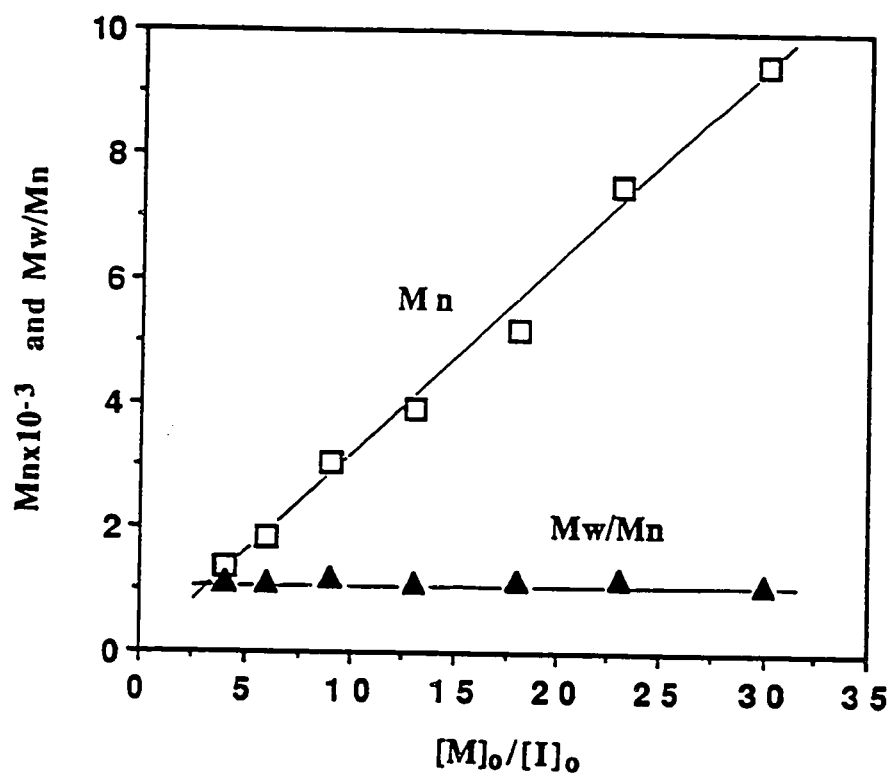


Figure 2. The dependence of the number average molecular weight (M_n) and of the polydispersity (M_w/M_n) of poly(6-5) on the $[M]_0/[I]_0$ ratio.

Figure 3 presents the heating and cooling DSC traces of 7-5, 7-7, 7-9, 6-5, 6-7, 6-9, 8-5, 8-7 and 8-9. As we can observe from this figure, only the alcohol derivatives 7-9, 7-7 and 7-5 display an enantiotropic nematic mesophase. Both the monomers (6-5, 6-7 and 6-9) and the monomeric model compounds (8-5, 8-7 and 8-9) exhibit a monotropic nematic mesophase. The phase transition temperatures and the corresponding thermodynamic parameters of these monomers and models are summarized in Table IV.

The DSC traces obtained during the first and subsequent heating scans are identical for all cases of poly(6-9), poly(6-7) and poly(6-5). The experimental data collected from both scans are reported in Tables I, II and III. However, only second heating and first cooling DSC scans will be presented in more detail. Heating and cooling DSC traces of poly(6-9) with degrees of polymerization from about 3 to 32 are presented in Figure 4. The heating DSC scans are identical irrespective of the thermal history of the sample. Therefore, first, second and subsequent heating scans are identical. The DSC traces obtained from the second heating and first cooling scans are exhibited in Figure 4. However, data collected from both first and second heating scans are presented in Table I and plotted in Figure 5a. The phase transition temperatures determined from the cooling scan are plotted in Figure 5b. Over the entire range of molecular weights, poly(6-9) displays only an enantiotropic s_A mesophase. This mesophase exhibits a classic focal conic fan shaped texture. As we have discussed at the beginning of this section, 8-9 displays both nematic and monotropic s_A mesophases. Since poly(6-9) with a degree of polymerization of about three shows only an enantiotropic s_A phase, it means that the slope of the T_{n-sA} - M_n dependence is higher than that of the T_{n-i} - M_n dependences. The intercept of these two dependences occurs below poly(6-9) reaches a degree of polymerization equal to three. A

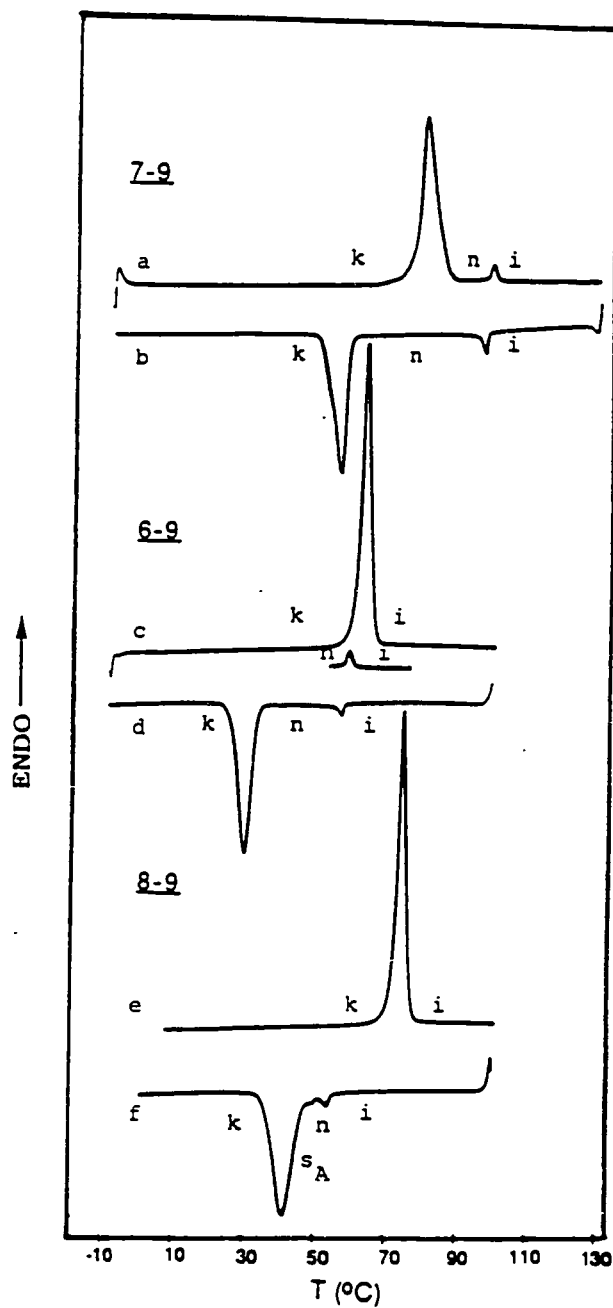
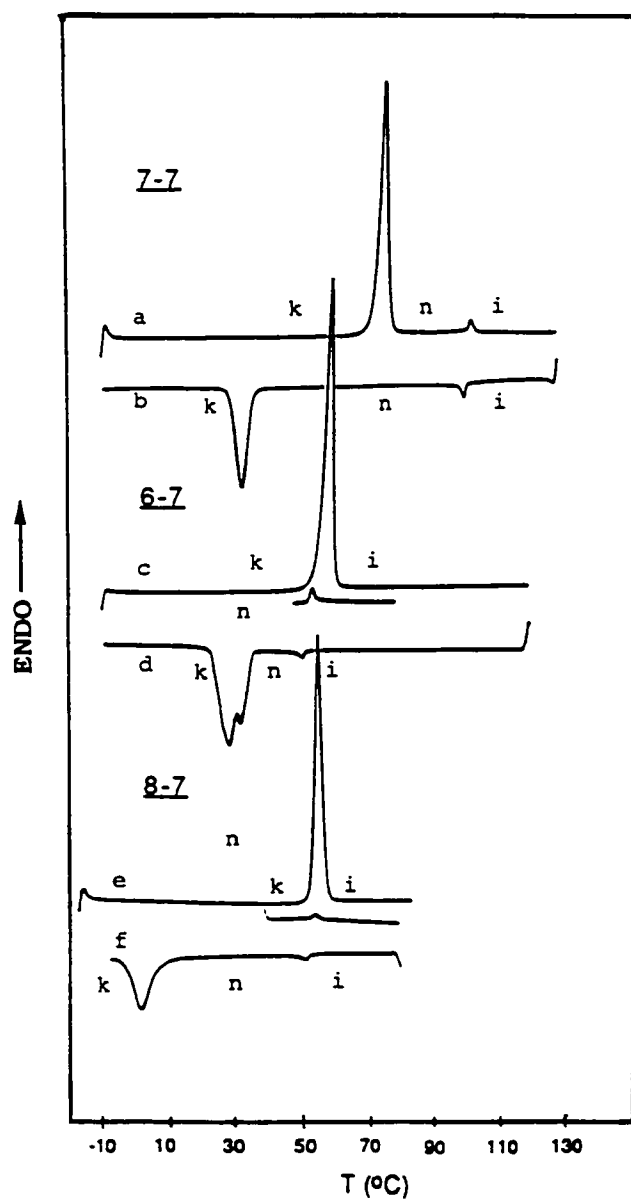


Figure 3a. Heating and cooling DSC scans of 7-9 (a, b), 6-9 (c, d) and 8-9 (e, f).



Figuer 3b. Heating and cooling DSC scans of 7-7 (a, b), 6-7 (c, d) and 8-7 (e, f).

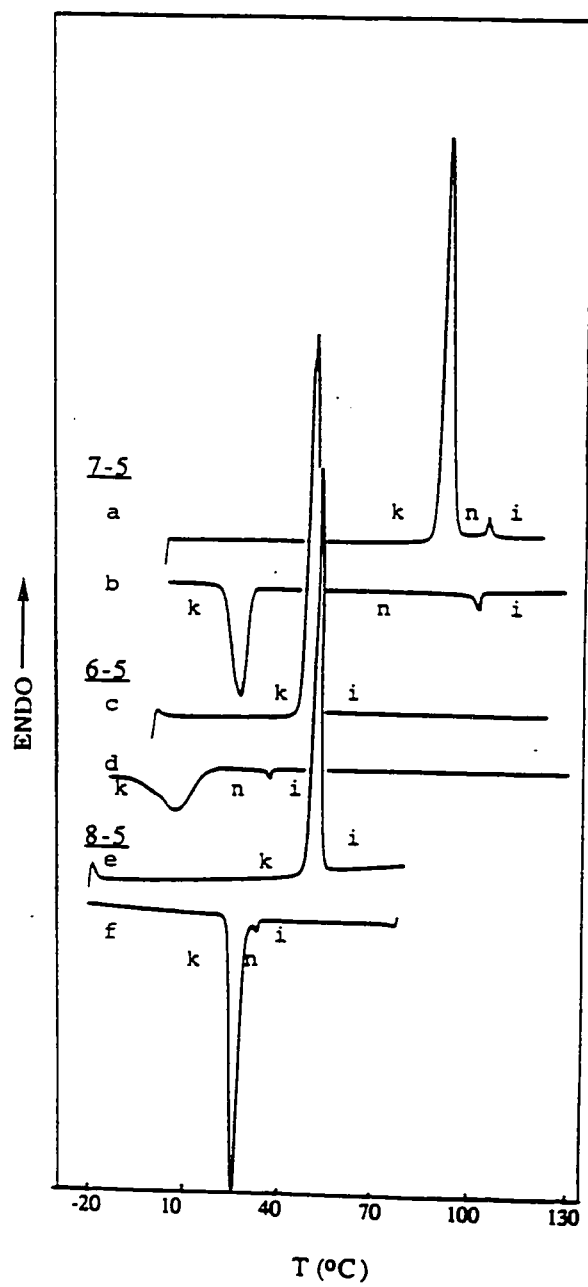


Figure 3c. Heating and cooling DSC scans of 7-5 (a, b), 6-5 (c, d) and 8-5 (e, f).

Table IV. Thermal Characterization of 4-Cyano-4'-(ω -hydroxyalkan-1-yloxy)biphenyls (7-5), (7-7) and (7-9), ω -[(4-Cyano-4'-biphenyl)oxy]alkyl Vinyl Ethers (6-5), (6-7) and (6-9), and of ω -[(4-Cyano-4'-biphenyl)oxy]alkyl Ethyl Ethers (8-5), (8-7) and (8-9).

Compound	phase transitions (0°C) and corresponding enthalpy changes (kcal/mol)	
	heating	cooling
<u>7-5</u>	k 95.5 (7.59) n 108.1 (0.18) i	i 104.4 (0.27) n 28.6 (3.63) k
<u>6-5</u>	k 52.4 (7.94) i	i 38.6 (0.086) n 9.8 (6.20) k
<u>8-5</u>	k 53.5 (6.96) i	i 34.5 (0.050) n 27.6 (5.79) k
<u>7-7</u>	k 95.5 (9.67) n 108.1 (0.18) i	i 100.2 (0.27) n 33.0 (3.96) k
<u>6-7</u>	k 58.7 (9.9) i [n 54.5 (0.21) i]*	i 50.6 (0.17) n 29.4 (7.67) k
<u>8-7</u>	k 56.0 (9.7) i [n 55.4 (0.21)]*	i 50.9 (0.15) n 1.6 (5.56) k
<u>7-9</u>	k 81.4 (9.10) n 98.9 (0.34) i	i 96.0 (0.35) n 54.9 (6.45) k
<u>6-9</u>	k 63.1 (10.20) i [n 59.2 (0.36) i]*	i 56.2 (0.33) n 28.9 (7.31) k
<u>8-9</u>	k 75.4 (10.22) i	i 53.2 (0.29) n 50.3 (-)* s _A 41.3 (8.23)* k

*[] virtual data

* overlapped peaks

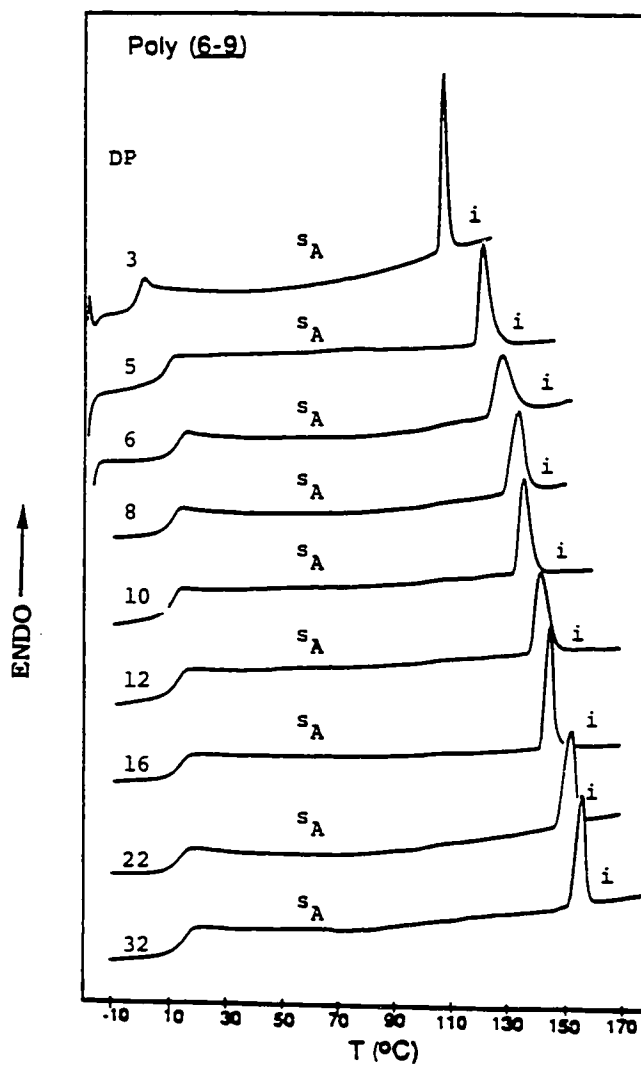


Figure 4a. DSC traces displayed during the second heating scan by poly(6-9) with different degrees of polymerization (DP). DP is printed on the top of each DSC scan.

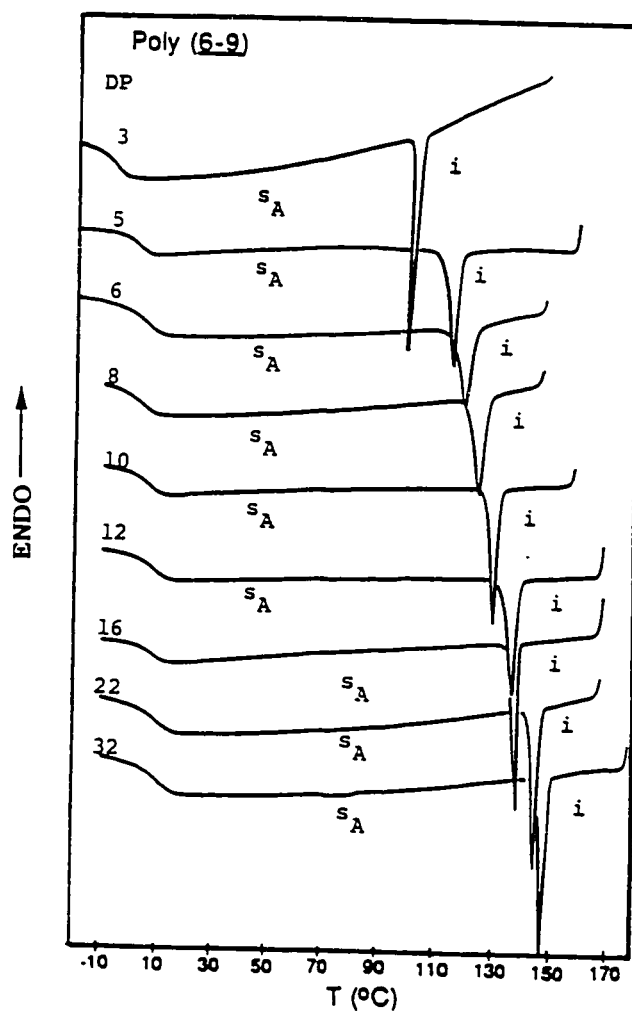


Figure 4b. DSC traces displayed during the first cooling scan by poly(6-9) with different degrees of polymerization (DP). DP is printed on the top of each DSC scan.

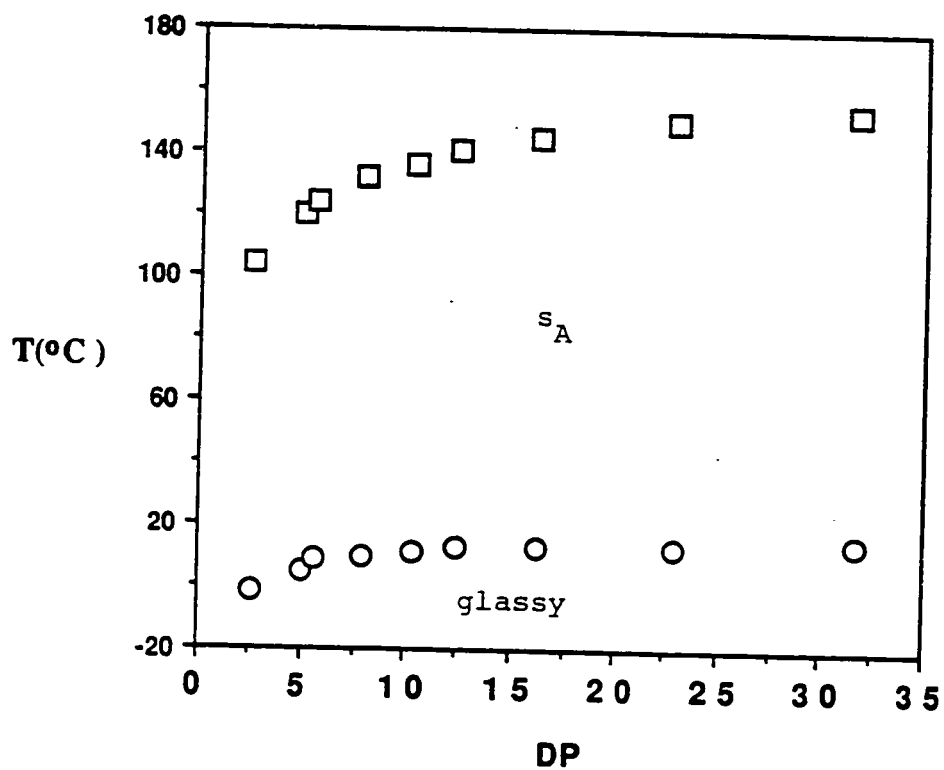


Figure 5a. The dependence of phase transition temperatures on the degree of polymerization of poly(6-9). (data from second heating scan): O- T_g ; \square - T_{S_A-i} .

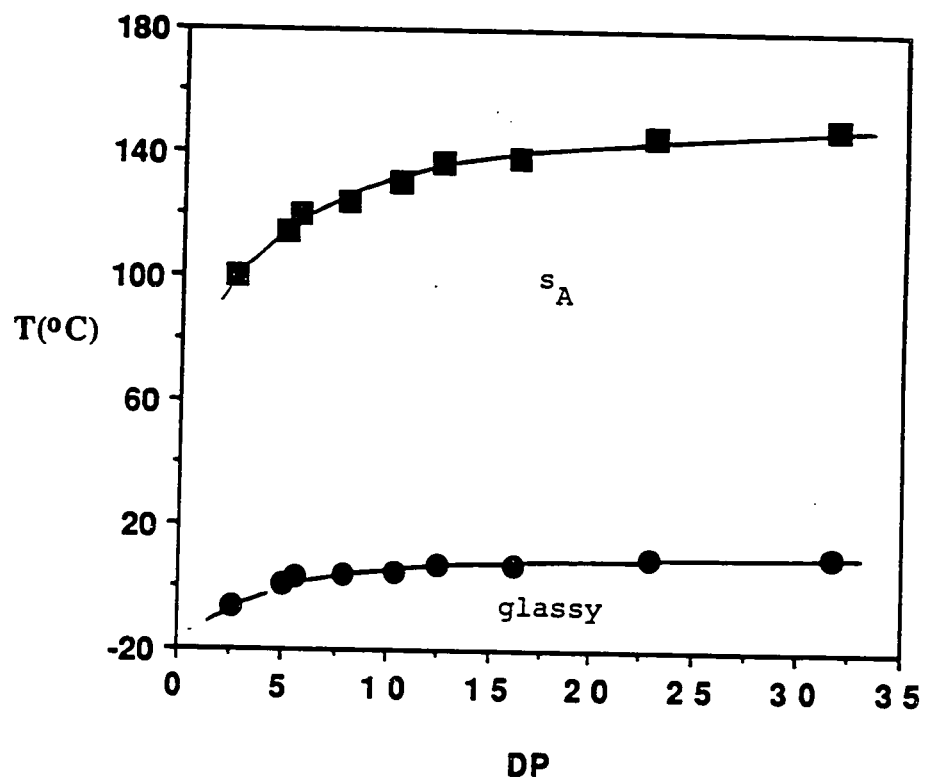


Figure 5b. The dependence of phase transition temperatures on the degree of polymerization of poly(6-9). (data from first cooling scan): ●- T_g ; ■- T_{sA} .

dependence like this, which however was expanding over a larger range of molecular weights was observed for both poly(6-6) and poly(6-8) as described in Chapter III. The overall behavior of poly(6-9) is of interest since this polymer does not present side chain crystallization at any molecular weight (Figure 5a, b).

The DSC traces collected from the second heating scan and first cooling scans of poly(6-7) are presented in Figure 6. The DSC traces of the first, second and subsequent heating scans are identical over the entire range of molecular weights. Poly(6-7) exhibits only an enantiotropic s_A mesophase. The monomeric model compound 7-7 exhibits a monotropic nematic mesophase. Therefore, we can speculate that the change from nematic to s_A occurs at a degree of polymerization between one and 3. The dependences of T_g , T_{s_A-i} and T_{i-s_A} versus molecular weight obtained from the first and second heating, and first cooling scans are summarized in Table II. The corresponding plots for the data obtained from the second heating and first cooling scans are presented in Figure 7.

Figure 8 presents the DSC traces of poly (6-5). Poly(6-5)s with degrees of polymerization below 10 exhibit an enantiotropic nematic mesophase while 7-5, which represents the "polymer" with a degree of polymerization equal to one, displays only a monotropic nematic mesophase. Poly(6-5) with degrees of polymerization from 10 to 30 exhibit enantiotropic nematic and s_A mesophases. The dependence of glass transition and of mesomorphic transition temperatures of poly(6-5) are plotted in Figure 9 as a function of the degree of polymerization. We can observe that the slope of the s_A -nematic versus molecular weight dependence is steeper than that of the nematic-isotropic versus molecular weight dependence. This trend provides a narrowing of the nematic range of poly(6-5) by increasing the degree of polymerization.

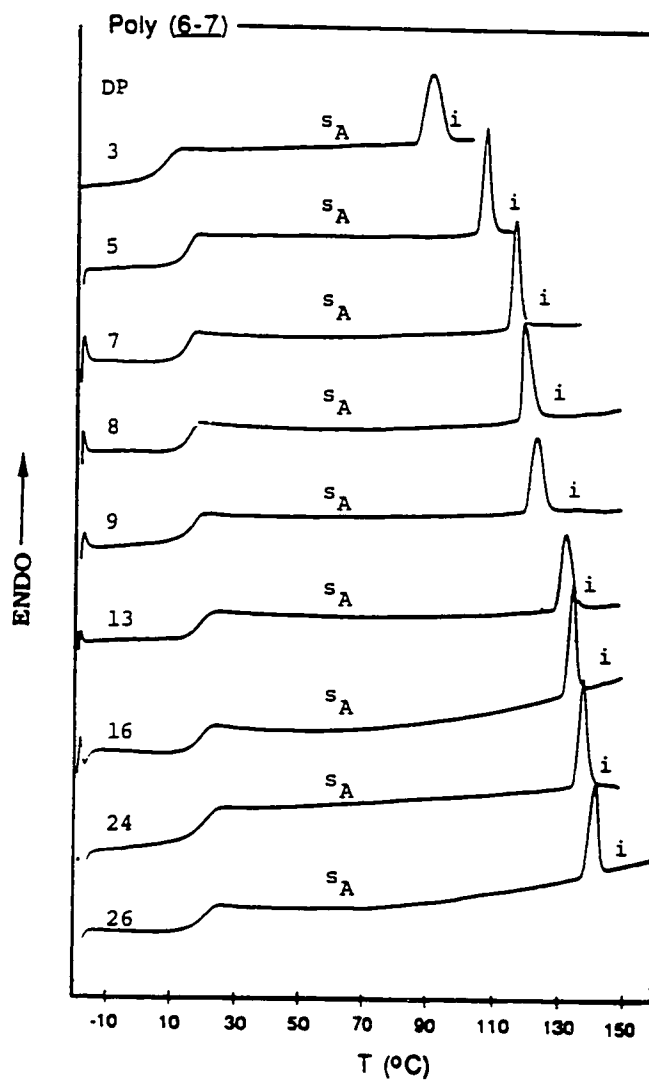


Figure 6a. DSC traces displayed during the second heating scan by poly(6-7) with different degrees of polymerization (DP). DP is printed on the top of each DSC scan.

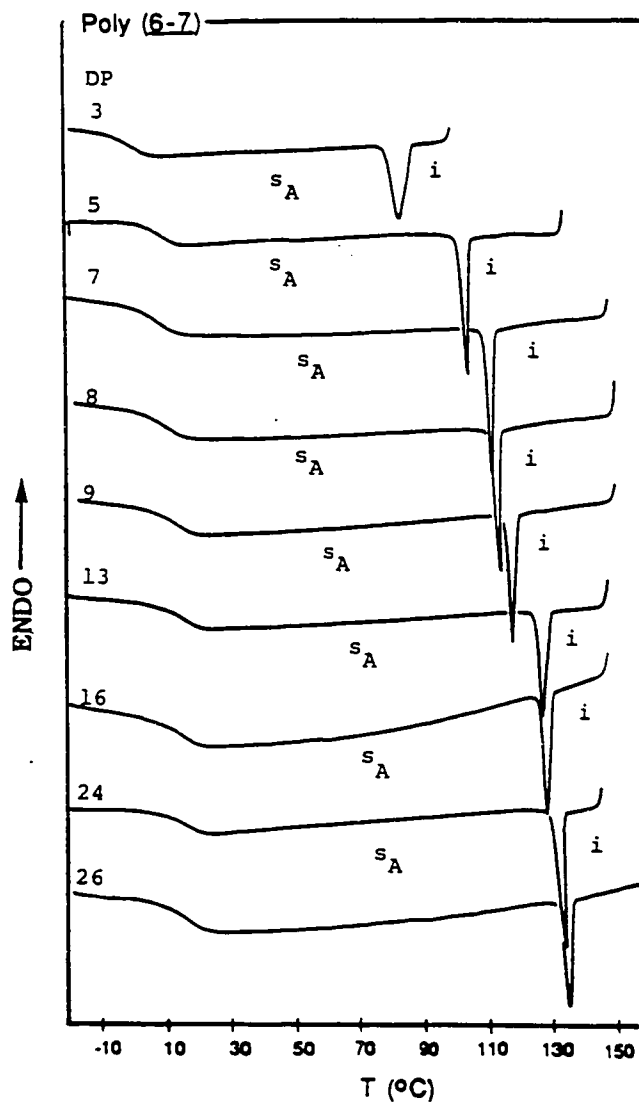


Figure 6b. DSC traces displayed during the first cooling scan by poly(6-7) with different degrees of polymerization (DP). DP is printed on the top of each DSC scan.

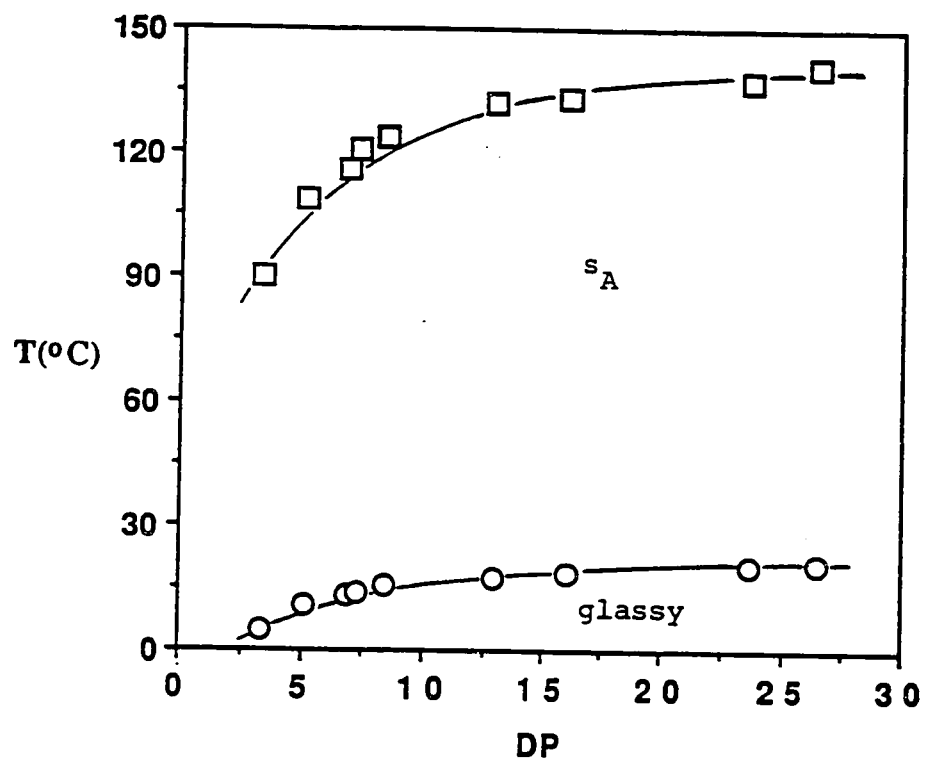


Figure 7a. The dependence of phase transition temperatures on the degree of polymerization of poly(6-7). (data from second heating scan): O- T_g ; □- T_{sA-i} .

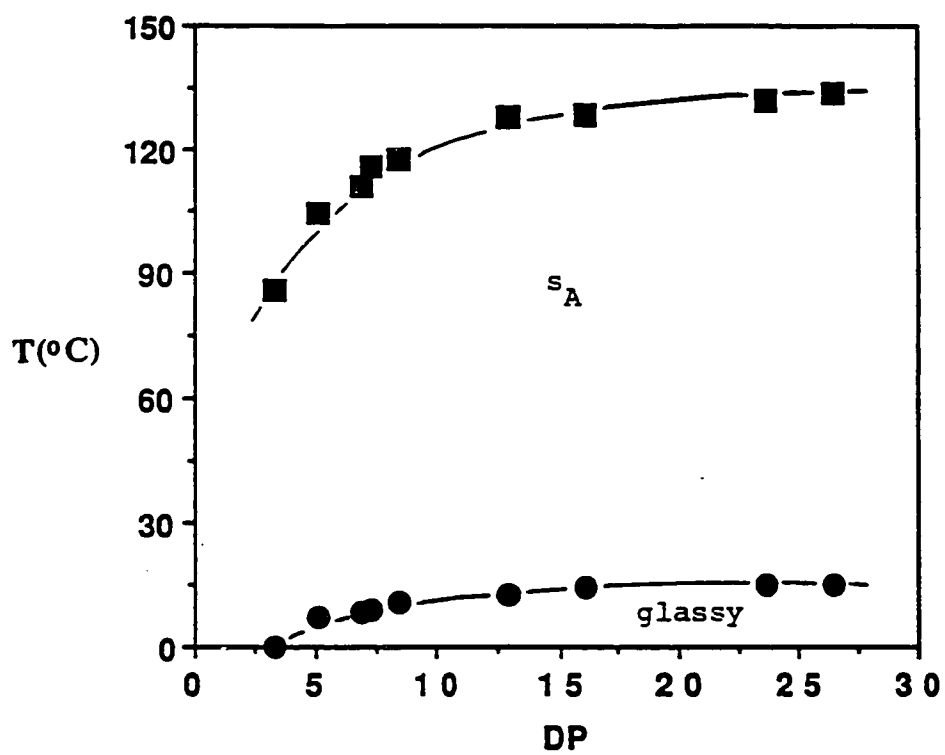


Figure 7b. The dependence of phase transition temperatures on the degree of polymerization of poly(6-7). (data from first cooling scan): ● - T_g ; ■ - T_{i-s_A} .

A n_{re} phase is expected below the s_A phase of these polymers due to the ability of liquid crystalline compounds containing mesogens with cyano groups to generate a s_{Ad} phase below the high temperature n phase as described in the introduction part of this chapter.^{16c,17d} The inspection of poly(6-5) with DP=10 to DP=31 on the optical polarized microscope uncovers a n_{re} mesophase (Figure 9). Although presently we do not have yet definitive evidence from X-ray diffraction experiments, we will assume that the s_A phase from above the n_{re} phase is a s_{Ad} phase. Since the transition from the s_{Ad} to n_{re} and n_{re} to s_{Ad} does not display a first order transition on the DSC curve, this transition was determined by optical polarized microscopy. Representative optical polarized micrographs of the texture exhibited by the high temperature nematic, s_{Ad} and n_{re} phases of poly(6-5) with a degree of polymerization equal to 30 are presented in Figure 10.

In conclusion, poly(6-9) and poly(6-7) that consist of medium length spacers containing an odd number of methylene units do not generate polymorphism at different molecular weights. However, poly(6-5) exhibits unusual $i-n-s_A-n_{re}$ sequence over a broad range of molecular weights. Therefore, poly(6-5) generates rich polymorphism above a certain molecular weight.

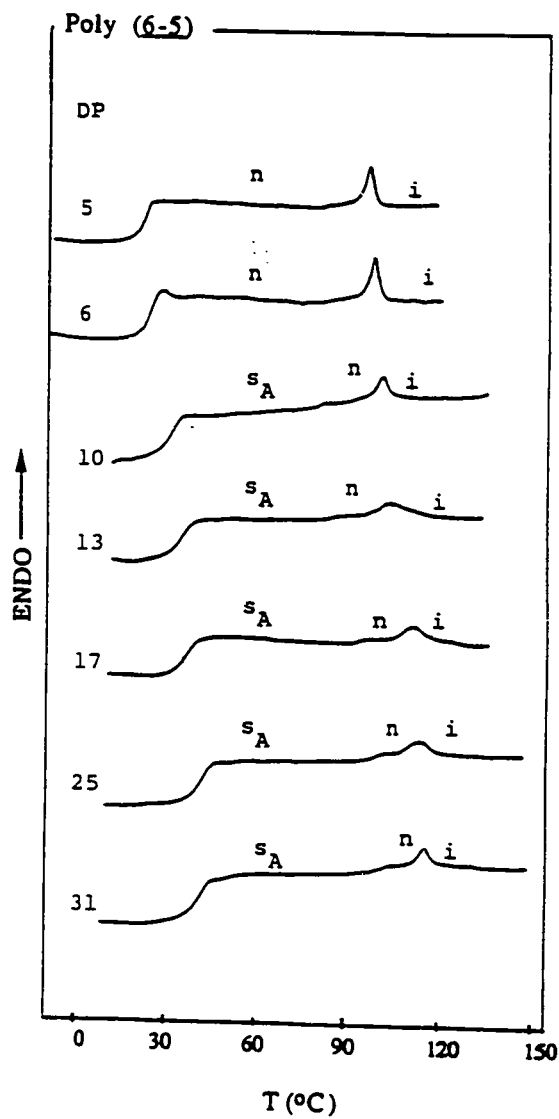


Figure 8a. DSC traces displayed during the second heating scan by poly(6-5) with different degrees of polymerization (DP). DP is printed on the top of each DSC scan.

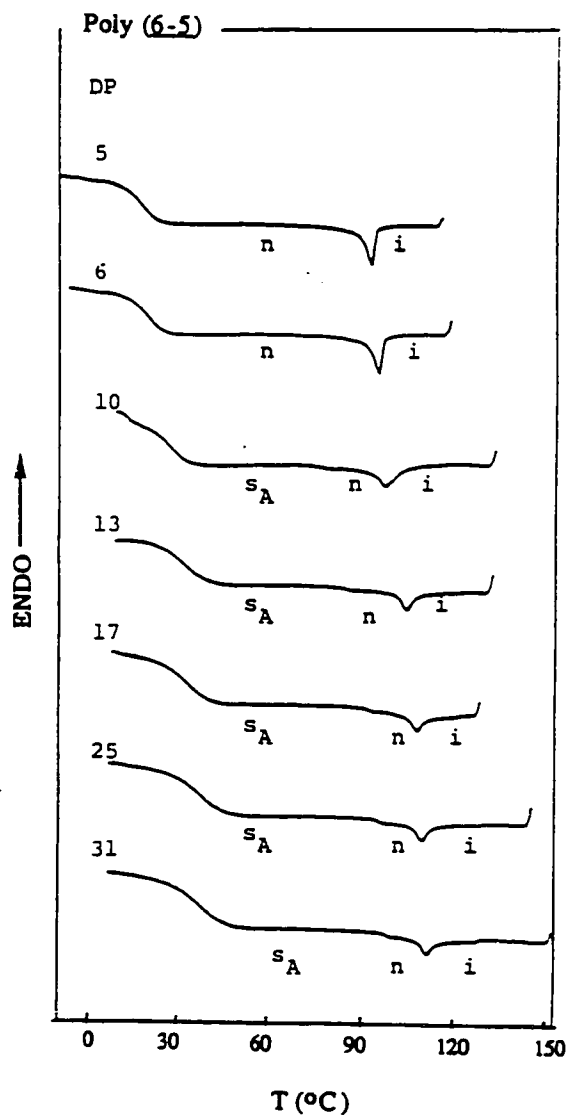


Figure 8b. DSC traces displayed during the first cooling scan by poly(6-5) with different degrees of polymerization (DP). DP is printed on the top of each DSC scan.

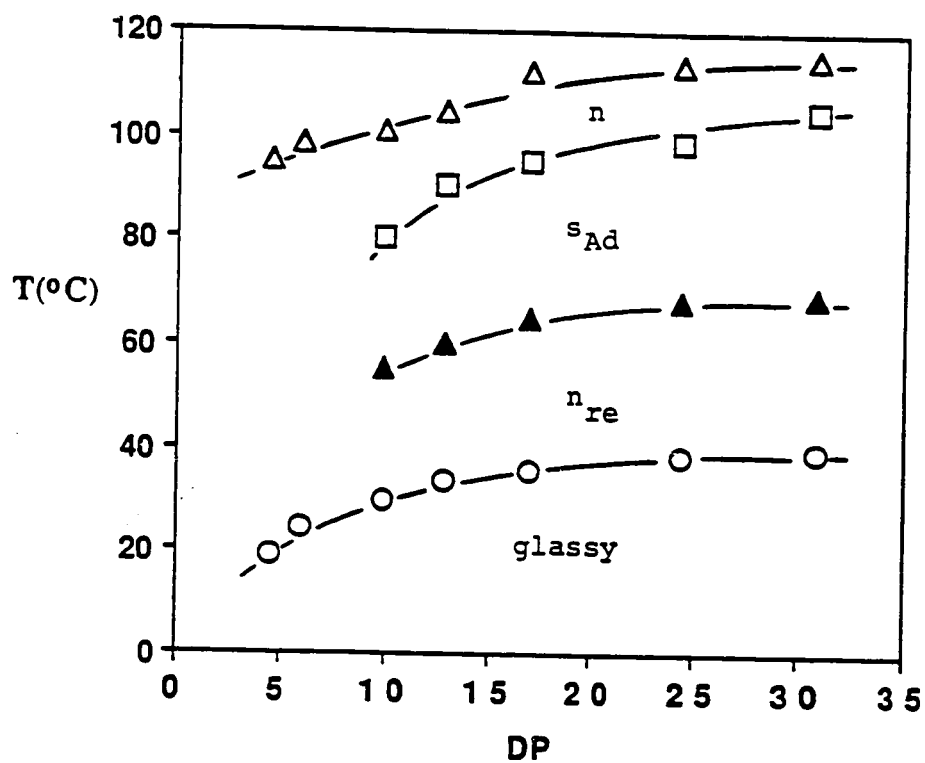


Figure 9a. The dependence of phase transition temperatures on the degree of polymerization of poly(6-5). (data from second heating scan): O- T_g ; ▲- $T_{n-re-sAd}$; □- T_{sAd-n} ; Δ- T_{n-i}

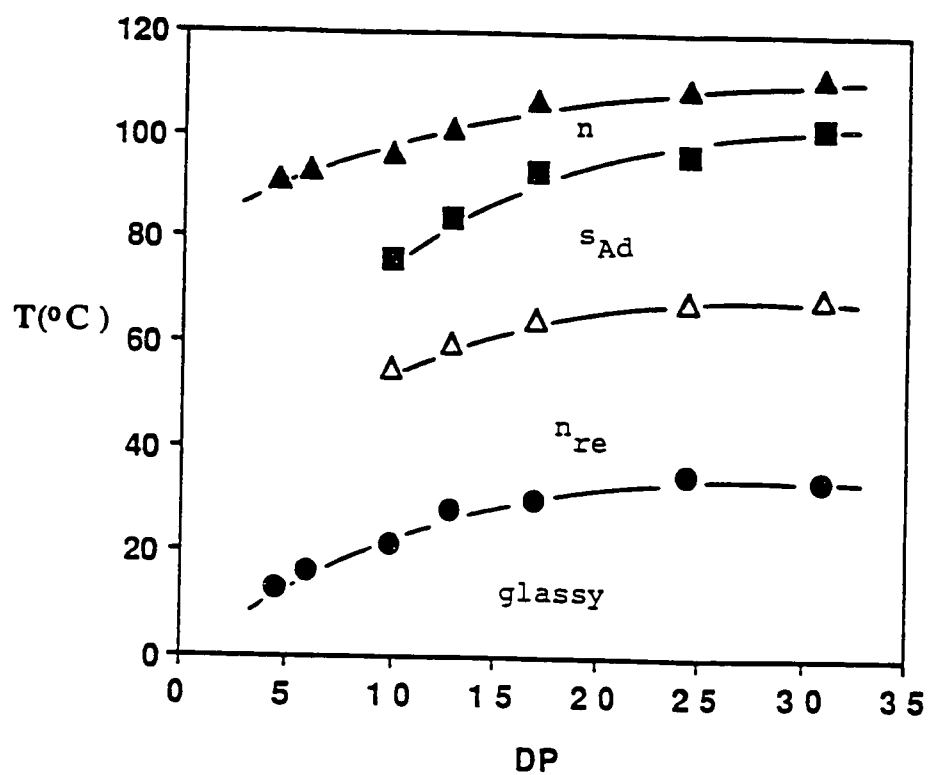


Figure 9b. The dependence of phase transition temperatures on the degree of polymerization of poly(6-5). (data from first cooling scan): \bullet - T_g ; Δ - $T_{sAd-nre}$; \blacksquare - T_{n-sAd} ; \blacktriangle - T_{i-n} .

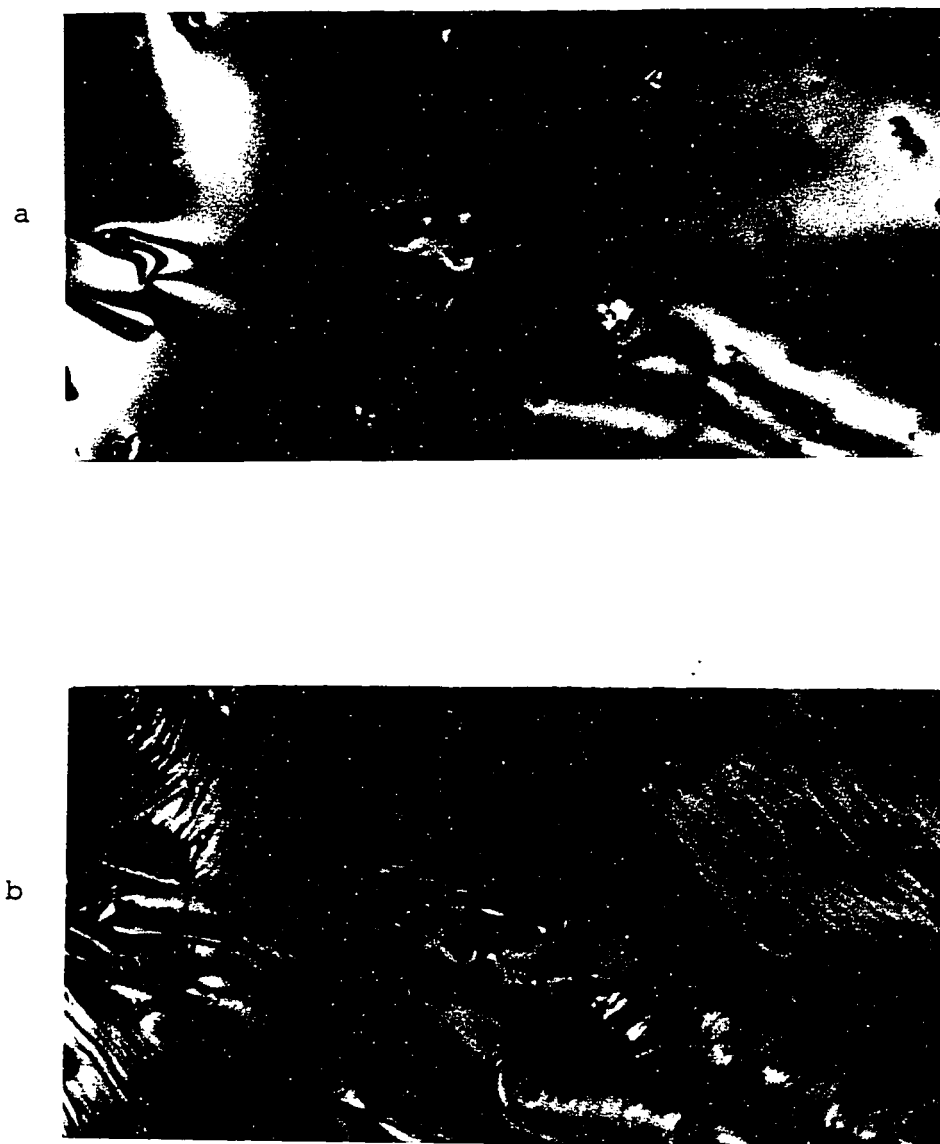
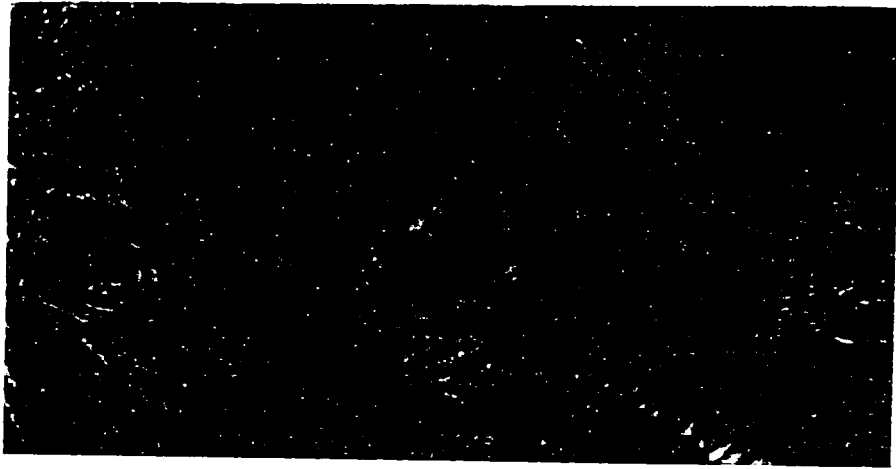


Figure 10. Representative optical polarized micrographs (100x) of the phases exhibited by poly(6-5) with degree of polymerization of 31: a) high temperature n phase at 109.2°C; b) transition from n to s_{Ad} phase at 102.4 °C; c) s_{Ad} phase 89.7°C; d) n_{re} phase at 54.2°C.

c



d

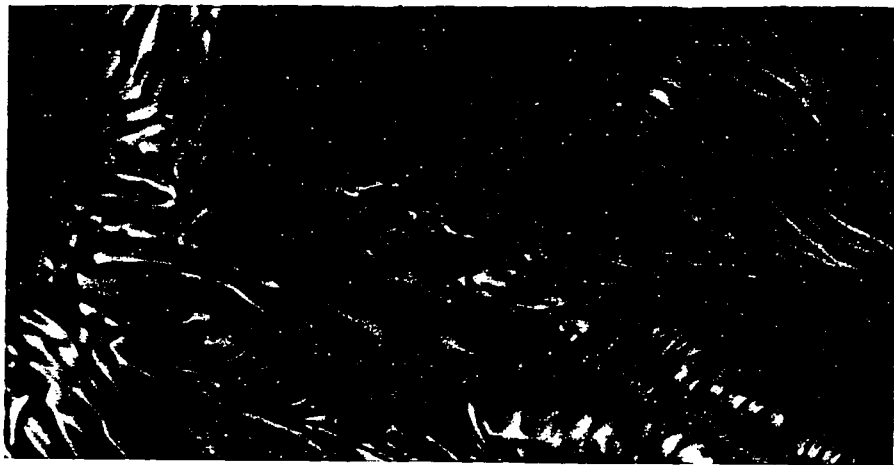


Figure 10. (continued)

REFERENCES

1. J. M. Rodriguez-Parada and V. Percec, *J. Polym. Sci., Polym. Chem. Ed.*, **24**, 1363 (1986)
2. V. Percec and D. Tomazos, *Polym. Bull.*, **18**, 239 (1987)
3. V. Percec, D. Tomazos and C. Pugh, *Macromolecules*, **22**, 3259 (1989)
4. T. Kodaira and K. Mori, *Makromol Chem., Rapid Commun.*, **11**, 645 (1990)
5. T. Sagane and R. W. Lenz, *Polym. J.*, **20**, 923 (1988)
6. T. Sagane and R. W. Lenz, *Polymer*, **30**, 2269 (1989)
7. T. Sagane and R. W. Lenz, *Macromolecules*, **22**, 3753 (1989)
8. V. Heroguez, A. Deffieux and M. Fontanille, *Makromol Chem., Rapid Commun.*, **32**, 199 (1990)
9. V. Heroguez, M. Schappacher, E. Papon and A. Deffieux, *Polym. Bull.*, **25**, 307 (1991)
10. E. Papon, A. Deffieux, F. Hardouin and M. F. Achard, *Liq. Cryst.*, in press
11. H. Jonsson, V. Percec and A. Hult, *Polym. Bull.*, **25**, 115 (1991)
12. V. Percec, C. S. Wang and M. Lee, *Polym. Bull.*, **26**, 15 (1991)
13. V. Percec, Q. Zheng and M. Lee, *J. Mater. Chem.*, **1**, 611 (1991)
14. R. Rodenhouse, V. Percec and A. E. Feiring, *J. Polym. Sci.: Part C: Polym. Lett.*, **28**, 345 (1990)
15. S. G. Kostromin, N. D. Cuong, E. S. Garina and V. P. Shibaev, *Mol. Cryst. Liq. Cryst.*, **193**, 177 (1990)
16. (a) P. E. Cladis, *Phys. Rev. Lett.*, **35**, 48 (1975); (b) P. E. Cladis, R. K. Bogardus, W. B. Daniels and G. N. Taylor, *Phys. Rev. Lett.*, **39**, 720 (1977); (c) D. Guillon, P. E. Cladis and J. Stamatoff, *Phys. Rev. Lett.*, **41**, 1598 (1978); (d) P. E. Cladis, R. K. Bogardus and D. Aadsen, *Phys. Rev. A.*, **18**, 2292 (1978); (e) N. H. Tinh, *J. Chim. Phys.*, **80**, 83 (1983); (f) J. W. Goodby, T. M. Leslie, P. E. Cladis and P. L. Finn, in "Liquid Crystals and Ordered Fluids", A. C. Griffin and J. F. Johnson, Eds., Plenum, Crystals and Ordered Fluids", A. C. Griffin and J. F. Johnson, Eds., Plenum, New York, 1984, p. 203
17. For some representative reviews see: (a) G. Sigaud, N. H. Tinh, F. Hardouin and H. Gasparoux, *Mol. Crst. Liq. Cryst.*, **69**, 81 (1981); (b) F. Hardouin, A.

- M. Levelut, M. F. Archard and G. Sigaud, *J. Chim. Phys.*, **80**, 53 (1983); (c) F. Hardouin, *Physica*, **140A**, 359 (1986); (d) P. E. Cladis, *Mol. Cryst. Liq. Cryst.*, **165**, 85 (1988)
18. P. Le Barny, J. C. Dubois, C. Friedrich and C. Noel *Polym. Bull.*, **15**, 341 (1986)
 19. T. I. Gubina, S. G. Kostromin, R. V. Talroze, V. P. Shibaev and N. A. Plate, *Vyskomol. Soed. Ser. B.*, **28**, 394 (1986)
 20. V. Shibaev, *Mol. Cryst. Liq. Cryst.*, **155**, 189 (1988)
 21. N. Lacoudre, A. Le Borgue, N. Spassky, J. P. Vairon, P. Le Barny, J. C. Dubois, S. Esselin, C. Friedrich and C. Noel, *Mol. Cryst. Liq. Cryst.*, **155**, 113 (1988)
 22. N. Spassky, N. Lacoudre, A. Le Borgue, J. P. Vairon, C. L. Jun, C. Friedrich and C. Noel, *Makromol. Chem., Makromol. Symp.*, **24**, 271 (1989)
 23. T. A. Gubina, S. Kise, S. G. Kostromin, R. V. Talroze, V. P. Shibaev and N. A. Plate, *Liq. Cryst.*, **4**, 197 (1989)
 24. S. G. Kostromin, V. P. Shibaev and S. Diele, *Makromol. Chem.*, **191**, 2521 (1990)
 25. C. Legrand, A. Le Borgue, C. Bunel, A. Lacoudre, P. Le Barny, N. Spassky and J. P. Vairon, *Makromol. Chem.*, **191**, 2979 (1990)

Chapter 6

INFLUENCE OF MOLECULAR WEIGHT ON THE PHASE TRANSITIONS OF POLY{ ω -[(4-CYANO-4'-BIPHENYL)OXY]ALKYL VINYL ETHER}S WITH BUTYL, PROPYL AND ETHYL ALKYL GROUPS

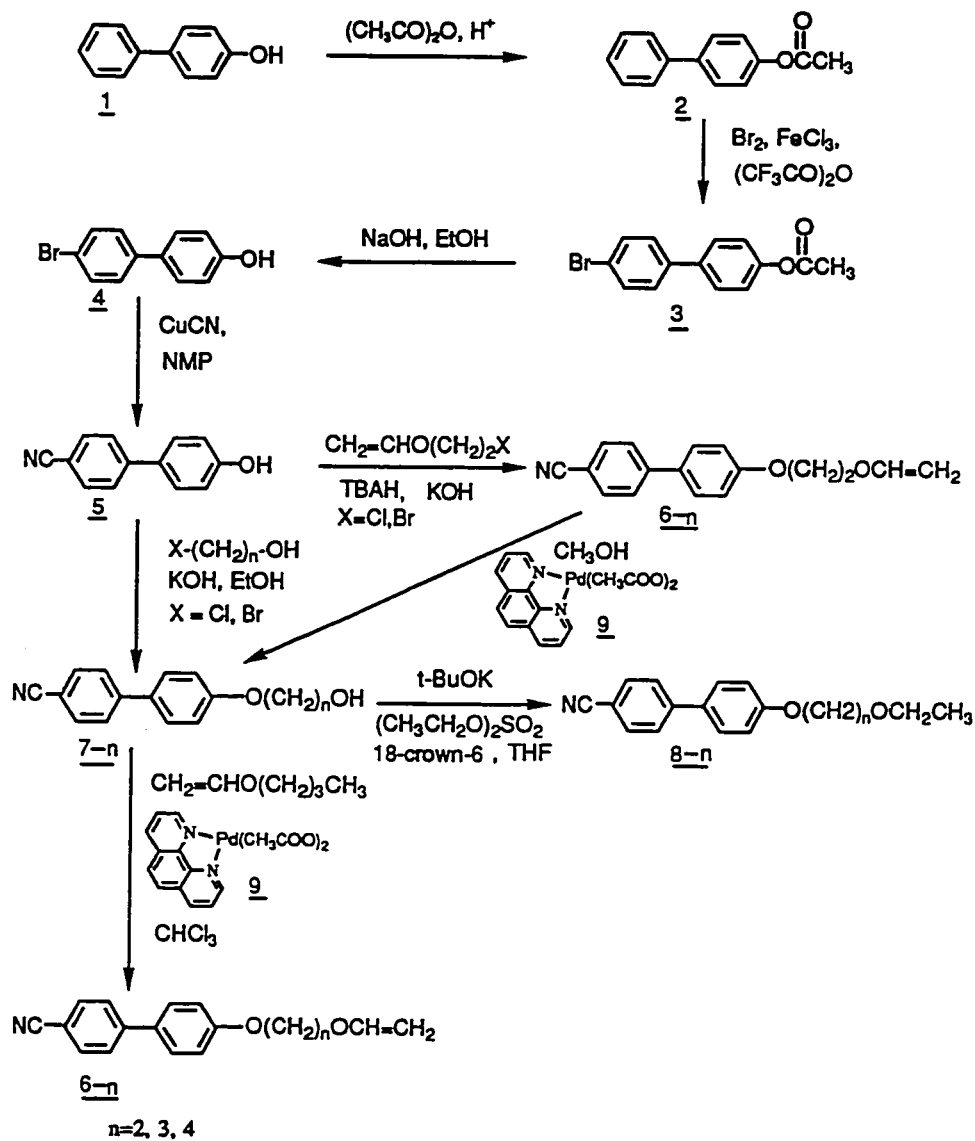
6.1.-INTRODUCTION

Previous chapters from this series have demonstrated that the transition temperature, nature and the number of mesophase of side chain liquid crystalline polymers are molecular weight dependent.

This chapter will describe the results on the influence of molecular weight on the phase behavior of the resulting polymers of last three monomers from the series of ω -[(4-cyano-4'-biphenyl)oxy]alkyl vinyl ethers with flexible spacers containing from two to eleven methylene units, i.e., 2-[4-cyano-4'-biphenyl)oxy]ethyl vinyl ether (6-2), 3-[4-cyano-4'-biphenyl)oxy]propyl vinyl ether (6-3) and 4-[4-cyano-4'-biphenyl)oxy]butyl vinyl ether (6-4). Their phase behavior will be compared to that of the model compounds of their monomeric structural units. Then, the mesomorphic behavior of poly{ ω -[(4-cyano-4'-biphenyl)oxy]alkyl vinyl ether}s with alkyl groups containing from two to eleven methylenic units will be comparatively discussed at four different degrees of polymerization: 30, 23, 13 and 4. The implication of different phase transitions at various molecular weights on the molecular design of novel macromolecular architectures based on side chain liquid crystalline polymers is briefly discussed.

6.2.-EXPERIMENTAL

Scheme I outlines the synthesis of monomers and model compounds.



Scheme I. Synthesis of 2-[(4-cyano-4'-biphenyl)oxy]ethyl vinyl ether (**6-2**), 3-[(4-cyano-4'-biphenyl)oxy]propyl vinyl ether (**6-3**) and 4-[4-cyano-4'-biphenyl]oxybutyl vinyl ether (**6-4**).

6.2.1.-Materials

3-Bromo-1-propanol (95%, Aldrich) and 4-chloro-1-butanol (94%, Lancaster Synthesis) were used as received. 4-Cyano-4'-hydroxybiphenyl of purities higher than 98 % and 1,10 phenanthroline palladium (II) diacetate were synthesized as described in previous chapters. Methyl sulfide was refluxed over 9-borabicyclo[3,3,1]nonane (crystalline, 98%, Aldrich) and then distilled under argon. Dichloromethane (99.6%, Aldrich) used as polymerization solvent was first washed with concentrated H₂SO₄, then with water, dried over magnesium sulfate, refluxed over calcium hydride and freshly distilled under argon before each use. Trifluoromethane sulfonic acid (triflic acid, 98%, Aldrich) was distilled under vacuum.

6.2.2.- Synthesis of Monomers

2-[(4-Cyano-4'-biphenyl)oxy]ethyl vinyl ether (6-2)

A mixture of 2g (10.25 mmol) of 4-cyano-4'-hydroxybiphenyl, 3.16ml (32.8mmol) 2-chloroethyl vinyl ether, 0.45g (11.07mmol) of powdered NaOH, 0.176g of tetrabutylammonium hydrogen sulfate (0.533mmol), 10.5ml toluene and 2ml dimethyl sulfoxide was stirred at 90°C for 6 hr. After cooling, the reaction mixture was washed with dilute NaOH, water, and dried over MgSO₄. The solvent was evaporated in a rotavapor and the resulting solid was recrystallized from methanol to yield 2.3g(87%) of white crystals which were further purified by column chromatography (silica gel, CH₂Cl₂ eluent). Purity: 99% (HPLC). mp, 118°C (lit.1, mp, 105°C). ¹H-NMR (CDCl₃, TMS, δ, ppm): 4.07(3 protons, -CH₂OCH=CH₂ trans, m), 4.27 (3 protons, PhOCH₂ and -OCH=CH₂ cis, m), 6.55 (1 proton, -OCH=CH₂, q), 7.02 (2 aromatic protons, o to alkoxy, d), 7.53 (2 aromatic protons, m to alkoxy, d), 7.69 (4 aromatic protons, o and m to -CN, d of d).

Synthesis of 4-cyano-4'-(2-hydroxyethan-1-yloxy)biphenyl (7-2)

2-[(4-Cyano-4'-biphenyl)oxy]ethyl vinyl ether (0.5 g, 1.885 mmol) was added to a mixture of 1,10-phenanthroline palladium (II) diacetate (0.038 g, 0.094 mmol) and methanol (15 ml). The mixture was refluxed for 12 hr. After cooling and filtration (to remove the catalyst) the solvent was distilled in a rotavapor and the product was recrystallized from a 1:9 mixture of acetone and n-hexane to yield 0.38 g of white crystals (84.2%) which were further purified by column chromatography (silica gel, CHCl_3 eluent). mp, 128.7°C (DSC). $^1\text{H-NMR}$ (CDCl_3 , TMS, δ , ppm), 4.02 (2 protons, $-\text{CH}_2\text{OH}$, t), 4.16 (2 protons, PhOCH_2- , t), 7.06 (2 aromatic protons, o to alkoxy, d), 7.53 (2 aromatic protons, m to alkoxy, d), 7.67 (4 aromatic protons, o and m to $-\text{CN}$, d of d).

Synthesis of 2-[(4-cyano-4'-biphenyl)oxy]ethyl ethyl ether (8-2)

4-Cyano-4'-(2-hydroxyethan-1-yloxy)biphenyl (0.35 g, 1.463 mmol) was added to a solution containing potassium t-butoxide (0.164 g, 1.463 mmol), a catalytic amount of 18-crown-6 and dry tetrahydrofuran (7 ml). Diethyl sulfate (0.21 ml, 1.61 mmol) was added, and the reaction mixture was refluxed for 5 hr under argon. After cooling, the reaction mixture was poured into chloroform. The chloroform solution was extracted with 10% aqueous KOH, washed with water, dried over magnesium sulfate and the solvent was removed on a rotavapor. The resulting product was purified by column chromatography (silica gel, CH_2Cl_2 eluent) and then was recrystallized from methanol to yield 0.17 g (42.7%) of white crystals. Purity: 99% (HPLC). mp, 68.9°C (DSC). $^1\text{H-NMR}$ (CDCl_3 , TMS, δ , ppm): 1.26 (3 protons, $-\text{CH}_2\text{CH}_3$, t), 3.65 (2 protons, $-\text{CH}_2\text{CH}_3$, q), 3.83 (2 protons, $-\text{CH}_2\text{OCH}_2\text{CH}_3$, t), 4.18 (2 protons,

PhOCH₂-, t), 7.05 (2 aromatic protons, o to alkoxy, d), 7.52 (2 aromatic protons, m to alkoxy, d), 7.66 (4 aromatic protons, o and m to -CN, d of d).

Synthesis of 4-cyano-4'-(3-hydroxypropan-1-yloxy)biphenyl (7-3)

4-Cyano-4'-hydroxybiphenyl (1.47 g, 7.53 mmol), sodium hydride (0.3 g, 7.59 mmol) and tetrabutylammonium hydrogensulfate (0.24 g, 0.71 mmol) were added to a mixture of toluene-DMSO (5:1) (22.1 ml). 3-Bromo-1-propanol (1.05 g, 7.55 mmol) was added to the resulting solution which was heated to 80°C for 28 hr. After cooling, the mixture was poured into water and then filtered. The obtained solid was dissolved in ethyl ether and then extracted with dilute aqueous NaOH, washed with water, dried over magnesium sulfate and then the solvent was removed in a rotavapor. The resulting product was recrystallized from methanol and then purified by column chromatography (silica gel, 1:1 ethyl acetate-hexane eluent) to yield 1.52 g (83%) of white crystals. mp, 114.6°C (DSC). Purity: 99.6% (HPLC). ¹H-NMR (CDCl₃, TMS, δ, ppm); 2.09 (2 protons, -CH₂CH₂CH₂-, m), 3.90 (2 protons, -CH₂OH, t), 4.19 (2 protons, PhOCH₂-, t), 7.02 (2 aromatic protons, o to alkoxy, d), 7.54 (2 aromatic protons, m to alkoxy, d), 7.66 (4 aromatic protons, o and m to -CN, d of d).

Synthesis of 3-[(4-cyano-4'-biphenyl)oxy]propyl vinyl ether (6-3)

4-Cyano-4'-(3-hydroxypropan-1-yloxy)biphenyl (2.0 g, 7.9 mmol) was added to a mixture of 1,10-phenanthroline palladium (II) diacetate (0.31 g, 0.79 mmol), n-butyl vinyl ether (43.1 ml) and dry chloroform (10.78 ml). The mixture was heated to 60°C for 6 hr. After cooling and filtration (to remove the catalyst), the solvent was distilled in a rotavapor and the product was purified by column chromatography (silica gel, CH₂Cl₂ eluent) and then was recrystallized from n-hexane to yield 1.83 g (83.0%)

of white crystals. Purity: 99.9% (HPLC). mp, 78.7°C (DSC). $^1\text{H-NMR}$ (CDCl_3 , TMS, δ , ppm): 2.18 (2 protons, $-\text{CH}_2\text{CH}_2\text{CH}_2-$, m), 3.90 (2 protons, $-\text{CH}_2\text{O}-$, t), 4.01 and 4.05 (1 proton, $-\text{OCH}=\text{CH}_2$ trans, d), 4.14 (2 protons, $-\text{CH}_2\text{OPh}$, t), 4.19 and 4.27 (1 proton, $-\text{OCH}=\text{CH}_2$ cis, d), 6.50 (1 proton, $-\text{OCH}=\text{CH}_2$, q), 7.02 (2 aromatic protons, o to alkoxy, d), 7.52 (2 aromatic protons, m to alkoxy, d), 7.67 (4 aromatic protons, o and m to $-\text{CN}$, d of d).

Synthesis of 3-[(4-cyano-4'-biphenyl)oxy]propyl ethyl ether (8-3).

4-Cyano-4'-(3-hydroxypropan-1-yloxy)biphenyl (0.5 g, 1.975 mmol) was added to a solution containing potassium t-butoxide (0.22 g, 1.975 mmol), a catalytic amount of 18-crown-6 and dry tetrahydrofuran (10 ml). Diethyl sulfate (0.284 ml, 2.17 mmol) was added and the reaction mixture was refluxed for 4 hr under argon. After cooling, the reaction mixture was poured into chloroform. The chloroform solution was extracted with 10% aqueous KOH, washed with water, dried over magnesium sulfate and the solvent was removed in a rotavapor. The resulting product was purified by column chromatography (silica gel, CH_2Cl_2 eluent) and then was recrystallized from methanol to yield 0.34 g (58.0%) of white crystals. Purity: 99.0% (HPLC). mp, 64.9°C (DSC). $^1\text{H-NMR}$ (CDCl_3 , TMS, δ , ppm): 1.21 (2 protons, $-\text{OCH}_2\text{CH}_3$, t), 2.08 (2 protons, $-\text{CH}_2\text{CH}_2\text{CH}_2-$, m), 3.50 (2 protons, $-\text{OCH}_2\text{CH}_3$, q), 3.62 (2 protons, $-\text{CH}_2\text{OCH}_2\text{CH}_3$, t), 4.13 (2 protons, PhOCH_2- , t), 7.02 (2 aromatic protons, o to alkoxy, d), 7.52 (2 aromatic protons, m to alkoxy, d), 7.66 (4 aromatic protons, o and m to $-\text{CN}$, d of d).

Synthesis of 4-cyano-4'-(4-hydroxybutan-1-yloxy)biphenyl (7-4)

4-Cyano-4'-hydroxybiphenyl (4.2 g, .0215 mol) and potassium carbonate (39 g, 0.3 mol) were added to a mixture of acetone-DMSO (10:1) (110 ml). 4-Chloro-1-butanol (11.67 g, 0.1075 mol) was added to the resulting reaction mixture which was heated to reflux for 3 days. After cooling, the mixture was poured into water and the separated solid was filtered. The obtained solid was recrystallized first from methanol and then from toluene to yield 2.82 g (49.1%) of white crystals. mp, 126.4 °C (DSC). ¹H-NMR (CDCl₃, TMS, δ, ppm): 1.55-2.15 (4 protons, -(CH₂)₂-, m), 3.75 (2 protons, -CH₂OH, t), 4.07 (2 protons, PhOCH₂-, t), 7.02 (2 aromatic protons, o to alkoxy, d), 7.51 (2 aromatic protons, m to alkoxy, d), 7.66 (4 aromatic protons, o and m to -CN, d of d).

Synthesis of 4-[4-Cyano-4'-biphenyl]oxylbutyl vinyl ether (6-4)

4-Cyano-4'-(4-hydroxybutan-1-yloxy)biphenyl (2.0 g, 7.48 mmol) was added to a mixture of 1,10-phenanthroline palladium (II) diacetate (0.29 g, 0.75 mmol), n-butyl vinyl ether (40.85 ml) and dry chloroform (10.2 ml). The mixture was heated to 60°C for 6 hr. After cooling and filtration (to remove the catalyst), the solvent was distilled in a rotavapor, the product was purified by column chromatography (silica gel, CH₂Cl₂ eluent) and then was recrystallized first from ethanol and then from n-hexane to yield 1.82 g (82.9%) of white crystals. Purity: 99.8% (HPLC). mp, 73.3°C. T_n-i, 77.1°C (DSC). ¹H-NMR (CDCl₃, TMS, δ, ppm); 1.91 (4 protons, -(CH₂)₂-, m), 3.78 (2 protons, -CH₂OCH=CH₂, t), 4.06 (3 protons, -OCH=CH₂ trans and PhOCH₂-, m), 4.16 and 4.23 (1 proton, OCH=CH₂ cis, d), 6.50 (1 proton, OCH=CH₂, q), 7.02 (2 aromatic protons, o to alkoxy, d), 7.52 (2 aromatic protons, m to alkoxy, d), 7.67 (4 aromatic protons, o and m to -CN, d of d).

Synthesis of 4-[4-cyano-4'-biphenyl]oxybutyl ethyl ether (8-4).

4-Cyano-4'-(4-hydroxybutan-1-yloxy)biphenyl (0.5 g, 1.67 mmol) was added to a solution containing potassium t-butoxide (0.20 g, 1.67 mmol), a catalytic amount of 18-crown-6 and dry tetrahydrofuran (10 ml). Diethyl sulfate (0.25 ml, 1.9 mmol) was added and the reaction mixture was refluxed for 4 hr under argon. After cooling, the reaction mixture was poured into chloroform. The chloroform solution was extracted with 10% aqueous KOH, washed with water, dried over magnesium sulfate and the solvent was removed in a rotavapor. The resulting product was purified by column chromatography (silica gel, CH_2Cl_2 eluent) and then was recrystallized from methanol to yield 0.32 g (57.9%) of white crystals. Purity: 99% (HPLC). mp, 64.7°C (DSC). $^1\text{H-NMR}$ (CDCl_3 , TMS, δ , ppm): 1.22 (3 protons, $-\text{OCH}_2\text{CH}_3$, t), 1.65-2.11 (4 protons, $-(\text{CH}_2)_2-$, m), 3.50 (4 protons, $-\text{CH}_2\text{OCH}_2\text{CH}_3$, m), 4.05 (2 protons, PhOCH_2- , t), 7.02 (2 aromatic protons, o to alkoxy, d), 7.51 (2 aromatic protons, m to alkoxy, d), 7.66 (4 aromatic protons, o and m to $-\text{CN}$, d of d).

6.2.3.-Cationic Polymerization

Polymerizations were carried out in glass flasks equipped with teflon stopcocks and rubber septa under argon atmosphere at 0°C for 1 hr. All glassware was dried overnight at 130°C. The monomer was further dried under vacuum overnight in the polymerization flask. Then the flask was filled with argon, cooled to 0°C and the methylene chloride, dimethyl sulfide and triflic acid were added via a syringe. The monomer concentration was about 10 wt% of the solvent volume and the dimethyl sulfide concentration was 10 times larger than that of the initiator. The polymer molecular weight was controlled by the monomer/initiator ($[\text{M}]_0/[\text{I}]_0$) ratio. After quenching the polymerization with ammoniacal methanol, the reaction mixture was

precipitated into methanol. The filtered polymers were dried and precipitated from methylene chloride solutions into methanol until GPC traces showed no traces of monomer. Tables I, II and III summarize the polymerization results. Although the polymer yields are lower than expected due to losses during the purification process, the conversions were almost quantitative in all cases.

6.3.-RESULTS AND DISCUSSION

Polymerization results are reported in Tables I, II and III. All polymers have relative number average molecular weights which show a linear dependence of $[M]_0/[I]_0$, and narrow molecular weight distributions. Figure 1 presents representative plot which demonstrate the living polymerization character for the case of monomer 6-3. The polymerization mechanism is outlined in Scheme II.² The thermal characterization of all intermediary alcohols, monomers and model compounds is summarized in Table IV. The alcohol derivatives 7-2, 7-3 and 7-4 exhibit a monotropic nematic mesophase. 6-2 is crystalline, 6-3 exhibits a monotropic nematic mesophase, while 6-4 an enantiotropic nematic phase. The model compounds 8-2 and 8-3 are only crystalline. 8-4 displays a monotropic nematic mesophase.

Figure 2 presents the DSC traces of poly(6-2) with different molecular weights. The polymerization of 6-2 was investigated previously by Sagane and Lenz.¹ Our present data do not agree completely with their results. In the first DSC heating scan (Figure 2a), poly(6-2) presents an endothermic transition which overlaps the glass transition temperature. This transition does not appear on the second heating (Figure 2b) or on the cooling scans (Figure 2c). Since we could not yet assign this phase, we will label it with X (Table I). Irrespective of thermal history of the sample, when the degree of polymerization of poly(6-2) is lower than 4, the polymer presents also an

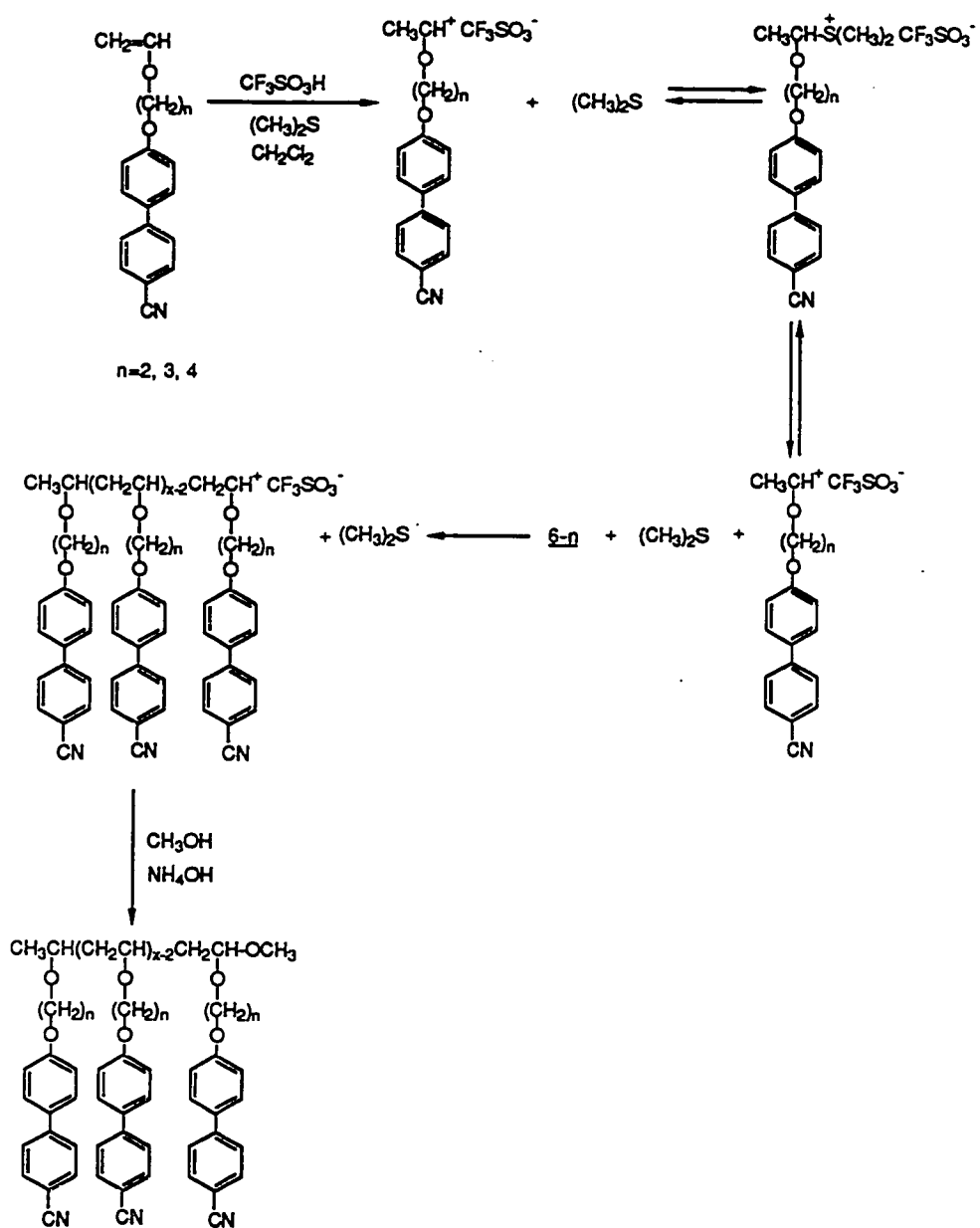
Scheme II. Cationic polymerization of 6-2, 6-3 and 6-4

Table I. Cationic Polymerization of 2-[4-Cyano-4'-biphenyl]oxyethyl Vinyl Ether (6:2) (polymerization temperature, 0°C; polymerization solvent, methylene chloride; $[M]_0=0.387$; $[(CH_3)_2S]_0/[I]_0=10$; polymerization time, 1hr) and Characterization of the Resulting Polymers. Data on first line are from first heating and cooling scans. Data on second line are from second heating scan.

Sample No.	[M] ₀ /[I] ₀	Polymer yield(%)	G P C		phase transitions(°C) and corresponding enthalpy changes (kcal/mru)		
			Mx10 ⁻³	Mw/Mn	D P	heating	cooling
1	3	35	0.5	1.22	2	g 34.5 X 37.5 (0.21) n 79.2 (0.061) i g 33.5 n 79.8 (0.061) i	i 76.3 (0.072) n 29.5 g
2	4	57	0.7	1.11	3	g 53.7 X 56.7 (0.29) n 81.1 (0.034) i g 51.0 n 80.2 (0.037) i	i 77.1 (0.040) n 43.5 g
3	5	55	0.9	1.21	4	g 60.1 X 66.7 (0.37) n 81.4 (0.008) i g 55.6 n 71.8 (0.027) i	i 70.8 (0.033) n 49.7 g
4	7	73	1.8	1.08	6	g 68.6 X 71.6 (0.34) i g 61.9 i	i 54.7 g
5	10	73	2.9	1.10	11	g 78.5 X 86.0 (0.18) i g 72.8 i	i 63.8 g
6	20	65	4.6	1.18	17	g 81.0 X 85.7 (0.25) i g 78.3 i	i 70.5 g

Table II. Cationic Polymerization of 3-[4-Cyano-4'-biphenyl]oxy]propyl Vinyl Ether (6-3) (polymerization temperature, 0°C; polymerization solvent, methylene chloride; $[M]_0=0.358$; $[(CH_3)_2S]_0/[I]_0=10$; polymerization time, 1hr) and Characterization of the Resulting Polymers. Data on first line are from first heating and cooling scans. Data on second line are from second heating scan.

Sample No.	$[M]_0/[I]_0$	Polymer yield(%)	G P C		phase transitions(°C) and corresponding enthalpy changes (kcal/mru)	
			Mnx10 ⁻³	Mw/Mn	D P	heating cooling
1	6	80	1.6	1.06	.6	g 38.2 X 41.3 (0.17) n 79.6 (0.10) i g 36.3 n 77.3 (0.11) i i 72.3 (0.083) n 30.8 g
2	10	88	2.6	1.14	9	g 41.3 X 46.6 (0.18) n 84.9 (0.067) i g 40.1 n 83.5 (0.065) i i 79.1 (0.071) n 38.5 g
3	13	87	3.3	1.20	12	g 45.1 X 49.6 (0.19) n 88.8 (0.078) i g 45.0 n 87.0 (0.095) i i 82.5 (0.083) n 42.7 g
4	18	83	5.1	1.18	18	g 59.5 X 64.5 (0.26) n 97.8 (0.094) i g 56.4 n 95.9 (0.070) i i 90.8 (0.078) n 50.3 g
5	23	82	6.0	1.11	22	g 61.7 X 66.4 (0.23) n 102.7 (0.078) i g 59.4 n 102.3 (0.086) i i 97.6 (0.078) n 52.1 g
6	30	79	8.1	1.21	29	g 64.4 X 68.4 (0.21) n 104.5 (0.070) i g 63.0 n 104.3 (0.081) i i 100.3 (0.075) n 54.1 g

Table III. Cationic Polymerization of 4-[4-Cyano-4'-biphenyl]oxybutyl Vinyl Ether (6-4) (polymerization temperature, 0°C; polymerization solvent, methylene chloride; $[M]_0=0.341$; $[(CH_3)_2S]/[I]_0=10$; polymerization time, 1hr) and Characterization of the Resulting Polymers. Data on first line are from first heating and cooling scans. Data on second line are from second heating scan.

Sample No.	$[M]_0/[I]_0$	Polymer yield(%)	G P C		phase transitions(°C) and corresponding enthalpy changes (kcal/mru)	
			Mnx10 ⁻³	Mw/Mn	D P	heating cooling
1	5	72	1.2	1.20	4	g 15.4 n 77.1 (0.056) i g 15.2 n 76.7 (0.067) i i 72.3 (0.047) n 10.3 g
2	7	80	1.5	1.10	5	g 24.5 n 75.2 (0.032) i g 24.0 n 74.8 (0.026) i i 67.8 (0.026) n 16.9 g
3	10	60	2.9	1.20	10	g 30.2 X 45.4 (0.29) n 83.3 (0.019) i g 28.4 n 77.2 (0.029) i i 69.5 (0.035) n 23.9 g
4	14	64	3.7	1.16	13	g 34.8 X 48.8 (0.49) n 85.5 (0.0029) i g 33.1 n 74.5 (0.003) i i 67.3 (0.009) n 23.2 g
5	18	81	5.0	1.22	17	g 35.7 X 52.2 (0.30) n 84.7 (0.0079) i g 34.3 n 83.2 (0.003) i i 69.5 (0.012) n 23.1 g
6	24	87	7.0	1.23	24	g 39.1 X 52.8 (0.39) n 87.4 (0.0058) i g 37.5 n 84.1 (0.012) i i 70.1 (0.003) n 28.0 g
7	30	89	8.5	1.18	29	g 47.2 X 58.2 (0.20) n 86.2 (0.015) i g 44.3 n 88.7 (0.011) i i 71.9 (0.003) n 36.4 g

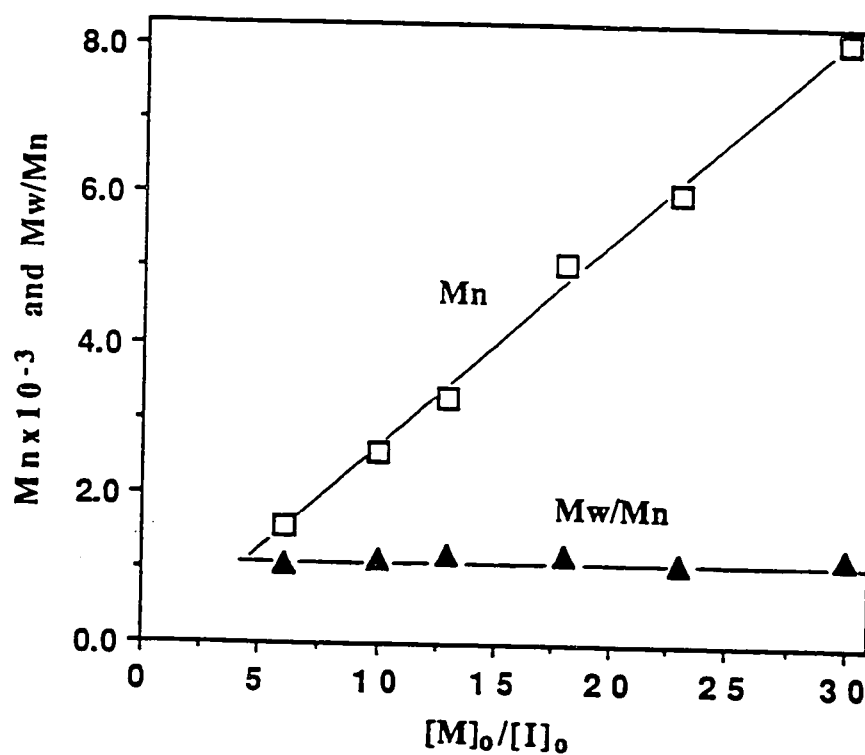


Figure 1. The dependence of the number average molecular weight (M_n) and of the polydispersity (M_w/M_n) of poly(6-3) on the $[M]_0/[I]_0$ ratio.

Table IV. Thermal Characterization of 4-Cyano-4'-(ω -hydroxyalkan-1-yloxy)biphenyls (7-2, 7-3 and 7-4), ω -[(4-Cyano-4'-biphenyl)oxy]alkyl Vinyl Ethers (6-2, 6-3 and 6-4) and ω -[(4-Cyano-4'-biphenyl)oxy]alkyl Ethyl Ethers (8-2, 8-3 and 8-4)

Compound	phase transitions (0°C) and corresponding enthalpy changes (kcal/mol)	
	heating	cooling
<u>7-2</u>	k 128.7 (6.84) i [n 126.5 (0.25) i]*	i 123.4 (0.31) n 105.4 (3.85) k
<u>6-2</u>	k 118.5 (8.21) i	i 83.4 (6.70) k
<u>8-2</u>	k 68.9 (5.46) i	i 13.3 (3.56) k
<u>7-3</u>	k 114.6 (7.45) i [n 115.3 (0.26) i]	i 112.7 (0.30) n 67.5 (2.87) k
<u>6-3</u>	k 78.74 (9.02) i	i -10.4 (0.08) n -51.4 (2.30) k
<u>8-3</u>	k 64.9 (7.83) i	i -5.9 (4.13) k
<u>7-4</u>	k 126.4 (5.95) i [n 124.8 (0.32) i]*	i 121.7 (0.31) n 99.3 (5.24) k
<u>6-4</u>	k 73.3 (7.82) n 77.1 (0.22) i	i 73.4 (0.29) n 48.4 (6.37) k
<u>8-4</u>	k 64.7 (7.87) i [n 50.5 (0.062) i]	i 47.4 (0.094) n 33.1 (5.38) k

[]* virtual data

enantiotropic nematic mesophase. Poly(6-2) with higher degrees of polymerization do not present this nematic phase. The disappearance of this phase at higher polymer molecular weights is due to the steep increase of the dependence of the glass transition temperature versus polymer molecular weight with the increase of polymer molecular weight. At degrees of polymerization of about 7 and higher, the glass transition of poly(6-2) is very close to the nematic-isotropic transition temperature. Therefore, the mesophase becomes kinetically controlled, and due to its close proximity to glass transition, it can not be observed by DSC. Upon shearing the polymer sample on the optical polarized microscope just above its T_g , we see the formation of the nematic phase. Figure 3 presents the dependence of glass transition, of the nematic-isotropic and of the x-nematic transition temperatures on molecular weight. This figure demonstrates that the slope of the T_g -Mn is higher than that of T_{n-i} -Mn and as a consequence, at higher polymer molecular weights, the nematic mesophase becomes kinetically controlled.

The first and second heating and the cooling DSC traces of poly(6-3) are presented in Figure 4a,b,c. This polymer presents an enantiotropic nematic mesophase. However, on the first heating scan, it also shows the x phase which overlaps the glass transition temperature (Figure 4a, Table II). Figures 4 and 5 show the dependence of glass transition and nematic-isotropic transition temperatures on molecular weight. The slopes of both dependences are almost identical. In the case of poly(6-2) the slope of T_g -Mn was higher than that of T_{n-i} -Mn. At the same time in the case of polymers with longer spacers, the slopes of the mesomorphic-isotropic phase transition temperatures versus Mn are higher than that of T_g -Mn as described in previous chapter.

In the first heating scan poly(6-4) with degrees of polymerization below five exhibits an enantiotropic nematic mesophase (Figure 6a, Table III). Polymers with

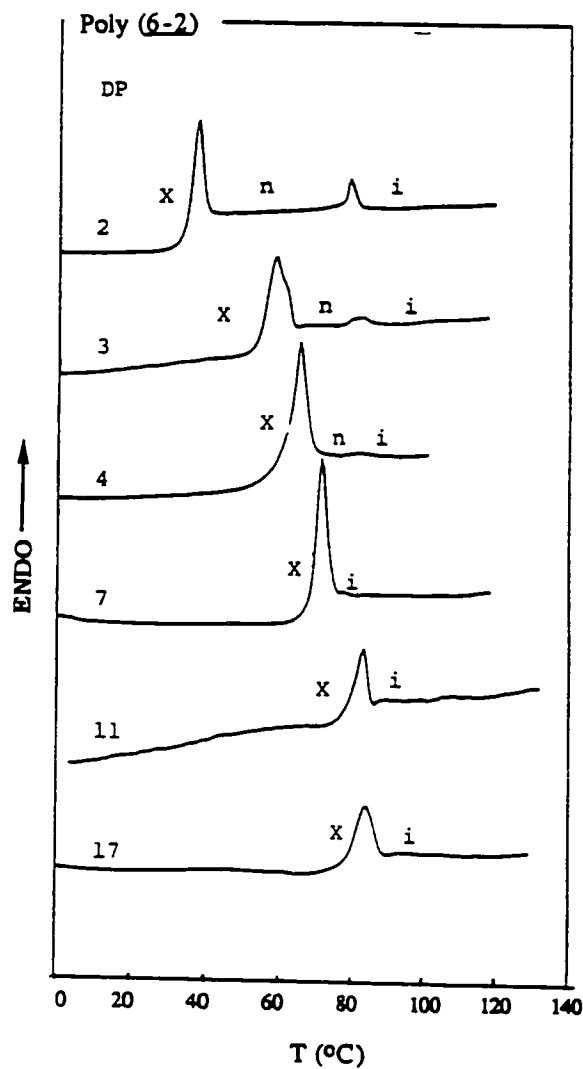


Figure 2a. DSC traces displayed during the first heating scan by poly(6-2) with different degrees of polymerization (DP). DP is printed on the top of each DSC scan.

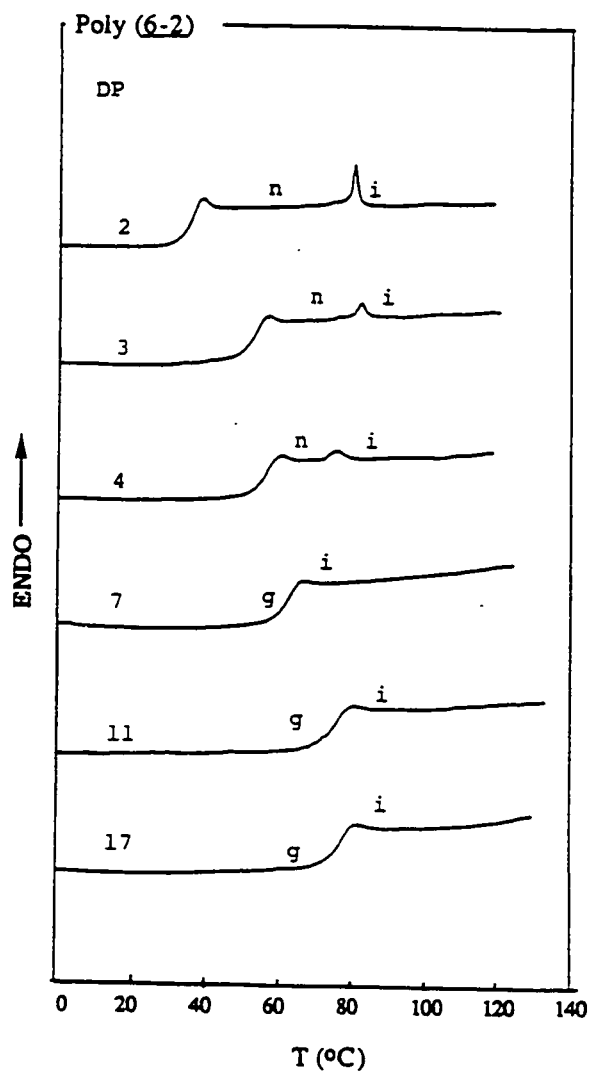


Figure 2b. DSC traces displayed during the second heating scan by poly(6-2) with different degrees of polymerization (DP). DP is printed on the top of each DSC scan.

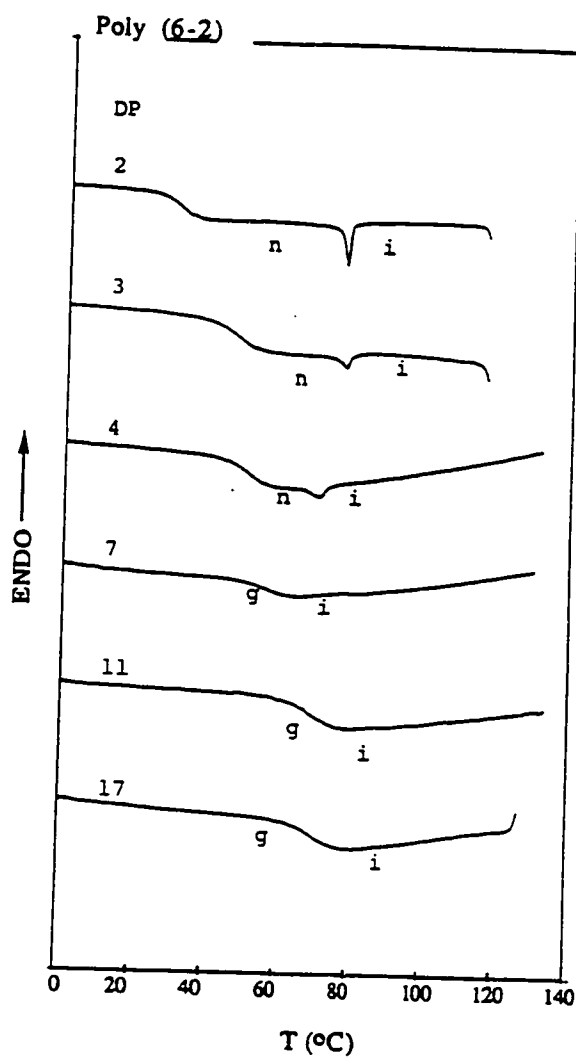


Figure 2c. DSC traces displayed during the first cooling scan by poly(6-2) with different degrees of polymerization (DP). DP is printed on the top of each DSC scan.

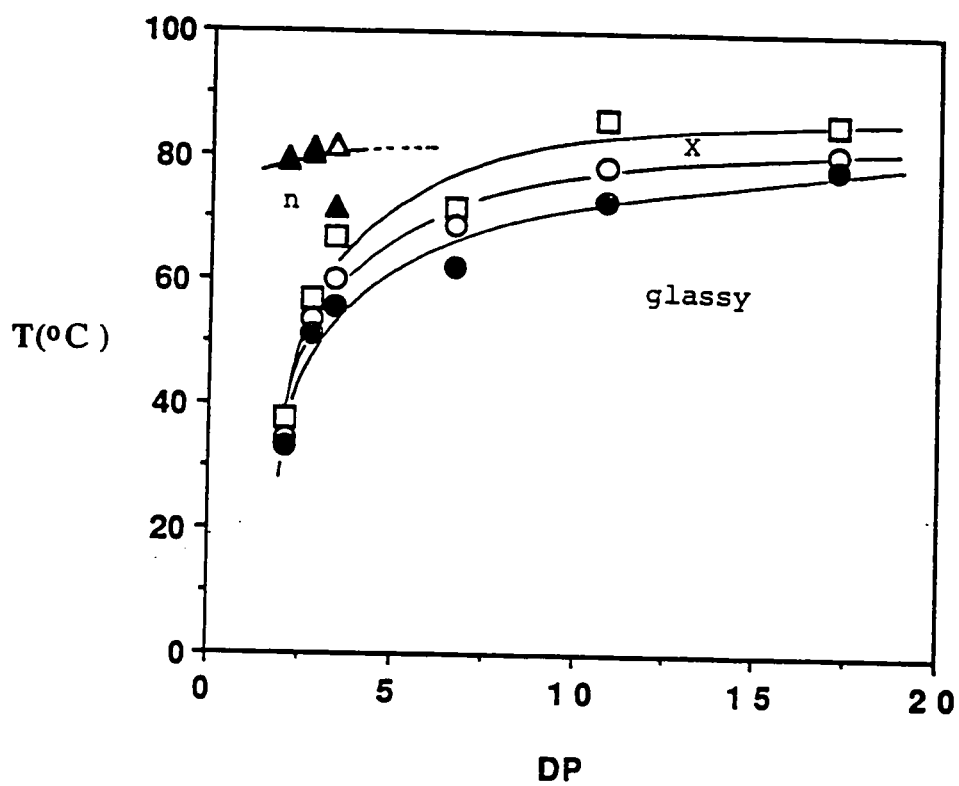


Figure 3. The dependence of phase transition temperatures on the degree of polymerization of poly(6-2). Data from first heating scan (fh) and second heating scan (sh): Δ -Tn-i(fh); \square -Tx-n(fh); O-Tg(fh); \blacktriangle -Tn-i(sh); \bullet -Tg(sh).

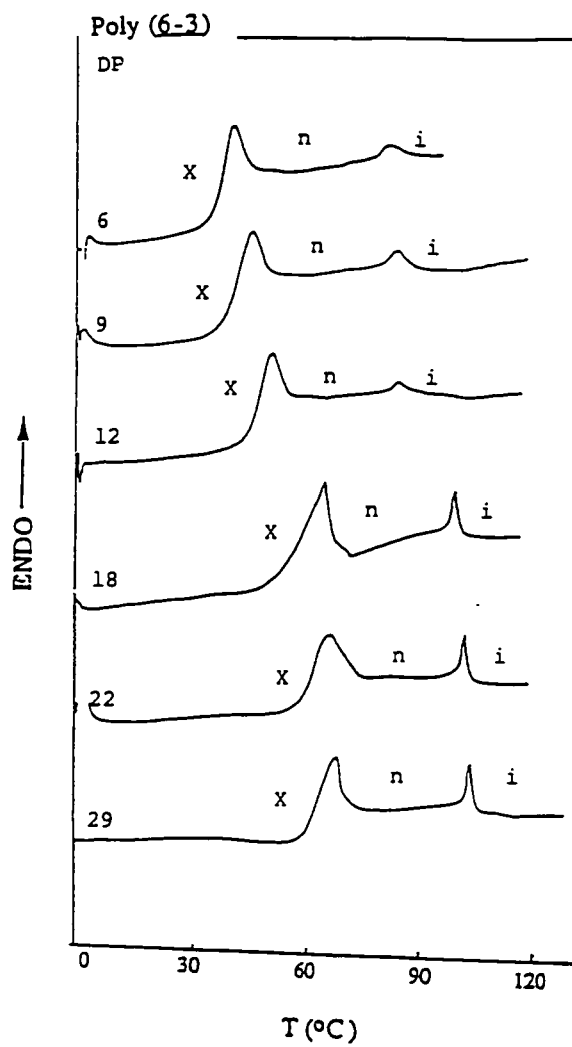


Figure 4a. DSC traces displayed during the first heating scan by poly(6-3) with different degrees of polymerization (DP). DP is printed on the top of each DSC scan.

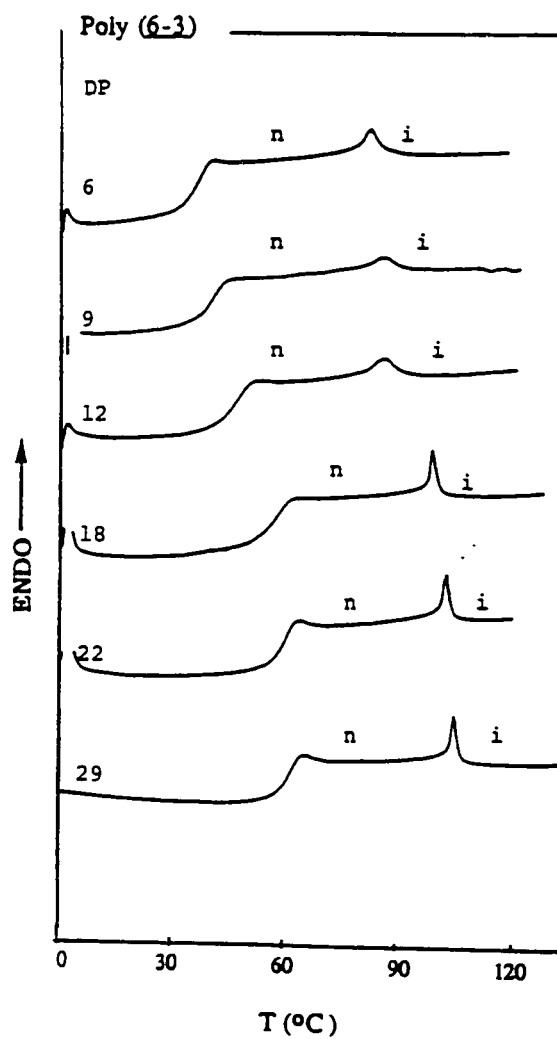


Figure 4b. DSC traces displayed during the second heating scan by poly(6-3) with different degrees of polymerization (DP). DP is printed on the top of each DSC scan.

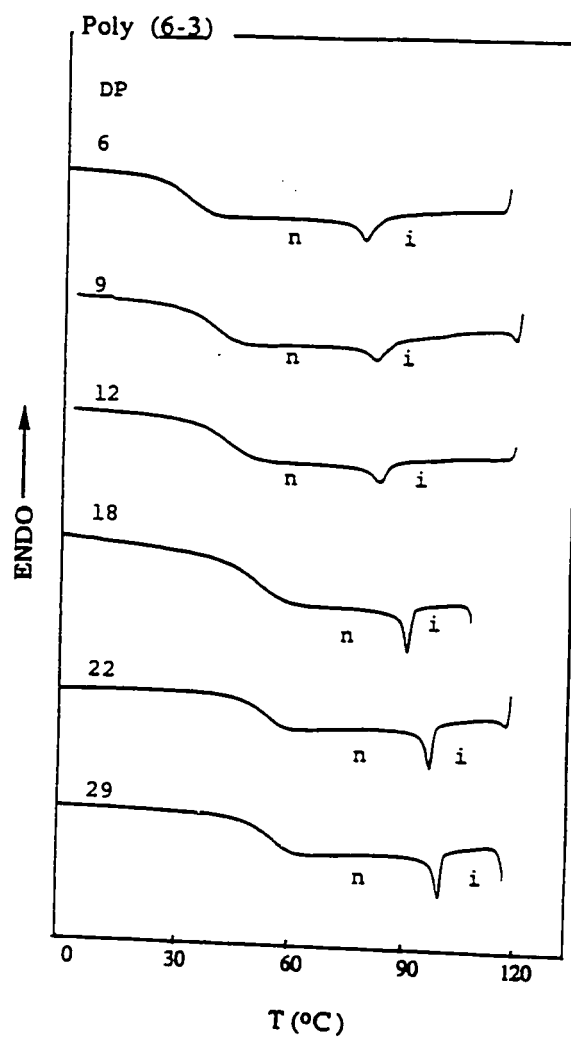


Figure 4c. DSC traces displayed during the first cooling scan by poly(6-3) with different degrees of polymerization (DP). DP is printed on the top of each DSC scan.

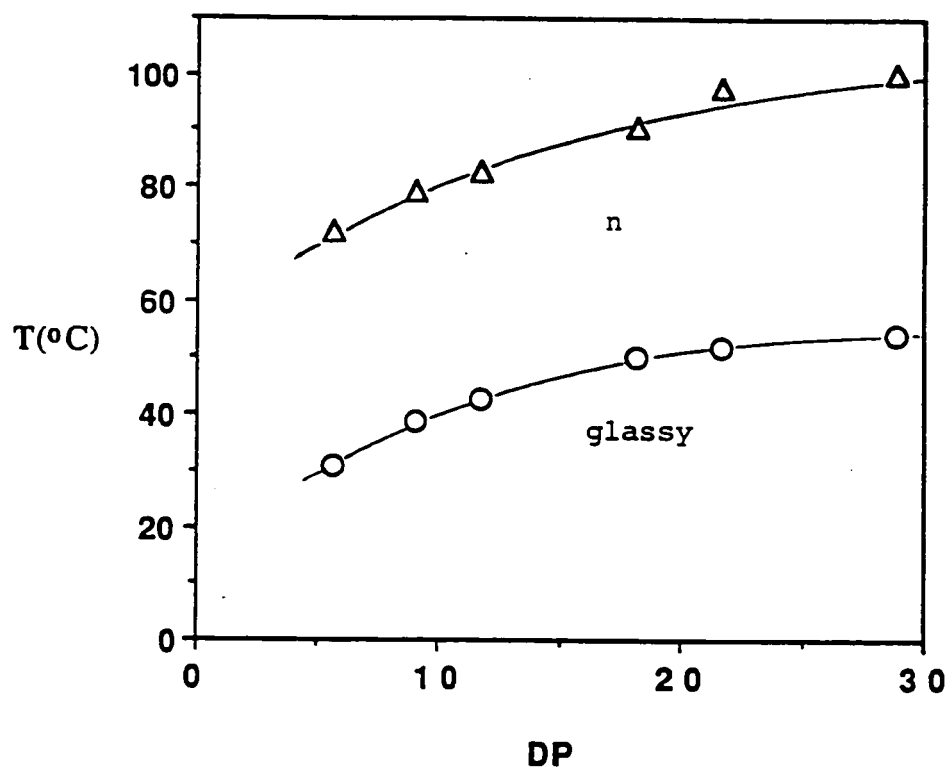


Figure 5. The dependence of phase transition temperatures on the degree of polymerization of poly(6-3). Data from first cooling scan: Δ - T_{n-i} ; O - T_g .

higher molecular weights exhibit the x phase followed by the enantiotropic nematic mesophase. The x phase can not be observed on the second heating and cooling scans (Figure 6b,c). The dependences of the phase transition temperatures of poly(6-4), collected from the first heating scans versus M_n , are plotted in Figure 7. Again we can observe similar slopes for the T_g - M_n and T_{n-i} - M_n dependences. It is very interesting to observe that the enthalpy changes associated with the nematic-isotropic transitions of poly(6-4) are very low.

In conclusion, mesomorphic poly(vinyl ether)s with long spacers exhibits smectic mesophases although their corresponding monomers and model compounds display nematic mesophases as shown in previous chapter. The corresponding polymers with short flexible spacers exhibit nematic mesophases. Their monomers and model compounds also exhibit nematic mesophases. In the case of polymers with short flexible spacers, the slopes of the T_g - M_n and T_{n-i} - M_n dependences are about equal, and therefore, these two dependences do not intercept each other. An exception is provided by poly(6-2) whose T_g - M_n slope is steeper than that of T_{n-i} - M_n dependence. Consequently, at a certain degree of polymerization the T_g - M_n dependence intercepts the T_{n-i} - M_n dependence, and therefore above this molecular weight the nematic phase becomes virtual. In the case of polymers with long flexible spacers, the slope of T_{s-i} - M_n is much steeper than that of T_g - M_n . In this case, the smectic mesophase is virtual below the molecular weight which corresponds to this interception and becomes enantiotropic above it. Last but not least, it is interesting to mention that the dimers and trimers of poly(6-2) as well as the low molecular weight oligomers of poly(6-3) have glass transition temperatures above room temperature and therefore, provide an interesting new approach to nematic glasses with fast dynamics. They may have the same potential applications as low molar mass glassy nematic liquid crystals.³

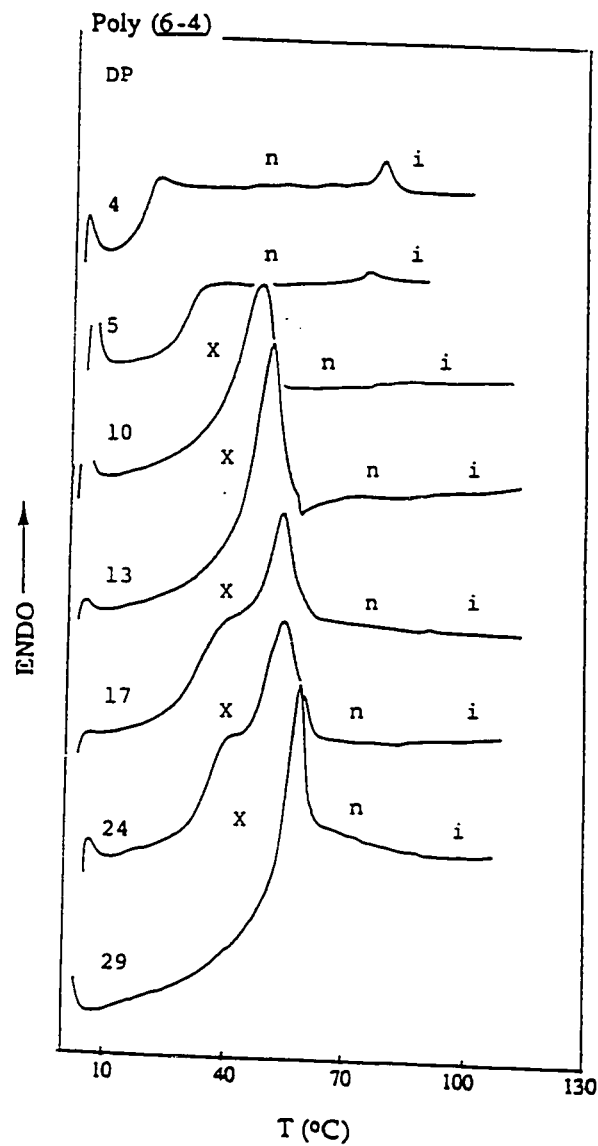


Figure 6a. DSC traces displayed during the first heating scan by poly (6-4) with different degrees of polymerization (DP). DP is printed on the top of each DSC scan.

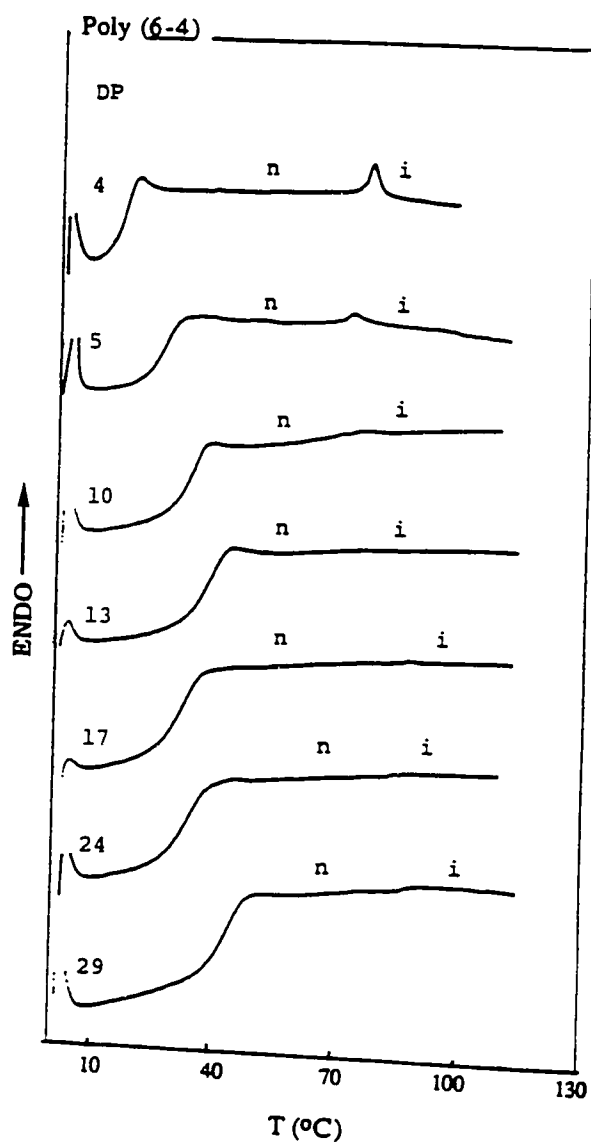


Figure 6b. DSC traces displayed during the second heating scan by poly (6-4) with different degrees of polymerization (DP). DP is printed on the top of each DSC scan.

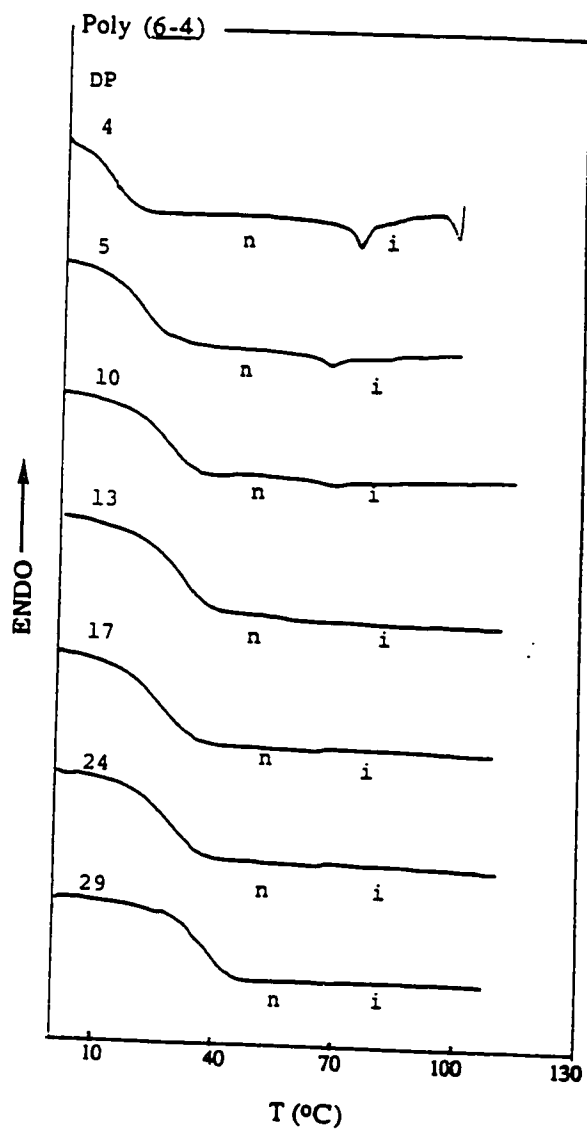


Figure 6c. DSC traces displayed during the first cooling scan by poly (6-4) with different degrees of polymerization (DP). DP is printed on the top of each DSC scan.

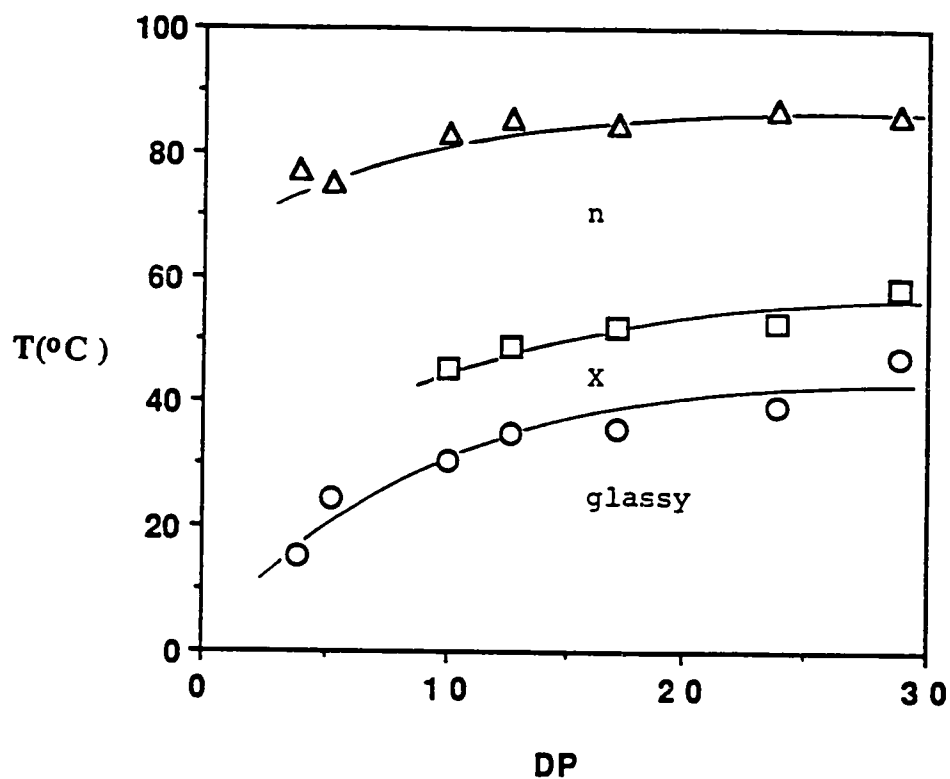


Figure 7. The dependence of phase transition temperatures on the degree of polymerization of poly(6-4). Data from first heating scan: Δ -T_{n-i}; \square -T_{x-n}; \circ -T_g.

The experiments described in this series of publication together with previous results on the same topic provided both by several research groups⁴⁻⁹ demonstrate the complexity of the influence of molecular weight on the phase transitions of side chain liquid crystal polymers. The only case which was explained so far refers to systems in which the virtual or monotropic mesophase of the monomer or of the monomeric structural unit transforms into a monotropic or enantiotropic mesophase after polymerization^{10,11}. The same explanation holds for situations when the monomeric structural unit exhibits an enantiotropic mesophase and the resulting polymer a broader range of temperature of its mesophase. However, the mechanism which changes the nature of the mesophase upon increasing the degree of polymerization is not yet known.

Let us now compare the phase behavior of poly(6-n) with $n=2$ to 11 at four different degrees of polymerization: 30, 23, 13 and 4. Figure 8a-d presents the thermal transition temperatures determined from the second heating scan, while Figure 9a-d presents the same thermal transition temperatures determined from the first heating scan. Thermal transition temperatures of poly(6-2), poly(6-3) and poly(6-4) were determined in this chapter. The results of poly(6-5), poly(6-7) and poly(6-9) were reported in Chapter IV, those of poly(6-6) and poly(6-8) in Chapter III, and those of poly(6-10) and poly(6-11) in Chapter II.

Figure 8a and b presents the thermal transitions, determined from second heating scans of poly(6-n), with degrees of polymerization of 30 and 23. Both plots demonstrate the same trend. Glass transition temperatures of poly(6-n) decrease with the increase of the polymer spacer length. Poly(6-2) with a degree of polymerization of 30 does not exhibit any mesophase. Poly(6-3) and poly(6-4) display a nematic

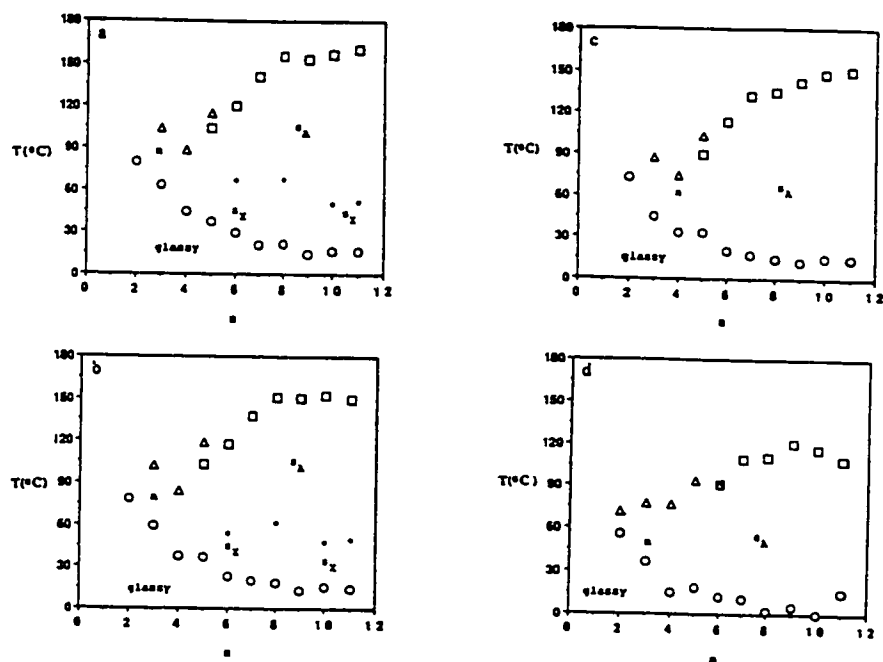


Figure 8. The dependence of phase transition temperatures on the length (n) of flexible spacer $[-(\text{CH}_2)_n-]$ of poly(6-n) at similar degrees of polymerization. a) data from second heating scan at DP=30: O-Tg; ◆-TsX-SA; □-TsA-i; Δ-Tn-i; b) data from second heating scan at DP=23; O-Tg; ◆-TsX-SA; □-TsA-i; Δ-Tn-i; c) data from second heating scan at DP=13: O-Tg; □-TsA-i; Δ-Tn-i; d) data from second heating scan at DP=4: O-Tg; □-TsA-i; Δ-Tn-i

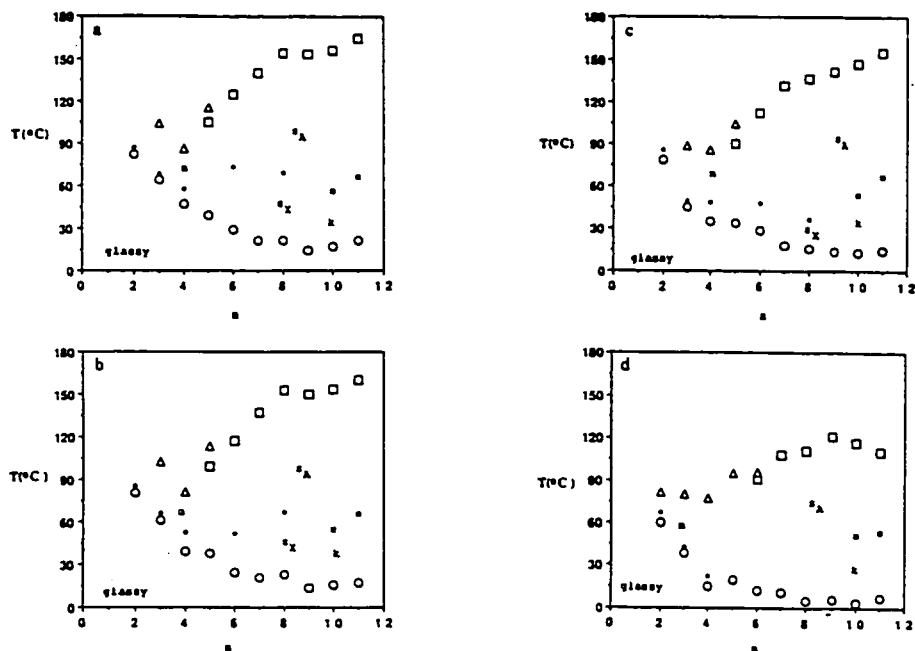


Figure 9. The dependence of phase transition temperatures on the length (n) of flexible $[-(\text{CH}_2)_n-]$ spacer of poly(6-n) at similar degrees of polymerization. a) data from first heating scan at $\text{DP}=30$: \circ - T_g ; \blacklozenge - $T_{sX-SA(n)}$; \blacksquare - T_{k-SA} ; \square - T_{sA-i} ; \triangle - T_{n-i} ; b) data from first heating scan at $\text{DP}=23$: \circ - T_g ; \blacklozenge - $T_{sX-SA(n)}$; \blacksquare - T_{k-SA} ; \square - T_{sA-i} ; \triangle - T_{n-i} ; c) data from first heating scan at $\text{DP}=13$: \circ - T_g ; \blacklozenge - $T_{sX-SA(n)}$; \blacksquare - T_{k-SA} ; \square - T_{sA-i} ; \triangle - T_{n-i} ; d) data from first heating scan at $\text{DP}=4$: \circ - T_g ; \blacklozenge - T_{sX-n} ; \blacksquare - T_{k-SA} ; \square - T_{sA-i} ; \triangle - T_{n-i} .

mesophase, while poly(6-5) a s_A and a nematic mesophase. Poly(6-6), poly(6-8), poly(6-10) and poly(6-11) exhibit s_X (an unidentified smectic mesophase) and a s_A mesophase. The isotropization transition temperature increases with the increase of the spacer length. Upon decreasing the degree of polymerization, all phase transition temperatures of poly(6- n) decreased.

For polymers with short spacers, the isotropization temperature seems to follow an odd-even effect which is opposite to that observed in the case of main chain liquid crystalline polymers containing flexible spacers.¹² That is, in the case of side chain liquid crystalline polymers the highest isotropization temperature is exhibited by the polymers containing odd spacers, while in the case of main chain liquid crystalline polymers by the polymers containing even spacers.¹² A similar behavior was observed in the case of side chain liquid crystalline polymethacrylates based on cyanobenzoyl ester and cyanophenyl ester mesogens and various spacer lengths.^{13,14} These data, together with those of various polymers containing 4-cyanobiphenyl and other mesogenic side groups with different spacer lengths and polymer backbones seem to indicate the same trend, and are discussed in a recent review article.⁹

Let us compare the phase behavior of poly(6- n) with degrees of polymerization 30 and 23, determined from second heating scan with that determined from the first heating scans. Data collected from first heating scans are presented in Figure 9a,b. With the exception of poly(6-2), the nature of the highest temperature mesophase of all other polymers is identical, regardless of the scan it was collected from. In the first heating scan, poly(6-2) exhibits a s_X mesophase. A s_X mesophase is also observed in the first heating scan of poly(6-3) and poly(6-4). In the first heating scan, poly(6-10) and poly(6-11) exhibit a crystalline phase, while in their second heating scan they exhibit a s_X phase.

Upon decreasing the degree of polymerization from 23 to 13, the phase behavior of poly(6-4) changes even more (Figure 8b and c). On the second heating scan, the highest temperature mesophases of poly(6-n)s with degree of polymerization 13 are identical to those of the corresponding polymers with degree of polymerization 23. However, with the exception of poly(6-5), no second mesophase is observed in the case of polymers with degree of polymerization of 13 (see Figure 8c versus b). In the first heating scan, a mesophase or crystalline phase is observed for the polymers with degrees of polymerization 13 (Figure 9c and 8c).

Poly(6-n) with degrees of polymerization of 4 exhibit an even more drastic change of their phase behavior, particularly in the case of polymers with short flexible spacers. Thus, in the second heating scan, poly(6-2) with a degree of polymerization of 4 exhibits a nematic phase, while in the first heating scan it exhibits a s_x and a nematic phase. Poly(6-3), poly(6-4), poly(6-5) and poly(6-6) display a nematic phase both in the second and first heating scans (Figure 8d and 9d). Both in the second and first heating scans, poly(6-6) with degree of polymerization 4 shows a s_A and a nematic phase which overlaps each other. The main difference between the first and second heating scans of the polymers with degrees of polymerization 4 is observed for polymers poly(6-2), poly(6-3), poly(6-10) and poly(6-11) which, in addition to the phases exhibited in the second heating scan (Figure 8d), in the first heating scan present a s_x phase in the case of the first two polymers, and a crystalline phase in the case of the last two polymers (Figure 9d).

The experimental results summarized in Figures 8 and 9 can be explained at least in a qualitative way. There are two combined effects which determine the influence of polymer molecular weight on its phase transitions.

The first one is a thermodynamic effect^{10,11} which through its entropic factor predicts that mesomorphic phase transition temperatures increase with the increase of the polymer molecular weight up to a certain value beyond which they remain constant. The T_g of the polymer exhibits the same trend. The slopes of dependences of various phase transitions versus molecular weight are spacer length dependent. Depending on the ratio between various slopes, a virtual phase transition may become enantiotropic either above or below a certain degree of polymerization. The first situation is representative for the s_X phase of poly(6-6), poly(6-8), poly(6-10) and poly(6-11) which becomes enantiotropic at high molecular weights (Figure 6a,b and c). The second situation is observed in the case of poly(6-2) which displays an enantiotropic nematic mesophase only at low molecular weights (Figure 8c,d). In this particular case, the slope of T_g - M_n dependence is steeper than that of the nematic-isotropic- M_n dependence and therefore, at higher molecular weights this enantiotropic nematic phase becomes virtual.

The second effect is a kinetic one. That is both liquid crystalline and crystalline phase transitions become kinetically controlled especially when they are in the close proximity of T_g and/or when the polymers have high molecular weights. This behavior is characteristic for the s_X phase of poly(6-2), poly(6-3) and poly(6-4) (Figure 9a-d) (due to its close proximity to T_g) and for the crystalline phases of poly(6-10) and poly(6-11) (Figures 8a-d and 9a-d).

The data reported from Chapter 2 to Chapter 6 on the influence of molecular weight on the phase behavior of poly{ ω -[(4-cyano-4'-biphenyl)oxy]alkyl vinyl ether}s provide the most comprehensive collection of results available to date on a polymer homologues series of side chain liquid crystalline polymers. They are important since they can be used to tailor make novel macromolecular architectures based on side chain

liquid crystalline polymers, as well as to provide a theoretical explanation for the trends obtained from these experiments.

REFERENCES

1. T. Sagane and R. W. Lenz, *Macromolecules*, **22**, 3763 (1989)
2. C. G. Cho, B. A. Feit and O. W. Webster, *Macromolecules*, **23**, 1918 (1990)
3. H. Dehne, A. Roger, D. Demus, S. Diele, H. Kresse, G. Pelzl, W. Wedler and W. Weissflog, *Liq. Cryst.*, **6**, 47 (1989) and references cited therein.
4. V. Percec and B. Hahn, *Macromolecules*, **22**, 1588 (1989)
5. S. G. Kostromin, R. V. Talroze, V. P. Shibaev and N. A. Plate, *Makromol. Chem., Rapid Commun.*, **3**, 803 (1982)
6. H. Stevens, G. Rehage and H. Finkelmann, *Macromolecules*, **17**, 851 (1984)
7. V. Shibaev, *Mol. Cryst. Liq. Cryst.*, **155**, 189 (1988)
8. S. Uchida, K. Morita, K. Miyoshi, K. Hashimoto and K. Kawasaki, *Mol. Cryst. Liq. Cryst.*, **155**, 93 (1988)
9. V. Percec and C. Pugh, in "Side Chain Liquid Crystal Polymers", McArdle, C. B. Ed., Chapman and Hall, New York, 1989, p. 30 and references cited therein.
10. V. Percec and A. Keller, *Macromolecules*, **23**, 4347(1990)
11. A. Keller, G. Ungar and V. Percec, in "Advances in Liquid Crystalline Polymers", R. A. Weiss and C. K. Ober Eds., ACS Symposium Series 435, Washington DC, 1990, p.308
12. V. Percec and Y. Tsuda, *Macromolecules*, **23**, 3509 (1990)
13. M. Mauzac, F. Hardouin, H. Richard, M. F. Achard, G. Sigaud and H. Gasparoux, *Eur. Polym. J.*, **22**, 137 (1986)
14. D. A. Gemmel, G. W. Gray and D. Lacey, *Mol. Cryst. Liq. Cryst.*, **122**, 205 (1985)

**PART II. MOLECULAR ENGINEERING OF LIQUID CRYSTALLINE
PHASES BY COPOLYMERIZATION**

Chapter 7

SYNTHESIS AND CHARACTERIZATION OF BINARY COPOLYMERS OF POLY{ ω -(4-CYANO-4'-BIPHENYL)OXY}ALKYL VINYL ETHER}S CONTAINING UNDECANYL AND HEXYL, PENTYL AND PROPYL, UNDECANYL AND PROPYL, AND UNDECANYL AND PENTYL PAIRS OF ALKYL GROUPS

7.1.-INTRODUCTION

7.1.1.-ISOMORPHISM OF LIQUID CRYSTALS

The existence of complete miscibility between two liquid crystalline phases in a binary system is an important criterion of the relationship among phases. If two phases show complete miscibility, they are isomorphic, and therefore, belong to one same type of mesophase. However, if two mesophases are immiscible, they are not isomorphic, but still may belong to the same type of phase. Most identical mesophases displayed by low molar mass liquid crystals are isomorphic and therefore are miscible, regardless of their chemical structure.¹⁻⁴ Consequently, these rules were extensively used to assign mesophases of low molar mass liquid crystals. Recently, these miscibility rules were applied to the identification of mesophases displayed by both main chain and side chain liquid crystal polymers. Similar mesophases of low molar mass liquid crystals and liquid crystalline polymers are frequently not isomorphic.⁴⁻⁷ The same is the case for similar phases of two different liquid crystalline polymers.⁸

When its structural units in a copolymer are isomorphic within a certain phase, the corresponding transition temperatures and thermodynamic parameters exhibit continuous dependences on composition. The validity of this continuous dependence has been demonstrated both for the case of nematic mesophases of liquid crystalline

polymers and the n, s_A mesophases of side chain liquid crystalline polymers. The isomorphic structural units of a copolymer behave like an ideal solution of those structural units. Therefore, the thermal behavior of this copolymer can be predicted by the Schroeder-van Laar equation (eq. 1).^{9,10}

$$F_1 = \left\{ 1 - \frac{\Delta H_1^\circ T_2 (T - T_1)}{\Delta H_2^\circ T_1 (T - T_2)} \right\}^{-1} \quad \text{Eq. 1}$$

where F_1 is the molar fraction of component 1, T_1 and ΔH_1 are the transition temperature and the enthalpy change of pure component 1, T_2 and ΔH_2 have the same meaning for component 2, while T_1 is the transition temperature corresponding to composition F_1 . Since $0 \leq F_1 \leq 1$, the permissible values of T are such that, for $T_2 > T_1$, T must be less than T_2 or greater than T_1 , otherwise $F_1 > 1$, which is not possible. Thus phase diagram that exhibits any temperature greater or lesser than the maximum or minimum T_2 or T_1 , respectively, violates the T criteria above and must therefore be discussed by the introduction of nonideality of solutions of structural units of copolymers.

7.1.2.-COPOLYMERIZATION

Copolymerization represents the simplest synthetic technique which can be used to tailor make phase transitions of both main chain^{11a} and side chain^{11b} liquid crystalline polymers. Indeed, copolymerization was frequently employed to manipulate the phase transitions of side chain liquid crystalline polymers.¹¹⁻¹⁵ However, most of the results reported in the literature can be considered only in a qualitative way, since

there are only very few cases in which information about both copolymer composition and molecular weight are available.^{11b-16}

A general classification of side chain liquid crystalline copolymers¹⁵ was recently discussed in a review article.^{11b} There are two main classes of side chain liquid crystalline copolymers. The first one refers to copolymers containing pairs of structural units with and without mesogenic units.^{11b-14,16-22} This class of copolymers was extensively investigated. The second class refers to copolymers based on pairs of structural units containing mesogenic units in each one. There are at least four different groups which should be considered in this second class: a) copolymers from monomer pairs containing identical mesogens and polymerizable groups, but different spacer lengths; b) copolymers from monomer pairs containing identical mesogens and spacer lengths but different polymerizable groups; c) copolymers from monomer pairs containing dissimilar mesogens, but either similar or different spacer lengths and polymerizable groups; d) copolymers from monomer pairs containing constitutional isomeric units, and similar or dissimilar spacers and polymerizable groups. Presently, there is a relatively good understanding of the last class of copolymers.^{23,24} When the structural units of these copolymers are isomorphic in their liquid crystalline phase but not in their crystalline phase, copolymerization could be used to transform virtual or monotropic mesophases into enantiotropic mesophases. A general discussion considering the isomorphism in liquid crystalline polymers and copolymers was published elsewhere.⁸

The following general trends were observed so far when copolymers from the second class of type a, b and c were investigated. When the structural units of the copolymer were isomorphic within the liquid crystalline phase, a continuous or even linear dependence of the phase transition temperature versus copolymer composition

was observed.²⁵ When the structural units of the copolymer were nonisomorphic within the mesophase, a discontinuous dependence of phase transitions versus composition was observed.²⁵⁻²⁸

Although the compositions of these copolymers were reported, molecular weight information was not presented. Liquid crystalline copolysiloxanes are prepared by hydrosilation reactions. They are considered to be statistical copolymers with a random distribution of their structural units.^{11b,25} Copolymers synthesized by chain copolymerization reactions exhibit a heterogeneous composition unless they are prepared at low conversions.^{11b,29} At the same time, there is no single example in the literature in which the molecular weights of statistical side chain liquid crystalline copolymers prepared by chain copolymerizations were reported.^{11b,13,15,26-28} Since mesomorphic transitions are molecular weight dependent,^{11b,21,30-40} the synthesis of copolymers with both well defined compositions and molecular weights are required. The ideal solution to the synthesis of copolymers by chain reactions would be to select monomer pairs which follow an azeotropic copolymerization and can be prepared by a living polymerization mechanism. Such systems require $r_1=r_2=1$ and are encountered mainly for comonomer pairs of almost similar structure.

Vinyl ethers containing an identical mesogenic group but different spacer lengths are presently the most suitable monomers for these investigations.³³⁻⁴¹ The living cationic polymerization of ω -[(4-cyano-4'-biphenyl)oxy]alkyl vinyl ethers with 2 to 11 methylene units as described in previous chapters and the characterization of the resulting polymers as a function of molecular weight were investigated. The availability of these data and monomers, provides access to a quantitative investigation of side chain liquid crystalline copolymers.

The goal of this chapter is to describe the synthesis and characterization of the following copolymers: poly{11-[(4-cyano-4'-biphenyl)oxy]undecanyl vinyl ether-co-6-[(4-cyano-4'-biphenyl)oxy]hexyl vinyl ether}X/Y {poly[(6-11)-co-(6-6)]X/Y}, poly{5-[(4-cyano-4'-biphenyl)oxy]pentyl vinyl ether-co-3-[(4-cyano-4'-biphenyl)oxy]propyl vinyl ether}X/Y {poly[(6-5)-co-(6-3)]X/Y}, poly{11-[(4-cyano-4'-biphenyl)oxy]undecanyl vinyl ether-co-3-[(4-cyano-4'-biphenyl)oxy]propyl vinyl ether}X/Y {poly[(6-11)-co-(6-3)]X/Y} and poly{11-[(4-cyano-4'-biphenyl)oxy]undecanyl vinyl ether-co-5-[(4-cyano-4'-biphenyl)oxy]pentyl vinyl ether}X/Y {poly[(6-11)-co-(6-5)]X/Y}. All copolymers were synthesized with degrees of polymerization of about 20, and molecular weight distributions of about 1.10. The mesomorphic phases exhibited by the parent polymers with degree of polymerization of 20 as determined from the second DSC scans are as follows: poly(6-11) and poly(6-6), enantiotropic s_A and s_X , poly(6-5) enantiotropic s_A and n , and poly(6-3), enantiotropic nematic. Therefore, the investigation of these three pairs of copolymers will elucidate the phase behavior of copolymers derived from pairs of homopolymers exhibiting the following high temperature mesophases: s_A and s_A , n and n , and s_A and n , and thus will provide a complete characterization of the class of copolymers (a).

7.2.-EXPERIMENTAL

7.2.1.-Materials

All materials were commercially available and were used as received or purified as described previously.^{36-38,40} Methyl sulfide (anhydrous, 99%, Aldrich) was refluxed over 9-borabicyclo[3.3.1]nonane (9-BBN, crystalline, 98%, Aldrich) and then distilled under argon. Dichloromethane (99.6%, Aldrich) used as a polymerization solvent was first washed with concentrated sulfuric acid, then with water, dried over

anhydrous magnesium sulfate, refluxed over calcium hydride and freshly distilled under argon before each use. Trifluoromethane sulfonic acid (triflic acid, 98%, Aldrich) was distilled under argon.

7.2.2.-Synthesis of Monomers

11-[(4-Cyano-4'-biphenyl)oxy]undecanyl vinyl ether (6-11)⁴⁰, 6-[(4-cyano-4'-biphenyl)oxy]hexyl vinyl ether (6-6),³⁸ 5-[(4-cyano-4'-biphenyl)oxy]pentyl vinyl ether (6-5)³⁷ and 3-[(4-cyano-4'-biphenyl)oxy]propyl vinyl ether (6-3)³⁶ were synthesized and purified as described in previous publications. Their purity was higher than 99% (HPLC). Their detailed characterization is described in the previous publications.

7.2.3.-Cationic Polymerizations and Copolymerization

Polymerizations were carried out in glass flasks equipped with teflon stopcocks and rubber septa under argon atmosphere at 0°C for 1 hr. All glassware was dried overnight at 130°C. The monomer was further dried under vacuum overnight in the polymerization flask. Then the flask was filled with argon, cooled to 0°C and the methylene chloride, dimethyl sulfide and triflic acid were added via a syringe. The monomer concentration was about 10 wt% of the solvent volume and the dimethyl sulfide concentration was 10 times larger than that of the initiator. The polymer molecular weight was controlled by the monomer/initiator ($[M]_0/[I]_0$) ratio. After quenching the polymerization with ammoniacal methanol, the reaction mixture was precipitated into methanol. When necessary, the polymers were reprecipitated until their GPC and HPLC traces showed complete absence of unreacted monomers. Tables I, II, III and IV summarize the polymerization results. Although polymer yields are lower than expected due to losses during the purification process, conversions determined by

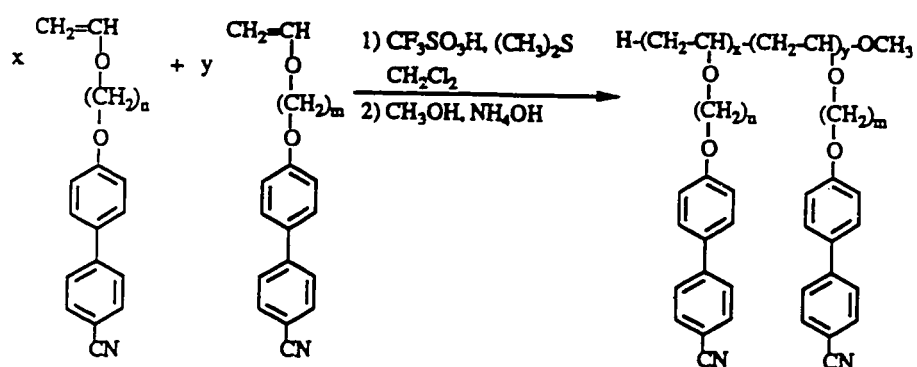
HPLC and GPC analysis before polymer purification were almost quantitative in all cases.

7.3.-RESULTS AND DISCUSSION

The synthesis, characterization and living cationic polymerization of ω -[(4-cyano-4'-biphenyl)oxy]alkyl vinyl ethers with alkyl groups from ethyl to undecanyl were described in the previous papers.³⁶⁻⁴⁰ Our preferred initiating system is $\text{CF}_3\text{SO}_3\text{H}/\text{S}(\text{CH}_3)_2$ ⁴² since it can be used to perform living cationic polymerizations in CH_2Cl_2 at 0°C . In addition, we have shown that this system can be used to initiate the living cationic polymerization and cyclopolymerization of monomers containing a variety of functional groups.⁴³⁻⁴⁶

The copolymerization of these monomer pairs is outlined in Scheme I. As discussed in the experimental section, the copolymer composition is equal to the monomer feed. Some ^1H -NMR experiments were used to test this assumption, which is based on the following additional experimental data. All copolymerizations lead to almost quantitative conversions (determined by HPLC and GPC), although the yields reported in Tables I to IV are lower than 100%. This is due to polymer losses during the purification experiments. The GPC traces of all copolymers show a monomodal molecular weight distribution characterized by a polydispersity of about 1.10 (Tables I and IV). Attempts were made to synthesize all copolymers investigated in this study with degrees of polymerization of about 20.

According to the nature of the highest temperature mesophase exhibited by the pair of homopolymers generated from the pair of monomers used in the synthesis of copolymers, we can classify these experiments in two classes. Copolymers based on monomer pairs whose parent homopolymers exhibit identical mesophases, and



Scheme I. Cationic polymerization of 6-n and 6-m

Table I. Cationic Copolymerization of 6-11 with 6-6 (polymerization temperature, 0°C; polymerization solvent, methylene chloride; $[M]_0 = [6-11] + [6-6] = 0.256-0.312M$; $[M]_0/[I]_0 = 20$; $[(CH_3)_2SiO]/[I]_0 = 10$; polymerization time, 1hr) and Characterization of the Resulting Polymers. Data on first line are from first heating and cooling scans. Data on second line are from second heating scan.

Sample No.	[6-11]/[6-6] (mol/mol)	Polymer yield(%)	Mnx10 ⁻³	Mw/Mn	D P	phase transitions (°C) and corresponding enthalpy changes (kcal/mru)	
						heating	cooling
1	0/10	85	6.1	1.10	19	g 31.3 sX 68.9 (0.30) sA 127.3 (0.19) i g 29.1 sX 67.7 (0.31) sA 126.9 (0.18) i g 25.6 sX 55.7 (0.21) sA 130.4 (0.20) i g 25.9 sX 53.5 (0.19) sA 130.2 (0.22) i g 22.2 sX 48.9 (0.25) sA 137.7 (0.32) i g 18.9 sA 137.1 (0.30) i g 19.7 sX 37.4 (0.22) sA 140.4 (0.42) i g 17.7 sA 140.5 (0.41) i g 16.5 sA 144.9 (0.52) i g 15.4 sA 144.7 (0.56) i g 15.4 sA 148.1 (0.54) i g 14.7 sA 147.7 (0.56) i g 14.8 sA 151.7 (0.62) i g 17.5 sA 151.5 (0.61) i g 14.3 sA 153.7 (0.68) i g 11.0 sA 153.3 (0.71) i g 12.6 k 47.5 (0.19) sA 154.3 (0.74) i g 10.8 sA 154.2 (0.76) i g 12.8 k 53.6 (2.18) sA 155.8 (0.84) i g 12.1 sA 155.3 (0.82) i g 14.5 k 57.1 (3.45) sA 157.2 (0.90) i g 14.0 sX 44.2 (0.93) sA 156.4 (0.87) i	i 120.3 (0.17) sA 57.4 (0.34) sX 25.9 g i 123.1 (0.22) sA 41.0 (0.30) sX 21.4 g i 132.0 (0.33) sA 15.4 g i 134.4 (0.42) sA 13.0 g i 138.8 (0.49) sA 10.2 g i 141.5 (0.57) sA 9.2 g i 146.6 (0.63) sA 9.0 g i 148.8 (0.71) sA 9.5 g i 148.2 (0.75) sA 8.9 g i 149.3 (0.81) sA 9.0 g i 149.4 (0.89) sA 18.9 (0.63) sX 8.8 g
2	1/9	86	7.0	1.09	21		
3	2/8	88	5.9	1.09	18		
4	3/7	80	6.7	1.14	20		
5	4/6	84	6.9	1.16	19		
6	5/5	82	6.4	1.15	18		
7	6/4	82	6.3	1.15	17		
8	7/3	74	7.0	1.13	19		
9	8/2	75	6.8	1.15	18		
10	9/1	80	8.1	1.12	21		
11	10/0	81	8.2	1.12	19		

Table II. Cationic Copolymerization of 6-5 with 6-3 (polymerization temperature, 0°C; polymerization solvent, methylene chloride; $[M]_0 = [6-5] + [6-3] = 0.326$ -0.358M; $[M]_0/[I]_0 = 20$; $[(CH_3)_2S]/[I]_0 = 10$; polymerization time, 1hr) and Characterization of the Resulting Polymers. Data on first line are from first heating and cooling scans. Data on second line are from second heating scan.

Sample No.	[6-5]/[6-3] (mol/mol)	Polymer yield(%)	$M_n \times 10^{-3}$	M_w/M_n	DP GPC	phase transitions (°C) and corresponding enthalpy changes (kcal/mru)	
						heating	cooling
1	0/10	80	5.9	1.09	21	g 61.3 X 68.8 (0.19) n 102.9 (0.12) i g 60.0 n 102.9 (0.10) i	i 97.6 (0.10) n 51.9 g
2	1/9	89	4.8	1.11	17	g 55.9 X 62.8 (0.14) n 101.4 (0.10) i g 554.9 n 101.7 (0.09) i	i 95.5 (0.09) n 46.8 g
3	2/8	84	4.9	1.09	18	g 51.2 X 58.5 (0.17) n 103.1 (0.10) i g 50.8 n 103.4 (0.09) i	i 97.2 (0.10) n 42.1 g
4	3/7	84	5.2	1.15	18	g 47.9 X 55.1 (0.17) n 103.3 (0.10) i g 47.5 n 103.5 (0.11) i	i 97.4 (0.10) n 38.1 g
5	4/6	86	5.3	1.10	19	g 45.2 X 53.4 (0.18) n 104.9 (0.10) i g 44.5 n 105.1 (0.11) i	i 99.3 (0.45) n 37.1 g
6	5/5	71	5.3	1.12	18	g 42.3 X 46.9 (0.15) n 106.9 (0.11) i g 42.1 n 107.1 (0.09) i	i 101.4 (0.10) n 34.8 g
7	6/4	82	5.3	1.09	18	g 39.4 X 42.9 (0.14) n 107.3 (0.12) i g 38.8 n 107.4 (0.11) i	i 101.7 (0.11) n 32.1 g
8	7/3	78	5.2	1.10	18	g 33.4 X 41.1 (0.18) n 110.6 (0.11) i g 34.2 n 110.7 (0.12) i	i 103.4 (0.11) n 31.5 g
9	8/2	84	5.1	1.11	17	g 32.2 X 39.3 (0.12) n 111.6 (0.09) i g 31.4 n 111.7 (0.11) i	i 106.9 (0.12) n 28.7 g
10	9/1	85	4.8	1.11	16	g 27.3 sA 89.2 (-) n 112.6 (0.10) i g 27.7 sA 88.4 (-) n 112.8 (0.12) i	i 107.8 (0.11) n 81.7 (-) sA 25.7 g
11	10/0	80	5.4	1.13	18	g 28.1 sA 102.3 (-) n 113.2 (0.14) i g 28.5 sA 102.1 (-) n 113.5 (0.13) i	i 108.9 (0.12) n 90.3 (-) sA 25.5 g

Table III. Cationic Copolymerization of 6-11 with 6-3 (polymerization temperature, 0°C; polymerization solvent, methylene chloride; $[M]_0/[I]_0=20$; $[(CH_3)_2S]/[I]_0=10$; polymerization time, 1hr) and Characterization of the Resulting Polymers. Data on first line are from first heating and cooling scans. Data on second line are from second heating scan.

Sample No.	[6-11]/[6-3] (mol/mol)	Polymer yield(%)	Mnx 10 ⁻³	Mw/Mn G P C	DP	phase transitions (°C) and corresponding enthalpy changes (kcal/mru)	
						heating	cooling
1	0/10	80	5.9	1.09	21	g 61.3 X 68.8 (0.19) n 102.9 (0.12) i g 60.0 n 102.9 (0.10) i	i 97.6 (0.10) n 51.9 g
2	1/9	78	5.7	1.12	18	g 54.1 X 61.3 (0.26) n 106.1 (0.13) i g 52.8 n 106.0 (0.14) i	i 100.7 (0.12) n 44.2 g
3	2/8	86	6.0	1.10	19	g 44.7 X 51.8 (0.33) n 110.2 (0.17) i g 44.2 n 110.4 (0.16) i	i 104.9 (0.15) n 36.7 g
4	3/7	74	5.6	1.08	17	g 37.9 X 43.6 (0.42) sA 98.3 (0.019) n 114.2 (0.20) i g 34.8 sA 98.2 (0.022) n 114.5 (0.19) i	i 108.5 (0.22) n 91.8 (0.026) sA 27.8 g
5	4/6	79	6.0	1.08	18	g 29.8 X 36.4 (0.18) sA 121.1 (0.44) i g 27.7 sA 121.0 (0.45) i	i 116.1 (0.45) sA 22.5 g
6	5/5	82	6.6	1.10	19	g 23.1 sA 128.7 (0.56) i g 22.5 sA 129.0 (0.55) i	i 122.8 (0.54) sA 17.9 g
7	6/4	76	6.7	1.10	19	g 18.5 sA 134.0 (0.63) i g 17.5 sA 134.5 (0.61) i	i 129.2 (0.59) sA 13.9 g
8	7/3	65	6.3	1.07	17	g 16.5 sA 139.4 (0.66) i g 15.6 sA 140.2 (0.70) i	i 135.0 (0.67) sA 10.5 g
9	8/2	70	7.6	1.10	20	g 14.6 k 47.4 (0.12) sA 144.3 (0.76) i g 14.0 sA 144.9 (0.74) i	i 139.9 (0.74) sA 9.8 g
10	9/1	67	7.5	1.09	19	g 14.8 k 50.6 (2.15) sA 150.8 (0.84) i g 14.1 sA 150.3 (0.81) i	i 144.3 (0.80) sA 9.0 g
11	10/0	81	8.2	1.12	19	g 14.5 k 57.1 (3.45) sA 157.2 (0.90) i g 14.0 sX 44.2 (0.93) sA 156.4 (0.87) i	i 149.4 (0.89) sA 18.9 (0.63) sX 8.8 g

Table IV. Cationic Copolymerization of 6-11 with 6-5 (polymerization temperature, 0°C; polymerization solvent, methylene chloride; $[M]_0 = [6-11] + [6-5] = 0.256$ -0.326M; $[M]_0/[1]_0 = 20$; $[(CH_3)_2S]/[I]_0 = 10$; polymerization time, 1hr) and Characterization of the Resulting Polymers. Data on first line are from first heating and cooling scans. Data on second line are from second heating scan.

Sample No.	[6-11]/[6-5] (mol/mol)	Polymer yield(%)	Mnx10 ⁻³	Mw/Mn G P C	D P	phase transitions (°C) and corresponding enthalpy changes (kcal/mru)	
						heating	cooling
1	0/10	87	5.4	1.13	18	g 28.1 n _{re} 69 ^a s _A 102.3 (-) n 113.2 (0.12) i g 28.5 n _{re} 69 ^a s _A 102.1 (-) s _A 113.5 (0.10) i g 25.4 n _{re} 40.3 ^a s _A 114.5 (-) n 118.2 (0.21) i g 25.2 n _{re} 40.3 ^a s _A 114.7 (-) n 118.4 (0.20) i g 22.7 s _A 123.2 (0.28) i g 20.4 s _A 122.7 (0.27) i g 18.4 s _A 130.8 (0.40) i g 17.7 s _A 130.6 (0.37) i g 16.2 s _A 134.0 (0.50) i g 15.3 s _A 133.7 (0.48) i g 15.4 s _A 139.1 (0.56) i g 14.7 s _A 138.5 (0.56) i g 15.2 s _A 143.1 (0.62) i g 15.7 s _A 143.5 (0.64) i g 14.3 s _A 148.6 (0.70) i g 13.5 s _A 148.1 (0.68) i g 13.9 s _A 149.8 (0.79) i g 12.7 s _A 149.0 (0.77) i g 13.8 k 53.6 (3.01) s _A 153.9 (0.87) i g 12.5 s _A 153.6 (0.85) i g 14.5 k 57.1 (3.45) s _A 157.2 (0.90) i g 14.0 s _X 44.2 (0.93) s _A 156.4 (0.87) i	i 108.9 (0.11) n 90.3 (-) s _A 69 ^a n _{re} 25.5 g i 115.0 (0.20) n 109.4 (-) s _A 40.3 ^a n _{re} 20.1 g i 117.9 (0.27) s _A 15.2 g i 124.7 (0.38) s _A 12.8 g i 127.4 (0.45) s _A 10.3 g i 134.4 (0.56) s _A 9.7 g i 138.1 (0.60) s _A 9.0 g i 142.2 (0.67) s _A 9.2 g i 144.0 (0.77) s _A 9.0 g i 148.3 (0.80) s _A 9.0 g i 149.4 (0.89) s _A 18.9 (0.63) s _X 8.8 g
2	1/9	85	5.7	1.19	18		
3	2/8	77	5.8	1.09	17		
4	3/7	82	6.8	1.14	18		
5	4/6	77	6.4	1.16	19		
6	5/5	79	6.3	1.15	18		
7	6/4	82	6.3	1.15	17		
8	7/3	74	6.2	1.13	17		
9	8/2	75	6.8	1.15	18		
10	9/1	83	7.7	1.12	20		
11	10/0	81	8.2	1.12	19		

^a data obtained from optical polarized microscopy

copolymers based on monomer pairs whose parent homopolymers exhibit different mesophases. Poly[(6-11)-co-(6-6)]X/Y and poly[(6-5)-co-(6-3)]X/Y copolymers belong to the first class. The first copolymer is derived from a monomer pair whose parent homopolymers exhibit enantiotropic s_A phases as their highest temperature mesophase, while the second copolymer is derived from a monomer pair whose parent homopolymers exhibit enantiotropic n phases as their highest temperature mesophase. Poly[(6-11)-co-(6-3)]X/Y and poly[(6-11)-co-(6-5)]X/Y are based on a monomer pair whose parent homopolymers exhibit enantiotropic s_A and respectively enantiotropic n phases as their highest temperature mesophase. The phase behavior of these copolymers will be presented in the order discussed above. The phase behavior of all these copolymers will be discussed as obtained from their first and second heating and first cooling DSC scans.

7.3.1.-Poly[(6-11)-co-(6-6)]X/Y

The synthesis and characterization of poly[(6-11)-co-(6-6)]X/Y copolymers is summarized in Table I. The first and the second heating and the first cooling DSC traces of all homopolymers and copolymers are presented in Figure 1a,b,c. As determined from the first DSC scans, poly(6-11) with a degree of polymerization of 19 exhibits an enantiotropic s_A mesophase and a crystalline melting.⁴⁰ When the phase behavior of the same poly(6-11) is determined from second and subsequent DSC scans, it exhibits enantiotropic s_A and s_X (i.e., an unidentified smectic) mesophases⁴⁰ (Figure 1a,b,c). Regardless of the thermal history of the sample, poly(6-6) with degree of polymerization 19 exhibits enantiotropic s_A and s_X mesophases (Figure 1a,b,c).³⁸

The dependence of the temperatures associated with the s_A -isotropic and isotropic- s_A transitions can be easily observed from the DSC traces presented in Figure

1a (for the first heating scans), Figure 1b (for the second heating scans) and Figure 1c (for the first cooling scans). This transition temperature shows a continuous, almost linear dependence of copolymer composition, regardless of the DSC scan the temperature transitions are collected from. However, the temperature transitions associated with the s_X-s_A , $k-s_A$ from the first heating scans (Figure 1a), s_X-s_A and s_X-s_A from the second heating scans (Figure 1b), and s_A-s_X from the first cooling scans (Figure 1c) show a discontinuous dependence of copolymer composition.

The phase transition temperatures collected from the first heating scans are plotted in Figure 2a, those from the second heating scans in Figure 2b, while those from the first cooling scans in Figure 2c. The upward curvature of the s_A -isotropic and isotropic- s_A dependences versus copolymer composition (Figure 2a,b,c) can be explained by the Schroeder-van Laar equations.¹⁰ This upward curvature was calculated by using the Schroeder-van Laar equations and qualitatively agrees with that obtained experimentally. Thus, the phase diagram of these copolymers can be regarded as close to what is expected for an ideal solution resulting from the structural units of the copolymer.¹⁰ The enthalpy changes associated with the s_A -isotropic phase transitions determined from the first and second DSC scans and the isotropic- s_A phase transitions (Table I) are plotted in Figure 2d as a function of copolymer composition. This dependence is linear, thus demonstrating a weight average dependence of copolymer composition.

The conclusion derived from these results is as follows. Over the entire range of compositions, the structural units of the poly[(6-11)-co-(6-6)]X/Y copolymers are isomorphic within the s_A mesophase.⁸ However, the same two structural units are not isomorphic within the crystalline phase of poly(6-11) (Figure 2a), and are isomorphic only over a very narrow range of composition into the s_X mesophase of poly(6-6)

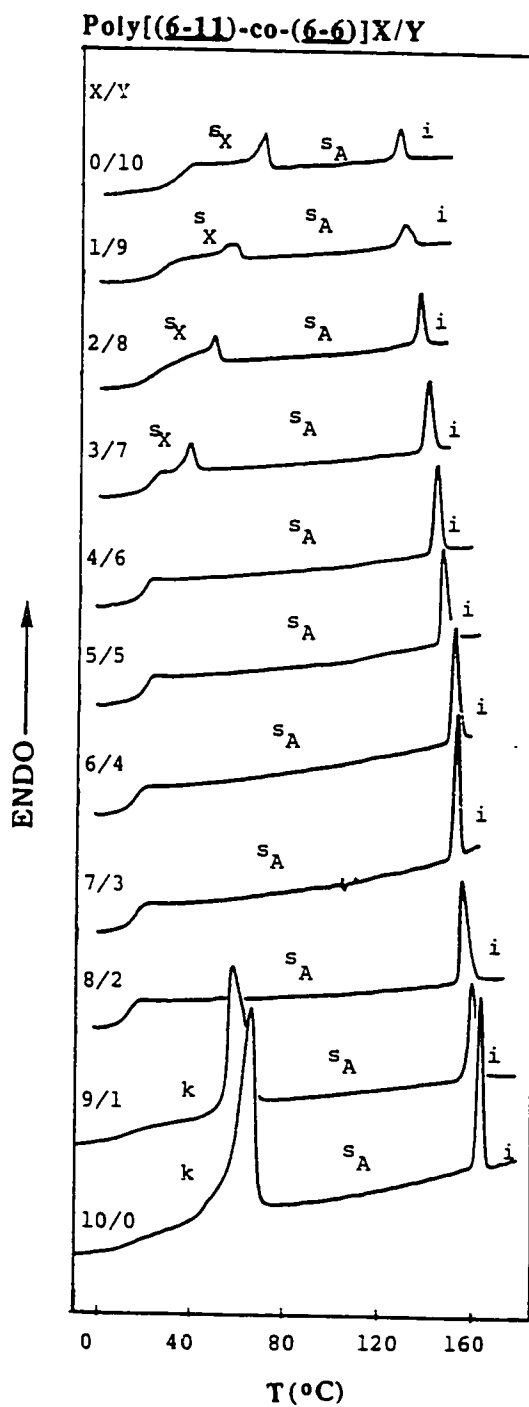


Figure 1a. DSC traces displayed during the first heating scan by poly(6-11), poly(6-6) and by poly[(6-11)-co-(6-6)]X/Y.

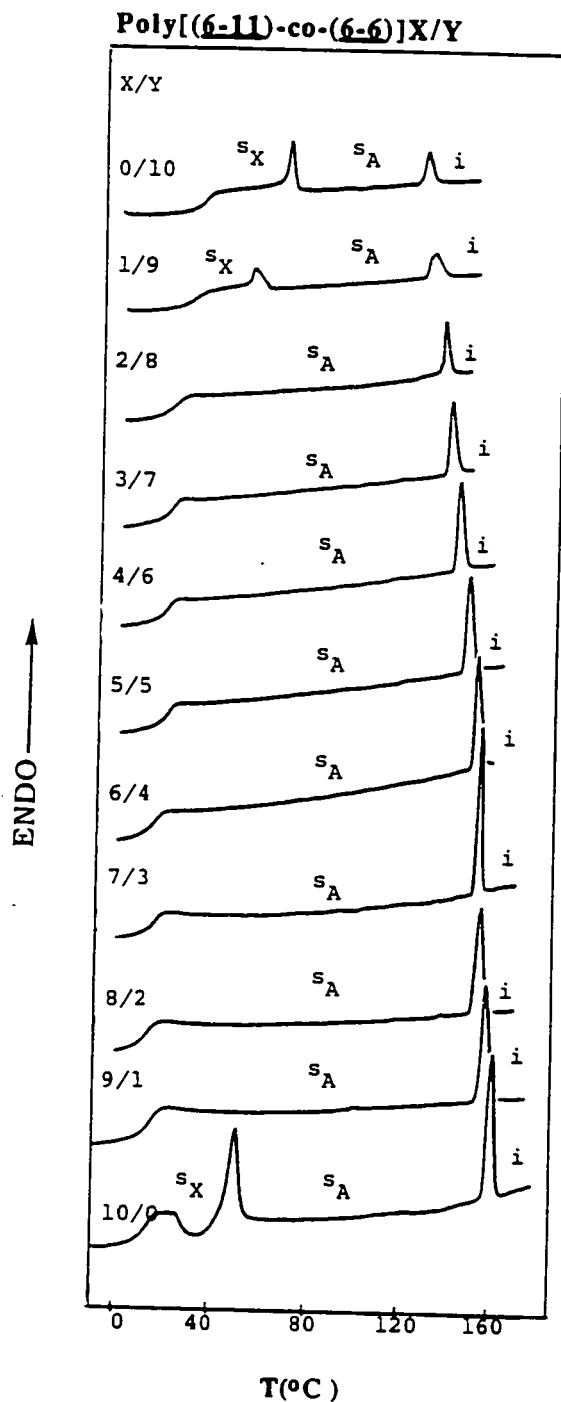


Figure 1b. DSC traces displayed during the second heating scan by poly(6-11), poly(6-6) and by poly[(6-11)-co-(6-6)]X/Y.

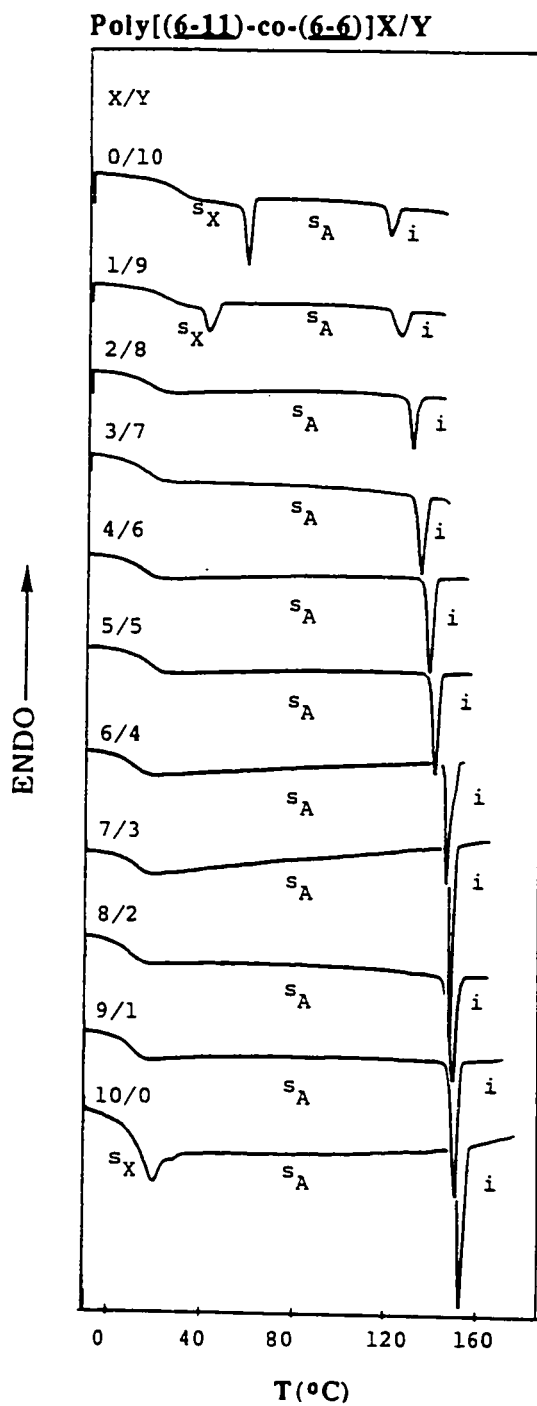


Figure 1c. DSC traces displayed during the first cooling scan by poly(6-11), poly(6-6) and by poly[(6-11)-co-(6-6)]X/Y.

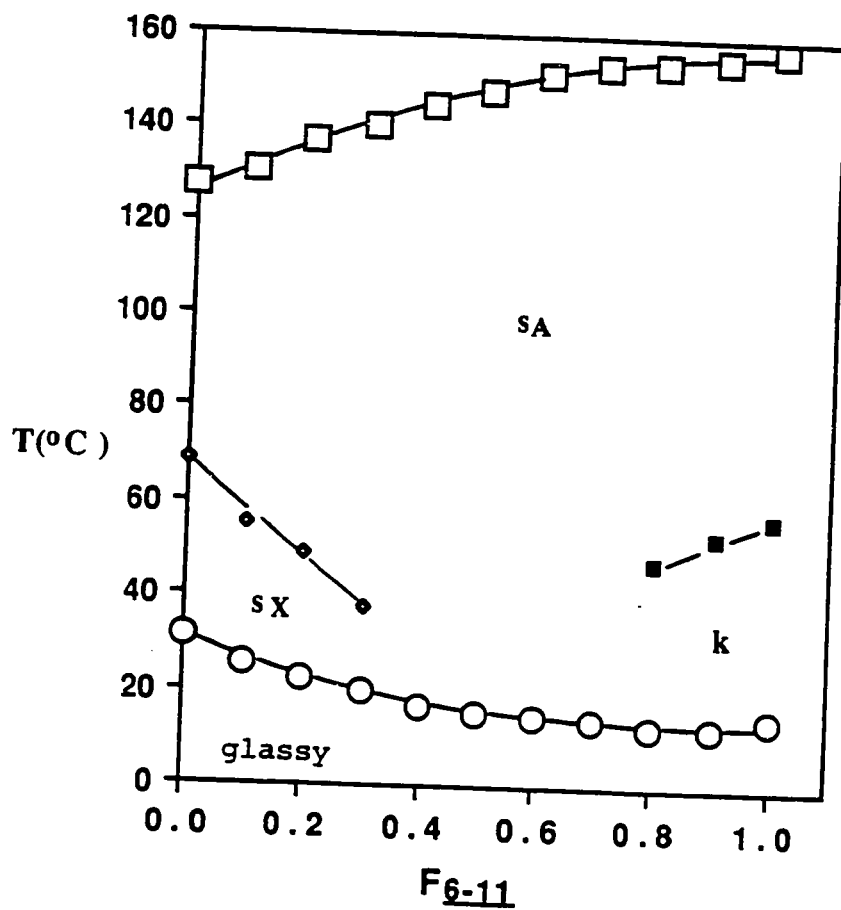


Figure 2a. The dependence of phase transition temperatures on the composition of poly[(6-11)-co-(6-6)]X/Y (data from the first heating scan): O- T_{g} ; \diamond - $T_{\text{SX-SA}}$; \blacksquare - $T_{\text{Tk-SA}}$; \square - $T_{\text{SA-i}}$

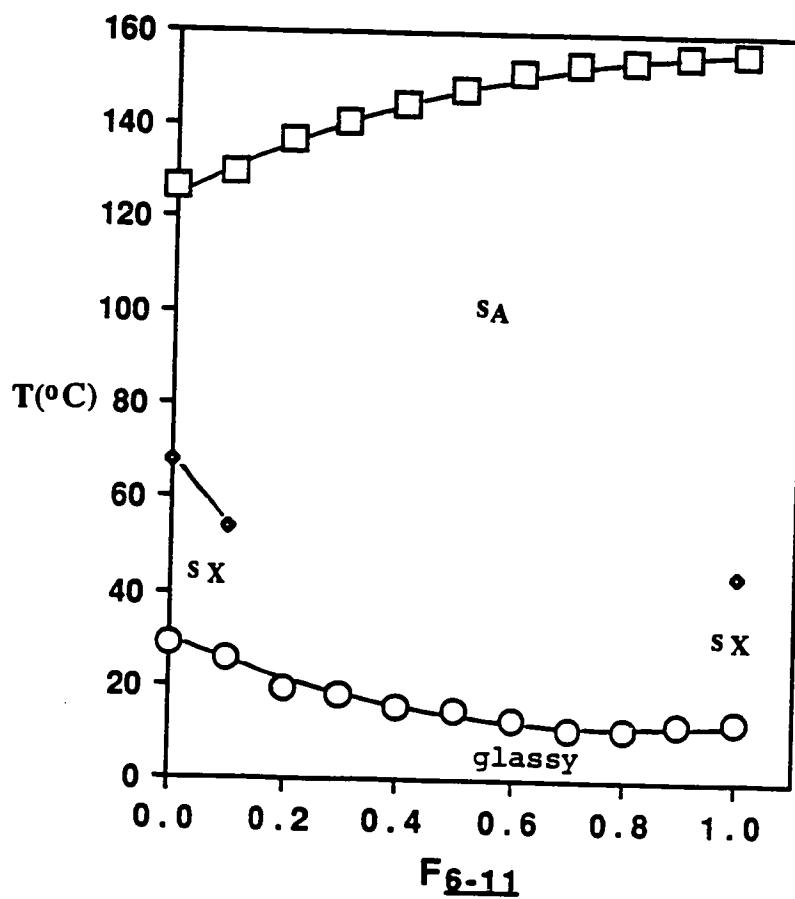


Figure 2b. The dependence of phase transition temperatures on the composition of poly[(6-11)-co-(6-6)]X/Y. (data from the second heating scan): O- T_g ; \diamond - T_{sX-SA} ; \square - T_{sA-i}

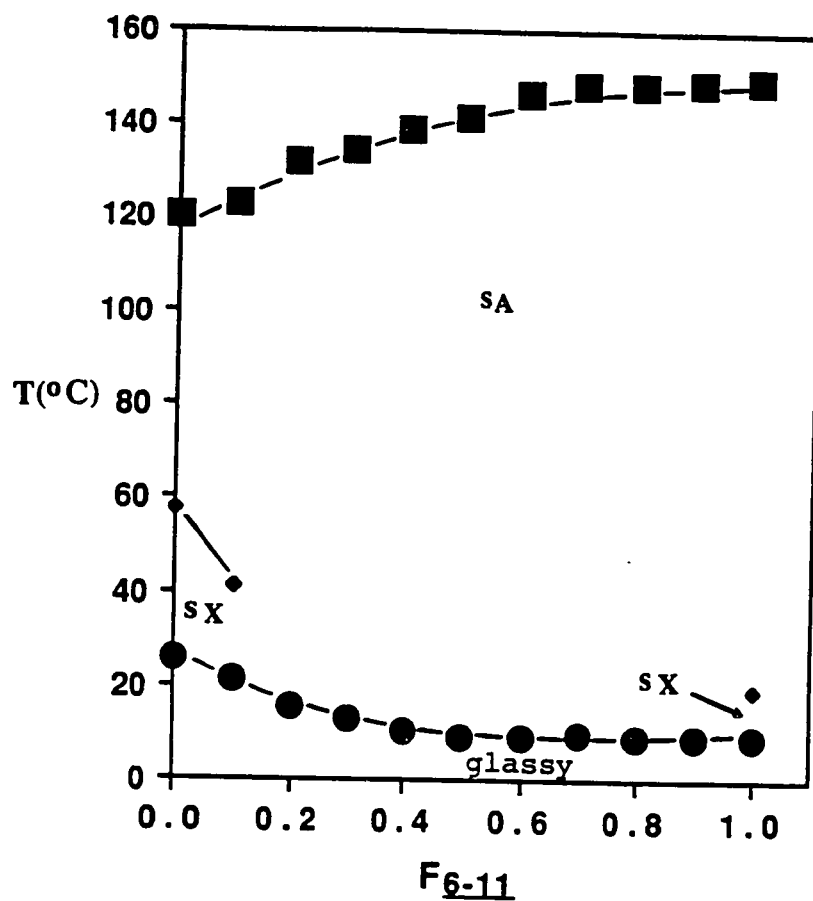


Figure 2c. The dependence of phase transition temperatures on the composition of poly[(6-11)-co-(6-6)]X/Y (data from the first cooling scan): ■- T_{i-sA} ; ◆- T_{sA-sX} ; ●- T_g .

(Figures 1a,b,c and 2a,b,c). As a consequence, poly[(6-11)-co-(6-6)]X/Y with X/Y=2/8 to 9/1 exhibit only an enantiotropic s_A phase over a very large range of temperatures.

From the preparative point of view, the results of this experiment provide a technique which can be used to molecular engineer noncrystallizable copolymers which exhibit a s_A mesophase over a very large range of temperatures. At the same time, it teaches us how to tailor make the degree of order of the s_A mesophase by living copolymerization experiments (Figure 2d) (i.e., how to design a polymer exhibiting a s_A mesophase with a well established enthalpy change associated with the s_A -isotropic phase transition).

7.3.2.-Poly[(6-5)-co-(6-3)]X/Y

Table II summarizes the synthesis and characterization of poly[(6-5)-co-(6-3)]X/Y. The DSC traces of the first heating scans are presented in Figure 3a, those of the second heating scans in Figure 3b and those of the first cooling scans in Figure 3c. Poly(6-5) with a degree of polymerization of 18 exhibits enantiotropic s_A and n mesophases both in the first and second DSC scans.³⁷ As characterized from the first DSC heating scan, poly(6-3) with a degree of polymerization of 21 exhibits monotropic s_X and enantiotropic n mesophases.³⁶ However, when the same polymer is characterized from the second DSC heating scan, it exhibits only an enantiotropic n mesophase (Figure 3a,b,c).³⁶ Let us investigate the phase behavior of poly[(6-5)-co-(6-3)]X/Y as obtained from the first DSC heating scans (Figure 3a). The n mesophase exhibits a linear dependence of copolymer composition which can be explained by the Schroeder-van Laar equations for an ideal solution.¹⁰ That is, the structural units of both poly(6-5) and poly(6-3) are isomorphic within the n phase over the entire range of

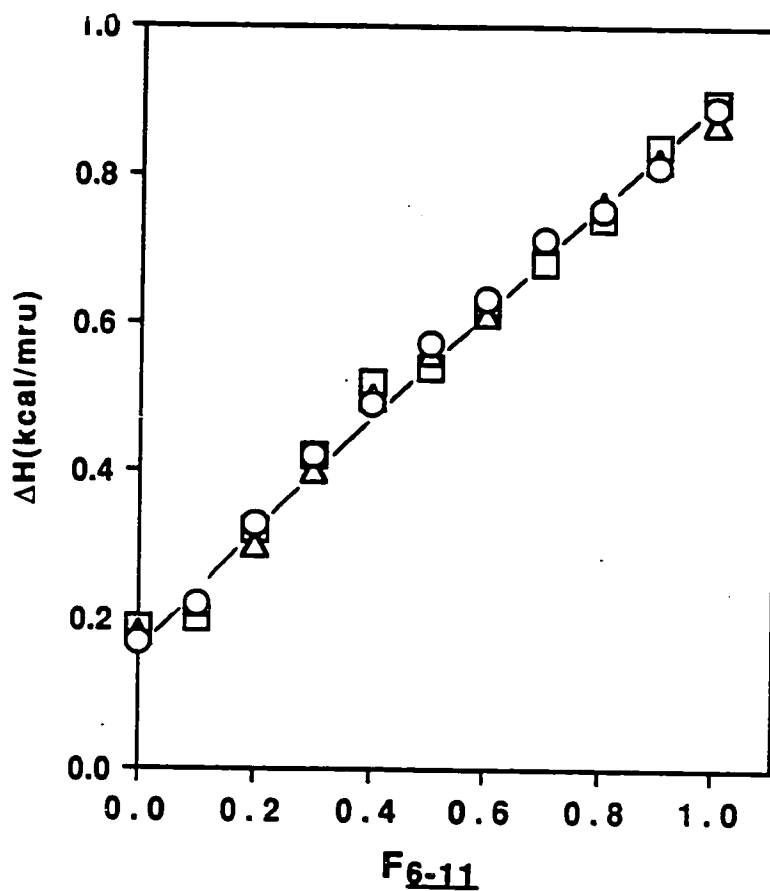


Figure 2d. The dependence of the enthalpy changes associated with the mesomorphic-isotropic and isotropic-mesomorphic phase transitions on the composition of poly[(6-11)-co-(6-6)]X/Y. □-ΔH_{sA-i} (data from the first heating scan); Δ-ΔH_{sA-i} (data from the second heating scan); O-ΔH_{i-sA} (data from the first cooling scan).

compositions. The s_X mesophase is also showing a continuous dependence of copolymer composition over the range of compositions from $X/Y=0/10$ to $8/2$. Poly[(6-5)-co-(6-3)]9/1 does not exhibit this mesophase.

The s_A mesophase appears also over a narrow range of copolymer composition, i.e., in the case of copolymer poly[(6-5)-co-(6-3)]9/1. In the second DSC heating scan, the s_X mesophase does not appear, while the s_A and n mesophases follow the same trend as the one observed in the first DSC heating scans (Figure 3a,b). The s_X mesophase does not form during the second heating scan since this phase is almost overlapping the glass transition temperature of these copolymers and therefore, it is strongly kinetically controlled. The cooling DSC scans (Figure 3c) are following the same pattern as the second heating DSC scans (Figure 3b). The phase behavior of poly[(6-5)-co-(6-3)] X/Y determined from the first heating, the second heating and the first cooling DSC scans is plotted in Figure 4a,b,c. All these plots show linear dependences of the n -i, and i -n phase transition temperatures versus copolymer composition.

Figure 4d plots the dependence of the enthalpy change associated with the n -i phase transition from the first and the second DSC heating scan and i -n phase transition, as a function of copolymer composition. The values of these enthalpy changes are much lower than those of the values associated with the s_A -i phase transition from Figure 2d and therefore, are subjected to a larger experimental error. Nevertheless, the plot from Figure 4a shows a linear dependence of copolymer composition.

In conclusion, the n mesophase of poly[(6-5)-co-(6-3)] X/Y exhibits, as the s_A mesophase of poly[(6-11)-co(6-6)] X/Y , a linear dependence of composition over the entire range of copolymer compositions. From preparative point of view, the results of

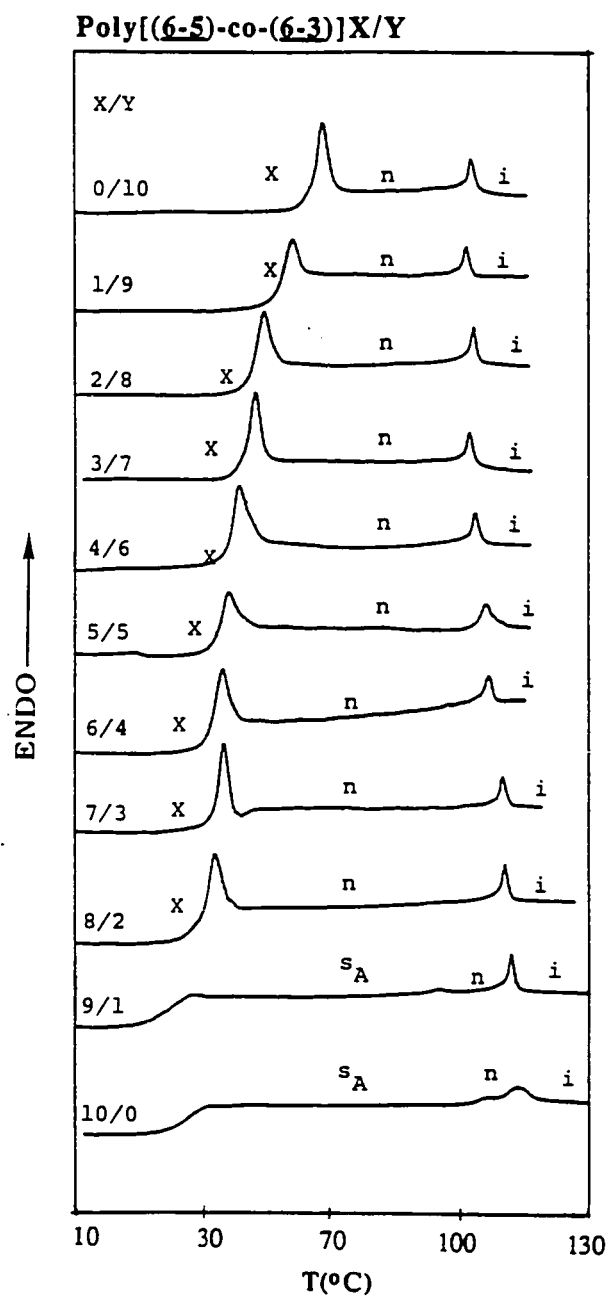


Figure 3a. DSC traces displayed during the first heating scan by poly(6-5), poly(6-3) and by poly[(6-5)-co-(6-3)]X/Y.

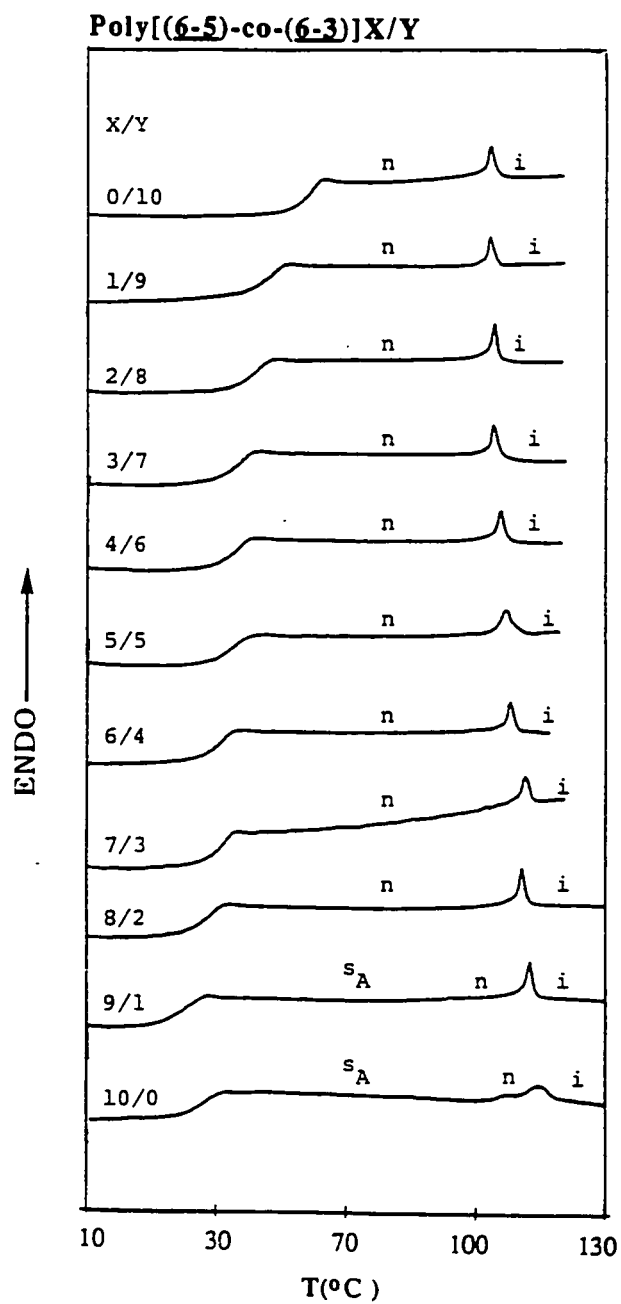


Figure 3b. DSC traces displayed during the second heating scan by poly(6-5), poly(6-3) and by poly[(6-5)-co-(6-3)]X/Y.

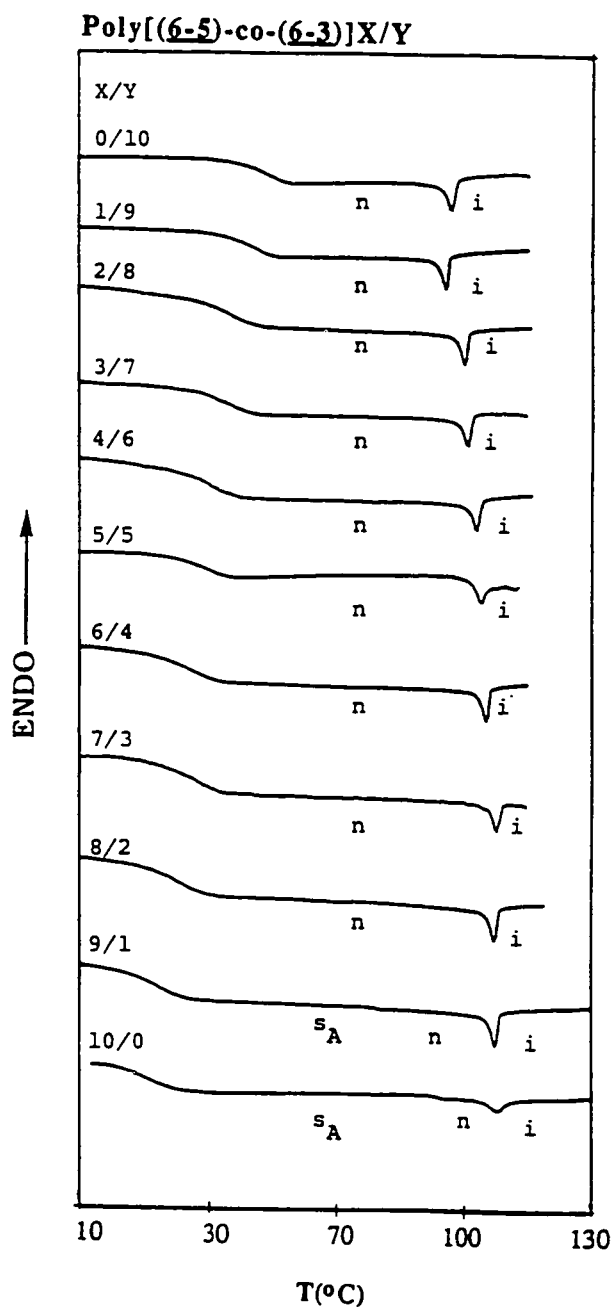


Figure 3c. DSC traces displayed during the first cooling scan by poly(6-5), poly(6-3) and by poly[(6-5)-co-(6-3)]X/Y.

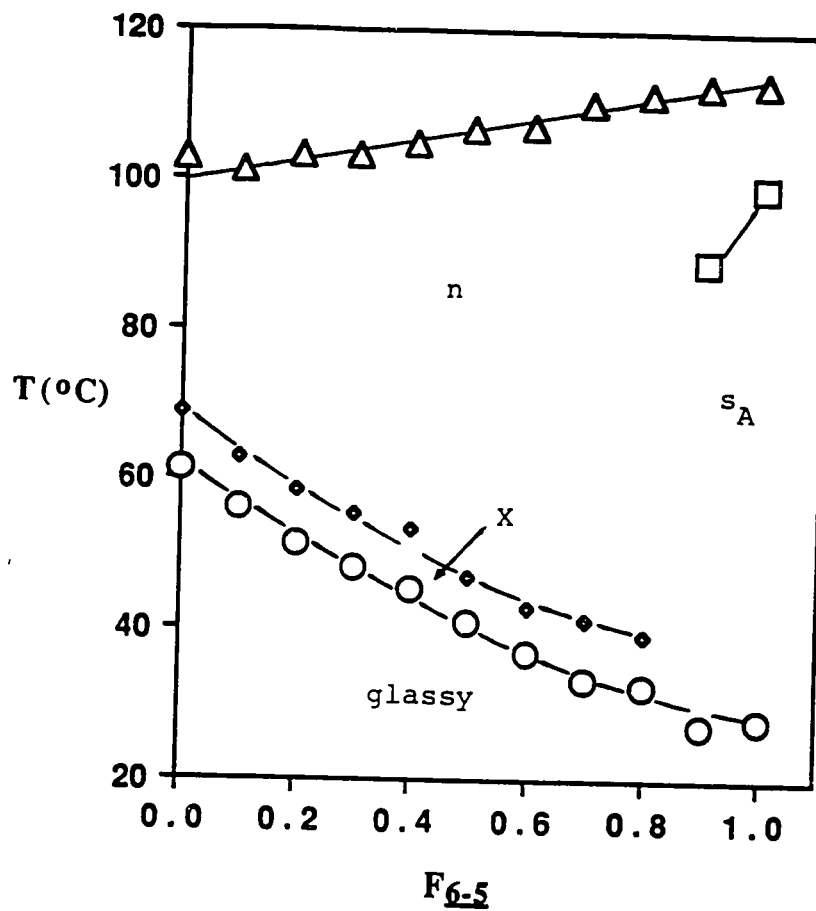


Figure 4a. The dependence of phase transition temperatures on the composition of poly[(6-5)-co-(6-3)]X/Y (data from the first heating scan): O- T_g ; \diamond - T_{X-n} ; \square - T_{sA-n} ; Δ - T_{n-i}

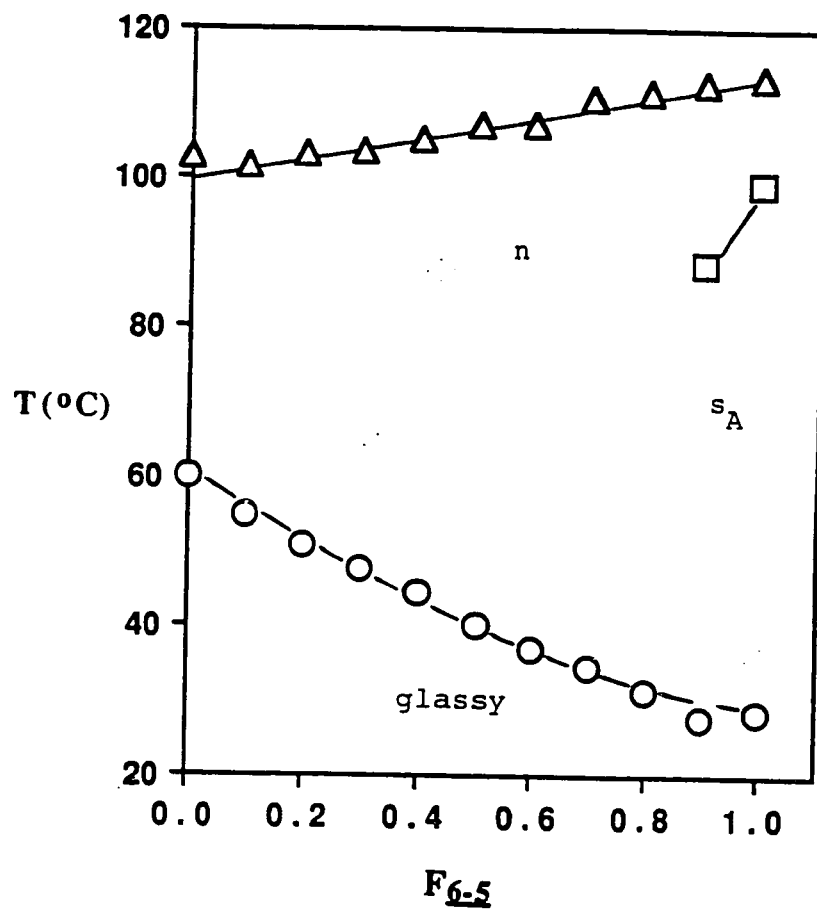


Figure 4b. The dependence of phase transition temperatures on the composition of poly[(6-5)-co-(6-3)]X/Y (data from the second heating scan): O- T_g ; \square - T_{sA-n} ; Δ - T_{n-i}

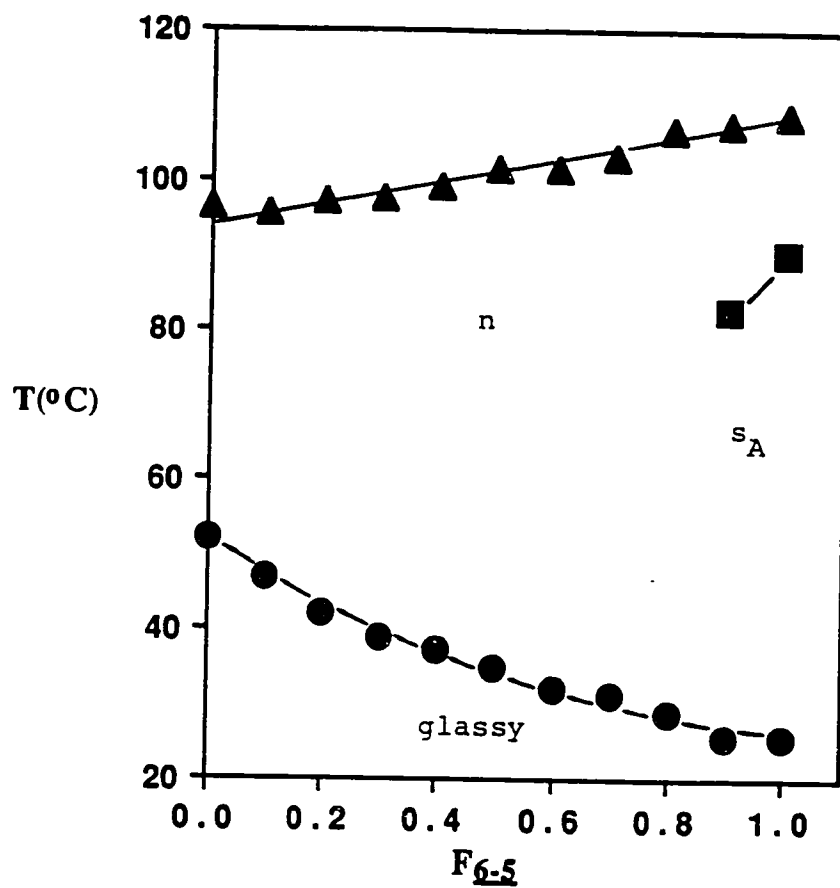


Figure 4c. The dependence of phase transition temperatures on the composition of poly[(6-5)-co-(6-3)]X/Y (data from the first cooling scan): ▲- T_n ; ■- T_n - S_A ; ●- T_g

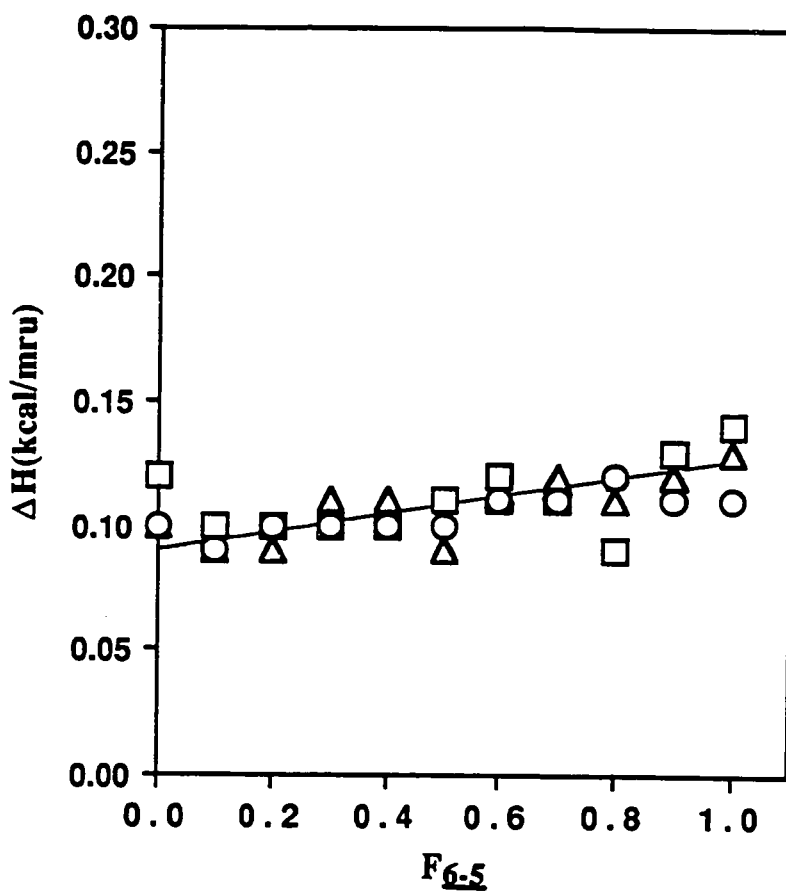


Figure 4d. The dependence of the enthalpy changes associated with the mesomorphic-isotropic and isotropic-mesomorphic phase transitions on the composition of poly[(6-11)-co-(6-6)]X/Y. □- ΔH_{sA-i} (data from the first heating scan); Δ - ΔH_{sA-i} (data from the second heating scan); O- ΔH_{i-sA} (data from the first cooling scan).

the investigation of the copolymers poly[(6-5)-co-(6-3)]X/Y teaches us how to design noncrystallizable nematic polymers containing a cyano group in the mesogen and a very broad range of temperature of the mesophase. There are very few examples of side chain liquid crystalline polymers containing cyano groups and exhibiting nematic mesophases.^{11b,12} Most frequently, nematic polymers containing cyano groups are synthesized by inserting a lateral substituent within the structure of the mesogenic unit,⁴⁸ and by using combinations of laterally and terminally attached mesogenic side groups.⁴⁹

7.3.3.-Poly[(6-11)-co-(6-3)]X/Y

This copolymer system is different from the two systems described above since the higher temperature mesophase of poly(6-11) is s_A , while that of poly(6-3) is nematic. Table III summarizes the experimental data of the copolymer poly[(6-11)-co-(6-3)]X/Y.

Let us start by investigating the DSC traces of the first heating scan (Figure 5a). The s_X phase of poly(6-3) shows a linear dependence of copolymer composition up to a value of $X/Y=4/6$. Copolymers with $X/Y=5/5$ to $7/3$ exhibit a single s_A mesophase. Only copolymers with $X/Y=10/0$ to $8/2$ exhibit the s_A mesophase and a crystalline phase. Copolymers with $X/Y=0/10$ to $3/7$ exhibit the n and the s_X mesophases. All copolymers from $X/Y=3/7$ to $10/0$ exhibit the s_A mesophase. Only the copolymer with $X/Y=3/7$ exhibits both a n and a s_A mesophase. Figure 6a plots all the phase transitions from the first DSC heating scan as a function of copolymer composition. As we can observe from Figure 6a, both the n and the s_A phases are showing linear dependences of copolymer composition. However, the phase diagram of this copolymer exhibits a triple point at $X/Y=4/6$. Poly[(6-11)-co-(6-3)] $3/7$ exhibits both enantiotropic nematic

and s_A mesophases. On the optical polarized microscope, this copolymer exhibits a reentrant nematic (n_{re}) mesophase, which appears both on heating and cooling at 55.6 °C (Figure 7a-d). To our knowledge, so far n_{re} mesophases were observed only in polyacrylates with cyano side groups and spacers containing six methylenic units.⁵³⁻⁶¹

In the second DSC heating scan (Figure 5b), the s_X mesophase does not appear. This is again due to its close proximity to the glass transition temperature of the copolymers. Only poly(6-11) exhibits on the second heating DSC scan a crystalline phase. The cooling DSC traces of these copolymers resemble those of the second heating scan (Figure 5c and b). The data collected from the second DSC heating scans and the first cooling scans are plotted in Figure 6b,c.

Finally, the enthalpy changes associated with the highest temperature mesophase of these copolymers are plotted in Figure 6d. Data collected from the first and the second heating and the first cooling DSC scans are plotted together. This plot shows very clearly the continuous character of the dependence of enthalpy change versus copolymer composition.

From preparative point of view, this copolymerization experiments provide a very simple technique which can be used to design a copolymer exhibiting two enantiotropic mesophases, by starting from two monomers whose parent homopolymers exhibit these two mesophases, and suggest a technique for the preparation of polymers displaying n_{re} mesophase.

7.3.4.-Poly[(6-11)-co-(6-5)]X/Y

Table IV summarizes the results of the copolymerization of 6-11 with 6-5. Attempts were made to prepare copolymers with a degree of polymerization (DP) of 20. Figure 8a presents the DSC traces of poly[(6-11)-co-(6-5)]X/Y copolymers obtained

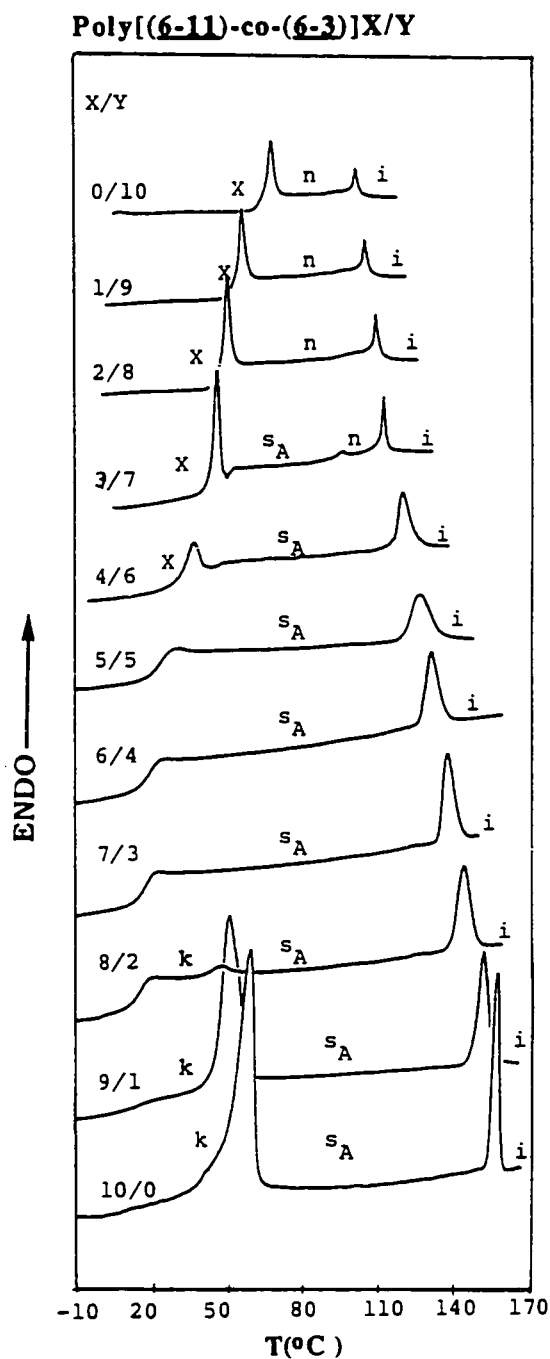


Figure 5a. DSC traces displayed during the first heating scan by poly(6-11), poly(6-3) and by poly[(6-11)-co-(6-3)]X/Y.

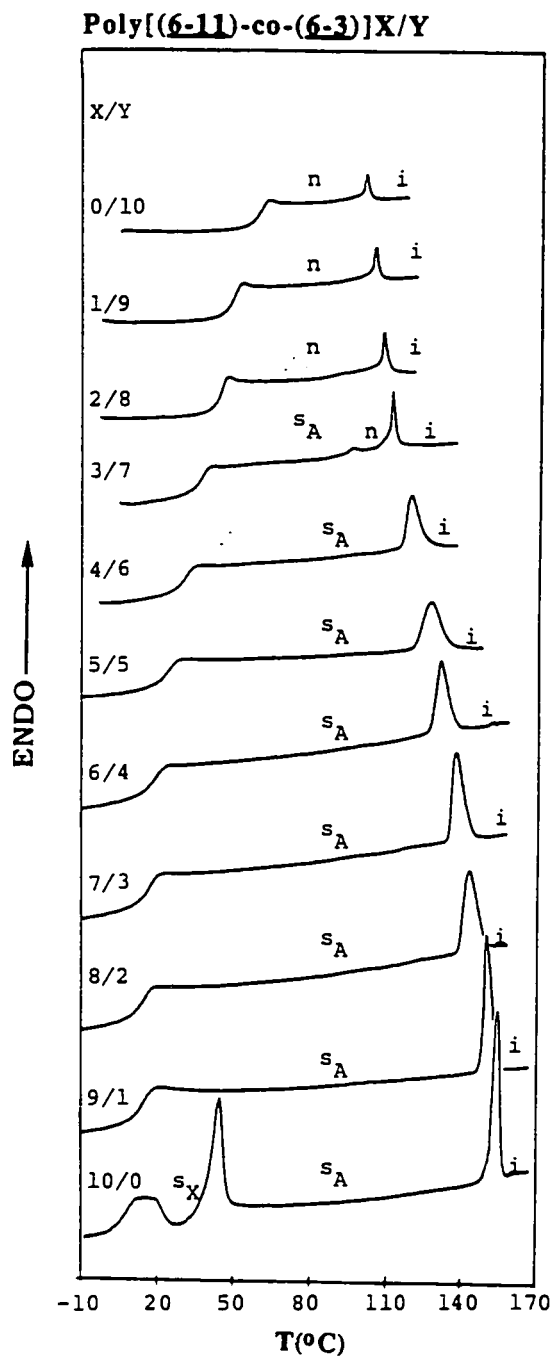


Figure 5b. DSC traces displayed during the second heating scan by poly(6-11), poly(6-3) and by poly[(6-11)-co-(6-3)]X/Y.

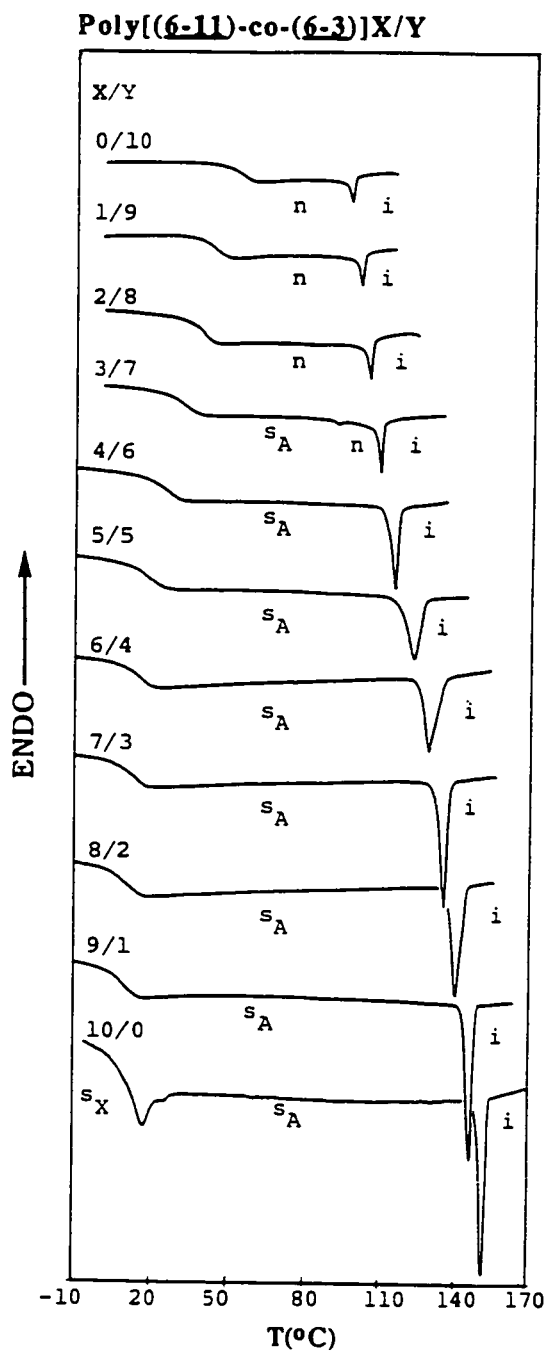


Figure 5c. DSC traces displayed during the first cooling scan by poly(6-11), poly(6-3) and by poly[(6-11)-co-(6-3)]X/Y.

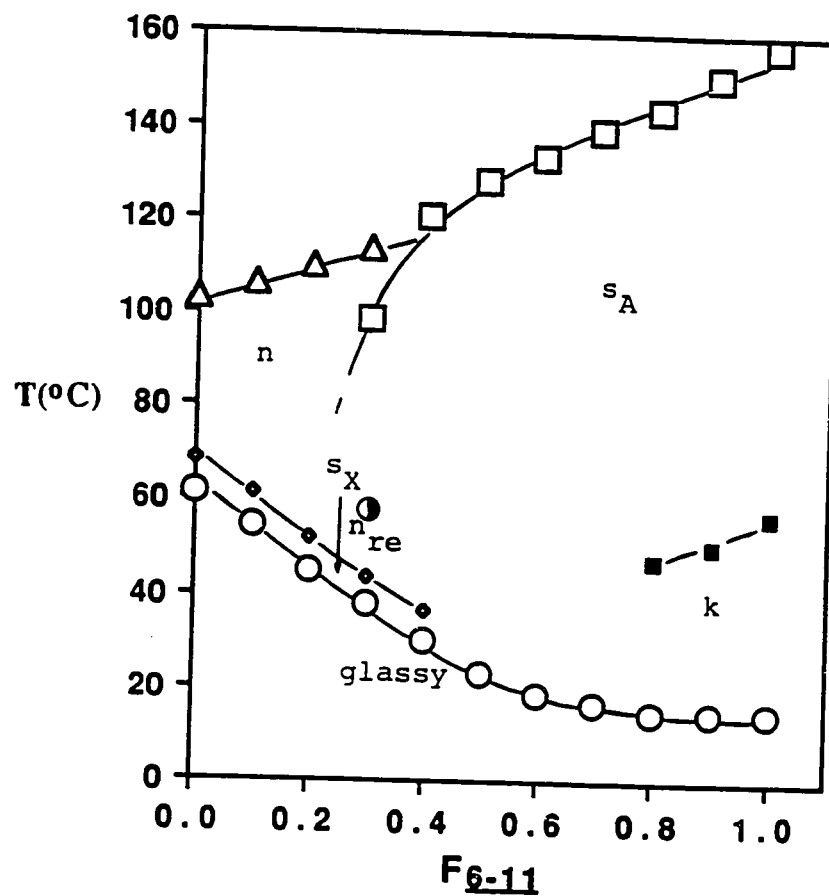


Figure 6a. The dependence of phase transition temperatures on the composition of poly[(6-11)-co-(6-3)]X/Y (data from the first heating scan): \circ - T_g ; \diamond - T_{X-SA} ; \blacksquare - T_{k-SA} ; \bullet - $T_{n-re-SA}$; \square - T_{sA-i} ; Δ - T_{n-i}

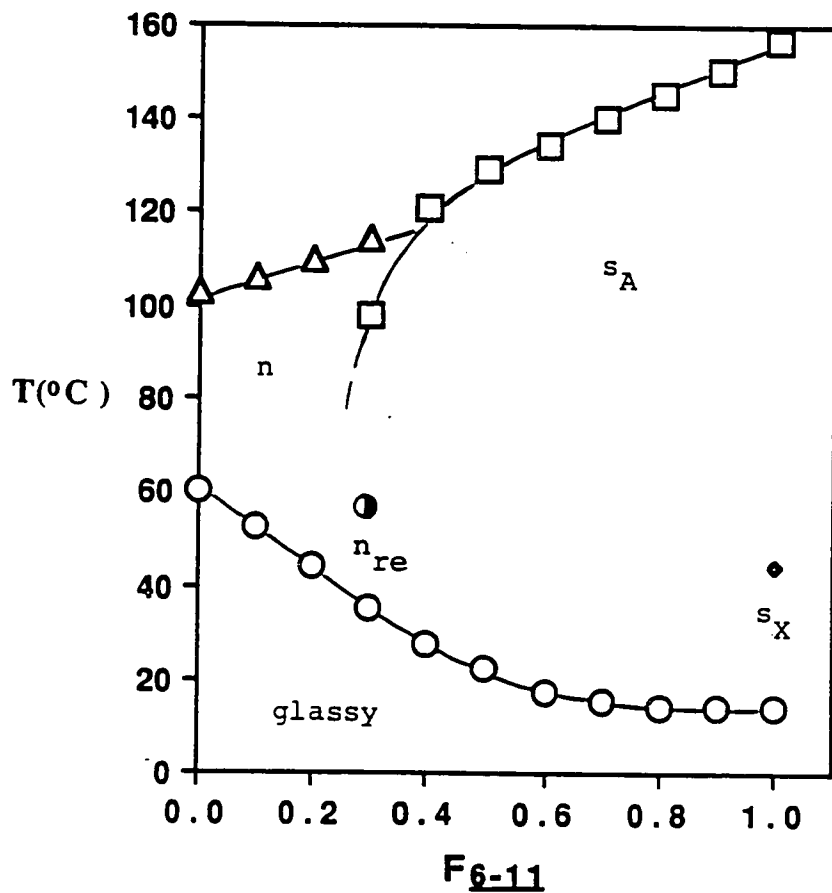


Figure 6b. The dependence of phase transition temperatures on the composition of poly[(6-11)-co-(6-3)]X/Y. (data from the second heating scan): O- T_g ; \diamond - T_{sX-SA} ; O- T_{nre-SA} ; \square - T_{SA-i} ; Δ - T_{n-i}

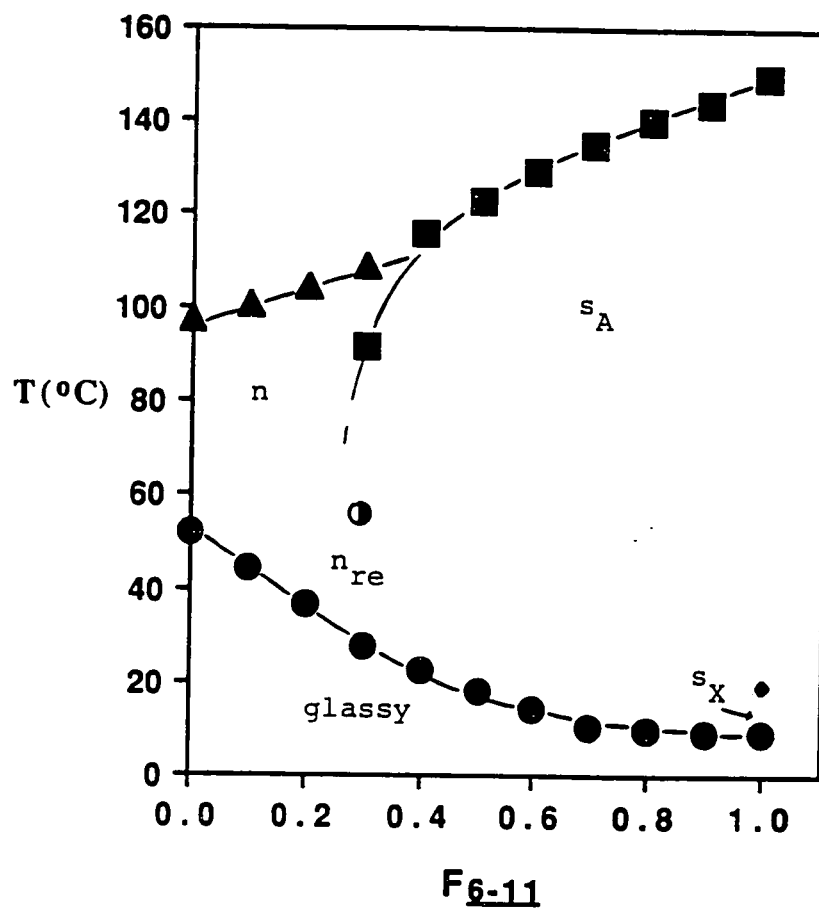


Figure 6c. The dependence of phase transition temperatures on the composition of $\text{poly}[(6-11)\text{-co-(6-3)}]X/Y$ (data from the first cooling scan): \blacktriangle - T_{i-n} ; \blacksquare - T_{i-sA} ; \circ - $T_{sAd-nre}$; \blacklozenge - T_{sA-sX} ; \bullet - T_g .

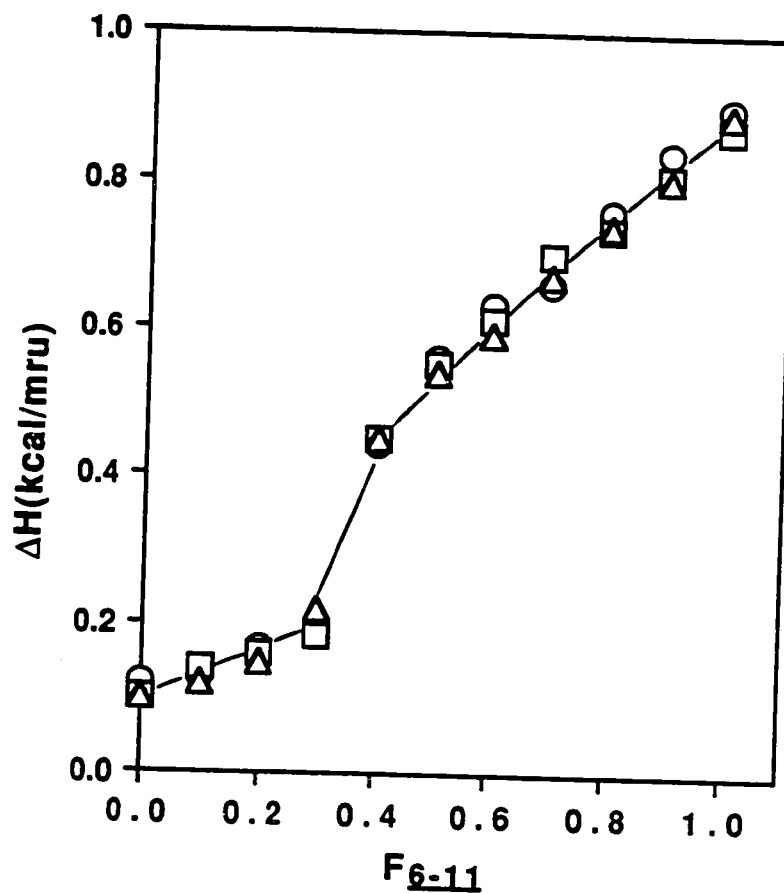
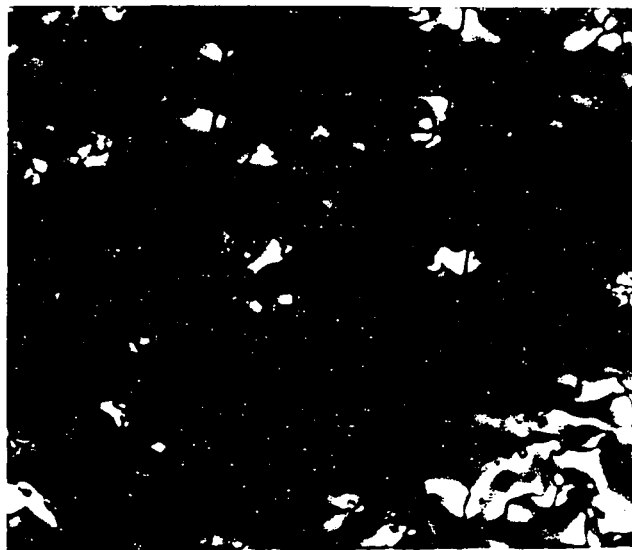


Figure 6d. The dependence of the enthalpy changes associated with the mesomorphic-isotropic and isotropic-mesomorphic phase transitions on the composition of poly[(6-11)-co-(6-3)]X/Y. □-ΔH_{sA-i} (data from the first heating scan); Δ-ΔH_{sA-i} (data from the second heating scan); ○-ΔH_{i-sA} (data from the first cooling scan).

a



b

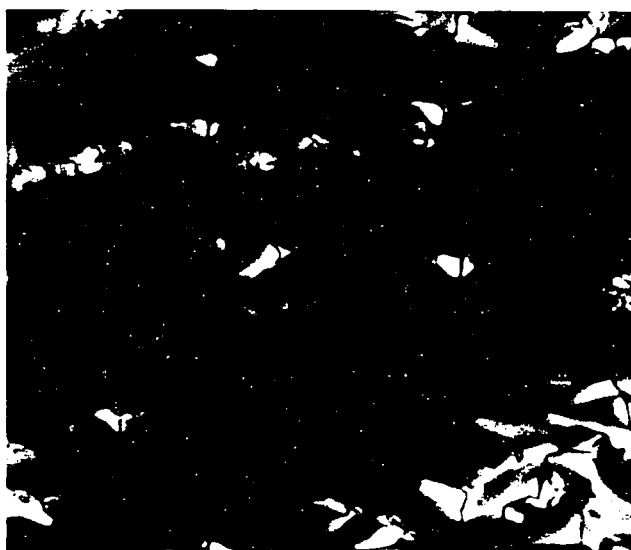
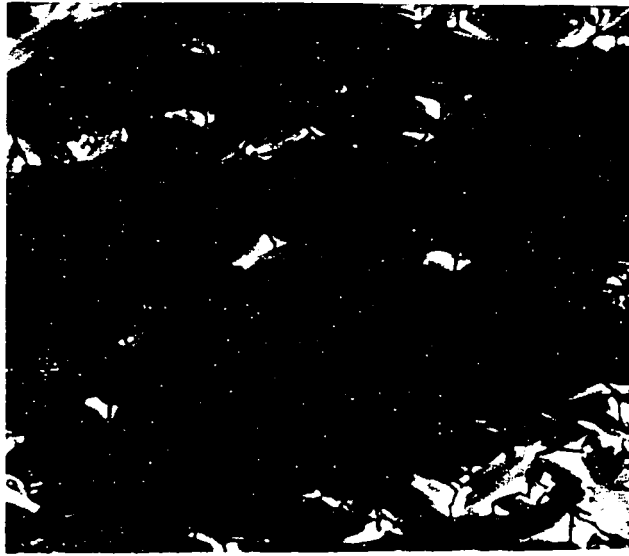


Figure 7: Representative optical polarized micrographs (100x) of the phases exhibited by poly[(6-11)-co-(6-3)]3/7 with degree of polymerization of 20: a) n phase at 99°C; b) transition from n to s_{Ad} at 92.5°C; c) s_{Ad} phase at 83.3°C; d) transition from s_{Ad} to n_{re} at 55.6°C; e) n_{re} phase at 52.9°C

c



d



Figure 7 (continued)

e

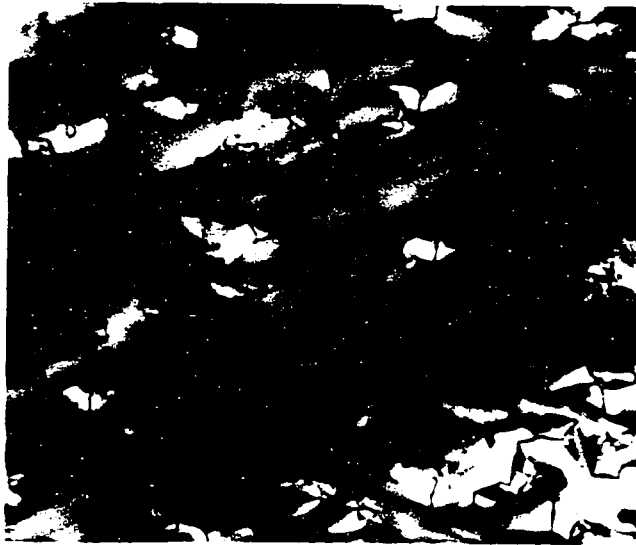


Figure 7. (continued)

from the first heating scan. The DSC traces obtained from the second and subsequent heating scans are presented in Figure 8b, and those obtained from the cooling scans in Figure 8c. Second and subsequent heating scans display identical DSC traces. Only poly[(6-11)-co-(6-5)]X/Y with X/Y=9/1 and 10/0 exhibit first DSC scans which differ from those of the second heating scans. All cooling scans of these copolymers are identical. In the first and subsequent heating scans, poly(6-5) exhibits enantiotropic n and s_{Ad} mesophases (Figure 9a,b). In the first DSC heating scan, poly[(6-11)-co-(6-5)]X/Y with X/Y=9/1 and 10/0 exhibit a crystalline melting followed by an enantiotropic s_A mesophase (Figure 8a). In the second heating scan, poly(6-11) exhibits enantiotropic s_A and s_X mesophases, while poly[(6-11)-co-(6-5)]X/Y with X/Y=9/1 only an enantiotropic s_A mesophase (Figure 8b). This behavior is due to the slow crystallization process induced by the close proximity of the crystallization transition temperature to the glass transition temperature. All copolymers with X/Y=10/0 to 2/8 display an enantiotropic s_A mesophase. The copolymer with X/Y=1/9 and poly(6-5) exhibit enantiotropic n and s_A phases (Figure 8a,b,c).

The inspection of poly(6-5) and poly[(6-11)-co-(6-5)]1/9 on the optical polarized microscope reveals n_{re} mesophases.⁵⁴⁻⁶² Therefore, the s_A phase of these two polymers is most probable a s_{Ad} phase. The dependences of phase transition temperatures of poly[(6-11)-co-(6-5)]X/Y on composition as determined from first heating, second heating, and cooling scans are plotted in Figure 9a,b,c. All phase transitions show continuous dependences of copolymer composition. Poly[(6-11)-co-(6-5)]2/8 exhibits a triple point on its phase behavior (Figure 9a,b). The upward curvature of the s_A -isotropic, s_A - n and of the entire transition temperature dependences versus copolymer composition (Figure 9a,b,c) can be explained by the Schroeder-van Laar equations,¹⁰ and qualitatively agree with the calculated ones. Figure 9d presents

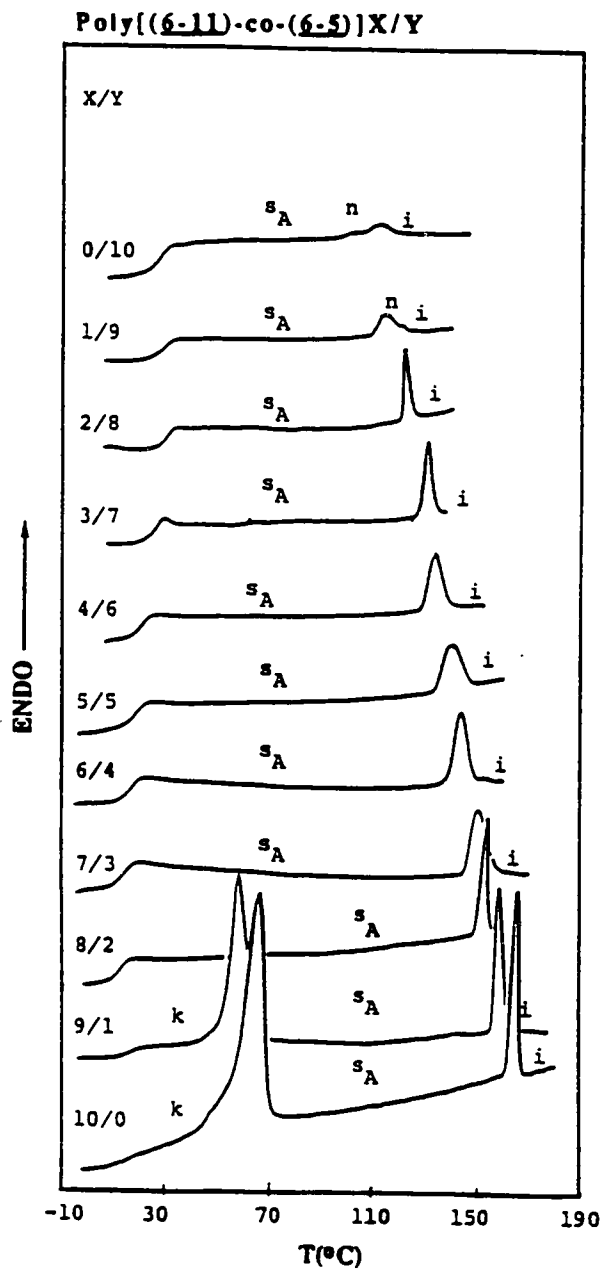


Figure 8a. DSC traces displayed during the first heating scan by poly(6-11), poly(6-5) and by poly[(6-11)-co-(6-5)]X/Y.

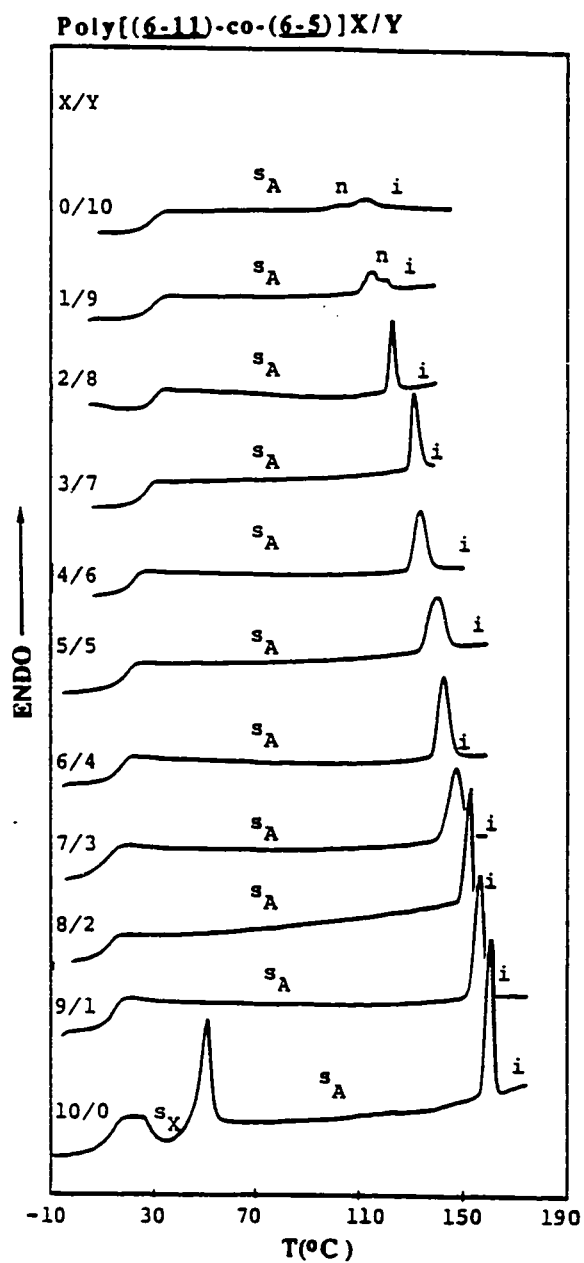


Figure 8b. DSC traces displayed during the second heating scan by poly(6-11), poly(6-5) and by poly[(6-11)-co-(6-5)]X/Y.

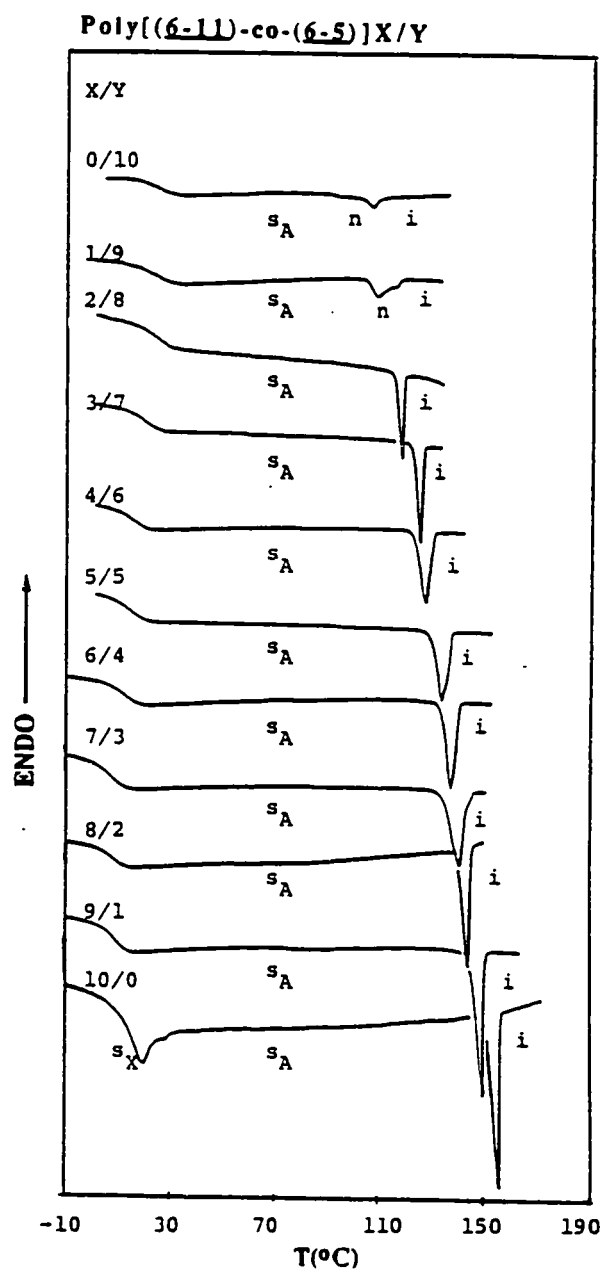


Figure 8c. DSC traces displayed during the first cooling scan by poly(6-11), poly(6-5) and by poly[(6-11)-co-(6-5)]X/Y.

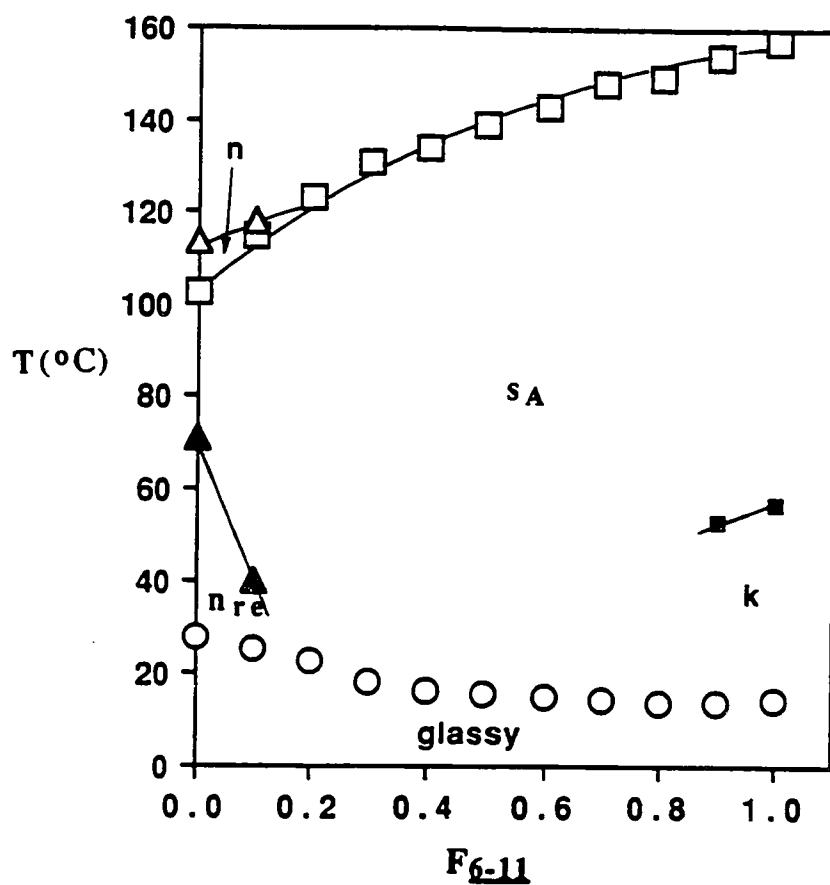


Figure 9a. The dependence of phase transition temperatures on composition of poly[(6-11)-co-(6-5)]X/Y: (data from first heating scan): O- T_g ; ■- T_k - s_A ; □- T_{sA-i} or - T_{sA-n} ; Δ- T_{n-i} ; ▲- $T_{n-re-sAd}$

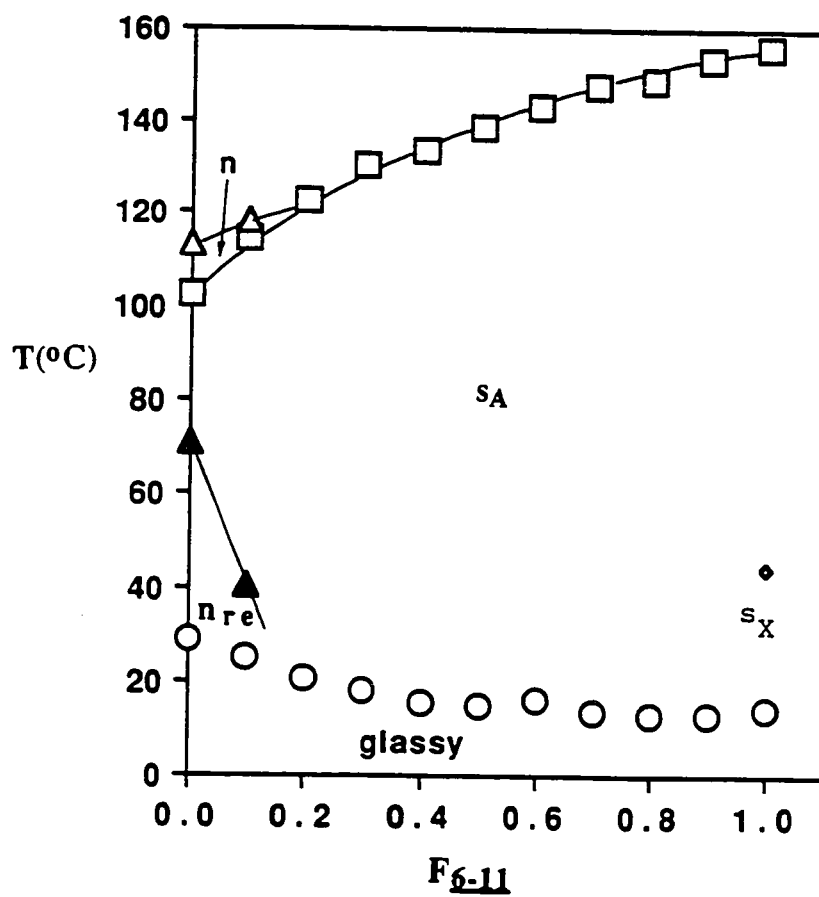


Figure 9b. The dependence of phase transition temperatures on composition of poly[(6-11)-co-(6-5)]X/Y: (data from second heating scan): O- T_g ; \diamond - T_{sX-sA} ; \square - T_{sA-i} or $-T_{sA-n}$; Δ - T_{n-i} ; \blacktriangle - $T_{nre-sAd}$

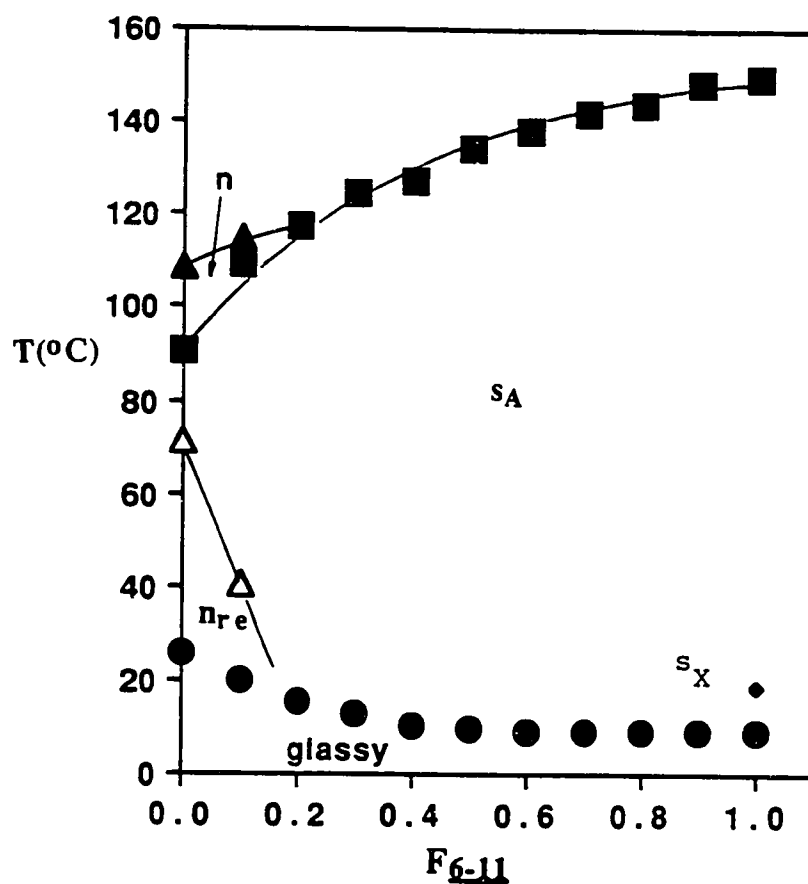


Figure 9c. The dependence of phase transition temperatures on composition of poly[(6-11)-co-(6-5)]X/Y: (data from first cooling scan): \circ - T_g ; Δ - T_{i-n} ; \square - T_{i-sA} or T_{n-sA} ; Δ - $T_{sAd-nre}$; \diamond - T_{sA-sX}

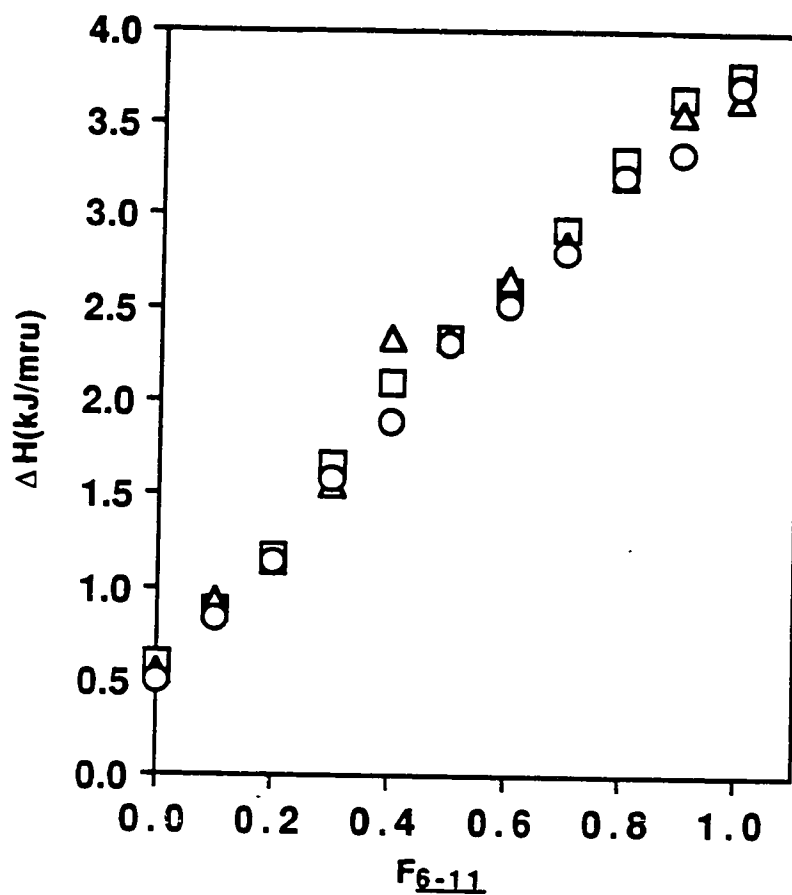


Figure 9d. The dependence of the enthalpy changes associated with the mesomorphic-isotropic and isotropic-mesomorphic phase transitions :
 □-ΔH_{n-i} (data from the first heating scan); Δ-ΔH_{n-i} (data from the second heating scan); ○-ΔH_{i-n} (data from the first cooling scan) versus copolymer composition.

the experimental and calculated data for the s_A -n and s_A -i transition temperatures of poly[(6-11)-co-(6-5)]X/Y copolymers. Thus, the phase diagram of these copolymers can be regarded as close to that expected for an ideal solution resulted from the structural units of the copolymer. The enthalpy changes associated with the s_A -isotropic, s_A -n and of the reversed phase transitions determined from the first and second heating, and first cooling DSC scans (Table IV) are plotted as a function of copolymer composition in Figure 9e. This dependence is linear. Therefore, it demonstrates a weight average dependence of copolymer composition.

In conclusion, the series of experiments described in this chapter are providing a complete and quantitative picture of the class of side chain liquid crystalline copolymers prepared from monomer pairs containing identical mesogens and polymerizable groups but different spacer length. This quantitative relationship can be summarized as follows: over the range of copolymer compositions where the two structural units of the copolymer are isomorphic within a certain mesophase, both the phase transition temperature and the enthalpy changes associated with this mesophase display a continuous or even linear dependence of composition. Alternatively, when the two structural units are nonisomorphic within a certain mesophase, a continuous dependence of both transition temperatures and enthalpy changes with a triple point at a certain copolymer composition is observed. This dependence is in complete agreement with the rules of isomorphism of monomer structural units (copolymer isomorphism) which were extensively investigated for the case of crystalline copolymers.^{51,52} A detailed discussion of the isomorphism of crystalline polymers, low molar mass liquid crystals and liquid crystalline polymers and copolymers was presented in detail elsewhere.⁸ The results described in this chapter will allow the molecular engineering of

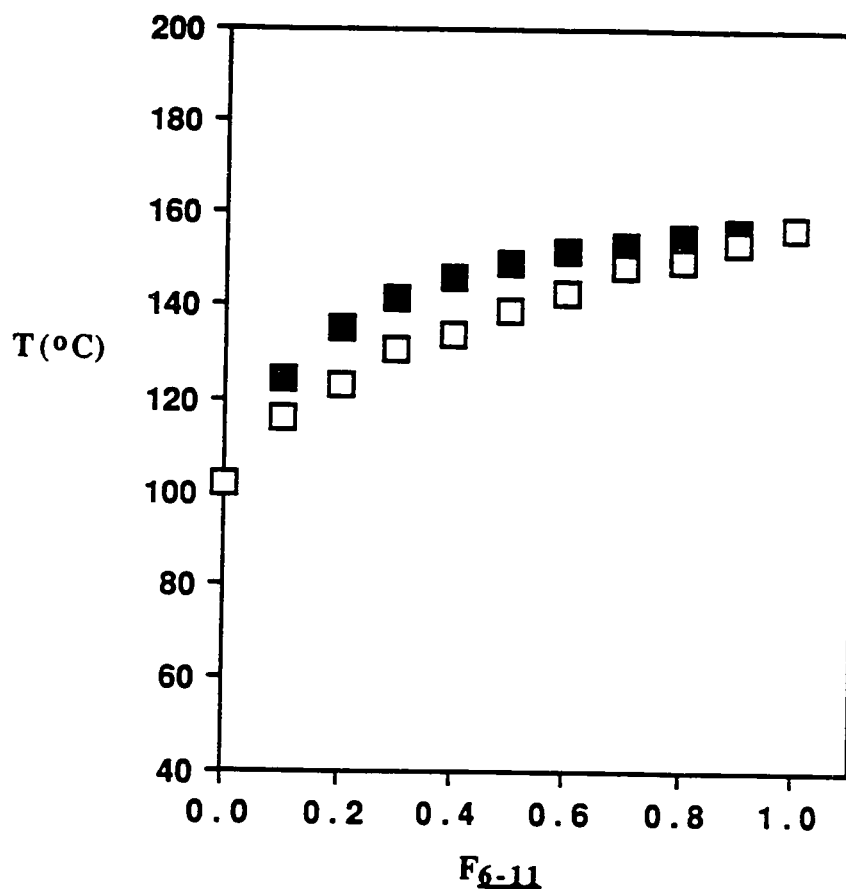


Figure 9e. The dependence of s_A -n and s_A -i phase transition temperatures on composition of poly[(6-11)-co-(6-5)]X/Y: (□) data calculated by Schroeder-van Laar equation; (■) experimental data from the first heating scan.

side chain liquid crystalline copolymers exhibiting one and more than one mesophase with well defined degree of order.

REFERENCES

1. H. Arnold and H. Sackmann, *Z. Phys. Chem. (leipzig)*, **213**, 145 (1960)
2. H. Sackmann and D. Demus, *Mol. Cryst. Liq. Cryst.*, **21**, 239 (1973)
3. D. Demus, S. Diele, S. Grande and H. Sackmann, "Advances in Liquid Crystals", (G. H. Brown Ed.), Academic Press, London, **6**, 1 (1983)
4. W. R. Krigbaum, *J. Appl. Polym. Sci., Polym. Symp.*, **41**, 105 (1985)
5. C. Casagrande, M. Veyssie and H. Finkelmann, *J. Phys. Lett.*, **43**, L-621 (1982)
6. H. Ringsdorf, H. W. Schmidt and A. Schneller, *Makromol. Chem., Rapid Commun.*, **3**, 745 (1982)
7. H. Benthack-Thomas and H. Finkelmann, *Makromol. Chem.*, **186**, 1895 (1985)
8. V. Percec and Y. Tsuda, *Polymer*, **32**, 661 (1991)
9. T. Schroeder, *Z. Phys. Chem.*, **11**, 449 (1893)
10. J. J. van Laar, *Z. Phys. Chem.*, **63**, 216 (1908); G. R. Van Hecke, *J. Phys. Chem.*, **83**, 2344 (1979)
11. a) V. Percec and R. Yourd, *Macromolecules*, **22**, 524 (1989); V. Percec, and Y. Tsuda, *Macromolecules*, **23**, 5 (1990); V. Percec and Y. Tsuda, *Macromolecules*, **23**, 3509 (1990); b) V. Percec and C. Pugh, in "Side Chain Liquid Crystal Polymers", C. B. McArdle Ed., Chapman and Hall, New York, 1989, p. 30 and references cited therein.
12. G. Gray, "Side Chain Liquid Crystal Polymers", C. B. McArdle Ed., Chapman and Hall, New York, 1989, p. 106
13. N. A. Plate and V. P. Shibaev, "Comb-Shaped Polymers and Liquid Crystals" Plenum Press, New York, 1987
14. M. Engel, B. Hisgen, R. Keller, W. Kreuder, B. Reck, H. Ringsdorf, H. W. Schmidt and P. Tschirner, *Pure Appl. Chem.*, **57**, 1009 (1985)
15. V. P. Shibaev and N. Plate, *Adv. Polym. Sci.*, **60/61**, 173 (1984)
16. H. W. Schmidt, *Angew. Chem. Int. Ed. Engl. Adv. Mater.*, **101**, 964 (1989)
17. S. Diele, S. Oelsner, F. Kuschel, B. Hisgen, H. Ringsdorf and R. Zentel, *Makromol. Chem.*, **188**, 1993 (1987)

18. S. Diele, S. Oelsner, F. Kuschel, B. Hisgen and H. Ringsdorf, H. *Mol. Cryst. Liq. Cryst.*, **155**, 399 (1988)
19. S. Westphal, S. Diele, F. Madicke, F. Kuschel, U. Scheim, K. Ruhlmann, B. Hisgen and H. Ringsdorf, *Makromol. Chem. , Rapid Commun.*, **9**, 489 (1988)
20. G. Nestor, G. W. Gray, D. Lacey and K. J. Toyne, *Liq. Cryst.* , **6**, 137 (1989)
21. V. Percec and B. Hahn, B. *Macromolecules* , **22**, 1588 (1989)
22. V. Percec, B. Hahn, M. Ebert and J. H. Wendorff, *Macromolecules* , **23**, 2092 (1990)
23. V. Percec and D. Tomazos, *Macromolecules* , **22**, 1512 (1989)
24. V. Percec and D. Tomazos, *Polymer* , **30**, 2124 (1989)
25. M. F. Achard, M. Mauzac, H. Richard, G. Sigaud and F. Hardouin, *Eup. Polym. J.*, **25**, 593 (1989)
26. G. Hardy, F. Cser and K. Nyitrai, *Isr. J. Chem.*, **18**, 233 (1979)
27. G. Hardy, F. Cser, K. Nyitrai and E. Bartha, *Ind. Eng. Chem. Res. Dev.* , **121**, 321 (1982)
28. J. Horvath, F. Cser and G. Hardy, *Prog. Coll. Polym. Sci.*, **71**, 59 (1985)
29. D. A. Tirrell, in "Encyclopedia of Polymer Science and Engineering", 2nd Ed., H. F. Mark, N. M. Bikales, C. G. Overberger and G. Menger Eds. Vol. 4, Wiley, New York 1986, p. 192
30. S. G. Kostromin, R. V. Talroze, V. P. Shibaev and N. A. Plate, *Makromol. Chem., Rapid Commun.*, **3**, 803 (1982)
31. H. Stevens, G. Rehage and H. Finkelmann, *Macromolecules* , **17**, 851 (1984)
32. V. Percec, D. Tomazos and C. Pugh, *Macromolecules* , **22**, 3259 (1989)
33. T. Sagane and R. W. Lenz, *Polym. J.*, **20**, 923 (1988)
34. T. Sagane and R. W. Lenz, *Polymer*, **30**, 2269 (1989)
35. T. Sagane and R. W. Lenz, *Macromolecules*, **22**, 3763 (1989)
36. V. Percec and M. Lee, *J. Macromol. Sci.-Chem.*, **A28**, 651 (1991)
37. V. Percec, M. Lee and C. Ackerman, *Polymer*, in press
38. V. Percec and M. Lee, *Macromolecules*, **24**, 1017 (1991)

39. V. Percec and M. Lee, *Macromolecules*, **24**, 2780 (1991)
40. V. Percec, M. Lee and H. Jonsson, *J. Polym. Sci., Polym. Chem. Ed.*, **29**, 327 (1991)
41. J. M. Rodriguez-Parada and V. Percec, *J. Polym. Sci., Part A: Polym. Chem.*, **24**, 1363 (1986)
42. C. G. Cho, B. A. Feit and O. W. Webster, *Macromolecules*, **23**, 1918 (1990)
43. R. Rodenhouse, V. Percec and A. E. Feiring, *J. Polym. Sci.: Part C: Polym. Lett.*, **28**, 345 (1990)
44. H. Jonsson, V. Percec and A. Hult, *Polym. Bull.*, **25**, 131 (1991)
45. V. Percec, A. S. Gomes and M. Lee, *J. Polym. Sci.: Part A: Polym. Chem. Ed.*, **29**, 1615 (1991)
46. R. Rodenhouse and V. Percec, *Adv. Mater.*, **3**, 101 (1991)
47. V. Percec and M. Lee, *Polym. Bull.*, in press
48. P. A. Gemmell, G. W. Gray and D. Lacey, *Mol. Cryst. Liq. Cryst.*, **122**, 205 (1985)
49. M. S. K. Lee, G. W. Gray, D. Lacey and K. Toyne, *J. Makromol. Chem., Rapid Commun.*, **10**, 325 (1989)
50. G. W. Gray, J. S. Hill and D. Lacey, *Angew. Chem. Int. Ed. Engl. Adv. Mater.*, **28**, 1120 (1989)
51. G. Allegra and I. W. Bassi, *Adv. Polym. Sci.*, **6**, 549 (1969)
52. G. Allegra and I. W. Bassi, in "Polymer Handbook" (Eds. Brandrup, J.; Immergert, E. H.), Wiley, New York, 1975, p. III-205
53. For some representative reviews see: (a) G. Sigaud, N. H. Tinh, F. Hardouin and H. Gasparoux, *Mol. Crst. Liq. Cryst.*, **69**, 81 (1981); (b) F. Hardouin, A. M. Levelut, M. F. Archard and G. Sigaud, *J. Chim. Phys.*, **80**, 53 (1983); (c) F. Hardouin, *Physica*, **140A**, 359 (1986); (d) P. E. Cladis, *Mol. Cryst. Liq. Cryst.*, **165**, 85 (1988)
54. P. Le Barny, J. C. Dubois, C. Friedrich and C. Noel *Polym. Bull.*, **15**, 341 (1986)
55. T. I. Gubina, S. G. Kostromin, R. V. Talroze, V. P. Shibaev and N. A. Plate, *Vyskomol. Soed. Ser. B.*, **28**, 394 (1986)
56. V. Shibaev, *Mol. Cryst. Liq. Cryst.*, **155**, 189 (1988)

57. N. Lacoudre, A. Le Borgue, N. Spassky, J. P. Vairon, P. Le Barny, J. C. Dubois, S. Esselin, C. Friedrich and C. Noel, *Mol. Cryst. Liq. Cryst.*, **155**, 113 (1988)
58. N. Spassky, N. Lacoudre, A. Le Borgue, J. P. Vairon, C. L. Jun, C. Friedrich and C. Noel, *Makromol. Chem., Makromol. Symp.*, **24**, 271 (1989)
59. T. A. Gubina, S. Kise, S. G. Kostromin, R. V. Talroze, V. P. Shibaev and N. A. Plate, *Liq. Cryst.*, **4**, 197 (1989)
60. S. G. Kostromin, V. P. Shibaev and S. Diele, *Makromol. Chem.*, **191**, 2521 (1990)
61. C. Legrand, A. Le Borgue, C. Bunel, A. Lacoudre, P. Le Barny, N. Spassky and J. P. Vairon, *Makromol. Chem.*, **191**, 2979 (1990)

Chapter 8

SYNTHESIS AND CHARACTERIZATION OF BINARY COPOLYMERS OF POLY{ ω -[(4-CYANO-4'-BIPHENYL)OXY]ALKYL VINYL ETHER}S CONTAINING UNDECANYL AND ETHYL, AND OCTYL AND ETHYL PAIRS OF ALKYL GROUPS

8.1.-INTRODUCTION

Previous chapter has provided a quantitative investigation of the phase behavior of copolymers derived from pairs of homopolymers exhibiting the following high temperature mesophases: s_A and s_A , n and n , and s_A and n .

This chapter describes the synthesis and characterization of poly{8-[(4-cyano-4'-biphenyl)oxy]octyl vinyl ether-co-2-[(4-cyano-4'-biphenyl)oxy]ethyl vinyl ether}X/Ys {poly[(6-8)-co-(6-2)]X/Y} and poly{11-[(4-cyano-4'-biphenyl)oxy]undecanyl vinyl ether-co-2-[(4-cyano-4'-biphenyl)oxy]ethyl vinyl ether}X/Ys {poly[(6-11)-co-(6-2)]X/Y} with constant degrees of polymerization, narrow molecular weight distributions and variable composition. As determined from the second differential calorimeter (DSC) scans, poly{2-[(4-cyano-4'-biphenyl)oxy]ethyl vinyl ether} [poly(6-2)] does not exhibit any mesophase^{1b}(i.e., is an amorphous polymer), poly{8-[(4-cyano-4'-biphenyl)oxy]octyl vinyl ether} [poly(6-8)] exhibits an enantiotropic smectic A mesophase,^{1c} and poly{11-[(4-cyano-4'-biphenyl)oxy]undecanyl vinyl ether} [poly(6-11)] displays both enantiotropic s_X and s_A mesophases.^{1a} Therefore, the investigation of these two pairs of copolymers will elucidate the phase behavior of copolymers derived from pairs of homopolymers exhibiting the highest temperature mesophases s_A and glassy phases.

8.2.-EXPERIMENTAL

8.2.1.-materials

4-Phenylphenol(98%),1,10-phenanthroline (anhydrous,99%) palladium (II) acetate (all from Lancaster Synthesis), ferric chloride anhydrous (98%), copper(I)cyanide(99%), n-butyl vinyl ether (98%), 9-borabicyclo[3.3.1]nonane (9-BBN, crystalline, 98%), 8-bromo-1-octanol (95%) (all from Aldrich), 2-chloro ethyl vinyl ether (Polysciences, bp, 109-110°C) and the other reagents were used as received. Methyl sulfide (anhydrous, 99%, Aldrich) was refluxed over 9-BBN and then distilled under argon. Dichloromethane (99.6%, Aldrich) used as polymerization solvent was first washed with concentrated sulfuric acid, then with water, dried over anhydrous magnesium sulfate, refluxed over calcium hydride and freshly distilled under argon before each use. n-Methyl-2-pyrrolidone (98%, Lancaster Synthesis) was dried by azeotropic distillation with benzene, shaken with barium oxide, filtered, and fractionally distilled under reduced pressure. Trifluoromethane sulfonic acid (triflic acid, 98%, Aldrich) was distilled under vacuum.

8.2.2.-Synthesis of Monomers

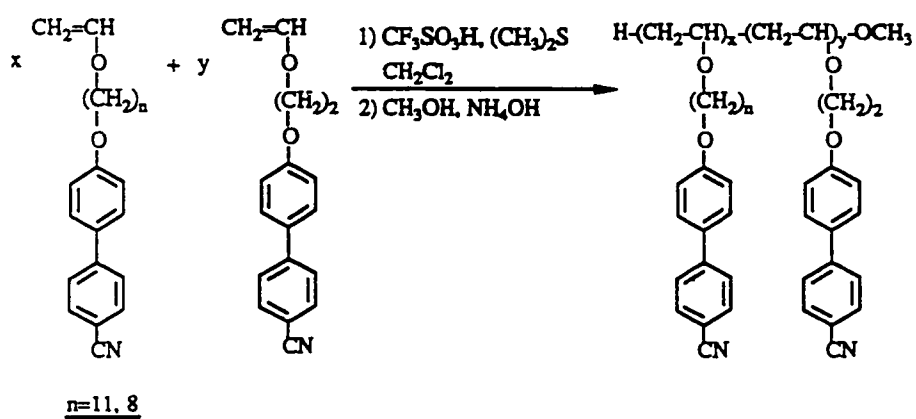
11-[(4-Cyano-4'-biphenyl)oxy]undecanyl vinyl ether (6-11)^{1a}, 8-[(4-cyano-4'-biphenyl)oxy]octyl vinyl ether (6-8)^{1c} and 2-[(4-cyano-4'-biphenyl)oxy]ethyl vinyl ether (6-2)^{1b} were synthesized and purified as described in previous publications. Their purity was higher than 99% (HPLC). Their detailed characterization is described in the previous publications.

8.2.3.-Cationic Polymerizations

Polymerizations were carried out in glass flasks equipped with teflon stopcocks and rubber septa under argon atmosphere at 0°C for 1 hr. All glassware was dried overnight at 130°C. The monomer was further dried under vacuum overnight in the polymerization flask. Then the flask was filled with argon, cooled to 0°C and the methylene chloride, dimethyl sulfide and triflic acid were added via a syringe. The monomer concentration was about 10 wt% of the solvent volume and the dimethyl sulfide concentration was 10 times larger than that of the initiator. The polymer molecular weight was controlled by the monomer/initiator ($[M]_0/[I]_0$) ratio. After quenching the polymerization with ammoniacal methanol, the reaction mixture was precipitated into methanol. The filtered polymers were dried and precipitated from methylene chloride solution into methanol until GPC traces showed no traces of monomer. Tables I and II summarize the polymerization results. Although polymer yields are lower than expected due to losses during the purification process, conversions were almost quantitative in all cases.

8.3.-RESULTS AND DISCUSSION

The influence of molecular weight on the phase transitions of poly(6-2), poly(6-8) and poly(6-11) was described in previous chapters. Our preferred initiating system is $\text{CF}_3\text{SO}_3\text{H}/\text{S}(\text{CH}_3)_2$ since it can be used to perform living cationic polymerizations in CH_2Cl_2 at 0°C. The phase behavior of poly(6-11), poly(6-8) and poly(6-2) are molecular weight dependent.^{1a-c} For example at low degrees of polymerization poly(6-8) displays enantiotropic smetic-A (s_A) and nematic (n) phases, at intermediary molecular weights an enantiotropic s_A phase, while at high molecular weights enantiotropic s_A and s_X phases. Scheme I presents the copolymerization of these monomer pairs. All copolymerizations lead to almost quantitative conversions



Scheme I. Cationic copolymerization of 6-1 and 6-2

Table I. Cationic Copolymerization of 6-8 with 6-2 (polymerization temperature, 0°C; polymerization solvent, methylene chloride; $[M]_0 = [6-8] + [6-2] = 0.285$ -0.377M; $[M]_0/[I]_0 = 20$; $[(CH_3)_2SiO]/[I]_0 = 10$; polymerization time, 1hr) and Characterization of the Resulting Polymers. Data on first line are from first heating and cooling scans. Data on second line are from second heating scan.

Sample No.	[6-8]/[6-2] (mol/mol)	Polymer yield(%)	Max 10 ⁻³	Mw/Mn	DP	phase transitions (°C) and corresponding enthalpy changes (kcal/mru)	
						heating	cooling
1	0/10	73	2.9	1.10	11	X 86.0 (0.18) i g 72.8 i	i 63.8 g
2	1/9	73	2.8	1.16	10	X 66.3 (0.38) i g 57.4 i	i 49.8 g
3	2/8	78	3.0	1.10	11	X 60.8 (0.41) n 75.2 (0.045) i g 48.3 n 74.8 (0.038) i	i 70.8 (0.042) n 41.0 g
4	3/7	81	2.9	1.13	10	X 54.6 (0.46) n 82.7 (0.049) i g 41.4 n 83.1 (0.061) i	i 80.2 (0.053) n 30.0 g
5	4/6	64	2.8	1.15	9	X 45.2 (0.39) n 94.1 (0.096) i g 36.0 n 93.8 (0.092) i	i 90.3 n (0.087) 27.8 g
6	5/5	65	2.8	1.17	9	g 33.7 sA 102.3 (0.092) i g 31.5 sA 102.5 (0.110) i	i 98.7 (0.110) n 22.6 g
7	6/4	72	3.1	1.15	9	g 24.9 sA 98.1 (-)* n 106.5 (0.16) i g 21.3 sA 94.6 (-)* n 104.2 (0.21) i	i 100.7 (0.18) n 90.8 (-)* sA 13.7 g
8	7/3	75	3.3	1.13	10	g 20.8 sA 109.3 (0.28) i g 18.2 sA 109.1 (0.26) i	i 104.8 (0.27) sA 12.5 g
9	8/2	70	3.3	1.10	10	g 18.2 sA 118.1 (0.32) i g 16.3 sA 117.0 (0.34) i	i 110.5 (0.35) sA 10.1 g
10	9/1	71	3.7	1.10	11	g 14.9 sA 121.3 (0.41) i g 14.3 sA 120.2 (0.43) i	i 115.2 (0.39) sA 10.8 g
11	10/0	62	3.6	1.15	10	g 11.6 sA 127.5 (0.43) i g 11.6 sA 127.3 (0.45) i	i 122.8 (0.46) sA 7.8 g

Table II. Cationic Copolymerization of 6-11 with 6-2 (polymerization temperature, 0°C; polymerization solvent, methylene chloride; $[M]_0 = [6-11] + [6-2] = 0.256-0.358M$; $[M]_0/[I]_0 = 20$; $[(CH_3)_2SiO]/[I]_0 = 10$; polymerization time, 1hr) and Characterization of the Resulting Polymers. Data on first line are from first heating and cooling scans. Data on second line are from second heating scan.

Sample No.	[6-11]/[6-2] (mol/mol)	Polymer yield(%)	Mnx10 ⁻³	Mw/Mn	DP	phase transitions (°C) and corresponding enthalpy changes (kcal/mru)	
						heating	cooling
1	0/10	65	4.6	1.18	17	X 85.7 (0.25) i g 78.3 i	i 70.5 g
2	1/9	72	4.1	1.26	15	X 70.5 (0.44) i g 64.8 i	i 56.6 g
3	2/8	74	4.2	1.09	15	X 64.4 (0.47) n 90.8 (0.038) i g 55.8 n 90.6 (0.044) i	i 86.7 (0.044) n 50.0 g
4	3/7	70	4.7	1.13	16	X 55.9 (0.055) n 98.5 (0.086) i g 44.1 n 98.5 (0.091) i	i 96.0 (0.085) n 41.6 g
5	4/6	71	4.7	1.12	15	X 42.8 (0.35) sA 103.2 (-) n 105.7 (0.18) i g 35.8 sA 103.0 n 105.6 (0.17) i	i 102.4 (-) n 96.5 (0.18) sA 30.8 g
6	5/5	62	5.6	1.15	17	g 30.3 sA 110.8 (0.34) i g 28.9 sA 110.6 (0.34) i	i 109.2 (0.35) sA 24.2 g
7	6/4	66	5.8	1.16	17	g 22.5 sA 119.1 (0.45) i g 20.0 sA 120.1 (0.47) i	i 116.6 (0.54) sA 17.5 g
8	7/3	62	7.0	1.16	20	g 16.7 sA 128.8 (0.58) i g 15.0 sA 127.1 (0.62) i	i 135.0 (0.67) sA 10.5 g
9	8/2	69	6.7	1.20	18	g 15.0 sA 136.3 (0.76) i g 14.8 sA 135.8 (0.71) i	i 130.1 (0.79) sA 8.4 g
10	9/1	54	9.0	1.12	23	g 16.7 k 52.1 (2.13) sA 145.8 (0.81) i g 13.3 sA 145.8 (0.80) i	i 138.9 (0.80) sA 7.5 g
11	10/0	72	7.6	1.09	19	g 15.0 k 62.7 (2.82) sA 153.3 (0.82) i g 12.5 sX 50.4 (1.74) sA 151.7 (0.87) i	i 142.8 (0.82) sA 19.8 (0.75) sX 8.5 g

(determined by HPLC and GPC), although the yields reported in Tables I to II are lower than 100%. This is due to polymer losses during the purification experiments. The GPC traces of all copolymers show a monomodal molecular weight distribution characterized by a polydispersity of about 1.1 (Tables I and II).

As determined from the second DSC heating scan, both poly[(6-8)-co-(6-2)]X/Y and poly[(6-11)-co-(6-2)]X/Y are based on a monomer pair whose parent homopolymers exhibit enantiotropic s_A and respectively glassy phases as their highest temperature mesophase. The phase behavior of these copolymers will be presented in the order discussed above and the phase behavior of all these copolymers will be discussed as obtained from their first and second heating and first cooling DSC scans.

8.3.1.-Poly[(6-8)-co-(6-2)]X/Y

All copolymerization experiments described in this paper were performed under experimental conditions where the resulting poly(6-2), poly(6-8) and poly(6-2-co-6-8) have a degree of polymerization of about 9-11 (Table I). Poly(6-8) with degree of polymerization equal to 10 displays an enantiotropic s_A mesophase^{1c} (Table I, Figure 1). Poly(6-2) with a degree of polymerization equal to 10 displays only in the first heating scan a monotropic X phase.^{8b} During the first and subsequent cooling scans and second and subsequent heating scans, poly(6-2) displays only a glass transition temperature (Table I, Figure 1). Therefore, the investigation of copolymers based on a structural unit whose homopolymer exhibits a X mesophase and a structural unit whose homopolymer exhibits a s_A mesophase when the data are collected from the first heating scan. Alternatively, when the data are collected from the second heating scan, the same copolymer system consists of a structural unit whose homopolymer is

amorphous and a structural unit whose homopolymer exhibits an enantiotropic s_A mesophase.

Upon copolymerization, the temperature associated with the X-isotropic phase transition decreases. Copolymers poly(6-8)-co-(6-2)5/5 to poly(6-8)-co-(6-2)10/0 do not exhibit the X phase. Therefore, the structural units derived from the monomers 6-2 and 6-8 are isomorphic within the X phase only over a very narrow range of compositions. A similar behavior can be observed for the s_A phase displayed by poly(6-8). Poly(6-8-co-6-2)X/Y with compositions from with X/Y=10/0 to 6/4 display a s_A phase. The temperature transition associated with this phase decreases by increasing the concentration of structural units derived from monomer 6-2. Poly(6-8-co-6-2)7/3 exhibits a triple point. Poly(6-8-co-6-2)6/4 exhibits both a nematic and a s_A mesophase. Inspection of this copolymer on the optical polarized microscope uncovers reentrant nematic mesophase (Table I).³ Therefore, the s_A phase of this copolymer is most probable a s_{Ad} phase. Poly(6-8-co-6-2)X/Y with X/Y from 5/5 to 2/8 exhibits a nematic phase.

The phase behavior of poly(6-8-co-6-2)X/Y determined from the first heating scan is plotted in Figure 2a. This figure demonstrates that both the s_A and n phases exhibit continuous dependences of copolymer composition within a certain range of compositions respectively. The very interesting result consists in the ability to prepare copolymers exhibiting a nematic mesophase from structural units derived from two homopolymers which display a smectic and X mesophases. This may result because within the s_A phase the backbone conformation of poly(6-8) is confined to the smectic layers.⁴ Simultaneously, since the spacer of poly(6-2) is short, the backbone of this polymer may exhibit an extended conformation within the X phase.⁵ Based on this account, the structural units of this copolymer are isomorphic in each of the two

mesophases only over the range of compositions where the polymer backbone can get distorted to accomodate either the X or s_A mesophases. Morphological experiments are required to support this speculative explanation.

The newly formed nematic mesophase extends over a broad range of copolymer composition (Figure 2a-c). The glass transition temperature of these copolymers decreases as expected by increasing the amount of 6-8 in the copolymer (Figure 2a). The DSC traces of the second heating scans of poly(6-2-co-6-8)X/Y are presented in Figure 1b. They are identical to those from the first heating scans from Figure 1a, except that X phase is missing and the change in the heat capacity at the glass transition temperatures of poly(6-8-co-6-2)X/Y from X/Y=0/10 to 4/6 is larger.

The thermal transition temperatures collected from Figure 1b are plotted in Figure 2b. This figure demonstrates that poly(6-8-co-6-2) displays a continuous dependence of the s_A and nematic phases on copolymer composition with a triple point at a certain composition. The absence of the X phase in the second heating scans is most probable the result of a kinetic effect which is due to the close proximity of the X phase from the glass transition. Therefore this X phase forms only when the polymers are precipitated from solution. If the polymer sample is redissolved and reprecipitated, the X phase reappear. Alternatively, if poly(6-2) and poly(6-8-co-6-2) are sheared above the glass transition temperature on the optical polarized microscope, an anisotropic texture forms. This behavior can be easily explained by thermodynamics.^{5,6} The cooling DSC scans of poly(6-8-co-6-2)X/Y are presented in Figure 1c. They provide the same conclusion as that derived from the second heating scans. The phase diagram of poly(6-2-co-6-8) obtained from the cooling DSC scans is plotted in Figure 2c and agrees very well with that from Figure 2b.

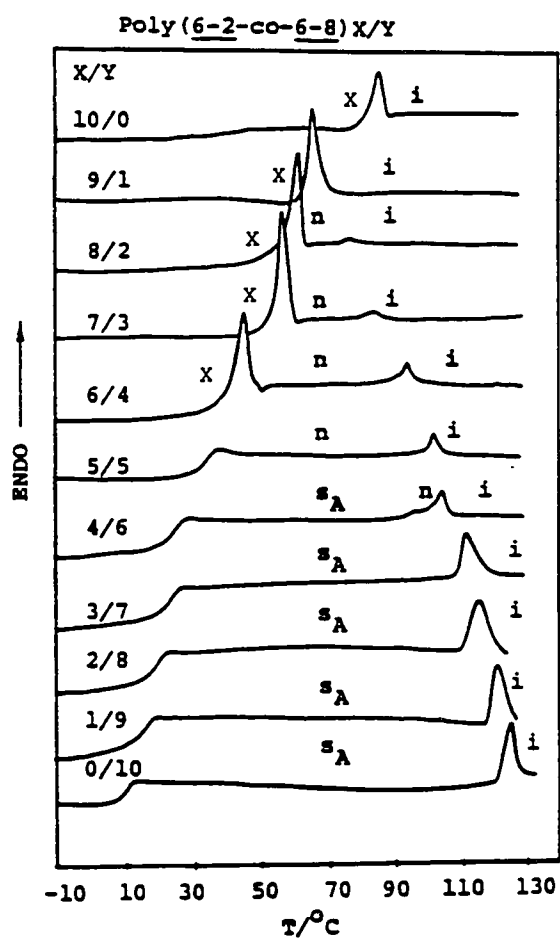


Figure 1a. DSC traces displayed during the first heating scan by poly(6-8), poly(6-2) and by poly[(6-8)-co-(6-2)]X/Y.

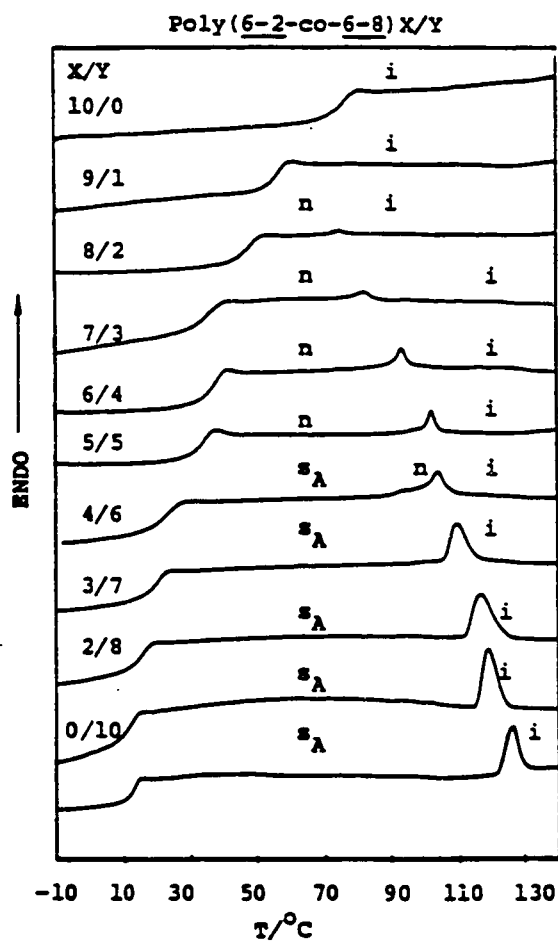


Figure 1b. DSC traces displayed during the second heating scan by poly(6-8), poly(6-2) and by poly[(6-8)-co-(6-2)]X/Y.

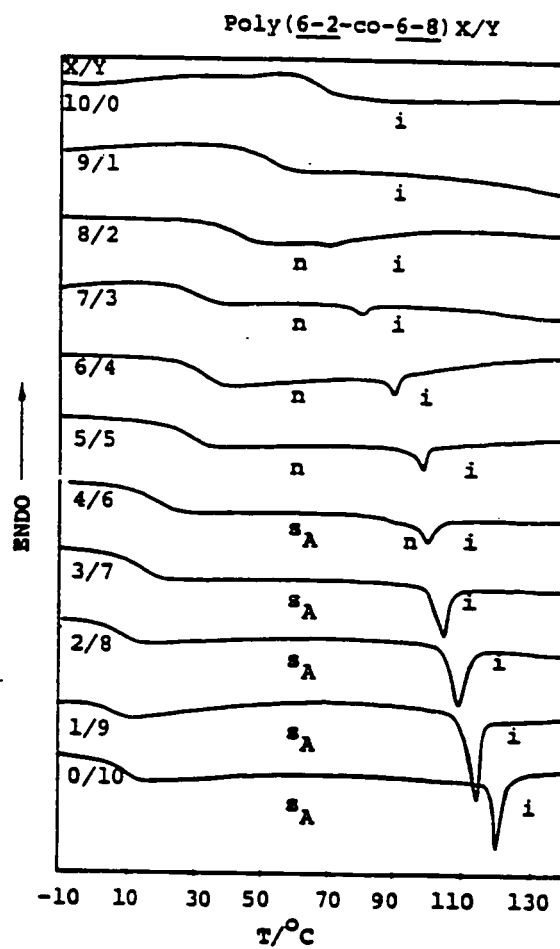


Figure 1c. DSC traces displayed during the first cooling scan by poly(6-8), poly(6-2) and by poly[(6-8)-co-(6-2)]X/Y.

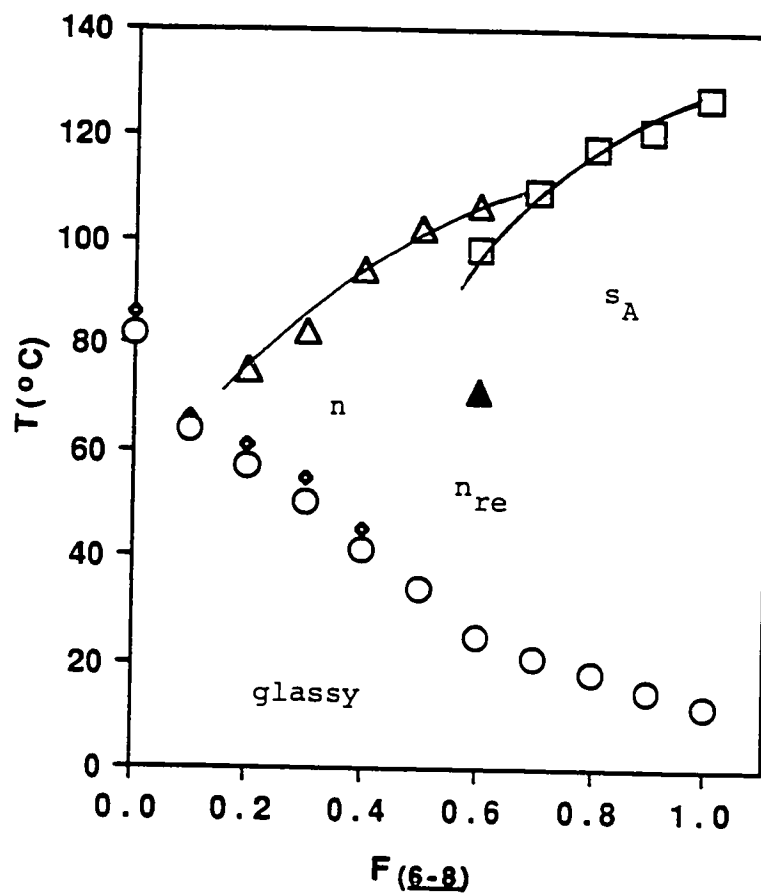


Figure 2a. The dependence of phase transition temperatures on composition of poly[(6-8)-co-(6-2)]X/Y (data from the first heating scan): O-Tg; \diamond -TsX-sA; Δ -Tn-i; \square -TsA-i; \blacktriangle -Tn-re-sAd

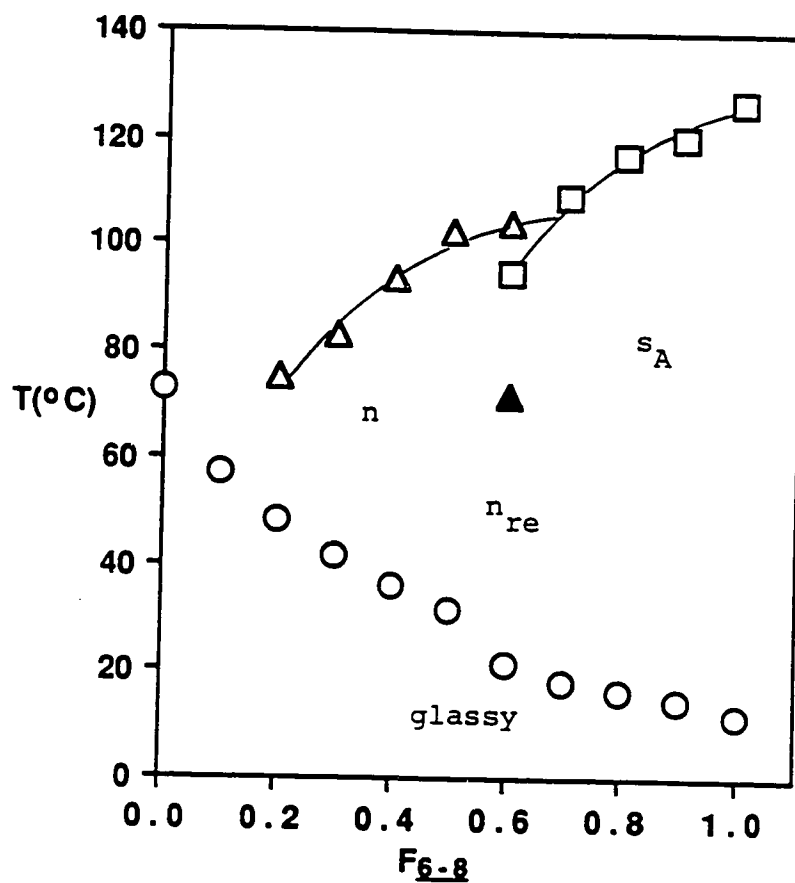


Figure 2b. The dependence of phase transition temperatures on composition of poly[(6-8)-co-(6-2)]X/Y (data from the second heating scan): O- T_g ; Δ - T_{n-i} ; \square - T_{SA-i} ; \blacktriangle - $T_{nre-sAd}$;

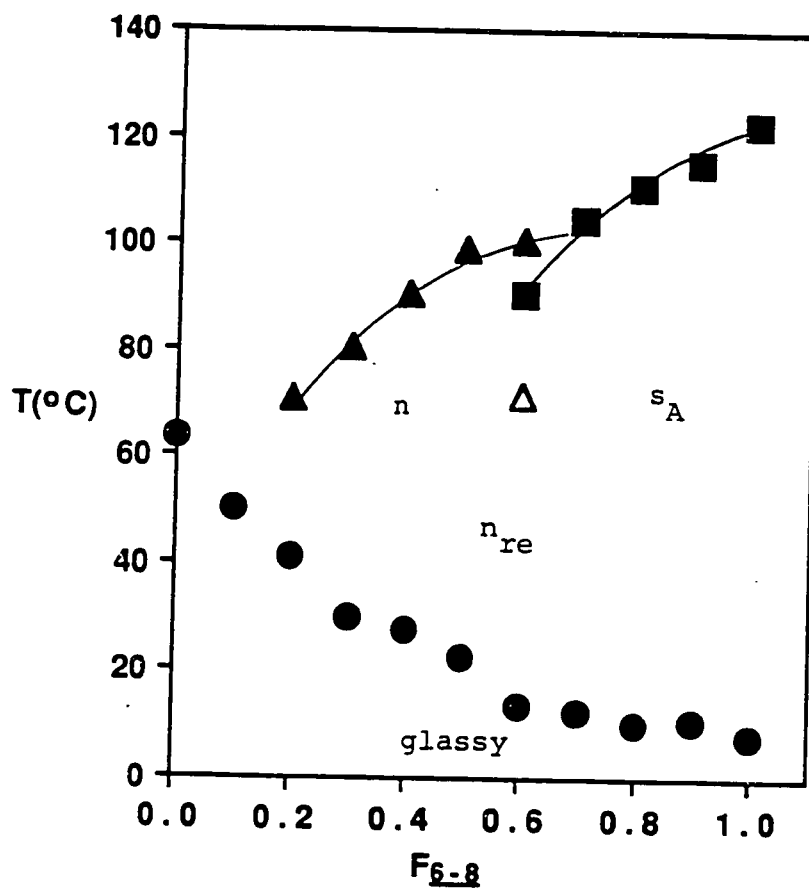


Figure 2c. The dependence of phase transition temperatures on composition of poly[(6-8)-co-(6-2)]X/Y (data from the first cooling scan): O- T_g ; Δ - T_{i-n} ; \square - T_{i-sA} ; Δ - $T_{sAd-nre}$

The dependence of the enthalpy changes associated with nematic-isotropic, isotropicnematic, s_A -isotropic and isotropic- s_A is plotted in Figure 3. The enthalpy changes of the nematic- s_A and s_A -isotropic as well as their reversed values of poly(6-8-co-6-2) 6/4 could not be separated and therefore, they were plotted as the sum of both transitions (Table 1, Figure 3). Even so, Figure 2d demonstrates that both the enthalpy changes associated with the s_A -phase and with the nematic phase transitions are located on straight lines. However, these lines have a different slope. These data prove that the structural units derived from 6-2 and 6-8 are isomorphous over a certain range of copolymer composition within the nematic phase and over another certain range of composition within the s_A phase. A classification of the various classes of homopolymer and copolymer isomorphism within liquid crystalline phase was presented in a previous publication.⁷

8.3.2.-Poly[(6-11)-co-(6-2)]X/Y

The influence of molecular weight on the phase transitions of poly(6-11) was reported in a previous publication.^{8a} In the first heating scan poly(6-11) exhibits a melting transition followed by an enantiotropic s_A mesophase. In the second heating scan poly(6-11) with degrees of polymerization lower than 3 exhibit a melting and an enantiotropic s_A mesophase. Polymers with degrees of polymerization between 4 and 15 exhibit only the enantiotropic s_A mesophase, while those with degrees of polymerization higher than 20 an enantiotropic s_X (unidentified smectic phase) and an enantiotropic s_A mesophase. The phase transitions of poly(6-11) with degrees of polymerization higher than 15 are almost molecular weight independent. Poly(6-2) with degrees of polymerization higher than 6 exhibit an inverse monotropic X phase only in the first heating scan.^{1b} In the second heating scan they exhibit only a glass

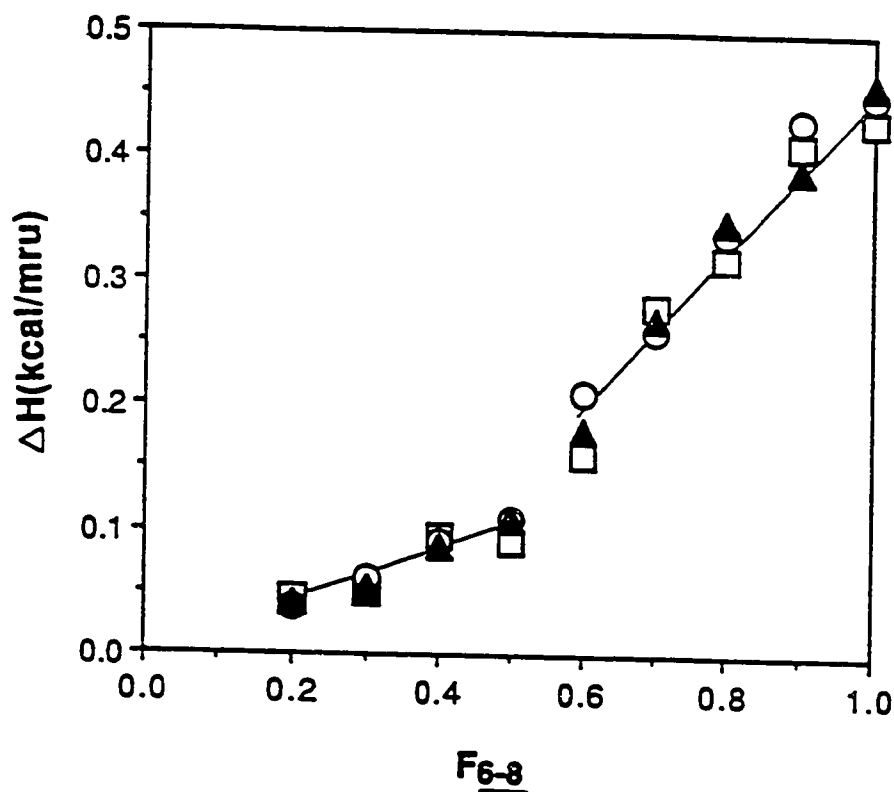


Figure 3. The dependence of the enthalpy changes associated with the mesomorphic-isotropic and isotropic-mesomorphic phase transitions on the composition of poly[(6-8)-co-(6-2)]X/Y. □- ΔH_{sA-i} (data from the first heating scan); ▲- ΔH_{sA-i} (data from the second heating scan); ○- ΔH_{i-sA} (data from the first cooling scan).

transition temperature. Therefore, in order to avoid the complication of the phase behavior due to the polymer molecular weight, we decided to investigate poly[(6-11)-co-(6-2)] with degrees of polymerization higher than 15. Table II summarizes the polymerization and copolymerization conditions, the molecular weights and the compositions of the resulting copolymers.

Figure 4a-c present the first and second heating and respectively the first cooling DSC scans of poly[(6-11)-co-(6-2)]X/Y where X/Y refers to the mole ratio between the 6-11 and 6-2 monomeric structural units in copolymer. In the first heating scan poly(6-2) and poly[(6-11)-co-(6-2)]1/9 display a monotropic X mesophase (Figures 1a). Poly[(6-11)-co-(6-2)] with X/Y=2/8 and 3/7 exhibit in the first heating scan a monotropic X phase and an enantiotropic nematic phase. In the second heating scan these copolymers exhibit only the enantiotropic nematic mesophase. Poly[(6-11)-co-(6-2)]5/5 exhibits a triple point on their phase behavior. Poly[(6-11)-co-(6-2)]4/6 presents the most interesting behavior since this copolymer exhibits the i-n-s_{Ad}-n_{re} sequence (Table II, Figure 7). Regardless of the DSC heating scan, poly[(6-11)-co-(6-2)] with X/Y=5/5 to 8/2 exhibit an enantiotropic s_A mesophase. Poly[(6-11)-co-(6-2)]9/1 displays a crystalline melting only in the first heating scan and an enantiotropic s_A phase in all other DSC scans, while poly(6-11) behaves as described in the previous publication^{1a}.

The thermal transition temperatures and their corresponding thermodynamic parameters are summarized in Table II. The thermal transition temperatures collected from the first and second heating scan are plotted in Figure 5a and Figure 5b respectively, and those from the first cooling scan in Figure 5c. Glass transition temperatures are also plotted in these figures. The enthalpy changes associated with these transitions are plotted in Figure 6.

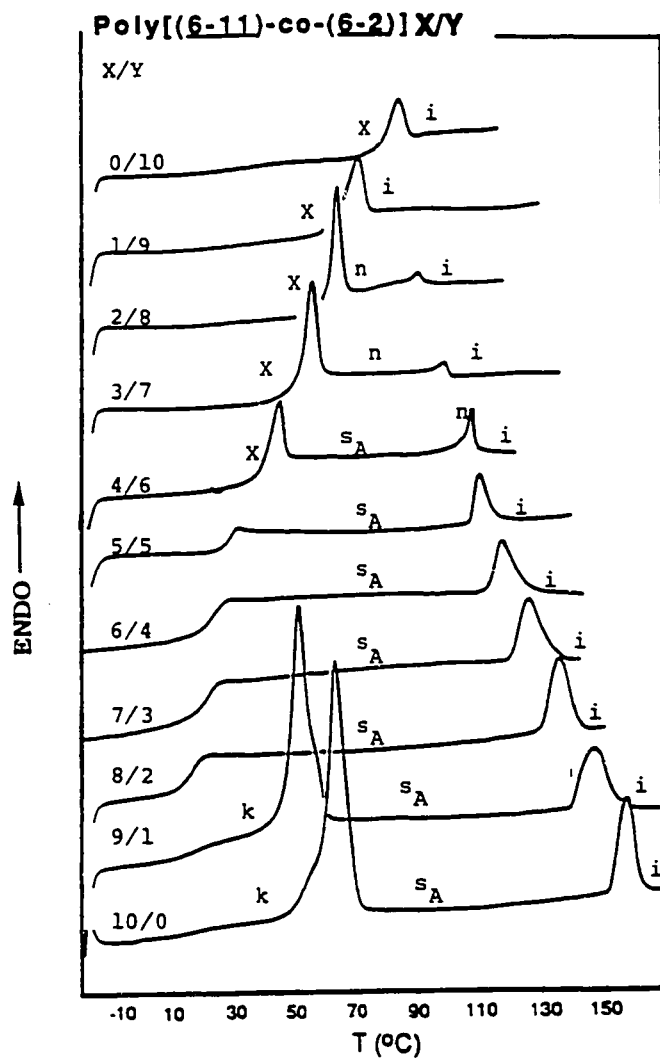


Figure 4a. DSC traces displayed during the first heating scan by poly(6-11), poly(6-2) and by poly[(6-11)-co-(6-2)]X/Y.

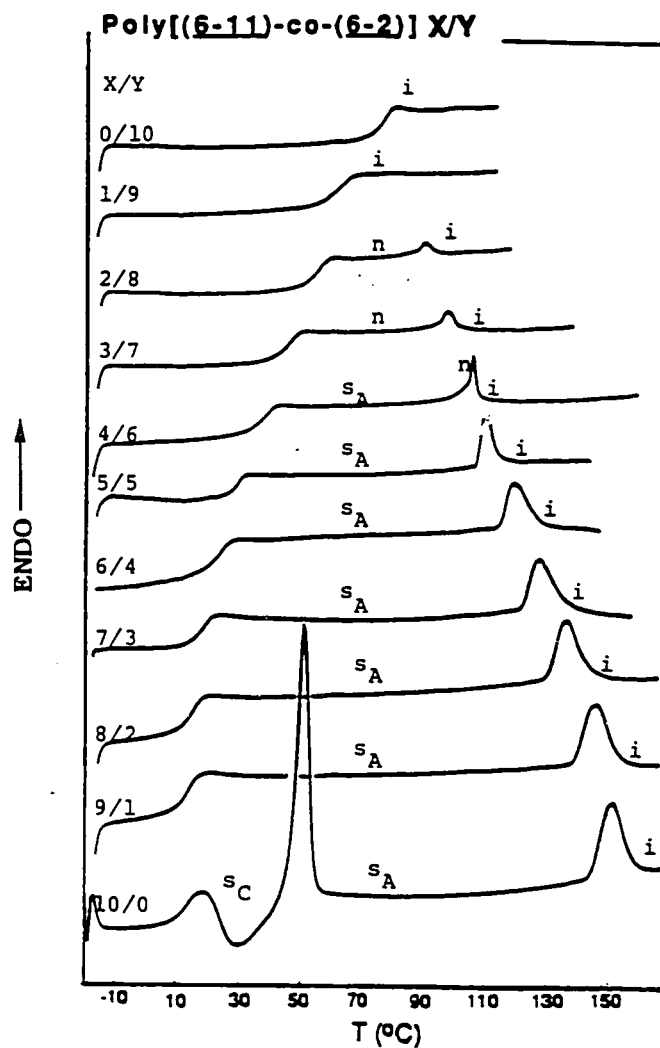


Figure 4b. DSC traces displayed during the second heating scan by poly(6-11), poly(6-2) and by poly[(6-11)-co-(6-2)]X/Y.

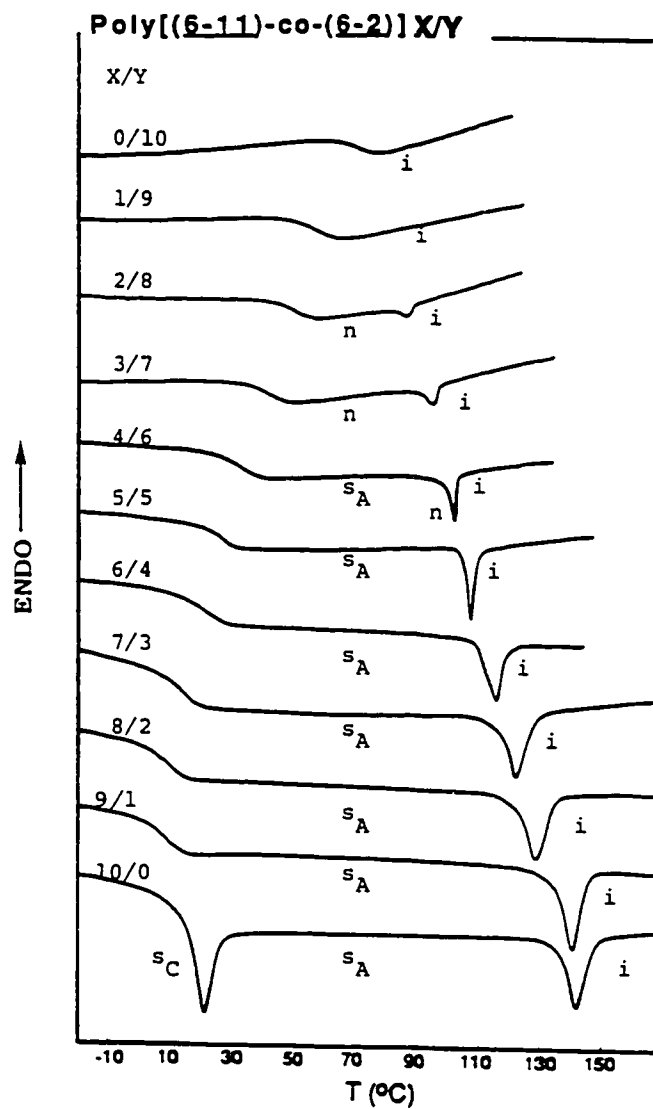


Figure 4c. DSC traces displayed during the first cooling scan by poly(6-11), poly(6-2) and by poly[(6-11)-co-(6-2)]X/Y.

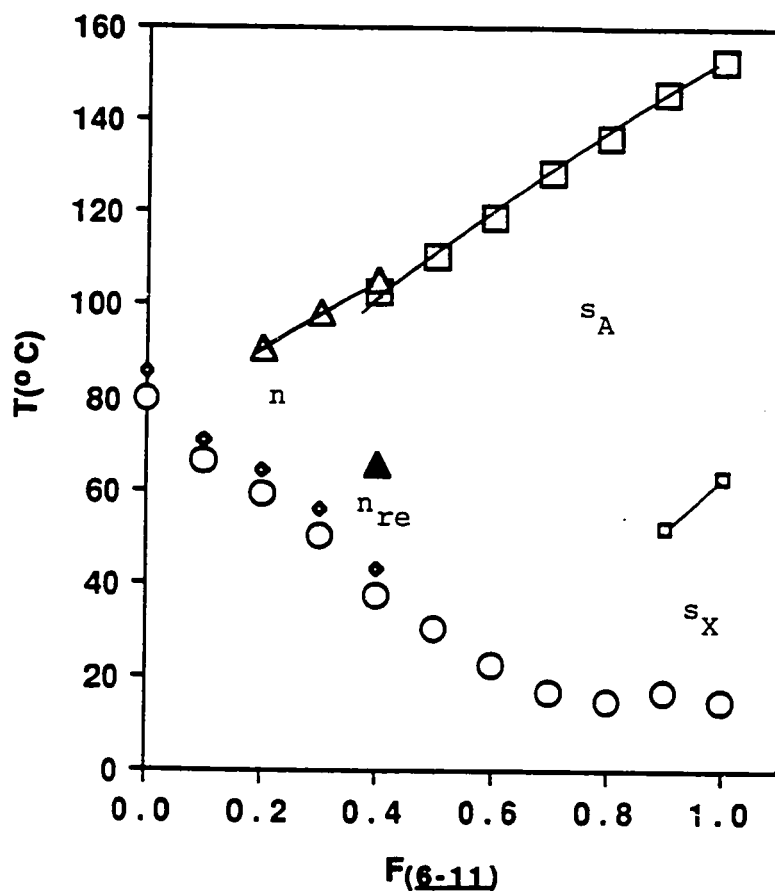


Figure 5a. The dependence of phase transition temperatures on composition of poly[(6-11)-co-(6-2)]X/Y (data from the first heating scan): O-Tg; \diamond -Ts_X-s_A; Δ -Tn-i; \square -Ts_A-i; \blacktriangle -Tn_{re}-sAd

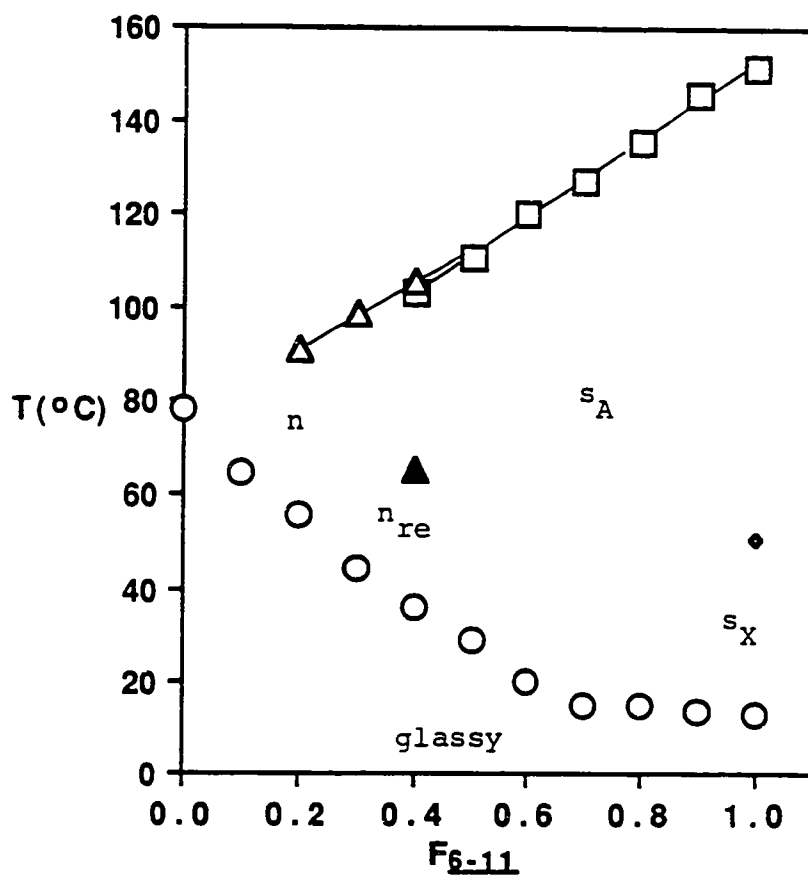


Figure 5b. The dependence of phase transition temperatures on composition of $\text{poly}[(6-11)\text{-co-}(6-2)]X/Y$ (data from the second heating scan): O - T_g ; Δ - T_{n-i} ; \square - T_{sA-i} ; \blacktriangle - $T_{n_{re}-sAd}$;

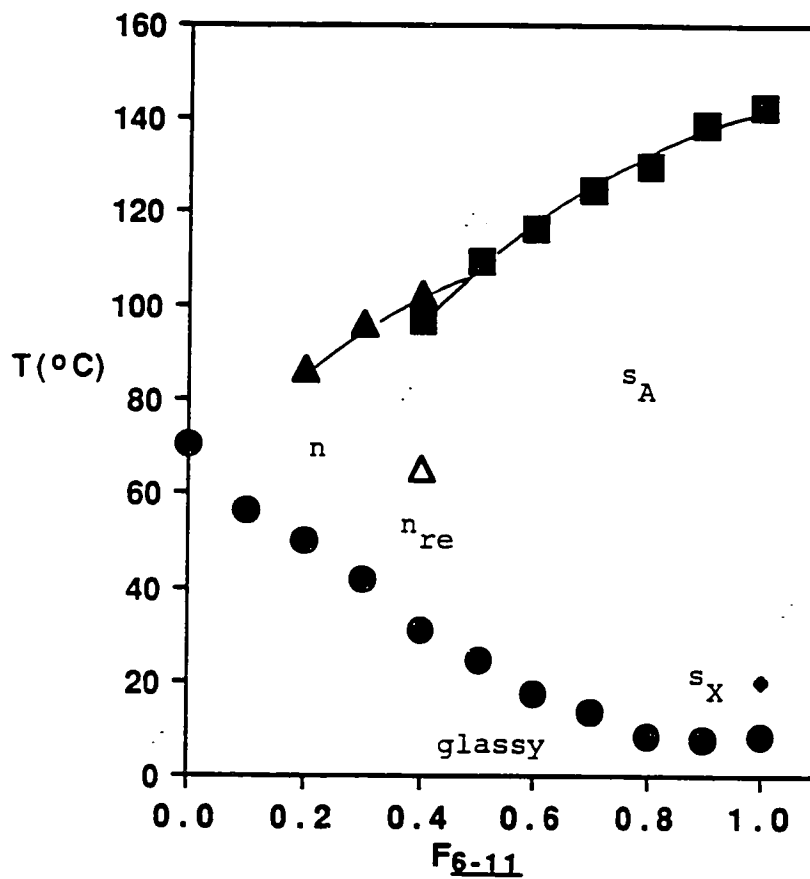


Figure 5c. The dependence of phase transition temperatures on composition of poly[(6-11)-co-(6-2)]X/Y (data from the first cooling scan): ●-Tg; ▲-Ti-n; ■-Ti-sA; Δ-TsAd-n_{re}

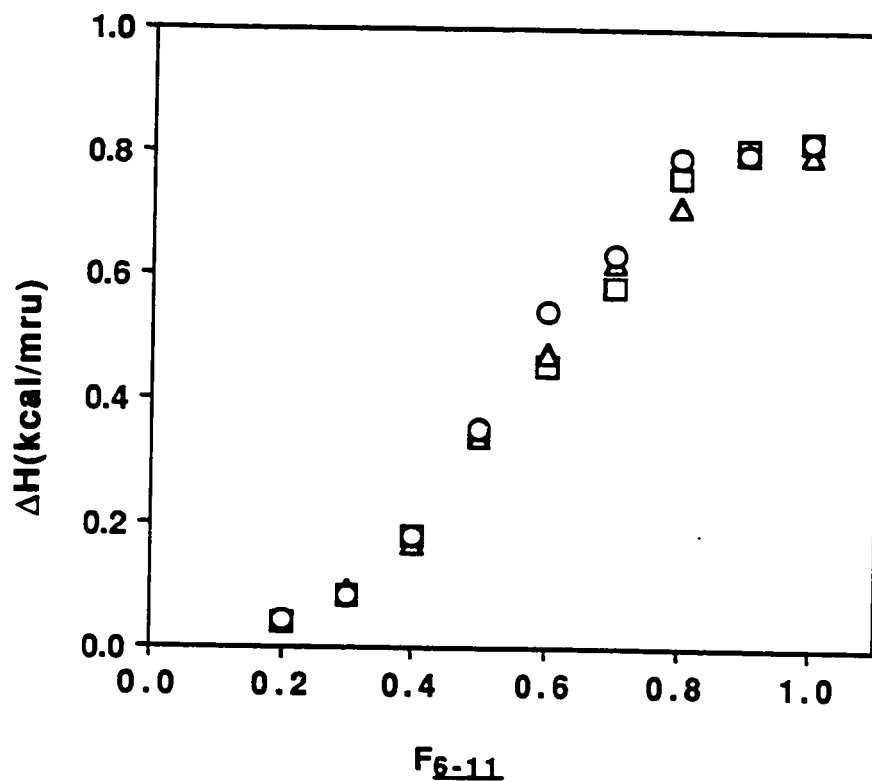


Figure 6. The dependence of the enthalpy changes associated with the mesomorphic-isotropic and isotropic-mesomorphic phase transitions on the composition of poly[(6-11)-co-(6-2)]X/Y. □-ΔH_{sA-i} (data from the first heating scan); Δ-ΔH_{sA-i} (data from the second heating scan); ○-ΔH_{i-sA} (data from the first cooling scan).

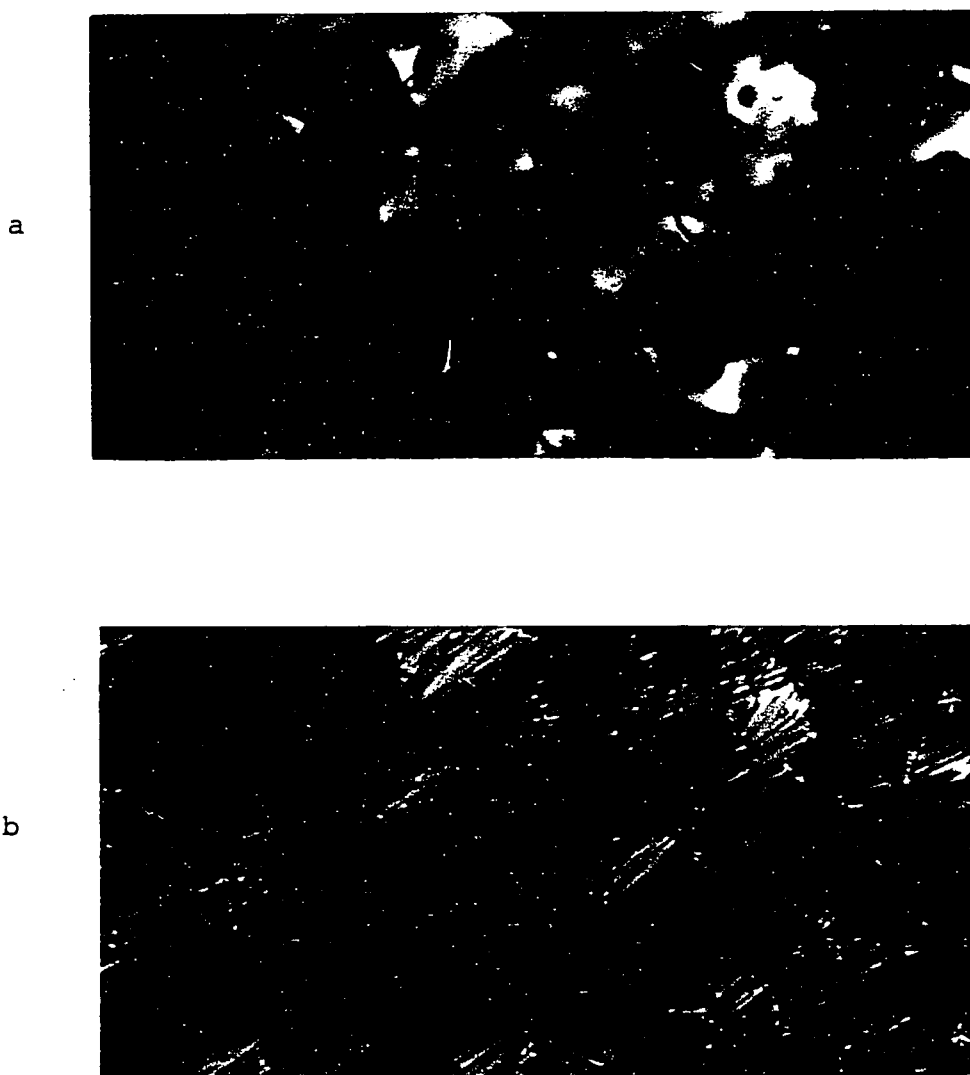


Figure 7. Representative optical polarized micrographs (100x) of the phases exhibited by poly[(6-8)-co-(6-2)]6/4 with degree of polymerization of 20: a) n phase at 103°C; b) s_{Ad} phase at 83°C; c) transition from n_{re} to s_{Ad} phase at 65 °C; d) n_{re} phase at 55°C

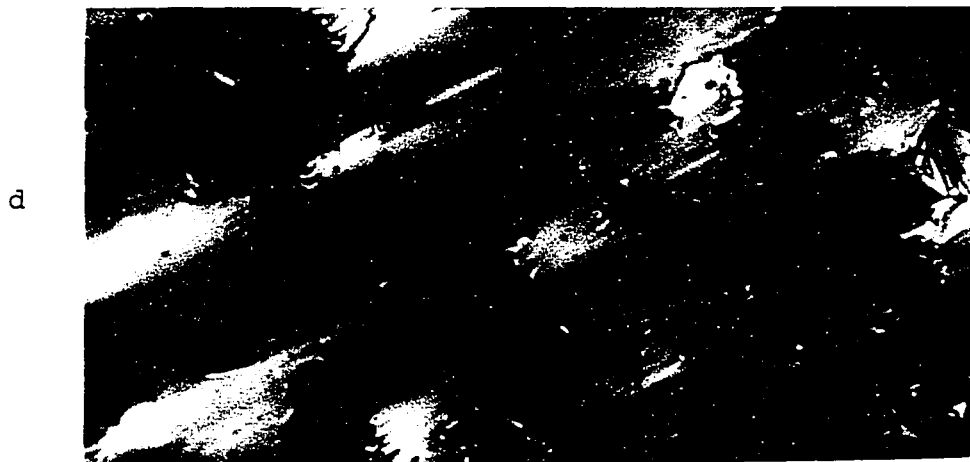
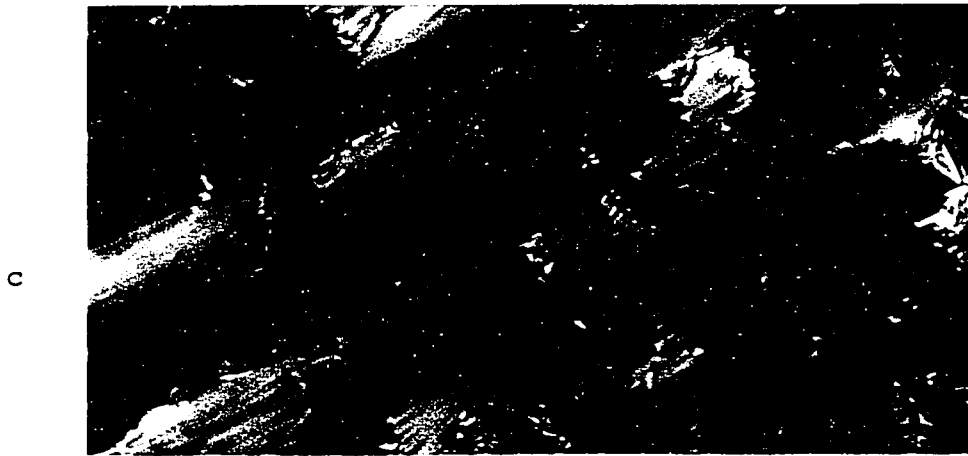


Figure 7. (continued)

In conclusion, the experimental results described in this chapter provide the quantitative copolymerization experiments performed with mesogenic vinyl ethers. Since these monomers can be polymerized by living cationic polymerization, both the molecular weight, molecular weight distribution and the composition of these copolymers can be conveniently controlled. The most important conclusions obtained from the results of poly[(6-8)-co-(6-2)]X/Y and poly[(6-11)-co-(6-2)]X/Y are as follows. Over a certain range of compositions the two structural units are isomorphic within the s_A phase, after which follows a triple point. After this triple point the two structural units are isomorphic within an induced nematic mesophase. Both copolymers generate within a certain range of compositions on the left side of the triple point the sequence i-n- s_A -n_{re}. This behavior allows the engineering of mesomorphic phase transition temperatures and of their thermodynamic parameters in a straightforward manner by statistical binary copolymerizations.

REFERENCES

1. (a)V. Percec, M. Lee and H. Jonsson, *J. Polym. Sci., Polym. Chem. Ed.*, **29**, 327 (1991); (b)V. Percec and M. Lee, *J. Macromol. Sci.-Chem.*, **A28**, 651 (1991); (c)V. Percec and M. Lee, *Macromolecules*, **24**, 1017 (1991);
2. C. G. Cho, B. A. Feit and O. W. Webster, *Macromolecules*, **23**, 1918 (1990)
3. (a) G. Sigaud, N. H. Tinh, F. Hardouin and H. Gasparoux, *Mol. Crst. Liq. Cryst.*, **69**, 81 (1981); (b) F. Hardouin, A. M. Levelut, M. F. Archard and G. Sigaud, *J. Chim. Phys.*, **80**, 53 (1983); (c) F. Hardouin, *Physica*, **140A**, 359 (1986); (d) P. E. Cladis, *Mol. Cryst. Liq. Cryst.*, **165**, 85 (1988)
4. V. Percec, B. Hahn, M. Ebert, J. H. Wendorff, *Macromolecules*, **23**, 2092 (1990)
5. A. Keller, G. Ungar and V. Percec, *Advances in Liquid Crystalline Polymers*, C. K. Ober and R. A. Weiss Eds. ACS Symposium series, Washington D. C., 1990
6. V. Percec and A. Keller, *Macromolecules*, **23**, 4347 (1990)
7. V. Percec and Y. Tsuda, *Polymer*, **32**, 661 (1991)

Chapter 9

SYNTHESIS AND CHARACTERIZATION OF BINARY COPOLYMERS OF 11-[4-CYANO-4'-BIPHENYL)OXY]UNDECANYL VINYL ETHER WITH (2S,3S)-(+)-2-CHLORO-3-METHYLPENTYL 4'-(8-VINYLOXYOCTYLOXY)BIPHENYL-4-CARBOXYLATE, AND OF (2S,3S)-(+)-2-CHLORO-3-METHYLPENTYL 4'-(8-VINYLOXYOCTYLOXY)BIPHENYL-4-CARBOXYLATE WITH 3-[4-CYANO-4'-BIPHENYL)OXY]PROPYL VINYL ETHER.

9.1.-INTRODUCTION

Copolymerization provides the most effective method for the molecular engineering of side chain liquid crystalline polymers.^{1,2} Copolymerization of monomer pairs each containing mesogenic units¹⁻¹⁰ can be classified into at least four different groups: (1) copolymers from monomer pairs containing identical mesogens and polymerizable groups but different spacer lengths; (2) copolymers from monomer pairs containing identical mesogens and spacer lengths but different polymerizable groups; (3) copolymers from monomer pairs containing dissimilar mesogens but either similar or different spacer lengths and polymerizable groups; (4) copolymers from monomer pairs containing constitutional isomeric units and similar or dissimilar spacers and polymerizable groups.²

For a quantitative approach to the understanding of side chain liquid crystalline copolymers, molecular weight, molecular weight distribution and copolymer composition should be well defined.¹¹ Copolymers synthesized by chain copolymerization reactions exhibit a heterogeneous composition since the copolymer composition differs from that of the monomer feed in the initial reaction mixture, exception being the azeotropic copolymerizations. Furthermore, the temperature and the nature of the mesophase are molecular weight¹²⁻¹⁶ and molecular weight distribution dependent.^{15,17} Therefore, for a quantitative investigation of side chain liquid

crystalline copolymers it is essential that these factors are well defined. The ideal solution to the synthesis of copolymers by chain reactions would be to select monomer pairs that can be copolymerized by an azeotropic living mechanism.¹⁸

Chapters 7 and 8 have investigated the first series of quantitative experiments on statistical binary copolymers with well defined composition, molecular weight and molecular weight distribution by living cationic polymerization corresponding to class 1, i.e., copolymers from monomer pairs containing identical mesogenic units and polymerizable groups but different spacer lengths. The general trend observed from these investigations is that over the entire range of copolymer compositions where the two structural units of the copolymer are isomorphic within a certain mesophase, both the phase transition temperatures and the enthalpy changes associated with this mesophase follow a continuous dependence of copolymer composition. The dependence of isotropization temperature on composition can also be predicted by the Schroeder-van Laar equation²¹ when the isomorphic structural units of the copolymer behave like an ideal solution of these structural units.^{19,20} When the two structural units are non-isomorphic within at a certain composition, a continuous dependence of both transition temperatures and enthalpy changes with a triple point at a certain copolymer composition can be observed.^{19b-e}

Presently, we are investigating the copolymers based on monomer pairs containing dissimilar mesogens and dissimilar spacer lengths but identical polymerizable groups which correspond to the class of copolymers 3. In the case of different chemical structure for each mesogen, the components of such polymer blends are generally immiscible and attempts to obtain homogeneous mixtures were not successful.⁶ Copolymers from this class are however of interest for the fundamental understanding of phase diagrams obtained by copolymerization.

This chapter will describe the synthesis and characterization of two copolymer series based on 11-[(4-cyano-4'-biphenyl)oxy]undecanyl vinyl ether (6-11) and 3-[(4-cyano-4'-biphenyl)oxy]propyl vinyl ether (6-3) with (2S,3S)-(+)-2-chloro-3-methylpentyl 4'-(8-vinyloxyoctyloxy)biphenyl-4-carboxylate (18-5). All copolymers were synthesized with a degree of polymerization of 20 and different compositions. When the mesomorphic phases exhibited by the parent homopolymers with a degree of polymerization of about 20 are determined from the second heating scans, poly(6-11)^{16a} exhibits enantiotropic s_A and s_X , poly(6-3)^{16b} enantiotropic nematic, and poly(15-8)^{20c} enantiotropic s_A , s_C^* and s_X mesophases. Therefore, it is expected that the investigation of these two series of copolymers will provide information about the phase behavior of the copolymers containing different mesogens and different spacer lengths derived from pairs of homopolymers exhibiting as the high temperature mesophases, s_A and s_A , and respectively, n and s_A . Therefore, this investigation will provide a quantitative understanding of the class of copolymers 3.

9.2.-EXPERIMENTAL

9.2.1-Materials

All materials were commercially available and were used as received or purified as described previously.^{16a,b} Methyl sulfide (anhydrous, 99%, Aldrich) was refluxed over 9-borabicyclo[3.3.1]nonane (9-BBN, crystalline, 98%, Aldrich) and then distilled under argon. Dichloromethane (99.6%, Aldrich) used as a polymerization solvent was first washed with concentrated sulfuric acid, then with water, dried over anhydrous magnesium sulfate, refluxed over calcium hydride and freshly distilled under argon before each use. Trifluoromethane sulfonic acid (triflic acid, 98%, Aldrich) was distilled under argon.

9.2.2.-Synthesis of Monomers

11-[(4-Cyano-4'-biphenyl)oxy]undecanyl vinyl ether (6-11),^{16a} 3-[(4-cyano-4'-biphenyl)oxy]propyl vinyl ether (6-3)^{16b} and (2S,3S)-(+)-2-chloro-3-methylpentyl 4'-(8-vinyloxyoctyloxy)biphenyl-4-carboxylate (15-8)^{20c} were synthesized and purified as described in previous publications. Their purity was higher than 99% (HPLC). Their detailed characterization was described in the previous publications.

9.2.3.-Cationic Polymerizations and Copolymerizations

Polymerizations were carried out in glass flasks equipped with teflon stopcocks and rubber septa under argon atmosphere at 0°C for 1 hr. All glassware was dried overnight at 130°C. The monomer was further dried under vacuum overnight in the polymerization flask. Then the flask was filled with argon, cooled to 0°C and the methylene chloride, dimethyl sulfide and triflic acid were added via a syringe. The monomer concentration was about 10 wt% of the solvent volume and the dimethyl sulfide concentration was 10 times larger than that of the initiator. The polymer molecular weight was controlled by the monomer/initiator ($[M]_0/[I]_0$) ratio. After quenching the polymerization with ammoniacal methanol, the reaction mixture was precipitated into methanol. When necessary, the polymers were reprecipitated until their GPC traces showed complete absence of unreacted monomers. Tables I and II summarize the polymerization results. Although polymer yields are lower than expected due to losses during the purification process, conversions determined by GPC analysis before polymer purification were almost quantitative in all cases.

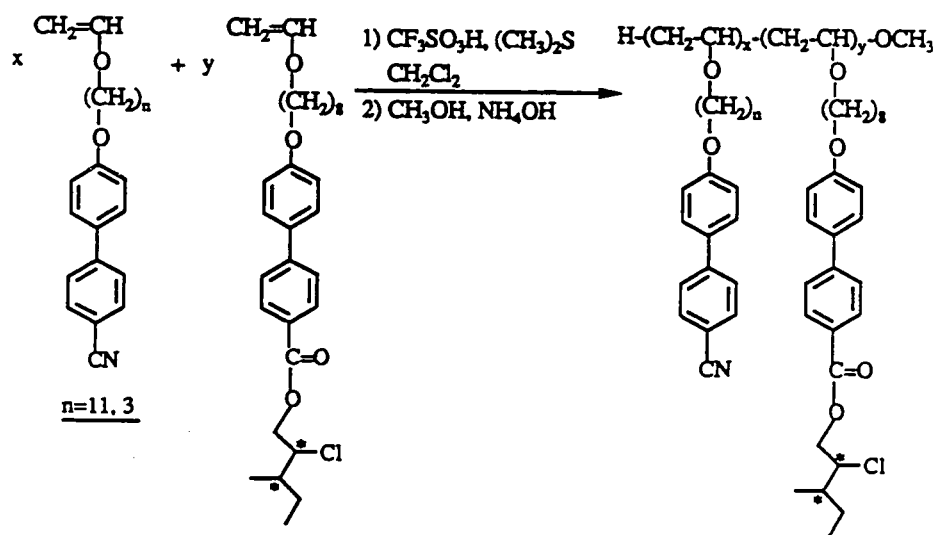
9.3.-RESULTS AND DISCUSSION

The synthesis, characterization and living polymerization of 11-[(4-cyano-4'-biphenyl)oxy]undecanyl vinyl ether (6-11),^{16a} 3-[(4-cyano-4'-biphenyl)oxy]propyl vinyl ether (6-3)^{16b} and (2S,3S)-(+)-2-chloro-3-methylpentyl 4'-(8-vinyloxyoctyloxy)biphenyl-4-carboxylate (15-8)^{20c} were described previously. Scheme I outlines the synthesis of copolymers. The initiating system $\text{CF}_3\text{SO}_3\text{H}/\text{S}(\text{CH}_3)_2$ ^{24,25} is known to induce living cationic polymerizations in CH_2Cl_2 at 0°C. The copolymerization results are listed in Tables I and II. The yields reported in Tables I and II are lower than quantitative due to polymer losses during the purification process. However, the conversions were quantitative and therefore, the copolymer composition is identical to that of the monomer feed (determined by 200 MHz ^1H -NMR spectroscopy). Figure 1 presents a typical 200 MHz ^1H -NMR spectrum of the aromatic region of poly[(15-8)-co-(6-3)]5/5 with its proton assignments. The ratio between the integrals of the signal at 6.95 ppm and 8.10 ppm was used to confirm the copolymer compositions. Therefore, these copolymerization systems follow an azeotropic pattern (i.e., $r_1=r_2=1.0$).

The GPC traces of all copolymers show a monomodal molecular weight distribution characterized by a polydispersity of about 1.15 (Tables I and II). Attempts were made to synthesize all copolymers with degrees of polymerization of about 20.

We have investigated the following two copolymer systems: poly[(6-11)-co-(15-8)]X/Y based on a monomer pair whose parent homopolymers exhibit enantiotropic s_A phases as their highest temperature mesophases and poly[(8-15)-co-(6-3)]X/Y based on a monomer pair whose parent homopolymers exhibit enantiotropic s_A and enantiotropic nematic phases as their highest temperature mesophases.

9.3.1.-Poly[(6-11)-co-(15-8)]X/Y



Scheme I. Cationic copolymerization of 6-n with 15-8

Table I. Cationic Copolymerization of [6-11] with [5-8] (polymerization temperature, 0°C; polymerization solvent, methylene chloride; $[M]_0 = [6-11] + [5-8] = 0.205$ mol/L; $[M]_0/[1]_0 = 20$; $[(CH_3)_2S]/[1]_0 = 10$; polymerization time, 1 hr) and Characterization of the Resulting Copolymers. Data on first line are from first heating and cooling scans. Data on second line are from second heating scan.

Sample No.	[6-11]/[5-8] (mol/mol)	Polymer yield(%)	Mn $\times 10^{-3}$	Mw/Mn	D P	phase transitions (°C) and corresponding enthalpy changes (kcal/mru)	
						G P C	heating cooling
1	0/10	77	8.6	1.08	18	g 16.7 sX 55.2 (0.13) sC* 93.4 (0.17) sA 104.7 (1.10) i g 16.1 sX 53.7 (0.13) sC* 92.1 (0.15) sA 103.7 (0.96) i	i 95.7 (0.93) sA 86.3 (0.14) sC* 45.9 (0.12) sX 13.6 g
2	1/9	84	10.1	1.22	21	g 25.1 k 45.2 (0.41) sC* 89.1 (0.07) sA 130.8 (1.20) i g 24.4 sX 42.8 (0.15) sC* 88.9 (0.11) sA 129.9 (0.11) i	i 122.5 (1.23) sA 79.3 (0.11) sC* 32.9 (0.21) sX 19.8 g
3	2/8	77	8.8	1.10	19	g 33.3 k 49.5 (0.15) k 58.0 (0.67) sC* 79.4 (-) sA 141.7 (1.35) i g 32.5 k 52.9 (0.60) sC* 78.2 (-) sA 140.6 (1.26) i	i 132.7 (1.27) sA 66.2 (-) sC* 44.5 (0.64) k 25.4 g
4	3/7	91	10.2	1.11	22	k 51.3 (0.10) k 63.1 (0.99) sA 149.5 (1.36) i k 61.7 (0.80) sA 150.4 (1.23) i	i 141.9 (1.18) sA 52.7 (0.77) k
5	4/6	89	9.4	1.10	21	k 62.3 (0.13) k 74.2 (1.16) sA 158.9 (1.35) i k 74.4 (1.09) sA 158.9 (1.24) i	i 150.6 (1.21) sA 65.1 (1.01) k
6	5/5	88	8.5	1.09	19	k 59.9 (0.23) k 79.1 (1.05) sA 160.7 (1.39) i k 75.4 (-) sX 78.6 (1.16) sA 160.8 (1.16) i	i 153.0 (1.19) sA 68.8 (1.17) sX 61.2 (-) k
7	6/4	93	9.6	1.17	22	k 58.6 (0.39) k 76.7 (0.96) sA 163.7 (1.21) i k 69.5 (-) sX 77.1 (1.03) sA 163.9 (1.06) i	i 155.9 (1.07) sA 67.1 (1.00) sX 55.8 (0.62) k
8	7/3	89	7.5	1.08	18	k 51.7 (0.29) k 69.4 (0.74) sA 160.3 (1.20) i k 68.3 (0.53) sA 161.0 (1.12) i	i 154.2 (1.14) sA 55.8 (0.42) k
9	8/2	85	7.4	1.07	18	g 13.2 k 51.5 (1.56) k 62.2 (-) sA 161.2 (1.20) i g 12.5 k 56.0 (0.29) sA 161.2 (0.99) i	i 154.6 (0.12) sA 35.3 (0.12) k 10.1 g
10	9/1	96	7.7	1.12	19	g 14.1 k 51.6 (2.21) k 56.4 (-) sA 157.7 (1.02) i g 12.0 sA 158.3 (0.94) i	i 151.9 (0.90) sA 8.1 g
11	10/0	81	8.2	1.12	19	g 14.5 k 57.1 (3.45) sA 157.2 (0.90) i g 14.0 sX 44.2 (0.93) sA 156.4 (0.87) i	i 149.4 (0.89) sA 18.9 (0.63) sX 8.8 g

^a overlapped peak

Table II. Cationic Copolymerization of 6-3 with 15-8 (polymerization temperature, 0°C; polymerization solvent, methylene chloride; $[M]_0 = [6-3] + [15-8] = 0.205$ -0.358M; $[M]_0/[I]_0 = 20$; $[(CH_3)_2S]_0/[I]_0 = 10$; polymerization time, 1hr) and Characterization of the Resulting Copolymers. Data on first line are from first heating and cooling scans. Data on second line are from second heating scan.

Sample	[15-8]/[6-3]	Polymer	Mnx10 ⁻³	Mw/Mn	D P	phase transitions (°C) and corresponding enthalpy changes (kcal/mru)	
No.	(mol/mol)	yield(%)	G P C			heating	cooling
1	0/10	87	5.9	1.04	21	g 61.3 sX 68.8 (0.19) n 102.9 (0.12) i g 60.0 n 102.9 (0.10) i	i 97.6 (0.10) n 51.9 g
2	1/9	86	5.4	1.12	18	g 55.1 sX 60.1 (0.44) Ch 96.8 (0.091) i g 53.0 Ch 96.8 (0.11) i	i 91.8 (0.10) Ch 42.3 g
3	2/8	85	5.6	1.14	18	g 43.2 sX 51.4 (0.17) Ch 90.6 (0.98) i g 41.3 Ch 90.1 (0.09) i	i 85.4 (0.10) Ch 37.1 g
4	3/7	83	6.2	1.12	18	g 33.9 sX 39.3 (0.13) sA 106.3 (0.54) i g 31.5 n 105.6 (0.41) i	i 97.8 (0.40) n 26.5 g
5	4/6	69	6.2	1.15	17	g 29.8 k 48.9 (0.37) sA 114.4 (0.65) i g 26.3 sA 114.0 (0.56) i	i 106.3 (0.56) sA 20.8 g
6	5/5	82	6.4	1.11	17	g 23.4 k 48.6 (0.43) sA 116.0 (0.92) i g 21.4 sA 115.3 (0.80) i	i 107.4 (0.80) sA 15.8 g
7	6/4	84	6.7	1.08	17	g 19.4 k 46.5 (0.45) sA 117.4 (1.18) i g 18.2 sA 116.5 (0.95) i	i 108.7 (0.92) sA 12.4 g
8	7/3	78	7.9	1.11	19	g 16.4 k 43.1 (0.05) sA 119.2 (1.19) i g 14.8 sA 118.7 (1.01) i	i 109.9 (1.00) sA 10.3 g
9	8/2	77	7.8	1.10	18	g 15.0 sX 23.9 (0.04) sC* 64.1 (0.04) sA 114.5 (1.15) i g 14.1 sX 37.4 (0.06) sC* 64.3 (0.05) sA 113.0 (1.00) i	i 104.9 (1.01) sA 59.9 (0.05) sC* 9.5 g
10	9/1	77	9.5	1.10	20	g 16.2 sX 40.7 (0.14) sC* 88.2 (0.09) sA 114.3 (1.16) i g 14.1 sX 37.4 (0.06) sC* 88.1 (0.11) sA 113.2 (0.99) i	i 105.5 (0.99) sA 83.8 sC* (0.13) 28.3 (0.07) sX 9.95 g
11	10/0	77	8.6	1.08	18	g 16.7 sX 55.2 (0.13) sC* 93.4 (0.17) sA 104.7 (1.10) i g 16.1 sX 53.7 (0.13) sC* 92.1 (0.15) sA 103.7 (0.96) i	i 95.7 (0.93) sA 86.3 (0.14) sC* 45.9 (0.12) sX 13.6 g

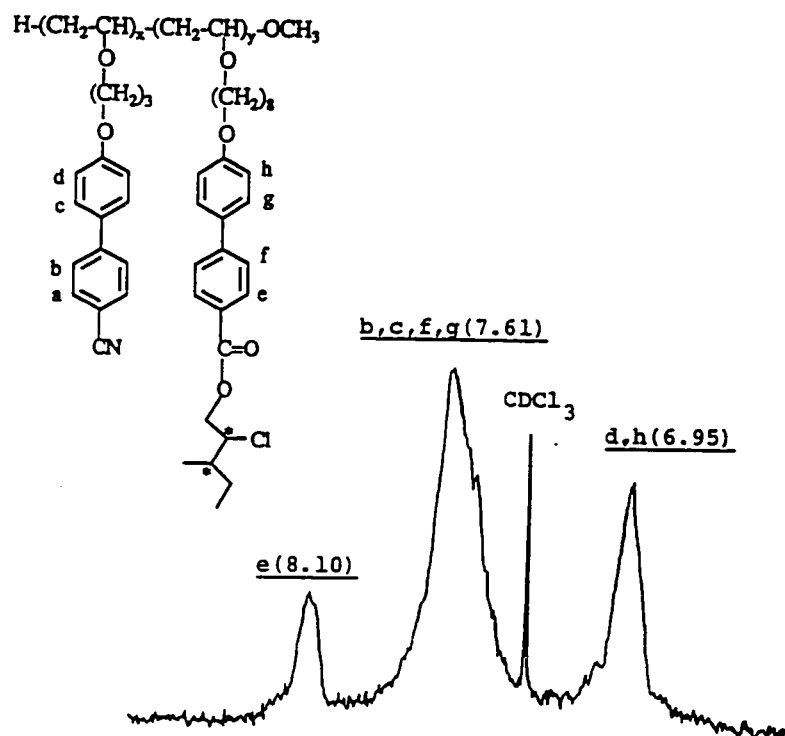


Figure 1. The aromatic region of the 200 MHz ^1H -NMR spectrum of poly[(15-8)-co-(6-3)]5/5.

The synthesis and characterization of poly[(6-11)-co-(15-8)]X/Y copolymers are summarized in Table I. The first and the second heating, and the first cooling DSC traces of all polymers and copolymers are presented in Figure 2a-c. As determined from the first DSC heating scans, poly(6-11)^{16a} with a degree of polymerization of 19 exhibits an enantitropic s_A mesophase and a crystalline melting. When the phase behavior of the same poly(6-11) is determined from the second and subsequent heating DSC scans, it exhibits enantitropic s_A and s_X (unidentified smectic) mesophases. Regardless of the thermal history of the sample, poly(15-8)^{20c} with a degree of polymerization of 18 exhibits enantitropic s_A , s_C^* and s_X mesophases (Figure 2a-c).

Let us first investigate the phase behavior of poly[(6-11)-co-(15-8)]X/Y as obtained from the first heating DSC scans (Figure 2a). The nature of the mesophase displayed by various copolymers is presented on this figure. Upon copolymerization, the temperature associated with the s_A -isotropic phase transition increases and therefore, the s_A mesophase exhibits a continuous dependence of composition with an upward curvature as clearly observed from their DSC traces (Figure 2a). That is, the structural units of both poly(6-11) and poly(15-8) are isomorphic within the s_A phase over the entire range of copolymer compositions.²⁶ However, this dependence shows a non-ideal solution like behavior since there is a significant deviation from what is expected for the same dependence predicted by the Schroeder-van Laar equation for an ideal solution resulting from the structural units of this copolymer (Figure 3b).²¹ All poly[(6-11)-co-(15-8)]X/Y copolymers exhibit a crystalline phase, while copolymers with X/Y=6/4 to 9/1 exhibit an induced s_X phase. Both the ability to obtain copolymers exhibiting a s_A mesophase with enhanced thermal stability and an induced smectic phase from structural units derived from two homopolymers which both display a s_A phase are interesting results for which do not have a definitive explanation.

However, the following speculative explanation is suggested. The new s_X mesophase may result because these copolymers contains strong polar cyano and less polar chiral alkyl groups. It is well known from studies of low molar mass liquid crystals that the mixture of strong polar and less polar mesogens may induce a smectic mesophase or/and enhance the thermal stability of the smectic mesophase.²⁷⁻³² We can speculate that polar cyano groups form the antiparallel associations between polar molecules with overlapped aromatic rings, while less polar chiral alkyl groups form a smectic structure with monomolecular layers. Therefore, upon copolymerization, dipolar associations of polar mesogens will rapidly collapse and the layer spacing decreases down to the line corresponding to what would be expected for a monomolecular layer. Consequently, both structural units will form denser packing upon copolymerization. Morphological experiments are required to support this speculative explanation.

However, upon copolymerization, the chiral smectic C and s_X phases of poly(15-8) are suppressed up to copolymer compositions of $X/Y=1/9$ and $X/Y=2/8$, respectively. Figure 3a plots the phase transitions from the first heating DSC scan as a function of copolymer composition. As we can observe from Figure 3a, the s_A phase shows a continuous dependence of composition with an upward curvature. In the second DSC heating scan (Figure 2b), the s_A mesophase exhibits again a continuous dependence with an upward curvature. However, copolymers with $X/Y=2/8$ to $X/Y=7/3$ exhibit an induced crystalline phase, while copolymers with $X/Y=4/6$ to $X/Y=8/2$ an induced enantiotropic s_X phase. Nevertheless, the transition temperatures associated with s_X and s_C^* phases of poly(15-8), and with the s_X phase of poly(6-11) decrease upon copolymerization. The cooling DSC traces of these copolymers are similar to those of the second DSC heating scans (Figure 2b,c). The data collected from

the second heating DSC scans and the first cooling scans are plotted in Figure 3c,d. Figure 3e plots the dependence of the enthalpy change associated with the s_A -i phase transition from first and second heating DSC scans and i- s_A phase transition from first cooling scan as a function of copolymer composition. This plot also shows the continuous character of the dependence of the enthalpy change associated with this phase transition versus copolymer composition.

These experimental results provide information on the isomorphism of two monomeric structural units derived from two different mesogens and spacer lengths within a smectic A phase. In contrast to binary copolymers based on structural units containing the same mesogen but different spacer lengths which are isomorphic within the same mesogen and behave as an ideal solution derived from the two structural units, structural units based on dissimilar mesogens are isomorphic but behave as a non-ideal solution.

9.3.2.-Poly[(15-8)-co-(6-3)]X/Y

This copolymer is synthesized from a pair of monomers whose parent homopolymers exhibit different mesophases before isotropization, that is, the highest temperature mesophase of poly(15-8)^{20c} is s_A , while that of poly(6-3)^{16b} is nematic. In addition, it is expected that this copolymer will generate, at a certain composition, also a cholesteric mesophase since poly(15-8) contains a chiral moiety. The synthesis and characterization of the copolymers poly[(15-8)-co-(6-3)]X/Y are presented in Table II.

Let us first discuss the phase behavior obtained from the first DSC heating scans (Figure 4a). The s_X phase of poly(6-3) shows a linear dependence up to a value of $X/Y=3/7$. As expected, a cholesteric mesophase was induced in copolymers with $X/Y=1/9$ and $2/8$. Copolymers with $X/Y=4/6$ to $6/4$ exhibit the s_A and an induced

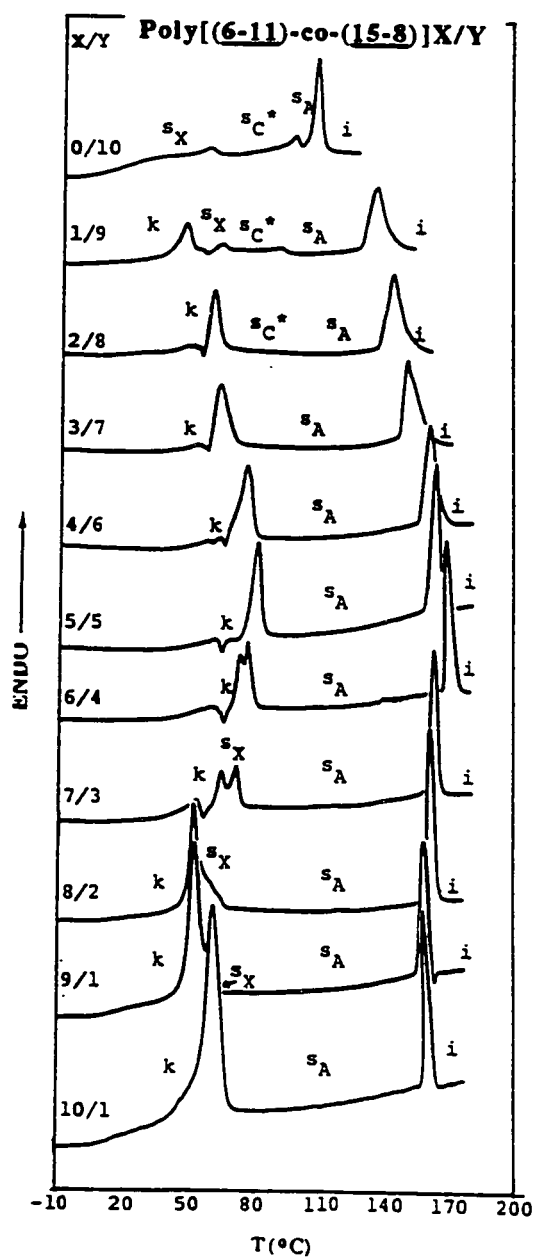


Figure 2a. DSC traces displayed during the first heating scan of poly(6-11), poly(15-8) and of $[\text{poly}(6-11)\text{-co-}(15-8)]X/Y$.

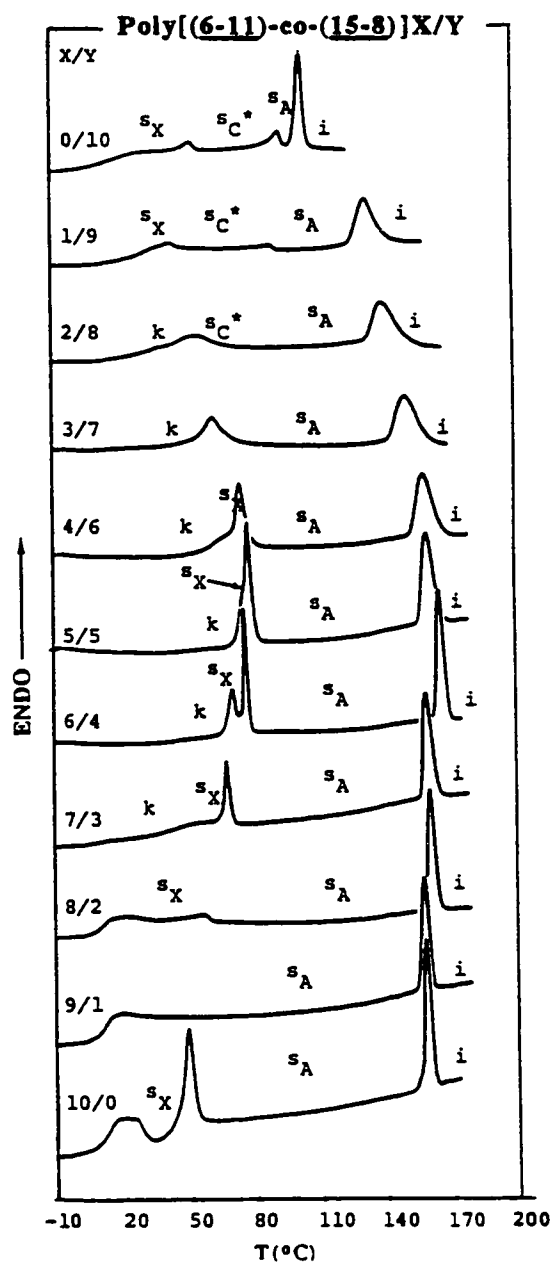


Figure 2b. DSC traces displayed during the second heating scan of poly(6-11), poly(15-8) and of [poly(6-11)-co-(15-8)]X/Y.

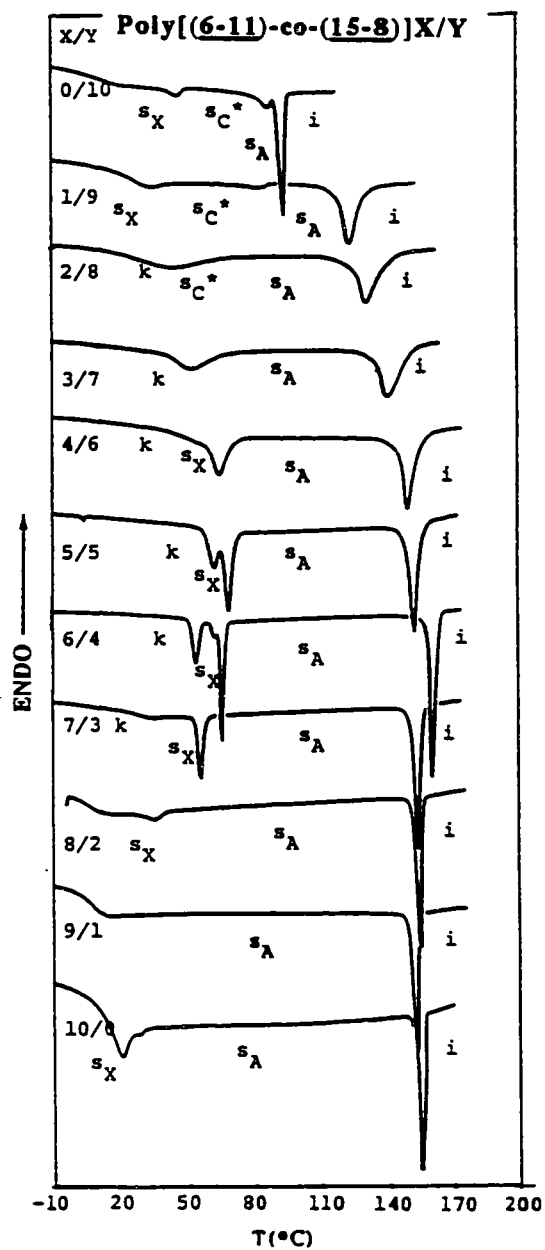


Figure 2c. DSC traces displayed during the first cooling scan of poly(6-11), poly(15-8) and of [poly(6-11)-co-(15-8)]X/Y.

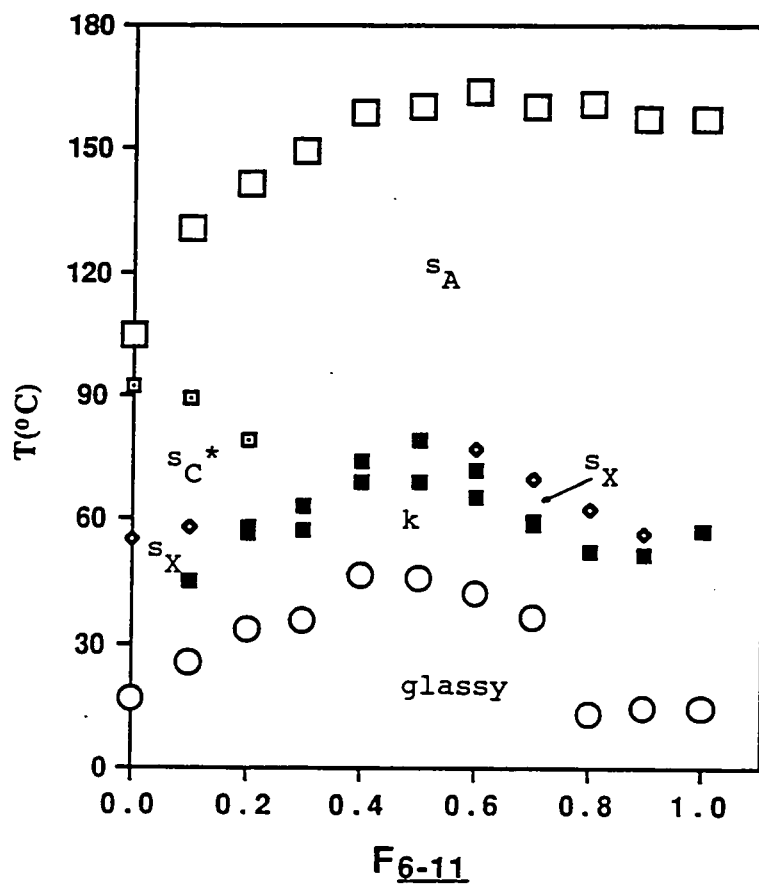


Figure 3a. The dependence of phase transition temperatures on the composition of [poly(6-11)-co-(15-8)]X/Y copolymers (data from first heating scan): \circ - T_g ; \blacksquare - T_k ; \diamond - $T_{sX-SA(SC^*)}$; \square - T_{sC^*-SA} ; \blacksquare - T_{sA-i} ;

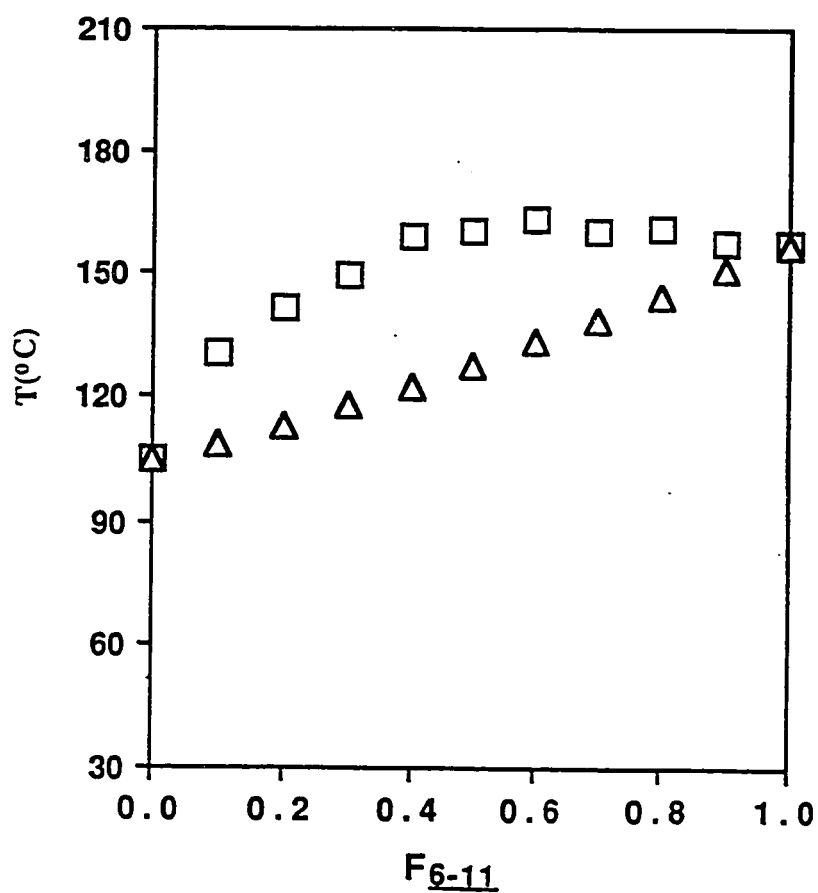


Figure 3b. The dependence of s_A -n and s_A -i phase transition temperatures on composition of poly[(6-11)-co-(6-5)]X/Y: (Δ) data calculated by Schroeder-van Laar equation; (\square) experimental data from the first heating scan

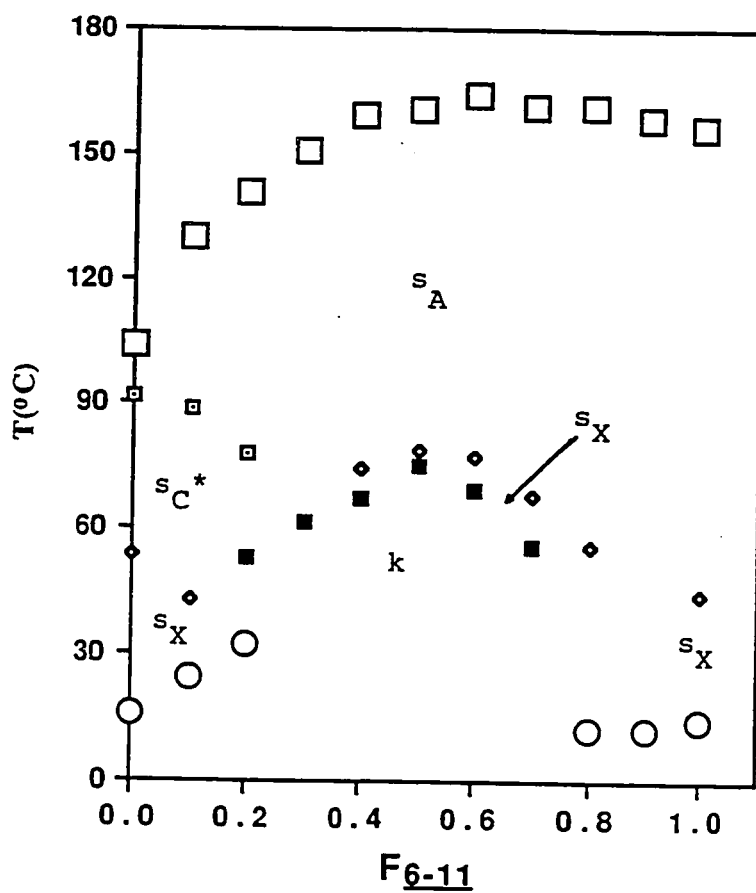


Figure 3c. The dependence of phase transition temperatures on the composition of [poly(6-11)-co-(15-8)]X/Y copolymers (data from second heating scan):
 O - T_g ; ■ - T_k ; ◊ - $T_{sX-SA}(s_C^*)$; ◻ - $T_{sC^*-s_A}$; □ - T_{s_A-i}

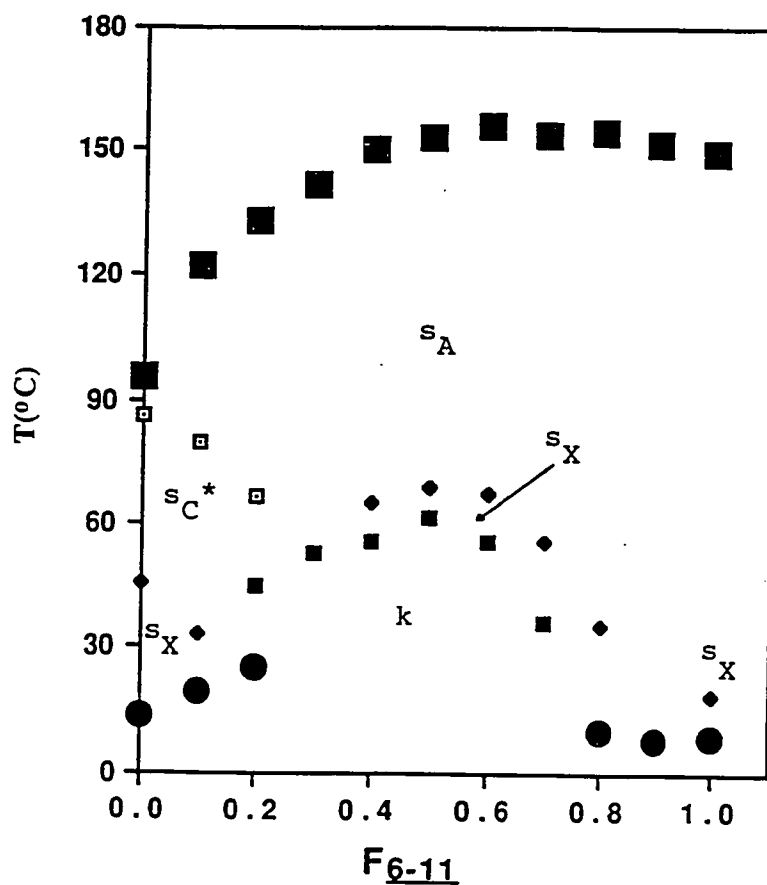


Figure 3d. The dependence of phase transition temperatures on the composition of [poly(6-11)-co-(15-8)]X/Y copolymers (data from first cooling scan): ● -T_g; ■ -T_k; ◆ -T_{sA}(s_{C*})-s_X; □ -T_{sA}-s_{C*}; ■ -T_{i-sA}

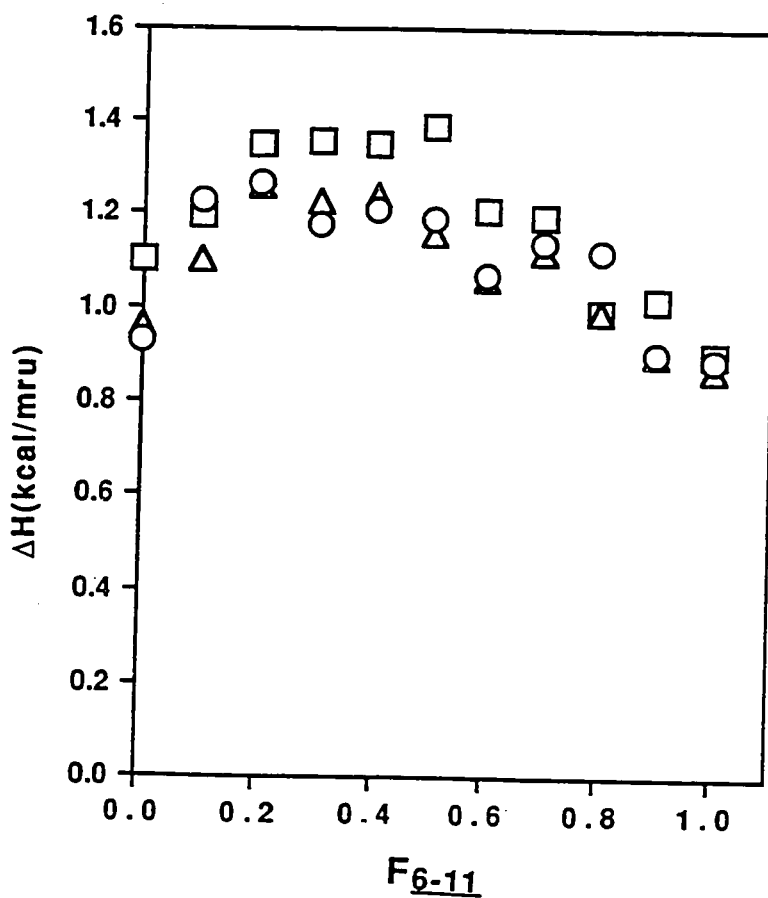


Figure 3e. The dependence of the enthalpy changes associated with the mesomorphic-isotropic and isotropic-mesomorphic phase transitions on the composition of [poly(6-11)-co-(15-8)]X/Y: □- ΔH_{s_A-i} (data from first heating scan); Δ- ΔH_{s_A-i} (data from second heating scan); ○- ΔH_{i-s_A} (data from first cooling scan)

crystalline phase, while copolymers with $X/Y=7/3$ to $10/0$ exhibit the s_A , s_C^* and s_X mesophases. The interest in these copolymers has arisen from their propensity to form cholesteric mesophase. It is well established that copolymerization of a monomer pair based on a monomer containing a chiral group with a monomer whose parent homopolymer exhibits a nematic mesophase generates cholesteric copolymers.³³⁻³⁷

Figure 5a plots all the phase transitions from the first heating DSC scans as a function of copolymer composition. As we can observe from Figure 5a, the nematic and cholesteric mesophases show a linear dependence of composition up to a value of $X/Y=2/8$. This indicates that the structural units of both poly(6-3) and poly(15-8) are isomorphic within the nematic and cholesteric phases over a certain range of copolymer compositions. In addition, the smectic A mesophase also shows a continuous character with an upward curvature over a certain range of copolymer composition which represents a similar behavior to that of poly[(6-11)-co-(15-8)] X/Y . In the second heating scan (Figure 4b), the induced crystalline and s_X phases do not appear. This is due to their close proximity to the glass transition temperature of the copolymers. Therefore, these two phases form only when the polymers are precipitated from solution. If the polymer is redissolved and reprecipitated, these phases reappear. However, the s_A , nematic and cholesteric mesophases follow the same trend as the one observed in the first DSC heating scans (Figure 4a). The cooling DSC scans of these copolymers show the same trend as those of the second heating scan (Figure 4b,c). The data collected from the second DSC heating scans and the first cooling scans are plotted in Figure 5b,c. The enthalpy changes associated with the highest temperature mesophase of these copolymers (Table II) are plotted in Figure 5d as a function of copolymer composition. A representative texture of the cholesteric mesophase is presented in Figure 6.

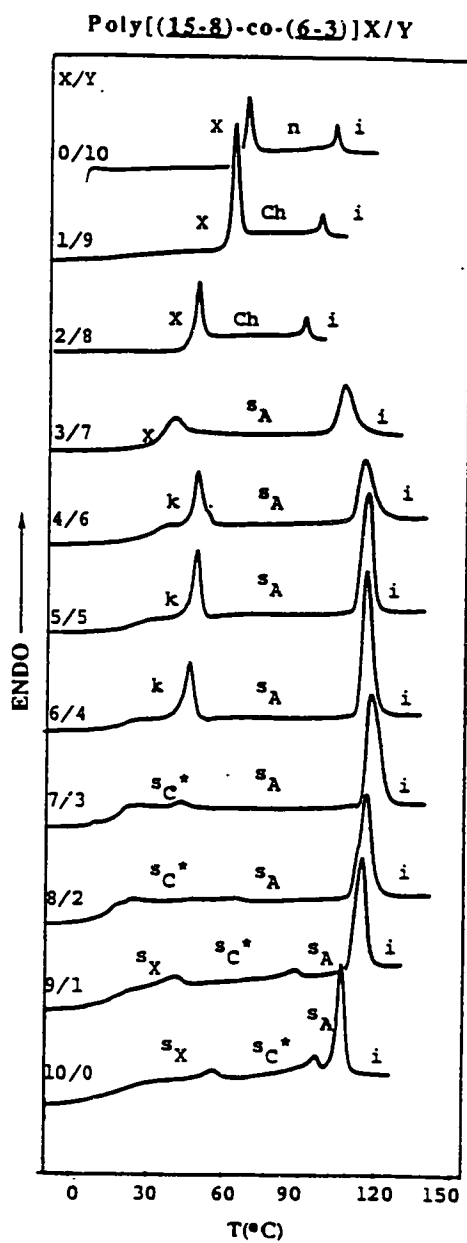


Figure 4a. DSC traces displayed during the first heating scan of poly(15-8), poly(6-3) and of [poly(15-8)-co-(6-3)]X/Y.

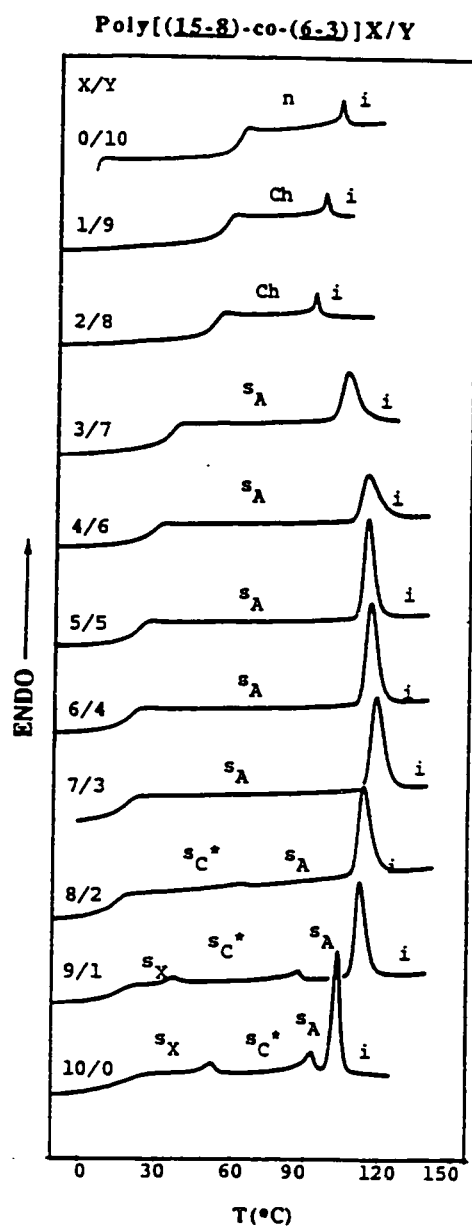


Figure 4b. DSC traces displayed during the second heating scan of poly(15-8), poly(6-3) and of [poly(15-8)-co-(6-3)]X/Y.

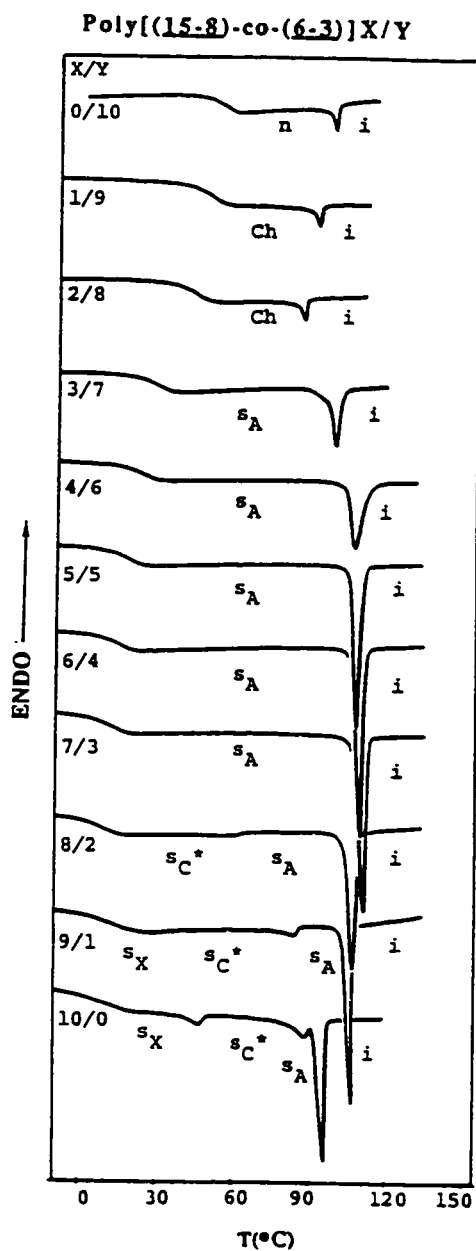


Figure 4c. DSC traces displayed during the first cooling scan of poly(15-8), poly(6-3) and of [poly(15-8)-co-(6-3)]X/Y.

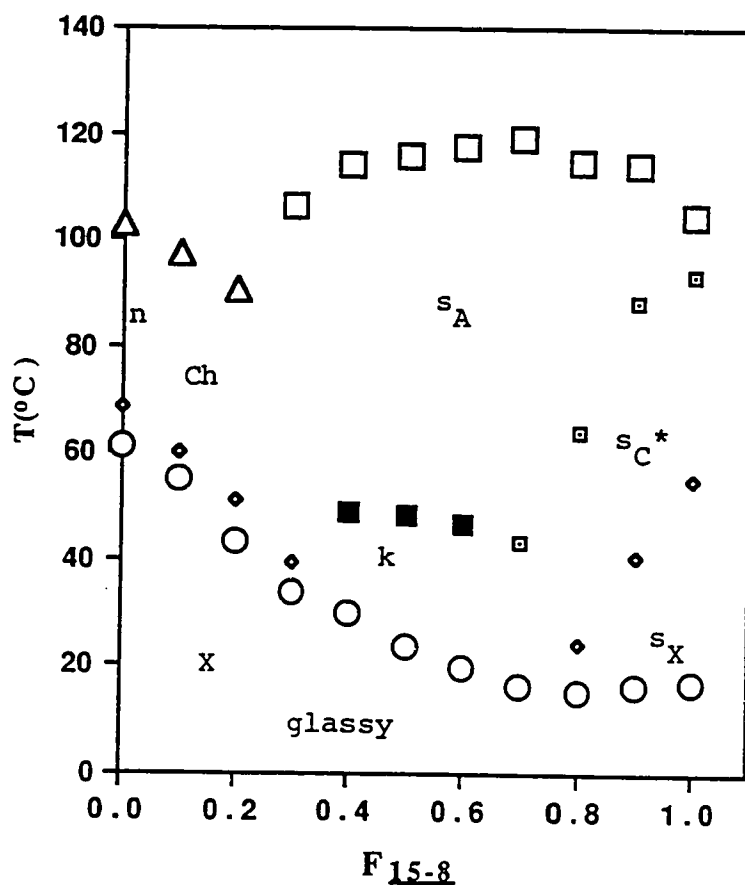


Figure 5a. The dependence of phase transition temperatures on the composition of [poly(15-8)-co-(6-3)]X/Y copolymers (data from first heating scan): O - Tg; ■ - Tk; ◊ - T_{X-n}(Ch); ◈ - T_{sX-sA}(sC*); □ - sC*-sA; ◼ - T_{sA-i}; Δ - T_{n(Ch)-i}

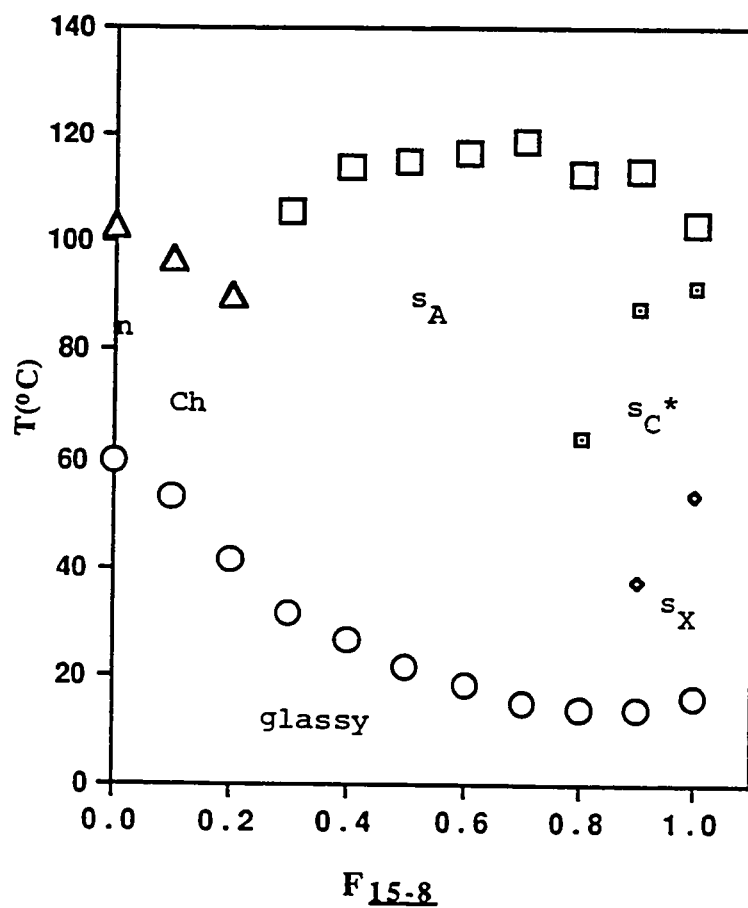


Figure 5b. The dependence of phase transition temperatures on the composition of [poly(15-8)-co-(6-3)]X/Y copolymers (data from second heating scan): O - T_g ; \diamond - $T_{sX-sA(sC^*)}$; \square - $s_{C^*}-s_A$; \square - T_{sA-i} ; Δ - $T_{n(Ch)-i}$

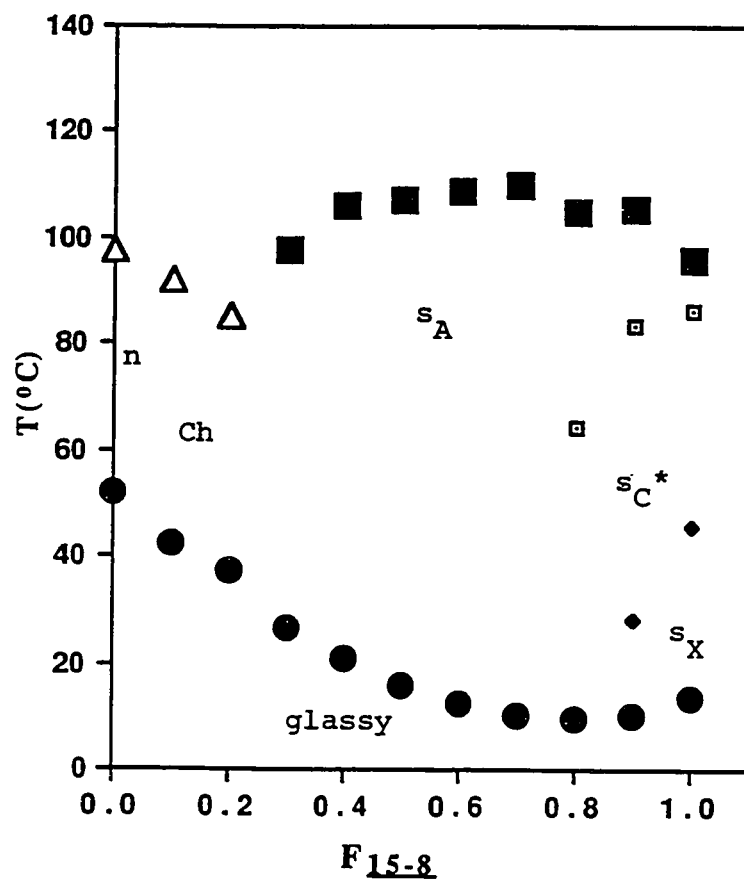


Figure 5c. The dependence of phase transition temperatures on the composition of [poly(15-8)-co-(6-3)]X/Y copolymers (data from first cooling scan): ● -T_g; ◆ -T_{sA(sC*)-sX}; □ -s_A-s_{C*}; ■ -Ti-s_A; Δ -Ti-n(Ch)

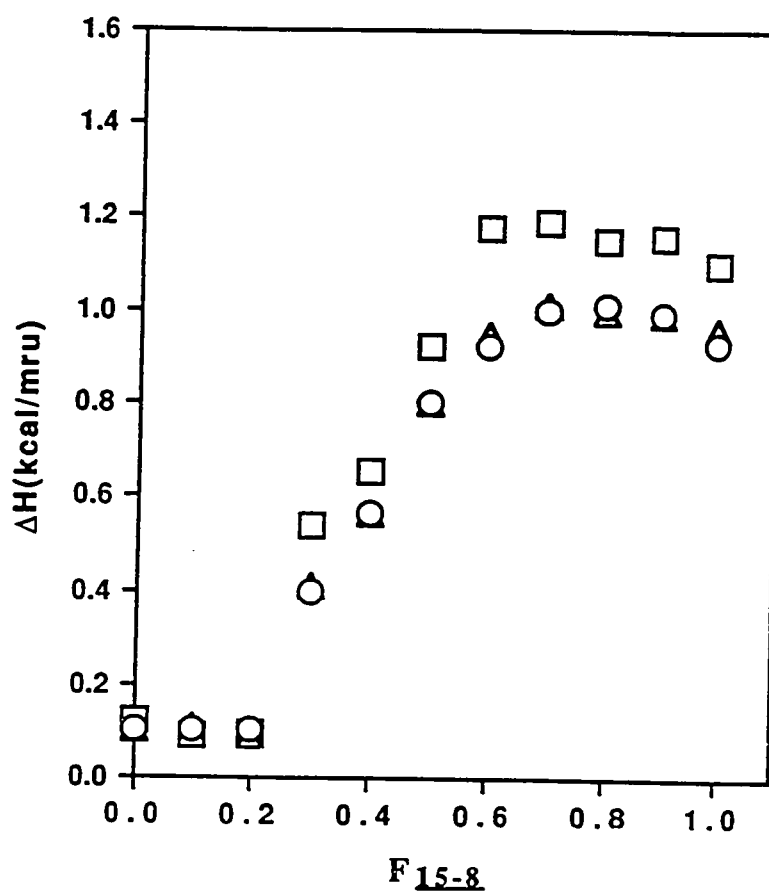


Figure 5d. The dependence of the enthalpy changes associated with the mesomorphic-isotropic and isotropic-mesomorphic phase transitions on the composition of [poly(15-8)-co-(6-3)]X/Y: □-ΔH_{sA-i} (data from first heating scan); Δ-ΔH_{sA-i} (data from second heating scan); O-ΔH_{i-sA} (data from first cooling scan)

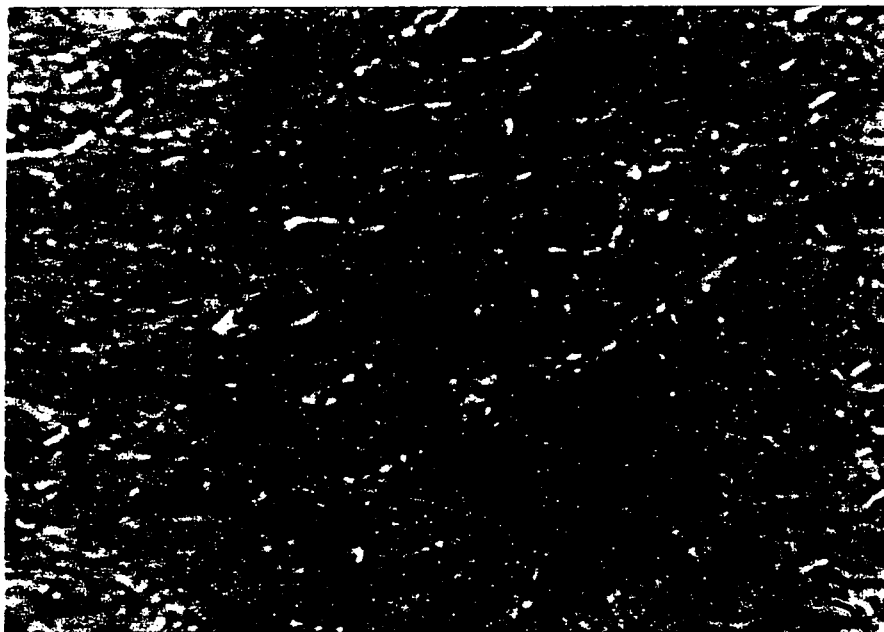


Figure 6. Representative optical polarized micrograph (100x) of: (a) [poly(15-8)-co-(6-3)]8/2 at 85 °C on the cooling scan (cholesteric phase).

The results obtained for the copolymers poly[(15-8)-co-(6-3)]X/Y show that the copolymerization of a monomer containing a chiral group with a monomer whose parent homopolymer exhibits a nematic mesophase provides a simple technique for the synthesis of copolymers exhibiting an enantiotropic cholesteric mesophase and exhibiting an enantiotropic smectic A phase with enhanced thermal stability.

In conclusion, the results described in this chapter have demonstrated that, when two structural units of a copolymer based on dissimilar mesogens are isomorphic within a certain mesophase, the transition temperature and enthalpy change associated with this mesophase show a continuous dependence over the entire range of copolymer composition. However, the dependence of the temperature transitions of this mesophase on copolymer composition, behaves as that of a solution derived from these two structural units which exhibits a non-ideal behavior.

REFERENCES

1. V. P. Shibaev and N. Plate, 1984, *Adv. Polym. Sci.*, **60/61**, 173
2. V. Percec and C. Pugh, in "Side Chain Liquid Crystal Polymers", McArdle, C. B. Ed., Chapman and Hall, New York, 1989, p. 30
3. G. Gray, in "Side Chain Liquid Crystal Polymers", McArdle, C. B. Ed., Chapman and Hall, New York, 1989, p. 106
4. N. A. Plate and V. P. Shibaev, "Comb-Shaped Polymers and Liquid Crystals" Plenum Press, New York, 1987
5. P. A. Gemmell, G. W. Gray and D. Lacey, *Mol. Cryst. Liq. Cryst.*, **122**, 205 (1985)
6. Y. S. Lapatov, V. V. Tsukruk, O. A. Lokhonya, V. C. Shilov, Y. B. Amerik, I. I. Konstantinov and V. S. Grebneva, *Polymer*, **28**, 1370 (1987)
7. H. Ringsdorf, H. W. Schmidt and A. Schneller, *Makromol. Chem., Rapid Commun.*, **3**, 745 (1982)
8. H. Finkelmann, U. Kiechle and G. Rehage, *Mol. Cryst. Liq. Cryst.*, **94**, 343 (1983)
9. G. M. Janini, R. J. Laub and T. J. Shaw, *Makromol. Chem., Rapid Commun.*, **6**, 57 (1985)
10. M. F. Achard, M. Mauzac, H. Richard, G. Sigaud and F. Hardouin, *Eur. Polym. J.*, **25**, 593 (1989)
11. G. W. Gray, W. D. Hawthorne, J. S. Hill, D. Lacey, M. S. K. Lee, G. Nestor and M. S. White, *Polymer*, **30**, 964 (1989)
12. S. G. Kostromin, R. V. Talroze, V. P. Shibaev and N. A. Plate, *Makromol. Chem., Rapid Commun.*, **3**, 803 (1982)
13. Stevens, H.; Rehage, G. and Finkelmann, H., *Macromolecules*, **17**, (1984) 851
14. V. Percec, D. Tomazos and C. Pugh, *Macromolecules*, **22**, 3259 (1989)
15. (a) T. Sagane and R. W. Lenz, *Polym. J.*, **20**, 923 (1988); (b) T. Sagane and R. W. Lenz, *Polymer*, **30**, 2269 (1989); (c) T. Sagane and R. W. Lenz, *Macromolecules*, **22**, 3763 (1989)
16. (a) V. Percec, M. Lee and H. Jonsson, *J. Polym. Sci., Polym. Chem. Ed.*, **29**, 327 (1991); (b) V. Percec and M. Lee, *J. Macromol. Sci.-Chem.*, **A28**, 651 (1991); (c) V. Percec and M. Lee, *Macromolecules*, **24**, 1017 (1991); (d) V.

- Percec and M. Lee, *Macromolecules*, **24**, 2780 (1991); (e) V. Percec, M. Lee and C. Ackerman, *Polymer*, in press
17. S. G. Kostromin, N. G. Cuong, E. S. Garina and V. P. Shibaev, *Mol. Cryst. Liq. Cryst.*, **193**, 77 (1990)
 18. M. Sawamoto, T. Ohtoyo, T. Higashimura, K. H. Guhrs and G. Heublein, *Polym. J.*, **17**, 929 (1985)
 19. (a) V. Percec and M. Lee, *Polym. Bull.*, **25**, 123 (1991); (b) V. Percec and M. Lee, *Polym. Bull.*, **25**, 131 (1991); (c) V. Percec and M. Lee, *Macromolecules*, **24**, 4963 (1991); (d) V. Percec and M. Lee, *Polymer*, **32**, 2862 (1991); (e) V. Percec and M. Lee, *J. Mater. Chem.*, **1**, 1007 (1991)
 20. (a) V. Percec, Q. Zheng and M. Lee, *J. Mater. Chem.*, **1**, 611 (1991); (b) V. Percec, Q. Zheng and M. Lee, *J. Mater. Chem.*, **1**, 1015 (1991); (c) V. Percec and Q. Zheng, *J. Mater. Chem.*, submitted.
 21. G. R. Van Hecke, *J. Phys. Chem.*, **83**, 2344 (1979)
 22. D. Demus and L. Richter, "Textures of Liquid Crystals", Verlag Chemie, Weinheim 1978
 23. G. W. Gray and G. W. Goodby, "Smectic Liquid Crystals. Texture and Structures", Leonard Hill, Glasgow 1984
 24. C. G. Cho, B. A. Feit and O. W. Webster, *Macromolecules*, **23**, 1918 (1990)
 25. C. H. Lin and K. Matyjaszewsky, *Polym. Prepr., Am. Chem. Soc. Div. Polym. Chem.*, **31**(1), 599 (1990)
 26. V. Percec and Y. Tsuda, *Polymer*, **32**, 673 (1991)
 27. M. Marcos, E. Melendez, M. B. Ros and J. L. Serrano, *Mol. Cryst. Liq. Cryst.*, **167**, 239 (1989)
 28. J. W. Park, C. S. Bak and M. M. Labes, *J. Am. Chem. Soc.*, **97**, 4398 (1975)
 29. C. S. Oh, *Mol. Cryst. Liq. Cryst.*, **42**, 1 (1977)
 30. B. Engelen, G. Hepkke, R. Hopf and F. Schneider, *Mol. Cryst. Liq. Cryst.*, **49**, 193 (1979)
 31. B. Engelen and F. Schneider, *Z. Naturforsch.*, **33a**, 1077 (1978)
 32. F. Hardouin, G. Sigaud, P. Keller, H. Richard, H. T. Nguyen, M. Mauzac and M. F. Achard, *Liq. Cryst.*, **5**, 463 (1989)
 33. E. Chiellini and G. Galli, Recent Advances in Liquid Crystalline Polymers, Chapoy, L., Ed., Elsevier Appl. Sci. Publishers, New York 1985

34. S. B. Evance, J. I. Weischenk, A. B. Padias, J. K. Hall and T. M. Leslie, *Mol. Cryst. Liq. Cryst.*, **183**, 361 (1990)
35. V. P. Shibaev, N. A. Plate and Y. S. Freizon, *J. Polym. Sci., Polym. Chem. Ed.*, **17**, 1655 (1979)
36. H. Finkelmann and G. Rehage, *Makromol. Chem., Rapid Commun.*, **1**, 733 (1980)
37. M. A. Maus, Y. S. Freizon, V. P. Shibaev and N. A. Plate, *Polym. Bull.*, **6**, 485 (1982)

PART III. MOLECULAR ENGINEERING OF LIQUID CRYSTAL POLYMERS
BY END FUNCTIONALIZATION AND BLOCK
COPOLYMERIZATION

Chapter 10
SYNTHESIS AND CHARACTERIZATION OF MACROMONOMERS AND
BLOCK COPOLYMERS BASED ON ω -[(4-CYANO-4'-BIPHENYL)OXY]ALKYL
VINYL ETHERS

10.1.1.-INTRODUCTION

In Part I, we have demonstrated that mesogenic vinyl ethers containing various functional groups can be polymerized by a living mechanism and these polymerizations allowed systematic investigations of the molecular weight effect on the phase transitions of the resulting polymers.¹ Binary copolymerization experiments were performed to investigate the influence of copolymer composition on the phase behavior of the copolymers with constant molecular weight. These results were used to tailor make polymers exhibiting nematic, smectic A, reentrant nematic, chiral smectic C, and cholesteric mesophases as described in Part II. In addition, we have demonstrated that a quantitative functionalization of a polymer chain end is possible^{1f} with the initiating system $\text{CF}_3\text{SO}_3\text{H}/\text{S}(\text{CH}_3)_2$ in CH_2Cl_2 .²

There are only few reports on the synthesis of AB block copolymers containing an amorphous A-block and a side chain liquid crystalline B-block.^{3,4} They were prepared by polymer homologous reactions of poly(styrene-*b*-butadiene) A-B block copolymer,³ and respectively by successive living polymerization of methyl methacrylate and a mesogenic methacrylate by group transfer polymerization.⁴ The theoretical interest on AB block copolymers containing liquid crystalline and amorphous segments was discussed in detail by Adams and Gronski.^{3a}

Presently, we are investigating the synthesis and characterization of macromonomers and block copolymers containing side chain liquid crystalline segments by living cationic polymerization. It is well known that the miscibility of

fluorocarbon and hydrocarbon molecules is very poor. As a consequence, fluorocarbon-hydrocarbon compounds are surface active systems and can assemble into aggregates both in nonaqueous solutions and in melt.⁵ Therefore, block copolymerization of mesogenic vinyl ethers with fluorocarbon-substituted vinyl ethers should allow the preparation of polymer materials with new microphase separated morphologies at very low degrees of polymerization of the hydrocarbon and fluorocarbon blocks.

Part A of this chapter will describe the synthesis of poly{3-[4-cyano-4'-biphenyl]oxy}propyl vinyl ether} [poly(6-3)] macromonomers by end capping the corresponding living polymer with 2-hydroxy ethyl methacrylate, 2-[2-(2-allyloxyethoxy)ethoxy]ethanol and 10-undecen-1-ol. Part B of this chapter describes the synthesis and thermal characterization of AB block copolymers based on ω -[(4-cyano-4'-biphenyl)oxy]alkyl vinyl ether (6-n) with alkyl being ethyl (6-2), propyl (6-3), nonyl (6-9) and undecanyl (6-11), and 1H,1H,2H,2H-perfluorodecyl vinyl ether (CF8), and of 2-(4-biphenyloxy)ethyl vinyl ether (BEVE) with 1H,1H,2H,2H-perfluorodecyl vinyl ether.

Part A. Synthesis and Characterization of Poly{3-[4-Cyano-4'-Biphenyl]oxy}propyl Vinyl Ether} Macromonomers.

10.2. EXPERIMENTAL

Scheme I outlines the synthesis of poly(6-3) macromonomers.

10.2.1.-Materials

All materials were commercially available and were used as received or purified as described previously.¹ 2-Hydroxyethyl methacrylate (98%, Aldrich), triethylene

glycol (anhydrous, >97%, Fluka), allyl chloride (98%, Aldrich), 10-undecenoic acid (99%, Aldrich), 2,6-lutidine (99%, Aldrich) and 1H,1H,2H,2H-perfluorodecan-1-ol (Strem Chemical) were used as received. Methyl sulfide (anhydrous, 99%, Aldrich) was refluxed over 9-borabicyclo[3.3.1]nonane (9-BBN, crystalline, 98%, Aldrich) and then distilled under argon. Dichloromethane (99.6%, Aldrich) used as a polymerization solvent was first washed with concentrated sulfuric acid, then with water, dried over anhydrous magnesium sulfate, refluxed over calcium hydride and freshly distilled under argon before each use. Trifluoromethane sulfonic acid (triflic acid, 98%, Aldrich) was distilled under argon.

10.2.2.-Synthesis of Monomers

3-[(4-Cyano-4'-biphenyl)oxy]propyl vinyl ether (6-3) with a purity higher than 99% (HPLC) was synthesized according to a previous publication.^{1b}

Synthesis of 10-Undecen-1-ol

10-Undecen-1-ol was synthesized by the reduction of 10-undecenoic acid with LiAlH₄ in dry THF and was purified by vacuum distillation (bp 132-133°C/15mm).⁶

Synthesis of 2-[2-(2-Allyloxyethoxy)ethoxy]ethanol

2-[2-(2-Allyloxyethoxy)ethoxy]ethanol was synthesized according to a modified literature procedure.⁷ Its detailed synthesis and characterization will be described elsewhere.⁸

10.2.3.-Polymerizations

Polymerizations were carried out in glass flasks equipped with teflon stopcocks and rubber septa under argon atmosphere at 0°C for 40 min. All glassware was dried overnight at 180°C. The 3-[4-cyano-4'-biphenyl)oxy]propyl vinyl ether (6-3) (0.4 g,

1.43 mmol) was further dried under vacuum overnight in the polymerization flask. After the flask was filled with argon, freshly distilled dry methylene chloride (4 ml) was added through a syringe and the solution was cooled to 0°C. Dimethyl sulfide (0.18 ml, 2.4 mmol) and triflic acid (21 μ l, 0.24 mmol) were then added via a syringe. After 40 min, 0.3 ml (2.4 mmol) of 2-hydroxy ethyl methacrylate was added followed by 0.1 ml of 2,6-lutidine. The cooling bath was removed and the mixture was allowed to warm up to room temperature. After 1 hr, the reaction mixture was precipitated into methanol. The filtered polymer was dried and precipitated from methylene chloride solution into methanol. The polymerization results are summarized in Table 1.

10.3.-RESULTS AND DISCUSSIONS

3-[4-Cyano-4'-biphenyl]propyl vinyl ether (6-3) was polymerized by initiation with $\text{CF}_3\text{SO}_3\text{H}/\text{S}(\text{CH}_3)_2$ in methylene chloride at 0°C. After 40 min a hydroxy end capping agent containing a double bond and 2,6-lutidine as proton scavenger were introduced into the solution to quench the polymerization. The reaction scheme is outlined in Scheme I. Figure 1 shows GPC traces of poly(6-3)s containing various end groups. These polymers show a very narrow molecular weight distributions and their molecular weights can be controlled by the ratio of $[\text{M}]_0/[\text{I}]_0$ (Table 1). The end group structure of these polymers was determined by $^1\text{H-NMR}$. Figure 2 shows the $^1\text{H-NMR}$ spectrum of 2-hydroxy ethyl methacrylate terminated poly(6-3) [poly(6-3)-I], Figure 3 presents the $^1\text{H-NMR}$ spectrum of 10-undecene-1-ol terminated poly(6-3) [poly(6-3)-II] and Figure 4 displays the $^1\text{H-NMR}$ spectrum of 2-[2-(2-allyloxyethoxy)ethoxy]ethanol terminated poly(6-3) [poly(6-3)-III]. The assignment of protonic resonances are also provided on these figures. The resonances of the expected unsaturated end-groups which are formed by quenching the living chain end with these

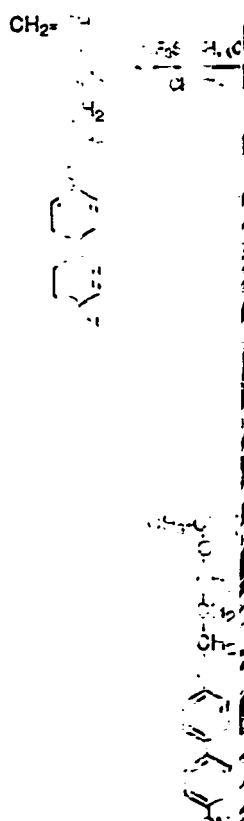
three end capping agents can be easily observed in all cases. In addition, end capping with hydroxy groups lead to acetal containing end groups which are characterized as signal k (Figures 2,3,4). The signals due to aromatic proton (signal d) and acetal proton (signal k) were integrated. The calculated degrees of polymerization are close to the theoretical one, i.e., $[M]_0/[I]_0=6.0$. The number of functional end-groups in each polymer chain was determined by measuring the integral ratio between the resonances which are corresponded to $=CH_2$ (signal p) and acetal proton (signal k), (Table 1). According to the NMR spectrum, the polymer chains are quantitatively end capped with an unsaturated functional group. These results demonstrate that the initiating system $CF_3SO_3H/(CH_3)_2S$ allows the preparation of poly(6-3) with well defined functional chain-ends.

The thermal characterization of poly(6-3) macromonomers by DSC is presented in Figure 5. All these macromonomers exhibit an enantiotropic nematic mesophase (Table 2, Figure 5). The thermal behavior of the macromonomers is similar to that of poly(6-3).⁶ However, the phase transition temperatures of poly(6-3)-II and III decrease by comparison to that of poly(6-3).

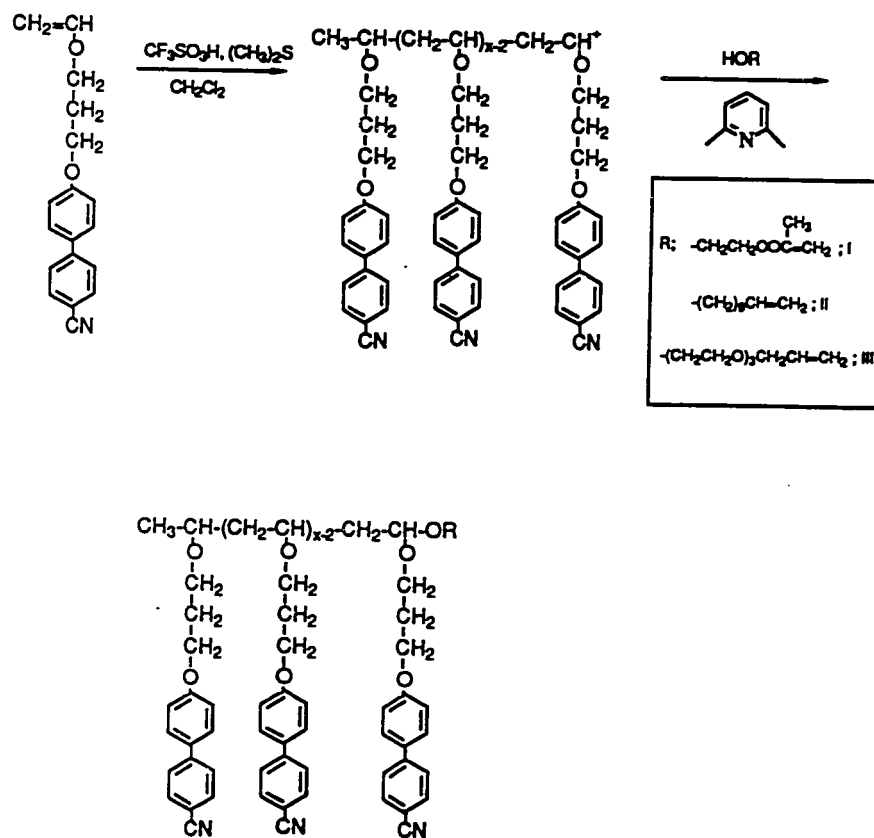
In conclusion, these experiments have demonstrated that the initiating system $CF_3SO_3H/(CH_3)_2S$ can be used in the synthesis of mesogenic macromonomers.

Table 1. Synthesis of Poly{3-[(4-Cyano-4'-biphenyl)oxy]propyl Vinyl Ether} Macromonomers

Sample No.	$[M]_0/[I]_0$	end capping agent	yield (%)	Mn theor.	Mn (GPC)	Mw/Mn	integration ratio p/k	DP (NMR)	Function-ality
1	6.0	I	82	1790	1600	1.09	1.92	5.5	0.96
2	6.0	II	80	1830	1800	1.11	2.08	5.2	1.04
3	6.0	III	78	1940	1800	1.13	2.06	6.8	1.03



Scheme 1 synthesis of



Scheme I. Synthesis of Macromonomers

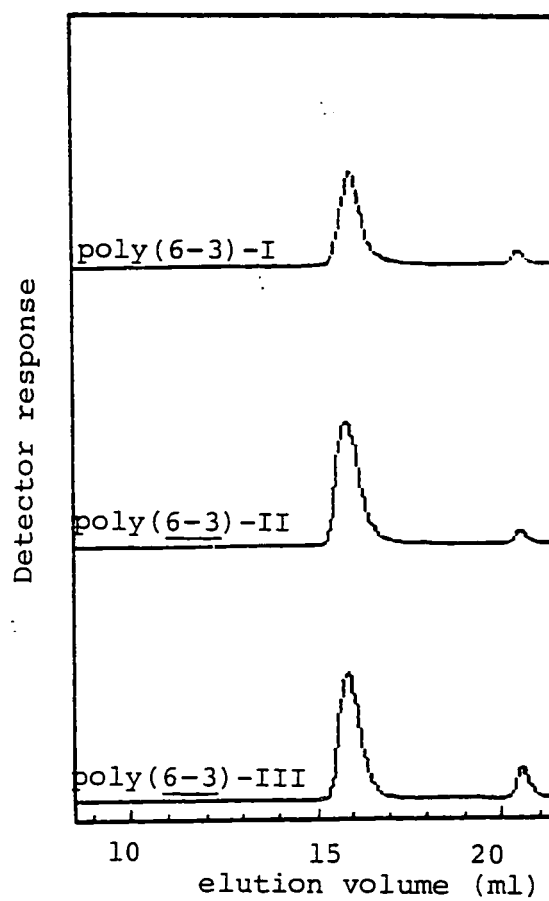


Figure 1. GPC traces of (A) poly(6-3)-I, (B) poly(6-3)-II and (C) poly(6-3)-III

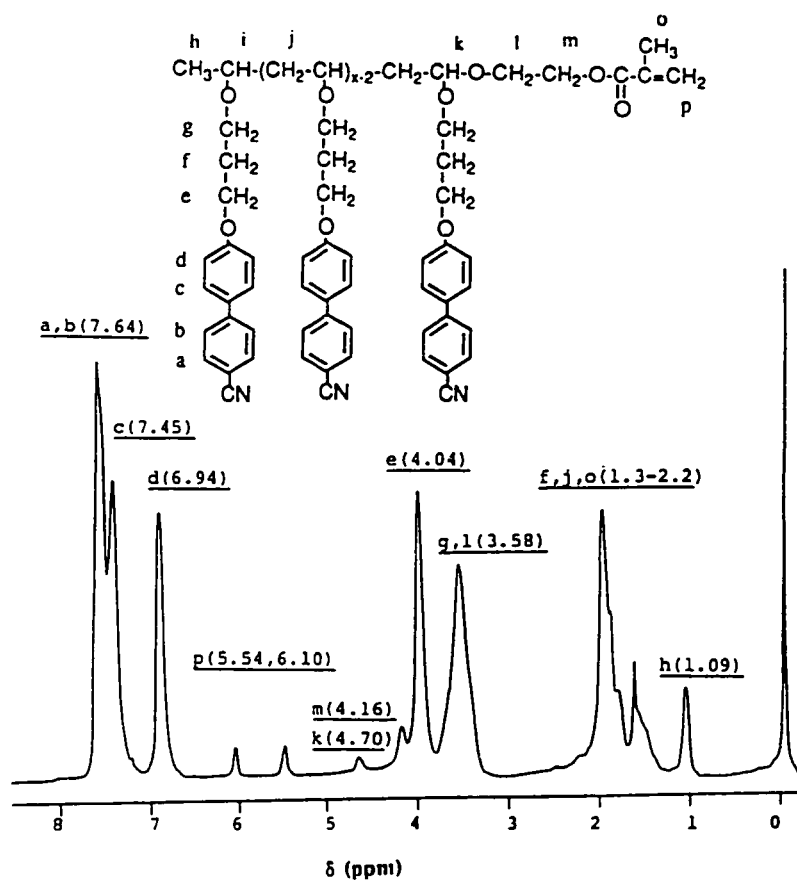


Figure 2. 200 MHz ^1H -NMR spectrum of poly(6-3)-I.

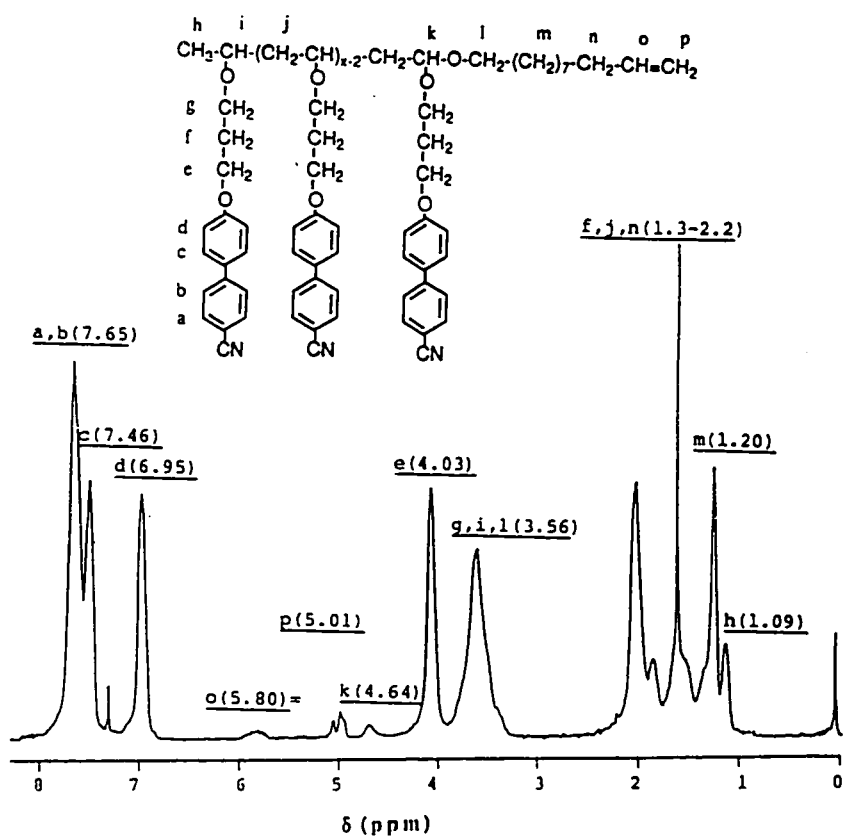


Figure 3. 200 MHz ¹H-NMR spectrum of poly(6-3)-II.

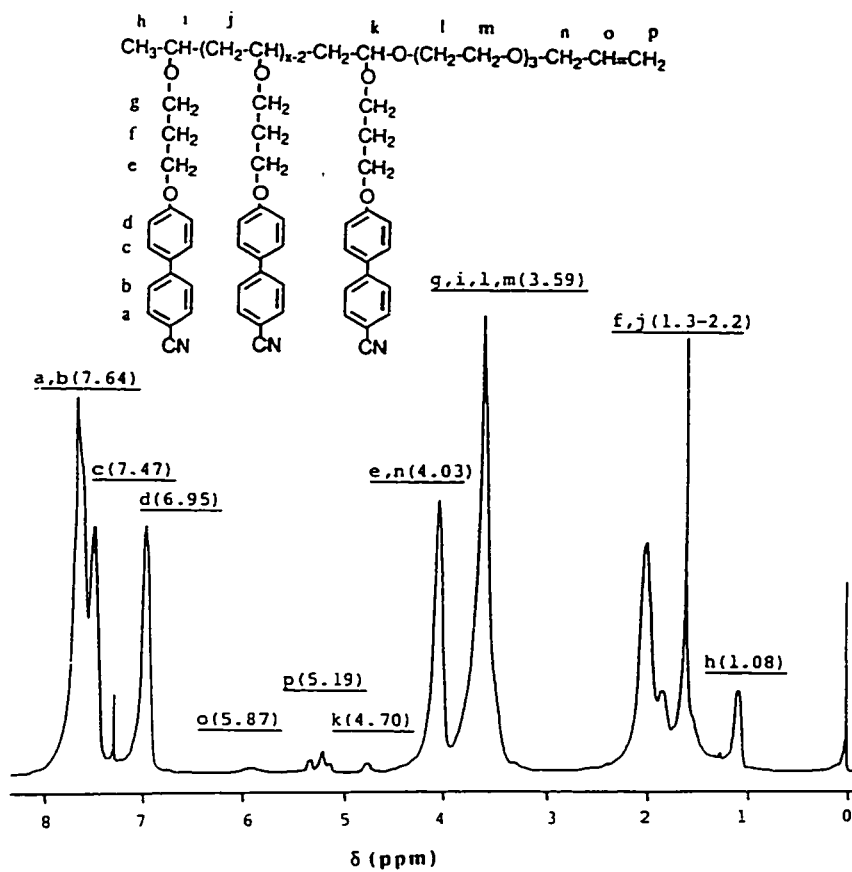
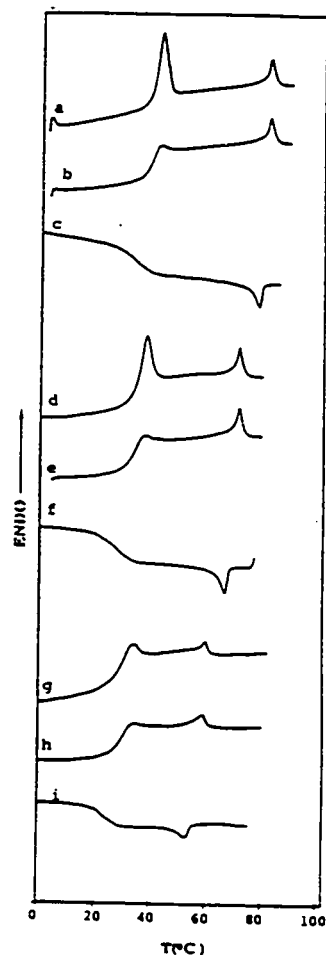


Figure 4. 200 MHz ¹H-NMR spectrum of poly(6-3)-III.

Table 2. Thermal Transitions and Their Corresponding Thermodynamic Parameters of the Macromonomers of Poly(6-3)

Macromonomer	phase transitions (°C) and corresponding enthalpy changes (kcal/mru)			
	heating		cooling	
poly(6-3)-I	g 36.2 X 42.5 (0.23) i (0.076)	n 81.1	i 75.7 (0.089) n 24.9 g	
poly(6-3)-II	g 35.9 n 80.4 (0.081) i			
	g 33.5 X 38.3 (0.17) i (0.082)	n 71.6	i 66.6 (0.088) n 25.8 g	
poly(6-3)-III	g 32.0 n 71.4 (0.090) i			
	g 25.8 X 33.6 (0.074) i (0.055)	n 59.1	i 53.0 (0.085) n 22.7 g	
	g 26.9 n 58.9 (0.066) i			

Figure 5. The DSC scans (20 °C/min) of poly(6-3)-I: (a) first heating scan, (b) second heating scan, (c) first cooling scan; of poly(6-3)-II: (d) first heating scan, (e) second heating scan, (f) first cooling scan; and of poly(6-3)-III: (d) first heating scan, (e) second heating scan, (f) first cooling scan



Part B: Synthesis and Characterization of AB Block Copolymers Based on ω -[4-cyano-4'-biphenyl]oxyalkyl Vinyl Ether, and 1H,1H,2H,2H-Perfluorodecyl Vinyl Ether, and of 2-(4-Biphenyloxy)ethyl Vinyl Ether with 1H,1H,2H,2H-Perfluorodecyl Vinyl Ether.

10.4.-EXPERIMENTAL

10.4.1.-Materials

Methyl sulfide (anhydrous, 99%, Aldrich) was refluxed over 9-borabicyclo[3.3.1]nonane (crystalline, 98%, Aldrich) and then distilled under argon. Dichloromethane (99.6%, Aldrich) used as polymerization solvent was first washed with concentrated sulfuric acid, then with water, dried over magnesium sulfate, refluxed over calcium hydride and freshly distilled under argon before each use. Trifluoromethane sulfonic acid (triflic acid, 98%, Aldrich) was distilled under vacuum. 1H,1H,2H,2H-Perfluorodecan-1-ol (Strem Chemicals, mp; 40-43 °C) was used as received.

10.4.2.-Techniques

¹H-NMR spectra were recorded on a Varian XL-300 spectrometer and Varian XL-200 spectrometer. TMS was used as internal standard.

10.4.3.-Synthesis of Monomers

2-[(4-Cyano-4'-biphenyl)oxy]ethyl vinyl ether (6-2),^{1b} 3-[(4-cyano-4'-biphenyl)oxy]propyl vinyl ether (6-3),^{1b} 9-[(4-cyano-4'-biphenyl)oxy]nonyl vinyl ether (6-9),^{1d} 11-[(4-cyano-4'-biphenyl)oxy]undecanyl vinyl ether (6-11),^{1a} 2-(4-biphenyloxy)ethyl vinyl ether (BEVE)^{1g} and 1H,1H,2H,2H-perfluorodecyl vinyl ether (CF8)⁹ were synthesized as described previously. Additional details for the synthesis of CF8 are presented below.

Synthesis of 1H,1H,2H,2H-Perfluorodecanyl vinyl ether (CF8).

1H,1H,2H,2H-Perfluorodecan-1-ol (14 g, 0.03 mol) was added to a mixture of 100 ml of n-butyl vinyl ether, 100 ml of chloroform, and 1,10-phenanthroline palladium(II) diacetate^{1a} (0.8 g, 2 mmol) and kept under argon. The yellow mixture slowly turned green while it was refluxed for 12h. After filtration, the solvent was removed in a rotary evaporator. The crude product was purified by column chromatography (silica gel, CH₂Cl₂ eluent) and then extracted with MeOH to remove residual n-butyl vinyl ether. The obtained product (yield 12 g, 74 %) was then dried over CaH₂ and freshly distilled under vacuum before each use. Purity: >99% (GC); bp: 71 °C (3 mm); 200MHz ¹H-NMR (CDCl₃, TMS, δ, ppm): 2.51 (2 protons, -CF₂-CH₂-, t), 4.00 (2 protons, -CH₂O-, t), 4.10 (1 proton, OCH=CH₂ trans, d), 4.23 (1 proton, OCH=CH₂ cis, d), 6.47 (1 proton, CH₂=CHO-, q).

10.4.4.-Synthesis of block copolymers

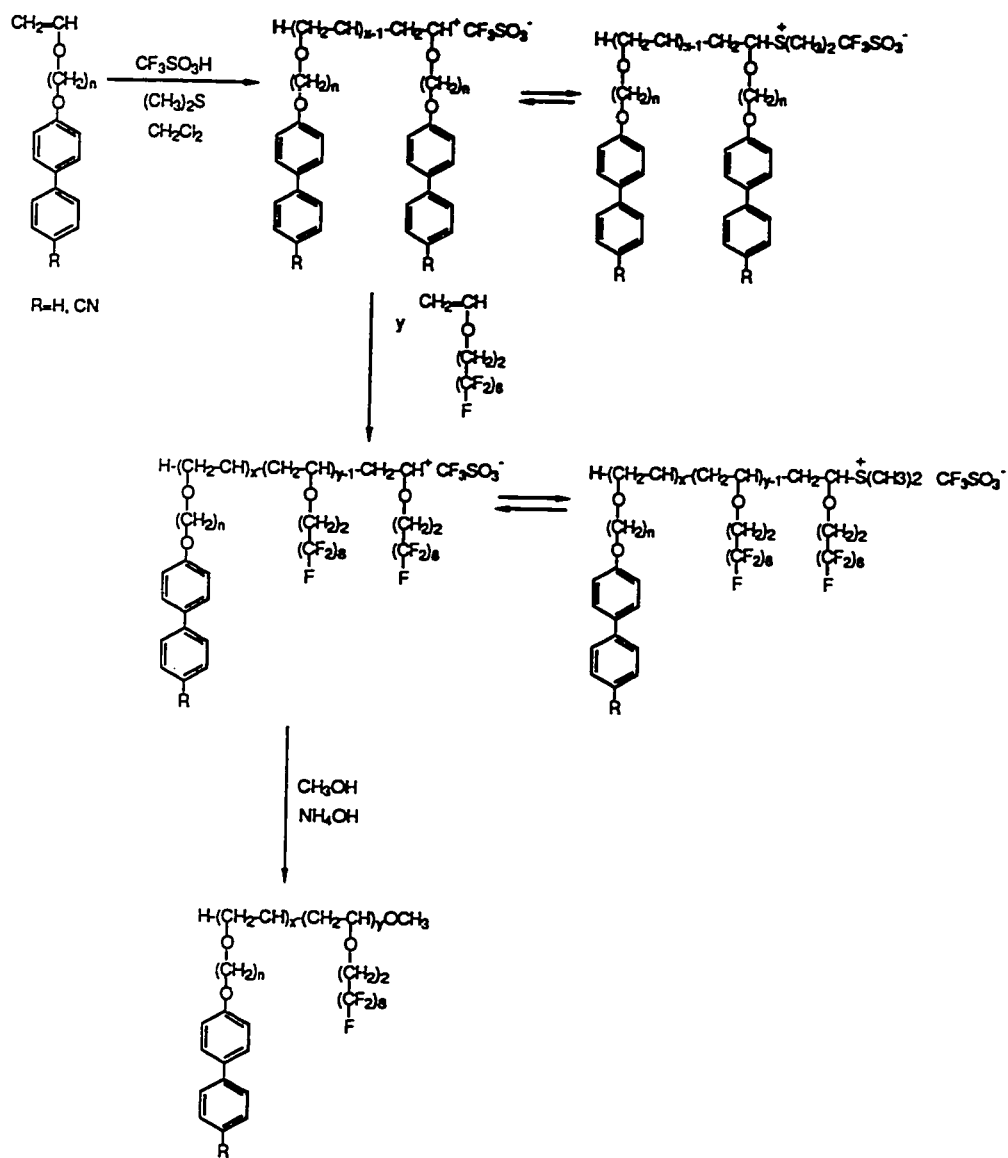
The synthesis of block copolymers was carried out in glass flasks equipped with teflon stopcocks and rubber septa under argon atmosphere at 0°C by sequentially polymerizing first the mesogenic vinyl ether and then CF8. All glassware was dried overnight at 130°C. The monomer was further dried under vacuum overnight in the polymerization flask. Then the flask was filled with argon, cooled to 0°C and the methylene chloride, dimethyl sulfide and triflic acid were added via a syringe. The first monomer concentration was about 10 wt% of the solvent volume and the dimethyl sulfide concentration was 20 times larger than that of the initiator. After 40 min of reaction time, when the polymerization of the first monomer had reached about 100% conversion, freshly distilled CF8 was injected into the polymerization solution. After two more hours, the polymerization was quenched with ammoniacal methanol. The

reaction mixture was then precipitated into methanol. The filtered polymers were dried and precipitated from methylene chloride solutions into methanol (two or three times) until GPC traces showed no traces of unreacted monomer. Tables III summarizes the polymerization results.

10.5.-RESULTS AND DISCUSSION

The mesogenic vinyl ethers, 6-n and BEVE were polymerized by initiation with $\text{CF}_3\text{SO}_3\text{H}/\text{S}(\text{CH}_3)_2$ in methylene chloride at 0°C .² After 40 min, CF8 was injected into the polymerization solution as a second monomer. The synthesis of block copolymers is outlined in Scheme II. Figure 6 shows typical GPC traces of poly(6-2) and of the resulting block copolymer. The polymerization of mesogenic vinyl ether had reached almost quantitative conversion in 40 min to produce the homopolymer with controlled molecular weight and narrow molecular weight distribution (Table III, Figure 6b). Subsequent sequential addition of CF8, led to block copolymers with a monomodal, narrow molecular weight distribution which however, was slightly broader than that of the parent mesomorphic homopolymers (Table III, Figure 6a). This sequence of polymerization was selected since poly(CF8) is insoluble in conventional solvents.^{6f} However, its insertion into a block copolymer leads to soluble block copolymers and demonstrates that CF8 can be polymerized by a living mechanism.

The structure and composition of the block copolymers were determined by 300 MHz ^1H -NMR spectroscopy. Figure 7 presents a typical 300 MHz ^1H -NMR spectrum of poly[(6-2)-b-CF8]5/5. This spectrum exhibits the aromatic protons of the (6-2) repeating units at 6.9-7.7 ppm and the methylene protons of the CF8 repeating units at 2.31 ppm. In addition, the resonances of the acetal and methoxy protons which are formed after quenching the living carbocationic polymerization with methanol are



Scheme II. Synthesis of block copolymers

Table I: Block Copolymers of Mesogenic Vinyl Ethers (M) and CF8 via Sequential Living Polymerization by $\text{CF}_3\text{SO}_3\text{H}/(\text{CH}_3)_2\text{S}$. $([\text{M}]_0/[\text{I}]_0=1.5, [(\text{CH}_3)_2\text{SO}]/[\text{I}]_0=20)$

No.	Block copolymer	$\text{Mn} \times 10^{-3}$		Mw/Mn		$\text{Mn} \times 10^{-3}$		Mw/Mn		$\text{Mn} \times 10^{-3}$		Mw/Mn		DP_A/DP_B		DP_A/DP_B		w_A/w_B		w_A/w_B		yield (%)
		(A)	(B)	(A)	(B)	(A)	(B)	(A)	(B)	(A)	(B)	(A)	(B)	(theo)	(GPC)	(theo)	(GPC)	(theo)	(NMR)	(theo)	(NMR)	
1	poly((6-2)-b-CF8)5/5	3.7		1.12		7.5		1.26		15/8		14/7		5:5		5:5		5.5/4.5		5.5/4.5		87
2	poly(BEVE-b-CF8)5/5	3.2		1.08		5.9		1.15		15/8		13/6		5:5		5:5		5.6/4.4		5.6/4.4		80
3	poly((6-3)-b-CF8)5/5	4.0		1.13		8.2		1.24		15/8		15/8		5:5		5:5		4.6/5.4		4.6/5.4		89
4	poly((6-9)-b-CF8)7/3	5.6		1.08		7.8		1.18		15/4		16/4		7:3		7:3		6.8/3.2		6.8/3.2		81
5	poly((6-11)-b-CF8)7/3	5.5		1.14		7.8		1.20		15/5		14/4		7:3		7:3		6.9/3.1		6.9/3.1		80

A=mesogenic segment; B=fluorinated segment; AB=block copolymer; DP_A , DP_B =degree of polymerization of segment A and B respectively; w_A and w_B =weight fractions of segment A and B in block copolymer respectively

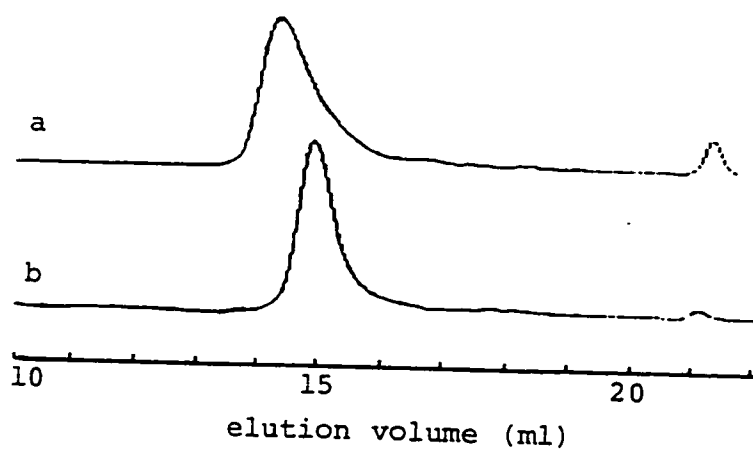


Figure 6. GPC traces of poly[(6-2)-b-CF8]5/5 (a) and of poly(6-2) (DP=14) (b)

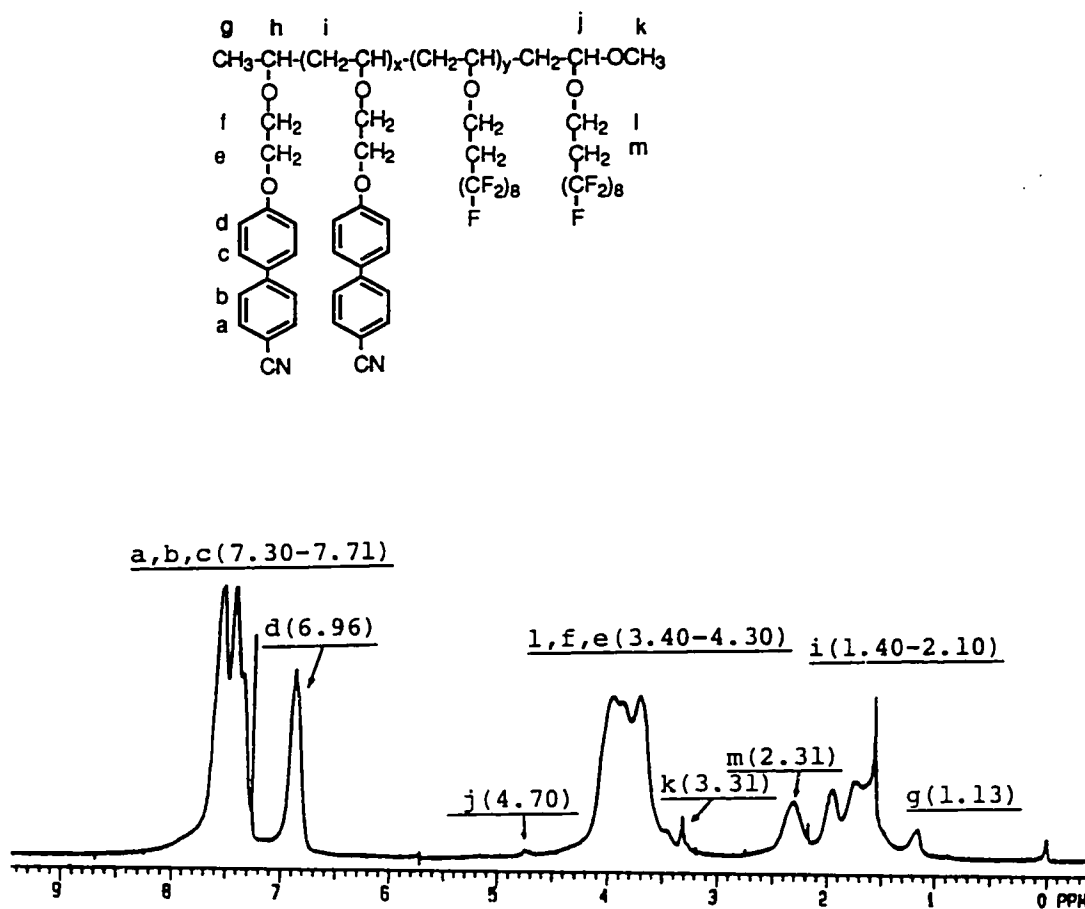


Figure 7. 300 MHz ¹H-NMR spectrum of poly[(6-2)-b-CF₈]5/5

observed at 4.70 and 3.31 ppm, respectively. No other signals indicative of side reactions are observed. The composition of block copolymers was determined from the ratio of the aromatic protons (o to alkoxy, signal d in Figure 7) to the methylene protons ($-\text{CH}_2\text{CF}_2-$, signal m in Figure 7). The composition of block copolymers determined from their NMR spectra and presented in weight ratio in Table I is in good agreement with the feed weight ratio of the two monomers.

The mesomorphic behavior of all block copolymers were characterized as to their mesomorphic behavior by DSC and optical polarized microscopy and compared to that of the homopolymers with similar degrees of polymerization of the A block.

Let us discuss the first the thermal behavior of poly[(6-2)-b-CF8]5/5 and poly[BEVE-b-CF8]5/5. Both block copolymers are synthesized from the mesogenic monomers whose parent homopolymers exhibit a glassy phase when it is determined from second DSC heating scan^{1b} (Table IV, Figures 8 and 9), and fluorinated monomer whose parent homopolymer displays a crystalline melting.⁹ In the first heating scan, poly[(6-2)-b-CF8]5/5 exhibits a crystalline melting which correspond to CF8 block followed by an X phase of the mesogenic block copolymer segment. The transition temperature of each phase in the block copolymer is very close to that of poly(6-2) (Table II) and poly(CF8).⁹ Second heating and cooling DSC scans of poly[(6-2)-b-CF8]5/5 display the same behavior except that the X phase does not appear since this mesophase is located in close proximity to the glass transition temperature of the mesogenic segment and therefore, it strongly kinetically controlled (Figure 3). The DSC traces of the first heating, second heating and cooling scans of poly[BEVE-b-CF8]5/5 are presented in Figure 9. Thermal behavior of poly[BEVE-b-CF8]5/5 is similar to that of poly[(6-2)-b-CF8]5/5 except that the melting transition of the mesogenic segment is absent in the first DSC heating scan.

One of the unique feature of these block copolymers is the persistence of mesomorphic behavior above the isotropization temperatures of the corresponding mesogenic homopolymers (Table IV, Figures 8,9). This is most probably due to a microphase separated morphology in the melt state. Since the refractive indices of these two segments are highly dissimilar, they exhibit an anisotropic texture on the optical polarized microscope. A characteristic example of the mesomorphic texture obtained for poly[(6-2)-b-CF8]5/5 at 190 °C is presented in Figure 10.

Poly[(6-3)-b-CF8]5/5 is based on the mesogenic monomer (6-3) whose parent homopolymer poly(6-3)^{1b} exhibits a nematic mesophase, This block copolymer exhibits a crystalline melting of the fluorinated segment, the X and nematic phases of the mesogenic segment, and the newly generated mesophase indicative of microphase separated morphology above the isotropization temperature (Table IV, Figure 11). Both the mesomorphic-mesomorphic transition temperature and the enthalpy change associated with the mesophase of poly[(6-3)-b-CF8]5/5 decreases in comparison to that of the parent homopolymers (Table IV). This trend agrees well with previous results available in the literature³ and is predicted by thermodynamic theory.^{10,11} The following speculative explanation about this phenomenon is possible. The decrease of enthalpy change may be caused by a disordering of the mesogens at the interphase. Although the phase boundary is sharp on a local scale, the interphase may be of very irregular structure which could oppose the ordering of the mesogens at the interphase.

The observation of textures of poly[(6-3)-b-CF8]5/5 by optical polarized microscopy reveals significant difference in comparison to the behavior of their respective homopolymers. Figure 12 shows the schlieren texture of both poly(6-3) and poly[(6-3)-b-CF8]5/5 which is characteristic of a nematic mesophase. However the domain size of the schlieren texture in block copolymer is much smaller than that of the

Table IV. Thermal characterization of the AB block copolymers and of the parent homopolymers. Data on first line are from first heating and cooling scans. Data on second line are from second heating scan

sample no.	polymer	phase transitions (°C) and corresponding enthalpy changes (kcal/mol)	
		heating	cooling
1	poly(6-2)	g 78.5 X 86.0 (0.18) i g 72.8 i	i 63.8 g
2	poly[(6-2)-b-CF8]	k -4.6 (-0.12) k 21.5 (0.30) g 75.1 X 83.1 (0.11) mes ^a 250 dec ^b k -0.9 (-0.11) k 20.1 (0.32) g 78.4 mes 250 dec	250 mes ^a 69.0 g -12.8 (0.18) k
3	poly(BEVE)	g 58.9 k 70.1 (1.04) i g 52.1 i	i 45.7 g
4	poly[(BEVE)-b-CF8]	k 30.2 (0.013) k 65.7 (0.82) mes 250 dec k 25.4 (0.010) g 50.0 mes 250 dec	250 mes 42.8 g 8.2 (0.011) k
5	poly(6-3)	g 59.5 X 64.5 (0.26) n 97.8 (0.094) i g 56.4 n 95.9 (0.07) i	i 90.8 (0.078) n 50.3 g
6	poly[(6-3)-b-CF8]	k -11.6 (-0.14) k 15.1 (0.37) g 60.0 X 64.0 (0.050) n 96.6 (0.04) mes ^a 250 dec ^b k -4.84 (-0.07) k 14.1 (0.35) g 59.0 n 95.2 (0.047) mes ^a 250 dec ^b	250 mes ^a 90.1 (0.042) n 52.0 g -14.5 (0.17) k
7	poly(6-2)	g 13.3 s _A 141.5 (0.62) i g 12.5 s _A 141.0 (0.60) i	i 136.7 (0.61) s _A 7.5 g
8	poly[(6-2)-b-CF8]	k -6.91 (0.054) g 12.3 k 22.6 (0.17) s _X 41.3 (0.03) s _A 140.1 (0.50) i g 10.2 k 22.1 (0.25) s _A 139.2 (0.47) i	i 134.5 (0.41) s _A 4.7 g -6.5 (0.11) k
9	poly(6-11)	g 17.0 k 66.3 (3.29) s _A 155.2 (0.82) i g 14.7 s _A 150.1 (0.77) i	i 143.4 (0.78) s _A 8.3 g
10	poly[(6-11)-b-CF8]	g 9.5 k 54.4 (-) k 64.4 (3.20) ^c s _A 146.2 (0.78) i g 8.4 k 20.5 (0.30) s _A 146.3 (0.72) i	i 140.0 (0.71) s _A 4.2 g -5.74 (0.09) k

^a mesophase, ^b decomposition, ^c overlapped peak

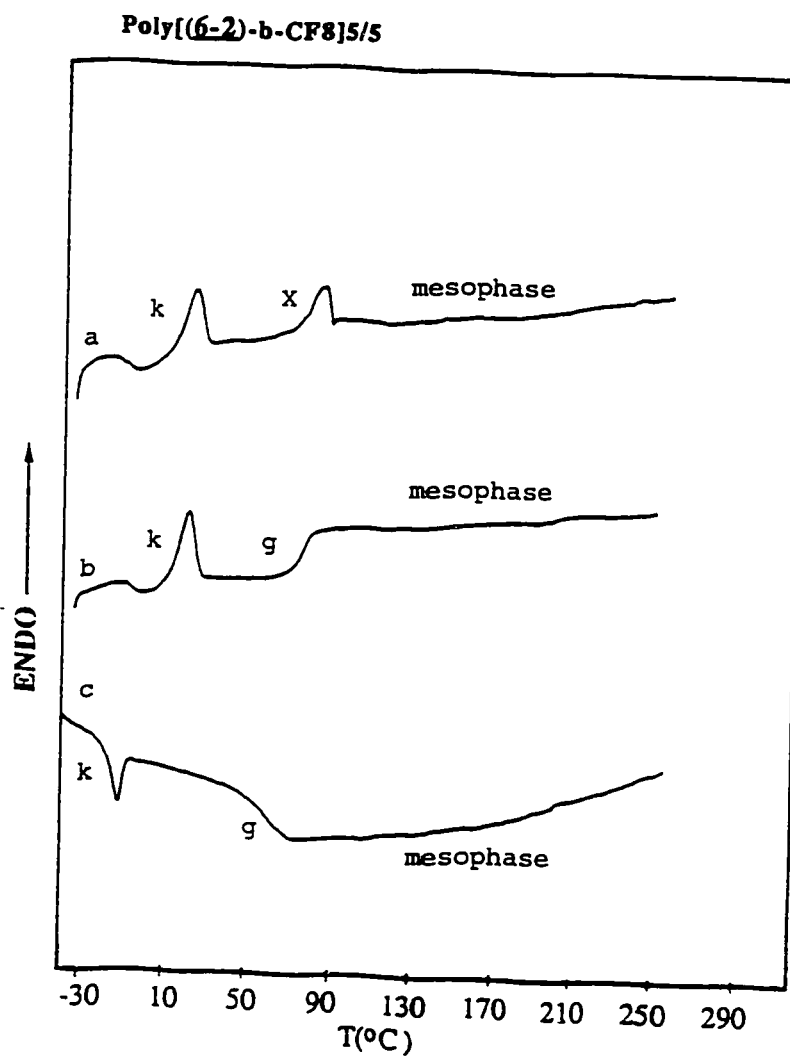


Figure 8. DSC traces displayed by the first heating (a), second heating (b) and the first cooling scans (c) of poly[(6-2)-b-CF₈]5/5

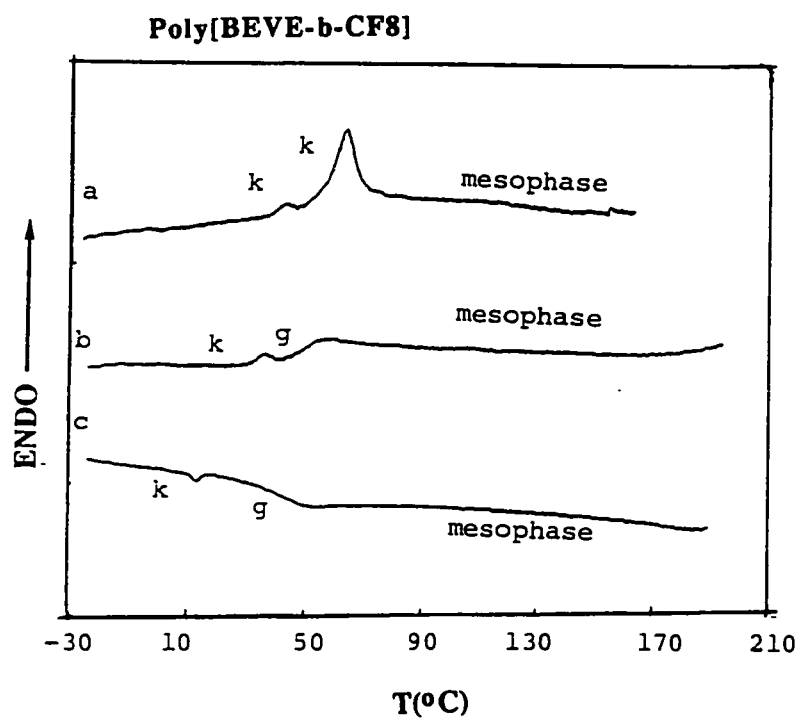


Figure 9. DSC traces displayed by the first heating (a), second heating (b) and the first cooling scans (c) of poly[BEVE-b-CF8]5/5

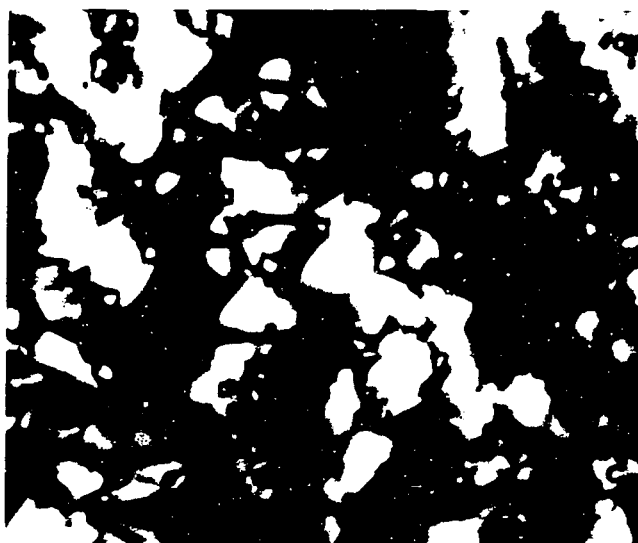


Figure 10. Representative optical polarized micrograph (100x) of the mesophase displayed by poly[(6-2)-b-CF8]5/5 at 190 °C after annealing 1 day.

parent homopolymer even after overnight annealing.

DSC traces of poly[(6-9)-b-CF8]7/3 and poly[(6-11)-b-CF8]7/3 are presented in Figures 13 and 14 respectively. Both block copolymers are synthesized from mesogenic monomers whose parent homopolymers exhibit a s_A phase as their highest temperature mesophase. In the case of the first heating DSC scan of poly[(6-9)-b-CF8]7/3, this block copolymer exhibits the melting of the fluorinated segment and the s_A phase of the mesogenic segment which is indicative of a microphase separated morphology. The first order transition at 41.3°C (Table IV, Figure 13) may result from different crystalline size of the fluorinated segment. In second and first cooling scans this first order transition does not appear, and there are only transitions which correspond to those of each homopolymer. Both the transition temperature from s_A to the isotropic state and the enthalpy change associated with this mesophase decrease when they are compared to those of the corresponding mesogenic homopolymers poly(6-9)^{1d} and poly(6-11)^{1a} (Table II).

Figure 9 displays representative optical polarized micographs of the s_A phase of poly(6-9) (a) and of poly[(6-9)-b-CF8]7/3 (b). The s_A phase of poly(6-9) displays a typical focal conic texture. The s_A phase of poly[(6-9)-b-CF8]7/3, on the other hand, exhibits striations on the focal conic texture which is clearly different from that of the parent homopolymer. It is believed that these striations are manifestations of microphase separation of the fluorinated block within the s_A phase.

Figure 15 presents first and second heating, and first cooling DSC scans of poly[(6-11)-b-CF8]7/3. The thermal behavior of this block copolymer is similar to that of poly[(6-9)-b-CF8]7/3 except that there is a melting transition of the mesogenic segment in the case of first heating scan.

Distinct from the behavior of the block copolymers based on mesogenic monomers with two and three methylene units in the spacer, the optical micrographs of poly[(6-9)-b-CF₈]7/3 and poly[(6-11)-b-CF₈]7/3 display a lack of mesomorphic behavior in melt state. This phenomenon illustrates the role of longer length spacer in decreasing the immiscibility between the mesogenic segment and fluorinated segment, and/or its influence on the difference between the refractive indices of the two segments.

In conclusion, block copolymers containing side chain liquid crystalline segments in one block and fluorocarbon segments in the second block can be synthesized by living cationic polymerization. The resulting block copolymers show narrow molecular weight distribution and the weight ratio composition of block copolymers is in good agreement with the feed weight ratio of the each monomer. The thermal behavior of all block copolymers synthesized in this paper was determined by DSC and optical polarized microscopy and shows a microphase separated morphology, although the degrees of polymerization of the mesogenic and fluorocarbon blocks are very low. For mesogenic monomers with short spacer lengths the microphase separated morphology is also maintained in the melt phase up to a temperature where the fluorinated and mesogenic segments become miscible.

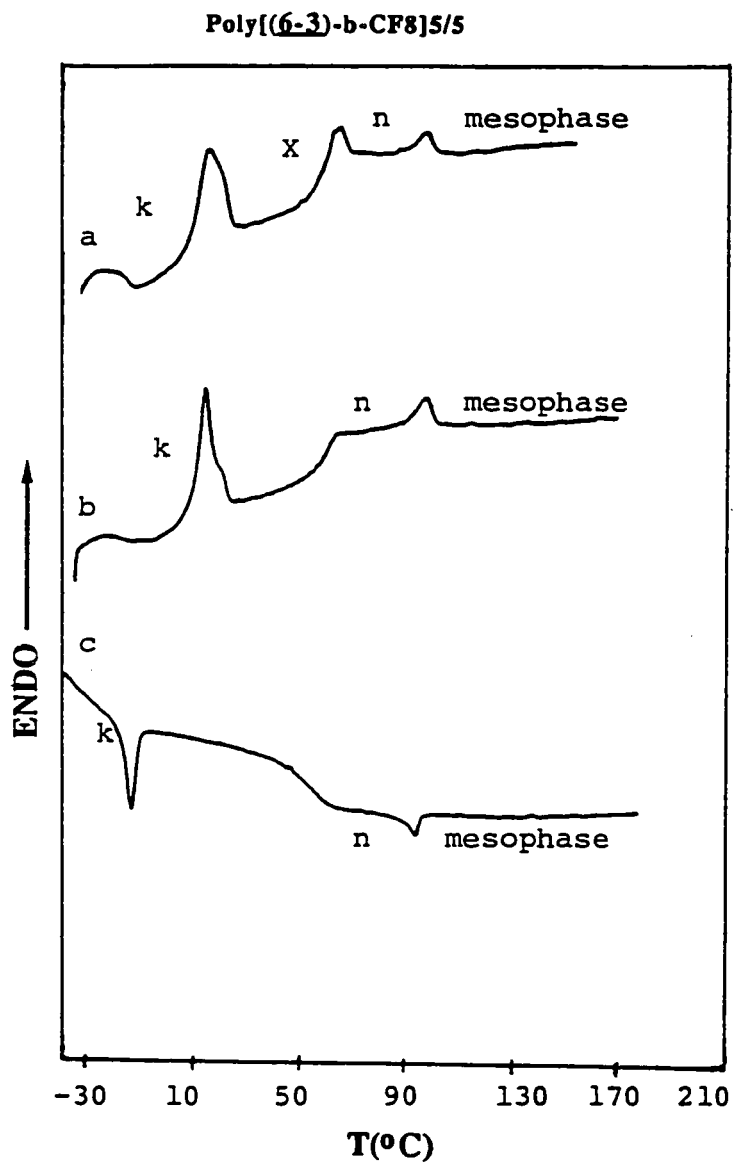


Figure 11. DSC traces displayed by the first heating (a), second heating (b) and the first cooling scans (c) of poly[(6-3)-b-CF8]5/5

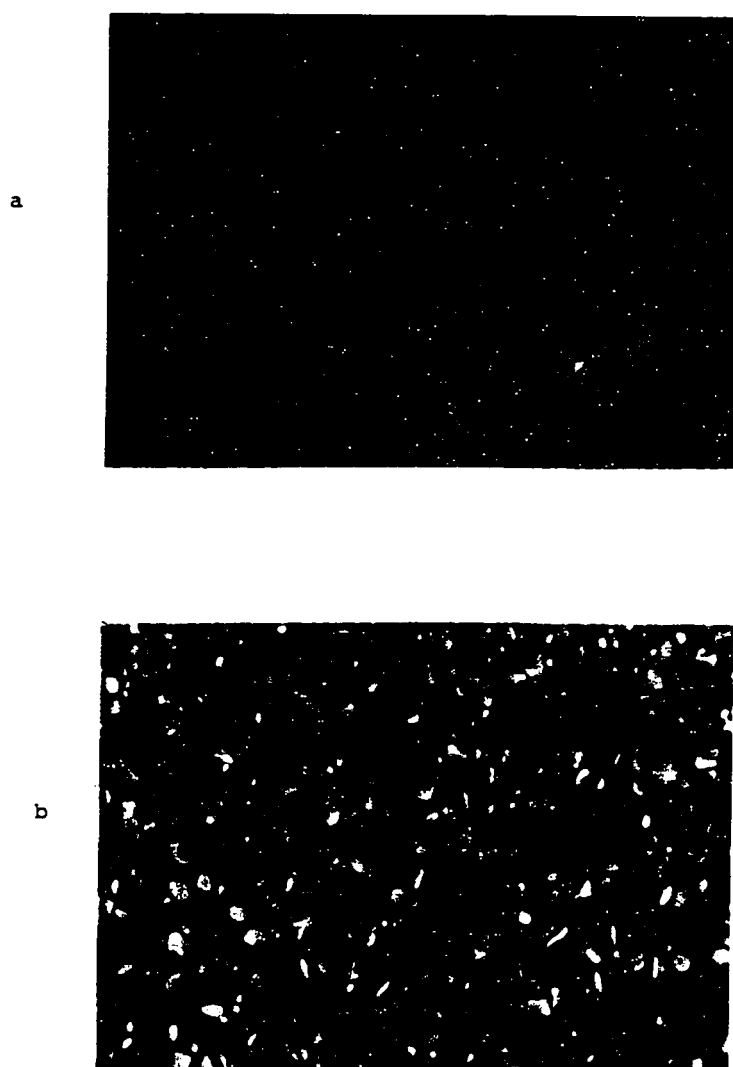


Figure 12. Representative optical polarized micrographs (100x) of the mesophase displayed by poly(6-3) (DP=16) at 90 °C (a) and poly[(6-3)-b-CF8]5/5 (b) at 90 °C after annealing overnight.

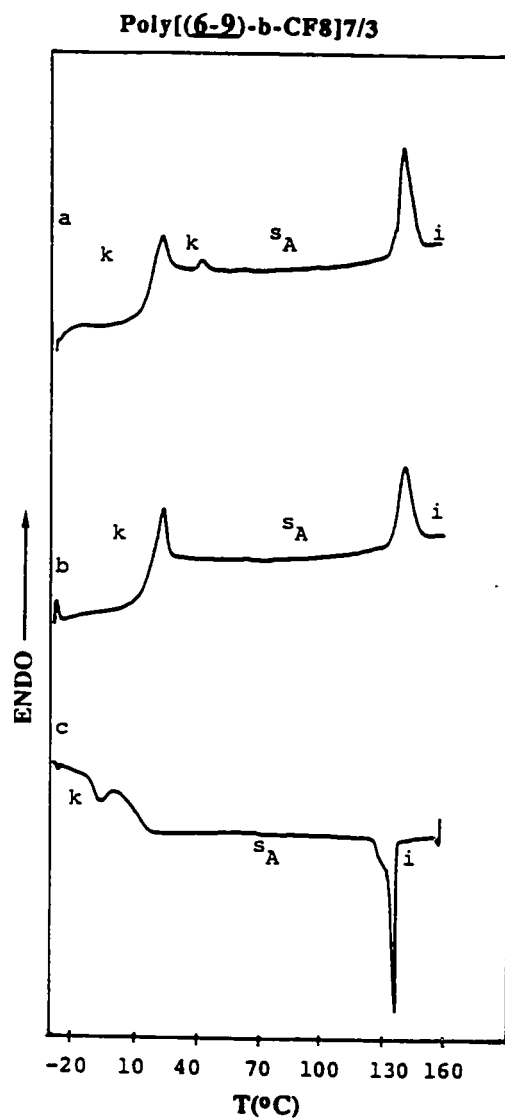


Figure 13. DSC traces displayed by the first heating (a), second heating (b) and the first cooling scans (c) of poly[(6-9)-b-CF₈]7/3



Figure 14. Representative optical polarized micrographs (100x) of the mesophase displayed by poly(6-9) (DP=16) (a) and poly[(6-9)-b-CF₈]7/3 (b) at 130 °C.

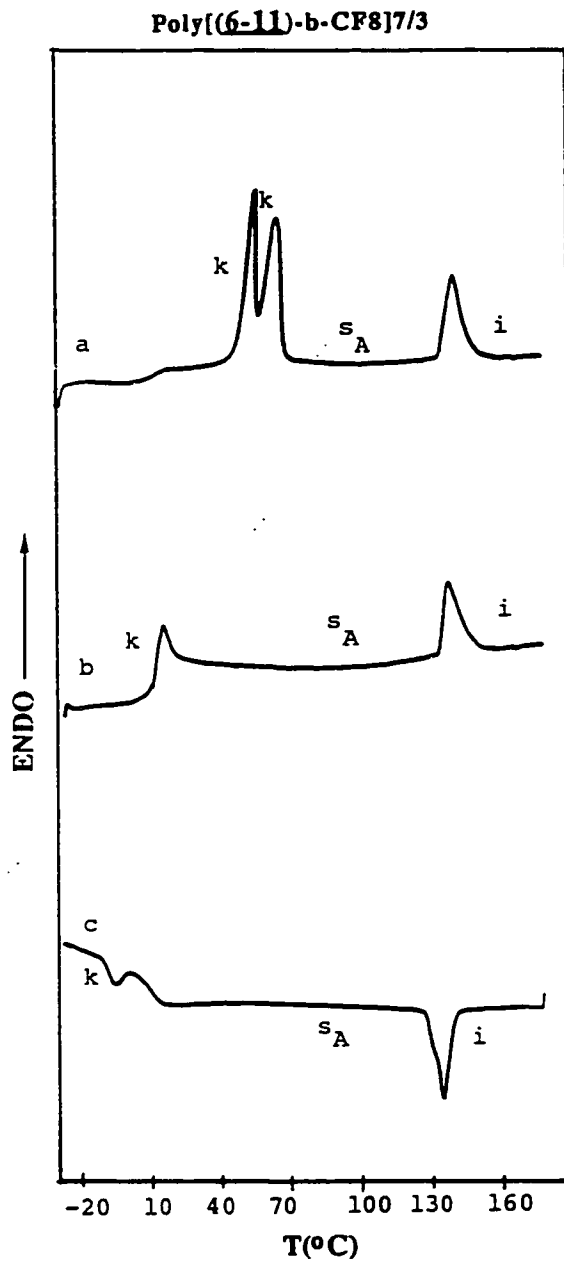


Figure 15. DSC traces displayed by the first heating (a), second heating (b) and the first cooling scans (c) of poly[(6-11)-b-CF8]7/3

REFERENCES

1. (a) V. Percec, M. Lee and H. Jonsson, *J. Polym. Sci.: Part A: Polym. Chem.*, **29**, 327(1991); (b) V. Percec and M. Lee, *J. Macromol. Sci.-Chem.*, **A 28**, 651(1991); (c) V. Percec and M. Lee, *Macromolecules*, **24**, 1017(1991); (d) V. Percec and M. Lee, *Macromolecules*, **24**, 2780(1991); (e) V. Percec, M. Lee and C. Ackerman, *Polymer*, in press; (f) V. Percec, M. Lee, P. Rinaldi and V. Litmann, *J. Polym. Sci.: Part A: Polym. Chem.*, in press; (g) V. Percec and M. Lee, *J. Macromol. Sci.-Chem.*, submitted
2. C. G. Cho, B. A. Feit and O. W. Webster, *Macromolecules*, **23**, 1918(1990); C. H. Lin and K. Matyjaszewsky, *Polym. Prepr. Am. Chem. Soc. Div. Polym. Chem.*, **31**(1), 599(1990).
3. (a) J. Adams and W. Gronski, *Makromol. Chem., Rapid Commun.*, **10**, 553 (1989); (b) J. Adams and W. Gronski, in "Liqui Crystalline Polymers", R. A. Weiss and C. K. Ober Eds., ACS Symposium Series 435, Am. Chem. Soc., Washington DC, 1990, p. 174
4. M. Hefft and J. Springer, *Makromol. Chem., Rapid Commun.*, **11**, 397 (1990)
5. J. Hopken, C. Pugh, W. Richtering and M. Moller, *Makromol. Chem.*, **189**, 911 (1988); Y. Ishikawa, H. Kuwahara and T. Kunitake, *J. Am. Chem. Soc.*, **111**, 8530 (1989); C. Viney, R. J. Twieg, T. P. Russell and L. E. Depero, *Liq. Cryst.*, **5**, 1783 (1989); M. P. Turberg and J. E. Brady, *J. Am. Chem. Soc.*, **110**, 7797 (1988); C. P. Jariwala, P. E. G. Sundell, C. E. Hoyle and L. J. Mathias, *Macromolecules*, **24**, 6352 (1991)
6. V. Percec, C. S. Hsu and D. Tomazos, *J. Polym. Sci.:Part A: Polym. Chem. Ed.*, **24**, 1363(1986);
7. T. Gibson, *J. Org. Chem.*, **45**, 1095(1980)
8. V. Percec and D. Tomazos, to be published.
9. Hopken, M. Moller, M. Lee and V. Percec, *Makromol. Chem.*, in press
10. A. Poniewierski, T. J. Sluckin, *Liquid Cryst.*, **2**, 281 (1987)
11. P. Sheng, *Phys. Rev. A* **26**, 1610 (1982)

BIBLIOGRAPHY

CHAPTER 1

1. F. Reinitzer, *Monatsh. Chem.* **9**, 421 (1888)
2. L. Gatterman and A. Rischke, *Ber. Deut. Chem. Ges.*, **23**, 1738 (1890)
3. D. Vorlander, *Kristallinisch-flussige Substanzen*, Enke Verlag, Stuttgart, (1908)
4. L. Onsager, *Ann. N. Y. Acad. Sci.*, **51**, 627 (1949)
5. P. J. Flory, *Proc. Royal Soc., London*, **234A**, 73 (1956)
6. A. Roviello and A. Sirigu, *J. Polym. Sci.: Polym. Lett.*, **13**, 455 (1975)
7. W. J. Jackson and H. F. Kuhfuss, *J. Polym. Sci.: Polym. Chem.*, **14**, 2043 (1976)
8. H. F. Kuhfuss and W. J. Jackson. *U. S. Patent*, 3,778,410 (1973); 3,804,805 (1974)
9. A. Caferri, W. R. Krigbaum and R. B. Meyer, "Polymer Liquid Crystals", Academic Press, New York (1982)
10. C. K. Ober, J. I. Jin and R. W. Lenz, *Adv. Polym. Sci.*, **59**, 103 (1984)
11. H. Finkelmann and G. Rehage, *Adv. Polym. Sci.*, **60/61**, 99 (1984)
12. C. B. McArdle, "Side Chain Liquid Crystalline Polymers", Chapman and Hall, New York, 1989
13. N. A. Plate and V. P. Shibaev, "Comb Shaped Polymers and Liquid Crystals", Plenum, New York, 1987
14. V. P. Shibaev and N. A. Plate, *Pure and Appl. Chem.*, **57**, 1589 (1985)
15. A. Blumstein, "Liquid Crystalline Order in Polymers", Academic Press, New York 1978
16. V. Percec and A. Keller, *Macromolecules*, **23**, 4347 (1990)
17. A. Keller, G. Ungar and V. Percec, "Advances in Liquid Crystalline Polymers", (R. A. Weiss and C. K. Ober Ed.), ACS Symposium Series 435, Am. Chem. Soc., Washington D. C., 1990
18. G. W. Gray and J. W. Goodby, "Smectic Liquid Crystals", Leonard Hill, Glasgow, 1984

19. C. Noel, "Polymeric Liquid Crystals", (A. Blumstein Ed.), Plenum Press, New York, 1985
20. C. Noel, *Makromol. Chem., Makromol. Symp.*, **22**, 95 (1988)
21. T. S. Chung, *Polym. Eng. Sci.*, **26**, 901 (1986)
22. C. Noel, "Recent Advances in Liquid Crystalline Polymers", (L. L. Chapoy Ed.), Elsevier Applied Science, **2**, 297 (1988)
23. H. J. Coles, "Developments in Crystalline Polymers", (D. C. Bassett Ed.), Elsevier Applied Science, **2**, 297 (1988)
24. V. P. Shibaev and N. A. Plate, *Vyskomol. Soed. Ser.*, **A19**, 23 (1977)
25. A. K. Alimoglu, A. Ledwith, P. A. Gemmell, G. W. Gray and D. Lacey, *Polymer*, **25**, 1342 (1987)
26. R. Duran and P. Gramain, *Makromol. Chem.*, **188**, 2001 (1987)
27. A. Frosini, G. Levita, D. Lupinacci and P. L. Magagnini, *Mol. Cryst. Liq. Cryst.*, **66**, 21 (1981)
28. G. Decobert, J. C. Dubois, S. Esselin and C. Noel, *Liq. Cryst.*, **1**, 307 (1986)
29. R. Zentel and H. Ringsdorf, *Makromol. Chem., Rapid Commun.*, **5**, 393 (1984)
30. J. Horvath, K. Nyitrai, F. Cser and G. Hardy, *Eur. Polym. J.*, **21**, 251 (1985)
31. M. Portugall, H. Ringsdorf and R. Zentel, *Makromol. Chem.*, **183**, 2311 (1982)
32. B. Hahn, J. H. Wendorff, M. Portugall and H. Ringsdorf, *Coll. Polym. Sci.*, **259**, 875 (1981)
33. W. Kreuder, O. W. Webster and H. Ringsdorf, *Makromol. Chem., Rapid Commun.*, **7**, 5 (1986)
34. C. Pugh and V. Percec, *ACS Polym. Prepr.*, **26(2)**, 303 (1985)
35. J. Rodriguez-Parada and V. Percec, *J. Polym. Sci., Polym. Chem. Ed.*, **24**, 1363 (1986)
36. J. Rodriguez-Parada and V. Percec, *J. Polym. Sci., Polym. Chem. Ed.*, **25**, 2269 (1986)
37. V. Percec and D. Tomazos, *Polym. Bull.*, **18**, 239 (1987)

38. B. Reck and H. Ringsdorf, *Makromol. Chem., Rapid Commun.*, **6**, 291 (1985)
39. R. Berg, V. Krone and H. Ringsdorf, *Makromol. Chem., Rapid Commun.*, **7**, 381 (1986)
40. P. Keller, *Macromolecules*, **17**, 2937 (1984)
41. P. Keller, *Macromolecules*, **18**, 2337 (1985)
42. H. Finkelmann and G. Rehage, *Makromol. Chem., Rapid Commun.*, **1**, 31, (1980)
43. V. Percec and B. Hahn, *Macromolecules*, **22**, 1588 (1989)
44. H. Finkelmann, M. Happ, M. Portugall and H. Ringsdorf, *Makromol. Chem.*, **179**, 2541 (1978)
45. H. Finkelmann, H. Ringsdorf and J. H. Wendorff, *Makromol. Chem.*, **179**, 273 (1978)
46. C. Boeffel, B. Hisgen, U. Pschorn, H. Ringsdorf and F. W. Spiess, *Israel J. Chem.*, **23**, 388 (1983)
47. H. Geib, B. Hisgen, U. Pschorn, H. Ringsdorf and F. W. Spiess, *J. Am. Chem. Soc.*, **104**, 917 (1982)
48. H. W. Spiess, *Pure Appl. Chem.*, **57**, 1617 (1985)
49. C. Pugh and V. Percec, *Polym. Bull.*, **16**, 513 (1986)
50. C. Pugh and V. Percec, *Polym. Bull.*, **16**, 521 (1986)
51. C. S. Hsu, J. M. Rodrigues-Parada and V. Percec, *Makromol. Chem.*, **188**, 1017 (1987)
52. C. S. Hsu, J. M. Rodrigues-Parada and V. Percec, *J. Polym. Sci.; Polym. Chem.*, **25**, 2425 (1987)
53. V. Percec and D. Tomazos, *Polymer*, **31**, 1658 (1990)
54. A. Blumstein, S. Vilasager, S. Ponrathnam, S. B. Clough R. B. Blumstein and G. Maret, *J. Polym. Sci.; Polym. Chem. Ed.* **20**, 877 (1982)
55. V. Percec and H. Nava and H. Jonsson, *J. Polym. Sci.; Polym. Chem. Ed.* **25**, 1943 (1987)
56. S. G. Kostromin, R. V. Talrose, V. P. Shibaev and N. A. Plate, *Makromol. Chem., Rapid Commun.*, **3**, 803 (1982)
57. M. Sawamoto, *Prog. Polym. Sci.*, **16**, 111 (1991)

58. T. Higashimura and M. Sawamoto, *Adv. Polym. Sci.*, **62**, 49 (1984)
59. M. Miyamoto, M. Sawamoto and T. Higashimura, *Macromolecules*, **17**, 265 (1984)
60. M. Sawamoto and T. Higashimura, *Makromol. Chem., Makromol. Symp.*, **3**, 83 (1986)
61. K. Matyjaszewski, *Makromol. Chem., Makromol. Symp.*, **13/14**, 457 (1988)
62. T. Higashimura, S. Aoshima and Y. Kishimoto, *Polym. Bull.*, **18**, 111 (1987)
63. T. Higashimura and S. Aoshima, *Macromolecules*, **22**, 1009 (1989)
64. C. G. Cho, B. A. Feit and O. W. Webster, *Macromolecules*, **23**, 1918 (1990)
65. C. H. Lin and K. Matyjaszewski, *Polym. Prepr., Am. Chem. Soc. Div. Polym. Chem.*, **31(1)**, 599 (1990)
66. T. Sagane and R. W. Lenz, *Polym. J.* **20**, 923 (1988); *Macromolecules*, **22**, 3763 (1989); *Polymer*, **30**, 2269 (1989)
67. V. Percec, Q. Zheng and M. Lee, *J. Mater. Sci.*, **1**, 611 (1991)
68. V. percec, C. S. Wang and M. Lee, *Polym. Bull.*, **26**, 15 (1991)
69. H. Jonsson, V. Percec and A. Hult, *Polym. Bull.*, **25**, 115 (1991)
70. H. Stevens, G. Rehage and H. Finkelmann, *Macromolecules*, **17**, 851 (1984)
71. V. Percec, D. Tomazos and C. Pugh, *Macromolecules*, **22**, 3259 (1989)
72. D. Demus and L. Richter, "Textures of Liquid Crystals" Verlag Chemie, Weinheim 1978
73. G. W. Gray and J. W. Goodby, "Smectic Liquid Crystals, Textures and Structures", Leonard Hill, Glasgow, 1984

CHAPTER 2

1. V. Percec and C. Pugh, in "Side Chain Liquid Crystal Polymers", McArdle, C. B. Ed., Chapman and Hall, New York, 1989, p. 30 and references cited therein
2. S. G. Kostromin, R. V. Talroze, V. P. Shibaev and N. A. Plate, *Makromol. Chem., Rapid Commun.*, **3**, 803 (1982)
3. H. Stevens, G. Rehage and H. Finkelmann, *Macromolecules*, **17**, 851 (1984)

4. V. Shibaev, *Mol. Cryst. Liq. Cryst.*, **155**, 189 (1988)
5. S. Uchida, K. Morita, K. Miyoshi, K. Hashimoto and K. Kawasaki, *Mol. Cryst. Liq. Cryst.*, **155**, 93 (1988)
6. V. Percec and B. Hahn, *Macromolecules*, **22**, 1588 (1989)
7. V. Percec, D. Tomazos and C. Pugh, *Macromolecules*, **22**, 3259 (1989)
8. T. Sagane and R. W. Lenz, *Polym. J.*, **20**, 923 (1988)
9. T. Sagane and R. W. Lenz, *Polymer*, **30**, 2269 (1989)
10. T. Sagane and R. W. Lenz, *Macromolecules*, **22**, 3763 (1989)
11. V. Percec and A. Keller, *Macromolecules*, **23**, 4347 (1990)
12. A. Keller, G. Ungar and V. Percec, in "Advances in Liquid Crystalline Polymers", C. K. Ober and R. A. Weiss, Eds., ACS Symposium Series 435; Washington D.C., p.308 (1990)
13. J. M. Rodriguez-Parada and V. Percec, *J. Polym. Sci:Part A: Polym. Chem.*, **24**, 1363 (1986)
14. R. Rodenhouse, V. Percec and A. E. Feiring, *J. Polym. Sci: Part C:Polym. Lett.*, **28**, 345 (1990)
15. J. Adams and W. Gronski, *Makromol. Chem., Rapid Commun.*, **10**, 553(1989)
16. J. E. McKeon and P. Fitton, *Tetrahedron*, **28**, 233 (1972)
17. C. S. Hsu, J. M. Rodriguez-Parada and V. Percec, *J. Polym. Sci. Part A:Polym. Chem.*, **25**, 2425 (1987)
18. G. W. Gray, H. J. Harrison, J. A. Nash, J. Constant, D. S. Hulme, J. Kirton and E. P. Raynes, in "Ordered Fluids and Liquid Crystals", Vol. II, R. S. Porter and J. F. Johnson, Eds., Plenum, New York, 1974, p.617
19. J. E. McKeon, P. Fitton and A. A. Griswold, *Tetrahedron*, **28**, 227 (1972)
20. V. Percec and D. Tomazos, *Polym. Bull.*, **18**, 239 (1987)
21. T. Higashimura, S. Aoshima and M. Sawamoto, *Makromol. Chem., Macromol. Symp.*, **13/14**, 457 (1988)
22. M. Sawamoto, S. Aoshima and T. Higashimura, *Makromol. Chem., Macromol. Symp.*, **13/14**, 513 (1988)
23. T. Higashimura and M. Sawamoto, in "Comprehensive Polymer Science", Vol.3, G. Allen and J. Bevington Eds., Pergamon Press, Oxford, 1989, p.684

24. C. G. Cho, B. A. Feit and O. W. Webster, *Macromolecules*, **23**, 1918 (1990)

CHAPTER 3

1. V. Tsukruk, V. Shilov and Y. Lipatov, *Macromolecules*, **19**, 1308 (1986)
2. (a) V. Tsukruk, V. Shilov and Y. Lipatov, *Acta Polym.*, **36**, 403 (1985); (b) V. Tsukruk, V. Shilov and Y. Lipatov, *J. Macromol. Sci., Macromol. Chem. Phys.*, **C24**, 173 (1984).
3. C. Noel, in "Side Chain Liquid Crystal Polymers" McArdle, C. B., Eds., Chapman and Hall, New York, 1989, p. 159
4. W. Hefrich, *J. Phys. (Paris) Coll.*, **40**, C3 (1979)
5. G. W. Gray and G. W. Goodby, "Smectic Liquid Crystals, Leonard Hill, Glasgow, 1984

CHAPTER 4

1. V. Percec and A. Keller, *Macromolecules*, **23**, 4347 (1990)
2. A. Keller, G. Ungar and V. Percec, in "Advances in Liquid Crystalline Polymers", C. K. Ober and R. A. Weiss, Eds., ACS Symposium Series 435; Washington D.C., p.308 (1990)
3. V. Shibaev, *Mol. Cryst. Liq. Cryst.*, **155**, 189 (1988)
4. T. Sagane and R. W. Lenz, *Polym. J.*, **20**, 923 (1988)
5. T. Sagane and R. W. Lenz, *Polymer*, **30**, 2269 (1989)
6. T. Sagane and R. W. Lenz, *Macromolecules*, **22**, 3763 (1989)
7. J. E. McKeon and P. Fitton, *Tetrahedron*, **28**, 233 (1972)
8. C. S. Hsu, J. M. Rodriguez-Parada and V. Percec, *J. Polym. Sci. Part A: Polym. Chem.*, **25**, 2425 (1987)
9. G. W. Gray, H. J. Harrison, J. A. Nash, J. Constant, D. S. Hulme, J. Kirton and E. P. Raynes, in "Ordered Fluids and Liquid Crystals", Vol. II, R. S. Porter and J. F. Johnson, Eds., Plenum, New York, 1974, p.617
10. J. E. McKeon, P. Fitton and A. A. Griswold, *Tetrahedron*, **28**, 227 (1972)
11. J. M. Rodriguez-Parada and V. Percec, *J. Polym. Sci.:Part A: Polym. Chem.*, **24**, 1363 (1986)

12. R. Rodenhouse, V. Percec and A. E. Feiring, *J. Polym. Sci: Part C: Polym. Lett.*, **28**, 345 (1990)
13. T. Higashimura, S. Aoshima and M. Sawamoto, *Makromol. Chem., Macromol. Symp.*, **13/14**, 457 (1988)
14. M. Sawamoto, S. Aoshima and T. Higashimura, *Makromol. Chem., Macromol. Symp.*, **13/14**, 513 (1988)
15. T. Higashimura and M. Sawamoto, in "Comprehensive Polymer Science", Vol.3, G. Allen and J. Bevington Eds., Pergamon Press, Oxford, 1989, p.684
16. C. G. Cho, B. A. Feit and O. W. Webster, *Macromolecules*, **23**, 1918 (1990)
17. C. H. Lin and K. Matyjaszewski, *Polym. Prepr., Am. Chem. Soc.*, **31**(1), 599 (1990)
18. V. Percec and C. Pugh, in "Side Chain Liquid Crystal Polymers", McArdle, C. B. Ed., Chapman and Hall, New York, 1989, p. 30 and references cited therein
19. R. S. Kumar, S. B. Clough and A. Blumstein, *Mol. Cryst. Liq. Cryst.*, **157**, 387 (1988)
20. V. Percec, D. Tomazos and C. Pugh, *Macromolecules*, **22**, 3259 (1989)
21. M. Warner, In "Side Chain Liquid Crystal Polymers" C. B. McArdle Ed., Chapman and Hall, New York, 1989, p 7 and references cited therein.
22. C. Noel, In "Side Chain Liquid Crystal Polymers", C. B. McArdle Ed., Chapman and Hall, New York, 1989, p 159.
23. G. Pepy, J. P. Cotto, F. Hardouin, P. Keller, M. Lambert, F. Mousa, L. Noirez, A. Lapp and C. Strazzielle, *Makromol. Chem. Macromol. Symp.*, **15**, 251 (1988)
24. Percec, V. Tomazos, D. *Polymer*, **31**, 1658 (1990)

CHAPTER 5

1. J. M. Rodriguez-Parada and V. Percec, *J. Polym. Sci., Polym. Chem. Ed.*, **24**, 1363 (1986)
2. V. Percec and D. Tomazos, *Polym. Bull.*, **18**, 239 (1987)
3. V. Percec, D. Tomazos and C. Pugh, *Macromolecules*, **22**, 3259 (1989)
4. T. Kodaira and K. Mori, *Makromol Chem., Rapid Commun.*, **11**, 645 (1990)
5. T. Sagane and R. W. Lenz, *Polym. J.*, **20**, 923 (1988)

6. T. Sagane and R. W. Lenz, *Polymer*, **30**, 2269 (1989)
7. T. Sagane and R. W. Lenz, *Macromolecules*, **22**, 3763 (1989)
8. V. Heroguez, A. Deffieux and M. Fontanille, *Makromol Chem., Rapid Commun.*, **32**, 199 (1990)
9. V. Heroguez, M. Schappacher, E. Papon and A. Deffieux, *Polym. Bull.*, **25**, 307 (1991)
10. E. Papon, A. Deffieux, F. Hardouin and M. F. Achard, *Liq. Cryst.*, in press
11. H. Jonsson, V. Percec and A. Hult, *Polym. Bull.*, **25**, 115 (1991)
12. V. Percec, C. S. Wang and M. Lee, *Polym. Bull.*, **26**, 15 (1991)
13. V. Percec, Q. Zheng and M. Lee, *J. Mater. Chem.*, **1**, 611 (1991)
14. R. Rodenhouse, V. Percec and A. E. Feiring, *J. Polym. Sci: Part C: Polym. Lett.*, **28**, 345 (1990)
15. S. G. Kostromin, N. D. Cuong, E. S. Garina and V. P. Shibaev, *Mol. Cryst. Liq. Cryst.*, **193**, 177 (1990)
16. (a) P. E. Cladis, *Phys. Rev. Lett.*, **35**, 48 (1975); (b) P. E. Cladis, R. K. Bogardus, W. B. Daniels and G. N. Taylor, *Phys. Rev. Lett.*, **39**, 720 (1977); (c) D. Guillon, P. E. Cladis and J. Stamatoff, *Phys. Rev. Lett.*, **41**, 1598 (1978); (d) P. E. Cladis, R. K. Bogardus and D. Aadsen, *Phys. Rev. A.*, **18**, 2292 (1978); (e) N. H. Tinh, *J. Chim. Phys.*, **80**, 83 (1983); (f) J. W. Goodby, T. M. Leslie, P. E. Cladis and P. L. Finn, in "Liquid Crystals and Ordered Fluids", A. C. Griffin and J. F. Johnson, Eds., Plenum, Crystals and Ordered Fluids", A. C. Griffin and J. F. Johnson, Eds., Plenum, New York, 1984, p. 203
17. For some representative reviews see: (a) G. Sigaud, N. H. Tinh, F. Hardouin and H. Gasparoux, *Mol. Crst. Liq. Cryst.*, **69**, 81 (1981); (b) F. Hardouin, A. M. Levelut, M. F. Archard and G. Sigaud, *J. Chim. Phys.*, **80**, 53 (1983); (c) F. Hardouin, *Physica*, **140A**, 359 (1986); (d) P. E. Cladis, *Mol. Cryst. Liq. Cryst.*, **165**, 85 (1988)
18. P. Le Barny, J. C. Dubois, C. Friedrich and C. Noel *Polym. Bull.*, **15**, 341 (1986)
19. T. I. Gubina, S. G. Kostromin, R. V. Talroze, V. P. Shibaev and N. A. Plate, *Vyskomol. Soed. Ser. B.*, **28**, 394 (1986)
20. V. Shibaev, *Mol. Cryst. Liq. Cryst.*, **155**, 189 (1988)

21. N. Lacoudre, A. Le Borgue, N. Spassky, J. P. Vairon, P. Le Barny, J. C. Dubois, S. Esselin, C. Friedrich and C. Noel, *Mol. Cryst. Liq. Cryst.*, **155**, 113 (1988)
22. N. Spassky, N. Lacoudre, A. Le Borgue, J. P. Vairon, C. L. Jun, C. Friedrich and C. Noel, *Makromol. Chem., Makromol. Symp.*, **24**, 271 (1989)
23. T. A. Gubina, S. Kise, S. G. Kostromin, R. V. Talroze, V. P. Shibaev and N. A. Plate, *Liq. Cryst.*, **4**, 197 (1989)
24. S. G. Kostromin, V. P. Shibaev and S. Diele, *Makromol. Chem.*, **191**, 2521 (1990)
25. C. Legrand, A. Le Borgue, C. Bunel, A. Lacoudre, P. Le Barny, N. Spassky and J. P. Vairon, *Makromol. Chem.*, **191**, 2979 (1990)

CHAPTER 6

1. T. Sagane and R. W. Lenz, *Macromolecules*, **22**, 3763 (1989)
2. C. G. Cho, B. A. Feit and O. W. Webster, *Macromolecules*, **23**, 1918 (1990)
3. H. Dehne, A. Roger, D. Demus, S. Diele, H. Kresse, G. Pelzl, W. Wedler and W. Weissflog, *Liq. Cryst.*, **6**, 47 (1989) and references cited therein.
4. V. Percec and B. Hahn, *Macromolecules*, **22**, 1588 (1989)
5. S. G. Kostromin, R. V. Talroze, V. P. Shibaev and N. A. Plate, *Makromol. Chem., Rapid Commun.*, **3**, 803 (1982)
6. H. Stevens, G. Rehage and H. Finkelmann, *Macromolecules*, **17**, 851 (1984)
7. V. Shibaev, *Mol. Cryst. Liq. Cryst.*, **155**, 189 (1988)
8. S. Uchida, K. Morita, K. Miyoshi, K. Hashimoto and K. Kawasaki, *Mol. Cryst. Liq. Cryst.*, **155**, 93 (1988)
9. V. Percec and C. Pugh, in "Side Chain Liquid Crystal Polymers", McArdle, C. B. Ed., Chapman and Hall, New York, 1989, p. 30 and references cited therein.
10. V. Percec and A. Keller, *Macromolecules*, **23**, 4347(1990)
11. A. Keller, G. Ungar and V. Percec, in "Advances in Liquid Crystalline Polymers", R. A. Weiss and C. K. Ober Eds., ACS Symposium Series 435, Washington DC, 1990, p.308
12. V. Percec and Y. Tsuda, *Macromolecules*, **23**, 3509 (1990)

13. M. Mauzac, F. Hardouin, H. Richard, M. F. Achard, G. Sigaud and H. Gasparoux, *Eur. Polym. J.*, **22**, 137 (1986)
14. D. A. Gemmel, G. W. Gray and D. Lacey, *Mol. Cryst. Liq. Cryst.*, **122**, 205 (1985)

CHAPTER 7

1. H. Arnold and H. Sackmann, *Z. Phys. Chem. (leipzig)*, **213**, 145 (1960)
2. H. Sackmann and D. Demus, *Mol. Cryst. Liq. Cryst.*, **21**, 239 (1973)
3. D. Demus, S. Diele, S. Grande and H. Sackmann, "Advances in Liquid Crystals", (G. H. Brown Ed.), Academic Press, London, **6**, 1 (1983)
4. W. R. Krigbaum, *J. Appl. Polym. Sci., Polym. Symp.*, **41**, 105 (1985)
5. C. Casagrande, M. Veyssie and H. Finkelmann, *J. Phys. Lett.*, **43**, L-621 (1982)
6. H. Ringsdorf, H. W. Schmidt and A. Schneller, *Makromol. Chem., Rapid Commun.*, **3**, 745 (1982)
7. H. Benthack-Thomas and H. Finkelmann, *Makromol. Chem.*, **186**, 1895 (1985)
8. V. Percec and Y. Tsuda, *Polymer*, **32**, 661 (1991)
9. T. Schroeder, *Z. Phys. Chem.*, **11**, 449 (1893)
10. J. J. van Laar, *Z. Phys. Chem.*, **63**, 216 (1908); G. R. Van Hecke, *J. Phys. Chem.*, **83**, 2344 (1979)
11. a) V. Percec and R. Yourd, *Macromolecules*, **22**, 524 (1989); V. Percec, and Y. Tsuda, *Macromolecules*, **23**, 5 (1990); V. Percec and Y. Tsuda, *Macromolecules*, **23**, 3509 (1990); b) V. Percec and C. Pugh, in "Side Chain Liquid Crystal Polymers", C. B. McArdle Ed., Chapman and Hall, New York, 1989, p. 30 and references cited therein.
12. G. Gray, "Side Chain Liquid Crystal Polymers", C. B. McArdle Ed., Chapman and Hall, New York, 1989, p. 106
13. N. A. Plate and V. P. Shibaev, "Comb-Shaped Polymers and Liquid Crystals" Plenum Press, New York, 1987
14. M. Engel, B. Hisgen, R. Keller, W. Kreuder, B. Reck, H. Ringsdorf, H. W. Schmidt and P. Tschirner, *Pure Appl. Chem.*, **57**, 1009 (1985)
15. V. P. Shibaev and N. Plate, *Adv. Polym. Sci.*, **60/61**, 173 (1984)

16. H. W. Schmidt, *Angew. Chem. Int. Ed. Engl. Adv. Mater.*, **101**, 964 (1989)
17. S. Diele, S. Oelsner, F. Kuschel, B. Hisgen, H. Ringsdorf and R. Zentel, *Makromol. Chem.*, **188**, 1993 (1987)
18. S. Diele, S. Oelsner, F. Kuschel, B. Hisgen and H. Ringsdorf, *Mol. Cryst. Liq. Cryst.*, **155**, 399 (1988)
19. S. Westphal, S. Diele, F. Madicke, F. Kuschel, U. Scheim, K. Ruhlmann, B. Hisgen and H. Ringsdorf, *Makromol. Chem., Rapid Commun.*, **9**, 489 (1988)
20. G. Nestor, G. W. Gray, D. Lacey and K. J. Toyne, *Liq. Cryst.*, **6**, 137 (1989)
21. V. Percec and B. Hahn, *Macromolecules*, **22**, 1588 (1989)
22. V. Percec, B. Hahn, M. Ebert and J. H. Wendorff, *Macromolecules*, **23**, 2092 (1990)
23. V. Percec and D. Tomazos, *Macromolecules*, **22**, 1512 (1989)
24. V. Percec and D. Tomazos, *Polymer*, **30**, 2124 (1989)
25. M. F. Achard, M. Mauzac, H. Richard, G. Sigaud and F. Hardouin, *Eur. Polym. J.*, **25**, 593 (1989)
26. G. Hardy, F. Cser and K. Nyitrai, *Isr. J. Chem.*, **18**, 233 (1979)
27. G. Hardy, F. Cser, K. Nyitrai and E. Bartha, *Ind. Eng. Chem. Res. Dev.*, **121**, 321 (1982)
28. J. Horvath, F. Cser and G. Hardy, *Prog. Coll. Polym. Sci.*, **71**, 59 (1985)
29. D. A. Tirrell, in "Encyclopedia of Polymer Science and Engineering", 2nd Ed., H. F. Mark, N. M. Bikales, C. G. Overberger and G. Menger Eds. Vol. 4, Wiley, New York 1986, p. 192
30. S. G. Kostromin, R. V. Talroze, V. P. Shibaev and N. A. Plate, *Makromol. Chem., Rapid Commun.*, **3**, 803 (1982)
31. H. Stevens, G. Rehage and H. Finkelmann, *Macromolecules*, **17**, 851 (1984)
32. V. Percec, D. Tomazos and C. Pugh, *Macromolecules*, **22**, 3259 (1989)
33. T. Sagane and R. W. Lenz, *Polym. J.*, **20**, 923 (1988)
34. T. Sagane and R. W. Lenz, *Polymer*, **30**, 2269 (1989)
35. T. Sagane and R. W. Lenz, *Macromolecules*, **22**, 3763 (1989)

36. V. Percec and M. Lee, *J. Macromol. Sci.-Chem.*, **A28**, 651 (1991)
37. V. Percec, M. Lee and C. Ackerman, *Polymer*, in press
38. V. Percec and M. Lee, *Macromolecules*, **24**, 1017 (1991)
39. V. Percec and M. Lee, *Macromolecules*, **24**, 2780 (1991)
40. V. Percec, M. Lee and H. Jonsson, *J. Polym. Sci., Polym. Chem. Ed.*, **29**, 327 (1991)
41. J. M. Rodriguez-Parada and V. Percec, *J. Polym. Sci., Part A: Polym. Chem.*, **24**, 1363 (1986)
42. C. G. Cho, B. A. Feit and O. W. Webster, *Macromolecules*, **23**, 1918 (1990)
43. R. Rodenhouse, V. Percec and A. E. Feiring, *J. Polym. Sci.: Part C: Polym. Lett.*, **28**, 345 (1990)
44. H. Jonsson, V. Percec and A. Hult, *Polym. Bull.*, **25**, 131 (1991)
45. V. Percec, A. S. Gomes and M. Lee, *J. Polym. Sci.: Part A: Polym. Chem. Ed.*, **29**, 1615 (1991)
46. R. Rodenhouse and V. Percec, *Adv. Mater.*, **3**, 101 (1991)
47. V. Percec and M. Lee, *Polym. Bull.*, in press
48. P. A. Gemmell, G. W. Gray and D. Lacey, *Mol. Cryst. Liq. Cryst.*, **122**, 205 (1985)
49. M. S. K. Lee, G. W. Gray, D. Lacey and K. Toyne, *J. Makromol. Chem., Rapid Commun.*, **10**, 325 (1989)
50. G. W. Gray, J. S. Hill and D. Lacey, *Angew. Chem. Int. Ed. Engl. Adv. Mater.*, **28**, 1120 (1989)
51. G. Allegra and I. W. Bassi, *Adv. Polym. Sci.*, **6**, 549 (1969)
52. G. Allegra and I. W. Bassi, in "Polymer Handbook" (Eds. Brandrup, J.; Immergert, E. H.), Wiley, New York, 1975, p. III-205
53. For some representative reviews see: (a) G. Sigaud, N. H. Tinh, F. Hardouin and H. Gasparoux, *Mol. Crst. Liq. Cryst.*, **69**, 81 (1981); (b) F. Hardouin, A. M. Levelut, M. F. Archard and G. Sigaud, *J. Chim. Phys.*, **80**, 53 (1983); (c) F. Hardouin, *Physica*, **140A**, 359 (1986); (d) P. E. Cladis, *Mol. Cryst. Liq. Cryst.*, **165**, 85 (1988)
54. P. Le Barny, J. C. Dubois, C. Friedrich and C. Noel *Polym. Bull.*, **15**, 341 (1986)

55. T. I. Gubina, S. G. Kostromin, R. V. Talroze, V. P. Shibaev and N. A. Plate, *Vyskomol. Soed. Ser. B.*, **28**, 394 (1986)
56. V. Shibaev, *Mol. Cryst. Liq. Cryst.*, **155**, 189 (1988)
57. N. Lacoudre, A. Le Borgue, N. Spassky, J. P. Vairon, P. Le Barny; J. C. Dubois, S. Esselin, C. Friedrich and C. Noel, *Mol. Cryst Liq. Cryst.*, **155**, 113 (1988)
58. N. Spassky, N. Lacoudre, A. Le Borgue, J. P. Vairon, C. L. Jun, C. Friedrich and C. Noel, *Makromol. Chem., Makromol. Symp.*, **24**, 271 (1989)
59. T. A. Gubina, S. Kise, S. G. Kostromin, R. V. Talroze, V. P. Shibaev and N. A. Plate, *Liq. Cryst.*, **4**, 197 (1989)
60. S. G. Kostromin, V. P. Shibaev and S. Diele, *Makromol. Chem.*, **191**, 2521 (1990)
61. C. Legrand, A. Le Borgue, C. Bunel, A. Lacoudre, P. Le Barny, N. Spassky and J. P. Vairon, *Makromol. Chem.*, **191**, 2979 (1990)

CHAPTER 8

1. (a) V. Percec, M. Lee and H. Jonsson, *J. Polym. Sci., Polym. Chem. Ed.*, **29**, 327 (1991); (b) V. Percec and M. Lee, *J. Macromol. Sci.-Chem.*, **A28**, 651 (1991); (c) V. Percec and M. Lee, *Macromolecules*, **24**, 1017 (1991);
2. C. G. Cho, B. A. Feit and O. W. Webster, *Macromolecules*, **23**, 1918 (1990)
3. (a) G. Sigaud, N. H. Tinh, F. Hardouin and H. Gasparoux, *Mol. Crst. Liq. Cryst.*, **69**, 81 (1981); (b) F. Hardouin, A. M. Levelut, M. F. Archard and G. Sigaud, *J. Chim. Phys.*, **80**, 53 (1983); (c) F. Hardouin, *Physica*, **140A**, 359 (1986); (d) P. E. Cladis, *Mol. Cryst. Liq. Cryst.*, **165**, 85 (1988)
4. V. Percec, B. Hahn, M. Ebert, J. H. Wendorff, *Macromolecules*, **23**, 2092 (1990)
5. A. Keller, G. Ungar and V. Percec, *Advances in Liquid Crystalline Polymers*, C. K. Ober and R. A. Weiss Eds. ACS Symposium series, Washington D. C., 1990
6. V. Percec and A. Keller, *Macromolecules*, **23**, 4347 (1990)
7. V. Percec and Y. Tsuda, *Polymer*, **32**, 661 (1991)

CHAPTER 9

1. V. P. Shibaev and N. Plate, 1984, *Adv. Polym. Sci.*, **60/61**, 173
2. V. Percec and C. Pugh, in "Side Chain Liquid Crystal Polymers", McArdle, C. B. Ed., Chapman and Hall, New York, 1989, p. 30
3. G. Gray, in "Side Chain Liquid Crystal Polymers", McArdle, C. B. Ed., Chapman and Hall, New York, 1989, p. 106
4. N. A. Plate and V. P. Shibaev, "Comb-Shaped Polymers and Liquid Crystals" Plenum Press, New York, 1987
5. P. A. Gemmell, G. W. Gray and D. Lacey, *Mol. Cryst. Liq. Cryst.*, **122**, 205 (1985)
6. Y. S. Lapatov, V. V. Tsukruk, O. A. Likhonina, V. C. Shilov, Y. B. Amerik, I. I. Konstantinov and V. S. Grebneva, *Polymer*, **28**, 1370 (1987)
7. H. Ringsdorf, H. W. Schmidt and A. Schneller, *Makromol. Chem., Rapid Commun.*, **3**, 745 (1982)
8. H. Finkelmann, U. Kiechle and G. Rehage, *Mol. Cryst. Liq. Cryst.*, **94**, 343 (1983)
9. G. M. Janini, R. J. Laub and T. J. Shaw, *Makromol. Chem., Rapid Commun.*, **6**, 57 (1985)
10. M. F. Achard, M. Mauzac, H. Richard, G. Sigaud and F. Hardouin, *Eur. Polym. J.*, **25**, 593 (1989)
11. G. W. Gray, W. D. Hawthorne, J. S. Hill, D. Lacey, M. S. K. Lee, G. Nestor and M. S. White, *Polymer*, **30**, 964 (1989)
12. S. G. Kostromin, R. V. Talroze, V. P. Shibaev and N. A. Plate, *Makromol. Chem., Rapid Commun.*, **3**, 803 (1982)
13. Stevens, H.; Rehage, G. and Finkelmann, H., *Macromolecules*, **17**, (1984) 851
14. V. Percec, D. Tomazos and C. Pugh, *Macromolecules*, **22**, 3259 (1989)
15. (a) T. Sagane and R. W. Lenz, *Polym. J.*, **20**, 923 (1988); (b) T. Sagane and R. W. Lenz, *Polymer*, **30**, 2269 (1989); (c) T. Sagane and R. W. Lenz, *Macromolecules*, **22**, 3763 (1989)
16. (a) V. Percec, M. Lee and H. Jonsson, *J. Polym. Sci., Polym. Chem. Ed.*, **29**, 327 (1991); (b) V. Percec and M. Lee, *J. Macromol. Sci.-Chem.*, **A28**, 651 (1991); (c) V. Percec and M. Lee, *Macromolecules*, **24**, 1017 (1991); (d) V. Percec and M. Lee, *Macromolecules*, **24**, 2780 (1991); (e) V. Percec, M. Lee and C. Ackerman, *Polymer*, in press

17. S. G. Kostromin, N. G. Cuong, E. S. Garina and V. P. Shibaev, *Mol. Cryst. Liq. Cryst.*, **193**, 77 (1990)
18. M. Sawamoto, T. Ohtoyo, T. Higashimura, K. H. Guhrs and G. Heublein, *Polym. J.*, **17**, 929 (1985)
19. (a) V. Percec and M. Lee, *Polym. Bull.*, **25**, 123 (1991); (b) V. Percec and M. Lee, *Polym. Bull.*, **25**, 131 (1991); (c) V. Percec and M. Lee, *Macromolecules*, **24**, 4963 (1991); (d) V. Percec and M. Lee, *Polymer*, **32**, 2862 (1991); (e) V. Percec and M. Lee, *J. Mater. Chem.*, **1**, 1007 (1991)
20. (a) V. Percec, Q. Zheng and M. Lee, *J. Mater. Chem.*, **1**, 611 (1991); (b) V. Percec, Q. Zheng and M. Lee, *J. Mater. Chem.*, **1**, 1015 (1991); (c) V. Percec and Q. Zheng, *J. Mater. Chem.*, submitted.
21. G. R. Van Hecke, *J. Phys. Chem.*, **83**, 2344 (1979)
22. D. Demus and L. Richter, "Textures of Liquid Crystals", Verlag Chemie, Weinheim 1978
23. G. W. Gray and G. W. Goodby, "Smectic Liquid Crystals. Texture and Structures", Leonard Hill, Glasgow 1984
24. C. G. Cho, B. A. Feit and O. W. Webster, *Macromolecules*, **23**, 1918 (1990)
25. C. H. Lin and K. Matyjaszewsky, *Polym. Prepr., Am. Chem. Soc. Div. Polym. Chem.*, **31**(1), 599 (1990)
26. V. Percec and Y. Tsuda, *Polymer*, **32**, 673 (1991)
27. M. Marcos, E. Melendez, M. B. Ros and J. L. Serrano, *Mol. Cryst. Liq. Cryst.*, **167**, 239 (1989)
28. J. W. Park, C. S. Bak and M. M. Labes, *J. Am. Chem. Soc.*, **97**, 4398 (1975)
29. C. S. Oh, *Mol. Cryst. Liq. Cryst.*, **42**, 1 (1977)
30. B. Engelen, G. Hepkcke, R. Hopf and F. Schneider, *Mol. Cryst. Liq. Cryst.*, **49**, 193 (1979)
31. B. Engelen and F. Schneider, *Z. Naturforsch.*, **33a**, 1077 (1978)
32. F. Hardouin, G. Sigaud, P. Keller, H. Richard, H. T. Nguyen, M. Mauzac and M. F. Achard, *Liq. Cryst.*, **5**, 463 (1989)
33. E. Chiellini and G. Galli, Recent Advances in Liquid Crystalline Polymers, Chapoy, L., Ed., Elsevier Appl. Sci. Publishers, New York 1985
34. S. B. Evance, J. I. Weischenk, A. B. Padias, J. K. Hall and T. M. Leslie, *Mol. Cryst. Liq. Cryst.*, **183**, 361 (1990)

35. V. P. Shibaev, N. A. Plate and Y. S. Freizon, *J. Polym. Sci., Polym. Chem. Ed.*, **17**, 1655 (1979)
36. H. Finkelmann and G. Rehage, *Makromol. Chem., Rapid Commun.*, **1**, 733 (1980)
37. M. A. Maus, Y. S. Freizon, V. P. Shibaev and N. A. Plate, *Polym. Bull.*, **6**, 485 (1982)

CHAPTER 10

1. (a) V. Percec, M. Lee and H. Jonsson, *J. Polym. Sci.: Part A: Polym. Chem.*, **29**, 327(1991); (b) V. Percec and M. Lee, *J. Macromol. Sci.-Chem.*, **A** **28**, 651(1991); (c) V. Percec and M. Lee, *Macromolecules*, **24**, 1017(1991); (d) V. Percec and M. Lee, *Macromolecules*, **24**, 2780(1991); (e) V. Percec, M. Lee and C. Ackerman, *Polymer*, in press; (f) V. Percec, M. Lee, P. Rinaldi and V. Litmann, *J. Polym. Sci.: Part A: Polym. Chem.*, in press; (g) V. Percec and M. Lee, *J. Macromol. Sci.-Chem.*, submitted
2. C. G. Cho, B. A. Feit and O. W. Webster, *Macromolecules*, **23**, 1918(1990); C. H. Lin and K. Matyjaszewsky, *Polym. Prepr. Am. Chem. Soc. Div. Polym. Chem.*, **31**(1), 599(1990).
3. (a) J. Adams and W. Gronski, *Makromol. Chem., Rapid Commun.*, **10**, 553 (1989); (b) J. Adams and W. Gronski, in "Liquid Crystalline Polymers", R. A. Weiss and C. K. Ober Eds., ACS Symposium Series 435, Am. Chem. Soc., Washington DC, 1990, p. 174
4. M. Hefft and J. Springer, *Makromol. Chem., Rapid Commun.*, **11**, 397 (1990)
5. J. Hopken, C. Pugh, W. Richtering and M. Moller, *Makromol. Chem.*, **189**, 911 (1988); Y. Ishikawa, H. Kuwahara and T. Kunitake, *J. Am. Chem. Soc.*, **111**, 8530 (1989); C. Viney, R. J. Twieg, T. P. Russell and L. E. Depero, *Liq. Cryst.*, **5**, 1783 (1989); M. P. Turberg and J. E. Brady, *J. Am. Chem. Soc.*, **110**, 7797 (1988); C. P. Jariwala, P. E. G. Sundell, C. E. Hoyle and L. J. Mathias, *Macromolecules*, **24**, 6352 (1991)
6. V. Percec, C. S. Hsu and D. Tomazos, *J. Polym. Sci.: Part A: Polym. Chem. Ed.*, **24**, 1363(1986);
7. T. Gibson, *J. Org. Chem.*, **45**, 1095(1980)
8. V. Percec and D. Tomazos, to be published.
9. Hopken, M. Moller, M. Lee and V. Percec, *Makromol. Chem.*, in press
10. A. Poniewierski, T. J. Sluckin, *Liquid Cryst.*, **2**, 281 (1987)

11. P. Sheng, *Phys. Rev. A* **26**, 1610 (1982)